PPG-821
UCLA-ENG-84-30

# FINESSE

## A Study of Issues, Experiments and Facilities for Fusion Nuclear Technology Research & Development

Interim Report

Volume IV

**October 1984**

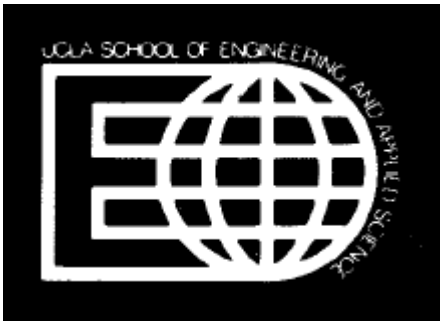


Center for Plasma Physics and Fusion Engineering
University of California, Los Angeles
Los Angeles, California

DISCLAIMER

This report was prepared as an account of work sponsored by the United States Government. Neither the United States nor the United States Department of Energy, nor any of their employees, makes any warranty, express or implied, or assumes any legal liability or responsibility for the accuracy, completeness, or usefulness of any information, apparatus, product, or process disclosed, or represents that its use would not infringe privately owned rights. Reference herein to any specific commercial product, process, or service by trade name, mark, manufacturer, or otherwise, does not necessarily constitute or imply its endorsement, recommendation, or favoring by the United States Government or any agency thereof. The views and opinions of authors expressed herein do not necessarily state or reflect those of the United States Government or any agency thereof.

Printed in the United States of America

Available from:

National Technical Information Service
U.S. Department of Commerce
5285 Port Royal Road
Springfield, Virginia 22161

Price: Printed Copy
Microfiche A01

Distribution Category:
Magnetic Fusion (UC-20)

University of California, Los Angeles
PPG-821
UCLA-ENG-84-30

# FINESSE: A Study of the Issues, Experiments and Facilities for Fusion Nuclear Technology Research and Development

Interim Report

Volume IV

## Contributors

M. Abdou, UCLA
C. Baker, ANL
T. Bauer, ANL
G. Bell, TRW
D. Berwald, TRW
M. Billone, ANL
J. Blanchard, UCLA
R. Burke, HEDL
R. Conn, UCLA
J. Crocker, EG&G
J. Davis, MDAC
G. Deis, EG&G
R. DiMelfi, UCLA
J. Doggett, LLNL
M. Fenstermacher, TRW
J. Garner, TRW
P. Gierszewski, UCLA/CFFTP
J. Gordon, TRW
S. Grotz, UCLA
J. Grover, HEDL
C. Gung, UCLA
G. Hollenberg, HEDL
J. Holmes, HEDL
D. Jassby, PPPL
K. Kleefeldt, UCLA/KfK
T. Kraft, ANL
Y. Liu, ANL
H. Madarame, UCLA/U. of Tokyo
L. Masson, EG&G
L. Miller, EG&G
G. D. Morgan, MDAC
R. Nygren, ANL
E. Opperman, HEDL
G. Orient, UCLA
Y. Oyama, UCLA/JAERI
M. Perrin, MDAC
R. Puigh, HEDL
D. Reuster, MDAC
D. Rose, ANL
Y. Seki, UCLA/JAERI
K. Shin, UCLA/Kyoto U.
W. Steele, TRW
J. Straalsund, HEDL
J. Szabo, UCLA
K. Taghavi, UCLA
K. Thomassen, LLNL
M. Tillack, UCLA
R. Whitley, TRW
M. Youssef, UCLA

October 1984

FINESSE: A Study of the Issues, Experiments and Facilities for Fusion Nuclear Technology Research and Development

Interim Report

Volume IV

Task Leaders

M. Abdou, UCLA: Principal Investigator

D. Berwald, TRW: Development Scenarios, Mirror Facilities

M. Billone, ANL: Tritium Extraction Modelling

J. Davis, MDAC: Failure Modes

G. Deis, EG&G: Fission Reactor Utilization

P. Gierszewski, UCLA/CFFTP: Testing Needs, Testing Requirements

G. Hollenberg, HEDL: Solid Breeders

J. Holmes, HEDL: Point Neutron Sources

D. Jassby, PPPL: Tokamak Facilities

G. Morgan, MDAC: Reference Generic Designs

R. Nygren, ANL: Non-Neutron Test Stands

J. Straalsund, HEDL: Materials, Interactive Effects

M. Tillack, UCLA: Issues, Testing Requirements

R. Whitley, TRW: Availability Modelling

VOLUME IV

TABLE OF CONTENTS


Page

7. NEUTRONICS TESTS

7.1 Introduction..... 7-1

7.2 Objectives of Neutronics Tests..... 7-2

7.3 Test Field and Geometrical Arrangement for Neutronics Testing..... 7-6

7.3.1 The Instrumentation and Operating Condition Requirements in a Fusion Test Device..... 7-7

7.3.2 Considerations for the Test Module Size Requirements and the Experimental Arrangement..... 7-19

7.3.2.1 Adjusting Neutron Spectrum Incident on the Test Module..... 7-21

7.3.2.2 Impact of the Poloidal Boundary Condition of the Test Module on Tritium Production..... 7-29

7.3.2.3 Impact of the Toroidal Boundary of the Test Module on First Wall Spectrum and Tritium Production... 7-33

7.3.2.4 Remarks on the Results from the Nuclear Analysis in the Poloidal and the Toroidal Models..... 7-45

7.4 Neutronics Testing Requirements Summary..... 7-47

7.4.1 Test Device Operating Condition Requirements..... 7-47

7.4.2 Test Module Requirements..... 7-48

References..... 7-56

8. FLUENCE CONSIDERATIONS

8.1 Introduction..... 8-1

8.2 Material Property Extrapolations..... 8-1

8.2.1 Introduction..... 8-1

8.2.2 Swelling..... 8-2

8.2.3 Creep..... 8-7

8.2.4 Tensile Strength/Ductility..... 8-9

8.2.5 Fracture Toughness..... 8-13

8.2.6 Ductile to Brittle Transition Temperature..... 8-19

8.2.7 Fatigue Crack Growth..... 8-20

8.2.8 Conclusions ..... 8-21
8.3 Uncertainty Projection Approach ..... 8-23
8.4 Interactive Testing ..... 8-25
8.5 Conclusions ..... 8-31
References ..... 8-34

9. INSTRUMENTATION AND TEST MATRIX
9.1 Instrumentation ..... 9-1
9.1.1 Introduction ..... 9-1
9.1.2 Generic Instrumentation Issues ..... 9-1
9.1.3 Test Instrumentation Requirements ..... 9-3
References ..... 9-12
9.2 Test Matrix ..... 9-13
9.2.1 Single Specimen Test Matrix and Preliminary Results ..... 9-16
References ..... 9-22

10. NON-NEUTRON TEST STANDS
10.1 Usefulness of Non-Nuclear Tests ..... 10-2
10.2 Test Stands for Single Effects, Interactive and Partially Integrated Testing ..... 10-4
10.2.1 Test Stands for Limiters and First Walls ..... 10-10
10.2.2 Test Stands for Solid Breeder Blankets ..... 10-11
10.2.3 Test Stands for Liquid Metal Blankets ..... 10-13
10.3 Existing Test Stands and Future Needs ..... 10-14
10.3.1 Test Stands for Blankets ..... 10-14
10.3.2 Test Stands for High Heat Flux Components ..... 10-16
References ..... 10-20

11. ACCELERATOR-BASED POINT NEUTRON SOURCES
11.1 Introduction ..... 11-1
11.2 Point Neutron Sources for Fusion Experiments ..... 11-1
11.2.1 Rotating Target Neutron Source (RTNS-II) at LLNL ..... 11-2
11.2.2 Intense Neutron Source (INS) at LANL ..... 11-2
11.2.3 LAMPF A-6 Target Station at LLNL ..... 11-2
11.2.4 Fusion Materials Irradiation Test (FMIT) Facility at HEDL ..... 11-3

11.3 Point Source Potential..... 11-3
11.4 Conclusion..... 11-4
References..... 11-6

12. UTILIZATION OF FISSION REACTORS
12.1 Key Issues for Fission Utilization..... 12-2
12.1.1 Radiation Damage..... 12-2
12.1.2 Power Density..... 12-3
12.1.3 Lithium Burnup Rate..... 12-4
12.1.4 Test Volume..... 12-4
12.1.5 Non-Nuclear Conditions..... 12-5
12.1.6 Reactivity Considerations..... 12-5
12.1.7 Availability for Testing..... 12-5
12.1.8 Cost..... 12-6
12.2 Technical Approach..... 12-6
12.2.1 Facility Survey..... 12-7
12.2.2 One-Dimensional Criticality Study.....12-12
12.2.3 Two-Dimensional Parameter Study.....12-13
12.2.4 Test Development/Analysis.....12-15
12.2.5 Summary of Technical Approach.....12-20
12.3 Analysis of Key Issues.....12-21
12.3.1 Radiation Damage.....12-21
12.3.2 Power Density/Lithium Burnup Rate.....12-23
12.3.3 Test Volume.....12-35
12.3.4 Non-Nuclear Conditions.....12-37
12.3.5 Reactivity Considerations.....12-39
12.3.6 Availability for Testing.....12-41
12.3.7 Cost.....12-41
12.4 Conclusions on Technical Usefulness of Fission Testing.....12-42
12.5 Overall Conclusions on Utilization of Fission Reactors.....12-43
References.....12-44

13. TANDEM MIRROR TEST FACILITIES
13.1 Background and Introduction..... 13-1
13.2 The Technology Demonstration Facility..... 13-5
13.2.1 TDF Design Objectives..... 13-6

13.2.2 Physical Description..... 13-7
13.2.3 Operating Description..... 13-8
13.2.4 Engineering Description.....13-15
13.2.5 Critical Engineering Issues.....13-20
13.2.5.1 Magnets.....13-20
13.2.5.2 Neutral Beams.....13-21
13.2.5.3 Shielding.....13-22
13.2.5.4 Tritium.....13-23
13.2.5.5 Test Facilities.....13-24
13.2.5.6 Maintenance.....13-24
13.3 The MFTF-α+T Upgrade of MFTF-B.....13-27
13.3.1 MFTF-α+T Design Objectives.....13-27
13.3.2 Physical Description and Configuration.....13-28
13.3.3 Physics Mode.....13-32
13.3.4 Engineering Description.....13-34
13.3.4.1 Magnet System.....13-34
13.3.4.2 Heating, Fueling and Drift Pumping.....13-36
13.3.4.3 Halo Scraper, Direct Converter and Vacuum Pumping.....13-38
13.3.4.4 Tritium Systems.....13-41
13.3.4.5 Maintenance.....13-41
13.3.5 Consideration of a More Ambitious Test Cell.....13-45
13.3.5.1 Parametric Analysis.....13-46
13.3.5.2 Optimized Cases.....13-49
13.3.5.3 Conclusions for MFTF-α+T Physics Modeling.....13-50
13.4 Resolving the FINESSE Nuclear Issues in a Tandem Mirror Nuclear Test Facility.....13-53
13.4.1 General Considerations.....13-53
13.4.2 Assessment of Tandem Mirror Nuclear Experimentation/ Testing vis-a-vis FINESSE Nuclear Issues List.....13-60
13.4.2.1 Methodology.....13-60
13.4.2.2 Results.....13-63
References.....13-84

14. TOKAMAK FUSION TEST FACILITIES
14.1 Objectives and Requirements..... 14-1

14.1.1 Introduction..... 14-1
14.1.2 Study Objective..... 14-1
14.1.3 Facility Requirements..... 14-1
14.2 Design Approach..... 14-4
14.2.1 Introduction..... 14-4
14.2.2 Principal Features..... 14-5
14.3 Design Description..... 14-6
14.3.1 Quasi-Ohmic Heating to Ignition..... 14-6
14.3.2 Device Operation.....14-10
14.3.3 Magnet Considerations.....14-10
14.3.4 Power Consumption and Cost.....14-11
14.4 Risks and Uncertainties of the Reference Approach.....14-13
14.4.1 Areas of Uncertainty.....14-13
14.4.2 Alternative Startup Method.....14-14
14.4.3 Comparison with Existing Tokamaks.....14-14
14.5 Conclusions.....14-16
Explanation of Symbols.....14-17

15. RELIABILITY DEVELOPMENT TESTING IMPACTS ON FUSION REACTOR AVAILABILITY
15.1 Introduction..... 15-1
15.2 Confidence Levels in Component Performance..... 15-2
15.3 The NAVAIR Approach to Development Testing..... 15-9
15.3.1 Description of Method.....15-13
15.3.2 Fusion Reactor Development Pathways.....15-14
15.3.3 Availability Models.....15-16
15.3.4 Baseline Analysis.....15-20
15.3.5 Parametric Studies.....15-30
15.3.6 Conclusions.....15-36
15.4 Summary and Conclusions.....15-37
References.....15-38

16. FUSION DEVELOPMENT SCENARIOS
16.1 Introduction and Motivation..... 16-1
16.2 Planning Considerations..... 16-2
16.2.1 Reactor Relevance..... 16-3
16.2.2 Tritium Production..... 16-3

16.2.3 Number of Blanket Options ..... 16-6
16.2.4 Test Objectives ..... 16-6
16.2.5 High Fluence ..... 16-8
16.3 Use of Existing Fusion and Non-Fusion Experimental and Test Facilities ..... 16-9
16.4 Fusion Experimental and Test Facilities ..... 16-11
16.4.1 Plasma Burning Experiment (PBX) ..... 16-11
16.4.2 Fusion Engineering Research Facility (FERF) ..... 16-13
16.4.3 Engineering Test Facility (ETF) ..... 16-14
16.4.4 Engineering Demonstration Facility (EDF) ..... 16-14
16.4.5 Other Facilities and Combinations ..... 16-15
16.5 Preliminary Fusion Development Scenario Evaluation ..... 16-15
16.5.1 Fusion Development Pathways ..... 16-15
16.5.2 Pathway Evaluation Guidelines ..... 16-18
16.5.3 Pathway Evaluations ..... 16-22
16.6 Summary and Conclusions ..... 16-32
16.6.1 Near-Term Experimental Program ..... 16-32
16.6.2 Preliminary Pathway Evaluations ..... 16-32
16.6.3 International Implications ..... 16-34
References ..... 16-36

APPENDIX A. EVALUATION OF EXPERIENCE FROM FAST BREEDER REACTORS
A.1 Introduction ..... A-1
A.2 History of LMFBR Development ..... A-4
A.2.1 Genesis ..... A-4
A.2.2 The National Laboratories and Early U.S. Fast Reactors ..... A-5
A.2.3 Early Industry Initiatives ..... A-11
A.2.4 Establishment of a Priority Breeder Program ..... A-14
A.2.5 LMFBR Program Planning ..... A-16
A.2.6 Fast Flux Test Facility ..... A-17
A.2.7 Developments Leading to LMFBR Commercialization ..... A-19
A.2.8 Institutional Constraints on LMFBR Development ..... A-24
A.2.9 Overview of Foreign Fast Reactor Program ..... A-27
A.3 Technical Program Developments and Problems ..... A-29
A.3.1 Fuels and Materials ..... A-29
A.3.2 Components Development ..... A-35

A.3.3 Safety..... A-45
A.3.4 Experimental Reactors and Plant Design..... A-57
A.4 Summary Observations and Conclusions..... A-64
References..... A-72

APPENDIX B. OBSERVATIONS OF EXPERTS FROM THE FISSION FIELD
B.1 Introduction..... B-1
B.2 Major Problems..... B-2
B.3 Regulations..... B-4
B.4 Setbacks and Failures..... B-6
B.5 Public Acceptance..... B-8
B.6 Power Density..... B-10
B.7 Plant Size..... B-11
B.8 Scaling..... B-14
B.9 Integrated Testing..... B-17
B.10 Personnel and Organizational Structure..... B-18
B.11 Lessons..... B-21
B.12 Reviewers' Comments..... B-23

APPENDIX C. EVALUATION OF EXPERIENCE FROM THE AEROSPACE INDUSTRY
C.1 Aerospace Approach to Design..... C-1
C.1.1 Establishment of Design Goals..... C-1
C.1.2 Establishment of Design Configuration..... C-2
C.1.3 Testing to Build Confidence in the Design..... C-2
C.2 Example of Aerospace Approach to Design..... C-3

APPENDIX D. CHARACTERIZATION OF FUSION NUCLEAR SYSTEMS OPERATING ENVIRONMENT
D.1 Introduction..... D-1
D.2 Radiation Field..... D-2
D.2.1 Introduction..... D-2
D.2.2 The $Li_2O$ Helium-Cooled Blanket with PCA Structure..... D-5
D.2.3 The $Li_2O$ Helium-Cooled Blanket with Ferritic Steel as Structure..... D-13
D.2.4 The $Li_{17}Pb_{83}$ Self-Cooled Blanket with PCA Structure..... D-20
D.2.5 The Liquid Lithium Self-Cooled Blanket with V15Cr5Ti Structure..... D-28

D.2.6 The $LiAlO_2$ Water-Cooled Blanket, with Ferritic Steel Structure..... D-35
D.2.7 Summary Table for the Nuclear Performance..... D-45
D.2.7.1 Tritium Breeeding..... D-45
D.2.7.2 Heat Deposition and Power Multiplication..... D-45
D.2.7.3. Damage Parameters..... D-45
D.2.8 Reference Fluxes at Key Locations..... D-47
References..... D-54
D.3 First Wall Blanket..... D-55
D.3.1 Li/Li/V Concept (Tokamak)..... D-56
D.3.2 $Li_2O$/He/FS Concept (Tokamak)..... D-56
D.3.3 $LiAlO_2/H_2O$/PCA/Be Concept (Tokamak)..... D-57
D.3.4 LiPb/LiPb/V Concept (TMR)..... D-58
References..... D-83
D.4 Plasma-Interactive Components..... D-84
D.4.1 Introduction..... D-84
D.4.2 Plasma Edge Conditions as the Base for Operating Parameters..... D-85
D.4.3 Operating Parameters..... D-86
D.4.3.1 Heat Flux..... D-86
D.4.3.2 Particle Flux and Species..... D-87
D.4.3.3 Neutron Flux and Fluence..... D-87
D.4.3.4 Burn Time and Number of Cycles..... D-88
D.4.3.5 Materials and Operating Temperature..... D-88
D.4.3.6 Manetic Field..... D-90
References..... D-91
D.5 Tritium and Vacuum Systems..... D-92
D.5.1 Fuel Cycle..... D-92
D.5.2 Breeder Cycle..... D-96
D.5.3 Secondary Systems..... D-97
D.5.4 Instrumentation and Control..... D-100
References..... D-102

APPENDIX E. MODELLING OF MFTF-α+T HIGH GAMMA MODE PERFORMANCE
E.1 Introduction..... G-1
E.2 MFTF-α+T High Gamma Mode Operation..... G-1

E.2.1 Device Description..... G-1
E.2.2 Physics Description..... G-2
E.3 Description of the Physics Model..... G-5
E.4 Baseline Parameters..... G-11
E.4.1 Strong Effects..... G-11
E.4.2 Moderate Effects..... G-12
E.4.3 Mild Effects..... G-13
References..... G-21

APPENDIX F. SMALL SCALE, MULTIPLE EFFECTS TESTING AT US/DOE BREEDER REACTOR IN-PILE FACILITIES

F.1 Introduction..... F-1
F.2 Aims and Expectations..... F-1
F.3 Cost in Money and Time..... F-3
F.4 Strategy for Facility Use..... F-4
F.5 Breeder Reactor In-Pile Test Facilities..... F-5
F.5.1 EBR-II Instrumented Subassemblies..... F-5
F.5.2 FFTF Test Subassemblies..... F-7
F.5.3 TREAT..... F-8
F.5.4 FNEL and FFTF Remote Handling Capability..... F-11
F.6 Fusion Experiments in Breeder Reactor Facilities..... F-13
F.6.1 General Features..... F-13
F.6.2 EBR-II..... F-14
F.6.3 FFTF..... F-15
F.6.4 TREAT..... F-16
F.7 Conclusions..... F-17
References..... F-18

# CHAPTER 7

# NEUTRONICS TESTS

TABLE OF CONTENTS


Page

7.1 Introduction..... 7-1

7.2 Objectives of Neutronics Tests..... 7-2

7.3 Test Field and Geometrical Arrangement for Neutronics Testing..... 7-6

7.3.1 The Instrumentation and Operating Condition Requirements in a Fusion Test Device..... 7-7

7.3.2 Considerations for the Test Module Size Requirements and the Experimental Arrangement..... 7-19

7.3.2.1 Adjusting Neutron Spectrum Incident on the Test Module..... 7-21

7.3.2.2 Impact of the Poloidal Boundary Condition of the Test Module on Tritium Production..... 7-29

7.3.2.3 Impact of the Toroidal Boundary of the Test Module on First Wall Spectrum and Tritium Production..... 7-33

7.3.2.4 Remarks on the Results from the Nuclear Analysis in the Poloidal and the Toroidal Models..... 7-45

7.4 Neutronics Testing Requirements Summary..... 7-47

7.4.1 Test Device Operating Condition Requirements..... 7-47

7.4.2 Test Module Requirements..... 7-48

References..... 7-56

# 7. NEUTRONICS TESTS

## 7.1 Introduction

Neutronics tests will demonstrate the capability for predicting parameters that resolve neutronics issues, such as TBR, heating rate, etc., in a fusion reactor by using calculational codes and data base packages. Such tests should be conducted in a fusion test device since undertaking this task in a demo or commercial fusion reactor is costly.

Currently, there are several benchmark experiments using the accelerator-based point sources, e.g., FNS (JAERI),[1,2] etc. These experiments are essential for testing the feasibility of tritium breeding and other design choices in addition to validating calculational methods. However, the point sources have limitations such as neutron intensity and the geometrical arrangement which deviate from the large scale fusion reactor. Predicting a parameter in a large scale reactor will include many sources of uncertainties that do not exist in a simple and clean benchmark experiment.

In this chapter, we discuss the neutronics test requirements in a nuclear field and the design of those experiments that can achieve this goal. In Section 7.2 we describe the objectives of neutronics tests relating to the benchmark experiments. Considerations for instruments and measurements needed to perform these neutronics tests are described in Section 7.3. These test requirements specify the minimum fluence, operation time, environmental magnetic field effects, and minimum size requirements for the instrumentation. As expected, these requirements vary depending on the parameter to be measured. In addition, Section 7.3 includes a detailed analysis pertaining to studying the effect of varying the test module conditions (test module width, surface area exposed to the nuclear field, boundary conditions, etc.) on the nuclear performance in a configuration where the test module is partially covering the plasma of the test device. In Section 7.4 we summarize the nuclear test requirements where we included specifications such as the minimum test module geometrical size that provides a desired nuclear performance within a predetermined accuracy. Specifically, we focused on the tritium breeding as a critical neutronic issue where the minimum test module size in a partial coverage condition is specified for various geometrical arrangements such that the local and integrated values are within a given accuracy as compared to the values obtained in the full coverage condition.

## 7.2 Objectives of Neutronics Tests

The goal of neutronics is to predict the neutronics performance of parameters of interest in a fusion reactor. These parameters are described in Chapter 3. The accuracy of the prediction is confirmed only by comparing the analytical results to the experimental data. This will serve as a verification of the calculational neutronics codes and confirm their reliability for prediction.

Recently, many neutronics experiments[3] have been carried out in simple geometries to focus on nuclear data verification rather than validating calculational method. The difference between results obtained by calculation and by experimental measurement is generally less than 10% in those experiments. However, the required accuracy[4] in predicting, for example, the tritium breeding ratio is about 5%. This requires improving the discrepancy between calculational results and measured values such that the difference is well below 10%.

Neutronics experiments using an accelerator-based DT point source can be classified according to their objectives as follows:

1) Basic benchmark experiments

The objective in this case is to verify the nuclear data and calculational method. The experiment is carried out in a simple geometry and possibly a single material is employed to minimize the modeling uncertainty and the complexity associated with a multi-material arrangement. Through these experiments, improvements in nuclear data can easily be achieved and the discrepancies among calculational methods can be identified and corrected for.

2) Engineering benchmark experiments

These experiments are carried out to verify the calculational code, modeling approach and data base, e.g., kerma factors, activation data base, etc. These experimental systems are generally more complicated than basic benchmark experiments, and they include several materials.

Verifying the validity of nuclear data, calculational methods, data base and modeling methods could be completed through these benchmark experiments.

However, it is not definite that the improvement in data base and calculational methods based on results from these experiments can lead to a satisfactory prediction when applied to a demo or full-size commercial reactor. The latter are characterized by a volumetric neutron source that has a different angular and spatial distribution as compared to a point source. In addition, the reflected component of source neutrons from the surrounding boundaries will give more than 70% contribution to the neutron spectrum at the first wall (see Table 7.2-1). The surrounding boundary is the surface of the breeder blanket that forms a cylindrical cavity around the plasma source, and it is generally difficult to simulate its effect in an experiment that utilizes a point source. Furthermore, limitations such as geometry and neutron intensity in the accelerator-based point source experiment still exist especially in measuring neutronics effects in large components (e.g., divertor, limiter, etc.) and in reproducing the actual level of activation in these components.

From the above discussion, it is clear that the desired accuracy of the calculational methods and data base established through benchmark studies may not fall within the accuracy required for the theoretical prediction of a given parameter in a full-scale fusion reactor. The experimental stages to identify and reduce the calculational uncertainties are classified as shown in Figure 7.2-1. A key neutronic parameter such as the tritium production rate (TPR) can be predicted by the following relation according to the experimental stage under consideration:

$$\text{Predicted TPR in a demo reactor} \equiv \text{Calculated TPR in a demo reactor} \times \frac{\text{Measured TPR in a Test Module}}{\text{Calculated TPR in a Test Module}} \times (1 + \Delta_s) \ ,$$

where $(1 + \Delta_s)$ is a correction factor that reflects the calculational uncertainty in the demo reactor as compared to the test device module. This factor may be a function of the degree of complexity involved as we move from the test module to the demo reactor geometry. Obviously, $\Delta_s$, becomes smaller when the details of a demo are closely simulated in a fusion test device. Therefore, $(1 + \Delta_s)$ is viewed as a scaling factor that relates the measured parameter in the test device to the corresponding parameter in a demo reactor.

Table 7.2-1 Percentage (%) of the Uncollided Neutrons Incident on the First Wall

| Device (cm) | Test Device ($r_p$ = 15, $t_v$ = 10)* | Mirror ($r_p$ = 50, $t_v$ = 10) | Tokamak ($r_p$ = 253, $t_v$ = 20) |
|---|---|---|---|
| Uncollided | 23.9 | 20.5 | 18.4 |
| Reflected (Collided) | 76.1 | 79.5 | 81.6 |

* $r_p$ = plasma radius

$r_p + t_v$ = first wall radius

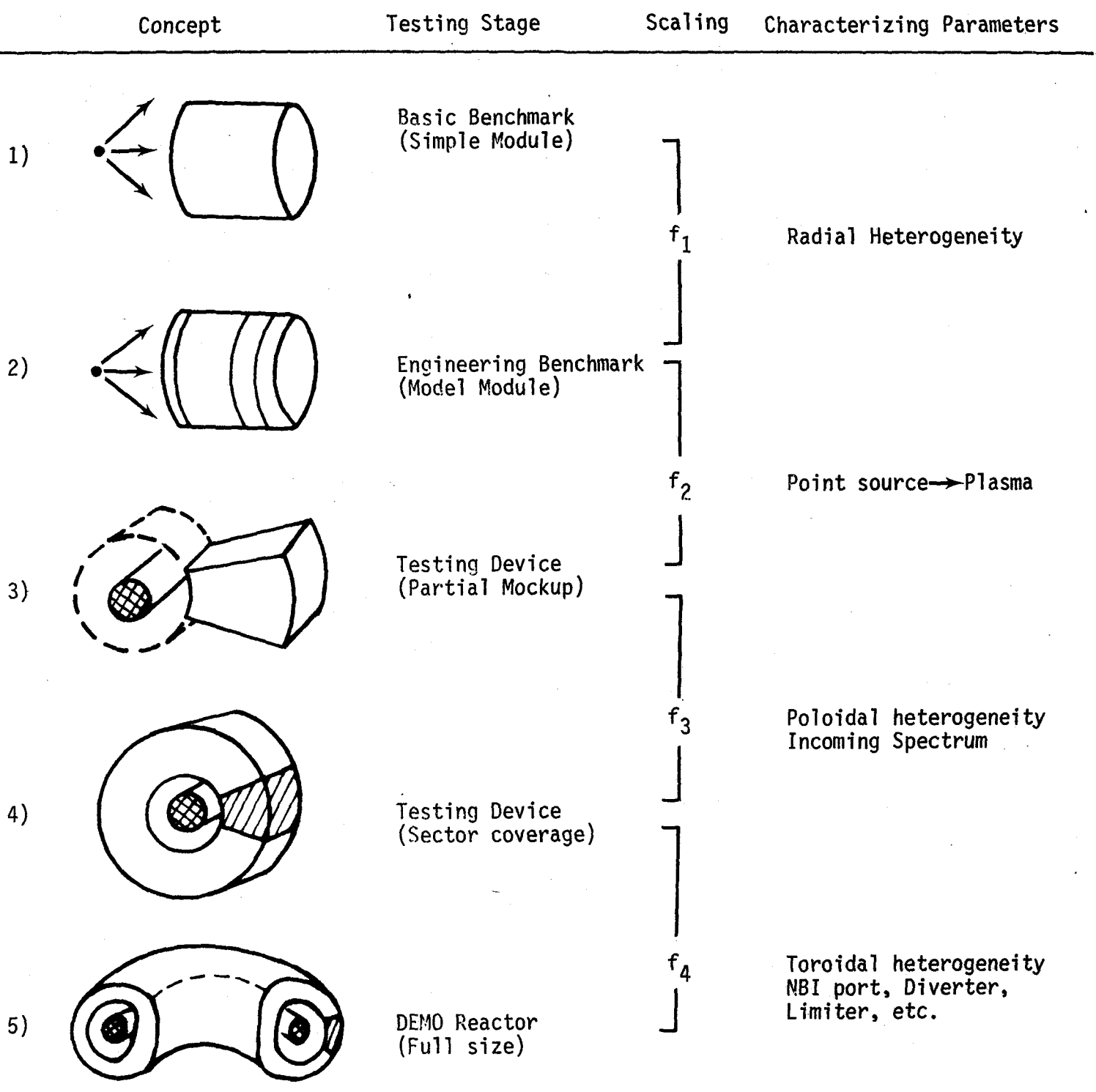


Figure 7.2-1 Stages for the experimental planning to perform neutronics testing and the uncertainty involved in each stage. ($f_i = 1+\Delta_i$)

Second fractional term is likely to be unity and should be closer to unity by improving the calculational model used.

Thus, the objectives of performing neutronics testing in a fusion test device can be summarized as follows:

1) Demonstrate the prediction capability of the neutronic calculational codes, the adequacy of the data base, and modeling approach.

2) Extrapolate the calculational uncertainty in benchmark experiments utilizing a point neutron source to the values expected in a demo reactor and assuring that this later uncertainty falls below a target accuracy.

3) Confirm the feasibility of a design parameter (e.g., TBR) in various blanket concepts by detailed mockup.

4) Verify the data base according to heavy irradiation; long term activation, damage function, etc.

The last objective does not require full simulation, but an intense neutron source is a necessity.

## 7.3 Test Field and Geometrical Arrangement for Neutronics Testing

In this section, we describe the experimental requirements in a fusion test device. These requirements are those related to the operating conditions of the test device itself in addition to those related to the geometrical configuration of the test module in the fusion test device.

The instrumentation for neutronics measurements dictates the operating conditions of the test device. These conditions are characterized by the neutron flux, fluence, and operation mode (continuous, pulsed...). The choice of a detector type also determines the minimum test space as will be discussed later.

Setting up the proper experimental configuration (size, geometry...) is an essential part in the experimental planning. In a fusion test device, the dimensions of the plasma and the first wall radius are smaller than those found in a full-scale demo or commercial reactor. In addition, the test module located in a fusion test device will not necessarily surround the plasma region (full coverage case). It is essential, therefore, to explore the effect of varying the test module size on the nuclear performance through-

out the test module and compare the results to those obtained in the full coverage case. The objective of this analysis is to determine the minimum size of the test module that leads to an acceptable nuclear performance as compared to the full coverage reference case within a desired target accuracy.

First, in Section 7.3.1 we give the test device operating conditions for adequate measurements of various responses. We devote Section 7.3.2 to the requirements imposed on the test module located in the fusion test device in terms of minimum size and geometrical arrangement to achieve the target accuracy mentioned above.

### 7.3.1 The Instrumentation and the Operating Condition Requirements in a Fusion Test Device

The experimental methods for measuring various neutronics parameter, e.g., source neutron yield, tritium production, nuclear heating, reaction rates, and neutron and gamma-ray spectra are briefly described in this section. The inherent limitations for measuring a particular parameter govern the optimum operating condition in a test device.[5] The source neutron yield is referred to as a part of the plasma diagnostic studies. This parameter is essential in comparing measured parameters to calculational prediction since most of the neutronics parameters are expressed in terms of result per unit source neutrons. The main limitations of the experimental techniques are: 1) counting rate, 2) counting statistics, 3) detector size, 4) operation environment, and 5) accuracy.

The counting rate limitation is inherent in counter methods. This limitation depends mainly on the neutron and gamma-ray separation technique. The required counting rate is generally about 1 kcps, including neutron and gamma-ray events. The counting statistic is a common requirement in all techniques, and it relates to the signal-to-background ratio and required neutron fluence. The detector size includes the electronics, the pre-amplifier, the photo-multiplier, etc., which cannot be disconnected from the probe in any counter methods. The operation environment includes temperature, magnetic field, magnetic field change, the degree of the intense neutron irradiation, etc. Temperature will influence some detectors such as the thermo-luminescence dosimeters (TLD's), the irradiation samples for tritium production measurement, etc. Magnetic field and its change will give the turbulence

to the electronics and the detector response, particularly in the counter methods. Neutron irradiation dictates the damage to the detector probes.

## Neutron Yield Measurements

Absolute total neutron yield measurement is practically impossible in fusion reactors since they have volumetric neutron sources. In the accelerator-based point D-T neutron source, the associated α-particles are measured and used to detect the D-T reaction rate. However, there is no direct method covering the entire source region in a large volumetric source. In this situation, we can only measure the neutron yield in a part of the source spatial zone.

The methods used for measuring neutron yield are the multi-foil activation (MFA) techniques, NE213 scintillation counter and fission chambers. These methods are characterized by being sensitive to the 14 MeV neutrons. The MFA technique and the NE213 counter can be used to measure the absolute neutron spectra. Fission chambers need some corrections to obtain neutron yield because their response depends on the neutron spectrum. The MFA technique consists of irradiating various foils of different materials, measuring the gamma-ray of the activated products and unfolding the spectrum using their differential cross sections. The NE213 scintillator and fission chambers are based on the counting methods (active methods).

The total source neutron yield or line source intensity may be estimated using the above detectors by semi-empirical method that is based on neutronic calculation. However, more elaborate diagnostics are required to measure the spatial distribution of the neutron source.

## Tritium Production Measurements

One of the methods used to measure tritium production rate is the β-counting method which consists of irradiating the lithium sample and counting the β-decay rate of tritium by scintillation counting method or internal gas proportional counter method. Typical results are shown in Figure 7.3.1-1.[6] The mass spectrometric method can also be used. In this method one measures the number of α-particles produced simultaneously by the tritium production reaction (e.g., $^{6}Li(n,\alpha)t$). However, a correction is needed to account for the α-particles coming from the $^{6}Li(n,dn)\alpha$ reaction, for example.

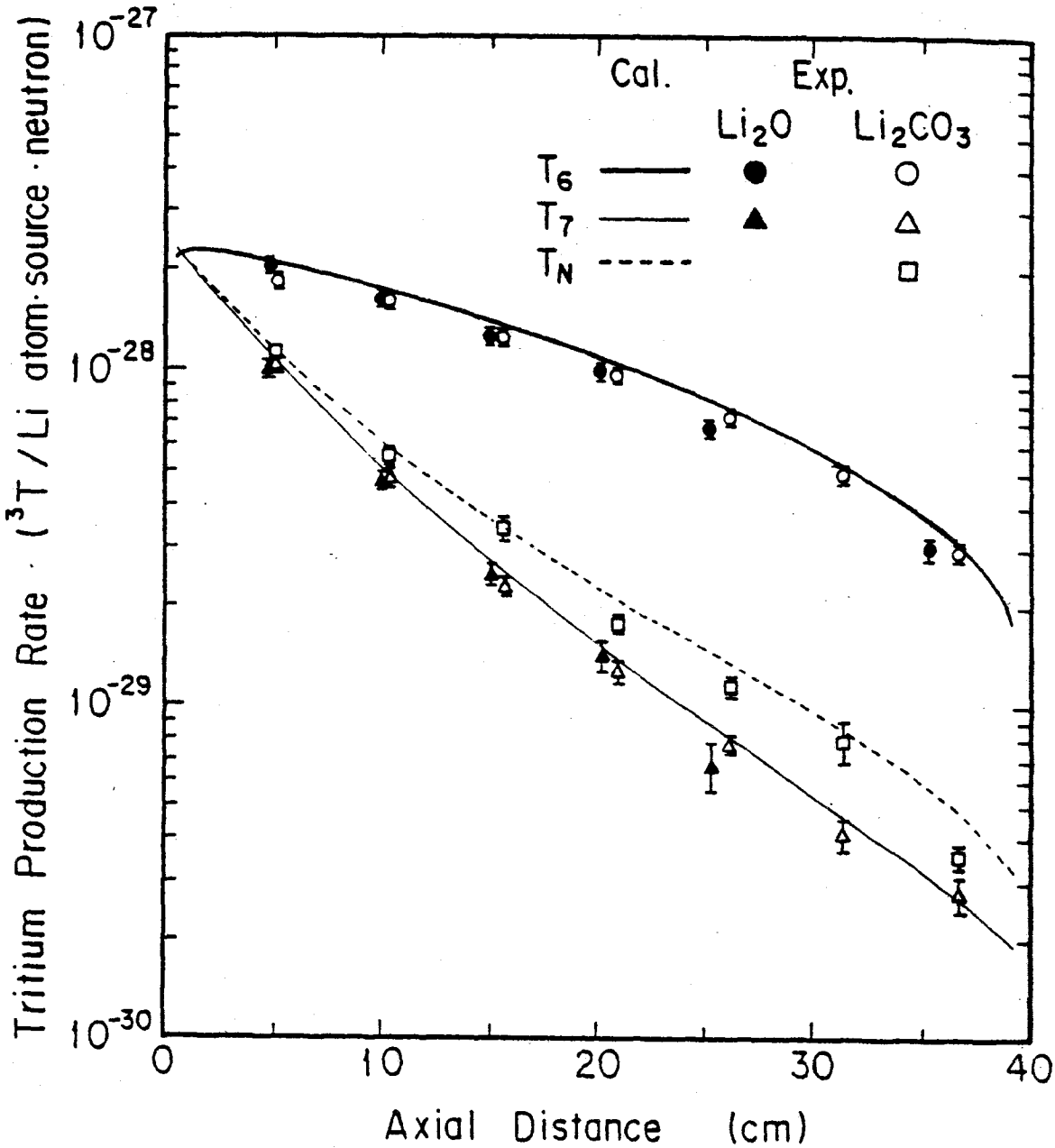


Figure 7.3.1-1 Tritium production rate distribution measurement in 40cm-thick $Li_2O$ cylindrical assembly at the Fusion Neutronics Source (FNS) facility at JAERI.

Some other methods are based on direct measurement for the $^{6}Li(n,\alpha)t$ reaction rate. Among these methods are the Li-glass scintillators, Li-radiator gas proportional counter, Li-radiator track recorder and LiF TLD's. The first two methods are a counter type. The last method consists of irradiating TLD's, annealing TLD's and measuring self-dose by β-decay of tritium produced in the TLD's. The most accurate methods are those based on the β-counting technique, but these methods need large neutron fluence because of their low sensitivity.

Nuclear Heating Measurements

Nuclear heating is produced by both neutron and gamma-ray interactions. The techniques used to measure the nuclear heating are calorimeters, thermoluminescence dosimeters (TLD's), and gas-filled counters.

Calorimeters are a direct method for heating measurements including neutron and gamma-ray heatings. They are generally used at steady state condition. For pulsed-operation mode, micro-calorimetry techniques with fast time response can be used but they require a wall load above 0.5 $MW/m^2$. Since these methods use thermocouples that are affected by the magnetic field change, this particular effect should be considered when measurements are performed in a fusion reactor.

The TLD's have generally been used for gamma-ray dose measurement. For heating rate measurement, it is required that the TLD's material be the same material as the surrounding media. The LiF(Mg) can be used in the blanket breeding zone that includes lithium. For gamma-ray heating measurements in other materials, more than one TLD with different effective atomic number are required and an interpolation between their responses is necessary. However, gamma heating measurements by TLD's methods require large correction due to the contribution from neutron heating. The TLD's are also applied to dosimeter by using cavity chamber theory which give the absorbed dose in the medium by gamma-rays interaction. In this case, a correction is needed which considers the differences between the mass energy absorption coefficient of the TLD cavity material and the medium where measurements is intended. Its correction depends on gamma-ray spectrum.

For neutron heating rate measurements, the gas-filled counters can be used. In this case, one measures the integrated energy of the charged parti-

cles emitted from the chamber wall (provided the chamber wall is made of the same material of the surrounding media where the measurement is intended). This method is in a development phase.

Reaction Rate Measurements

Reaction rate measurements are based on measuring the gas production rate and/or the rate of a particular transmutation or activation process. In performing these measurements, the foil activation method, the mass spectrometric method and fission chambers are used.

Some (n,p) and (n,α) reactions can be measured by the foil activation method. Transmutation and activation reactions such as the (n,2n'), (n,n'), and (n,γ ) reactions can also be measured by the foil activation method. The reaction types that are commonly used in this method are shown in Table 7.3.1-1. One should notice that in measuring the helium production rate, the mass spectrometric method can be applied. This is also the same technique used for tiritum production measurement. Although fission chambers give fission reaction rates, this method is not suitable for measuring other reaction types. Fission chambers are used mainly to extract information about the spectral indices at various locations.

Neutron Spectroscopy

The neutron spectrum may be measured by various techniques such as the multi-foil activation method (MFA), the proton recoil counter and the NE213 scintillator. The MFA technique and the NE213 scintillator are the same methods discussed in the neutron yield measurements. The proton-recoil counter and the NE213 scintillator are used to measure the recoil proton of the gas and the scintillator, respectively. These measurements require unfolding the spectrum by using response matrix. The energy ranges suitable for measurements are above 1 MeV for the NE213 scintillator, and 1 KeV to 1 MeV for the proton recoil counter. Some development is currently in progress to use the proton recoil counter in measuring neutron spectrum above 1 MeV. The energy range for the MFA depends on the reactions used in the unfolding process, but this method has large uncertainty in the energy range of 10-500 KeV. However, the accuracy is good in the high energy range.

Table 7.3.1-1 Table of Activation Reactions for Reaction Rate Measurements

| Reaction Type | Target | Product | Half Life | Reaction Type | Target | Product | Half life |
|---|---|---|---|---|---|---|---|
| (n,p) | $^{24}Mg$ | $^{24}Na$ | 15 hr | (n,2n) | $^{23}Na$ | $^{22}Na$ | 2.6yr |
| | $^{27}Al$ | $^{27}Mg$ | 9.5min | | $^{55}Mn$ | $^{54}Mn$ | 312d |
| | $^{46}Ti$ | $^{46}Sc$ | 84d | | $^{59}Co$ | $^{58}Co$ | 71d |
| | $^{47}Ti$ | $^{47}Sc$ | 3.4d | | $^{58}Ni$ | $^{57}Ni$ | 1.5d |
| | $^{48}Ti$ | $^{48}Sc$ | 44hr | | $^{63}Cu$ | $^{62}Cu$ | 16hr |
| | $^{54}Fe$ | $^{54}Mn$ | 2.6hr | | $^{65}Cu$ | $^{64}Cu$ | 12.7hr |
| | $^{59}Co$ | $^{59}Fe$ | 45d | | $^{90}Zr$ | $^{89}Zr$ | 3.3d |
| | $^{58}Ni$ | $^{58}Co$ | 71d | | $^{93}Nb$ | $^{92m}Nb$ | 10d |
| | $^{60}Ni$ | $^{60}Co$ | 5.3yr | | $^{197}Au$ | $^{196}Au$ | 6.2d |
| | $^{64}Zn$ | $^{64}Cu$ | 12.7hr | | | | |
| | | | | (n,γ) | $^{23}Na$ | $^{24}Na$ | 15hr |
| (n,α) | $^{27}Al$ | $^{24}Na$ | 15hr | | $^{55}Mn$ | $^{56}Mn$ | 2.6hr |
| | $^{59}Co$ | $^{56}Mn$ | 2.6hr | | $^{59}Co$ | $^{60}Co$ | 5.3yr |
| | | | | | $^{63}Cu$ | $^{64}Cu$ | 12.7hr |
| | | | | | $^{115}In$ | $^{116m}In$ | 26.9min |
| | | | | | $^{197}Au$ | $^{198}Au$ | 2.7d |

Small size NE213 scintillators[7] have been used for in-system spectrum measurements. The results shown in Figure 7.3.1-2 are based on the employment of this small scintillators.

Gamma-ray Spectroscopy

The techniques for in-system gamma-ray spectrum measurement are based on using the NE213 scintillator, the bismuth germanium oxide (BGO) scintillator, and the Si(Li) solid-state detector. The NE213 scintillator is used to measure the recoil electron spectrum and gamma-ray spectrum can be evaluated by unfolding this spectrum. This method requires a probe size larger than 5 cm in diameter for high energy gamma rays. The BGO scintillators are smaller in size but they need large correction due to the gamma-rays produced from neutron activation and reactions such as the (n,inelastic) reaction. The Si(Li) detectors have limitation since they can be used only in a limited energy range. In addition, this type of detector suffers from the radiation damage caused by fast neutrons.

At present, it appears that there is no adequate method to measure the gamma-ray spectrum. However, one can deduce gamma-ray effects such as heating from measurements performed by the TLD's. The methods for measuring the decay gamma-ray spectrum are the NaI(Tl), the BGO scintillators, and the Ge(Li) solid-state detectors. These techniques are used to measure the leakage gamma-ray spectrum and gamma-ray emission from irradiated samples after shutdown.

The techniques mentioned above are summarized in Table 7.3.1-2. The entries for power conditions shown on this table are estimated roughly and the accuracies shown are the uncertainty of the measurements. The typical size indicated in this table gives the space requirement where the detector is located. The entry "electromagnetic effect" shown indicates whether or not the detection method used involves electronics that will be influenced by the magnetic field. In Figure 7.3.1-3, we show the range of the fluence required for the measurements in each technique. Neutron fluence is normalized to the neutron wall load at the first wall. The techniques shown in Figure 7.3.1-3 can be divided into two groups. The first group includes those techniques that require a very low fluence of $\sim 1$ W•sec/m$^2$, while a low fluence of $\sim 1$ MW•sec/m$^2$ is reserved for the second group. All instruments belonging to the

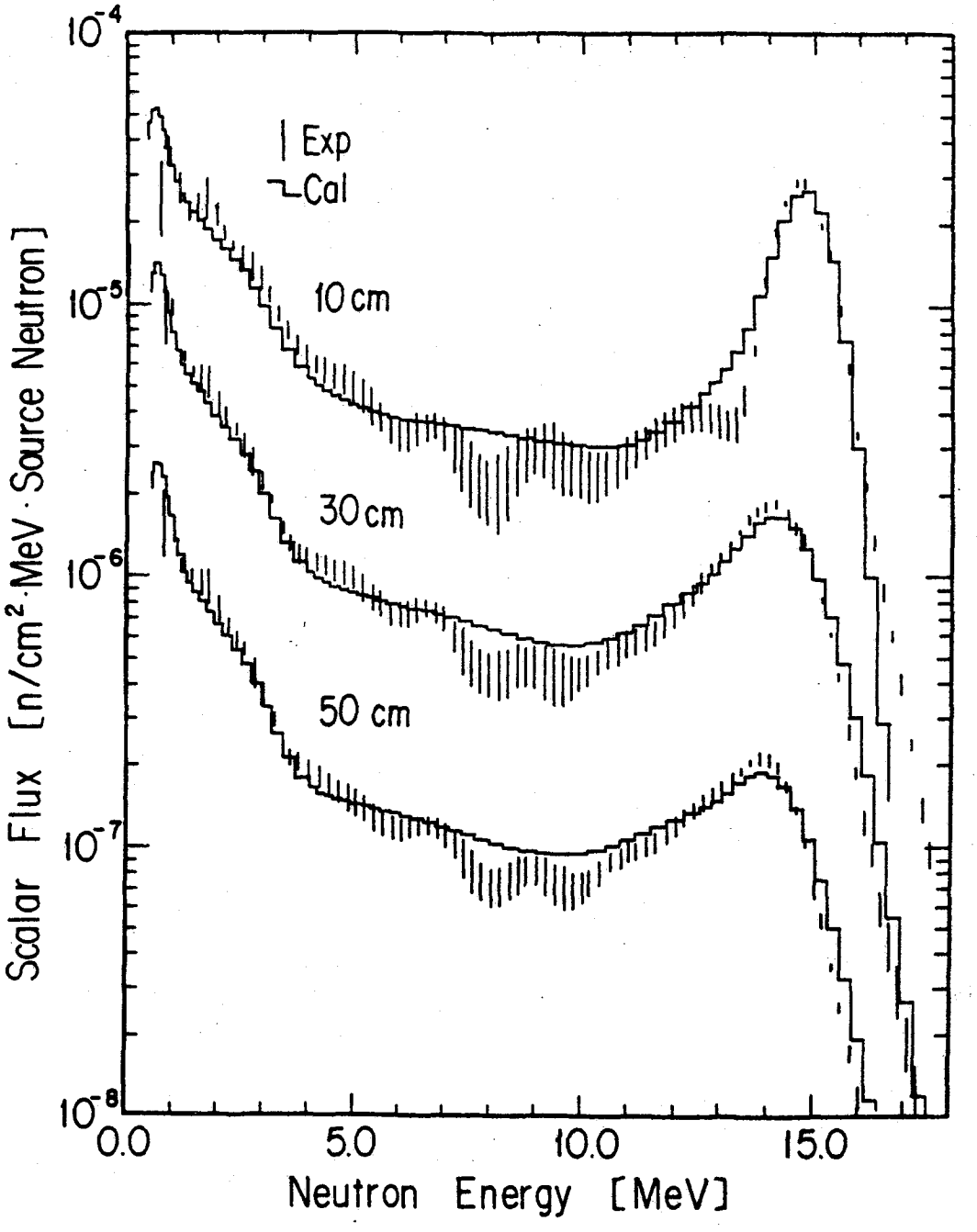


Figure 7.3.1-2 In-system neutron spectrum measurement by NE213 spectrometer in 60cm-thick $Li_2O$ cylindrical assembly at the Fusion Neutronics Source (FNS) facility at JAERI.

Table 7.3.1-2 Neutronics Experimental Techniques

| Parameter | Technique | Power Condition ($P_w$) Flux Limit | Power Condition ($P_w$) Fluence | Typical Size (mm) | Accuracy | Electro-magnetic Effect [a] | Comment |
|---|---|---|---|---|---|---|---|
| Total Burning (Neutron Yield) | MFA (Multi-Foil Activation) | No Limit | $>10^{-2}$ MWS/$m^2$ | 15$\phi$ x 2 (Depends on Fluence) | 2-20%[b] | No | |
| | NE213 | $<10^{-3}$ W/$m^2$[c] | $>10^{-2}$ WS/$m^2$ | 20 x 190 | <5% | Yes | |
| | $\mu$ Fission Chamber | $<10^{-2}$ W/$m^2$ | $>10^{-1}$ WS/$m^2$ | 5$\phi$ x 50 | 5% | Yes | |
| TPR | Radiochemical ($\beta$-counting) | No | $>10^{-1}$ MWS/$m^2$ | 10$\phi$ x 2 | <5% | No | <100°C |
| | Internal Gas Counter ($\beta$-counting) | No | $>10^{-2}$ MWS/$m^2$ | 10$\phi$ x 2 | <5% | No | <100°C |
| | Mass Spectrometric | No | >1 MWS/$m^2$ | 10$\phi$ x 2 | 5% | No | Compete Reaction, <100°C |
| | Track Recorder | No | ? | 10$\phi$ x 1 | ? | No | Development Needed |
| | Gas Proportional ($^6$Li) | $<10^{-3}$ MW/$m^2$ | $>10^{-1}$ MWS/$m^2$ | 50 x 300 | >10% | Yes | |
| | Li Glass ($^6$Li) | $<10^{-3}$ W/$m^2$ | $>10^{-2}$ WS/$m^2$ | 20$\phi$ x 180 | 5% | Yes | |
| | TLD's ($^6$Li) | No | $>10^{-1}$ MWS/$m^2$ | 2$\phi$ x 10 | >10% | No? | $\gamma$ Effect <100°C |

Table 7.3.1-2 Neutronics Experimental Techniques (contd.)

| Parameter | Technique | Power Condition ($P_w$) | | Typical Size (mm) | Accuracy | Electro-magnetic Effect | Comment |
|---|---|---|---|---|---|---|---|
| | | Flux Limit | Fluence | | | | |
| Heating | Calorimeters | No | $>10^{-1}$ MWS/m$^2$ | 6$\phi$ x 40 | 10% | Yes | |
| | TLD's | No | $>10^{2}$ WS/m$^2$ | 2$\phi$ x 10 | 10% | No? | e,$\alpha$ <100°C |
| | Gas-Filled Counter | $<10^{-2}$ W/m$^2$ | >1 WS/m$^2$ | 50$\phi$ x 300 | ? | Yes | e,p,$\alpha$ |
| | TLD Dosimeter | No | $>10^{2}$WS/m$^2$ | 2$\phi$ x 10 | 10% | No? | Chamber Theory?, <100°C |
| Reaction Rate | Foil | No | $>10^{-1}$ MWS/m$^2$ | 15$\phi$ x 2 | 2-5% | No | |
| | Mass Spectrometer (n,$\alpha$) | No | $>10^{-1}$ MWS/m$^2$ | 15$\phi$ x 2 | 5% | No | |
| | Fission Chamber (n, fission) | $<10^{-2}$ W/m$^2$ | $>10^{-1}$ MWS/m$^2$ | 5$\phi$ x 50 | 5% | Yes | |
| Neutron Spectroscopy | MFA | No | $>10^{-1}$ MWS/m$^2$ | 15$\phi$ x 2 | 2-20% | No | |
| | NE 213 | $<10^{-3}$ W/m$^2$ | >1 WS/m$^2$ | 20$\phi$ x 190 | <5% | Yes | 1 MeV < $E_n$ |
| | Proton Recoil | $<10^{-2}$ W/m$^2$ | $>10^{-1}$ WS/m$^2$ | 50$\phi$ x 300 | 5% | Yes | 1 KeV < $E_n$ < 1 MeV |

Table 7.3.1-2 Neutronics Experimental Techniques (cont'd.)

| Parameter | Technique | Power Condition ($P_w$) Flux Limit | Power Condition ($P_w$) Fluence | Typical Size (mm) | Accuracy | Electro-magnetic Effect | Comment |
|---|---|---|---|---|---|---|---|
| Gamma Ray Spectroscopy | NE213 | $< 10^{-4}$ W/m$^2$ | $> 10^{-3}$ WS/m$^2$ | 40 $\phi$ x 200 | 10% | Yes | |
| | Si (Li) | $< 10^{-4}$ W/m$^2$ | $> 10^{-3}$ WS/m$^2$ | 5 $\phi$ x 10 | 10% | Yes | Neutron Damage |
| | BGO[d] | | | | 10% | No | Neutron-Induced Reaction |
| | Ge(Li)[d] | | Not limited | | 5% | No | |
| | NaI (Tl)[d] | | | | 10% | No | Activation |

[a]Detector response and electronics will be influenced by strong magnetic field.
[b]Depend on energy region.
[c]Count rate limit ~ 1 kcps; it is required mainly by neutron-gamma separation technique.
[d]Used to leak spectrum or decay gamma spectrum.

Figure 7.3.1-3 Fluence Requirements for Various Experimental Techniques

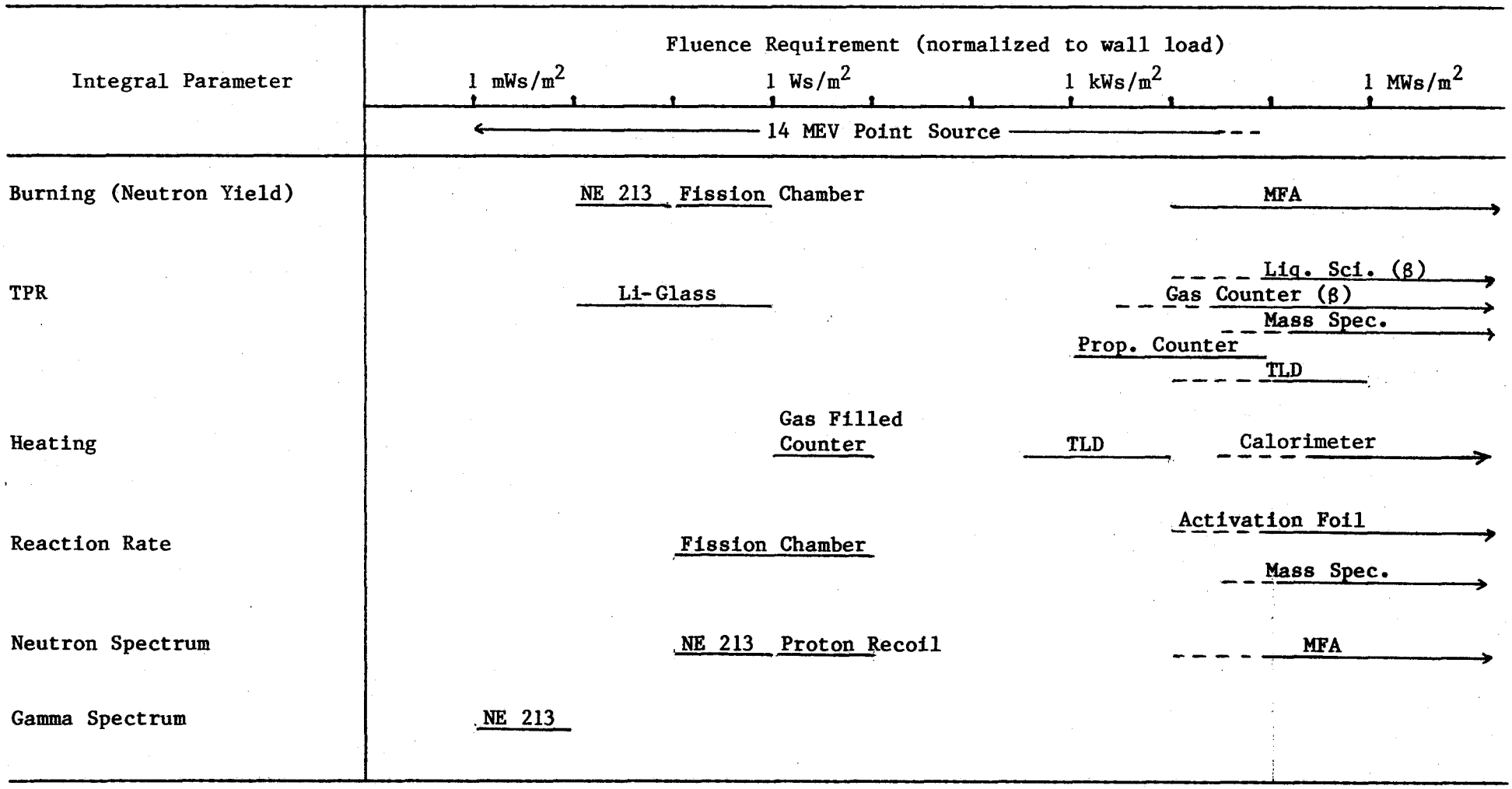


*For counter methods, the measuring time is assumed to be 10 ~ 100 sec.

very low fluence group are based on the counter methods and they may be influenced by the magnetic field and the magnetic field change. The relatively high fluence group is based on an after-irradiation counting method, so that detectors can be located simultaneously at various positions and measurements are performed under stable conditions after irradiation. Moreover, the detector size is relatively small and these detectors can easily be located in a test module of small size.

### 7.3.2 Considerations for the Test Module Size Requirements and the Experimental Arrangement

It is most likely that the test module in a fusion test device will partially occupy the region that surrounds the plasma in the fusion test device. Certain locations are expected to be reserved for one or more test modules while the rest of the surrounding zone is made up of a filling material other than the test module constituents. In this case, the source condition at the first wall of the test module is different from the corresponding situation where the test module completely surrounds the plasma (full coverage reference case). It is the objective of the present analysis in this section to identify the minimum size requirement of the test module such that the nuclear performance thoroughout the test module simulates in greater details the one found in the full coverage case. This necessitates adjusting the incoming neutron spectrum from regions facing the test module (reflective zone) as well as adjusting the conditions at the buffer zones that surround the test module.

A calculational survey has been carried out to investigate the requirements mentioned above. The one-dimensional transport code ANISN[8] was used in determining the thickness of the reflective zone used to adjust the incoming spectrum. In addition, the two-dimensional transport code DOT 4.3[9] has been employed in determining the buffer zone thickness. This zone is used to adjust the condition at the side of the test module. The procedure and modeling for the calculational survey are shown in Figure 7.3.2-1. The survey focuses on the tritium production rate measurement since this measurement requires the highest accuracy.

In this survey, we studied the impact of varying parameters such as the source reflector thickness, $t_B$, the width of the test module, $\theta_m$, and its

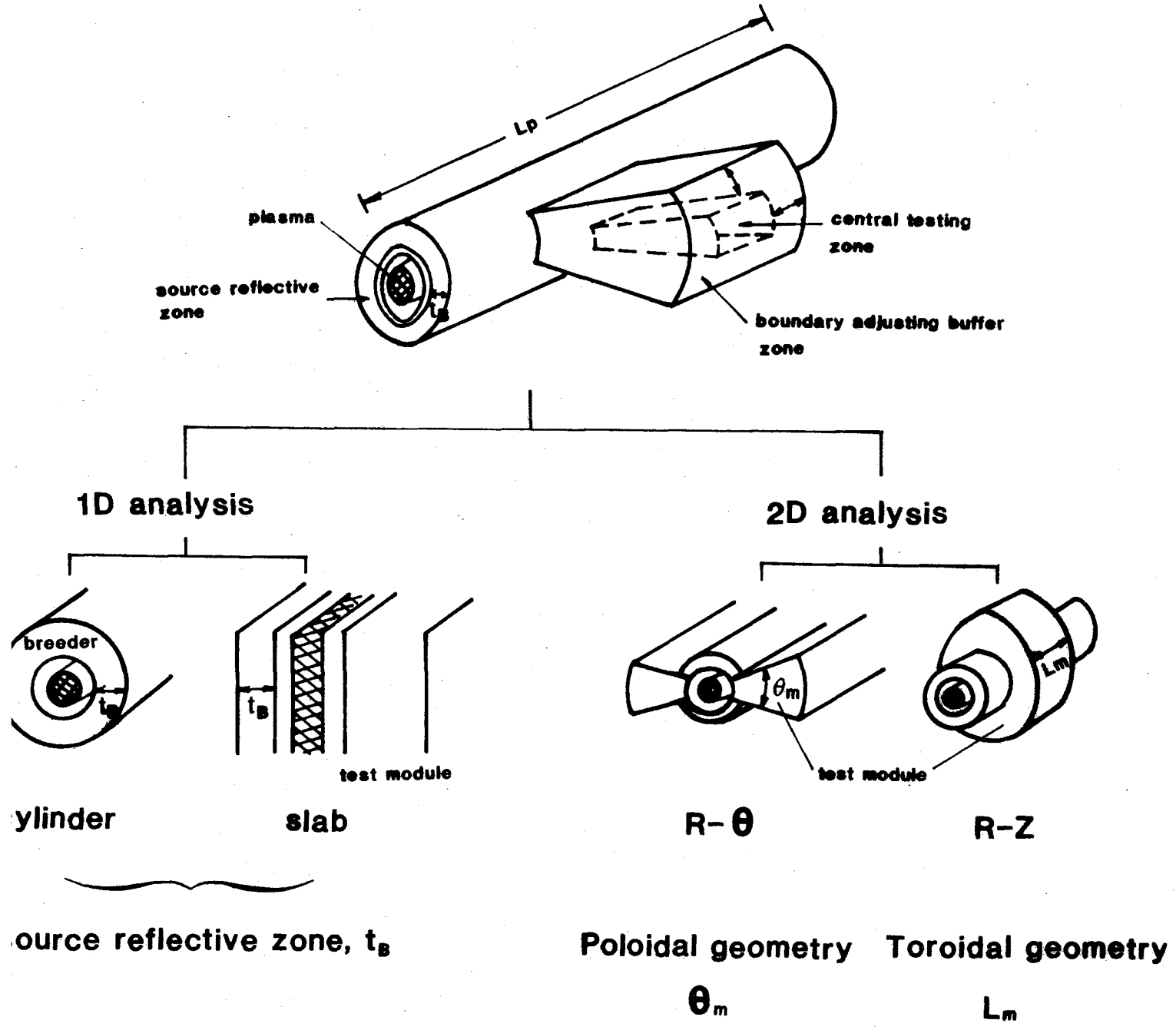


Figure 7.3.2-1 Procedure and models for the calculational survey.

length, $L_m$, on the tritium profiles throughout the test module. The blanket chosen for the survey is the lithium oxide helium-cooled blanket discussed in Chapter 5. The geometrical arrangement and the atomic densities used in the calculation are given in Table 7.3.2-1.

### 7.3.2.1 Adjusting Neutron Spectrum Incident on the Test Module

In a fusion reactor, the neutron spectrum coming into the first wall of a blanket is made up of the uncollided neutrons from the plasma region and the neutrons reflected by the first wall and blanket materials on the other side of the plasma. The ratio of the reflected to the uncollided neutrons is relatively large. These reflected neutrons play an important part in determining the nuclear performance through the blanket as discussed below.

#### Spectral Saturation

A 1-D cylindrical module was used to investigate the impact of varying the breeding thickness, $t_B$, on the spectrum at the first wall. The results from this full coverage case give the required thickness of the reflective zone facing the $Li_2O$ test module. In the cylindrical 1-D module (see Fig. 7.3.2-1), the reflective zone is made up of the test module geometrical arrangement. By increasing the thickness $t_B$ shown in Fig. 7.3.2-1, one notices that not all the breeder zone contributes to the first wall spectrum; only the front zone of the breeder region that has the highest impact as shown from the results displayed in Fig. 7.3.2.1-1. From this figure, one notices that the spectrum in the first wall reaches saturation quickly. The values shown in Fig. 7.3.2.1-1 are the ratios to the values obtained in the full mock-up of the test module case ($t_B$ = 42 cm, the reference case). The saturation is relatively slow for low energy neutrons, but the relative ratio comes within 30% for a breeder thickness of 20 cm.

The impact of the type of materials surrounding the test module on the spectrum in the first wall has also been investigated in a slab geometrical model. The slab geometrical model used in the calculation is shown in Fig. 7.3.2.1-2a. In contrast to the geometrical model used in the 1-D cylindrical case, it is possible to consider different geometrical arrangements to the left side of neutron source (where the thickness of breeder zone, $t_B$ is varied) while maintaining the full details of the test module to the right

Table 7.3.2-1

Test Device Parameter

| Parameter | Size (cm) | Material | Density Factor |
|---|---|---|---|
| Plasma Radius | 15 | Vac | |
| First Wall Radius | 25 | Vac | |
| First Wall Thickness | 6 | HT-9 | 18% |
| Breeder | 42 | $Li_2O$<br>HT-9<br>He | 85% x 0.85<br>8%<br>7% |
| Plenum | 22 | HT-9 | 15% |
| Shield | 30 | SS | 100% |

Atomic Densities of Materials

| HT-9 | | $Li_2O$ | | Stainless Steel | |
|---|---|---|---|---|---|
| Fe | 6.855-2* | $^7Li$ | 7.551-2 | Cr | 1.600-2 |
| Cr | 9.930-3 | $^6Li$ | 6.052-3 | Fe | 5.745-2 |
| Ni | 3.825-5 | O | 4.078-2 | Ni | 1.179-2 |
| Mo | 4.680-4 | | | | |
| Mn | 4.09-4 | | | | |
| Si | 4.00-4 | | | | |
| C | 7.48-4 | | | | |

*read as $6.855 \times 10^{-2} \times 10^{24}$ atom/cm$^3$

| group | $E_n$ | |
|---|---|---|
| 1 | 14.9～13.5 | MeV |
| 2 | 13.5～12.2 | |
| 15 | 2.47～1.35 | |
| 18 | 408 ～166 | KeV |
| 20 | 31.8～3.35 | |
| 22 | 354 ～37.3 | eV |
| 25 | <0.41 | |

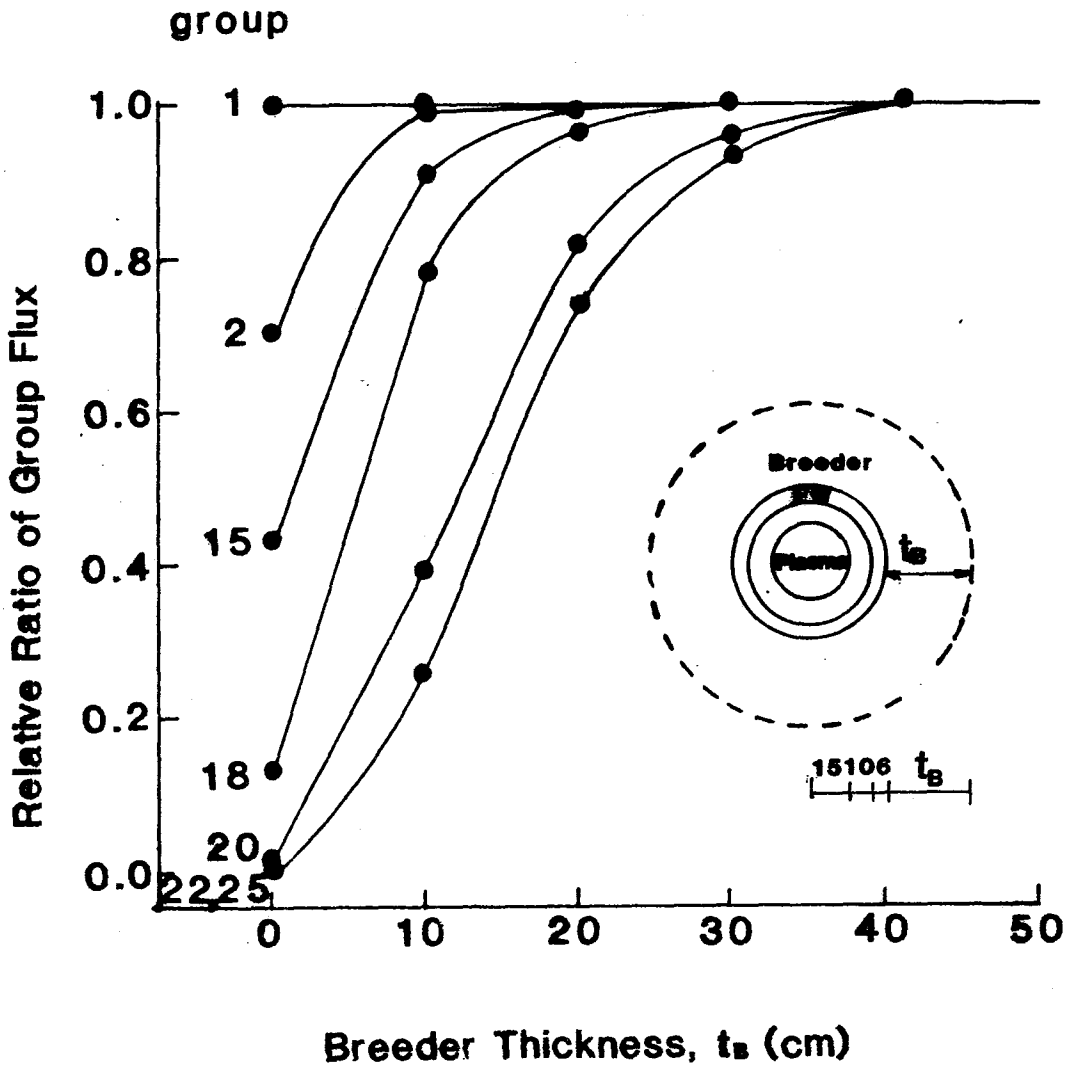


Figure 7.3.2.1-1 Level of spectral saturation as a function of the breeder thickness (1-D, cylindrical model).

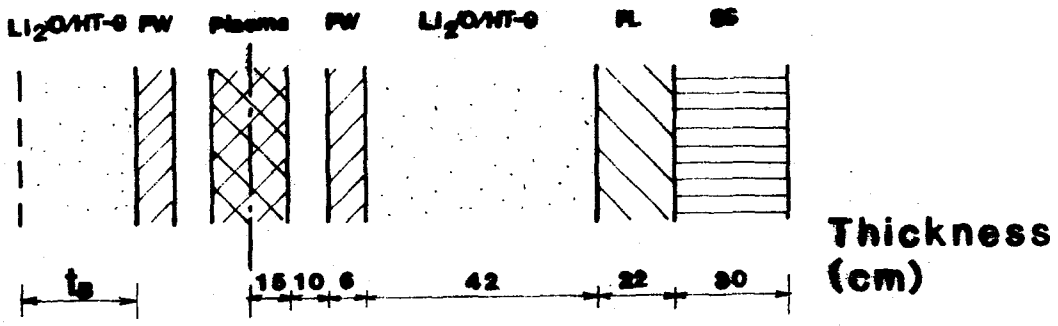


Figure 7.3.2.1-2(a) Slab model.

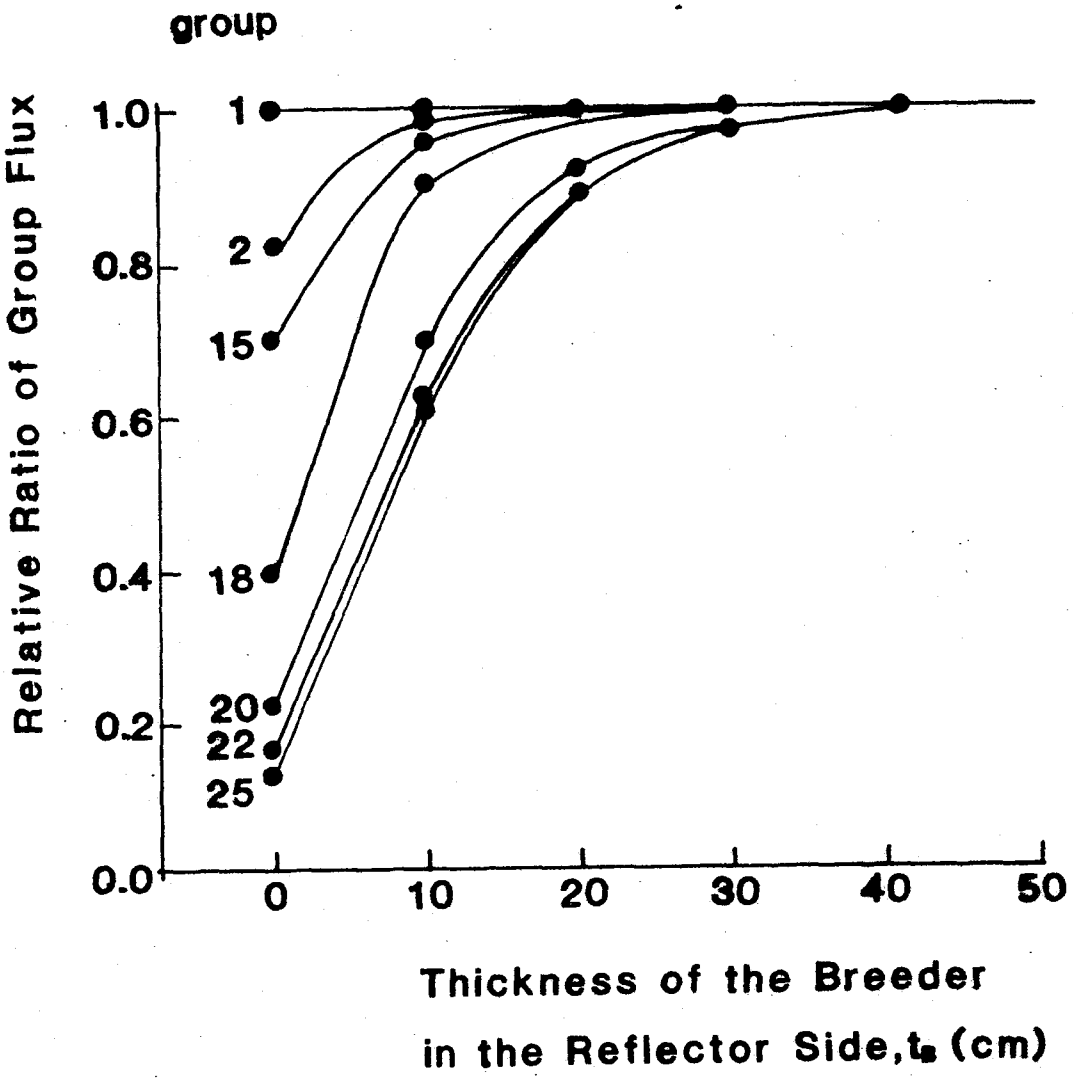


Figure 7.3.2.1-2(b) Level of spectral saturation as a function of the breeder thickness (1-D, slab model)

side of the source. Here, we varied the thickness $t_B$ and, as shown in Fig. 7.3.2.1-2b, the spectrum in the first wall saturates rapidly (as compared to the cylindrical model case) and the difference is within 10% for $t_B$ = 20 cm.

Reflector Materials

The results shown in Figs. 7.3.2.1-1 and 7.3.2.1-2 indicate that we can have a fairly accurate simulation of the first wall spectrum (within 5% deviation) if we keep the thickness of the breeding zone located in the reflector side (see Fig. 7.3.2.1-2) at ~ 30 cm.

A series of calculations has also been carried out to optimize the thickness of the breeding zone, $t_B$, by examining other material combinations in the breeding zone located in the reflector side. The fact that the low energy neutrons saturate more slowly as compared to the fast ones indicates that the front part of the breeding zone (in the reflector side) is more efficient in reflecting the high energy neutrons, while a thicker breeding zone is required to simulate the reflected slow energy neutrons.

To examine this effect, the back-end part of the breeding zone located in the reflector side was replaced by stainless steel. Several cases were considered in the 1-D slab geometrical model, and the results are summarized in Table 7.3.2.1-1. The case where the breeder thickness B = 0 represents no breeding zone, and only the first wall was included in the reflector side. The case shown with a breeding zone thickness of 5 cm followed by a 10 cm-thick stainless steel gives better agreement except for the thermal group ($E_n$ < 0.41 eV), where the discrepancy as compared to the reference case reaches ~ 15%.

The tritium production profiles from $^6Li$ throughout the breeder zone of the test module are shown in Fig. 7.3.2.1-3 for four cases selected from Table 7.3.2.1-1. As shown in this figure, the case where no breeding zone is included in the reflector side (B = 0) has a very different tritium production profile as compared to the reference case, (B = 42 cm), and the deviation reaches values above 30% even at the back end of the breeding zone of the test module. However, an excellent simulation of the tritium production profile can be obtained in the case where B = 5 cm, followed by a 10 cm-thick stainless steel zone as can also be noticed from the results given in Table 7.3.2.1-2.

Table 7.3.2.1-1 Ratio of Neutron Group Flux at the First Wall to the Corresponding Values in the Reference Case* (1-D Slab Geometry)

| Group | Neutron Energy | Case (cm) B = 0 | B = 10 | B = 20 | B = 5+ SS = 10 | B = 10 SS = 5 | B = 0 SS = 10 |
|---|---|---|---|---|---|---|---|
| 1 | 13.5 ~ 14.9 MeV | - 0.3 | 0.0 | 0.0 | 0.0 | 0.0 | + 0.2 |
| 2 | 12.2 ~ 13.5 | -17.9 | - 0.4 | 0.0 | 0.0 | 0.0 | - 7.1 |
| 15 | 1.35 ~ 2.47 | -48.0 | - 3.3 | - 0.4 | - 0.7 | - 0.1 | + 0.7 |
| 18 | 1.66 ~ 4.08 MeV | -61.0 | - 9.2 | - 1.2 | + 2.0 | - 2.6 | + 17.2 |
| 20 | 3.35 ~ 31.8 keV | -77.9 | -29.5 | - 7.0 | - 0.8 | - 9.5 | - 8.6 |
| 22 | 37.3 ~ 354 eV | -83.9 | -37.7 | -10.4 | + 6.9 | -11.4 | + 27.0 |
| 25 | <0.41 eV | -86.7 | -38.7 | -10.8 | +14.7 | -11.4 | +534.0 |

*Values cited in the table are the deviation from unity.

+ B: Breeder $Li_2O$/HT-9
SS: Stainless Steel

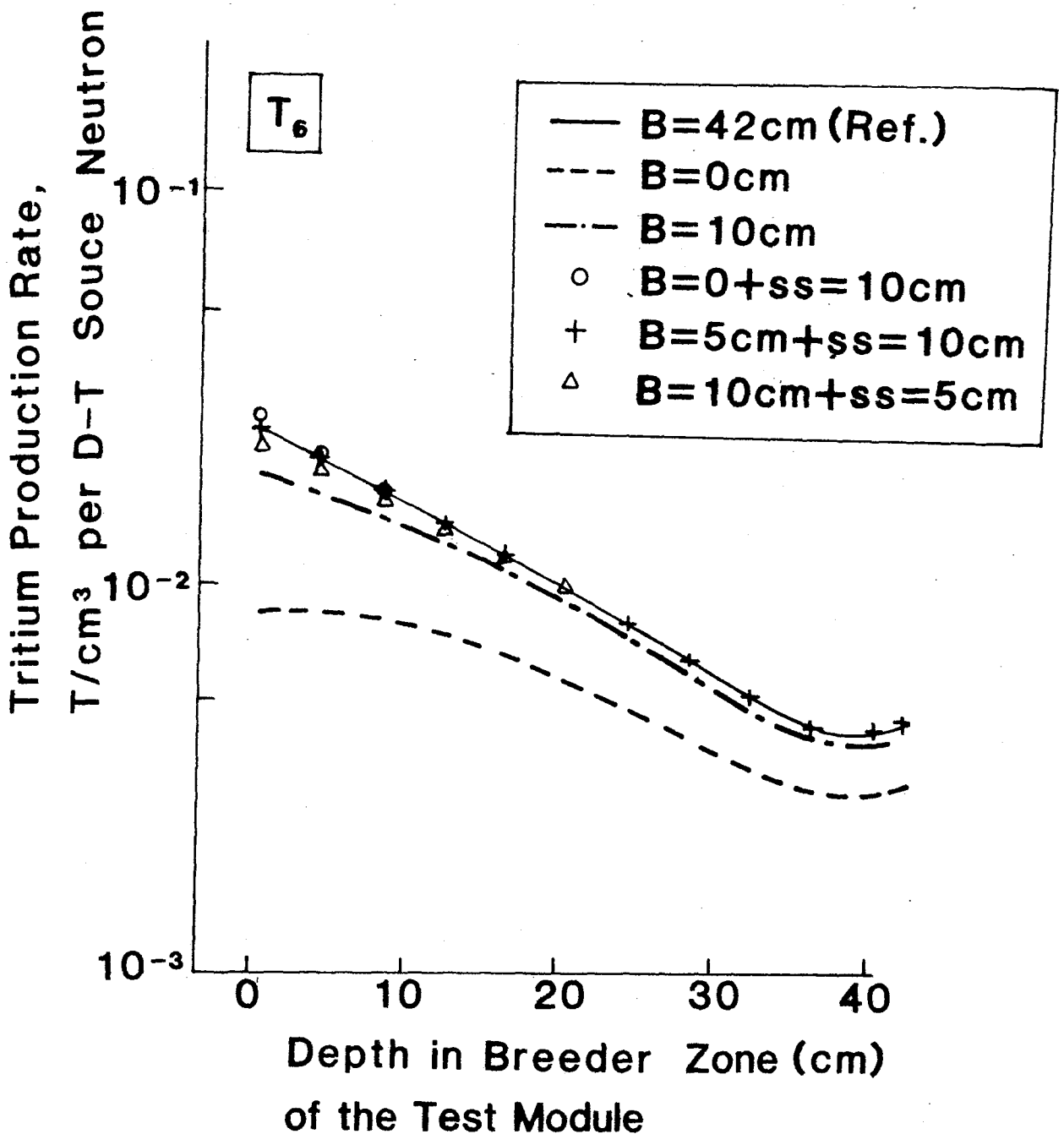


Figure 7.3.2.1-3 Tritium production profiles from $^{6}Li$ throughout the test module for various materials choices in the reflector zone.

Table 7.3.2.1-2 Total Tritium Production Rate ($T_6+T_7$) Normalized to the Values in the Reference Case.

| Case | Depth in the Breeder Zone | | |
|---|---|---|---|
| | 0.5 cm | 20.5 cm | 40.5 cm |
| Reference | 1.0 | 1.0 | 1.0 |
| B = 0 cm | 0.5796 | 0.6354 | 0.7109 |
| B = 10 cm | 0.8711 | 0.9185 | 0.9452 |
| B = 20 cm | 0.9699 | 0.9844 | 0.9906 |
| B = 0, SS = 10 cm | 1.0384 | 0.9899 | 0.9914 |
| B = 5, SS = 10 cm | 1.0060 | 0.9965 | 0.9959 |
| B = 10, SS = 5 cm | 0.9593 | 0.9737 | 0.9821 |

1-D Slab Model

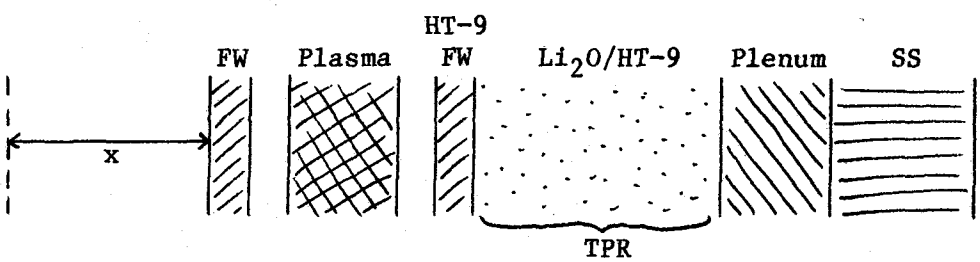


x = Parameter

### 7.3.2.2 Impact of the Poloidal Boundary Condition of the Test Module on Tritium Production

The impact of the poloidal boundary condition on the tritium breeding profile throughout the test module was examined using the two-dimensional transport code, DOT 4.3, in R-θ geometry as shown in Fig. 7.3.2.2-1. The geometrical model shown in this figure actually includes two test modules; the one not shown is on the other side of the reflective boundary. The profiles of the tritium production rate (TPR) from $^{6}Li$ and $^{7}Li$ were calculated individually in several cases where the angle substended by the front edge of the test module was varied. The TPR from $^{7}Li$ depends on the high energy neutron component and mainly the uncollided neutrons reaching the breeding zone. On the other hand, the TPR from $^{6}Li$ depends on the low energy neutron component in the module and those reflected by the surrounding boundaries. The tritium production profiles at the central axis throughout the breeding zone of the test module are shown in Fig. 7.3.2.2-2(a) and (b), for the TPR from $^{6}Li(T_6)$ and $^{7}Li(T_7)$, respectively. In these figures, the results from three cases are displayed, namely: the full coverage case (1-D, ANISN), and the partial coverage cases of $\theta_m = 24°$ and $48°$ as shown in Fig. 7.3.2.2-1. The reflector zone located in the poloidal boundary is made up of 5 cm-thick breeding material followed by 10 cm stainless steel. This arrangement and material choice are based on the results discussed in Section 7.3.2.1.

The profiles for the TPR from $^{7}Li$ are very similar in the three cases considered. However, the profiles for the TPR from $^{6}Li$ are different especially in the rear part of the breeding zone since the neutron spectrum in this location is considerably different from the spectrum found in the full coverage case.

First, one notices that as the thickness of the test module in θ direction increases, the $T_6$ profile comes closer to the profile in the full coverage case as shown in Fig. 7.3.2.2-2(a). This is also true for $T_7$ profiles [see Fig. 7.3.2.2-2(b)]. As $\theta_m$ increases (reflects increase in the test module width), the vacuum zone shown on Fig. 7.3.2.2-1 decreases in volume and thus more neutrons can be reflected and consequently both $T_6$ and $T_7$ increase at the center line of the breeding zone. The extreme case is when the vacuum region is replaced entirely by the test module (the full coverage

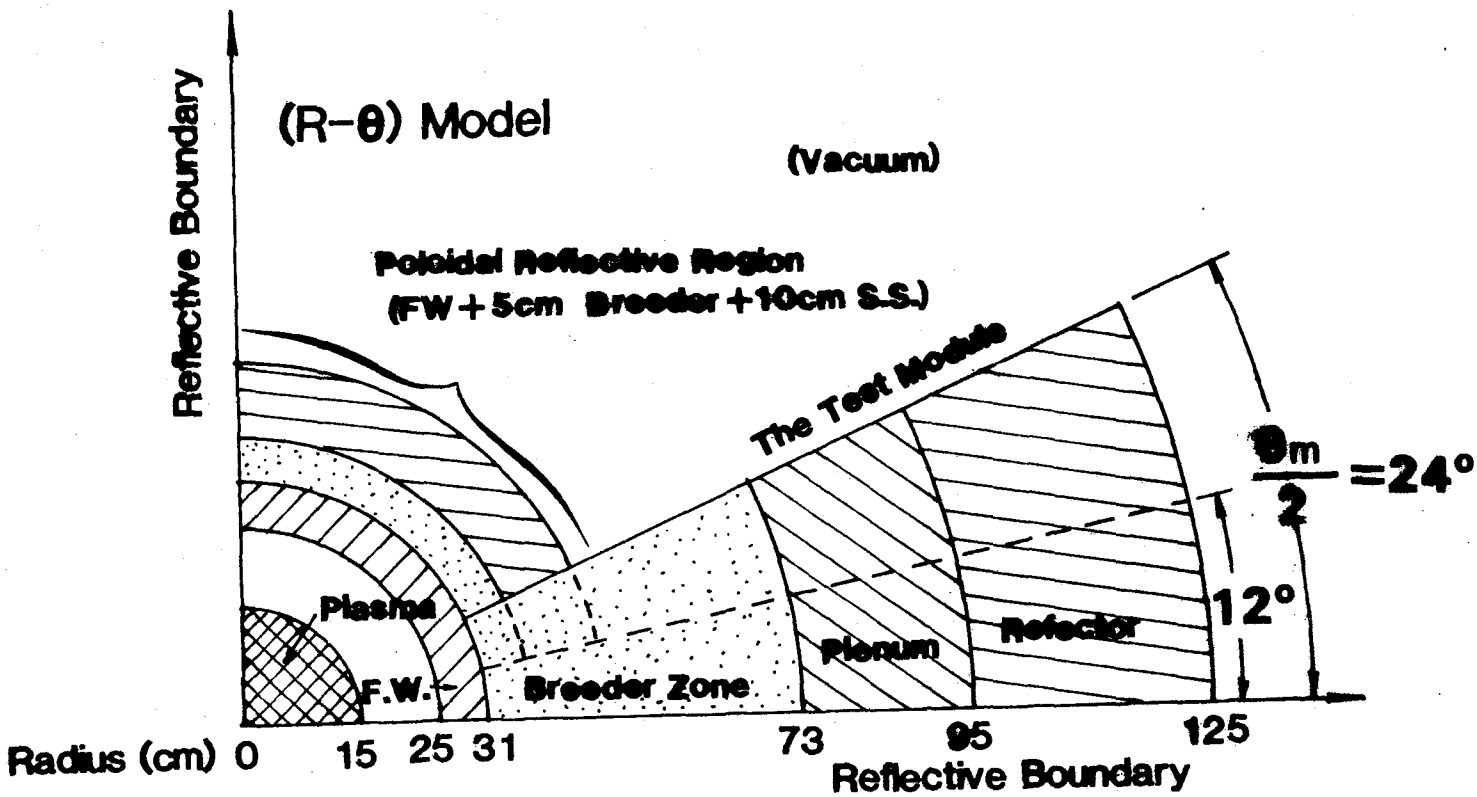


Figure 7.3.2.2-1 The R-θ geometrical model used to examine the poloidal boundary condition.

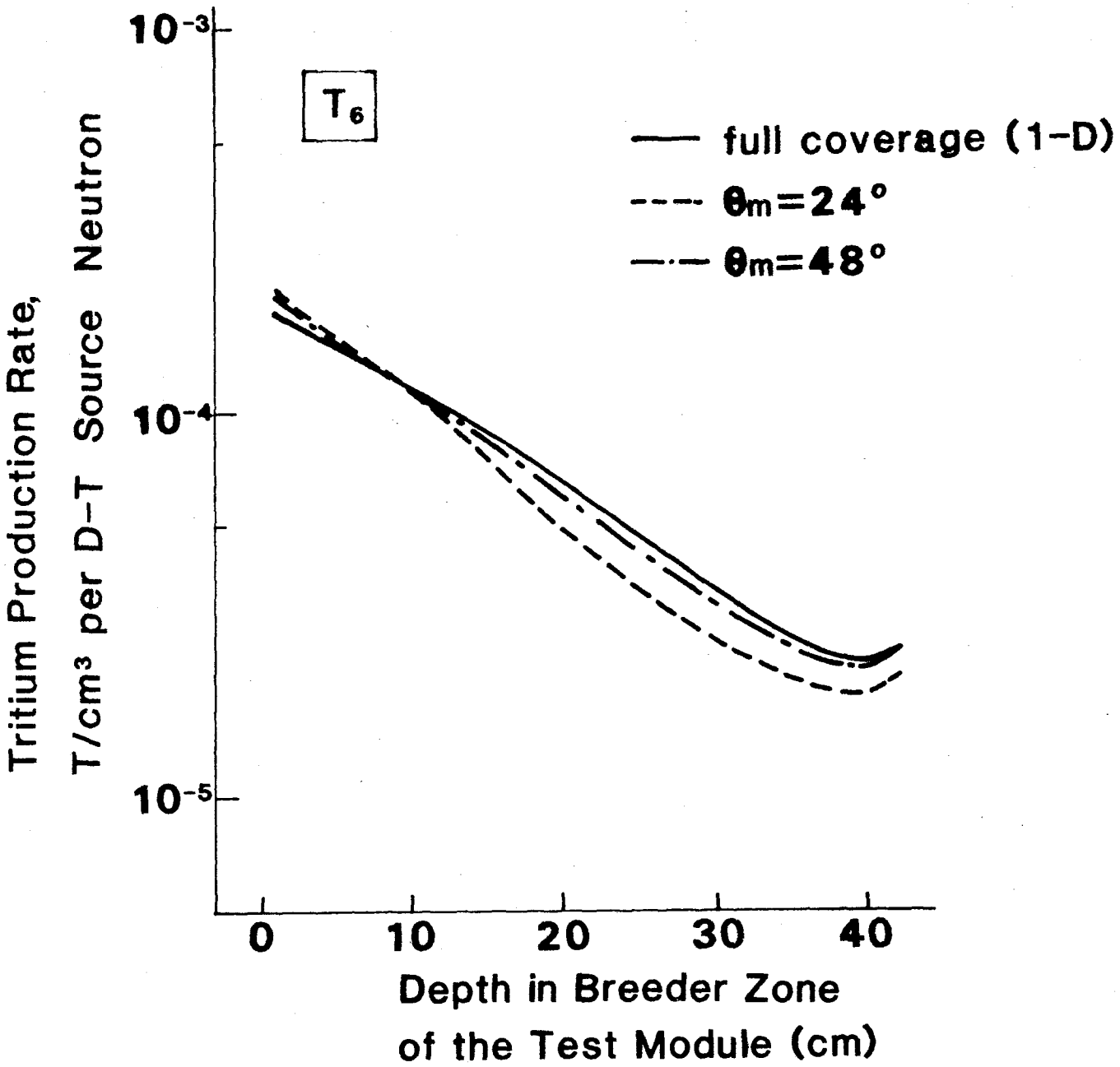


Figure 7.3.2.2-2(a) Tritium production profiles from $^{6}Li$ on the central axis of the breeding zone and throughout the test module (R-θ poloidal geometry).

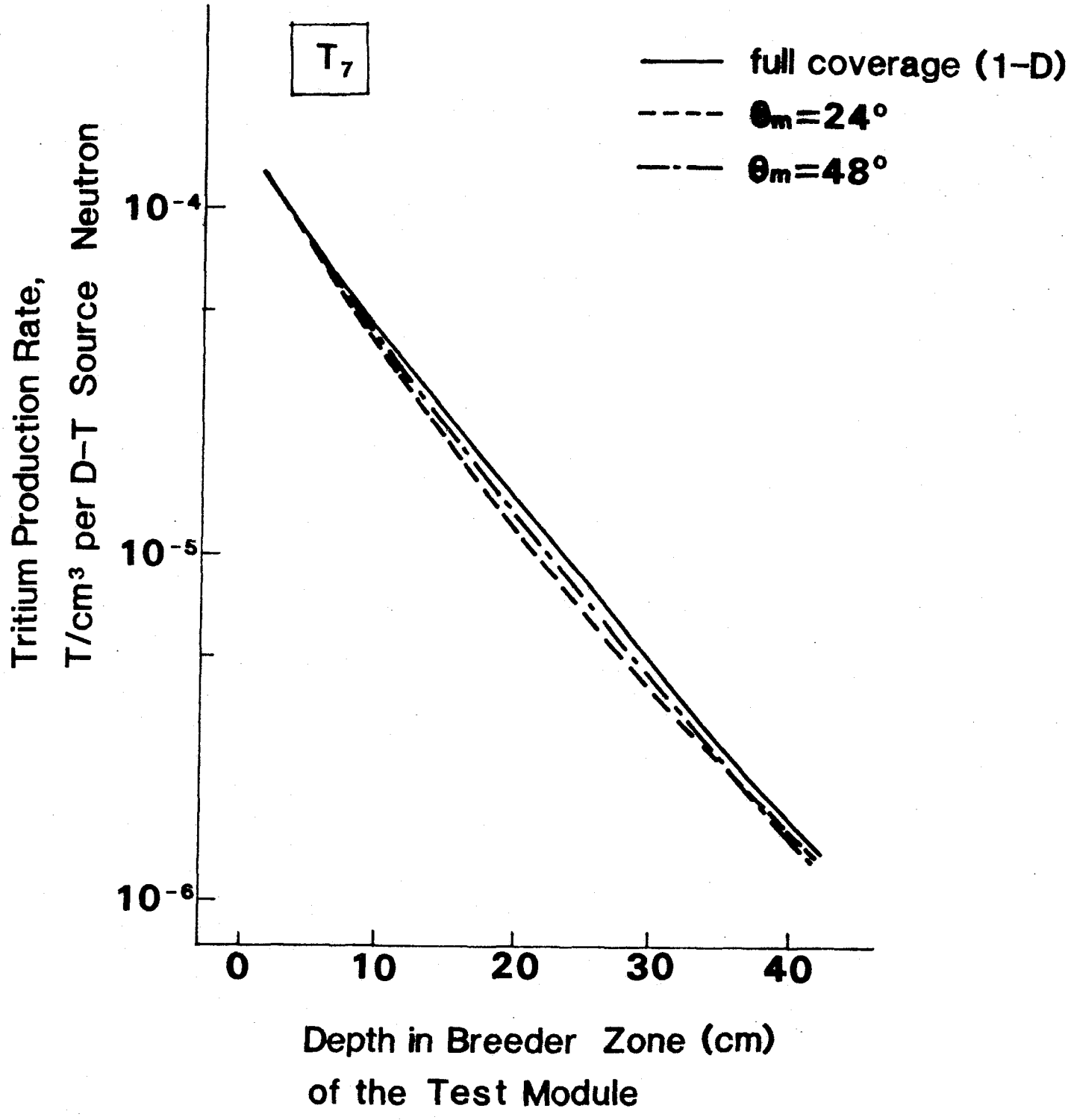


Figure 7.3.2.2-2(b) Tritium production profiles from $^{7}Li$ on the central axis of the breeding zone and throughout the test module (R-θ poloidal geometry)

case). The impact of this vacuum region on the $T_6$ and $T_7$ profiles across the breeding zone in θ-direction are shown in Fig. 7.3.2.2-3(a) and (b), respectively, at three locations: the front edge (top), the middle point, and the rear edge (bottom) of the breeding zone. For $T_6$, as we move outwards in the θ-direction, the profiles drop in values as compared to those at the center of the breeding zone. This is because moving towards the vacuum boundary decreases the number of reflected neutron that contribute to $T_6$, especially in the middle and the rear edge locations. At the front edge, there is a slight increase in $T_6$ due to the fact that neutrons reflected from the stainless steel zone located in the poloidal boundary (see Fig. 7.3.2.2-1) has more chance in contributing to $T_6$ as compared to locations deep in the breeding zone of the test module. The situation for $T_7$ is similar, i.e., a decrease in $T_7$ profile as we move towards the boundary, particularly in the middle point location. However, practically no change in this profile takes place at the front edge while $T_7$ profile at the back edge exhibits an increase as we move in the θ-direction. This later increase is due to the fact that the neutron spectrum gets harder as we move closer to vacuum edge. The increase in the high energy component of the spectrum is due to the contribution from the uncollided neutrons reaching the back edge of the breeding zone. Although this is also true at the middle location, the impact of the decrease in neutron reflection at locations closer to the boundary dominates the impact of the increase in the uncollided component.

### 7.3.2.3 Impact of the Toroidal Boundary of the Test Module on First Wall Spectrum and Tritium Production

In the previous section we examined the impact of the poloidal boundry conditions on the tritium production profiles throughout the test module. We devote this section to studying similar effects, but the toroidal boundary condition is varied in this case. The results have shown that the general trends regarding the variation in the tritium profiles are similar to those obtained in the previous section. However, variations in the plasma length in the toroidal direction affect significantly the neutron spectrum at the first wall of test module as it will be apparent from the results shown below.

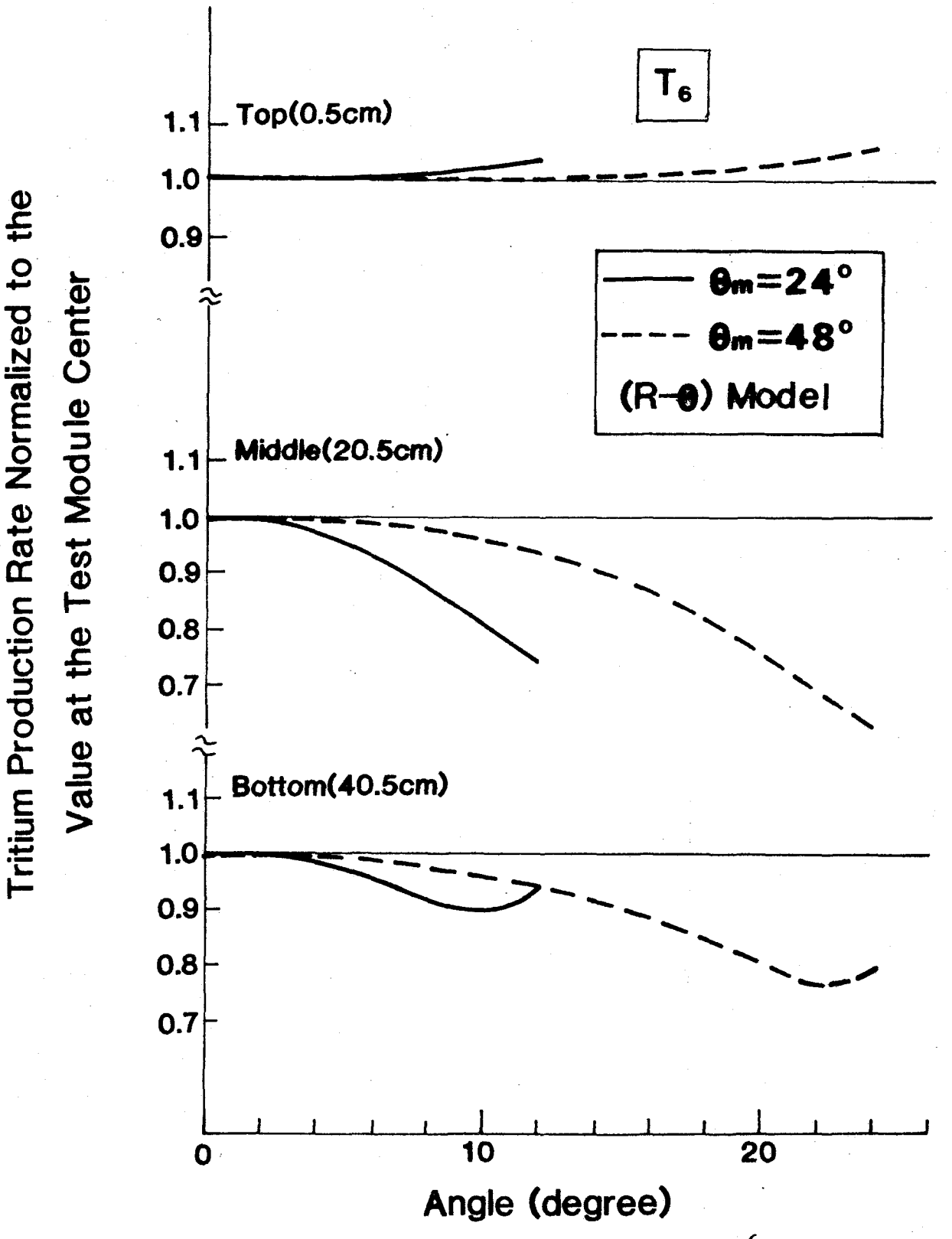


Figure 7.3.2.2-3(a) Tritium production profiles from $^{6}Li$ across the test module normalized to the central value (Top, Middle and Bottom locations are at distances of 0.5, 20.5 and 40.5 cm from the front edge of the breeding zone; R-θ poloidal geometry).

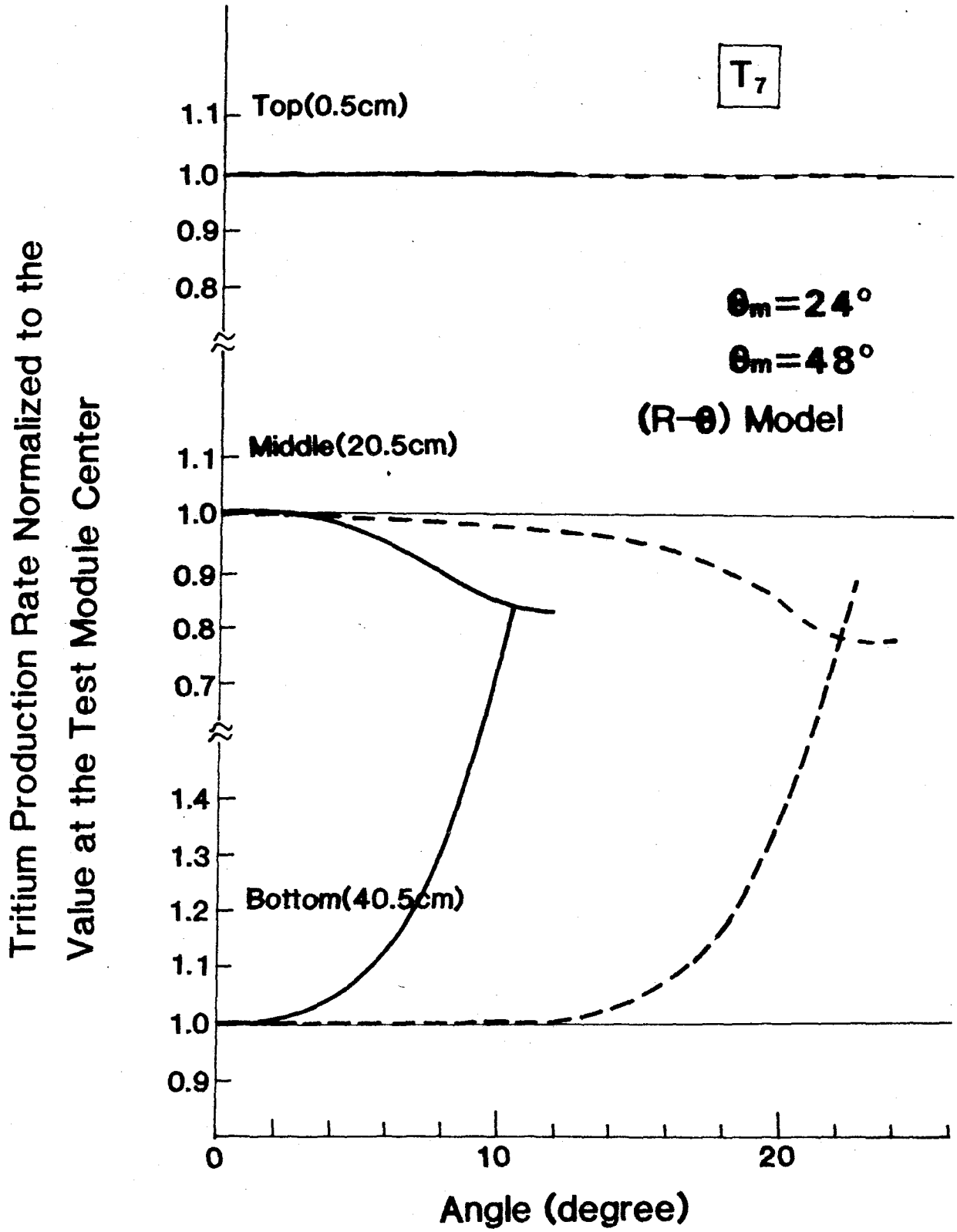


Figure 7.3.2.2-3(b) Tritium production profiles from $^{7}Li$ across the test module normalized to the central value (Top, Middle and Bottom locations are at distances of 0.5, 20.5 and 40.5 cm from the front edge of the breeding zone; R-θ poloidal geometry).

Impact of the Reflective Zone on the Test Module First Wall Spectrum

Various combinations of the plasma length, $L_p$, and the test module width, $L_m$, were considered in the 2-D, R-Z geometrical model shown in Fig. 7.3.2.3-1. As is the case for the R-θ model discussed in the previous section, the objective here is to investigate the impact of varying these geometrical parameters on the tritium production profile throughout and across the test module. Specifically, the variation in the plasma length was presented by the two cases, $L_p$ = 160 and 320 cm, and the variation in the test module width was studied for the three cases, $L_m$= 60, 100 and 140 cm. In these cases, the reflective condition at the left and the bottom boundaries in Fig. 7.3.2.3-1 were assumed while vacuum boundaries at the top and the right side were used in the calculation.

In order to examine the effect of the reflective zone shown in Fig. 7.3.2.3-1 on the spectrum at the first wall, the case for $L_p$= 160 cm and $L_m$= 60 cm was calculated with and without the reflective zone present and the results are summarized in Table 7.3.2.3-1. For comparison, we included in this table the case where a reflective boundary condition was assumed at the top boundary for the case with a plasma length $L_p$= 160 cm and test module width $L_m$= 100 cm and with the reflector zone included. This latter case assumes that the test module is repeated along the plasma length every 60 cm.

The results shown in Table 7.3.2.3-1 indicate that there is a substantial deviation in the neutron flux from the values obtained in the full coverage case (1-D calculation) if the reflective zone is excluded. This deviation (expressed in percentage) is more pronounced at low energy neutrons. Also, for a fixed plasma length ($L_p$= 160 cm) the deviation in the first wall spectrum at low energy is larger in the case of $L_m$= 100 cm as compared to the results for the case with $L_m$= 60 cm. In addition, one can notice from Table 7.3.2.3-1 that assuming a periodic boundary conditions at the configuration top for the case with $L_p$= 160 cm and $L_m$= 100 cm results in larger values for the spectrum at the first wall as compared to the spectrum in the reference case, and again this positive deviation is larger for the low energy neutrons. To investigate the impact of varying the plasma length on the first wall spectrum, we included in Table 7.3.2.3-1 the results for the case of $L_p$= 320 cm and $L_m$= 100 cm with a vacuum boundary at the top of the configuration. One notices that the deviation in the first wall spectrum in this case

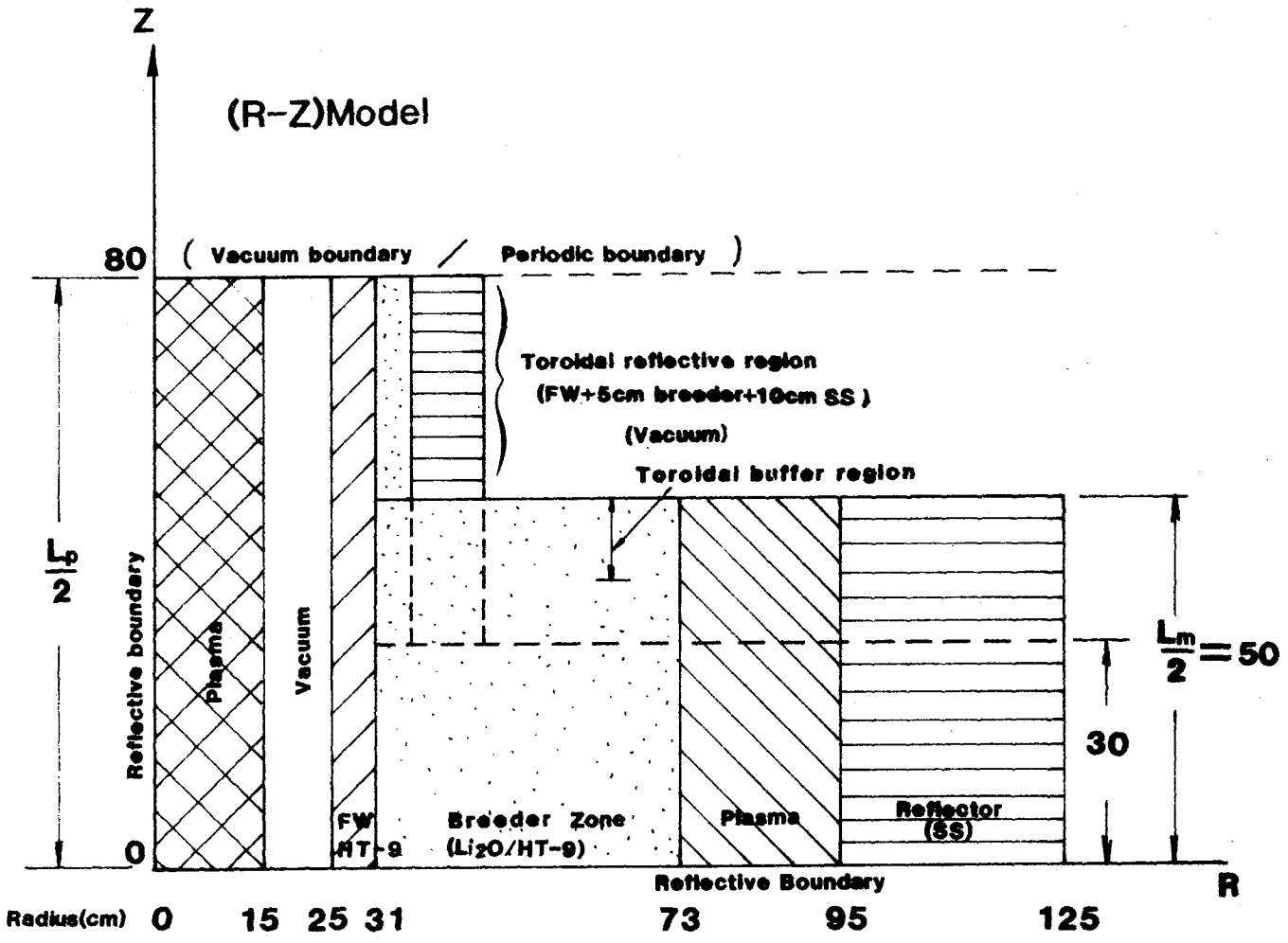


Figure 7.3.2.3-1 The R-Z geometrical model used to examine the toroidal boundary condition.

Table 7.3.2.3-1 Effect of the Reflective zone on the First Wall Spectrum
(Deviations from the full coverage case are shown in percentage)

| Neutron Group | Upper Energy | Plasma Length | | | | |
|---|---|---|---|---|---|---|
| | | $L_p$= 160cm | | | | $L_p$= 320cm |
| | | $L_m$=60cm* no ref. | $L_m$=60cm | $L_m$=100cm | $L_m$=100cm** Periodic | $L_m$=100cm |
| 1 | 14.9818 MeV | - 8.2 | - 8.2 | - 8.2 | + 3.7 | + 2.4 |
| 2 | 13.499 | - 23.9 | - 21.9 | - 19.0 | + 11.4 | + 4.0 |
| 3 | 12.214 | - 23.9 | - 20.6 | - 20.1 | + 6.1 | + 2.8 |
| 4 | 11.052 | - 21.5 | - 19.1 | - 18.9 | + 4.5 | - 0.3 |
| 5 | 9.0494 | - 21.9 | - 19.0 | - 18.8 | + 3.7 | - 0.5 |
| 6 | 7.4082 | - 22.8 | - 20.4 | - 20.3 | + 3.8 | - 0.9 |
| 7 | 5.4881 | - 27.8 | - 22.5 | - 22.0 | + 3.5 | - 1.8 |
| 8 | 3.0119 | - 40.1 | - 27.9 | - 28.4 | + 4.3 | - 3.5 |
| 9 | 742.74 keV | - 51.2 | - 31.1 | - 33.8 | + 8.1 | - 2.9 |
| 10 | 165.73 | - 67.1 | - 37.8 | - 41.3 | + 10.4 | - 3.7 |
| 11 | 3.3546 | - 73.9 | - 39.4 | - 46.0 | + 18.8 | + 0.1 |
| 12 | 37.267 eV | - 78.4 | - 42.6 | - 50.7 | + 23.1 | + 1.9 |
| 13 | 0.41399 | - 81.0 | - 45.4 | - 53.8 | + 25.1 | + 2.1 |
| | 1.00-5 | | | | | |

*without reflective zone
**periodic condition at the top boundary is adopted for the case of $L_p$= 160 cm and $L_m$= 100 cm.

is relatively small (~ 3% maximum) which indicates that for a fixed test module width, the impact of varying the plasma length on the first wall spectrum is large. By doubling the plasma length from $L_p$= 160 cm to $L_p$= 320 cm and for a fixed test module width ($L_m$= 100 cm), the maximum absolute deviation in the first wall spectrum drops from 54% to only 3%. In Fig. 7.3.2.3-2, the tritium production profiles from $^6$Li throughout the test module are displayed at the central line of the test module for the several cases shown in Table 7.3.2.3-1. From this figure, it is clear that the TPR values at the front edge of the breeding zone follows the same trends as the neutron spectrum at the first wall. In addition, the cases for ($L_p$= 160 cm, $L_m$= 100 cm, periodic condition) and ($L_p$= 320 cm, $L_m$ = 100 cm) closely reproduce the $T_6$ profile found in the reference case.

The Toroidal Buffer Region

The toroidal buffer region is defined as the zone located near the test module side boundaries and its width is measured from the test module boundaries. One would expect that the tritium production rate in this zone is different form the values at the test module center location. Similar buffer zones can be defined for the (R-θ) geometry discussed previously. In defining this buffer zone, it is necessary that the average deviation of the tritium production rate in the rest of the module from the value found in the reference full coverage case should not exceed a given percentage. To define the buffer zone in the R-Z model of Fig. 7.3.2.3-1, several test module lengths ($L_m$= 60 cm, $L_m$= 100 cm) were considered for a plasma length $L_p$= 320 cm. The profiles of $T_6$ and $T_7$ for these cases are shown in Figs. 7.3.2.3.-3(a) and (b), respectively, at the central line of the test module. Included in these figures is the result from the reference case where a full coverage for the test module is assumed and corresponds to the parameters $L_m$= ∞ . Deviation from the values in the reference case is found at the back-end of the test module. This discrepancy can be reduced by increasing the toroidal width of the test module. The $T_7$ profiles show a good agreement throughout the test module.

The $T_6$ and $T_7$ profiles across the test module in the toroidal Z direction have the same features as those found in the poloidal (R-θ) model discussed in the previous subsection. These profiles are shown in Figs. 7.3.2.3-4(a) and

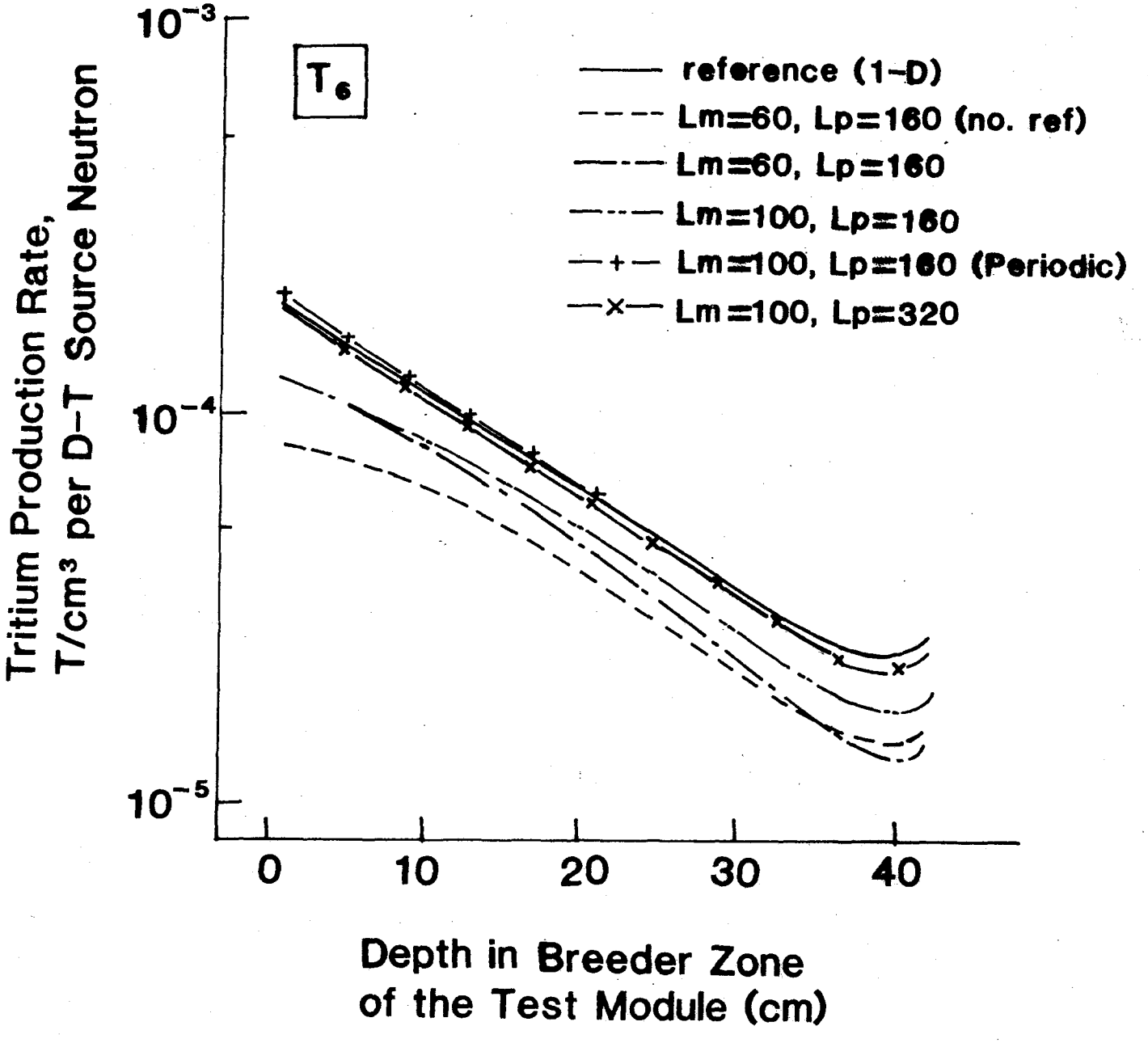


Figure 7.3.2.3-2 Effect of the reflective zone on the tritium production profiels from $^{6}Li$ throughout the test module.

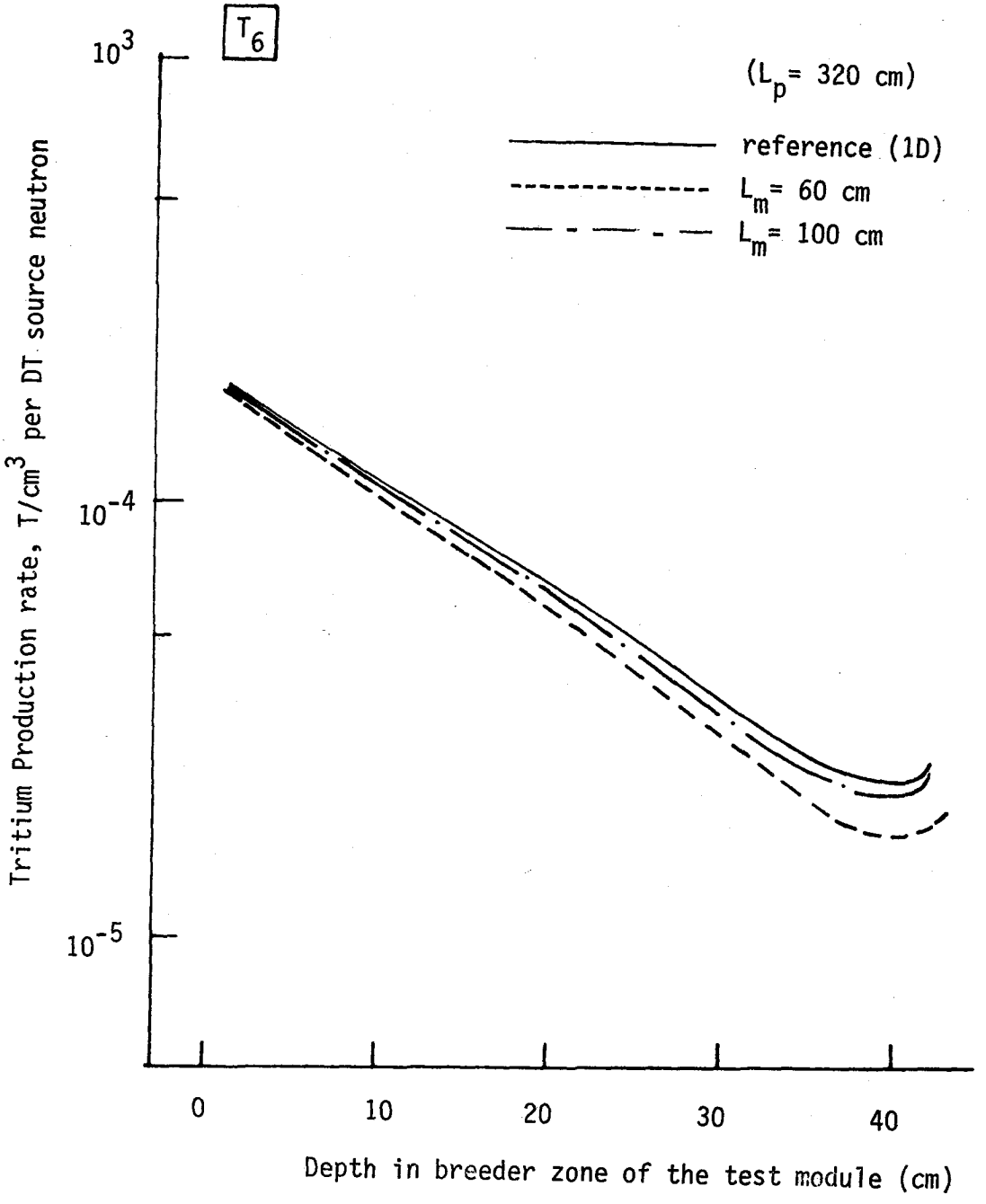


Fig. 7.3.2.3-3(a) Tritium production profiles from $^6$Li on the central axis of the breeding zone and throughout the test module (R-Z toroidal geometry).

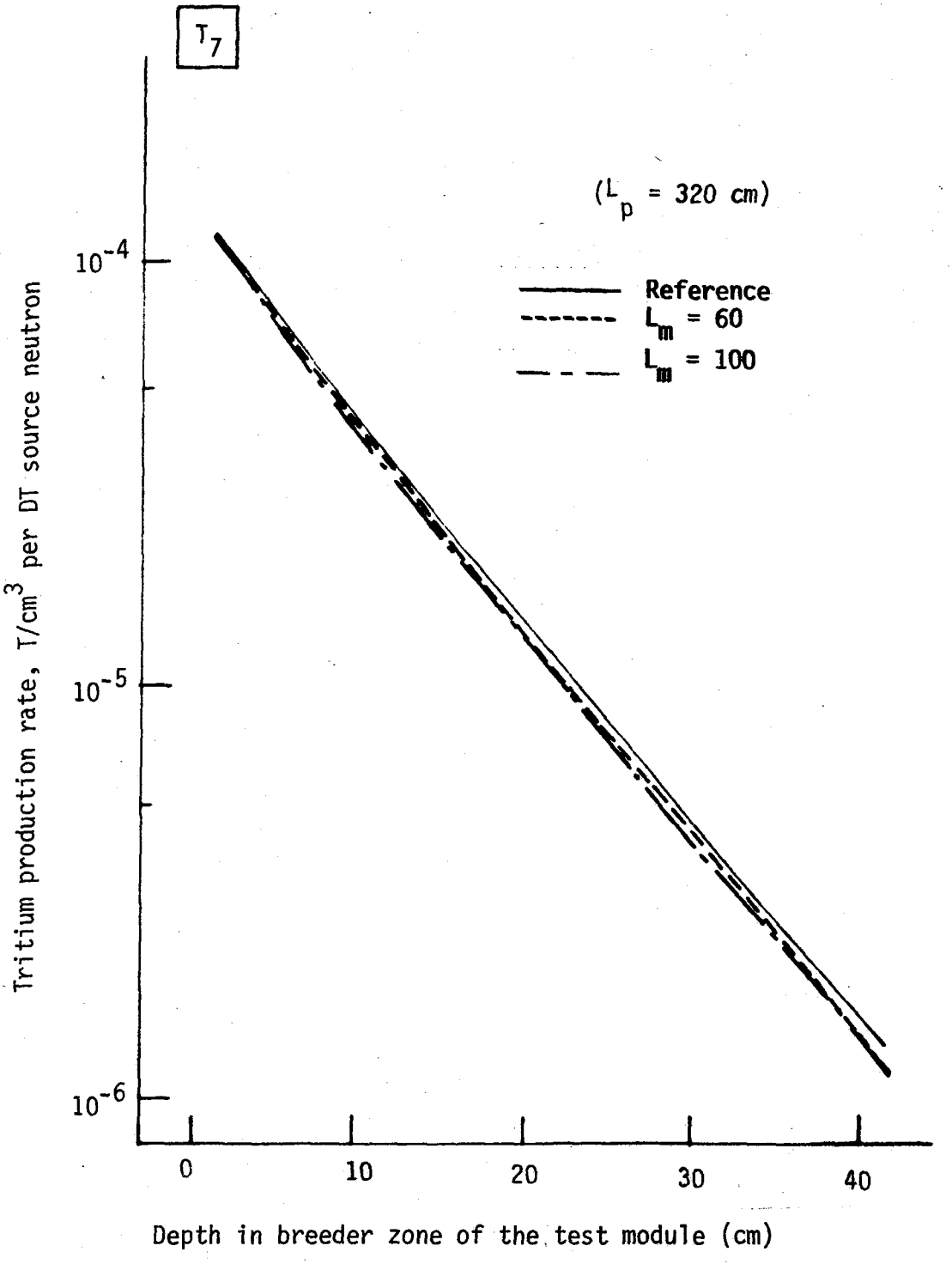


Fig. 7.3.2.3-3(b) Tritium production profiles from $^7$Li on the central axis of the breeding zone and throughout the test module (R-Z toroidal geometry).

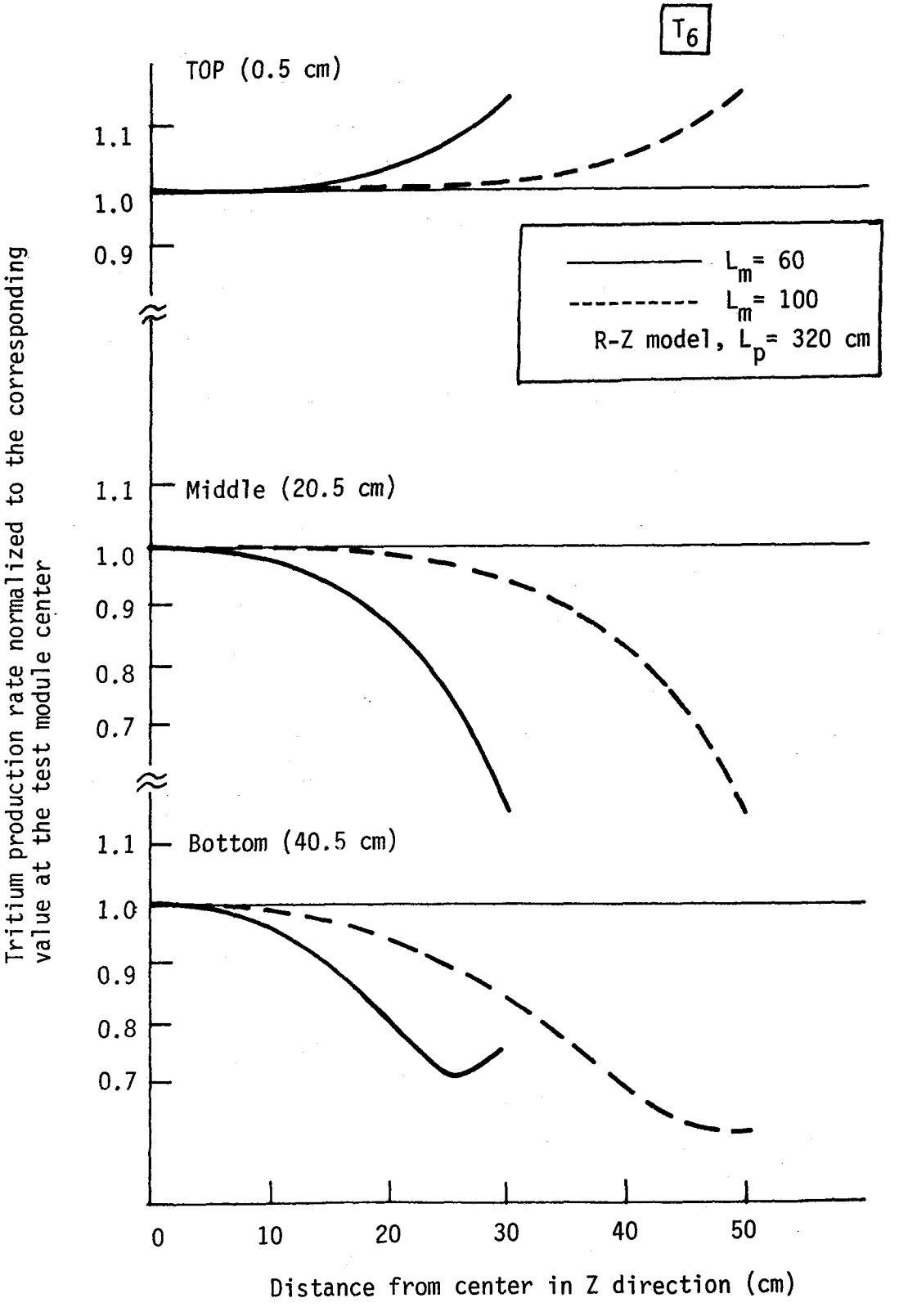


Fig. 7.3.2.3-4(a) Tritium production from $^{6}Li$ across the test module normalized to the central value (Top, middle and bottom locations are at distances of 0.5, 20.5 and 40.5 cm from the front edge of the breeding zone; R-Z toroidal geometry)

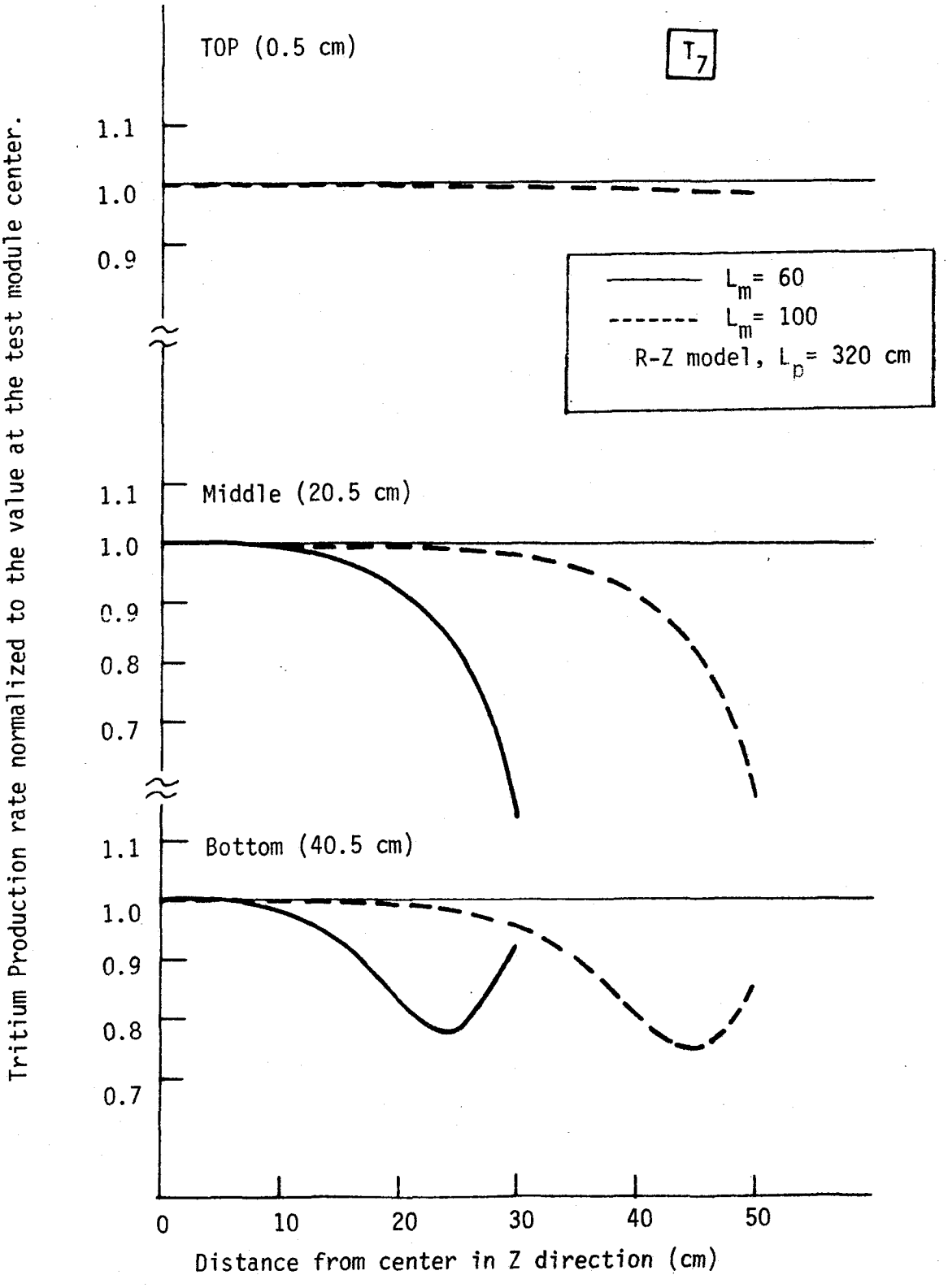


Fig. 7.3.2.3-4(b) Tritium production profiles from $^{7}Li$ across the test module normalized to the central value (Top, Middle and Bottom locations are at distances of 0.5, 20.5 and 40.5 cm from the front edge of breeding zone; R-Z toroidal geometry.)

(b). The only exception is the profile for $T_7$ at the rear edge of the breeding zone as shown in Fig. 7.3.2.3-4(b).

### 7.3.2.4 Remarks on the Results from the Nuclear Analysis in the Poloidal and the Toroidal Models

In the previous section, we discussed the degree of simulation one would expect between the tritium production profiles throughout a test module and the corresponding profiles in a full coverage case by adjusting the boundary conditions and the geometrical arrangement. The results for the (R-θ) and (R-Z) models used in the present analysis are summarized in Table 7.3.2.4-1. In this table, the total tritium production rate at the center line of the test module breeding zone is normalized to the corresponding value in the full coverage case (reference case) at three different locations.

In the (R-θ) model, better simulation is obtained by increasing the angle $\theta_m$ substended by the test module, i.e., by increasing the width of the test module. Our analysis has shown that by extending $\theta_m$ to ~ 48°, less than 5% deviation in the local tritium production rate from those values found in the refrence case is obtained, especially in the front and the back edge of the breeding zone. For this case, the corresponding deviation at the middle point of the breeding zone is larger (~ 7%) . We recall, these cited variations are those corresponding to the values at the center line of the breeding zone where tritium production measurement are most likely to be performed. However, by moving across the test module in the poloidal θ direction, different tritium production profiles are obtained as was discussed previously. Note that the poloidal reflective region (see Fig. 7.3.2.2-1) is ~ 15 cm thick and consists of 5 cm breeding material and 10 cm stainless steel (in addition to a first wall) which was obtained from the one-dimensional optimization procedures.

In the (R-Z) model, we have demonstrated the importance of simulating the conditions of the reflected neutrons since they have significant contribution to the tritium breeding from $^6Li$. In addition, by increasing the plasma length, better agreement with the results in the full coverage reference case is obtained for the same test module width ($L_m$= 100 cm). Furthermore, by periodic repetition of the test module ($L_m$= 100 cm) every 60 cm, a good agreement within less than 1% is obtained. This excellent simulation is expected

Table 7.3.2.4-1 The Total Tritium Production Rate at Three Locations in the Breeding Zone Normalized to the Values in the Reference Case

| Case | Depth in the Breeding Zone Top(0.5 cm) | Middle(20.5cm) | Bottom(40.5 cm) |
|---|---|---|---|
| 1-D cylinder model; reference | 3.1558-4[+] (1.000) | 7.5177-5 (1.000) | 2.5012-5 (1.000) |
| R-θ Model; | | | |
| $\theta_m$ = 24 deg | 0.898 | 0.754 | 0.830 |
| $\theta_m$ = 48 deg | 1.061 | 0.925 | 0.964 |
| $\theta_m$ = 72 deg | 1.060 | 0.983 | 1.044 |
| R-Z Model; | | | |
| ($L_p$ = 160 cm) | | | |
| $L_m$ = 60 cm | 0.769 | 0.760 | 0.615 |
| $L_m$ = 100 cm | 0.749 | 0.785 | 0.757 |
| $L_m$ = 140 cm | 0.739 | 0.787 | 0.802 |
| $L_m$ = 60 cm, no ref[*1] | 0.617 | 0.657 | 0.664 |
| $L_m$ = 100 cm, (periodic)[*2] | 1.068 | 1.011 | 1.011 |
| ($L_p$ = 320 cm) | | | |
| $L_m$ = 60 cm | 1.031 | 0.924 | 0.796 |
| $L_m$ = 100 cm | 0.989 | 0.950 | 0.919 |
| $L_m$ = 140 cm | 0.970 | 0.949 | 0.960 |

[+] $T/cm^3$/source neutron
[*1] without the reflective zone
[*2] periodic boundary conditions was adopted at the top

since the condition of the reflected neutrons is closely simulated in this case. However, since this particular geometrical arrangement is costly, one tends to choose the case where the plasma length $L_p$= 320 cm ($L_m$= 100 cm, first wall radius = 25 cm) and no periodic condition. This particular case shows that a deviation of ~ 3.5% in the local tritium production rate is obtained as compared to the reference case.

## 7.4 Neutronics Testing Requirements, Summary

As discussed in the previous sections, neutronics testing in a fusion test device will involve several types of measurements such as tritium production rate, source neutron yield, neutron and gamma-ray spectra, heating rates during operation, activation and afterheat measurements. Fortunately, all the neutronics responses with the exception of radioactivity parameters vary linearly with the neutron wall load. Thus, any value of neutron wall load or fluence in the testing device is, in principle, acceptable since the results of the neutronics measurements can be translated to the correpsonding values with a different wall load or fluence. The non-linearity in the dependence of the induced-activation on the wall load and the long-time required for measuring the behavior of long-lived isotopes impose, however, more complex requirements on the test conditions that depend on the particular materials constituting the test module.

The requirements for neutronics testing fall within two categories: (a) test device operating conditions, (b) test module conditions. The fusion test device conditions include parameters such as the wall load, fluence, and pulse length. The test module conditions are those related to the test module material and configuration, surface area exposed to nuclear field, minimum size requirement for optimal testing, and requirements on the test module boundary conditions and geometrical arrangement.

### 7.4.1 Test Device Operating Condition Requirements

As we discussed in Section 7.3.1 devoted to the instrumentation requirements, two modes of operation are possible; namely, the low fluence mode ( ~ 1 MW $\cdot$sec/$m^2$) and the very low fluence mode ( ~ 1 W$\cdot$sec/$m^2$). The low fluence mode can be achieved, for example, with a wall load of 1 MW/$m^2$ and 1 sec plasma burn time or, alternatively, 0.01 MW/$m^2$ and 100 sec. Thus, neutronics

tests impose modest requirements on the product of the wall load and plasma burn time with no stringent requirements on the magnitude of either parameter.

Measurements of tritium production rate, neutron and gamma-ray heating, reaction rates, and neutron spectra can be performed with the low fluence mode. However, operating the test device in the very low fluence mode is most suitable for measuring tritium production from $^{6}Li$, gamma-ray heating, neutron and gamma-ray spectra if a low activation level is desired. In practice, the main problem associated with low fluence operating mode is the activation of the test module and device components which may render the test device inaccessible just after shutdown. This will necessitate a long cooldown time to handle the reactor components. On the other hand, the main problem related to the very low fluence operation mode is the poor spatial resolution and instability of measurements. As expected, the methods used for measurements in the low fluence mode have better accuracy and spatial resolution as compared to those used in the very low fluence operation mode. For source characterization and neutron yield, which is viewed as a part of the plasma diagnostics, measurements can be undertaken in both operation modes. It should be noticed that performing other measurements such as tritium production measurements, should be done simultaneously with the source and neutron yield measurements during a particular plasma burn cycle to assure that the response measured (TPR, for example) corresponds to the same neutron source condition of that particular plasma burn cycle. The methods that can be used to measure various parameters under various operating conditions have been discussed previously and are summarized in Table 7.3.1-3.

### 7.4.2 Test Module Requirements

The requirements on the test module size and geometry are governed mainly by the objective and procedure for the particular neutronics test under consideration. If local measurement of tritium production is intended, for example, then the only useful information that can be obtained from such a neutronics test is to verify the consistency between analytical prediction and experimental measurements. Resolving the question of the adequacy of nuclear data base can be better achieved in a simple benchmark experiment as we pointed out earlier in Section 7.2. In this particular case, there is no need to duplicate the actual blanket of the demo or commercial reactor. However,

to improve the analytical prediction and to identify the various sources of uncertainties, one would proceed from a geometrically simple model benchmark experiment utilizing a point source to a more complicated one involving a volumetric plasma source in a fusion test device.

On the other hand, if the objective of the neutronics test is to verify an integrated parameter in a given blanket concept such as the tritium breeding ratio (TBR), the test module used in this experimental planning approach should duplicate in great detail the actual blanket module (look-alike test module). Furthermore, factors that affect the global TBR should be included in the fusion test device such as the actual penetrations for heating and fueling, full coverage geometrical arrangement, presence of the impurity control system, etc. This is an important point of concern since extrapolating measurements of the local tritium production rate (TPR) in a partial coverage case to a demo or commercial reactor involves many uncertainties. These arise from: a) uncertainty in specifying the neutron source condition at the first wall of the test module, b) uncertainties in predicting (by calculation or measurments) the energy-dependent angular flux at the test module boundaries, and c) uncertainties in extrapolating the effects of penetrations and other configurational features of a demo or commercial reactor that cannot be easily reproduced in a fusion test device. Since the estimated margin in TBR for candidate blanket concepts is small, very high accuracies in measurements are required and these uncertainties need to be carefully evaluated.

Our present nuclear analysis presented in the previous section emphasizes the above mentioned considerations. No attempt was made in this analysis to test the self-sufficiency in tritium production. Rather, the objective of the tests considered here has been to investigate those factors affecting the tritium production profiles (from $^{6}Li$ and $^{7}Li$, individually) in a geometrical arrangement where the test module partially covers the plasma source. The motivation behind this analysis is to identify the best geometrical arrangement and minimum test module size that simulates the tritium production profiles in the full coverage case. The factors studied are the test module width, the thickness and material choice for the reflective zone (the zone that surrounds the plasma source in locations other than the test module), the plasma length, and the conditions at the test module boundaries. The simula-

tion is expressed in terms of the percentage deviation of the local tritium production rate in the partial coverage case from the corresponding value obtained in the full coverage case.

A summary of the present nuclear analysis that specifies the minimum test module size (expressed in terms of the poloidal angle $\theta_m$ in the R-$\theta$ arrangement, or the test module width $L_m$ in the R-Z arrangement) are shown in Figs. 7.4.2-1 to 7.4.2-3. Fig. 7.4.2-1 shows the variation in the local tritium production rate (sum of $T_6$ and $T_7$) as a function of the poloidal angle $\theta_m$ at three locations on the central line of the test module and the values shown are normalized to the corresponding values in the full coverage case. Also shown in this figure is the maximum deviation (in %) from the tritium production rate at the central line of the test module as we move towards the side boundaries of the test module within a spatial zone characterized by two angles, $\theta_t = 10^o$ and $20^o$ ($\theta_t/2 = 5^o$ and $10^o$ measured from the test module central line). This deviation depends on the width of the test module (characterized by the angle $\theta_m$) and on the location throughout the test module (top, middle, bottom,...) as shown in Fig. 7.4.2-1. The information contained in this figure is useful in specifying the minimum test module width ($\theta_m$) and the location inside the test module such that the deviation in the local tritium production rate from the value found in the full coverage arrangement is within a prescribed percentage. For example, if the local tritium production rate at the front edge of the test module (evaluated at the test module central line) is required to be within 5% of the corresponding value in the full coverage case, the width of the test module should be the one that corresponds to either $\theta_m = 22^o$ (-5% deviation) or $\theta_m = 48°$ (+5% deviation). If measurements were to be performed at the back-edge of the test module central line, the corresponding values would be $\theta_m = 48°$ or $71°$ for the same target accuracy. The situation is different at the middle location where a test module width that corresponds to $\theta_m = 55°$ would give a 5% target accuracy. In addition to this prescribed deviation from the values in the full coverage case, one should add an additional deviation that comes from performing the measurements within the spatial zone characterized by the angle $\theta_t$. The results shown in Fig. 7.4.2-1 indicate that performing the measurements within a spatial zone that corresponds to $\theta_t = 10°$ at the front edge of the breeding zone is practically as good as performing these measurements within a spatial zone corresponding to $\theta_t = 20°$. However, if tritium production measurements

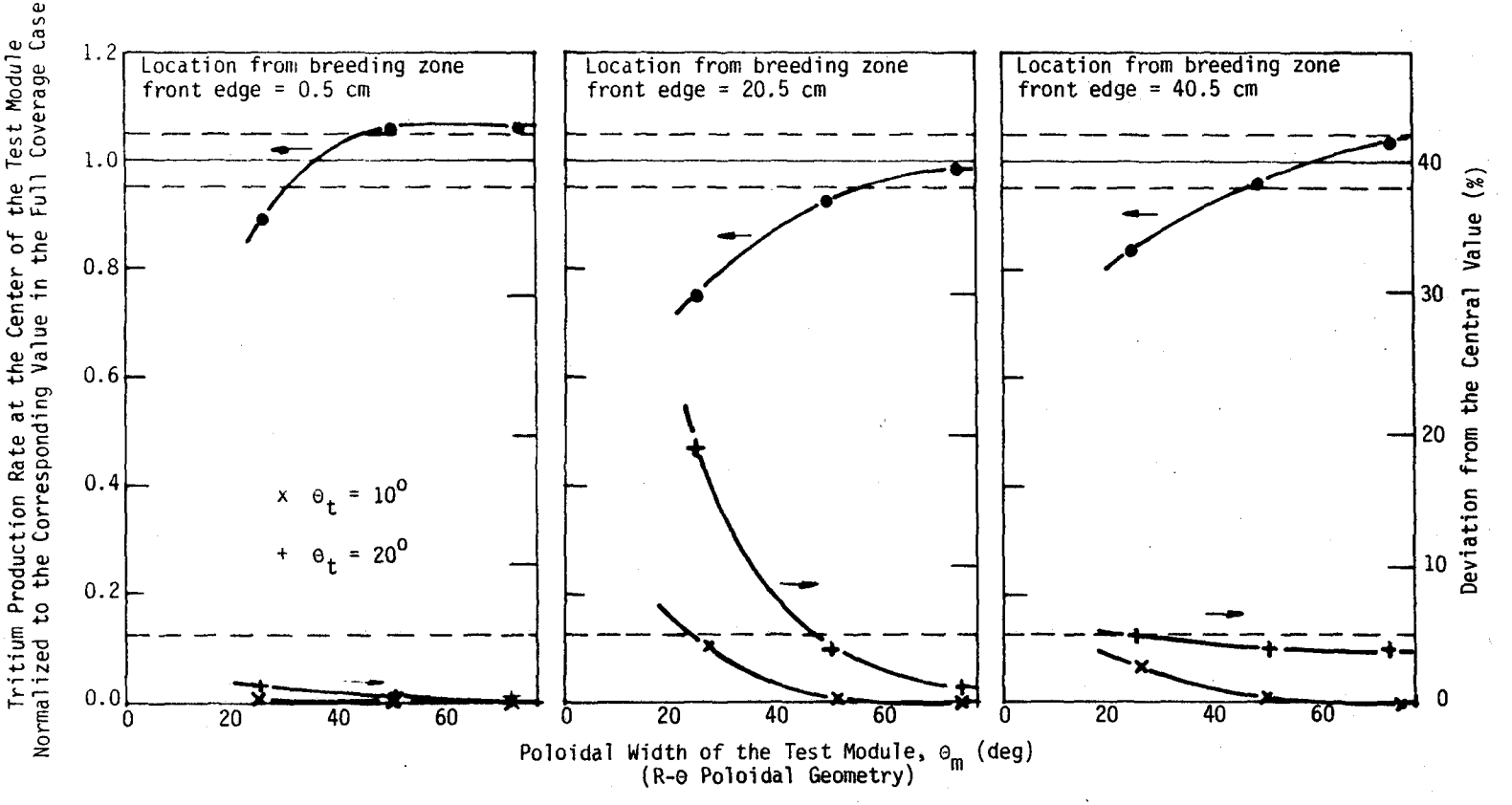


Fig. 7.4.2-1 The total tritium production rate ($T_6+T_7$) as a function of the test module width ($\theta_m^{6,7}$). Also shown is the deviation (%) from central values as a function of the test module width for two central zone widths, $\theta_t$= 10° and 20°. (R-θ geometry)

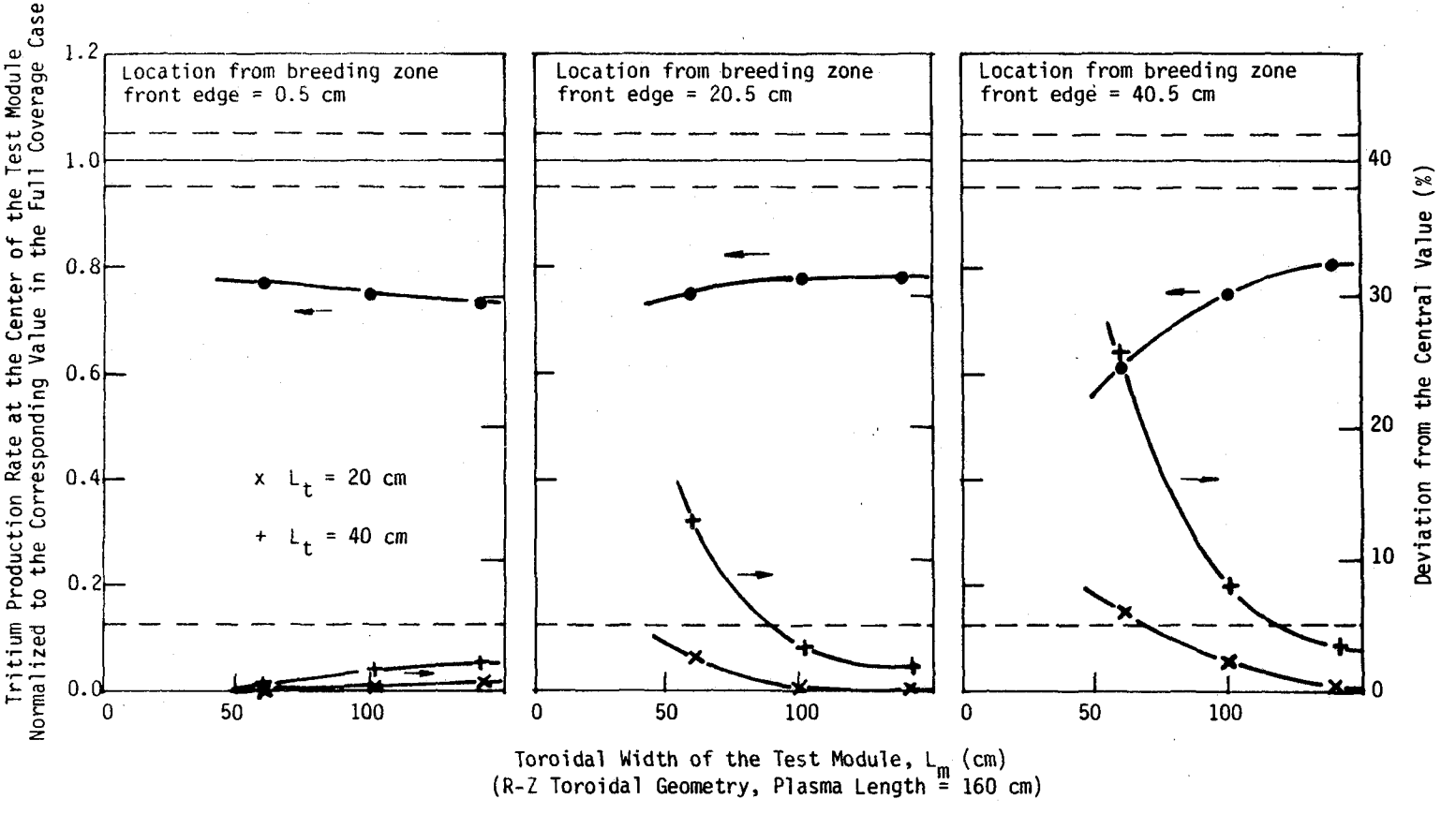


Fig. 7.4.2-2 The total tritium production rate ($T_6$+$T_7$) as a function of the test module width ($L_m$). Also shown is the deviation (%) from the central values as a function of the test module width for two central zone widths, $L_t$=20 and 40 cm in the case of plasma length $L_p$=160 cm.

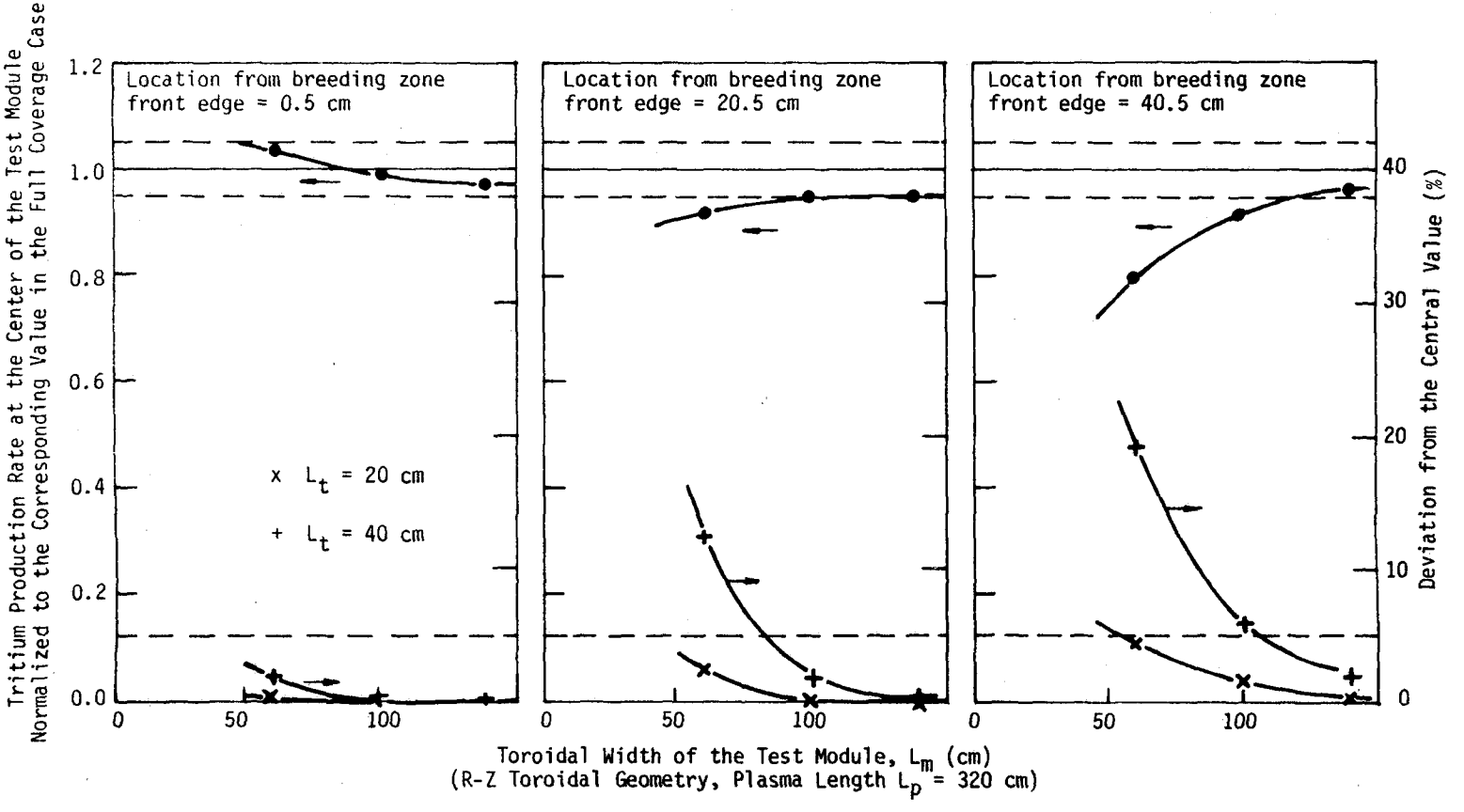


Fig. 7.4.2-3 The total tritium production rate ($T_6$+$T_7$) as a function of the test module width ($L_m$). Also shown is the deviation (%) from the central values as a function of the test module width for two central zone widths, $L_t$=20 and 40 cm in the case of plasma length $L_p$ = 320 cm.

were to be carried out at the middle location of the test module of a width $\theta_m = 55°$, an additional contribution of ~ 2.6% should be added in to the deviation obtained in the case where measurements are performed within a zone substended by $\theta_t = 20°$. This leads to about 7.6% deviation from the tritium production value at this location in the full coverage case. The corresponding deviation for the case with $\theta_m = 55°$ and $\theta_t = 10°$ is almost 5%.

Similar curves that specify the minimum test module size in the R-Z geometrical model are shown in Fig. 7.4.2-2 and 7.4.2-3 for the cases where the plasma length is $L_p = 160$ and 320 cm, respectively. In this geometrical arrangement, the test module width is characterized by the parameter $L_m$ while the test module-central zone where measurements are most likely to be performed is characterized by the parameter $L_t$. For the case with $L_p = 160$ cm, the tritium production value at the front-edge of the test module is less than ~ 80% of the corresponding value in the full coverage case and the situation even worsens as the test module width, $L_m$, increases. However, for the case with a plasma length $L_p = 320$ cm, the tritium production rate at the front-edge of the test module is within 5% of the corresponding value in the full coverage case provided the test module width is either $L_m = 50$ cm (+5% deviation) or $L_m = 150$ cm (- 5% deviation). For the former case, one should add ~ 3.4% deviation (total ~ 8.4%) if measurement were to be carried out within the central zone of $L_t = 40$ cm at that location.

To emphasize that it is impractical to perform a neutronics test that verifies the self-sufficiency of tritium breeding (TBR > 1) in a fusion test device where the test module is partially covering the plasma source, we show in Fig. 7.4.2-4 the integrated values of tritium production rate in various segments of the test module (characterized by the parameter $t_B$) and the overall tritium breeding rate as function of the test module width. The curves shown are for both the R-Θ and the R-Z arrangements. The values shown in this figure are normalized to the corresponding values in a volume equivalent to the test module volume in the full coverage case. In all the cases shown, the total tritium breeding ratio in the test module is smaller than the corresponding value in the full coverage case. This demonstrates the uncertainty involved in testing the self-sufficiency requirement in a demo or a commercial reactor. Performing such a test, therefore, will require a geometrical arrangement that duplicates the entire blanket (including penetrations) as has been shown in previous studies.[10]

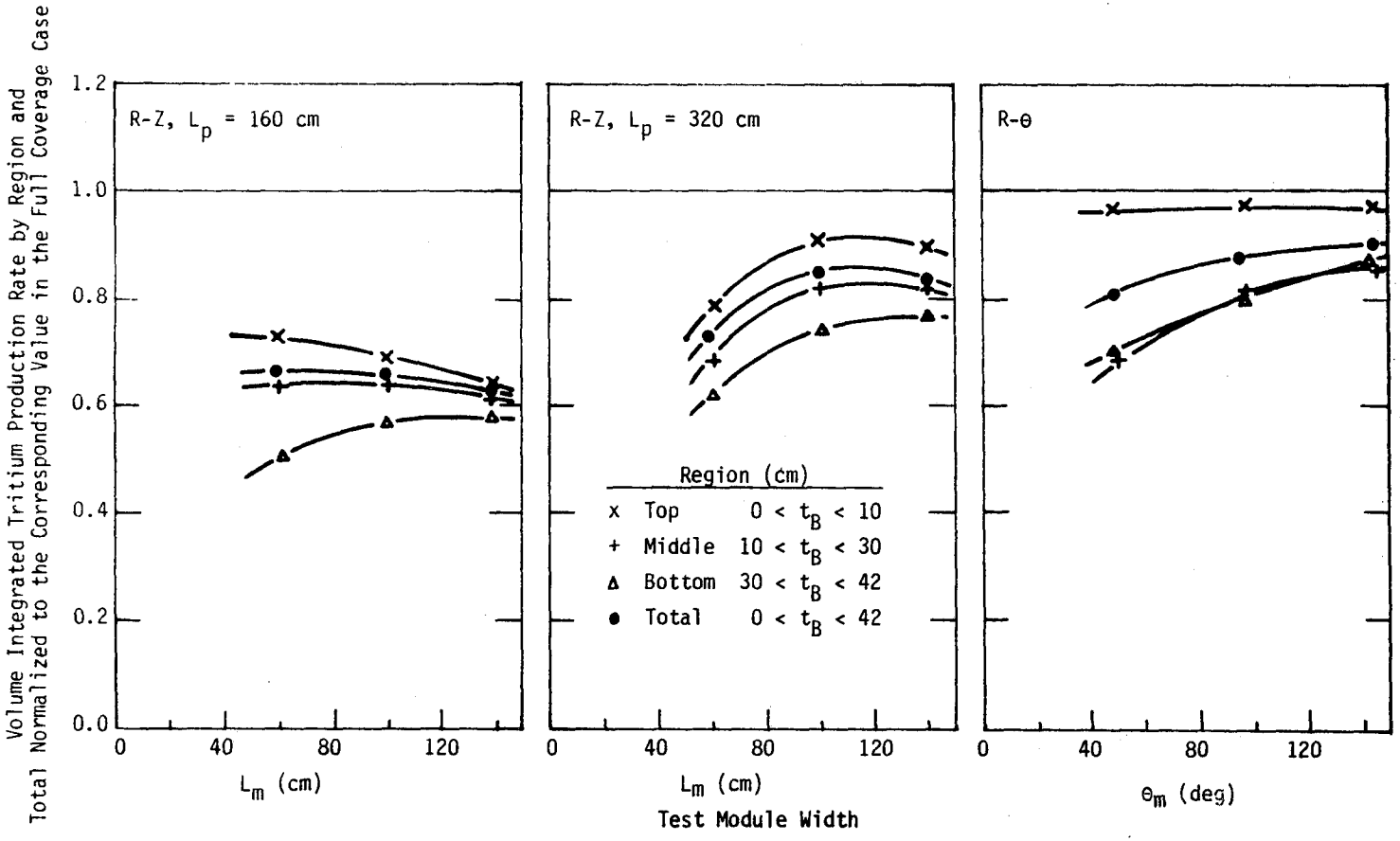


Fig. 7.4.2-4 Total tritium production rate integrated over various spatial segments and the overall tritium breeding rate as a function of the test module width ($L_m$ or $\theta_m$)

## References for Chapter 7


1. T. Nakamura, et al., "Integral Experiment on Lithium Oxide Spherical Assembly with Graphic Reflector and on Duct Streaming", 3rd IAEA Technical Committee Meeting and Workshop on Fusion Reactor Design and Technology, Tokyo (1981).

2. T. Nakamura, et al., "A D-T Neutron Source for Fusion Neutronics Experiments at the JAERI," Proc. Int. Ion Engineering Congress-ISIAT'83 & IPAT'83, Sept. 12-16, 1983, Kyoto, Japan, Vol. I, pp. 567-570 (1983).

3. L. Green, "Review of Integral Fusion Blanket Neutronic Experiments", The Technology of Controlled Nuclear Fusion, Proceedings of the Fourth Topical Meeting, Oct. 14-17, 1980, Vol. I, pp. 395-404 (1981).

4. M. A. Abdou, "Tritium Breeding in Fusion Reactors," ANL/FPP/TM-165, (1982).

5. M.A. Abdou, et. al., "Engineering Testing," FED-INTOR/TEST/82-4, Chapter XII of USA FED-INTOR/82-1 (1982).

6. H. Maekawa, et al., "measurements of Tritium Production-Rate Distribution in Simulated Blanket Assemblies at the FNS," NEACRP-L-268, JAERI-M 83-196.

7. Y. Oyama, et al., "Development of a Spherical NE213 Spectrometer with 14 mm Diameter," JAERI-M 84-124.

8. Jr. W.W. Engle, "A User's Manual for ANISN, a One-Dimensional Discrete Ordinates Code with Anisotropic Scattering," K-16932, Union Carbide Corp. (1976).

9. DOT IV, Version 4.3, "One- and Two -Dimensional Transport Code System," CCC-429. Radiation Shielding Information Center (Apr. 1982)

10. M.Z. Youssef and M.A. Abdou, "Neutronics Testing Requirements in Fusion Devices," Trans. Am. Nucl. Soc., 46, 234 (June 1984).

# CHAPTER 8

# FLUENCE CONSIDERATIONS

TABLE OF CONTENTS


Page

8.1 Introduction ..... 8-1

8.2 Material Property Extrapolations ..... 8-1
8.2.1 Introduction ..... 8-1
8.2.2 Swelling ..... 8-2
8.2.3 Creep ..... 8-7
8.2.4 Tensile Strength/Ductility ..... 8-9
8.2.5 Fracture Toughness ..... 8-13
8.2.6 Ductile to Brittle Transition Temperature ..... 8-19
8.2.7 Fatigue Crack Growth ..... 8-20
8.2.8 Conclusions ..... 8-21

8.3 Uncertainty Projection Approach ..... 8-23

8.4 Interactive Testing ..... 8-25

8.5 Conclusions ..... 8-31

References ..... 8-34

# 8. FLUENCE CONSIDERATIONS

## 8.1 Introduction

One of the primary goals of FINESSE is to outline a program for studying fusion reactor materials behavior and, in particular, for resolving the key issues associated with interactive effects. Many of these key issues have been identified in Chapter 3 of this report. It is well known from experiments performed in fission reactors that neutron fluence changes many material properties and, therefore influences many interactive effects. Since testing in a neutron environment, especially one simulating fusion neutrons will be very expensive, it becomes important to gage the value of the information gained as a function of neutron testing fluence for a given testing program. In order to achieve an optimum test program, several questions must be addressed. First we must have some method of determining to what fluence we must test a given element or module to be able to adequately understand the given effect in question. Next we must address the issue of what risk we assume if we do not test out to this neutron fluence.

The approach we have undertaken for addressing these questions will consist of the following steps. First the key material properties will be identified, and estimates of their changes with neutron fluence will be made. The next step will consist of performing uncertainty projections as defined in Refs. (1) and (2) to quantify the relative benefit of nuclear testing as a function of accumulated testing fluence for each of these material properties. Finally, the approach of uncertainty projections will be extended to address the issues associated with interactive effects testing.

## 8.2 Material Property Extrapolations

### 8.2.1 Introduction

The neutron flux associated with any fusion device is responsible for damage to the structural material, nuclear heating, and nuclear transmutations. The amount of damage is dependent upon both the neutron flux and

spectrum. This damage is responsible for changes in the materials' physical and mechanical properties. The neutron flux also give rise to bulk heating in any fusion component. This bulk heating is a factor in determining the temperature gradients in the component and must be accommodated in the design of the component. Finally, the neutron flux is responsible for transmutations in the component materials. Within the structural materials these transmutations can lead to changes in the materials properties such as loss in ductility through the introduction of helium into the material.

Our present understanding of the influence of neutron fluence upon material properties comes from the extensive testing of materials in fission reactors and point sources. Extensive testing has been performed on austenitic type alloys, and significant testing has been performed on the ferritic alloy HT9. For advanced alloys such as the vanadium based alloys, however, the extent of nuclear testing is quite limited. Within this section, our current understanding of the influence of neutron fluence on material properties will be described. Also, the extrapolation of the material properties with neutron exposure will be presented. These extrapolations are based upon available models, theories, and engineering judgment when necessary and are based upon data bases obtained from fission reactor irradiations. These extrapolations represent the best guess at this time as to the behavior of the material within a fission spectrum environment.

### 8.2.2 Swelling

The swelling of structural materials within a neutron environment has long been recognized as a material behavior which has a significant impact on both reactor design and life. The swelling of many structural materials and solid breeder materials have been adequately described with a bi-linear model of the form:[3]

$$\frac{\Delta V}{V_o} = R \{\phi t + \frac{1}{\alpha} \log_e [\frac{1 + \exp[\alpha(\tau - \phi t)]}{1 + \exp(\alpha\tau)}] \} \quad (8.2.2\text{-}1)$$

where R is the steady state swelling rate, $\alpha$ is the curvature parameter, and $\tau$ is the incubation parameter. Below the neutron fluence corresponding to $\tau$, little swelling occurs. After the neutron fluence corresponding to $\tau$, the material's volume increases at a steady rate given by R. In general, R, $\tau$, and $\alpha$ may depend upon the irradiation temperature.

Swelling data on PCA have been obtained to a peak neutron exposure corresponding of 22 dpa.[4] No swelling in the cold worked condition of this alloy has been observed for irradiation temperatures 400 to 650°C and neutron fluences to 22 dpa. Recent work on solution annealed titanium modified 316 SS suggest that after the incubation period the steady-state swelling rate can approach 1%/dpa.[5] This rate appears to be a universal constant observed in many austenitic alloys.[6] The extrapolated swelling behaviors for a cold worked titanium modified 316 SS such as PCA are given in Figures 8.2.2-1 to 8.2.2-3 for irradiation temperatures of 300, 400 and 500°C, respectively. The upper bounds for all three extrapolations assume a swelling rate of 1%/dpa. The lower bounds assume a relatively long transient regime (small value for $\alpha$). The values for the incubation parameter $\tau$ have been arbitrarily assumed to be approximately 100 dpa for the upper bound at all three temperatures. The incubation parameter for the lower bound has been set at approximately 170 dpa for 300°C and at approximately 150 dpa for 400 and 500°C.

Swelling data on HT9 have been obtained to a peak neutron exposure corresponding to 80 dpa with no observable swelling.[7] Swelling measurements performed on simple ferritic alloys have shown a steady-state swelling rate on the order of 0.06%/dpa with the peak swelling occurring in the temperature range of 380 to 430°C.[8] The extrapolated swelling behavior for HT9 are shown in Figures 8.2.2-4 to 8.2.2-6. The upper bounds for the extrapolations assume a swelling rate of 0.12%/dpa and incubation parameters in the range of 110 to 130 dpa. The lower bounds assume a swelling rate of 0.06%/dpa. The incubation parameters for the lower bounds were arbitrarily set at >250 dpa at 300°C, approximately 150 dpa at 400°C, and approximately 180 dpa at 500°C.

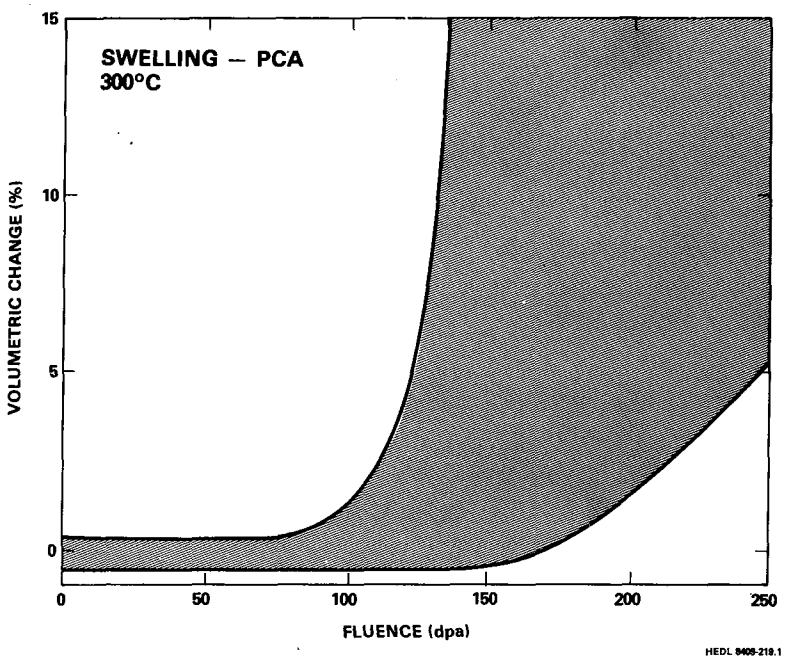


Figure 8.2.2-1. Anticipated range of stress-free swelling for PCA at 300°C as a function of neutron fluence.

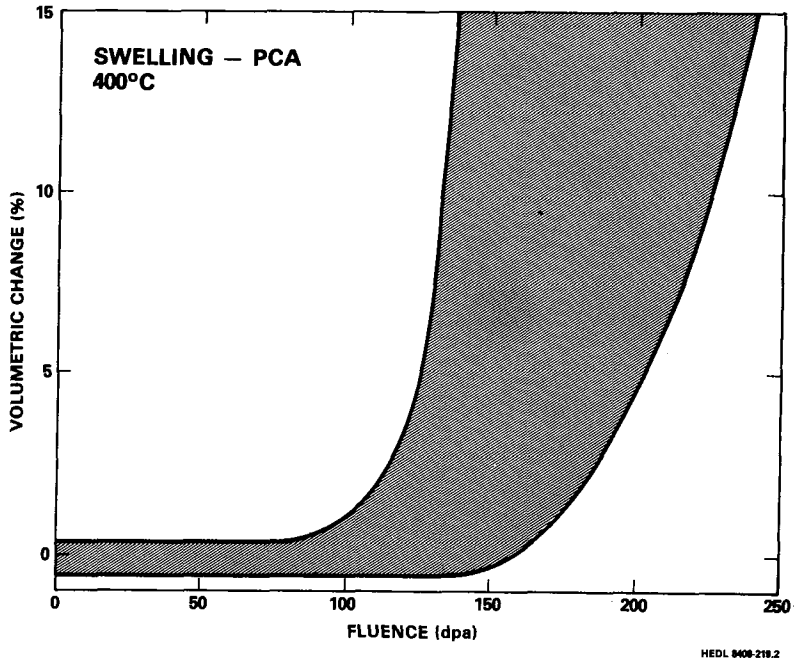


Figure 8.2.2-2. Anticipated range of stress-free swelling for PCA at 400°C as a function of neutron fluence.

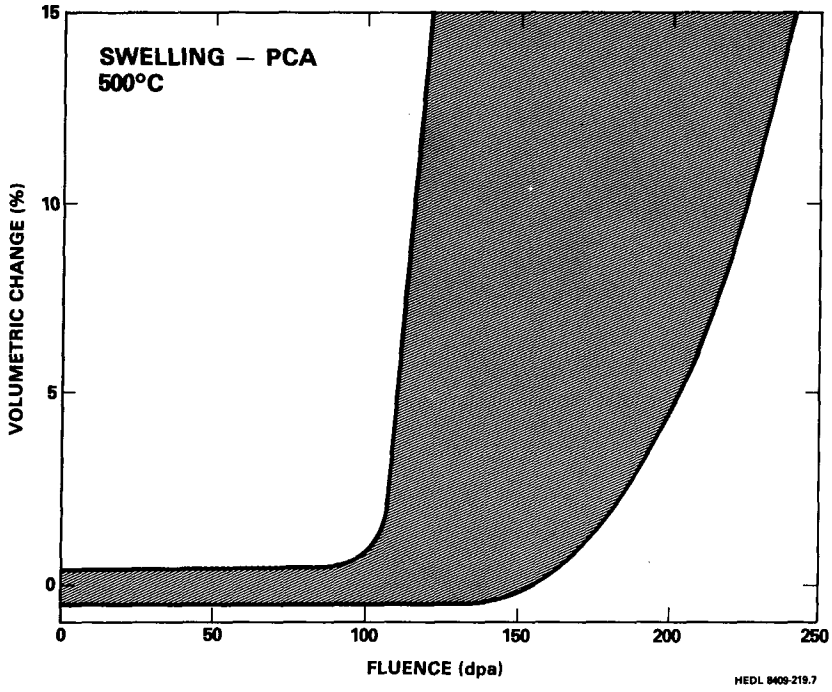


Figure 8.2.2-3. Anticipated range of stress-free swelling for PCA at 500°C as a function of neutron fluence.

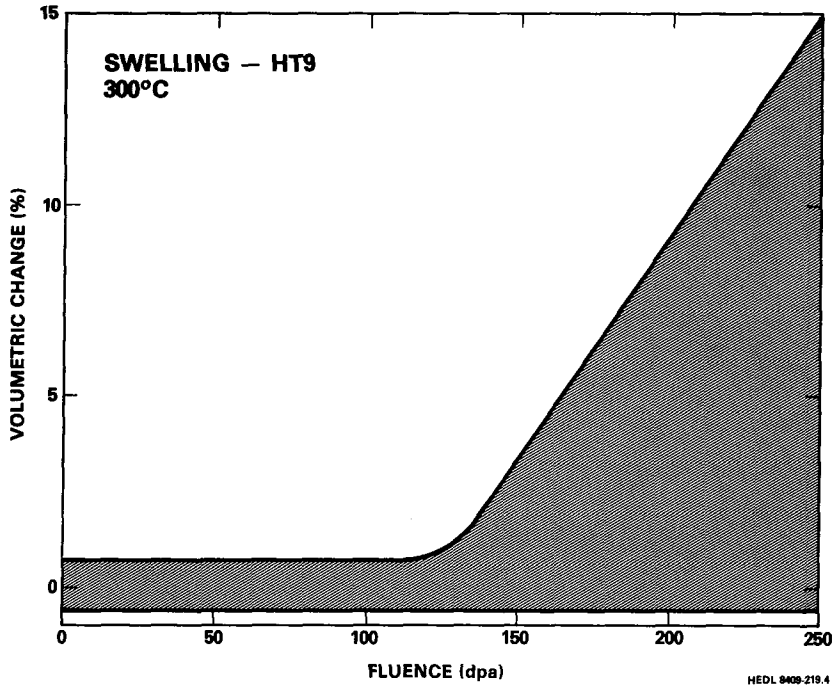


Figure 8.2.2-4. Anticipated range of stress-free swelling for HT9 at 300°C as a function of neutron fluence.

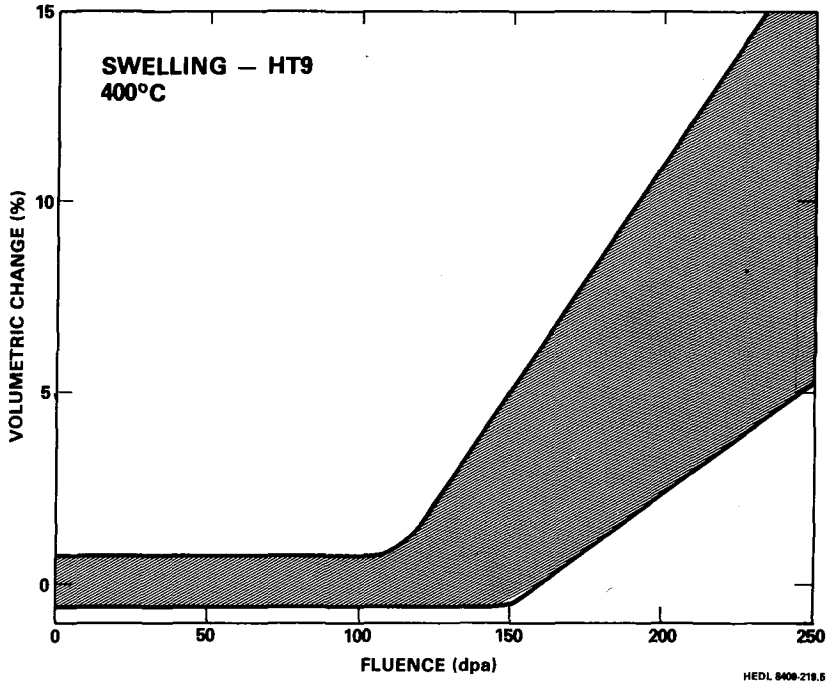


Figure 8.2.2-5. Anticipated range of stress-free swelling for HT9 at 400°C as a function of neutron fluence.

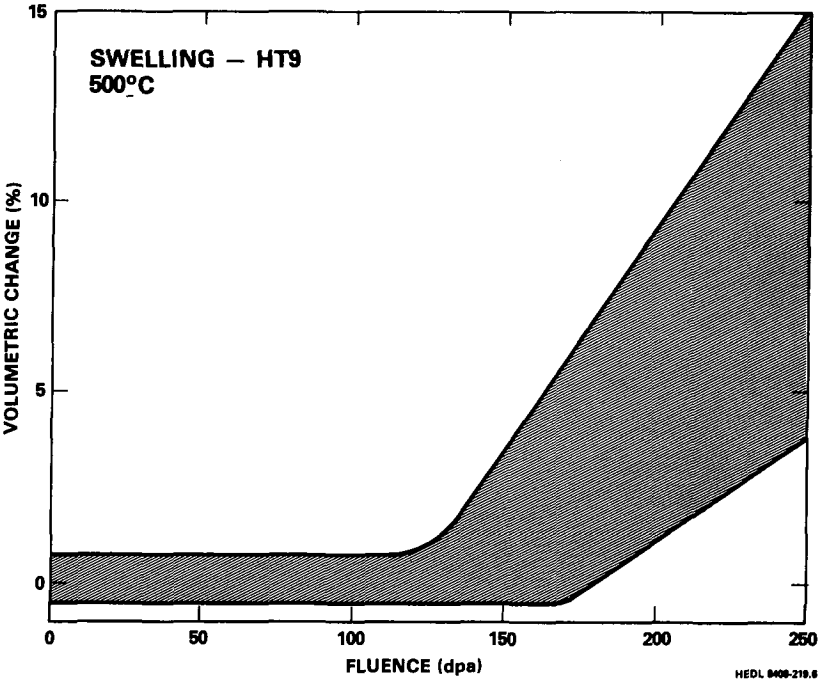


Figure 8.2.2-6. Anticipated range of stress-free swelling for HT9 at 500°C as a function of neutron fluence.

Swelling data on vanadium based alloys are very limited. Both neutron and ion irradiation swelling data on V-20Ti at 600°C indicate no swelling after a peak neutron exposure of 55 dpa.[9] We have assumed that the swelling behavior of the vanadium alloy V-15Cr-5Ti will be equivalent to that of HT9.

Recent swelling data on selected solid breeder materials have been obtained from the FUBR experiment in the experimental breeder reactor, EBR-II.[10] These data for $Li_2O$ are shown in Figure 8.2.2-7. Specifically, we find that to an atom burn-up of approximately $9 \times 10^{20}$ captures/$cm^3$, the $Li_2O$ material exhibits a linear increase in its volume as a function of increasing burn-up. The $LiAlO_2$, on the other hand, exhibits little if any change in its volume. The extrapolated range for swelling in $Li_2O$ is, therefore, given in Figure 8.2.2-8.

## 8.2.3 Creep

The creep of a structural material within a neutron environment can be described by a model of the form:

$$\dot{\varepsilon} = B_o \phi \sigma^n + D\dot{S}\sigma^n + \dot{\varepsilon}_T \qquad (8.2.3\text{-}1)$$

where $\dot{\varepsilon}$ is the effective creep strain rate, $B_o$ is the average creep coefficient, $\phi$ is the neutron flux, $\sigma$ is the stress, n is the stress exponent, $\dot{S}$ is the swelling rate, D is the swelling enhanced creep constant, and $\varepsilon_T$ is the thermal creep component of effective creep strain rate. This model has been successful in fitting in the in-reactor creep behavior of several austenitic stainless steels.[11,12] This equation has also been fit to the ferritic alloy 2-1/4Cr-1Mo[13] and has, therefore, been assumed to be valid for HT9 and vanadium based alloys as well.

Creep data on PCA have been reported only to a peak fluence of 5 dpa. However, creep data on cold worked titanium modified 316 SS to a peak neutron exposure of approximately 20 dpa[14] indicate the creep behavior

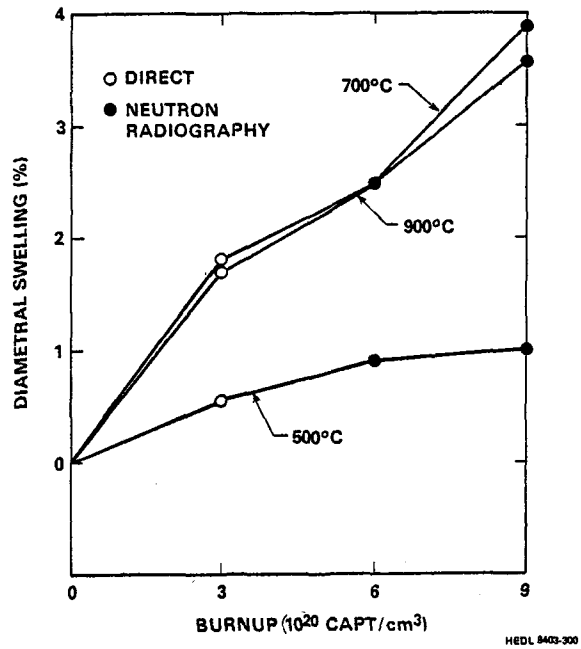


Figure 8.2.2-7. The swelling behavior of the solid breeder material $Li_2O$.

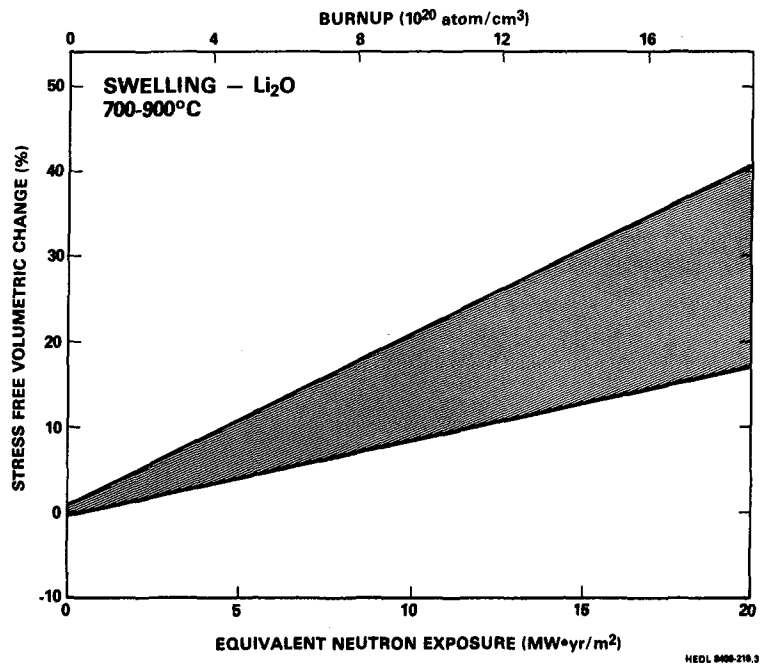


Figure 8.2.2-8. Anticipated range of stress-free swelling for $Li_2O$, as a function of atom burn-up.

of this alloy is similar to that of 20% CW 316 SS[15] at 400°C and exhibits less creep strain when compared to CW 316 SS at higher irradiation temperatures. These observations were used to construct the anticipated ranges for the in-reactor creep behavior of PCA which are shown in Figures 8.2.3-1 to 8.2.3-3. These anticipated ranges are valid for stresses less than 200 MPa. For PCA, a stress exponent of 1.0 is assumed based upon data on a cold worked titanium modified 316 SS.[14] Also, the value for the swelling enhanced creep constant was assumed to be within the range of 0 to 0.05 $MPa^{-1}$. Based upon creep data on 316 SS,[16] it is anticipated that thermal creep mechanisms in PCA will not become important until the irradiation temperatures are greater than 600°C. The upper bound in each figure reflect the observation that in a particular heat of cold worked 316 SS, the creep rate monotonically increases until the onset of swelling.[15] Other austenitic alloys exhibit a bi-linear creep rate more consistent with the model which we have chosen.[12] The lower bond in each of the figures assumes D = 0.

In-reactor creep data for HT9 have been reported to a peak fluence of 50 dpa for irradiation temperatures between 400 and 600°C.[17] These data suggest a stress exponent of approximately 1.5. In general, the HT9 creep strains are less than the creep strains for 316 SS and titanium modified 316 SS for irradiation temperatures between 450 to 600°C. These HT9 creep data suggest a linear fluence dependence. The anticipated ranges of creep behavior for this alloy are shown in Figures 8.2.3-4 and 8.2.3-5. These anticipated ranges of creep behavior are valid for stresses less than 150 MPa. The upper bonds assume D = 0.05 and uses the upper bound for swelling (given in Figures 8.2.2-4 to 8.2.2-6) in the creep model. The lower bond assumes D = 0. Thermal creep mechanisms become important in HT9 for irradiation temperatures greater than 550°C.

### 8.2.4 Tensile Strength/Ductility

Both the strength and ductility of a structural material change with increasing neutron fluence. Typically, this change in the material property occurs rapidly and tends to saturate for neutron exposures greater than

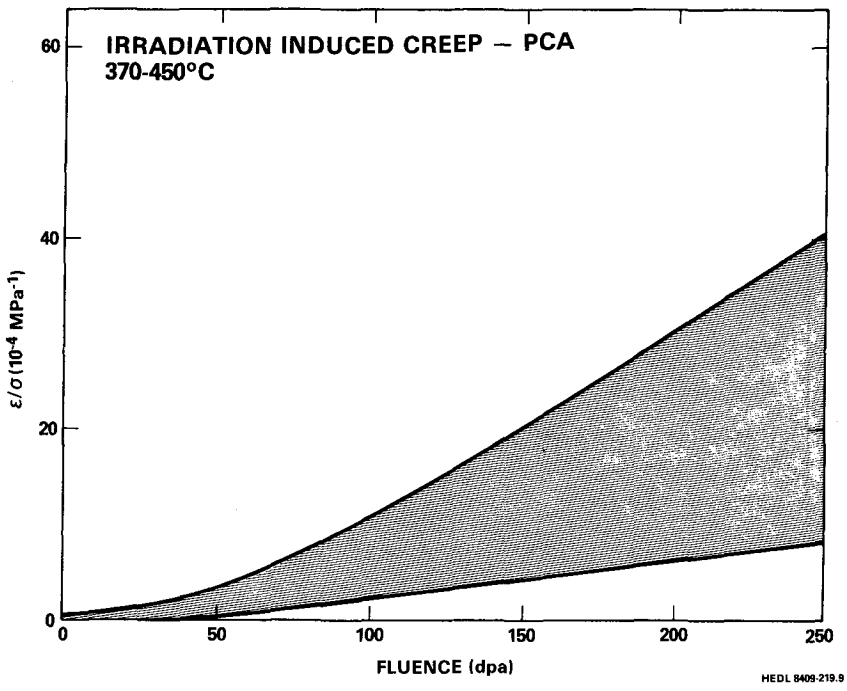


Figure 8.2.3-1. Anticipated range of stress normalized creep strains for PCA at 370 to 450°C as a function of neutron fluence.

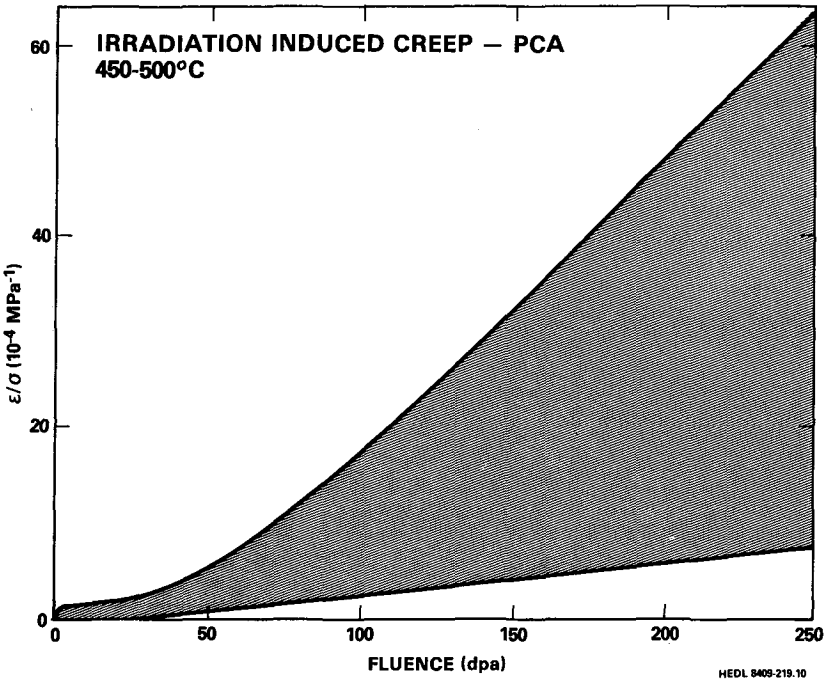


Figure 8.2.3-2. Anticipated range of stress normalized creep strains for PCA at 450 to 500°C as a function of Neutron fluence.

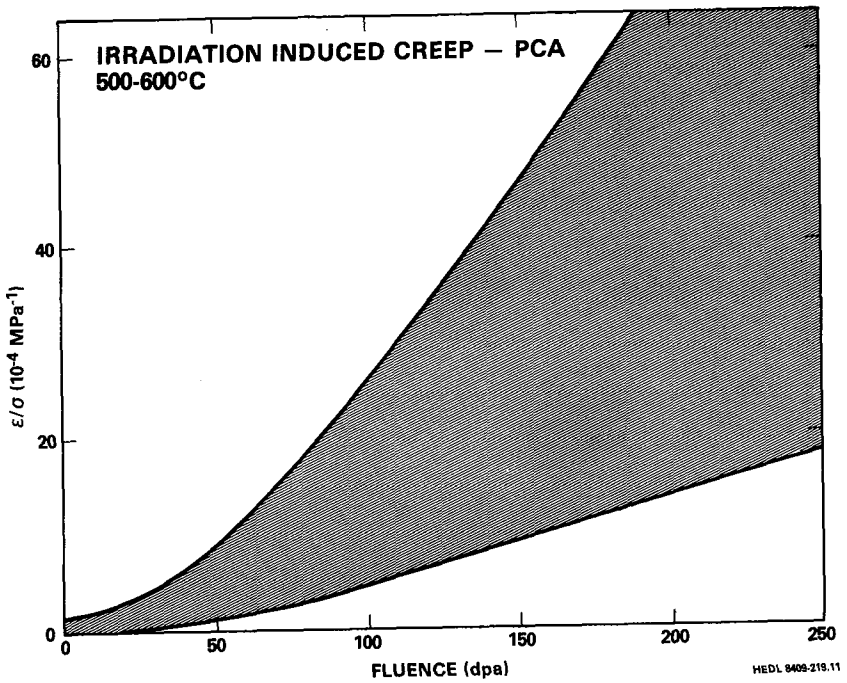


Figure 8.2.3-3. Anticipated range of stress normalized creep strains for PCA at 500 to 600°C as a function of neutron fluence.

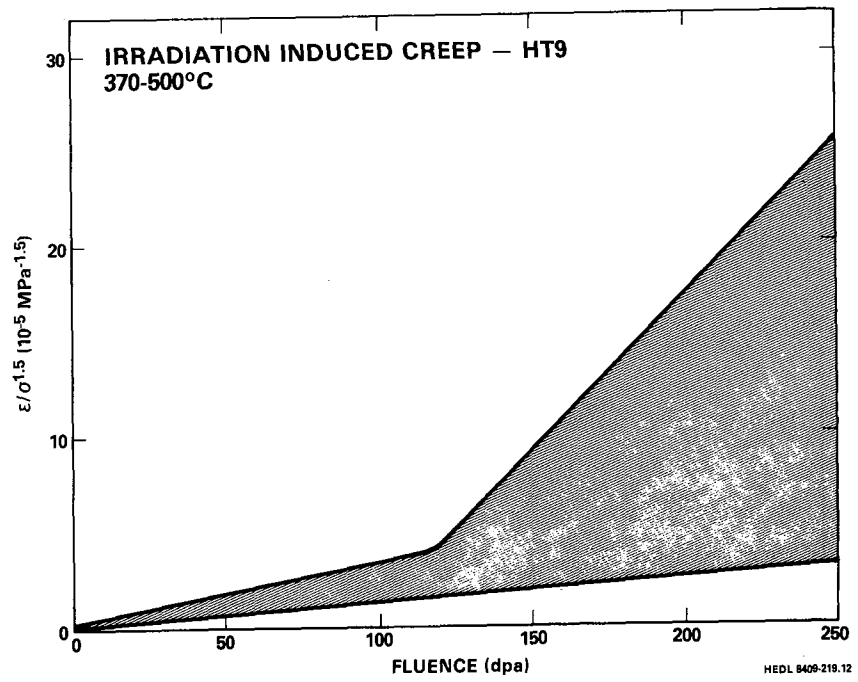


Figure 8.2.3-4. Anticipated range of stress normalized creep strains for HT9 at 370 to 500°C as a function of neutron fluence.

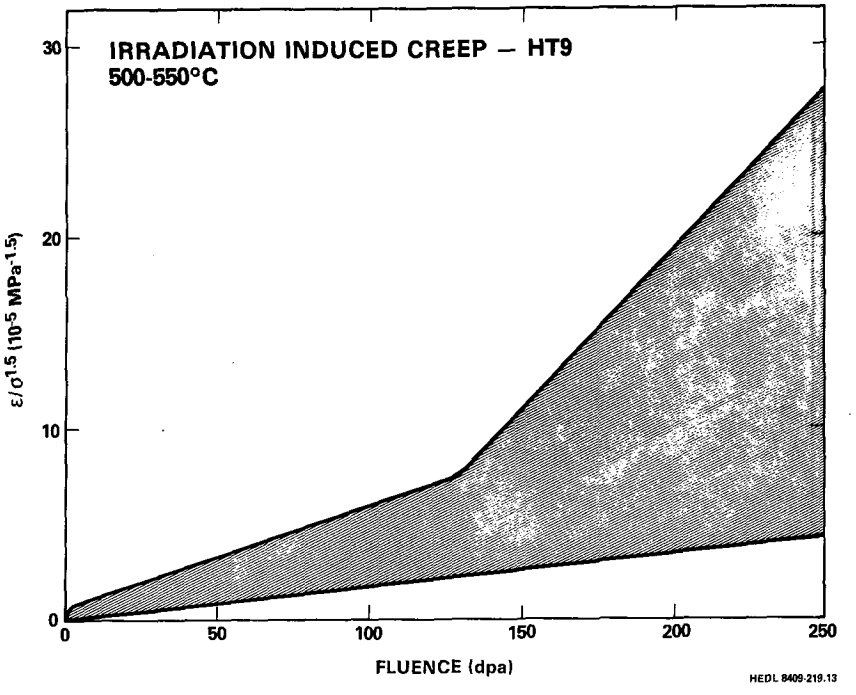


Figure 8.2.3-5. Anticipated range of stress normalized creep strains for HT9 at 500 to 550°C as a function of neutron fluence.

approximately 15 dpa. For low irradiation temperatures (typically less than 450°C), irradiation hardening occurs, and a corresponding decrease in the material's ductility is observed. Above this irradiation temperature the material's strength tends to decrease with increasing fluence and, correspondingly, the ductility increases. One of the complications in these general trends has been the impact of helium on the ductility. Specifically for irradiation temperatures greater than 550°C, helium has tended to reduce the ductility in 316 SS to values below 1% total elongation.[18]

Two different fluence dependent models exist for the strength of austenitic steels.[19,20] One model assumes the saturation in the strength and ductility of a material after neutron fluences greater than approximately 10 to 20 dpa.[19] Limited data on one heat of cold worked 316 SS, however, suggest that this saturation may not be valid at irradiation temperatures around 400°C.[21] These results are consistent with a different tensile strength model.[20] Within FINESSE, we have assumed the saturation model

to be valid for the three structural materials, PCA, HT9, and V-15Cr-5Ti. Irradiated PCA tensile data have been reported for a peak fluence of 22 dpa.[22] The anticipated yield strength for PCA as a function of neutron fluence are shown in Figures 8.2.4-1 to 8.2.4-3. The anticipated ductility for PCA is shown in Figures 8.2.4-4 and 8.2.4-5.

No tensile data have been reported in the open literature for HT9 tensile properties for any reasonable fluences. We have used unirradiated HT9 data and assumed that the fluence dependence for the HT9 tensile properties are similar to that of 316 SS. The anticipated range in the yield strength and ductility behaviors of HT9 with neutron fluence are shown in Figures 8.2.4-6 to 8.2.4-9.

Limited neutron irradiation tensile data on the vanadium alloy V-20Ti have been reported.[23] The anticipated yield strength and ductility for this alloy are given in Ref. (1). For these extrapolations, a saturation model for the tensile properties was assumed.

### 8.2.5 Fracture Toughness

The fracture toughness of a material represents another material behavior important to design. Toughness data on austenitic alloys have shown that this property also changes rapidly with relatively small (5 to 15 dpa) fluences and tends to saturate after a neutron exposure of approximately 15 dpa.[24] These observations are consistent with a model which relates the fracture toughness to the yield strength of the material.[25] The fracture toughness of PCA is assumed to be similar to that of 316 SS. Fracture toughness data on cold worked 316 SS to a peak fluence of 80 dpa suggest saturation in the value of $K_{Ic}$. The anticipated fluence dependence of fracture toughness for PCA at 370 to 450°C is shown in Figure 8.2.5-1. The anticipated fluence dependence for HT9 at 370 to 450°C is shown in Figure 8.2.5-2. The lower bound for HT9 is assumed to be equivalent to that of 316 SS and PCA. The upper bound for HT9 was arbitrarily set somewhat higher than that anticipated for 316 SS because of the lack of HT9 fracture

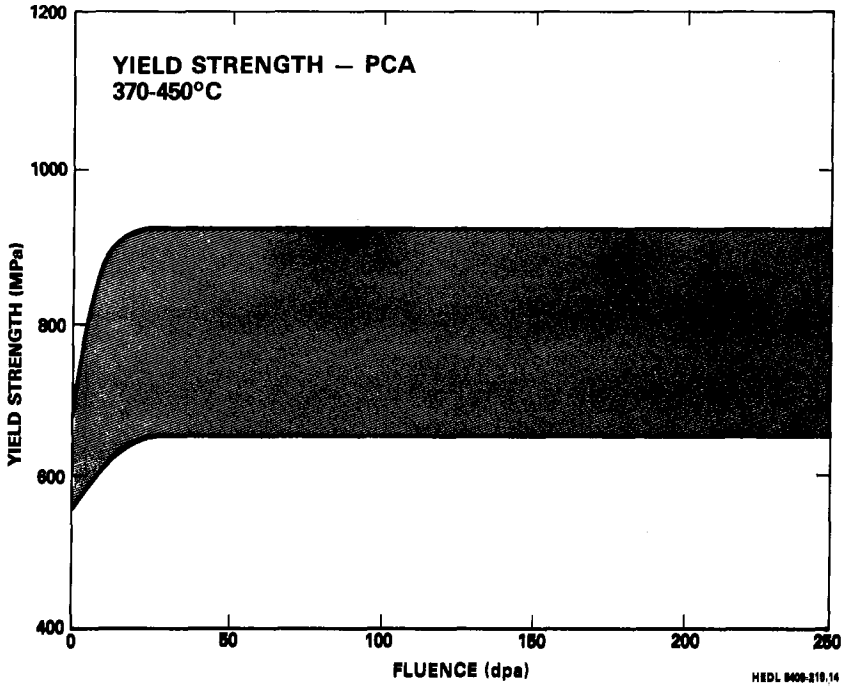


Figure 8.2.4-1. Anticipated range of yield strength for PCA at 370 to 450°C as a function of neutron fluence.

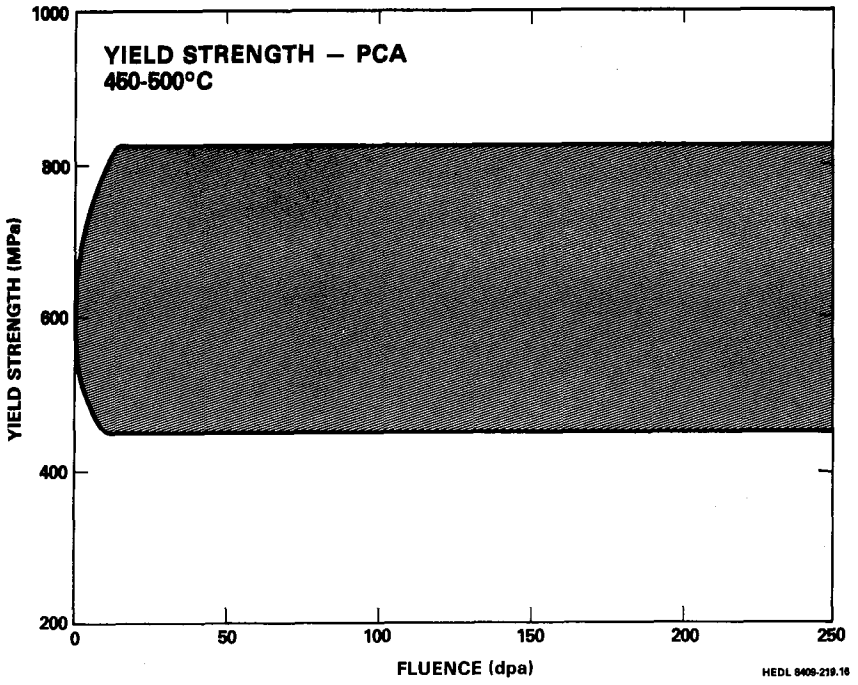


Figure 8.2.4-2. Anticipated range of yield strength for PCA at 450 to 500°C as a function of neutron fluence.

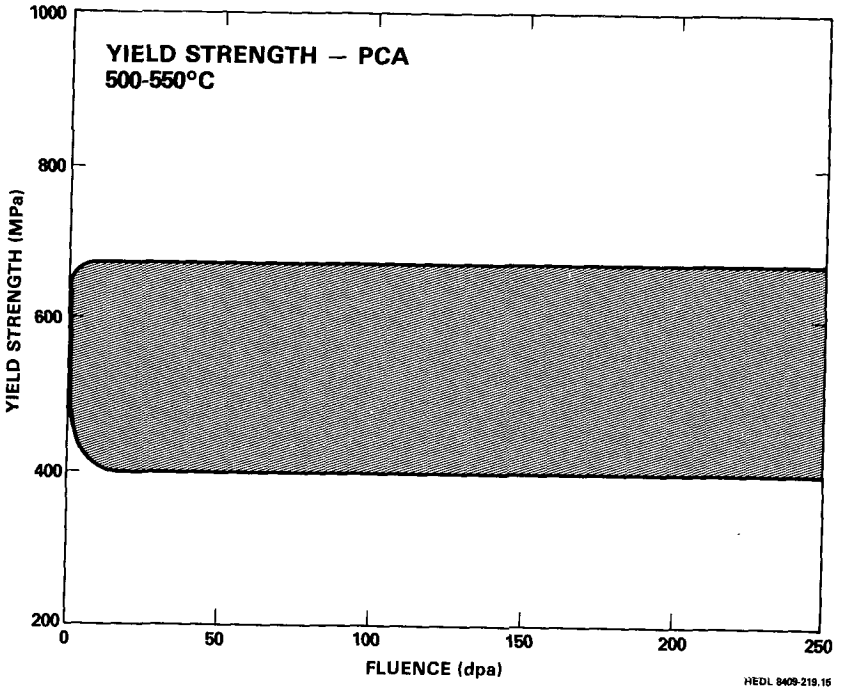


Figure 8.2.4-3. Anticipated range of yield strength for PCA at 500 to 550°C as a function of neutron fluence.

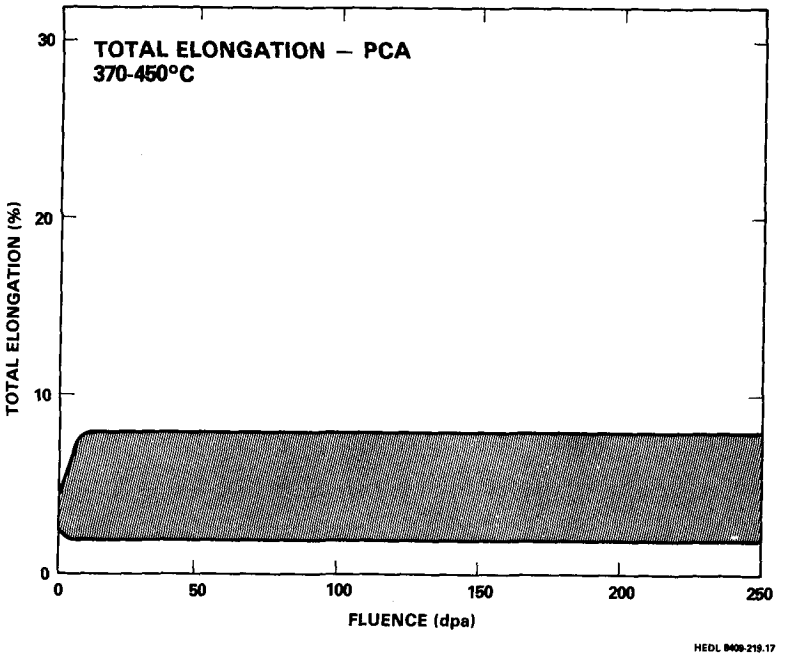


Figure 8.2.4-4. Anticipated range of total elongation for PCA at 370 to 450°C as a function of neutron fluence.

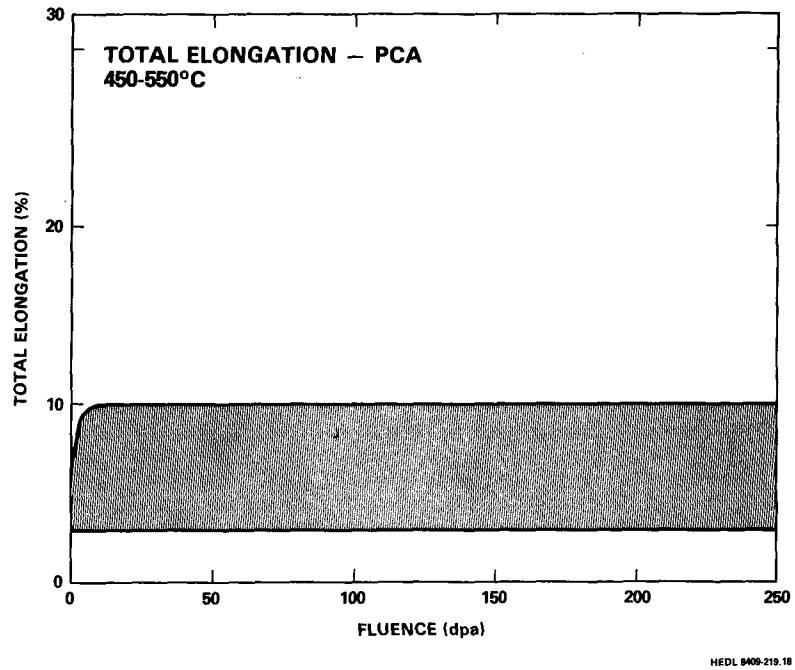


Figure 8.2.4-5. Anticipated range of total elongation for PCA at 450 to 550°C as a function of neutron fluence.

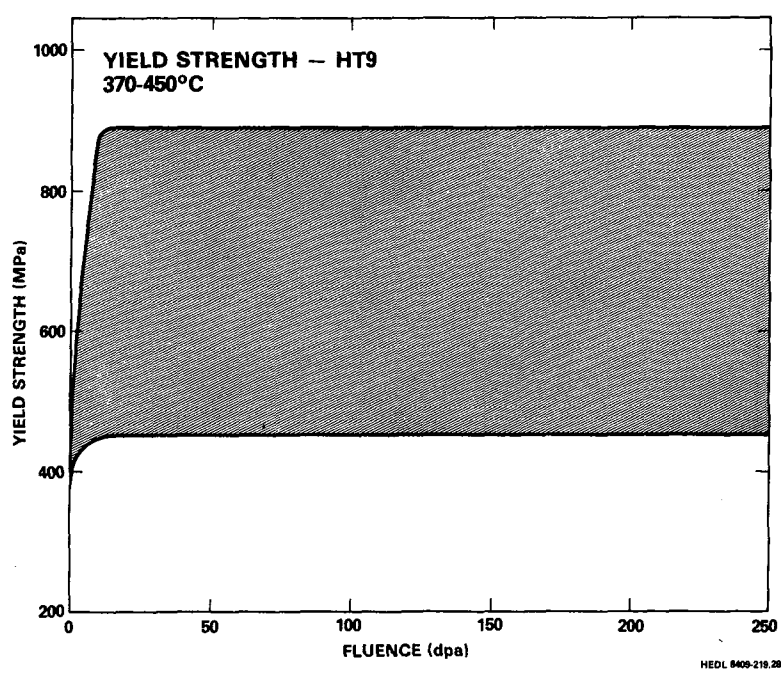


Figure 8.2.4-6. Anticipated range of yield strength for HT9 at 370 to 450°C as a function of neutron fluence.

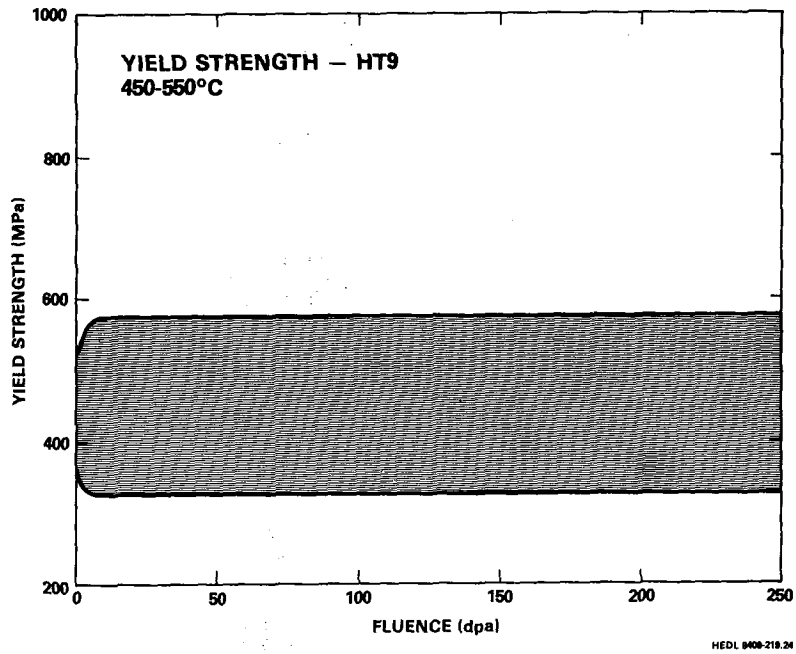


Figure 8.2.4-7. Anticipated range of yield strength for HT9 at 450 to 550°C as a function of neutron fluence.

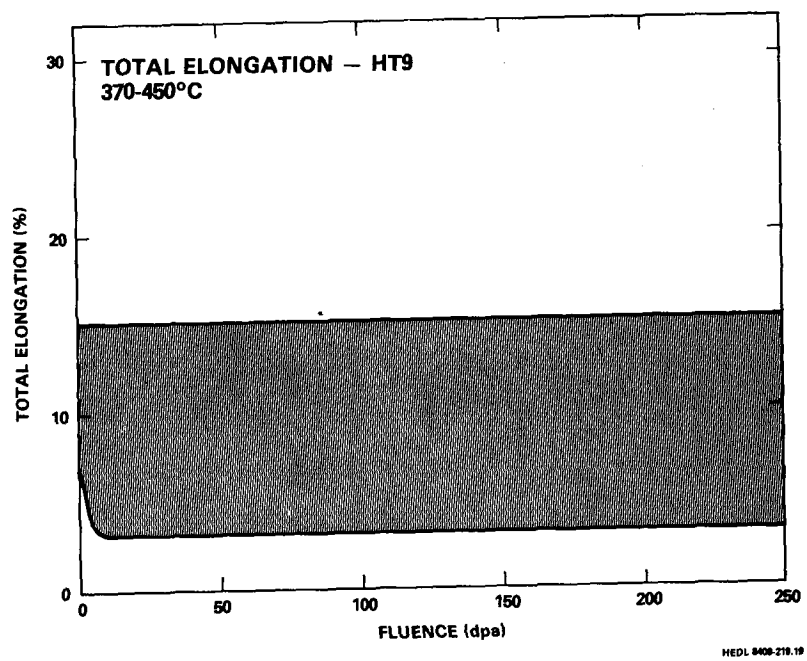


Figure 8.2.4-8. Anticipated range of total elongation for HT9 at 370 to 450°C as a function of neutron fluence.

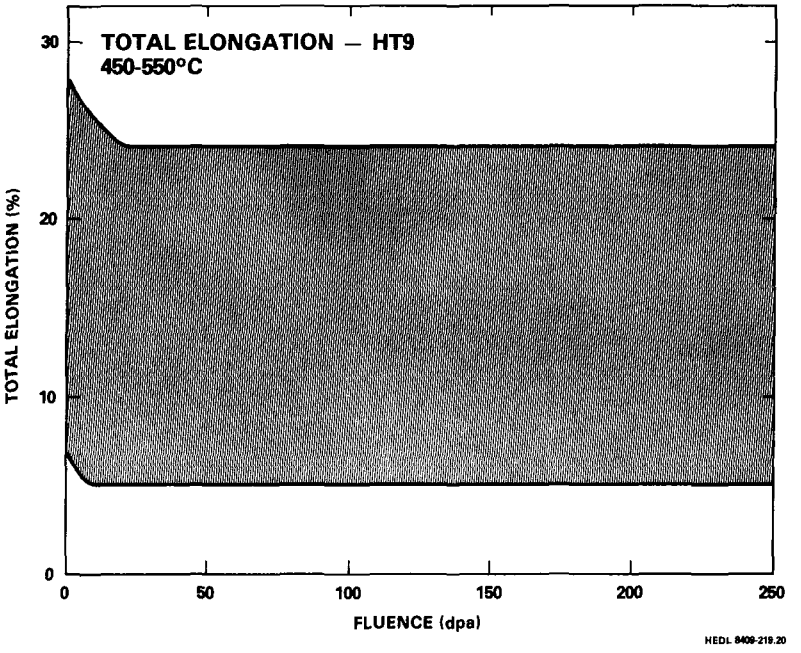


Figure 8.2.4-9. Anticipated range of total elongation for HT9 at 450 to 550°C as a function of neutron fluence.

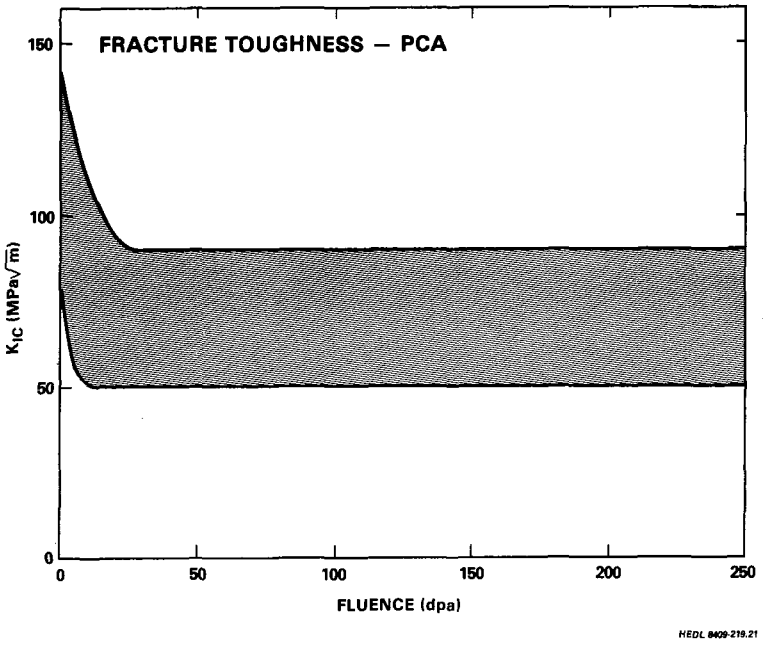


Figure 8.2.5-1. Anticipated range of fracture toughness for PCA as a function of neutron fluence.

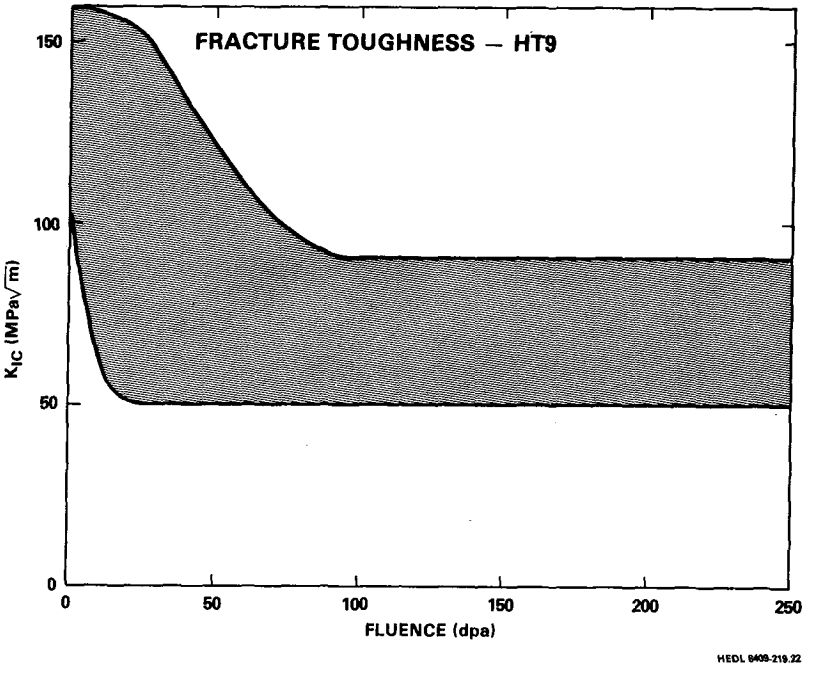


Figure 8.2.5-2. Anticipated range of fracture toughness for HT9 as a function of neutron fluence.

toughness data. Again, the fluence dependence for the fracture toughness of vanadium based alloys is assumed to be similar to that of HT9.

## 8.2.6 Ductile to Brittle Transition Temperature

The ductile to brittle transition temperature for a material can change as a function of accumulated neutron exposure. If the shift in this transition temperature were to occur into the operating temperature regime for a component then the component could experience catastrophic failure. Limited data on HT9 suggests that this alloy may experience such a shift. The anticipated change in the DBTT with fluence at 370 to 410°C is shown in Figure 8.2.6-1. At this temperature the shift could be as high as 150°C. Data suggests that this shift saturates at relatively small fluences on the order of 10 to 20 dpa. The concern for HT9 is the magnitude of this shift at lower irradiation temperatures of 300 to 350°C could be larger. A sample model for the observed shift in DBTT for ferritic alloys is given in Ref. (26)

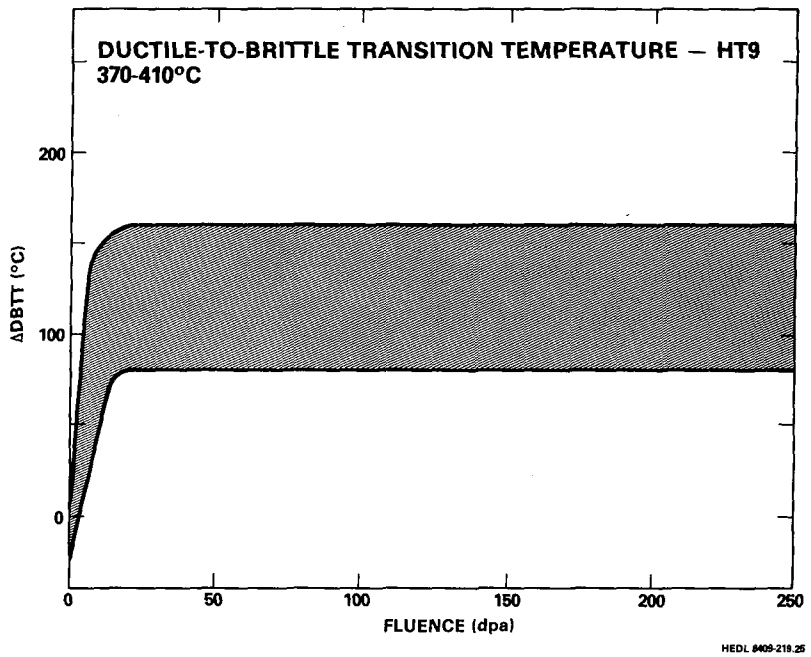


Figure 8.2.6-1. Anticipated range of DBTT for HT-9 at 370 to 410°C as a function of neutron fluence.

## 8.2.7 Fatigue Crack Growth

Both PCA and HT9 have similar crack growth behaviors[27] at relatively low values of $\Delta K$. Also, the irradiation effects on the crack growth rate appears to saturate for 316 SS in that the values for $K_{Ic}$ which limits the upper values of the crack growth rate at high $\Delta K$ saturate quickly with fluence. Limited postirradiation and in-reactor fatigue crack growth data[28] suggest that irradiation has little if any effect on the crack growth rates in the Paris regime for neutron exposures to 30 dpa. At present there are no data available on the effects of neutron irradiation on the threshold stress intensity factor for the structural alloys under consideration in this study. The anticipated fatigue crack growth rates for both HT9 and PCA are assumed to be equivalent to that of cold worked 316 SS given in Ref. (1).

## 8.2.8 Conclusions

The anticipated fluence dependence of the three major structural materials in this study are based upon data bases derived from fission reactor irradiations. The neutron environments associated with these fission reactors are significantly different to the neutron environment anticipated in a fusion device. A fairly comprehensive discussion on the impact of neutron flux and spectrum upon material properties has been given in Ref. (1) for austenitic alloys such as PCA, and their conclusions are applicable to the other alloys being considered in this study.

The anticipated ranges for the various key material properties have been expressed as a function of neutron fluence in units of dpa in an attempt to take into account the impact of spectral differences between the fission and fusion environments. Another exposure unit which has been introduced into the fusion program is MW• yr/$m^2$ which is sometimes used to express the 14 MeV neutron loading on a reactor first wall. However, the actual neutron fluence at the first wall and blanket depend upon the blanket materials and the reactor design. In this study, the correspondence assumed between these two units for neutron exposure is given in Table 8.2.8-1. Moreover, only neutron fluences near the first wall were considered.

The extensive fission reactor materials data bases tend to show that most changes in the material properties can be modeled as consisting of a transient regime where the material property is constantly changing with neutron fluence and a saturation regime where either the property remains constant or changes at a constant rate as a function of neutron fluence. It is this transient regime which is most sensitive to neutron flux, temperature, stress and perhaps also spectrum.

The fusion neutron energy spectrum will also be significantly different from that in fission reactors. These differences will lead to different transmutants which can impact material behavior.[1] The transmutation of

Table 8.2.8-1. Conversion Factors Used in this FINESSE Study to Relate Damage in the Materials to MW• yr/$m^2$

| Material | Conversion Factor | |
|---|---|---|
| | dpa/(MW• yr/$m^2$) | ($10^{20}$ Captures/$cm^3$) /(MW• yr/$m^2$) |
| PCA | 12 | - |
| HT-9 | 12 | - |
| V-15Cr-5Ti | 14 | - |
| $Li_2O$* | - | 0.95 |
| $LiAlO_2$** | - | 3.5 |

*Assumes no beryllium multiplier.
**Assumes beryllium multiplier.

major elements within PCA, HT9 and V-15Cr-5Ti are given in Ref. (1). Specifically, the fusion spectrum will give rise to different transmutations which may impact the phase evolution of austenitic alloys such a PCA and thereby impact the transient regime of a material property change. The ferritic alloy HT9 appears to be susceptible to this microchemical evolution as evidenced by its observed irradiation induced phases[8] and, therefore, may also be sensitive to spectrum. Data are only now becoming available on the phase stability of V-15Cr-5Ti after neutron irradiation.

In summary, we have developed extrapolated ranges of material property behavior which are consistent with present models. Both these models and their supporting data are predominantly from fission reactor sources of irradiation. The neutron environment associated with these fission sources are significantly different from the neutron environment anticipated in fusion devices. These differences in the two environments will probably alter the transient regime in both its magnitude and when it occurs. However, the exact impact of the fusion environment on material property changes with fluence accumulation is not known at this time. For this reason the fission based extrapolations of material properties were used in FINESSE to assess

when component interactions occurred within a given blanket concept. Inherent in our analysis is the assumption that the impact of a different neutron environment will not be significant with respect to this study.

## 8.3 Uncertainty Projection Approach

In the previous section the anticipated changes in the material property with fluence were given. In all cases the extrapolation of these data to high neutron doses was dependent upon an assumed fluence dependent model. In an attempt to quantify the information gained as one tested a given material property to higher and higher fluences the concept of uncertainty projections was developed.[2] The major facets of this approach are the existence of a fluence dependent model and a specific or assumed testing plan as a function of neutron exposure. With these given, a set of results are assumed for the testing plan. These hypothetical results have an inherent uncertainty and are consistent with the fluence dependence of the model. Projections of the uncertainty in the property are then made by extrapolating the fluence dependent model to some goal fluence and requiring the extrapolation also be consistent with the hypothetical results up to some peak fluence. Several examples of this approach can be found in Refs. (1) and (2).

This approach has been applied to the key material properties outlined in the previous section by making the following assumptions. The fluence dependent models used in extrapolating the material properties with fluence were assumed to be correct. A testing program was assumed to require specimen examinations at neutron exposures corresponding to 0.2, 1, 3, 5, 8, 10, 12, 14, 16, 18, and 20 MW• yr/$m^2$. The uncertainties associated with the hypothetical testing results were assumed to be consistent with breeder reactor experience. Finally, goal fluences corresponding to both 10 and 20 MW• yr/$m^2$ were considered.

The results of this analysis are summarized in Table 8.3-1 for the major structural and solid breeder materials under investigation in this study. We find that the results are dependent upon the goal fluence under consideration

Table 8.3-1. FINESSE-Neutron Fluence Goals for Material Properties

| | Required Neutron Exposure to Reduce Uncertainty ($MW \cdot yr/m^2$) | | | | | | |
|---|---|---|---|---|---|---|---|
| | Swelling | Creep | Fatigue/ Crack Growth | DBTT | Ductility/ Toughness | Thermal Expansion/ Conductivity | Cracking/ Sintering |
| HT/9 | 14-16 | [14-16] 1-3 | 1-3 | 1-3 | 1-3(5)* | --- | --- |
| PCA | 10-12 | [10-12] 1-3 | 1-3 | --- | 1-3 | --- | --- |
| V | 16-18 | [16-18] 1-3 | 1-3** | --- | 1-3(5)** | --- | --- |
| $Li_2O$ | 1-3 | 1-3 | --- | --- | --- | 0.2 | 0.2 |
| $LiAlO_2$ | --- | 1-3 | --- | --- | --- | 0.2 | 0.2 |

*5 $MW \cdot yr/m^2$ testing may be required to reduce uncertainty in fracture toughness in HT9.
**V-alloys assumed to require the same amount of testing as HT9. Bracketed goal fluences required for creep if goal life for use of data is beyond incubation fluence for swelling.

for the creep and swelling behaviors. Specifically, if the goal fluence is 10 MW yr/$m^2$, then swelling behaviors of the HT9 and V alloys are not an issue and the uncertainty in creep is significantly reduced after measurements are performed at 1 to 3 MW yr/$m^2$. If, on the other hand, the goal fluence is 20 MW yr/$m^2$, then swelling and creep uncertainties remain large until measurements are performed after the onset of swelling. The uncertainties in the other key properties for both the structural materials and the solid breeders are significantly reduced after measurements are performed at 3 to 5 MW yr/$m^2$. These results are consistent with the observation that one gains the most information concerning the change in a material's behavior by performing measurements in the transient regime for a given material property and that little additional information is gained once the property's changes are in the saturation or steady-state regime.

## 8.4 Interactive Testing

Most of the issues outlined in Chapter 3 of this report will require some form of interactive testing. By an interactive test we are referring to an experiment where two or more materials or material properties impact the overall integrity or performance of the combined system. The concept and role of interactive testing within the FINESSE framework is more fully discussed in Chapter 9. At present, specific interactive experiments have not been defined for the FINESSE project. However, one can consider the generic key issues outlined in Chapter 3 of this report.

The first step when considering these issues is to identify the key material properties and behaviors involved. Their independent behavior can be plotted as a function of fluence to aid in evaluating which properties lead to the interaction. In general, the exact fluence at which the interaction occurs will depend upon the specific design of the component. Nevertheless, the time of interaction will be bounded in many instances by other design constraints.

For example, let us consider the interaction between the HT9 cladding and the $Li_2O$ solid breeder material as a function of neutron fluence. The key material properties for the HT9 cladding are creep, ductility, and eventually swelling. The key material properties for the $Li_2O$ are thermal expansion, cracking/redistribution, swelling and creep. Initially the $Li_2O$ thermal expansion, cracking/redistribution and swelling lead to contact between the $Li_2O$ and HT9 cladding. The neutron exposure at which this occurs depends upon the initial gap size. Once the cladding and solid breeder material are in contact, the stress in the cladding will increase until a delicate balance in the creep mechanisms in both the $Li_2O$ and HT9 is achieved. Breach of the HT9 cladding may occur at this time due to irradiation embrittlement. Once the incubation fluence for HT9 swelling is reached, the swelling in the HT9 cladding will tend to relieve the stress buildup in the cladding. Therefore, the possibility of the cladding rupture due to this particular interaction decreases. As mentioned before, the actual neutron exposure at which contact occurs depends upon the designed gas gap. Decreasing the gap allows better heat transfer from the solid breeder material but shortens the neutron exposure at which contact occurs. Increasing the gas gap delays the time at which contact occurs, but also can increase the operating temperature for the solid breeder and impact tritium recovery.

In an attempt to quantify the information gained in interactive testing as a function of testing fluence, the concept of uncertainty projections (discussed earlier in Chapter 8.3) was extended to the key issues outlined in Chapter 3. The major material properties associated with each issue for a given blanket concept were identified and uncertainty projections were constructed assuming goal fluences of both 10 and 20 $MW \cdot yr/m^2$. These uncertainty projections were then transformed into normalized uncertainty ranges as a function of testing exposures. These normalized uncertainty ranges were then combined for all the major material properties. Finally, a plot of the absolute value of the derivative of this combined uncertainty range was constructed. This plot of the derivative of the combined uncertainty ranges reflects the regions in testing fluence where the uncertainty in the interaction are changing the fastest. Specifically, relatively small

values for the derivative represent testing fluences where additional uncertainty reductions are small. Similarly, relative maxima in this plot of the derivative reflect regions where the reduction in the combined uncertainties are the greatest. If we assume that this combined uncertainty which reflects each of the major material properties responsible for the interaction is directly correlated to the uncertainty associated with the interaction behavior itself, then this approach can be used to address at what fluences the uncertainty associated with the interaction are reduced. However, this approach cannot address the issue of which parts of the interaction are most important.

As an example of this approach, consider the mechanical interaction between the solid breeder and structure for HT9/$Li_2O$/He blanket concept and for a goal fluence of 10 MW• yr/$m^2$. The major material properties and behaviors pertinent to this interaction are $Li_2O$ thermal expansion, cracking/redistribution, creep and swelling, and HT9 creep and ductility. (If the goal fluence were 20 MW• yr/$m^2$, then HT9 swelling would also be a major material property with respect to the interaction.) The anticipated stress free swelling of $Li_2O$ is shown in Figure 8.4-1. Also shown in the figure are hypothetical results from measurements performed at 0.2, 1, 3, 5, 8, and 10 MW• yr/$m^2$. The extrapolations for each measurement are also shown, and they assume a linear swelling fluence dependence. The uncertainty in the hypothetical data are reflected by the size of the data symbols in the figure. At the goal fluence of 10 MW• yr/$m^2$, the anticipated range in $Li_2O$ volumetric swelling at 700 to 900°C is between 9.2 and 20%. Hypothetical measurements performed at 0.2 and 1.0 MW• yr/$m^2$ do not reduce the uncertainty anticipated at a fluence of 10 MW• yr/$m^2$. Measurements performed at 3, 5, and 8 MW• yr/$m^2$ do reduce the anticipated range of swelling in $Li_2O$ as shown in Figure 8.4.1. The projected uncertainty at 10 MW• yr/$m^2$ for stress free $Li_2O$ swelling is shown in Figure 8.4-2.

If we normalize the projected uncertainty range at 10 MW• yr/$m^2$ to a value of one and then normalize the projected uncertainty plot, we then obtain Figure 8.4-3 which depicts the decrease in the normalized uncertainty

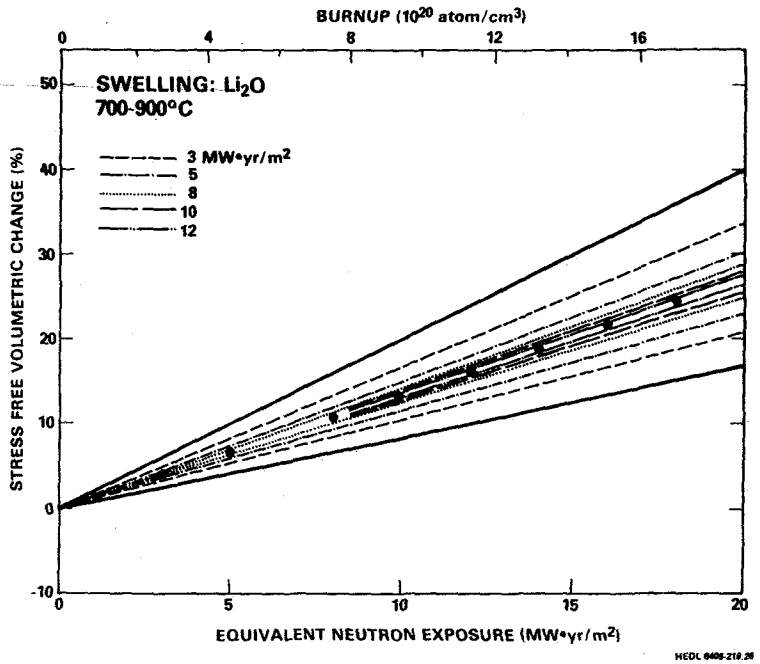


Figure 8.4-1. Graphical representation of the uncertainty projection approach for stress-free $Li_2O$ swelling.

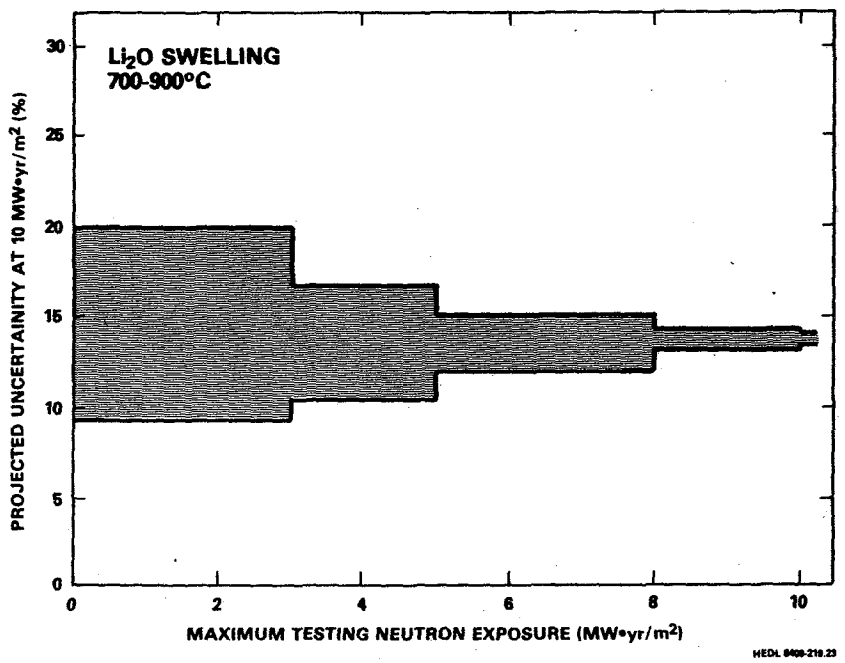


Figure 8.4-2. Projected uncertainty at a goal fluence of 10 MW• yr/m$^2$ for $Li_2O$ stress-free swelling.

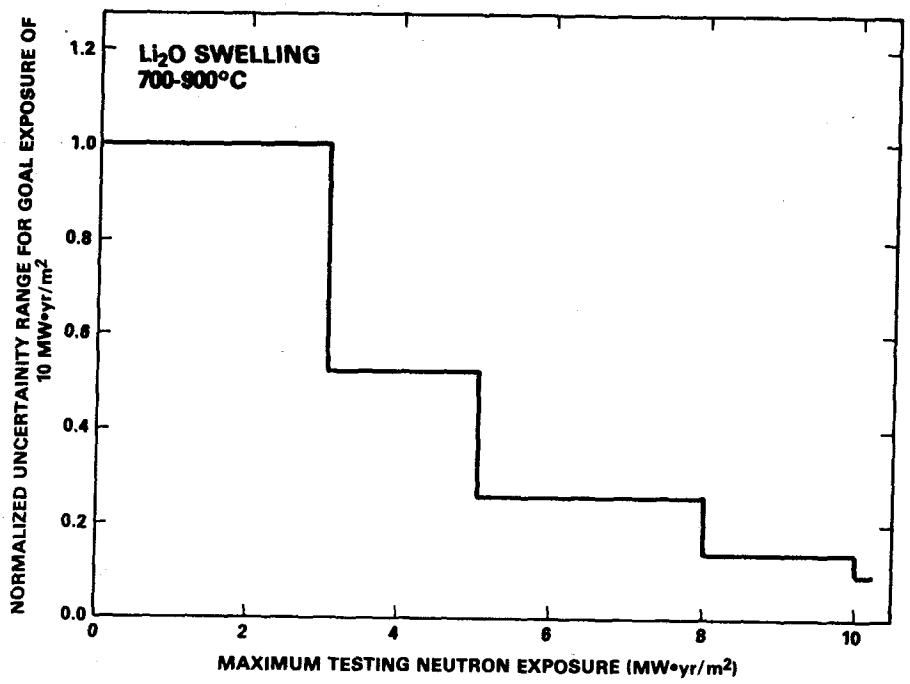


Figure 8.4-3. Normalized uncertainty range for a goal fluence of 10 MW• yr/$m^2$ for $Li_2O$ stress-free swelling.

range as a function of testing fluence. A similar procedure is applied to the other major material properties, and these normalized uncertainty ranges are combined as shown in Figure 8.4-4. Figure 8.4-4 has been smoothed to reflect the anticipated behavior independent of the originally assumed testing scenario. Finally, the absolute value for the derivative of the combined uncertainty ranges is derived from Figure 8.4-4 and shown in Figure 8.4-5 as a function of testing fluence. Figure 8.4-5 contains two relative maxima at testing fluences of approximately 0.2 and approximately 3.5 MW• yr/$m^2$. The first maxima corresponds to the reduction in the uncertainty associated with $Li_2O$ cracking and redistribution after a relatively short testing period. The relative maxima for a testing fluence of 3.5 MW• yr/$m^2$ reflects the decrease in material property uncertainties for $Li_2O$ creep and swelling and for HT9 creep and ductility. From this plot, one can infer that the uncertainty in the mechanical interaction between the HT9 cladding and the $Li_2O$ solid breeder is significantly reduced after testing in the fluence range of 3 to 5 MW• yr/$m^2$.

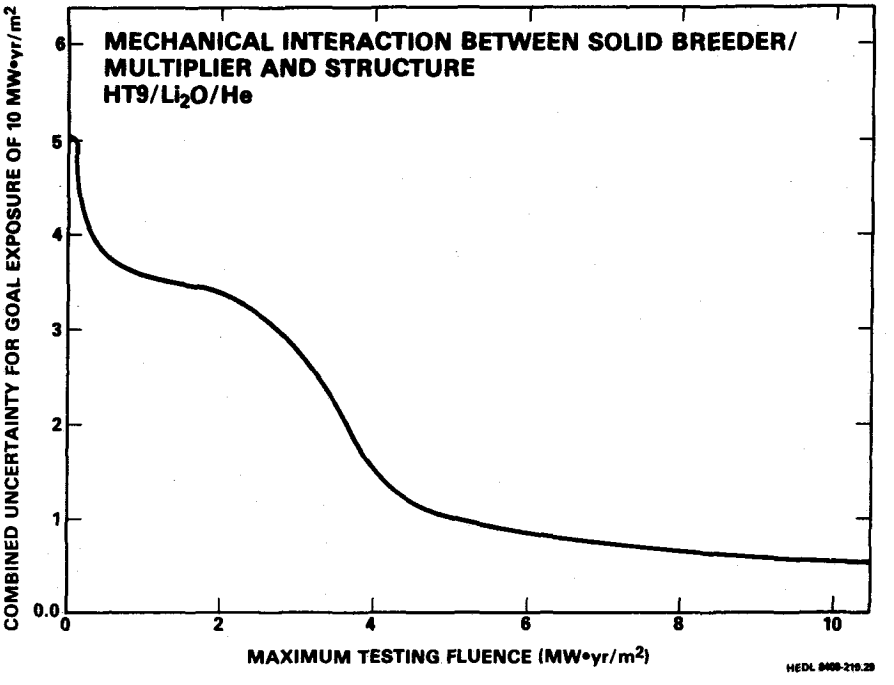


Figure 8.4-4. The combined uncertainty range for a goal fluence of 10 MW• yr/$m^2$ for the mechanical interaction between the

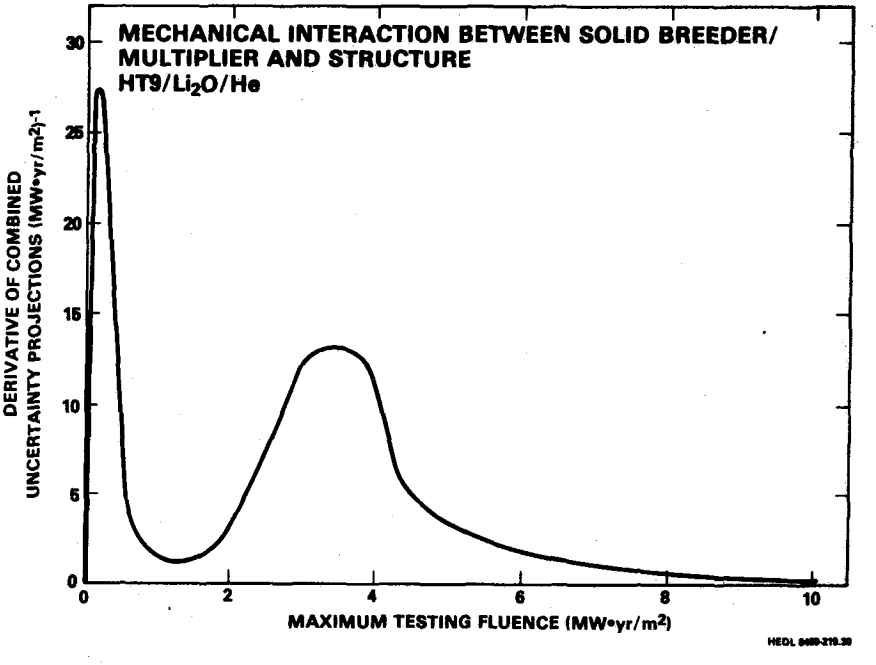


Figure 8.4-5. The absolute derivitive of the combined uncertainty range for the mechanical interaction between the $Li_2O$ solid breeder and HT9

This approach of using material property uncertainties to determine the required testing fluences has been applied to the key structural material issues for the HT9/$Li_2O$/He blanket concept which are tabulated in Chapter 3. The analysis was performed assuming goal fluences corresponding to 10 MW• yr/$m^2$ and 20 MW• yr/$m^2$. The results of this analysis are summarized in Table 8.4-1. This table lists the key issues associated with the structural materials, indicates the major material properties associated with the issue of material interaction, and finally, gives the anticipated testing goal based upon the analysis outlined in this section. In general, we found that interactive testing conducted at neutron exposures of 3 to 5 MW• yr/$m^2$ significantly reduce the uncertainty in the interaction as long as the goal fluence is below the neutron fluence at which swelling in the structural material starts. For a goal fluence of 20 MW• yr/$m^2$ nuclear testing out to neutron exposures of 16 to 18 MW• yr/$m^2$ are required to minimize all the uncertainty associated with the interaction.

## 8.5 Conclusions

Fluence is a major consideration in outlining a program for studying fusion reactor materials behavior and interactive effects. From extensive materials testing in the breeder reactor programs, we have found that changes in many material properties are strongly dependent upon accumulated fluence. Typically these changes in material properties with neutron fluence can be partitioned into two regimes: a transient regime where the material's property is changing rapidly with accumulated neutron fluence, and a saturation regime where either the material property or the rate of change in the material property remains constant with fluence. These changes in the material properties with fluence lead to many complex interactions when considering a fusion reactor component such as the blanket. And, in general, these interactions can become quite complex when considering complex systems.

To assess the impact of the testing fluence in FINESSE, we began by first assessing the impact of fluence upon the key material properties for

Table 8.4-1. Neutron Fluence Goals for HT9/$Li_2O$/He Concept

| Issue | Major Material Properties | Fluence Goal ($MW \cdot yr/m^2$) |
|---|---|---|
| Changes in properties and behavior of materials | [All material properties pertinent to design] | [See Table 8.3-1 for specimen fluence goals] |
| Mechanical interaction within the structure itself | HT9: Thermal differential expansion fatigue/crack growth, ductility, swelling* | 3-5; (16-18)* |
| Plasma-structure interaction | ----- | ----- |
| Premature failure of welds in full components | HT9 Thermal differential expansion, fatigue/crack growth, ductility, swelling* | 3-5; (16-18)* |
| Coolant-structure interaction | ----- | ----- |
| Magnetic field interaction with structure | HT9: Ductility, fracture toughness, fatigue/crack growth, creep | 3-5 |
| Mechanical interaction between solid Breeder/multiplier and structure | HT9: Ductility differential expansion, fatigue/crack growth, ductility, swelling* Li2O: Cracking/sintering; swelling; corrosion | 3-5; (16-18)* |

*Testing fluence goal required if data to be applied to design with goal life > 18 $MW \cdot yr/m^2$.

both the solid breeder and structural materials. By necessity, the anticipated fluence behaviors for these properties were derived from the data bases from fission reactor irradiations. Also, fission reactor based models were used to extrapolate the anticipated behaviors where no data exist. We are fairly certain that within a fusion neutron environment the anticipated fluence behavior could be different, but at present we have no means of assessing or predicting the magnitude of this difference in behaviors.

For individual materials properties, we have used the method of uncertainty projections in an attempt to quantify the information gained as a function of testing fluence. This approach indicates that one obtained the greatest amount of information concerning the property change when tests are performed in the transient regime. Also, once the material property has saturated with fluence, little additional is obtained from nuclear testing. The results of this analysis were summarized in Table 8.3-1.

In interactive effects testing, fluence still plays an important role in defining the nature and outcome of the interaction. To assess the impact of fluence upon interactive testing, we first identified the major materials properties associated with a given interaction. In an attempt to identify fluence regions which would provide the most information concerning an interaction, a method of extrapolating uncertainty projections to interactive effects testing was formulated. This approach assumes that the uncertainty in the interaction is directly related to the combined uncertainties associated with the major material properties of the interaction. This approach was applied to the key structural material related issues outlined in Chapter 3 of this report. The results of that analysis were summarized in Table 8.4-1 for the HT9/$Li_2O$/He blanket concept. In general, it was found that the major uncertainty in the interaction was significantly reduced after neutron testing in the fluence range corresponding to 3 to 5 MW•yr/$m^2$ so long as the goal fluence for the component under consideration was less than the incubation period for swelling of its structural material.

## References for Chapter 8


1. Engineering Testing, FED-INTOR/TEST/82-4,NIN, U.S. FED/INTOR Report - Critical Issues, USA FED-INTOR/82-1, Vol. 2 (1982).

2. R. J. Puigh, E. K. Opperman, R. E. Nygren and G. L. Wire, "An Analytical Approach for Projecting Material Property Uncertainties," Journal of Nuclear Materials 122 and 123 (1984) pp. 169-173.

3. J. F. Bates and M. K. Korenko, Nuclear Technology, Vol. 48 (May, 1980).

4. P. J. Maziasz and D. N. Braski, "Improved Swelling Resistance for PCA Austenitic Stainless Steel under HFIR Irradiation through Microstructure Control," Journal of Nuclear Materials 122 and 123 (1984) pp. 311-316.

5. F. A. Garner, H. B. Brager and R. J. Puigh, "Swelling Behavior of Titanium Modified Alloys in EBR-II," First International Conference on Fusion Reactor Materials, Tokyo, Japan (Dec. 1984).

6. F. A. Garner, "Recent Insights on the Swelling and Creep of Irradiated Austenitic Alloys, " Journal of Nuclear Materials, 122 and 123 (1984) pp. 459-471.

7. R. W. Powell, D. T. Peterson, M. K. Zimmerschied, and J. F. Bates, "Swelling of Several Commerical Alloys Following High Fluence Neutron Irradiation," Journal of Nuclear Materials 103 and 104 (1981) pp. 969-974.

8. D. S. Gelles and L. E. Thomas, "Effects of Neutron Irradiation on Microstructure in Experimental and Commerical Ferritic Alloys," Proceedings of the Third Topical Conference on Ferritic Alloys for Use in Nuclear Energy Technologies (June 19-23, 1983) Snowbird, UT.

9. J. Bentley and F. W. Wiffen, Nuclear Technology, 30 (1976), pp. 376-384.

10. G. W. Hollenberg, "Fast Neutron Irradiation Results on $Li_2O$, $Li_4SiO_4$, $Li_2ZrO_3$ and $LiAlO_2$," Proceedings of the Third Topical Meeting on Fusion Reactor Materials, Albuquerque, NM (Sept. 19-22, 1983) pp. 896-900.

11. R. A. Weiner, J. P. Foster and A. Boltax, "Irradiation Creep-Swelling Coupling: Microstructural Modeling and Data Analyses," Radiation Effects in Breeder Reactor Structural Materials AIME (June, 1977) pp. 865-878.

12. W. Schneider, K. Herschbach, and K. Ehrlich, "Interdependence of In-Pile Creep and Void Swelling on Ti- and Nb-Stablizied Stainless Steels," Effects of Radiation on Materials: Eleventh Conference ASTM STP 782 (June 1982) pp. 30-43.

13. D. S. Gelles and R. J. Puigh, "Evaluation of Ferritic Alloy 2-1/4Cr-1Mo After Neutron Irradiation-Irradiation Creep and Swelling," Effects of Radiation on Materials: Twelfth Conference, Williamburg, VA (June 1984) (in press).

14. M. M. Paxton, B. A. Chin and E. R. Gilbert, "The In-Reactor Creep of Selected Ferritic, Solid Solution Strengthened and Precipitation Hardened Alloys," Journal of Nuclear Materials 45 (1980) pp. 185-192.

15. R. J. Puigh, E. R. Gilbert and B. A. Chin," An In-Reactor Creep Correlation for 20% Cold Worked AISI 316 Stainless Steel," Effects of Radiation on Materials: Eleventh Conference, ASTM STP 782 (June 1982) pp. 68-121.

16. E. R. Gilbert and A. J. Lovell, "Temperature Dependence of In-Reactor Creep of 20% Cold Worked 316 Stainless Steel," Radiation Effects in Breeder Reactor Structural Materials (1977) pp. 269-276.

17. J. L. Straalsund and D. S. Gelles, "Assessment of the Performance Potential of the Martensitic Alloy HT9 for Liquid Metal Fast Breeder Reactor Applications," and B. A. Chin, "An Analysis of Creep Properties of a 12Cr-1Mo-W-V Steel," Proceedings of the Topical Conference on Ferritic Steel for Use in Nuclear Energy Technologies, Snowbird, UT (June 19-23, 1983).

18. R. E. Gold et al., "Technical Assessment of Vanadium-Based Alloys for Fusion Reactor Applications", COO-4540-1, U.S. Department of Energy, (April 1978).

19. D. N. Braski and P. J. Maziasz, "The Tensile Properties and Bend Ductility of PCA After Irradiation in HFIR," ADIP Semiannual Progress Report for Period Ending March 31, 1984, pp. 61-74.

20. R. L. Fish, N. S. Cannon and G. L. Wire, ASTM STP 683 (1979) p. 450.

21. R. L. Simons, "Tensile Property Correlation for 20% Cold Worked 316 Stainless Steel," DAFS Quarterly Progress Report (April-June 1981) p. 117.

22. M. L. Hamilton, N. S. Cannon and G. D. Johnson, "Mechanical Properties of Highly Irradiated 20 Percent Cold Worked Type 316 Stainless Steel," Effects of Radiation on Materials: Eleventh Conference ASTM STP 782 (June 1982) pp. 636-647.

23. R.E. Goldand D. L. Harrod, "Radiation Effects in Vanadium and Vaadium-base Alloys," International Metals Reviews, No. 5 and 6 (1980) pp. 232-254.

24. F. H. Huang, "The Fracture Characterization of Highly Irradiated Type 316 Stainless Steel", International Journal of Fracture, 25 (1984), pp. 181-193.

25. W. G. Wolfer and R. H. Jones, "Flow and Fracture of Alloys in the Fusion Environment," Journal of Nuclear Materials 103 and 104 (1981) pp. 1305-1314.

26. N. M. Ghoniem and R. W. Conn, "Assessment of Ferritic Steels for Steady State Fusion Reactors, "Technical Committee Meeting and Workshop on Fusion Reactor Design and Technology, Tokyo, Japan (October 5-16, 1981).

27. A. M. Ermi, "Fatigue Crack Growth in Path E Alloys," ADIP Semi-Annual Progress Report for Period Ending March 31, 1983, pp. 108-124.

28. A. M. Ermi and B. A. Chin, "An In-Situ Fatigue Crack Propagation Experiment, Journal of Nuclear Materials 103 and 104 (1981) pp. 1505-1510.

# CHAPTER 9

# INSTRUMENTATION AND TEST MATRIX

TABLE OF CONTENTS


Page

9.1 Instrumentation ..... 9-1
9.1.1 Introduction ..... 9-1
9.1.2 Generic Instrumentation Issues ..... 9-1
9.1.3 Test Instrumentation Requirements ..... 9-3
References ..... 9-12

9.2 Test Matrix ..... 9-13
9.2.1 Single Specimen Test Matrix and Preliminary Results ..... 9-16
References ..... 9-22

# 9. INSTRUMENTATION AND TEST MATRIX

## 9.1 Instrumentation

### 9.1.1 Introduction

As the design of experiments evolve, the requirements for instrumentation become evident. As experiments and associated instruments become increasingly complex, the need to identify instrument limitations and the impact of the instrument on the test becomes more critical. This chapter is an attempt to describe test requirements for instrumentation, as well as identify some limitations and impacts on the test design and operation. For each test requirement, several factors are considered:

-- Potential measurement devices
-- Impact of environment (neutrons, liquid metal, temperature, etc.)
-- Size and access restrictions
-- Instrument effects on test behavior
-- Assessment of measurement practicality

The emphasis in this section is placed on instrumentation relative to engineering testing, particularly those instruments that must be placed within the hostile test environment. There is no attempt to include instrumentation for plasma diagnostics and control. Neither are those instruments which can be located in shielded, remote regions and which are used in standard practice discussed.

### 9.1.2 Generic Instrumentation Issues

Chapter 3 of this report lists several generic issues related to instrumenting a fusion machine. As might be expected, these are also important issues to be considered in the design of test instrumentation. The following is a list of the more important considerations:

1. Transducer Lifetime

Temperature, radiation damage, heat flux, etc., can severely reduce the lifetime of a transducer. In many instances, however, it may be of value to have even short-lived instruments. As an example, beginning of life measurements of coolant channel flow distributions may be entirely adequate.

2. Breakdown of Insulation Resistance

Most instruments rely on some form of electrical insulation. Ionizing radiation may result in a breakdown of the insulating properties depending on the operating temperature and voltage.

3. Transmutation

Many instruments rely on basic material properties. Strain gauges are based on an understanding of electrical resistance; thermocouples are based on the thermoelectric effect of dissimilar materials. Changes in the material composition resulting from transmutation can cause decalibration of these instruments.

4. Darkening of Optical Windows, Lens, Etc.

Some measurements have been proposed which would require optical transmission devices. Infrared temperature mapping or laser interferometry are examples. Darkening or clouding of lens, prisms, windows, etc., will have to be contended with for such measurements to be made.

5. Cable Noise

The environment of large integrated tests will have many components that generate cable noise: RF, rapidly changing magnetic fields, charged particles, ionizing radiation, etc. Considerable care will be required to design instruments and data acquisition systems which eliminate, filter, or compensate for this noise.

### 9.1.3 Test Instrumentation Requirements

During the course of this study, there has been considerable discussion of potential test designs which has resulted in the identification of several required measurements. A discussion of the more important requirements is included herein.

#### 1. Temperature

Temperature measurement is one of the most basic and often requested requirements. This requirement ranges from measurement of bulk coolant inlet and outlet temperatures to the quantification of the temperature gradient through structural components. Temperature measurement experience in fission reactors, particularly during the Breeder Reactor Development Program, provides confidence that reliable measurements can be made. Considerable experience has been gained with thermocouples and resistance temperature devices, the latter being used primarily in shielded regions where size of the sensing device is not critical.

Type K thermocouples have been used extensively in the Breeder Reactor Development Program and have proven to be reliable to a fast fluence ($E \geq .1$ MeV) of $1.5 \times 10^{23}$ n/cm$^2$. There has been some concern expressed about the enhanced potential for transmutation in a 14 MeV environment and the effect on thermocouple calibration. Experience in a 14 MeV flux has been limited and the results mixed. There have been two tests completed at the RTNS-II facility to an accumulated fluence of $10^{18}$ n/cm$^2$ (14 MeV). One test showed some decalibration with fluence;[1] the other test showed little effect.[2] Further testing will be necessary to resolve the question.

Thermocouples range in diameters from 0.5 to 2.0 mm, and sheathed thermocouples have been purchased to 40' long. Generally, these devices are small and inobtrusive enough that they do not significantly perturb the environment. However, in applications where an array of thermocouples is necessary, such as the measurement of the temperature gradient through the first wall, this may not hold true.

In general, this is a highly practical measurement to make. As noted above, the exception to this may be in trying to determine temperature distribution through the use of arrays; care must be taken not to perturb the desired measurement.

2. Pressure

Pressure is another basic measurement for which there is considerable need. Again, a broad range of capabilities has been requested - from measurement of blanket inlet and outlet pressure to fluctuations resulting from flow turbulence.

Several devices are available for making these measurements, each with its own limitations. Piezoelectric pressure transducers, strain gauge pressure transducers, and null balance devices are some examples of pressure sensing devices that may be used.

The major limitation on these devices is associated with the radiation environment. Piezoelectric transducers have a very short lifetime in a radiation field, but they are the best candidate for measuring rapid fluctuations in a coolant channel. It may be that beginning of life measurements of this phenomena are sufficient, making these sensors a viable choice. Even in this case, some testing is required to define how long they will survive.

Strain gauge pressure transducers offer somewhat more radiation resistance. These gauges generally incorporate a diaphragm which is elastically deformed by the pressure and the deformation measured by strain gauges. Decalibration may result from changes in the diaphragm material, e.g., swelling, irradiation-induced creep, or changes in elastic properties. Changes in the strain gauge properties due to transmutation will also result in decalibration. In-situ calibration or the use of compensating transducers may extend the utility of these devices.

Another method which has been used in the breeder program extensively is the use of a tube filled with a medium which will transmit the pressure to the transducer located in a shielded region. The medium may range from a gas to

liquid metal depending on the application. Liquid metals which are incompressible, have low vapor pressure, and are not greatly effected by radiation may be used when fast response is required.

One device which has been successfully used in a reactor is a null balance. With this method, the system pressure is converted to a force through a diaphragm which moves an electrical contact and opens a circuit. An external pressure is applied to the diaphragm until the circuit is closed; at this point, the pressure is measured. Since this system utilizes the balancing of two forces, it is relatively independent of material properties and hence, quite radiation resistant. It does have the disadvantage of being relatively slow.

Pressure transducers are generally relatively large devices with diameters of 10 mm or more. Measurement of pressure in large areas such as coolant inlet lines or gas plenums should present no problem. Pressure measurement in individual coolant channels will become more difficult as the tests become more complex. It will be difficult, for example, to measure the pressure in very many coolant channels in a module or submodule test without perturbing some aspect of the test geometry or environment.

Within the constraints mentioned herein, the measurement is practical to make and experimenters should be able to anticipate availability of pressure data.

3. Strain

In-situ strain measurements are desirable for many tests. Several issues listed in Chapter 3 refer to structural interaction between various components. Measurement of strain at structural discontinuities and welds can provide much information about stress levels and expected lifetimes. It is also desirable to measure the strain of the thin cladding around the solid breeder.

The Canadians have had good success using welded strain gauges in reactors up to fast fluences of $2 \times 10^{23}$ n/cm$^2$.(3) As one might expect, radiation damage causes considerable decalibration of the gauge. The

resistance of the gauge changes dramatically to a fluence of $5 \times 10^{21}$ n/cm$^2$. Beyond this fluence, the damage appears to saturate and the gauges provide reliable data. This makes it very difficult to measure strains at the beginning of life unless some method of in-situ calibration is provided. There is no data available on the effects of 14 MeV neutrons. Testing will be required to quantify behavior in this environment.

The strain gauges are approximately 10 mm x 25 mm x 3 mm and can quite easily be applied to large structural components. Obviously, it will be very difficult to apply these gauges to 0.5 mm thick cladding. Furthermore, the sturdiness of the gauge would certainly perturb the strain rate of the cladding at the point of application.

It appears that strain measurements can be assumed practical for the larger structures; the currently available gauges do not appear practical for measuring the strain of thin members such as the cladding. It may be possible to develop smaller less sturdy gauges, however, which may be adequate.

Optical methods such as laser interferometry or direct optical measurements have also been proposed for strain measurements. These techniques generally require optical windows, lens, prisms, etc., which are subject to radiation damage as discussed earlier.[4]

Use of optical methods requires that an optical path be provided, and this in turn, results in a requirement for increased local shielding. Other than the shielding requirements, optical methods should have minimal impact on the test itself.

Providing resolution to the shielding problem and radiation damage to the optical transmission components can be achieved, this method may be the most practical for measuring the strain of large surfaces such as the first wall.

4. Bulk Heating Rate Measurements

Many design decisions are governed by bulk heat deposition rates. These rates are analytically estimated and, though physicists have a great deal of confidence in these calculations, fission reactor experience indicates that

there can be significant errors. Bulk heating measurements are necessary to confirm or correct the analytical models.

Calorimeters have been successfully used in fission reactors for many years, and this technology should be readily transferable to the fusion development programs. The calorimeter is simply a susceptor, such as stainless steel, contained in an evacuated capsule with highly polished surfaces. A thermocouple is positioned to measure the centerline temperature of the susceptor and another measures the capsule wall temperature. Knowing the temperature drop, it is possible to calculate the heat generation rate.[5]

These calorimeters should perform well in a fusion environment providing the 14 MeV neutrons do not degrade the thermocouple performance. The calorimeters are approximately 10 cm in diameter and 50 cm long. Access to a few key positions should not be difficult, and there should be no significant impact on the operation of the test. The measurement is considered to be highly practical.

5. Surface Heat Flux Measurements

In addition to the bulk heating, a significant amount of energy is deposited in the first wall and other components adjacent to the plasma in the form of surface heat flux. The primary sources of this surface flux are radiated energy from the plasma and charge exchange. Since the temperature gradient through the wall and hence the thermal stresses are dependent on this surface heat flux, it is a particularly important measurement.

The measurement of the surface heat flux in the intense fusion environment is very difficult. Several types of bolometers have been used on present machines with varying success. Some of these are not radiation tolerant and will not be adequate for future machines. There have been some metal resistance bolometers developed for JET which appear to have some potential.[6] These consist of a thin (4 μm) gold coating applied to a capton insulator with a 0.1 μm gold resistor on the backside. The change in temperature of the resistor is proportional to the temperature of the gold which is related to the surface heat flux. Platinum resistance bolometers have also been used on the PLT Tokamak.[7]

These bolometers are approximately 25 mm in diameter and 40 mm long. Generally, an array of bolometers is required to provide time and position dependent measurements. Providing adequate access is an engineering problem, but one that is workable. Other than the provisions for access, no impact on the test operation is anticipated.

The measurement is a difficult one and more development is required to qualify instruments such as the metal resistance bolometer; however, it does appear to be practical.

6. Coolant Channel Velocity Profiles

Design of coolant channels is a major aspect in the engineering of the first wall and blanket. Considerable testing will be required to verify that actual heat transfer rates are sufficient to remove the heat generated. The velocity profile in a coolant channel has a significant effect on the overall heat transfer coefficients. It is desirable, therefore, to have some method to measure the profile. An example of the need for measuring these profiles is the uncertainty associated with liquid metal flowing in high magnetic fields. The fields may suppress turbulence and mixing giving rise to a large boundary layer and reduced heat transfer coefficient.

Although the need for the measurements is evident, they will be very difficult to make, particularly in the fusion environment. The coolant channels are relatively small, and it will be difficult to place probes within the channels without perturbing that flow.

One method proposed is the use of hot film anemometers developed for use in liquid metals. These consist of a 70 μm quartz rod with an extremely thin layer of nickel and then a 2 μm layer of quartz deposited over that. These have been reported to provide reliable velocity measurement down to 2.5 mm/sec.[8] These are very delicate instruments and their survivability in the hostile fusion environment is suspect. Considerable development will be required if these are to be used in large integrated tests. A more reasonable application would be to characterize these profiles in bench tests, thereby removing the sensor from the extremely harsh fusion environment.

As noted above, these sensors are quite small; however, to measure a profile, an array will be required. Placing this array into channels which are part of a submodule or module will be extremely difficult. Again, a bench test is a more achievable goal. Even in a bench test, there is some concern that an array would perturb the profile and result in invalid data. Considerable testing will be required before the sensors can be deemed reliable.

7. Neutron Flux

Many of the parameters to be measured during testing are dependent on the neutron flux, accumulated fluence, and spectrum. To properly understand the response of structural materials, breeding ratios, swelling of solid breeder materials, etc., it will be necessary to accurately measure the neutron environment.

It may be possible to make in-situ measurements using active monitors such as self-powered neutron detectors (SPND's), flux monitors, etc. There are some definite limitations with these devices, however. Most devices generate a signal through the interaction of a neutron with a special material in the device. An example is the reaction of a neutron with rhodium in a SPND; this generates electrons creating a very low current. The difficulty is that at 14 MeV, there are few materials that interact with neutrons. It may be that these devices can only provide gross relative information rather than definitive neutron flux levels. Another problem is the low signal level; in the very noisy fusion environment, the signal-to-noise ratio may be so low that the information is entirely masked.

Passive devices such as activation foils and solid-state track recorders can provide accurate fluence and spectrum measurements; however, these cannot be evaluated until after they are removed from the test.

Passive devices are generally very small, less than 10 mm x 10 mm x 2 mm, and can be placed at several places within an assembly without perturbing the test. SPND's are approximately 2 mm in diameter and are also easily positioned. Other active devices such as flux monitors, fission counters,

etc., require larger sensors ( $\geq 10$ $cm^3$) and are not so easily located within an assembly.

8. Tritium Production Rates

One of the biggest questions in the design of a fusion machine is concerning the ability of the machine to generate tritium fast enough to fuel the machine. Knowing the tritium production rate through the blanket becomes very important. As there will be some spatial distribution of production rate, monitors will have to be placed in several positions throughout the blanket.

Two methods have been proposed for making these measurements. The first is on-line monitoring of the production rate and requires piping a carrier gas or liquid from the blanket to a counter such as an ionization chamber or a scintillation counter. This becomes a relatively complex system, and it may be difficult to provide enough information to define the spatial distribution. It would be useful for measuring the time variation in production.

Combined with an on-line system, some form of dosimetry could be used to provide the spatial information. Small sealed vials with blanket material within them can be strategically placed and removed after testing for analysis. The size of the breeder material vials will be dictated by the test geometry, but adequate access should be available to make this a practical measurement. By keeping the coupons small and limiting the number of on-line systems, these measurements should not perturb the test results.

9.1.4 Conclusions

The list of measurements included in this chapter cannot be considered complete. Many of the measurement requirements have not yet been defined; others have not yet been investigated. The list does serve to point out the need for instrumentation and the magnitude of the task to develop that instrumentation. The fusion environment poses some significant challenges for instrumentation of experiments. Even the most basic measurements, such as temperature measurement with thermocouples, will require some development before they can be made with confidence.

It does appear that with sufficient effort, techniques can be developed to provide the necessary information. It is also evident that it is unreasonable to expect all measurements to be made in a large scale integrated test such as a module or submodule. Some measurements should be made during bench testing, if possible. Other measurements such as tritium production rate measurements should combine simple methods like coupon analysis with the more ambitious on-line measurements. Through judicious test planning and instrument selection, it is anticipated that the necessary information can be gathered without jeopardizing the test through overcomplexity.

## References for Section 9.1


1. "Effects of Fusion Neutrons on Thermocouples," UCRL-85452, CM Logan/DW Heikkinen/BJ Schumacher/PA House, June, 1981.

2. Private Conversation Between JM Grover and CP Cannon, Westinghouse Hanford Company, July, 1984.

3. "Effects of Neutron Irradiation on the Resistance of Ni-Cr Weldable Strain Gauges," PJ Fehrenbach, et al., ANS Meeting, San Francisco, November, 1983.

4. "Radiation Hardening of Diagnostics for Fusion Reactors," GA-A16614 UC-20, JF Bauer, et al., General Atomic Company, December, 1981.

5. "FTR Energy Deposition Using HEDL Calorimeters," TC-2284, FS Moore/MR Wood, December, 1982.

6. "Proceeding of Course on Diagnostics for Fusion Reactor Conditions," Vol. I, Commission of the European Communities (EUR 8351-1 EM), September, 1982.

7. "Nuclear Aspects of Tokamak Fusion Test Reactor (TFTR) Diagnostics and Instrumentation," K. M. Young, Plasma Physics Laboratory, Princeton University, January, 1982.

8. "Applications of Laboratory and Theoretical MHD Duct Flow Studies in Fusion Reactor Technology," UKAEA Report #CLM-R169, JCR Hunt/RJ Holroyd, 1977.

## 9.2 Test Matrix

Test matrices that list the required nuclear tests and important testing parameters will be developed for FINESSE to help define and quantify the nuclear testing requirements. The test matrices will be based upon the issues and testing needs documented during the first year of the FINESSE study. In the interim report, the overall features of the test matrix will be discussed along with a preliminary assessment of the testing volume and required first wall area necessary to support fusion reactor development. The role of alternate facilities such as Point Neutron Sources (PNS), Fission Reactors (FR) and Non-Neutron Test Stands (TS) will also be discussed.

In Chapters 3 and 4 of this report, the nuclear issues and testing needs important to fusion development were categorized and listed in significant detail. This information provides the basis from which the test matrices are formulated. The data of particular interest are listed in Table 4.4 of Chapter 4 and contains the nuclear tests, associated testing parameters and the usefulness of non-fusion testing facilities such as fission reactors. The data was tabulated by the entire FINESSE team and represents a broad and diverse base of testing expertise. The information, however, is not in the correct form, nor is it sufficiently complete to directly determine hard and concise testing requirements. The test matrix will be used as a mechanism to combine the testing needs with input from test designers and facility operational personnel for the purpose of identifying facility requirements. A number of previous studies[1-3] used test matrices in a manner very similar to this. Figure 9.2-1 shows the relationship between the test matrix, facility requirements and the data compiled during the first year of the FINESSE.

As shown in the figure, the test matrix is closely interrelated to the design of actual testing hardware (e.g., the experiments) and to the operation and handling of the hardware in the testing facility. In order to understand and document the needs of an experimenter in an irradiation facility, the shape and size of the test hardware needs to be known as well as the manner in which that hardware is handled and operated. Clearly conceptual

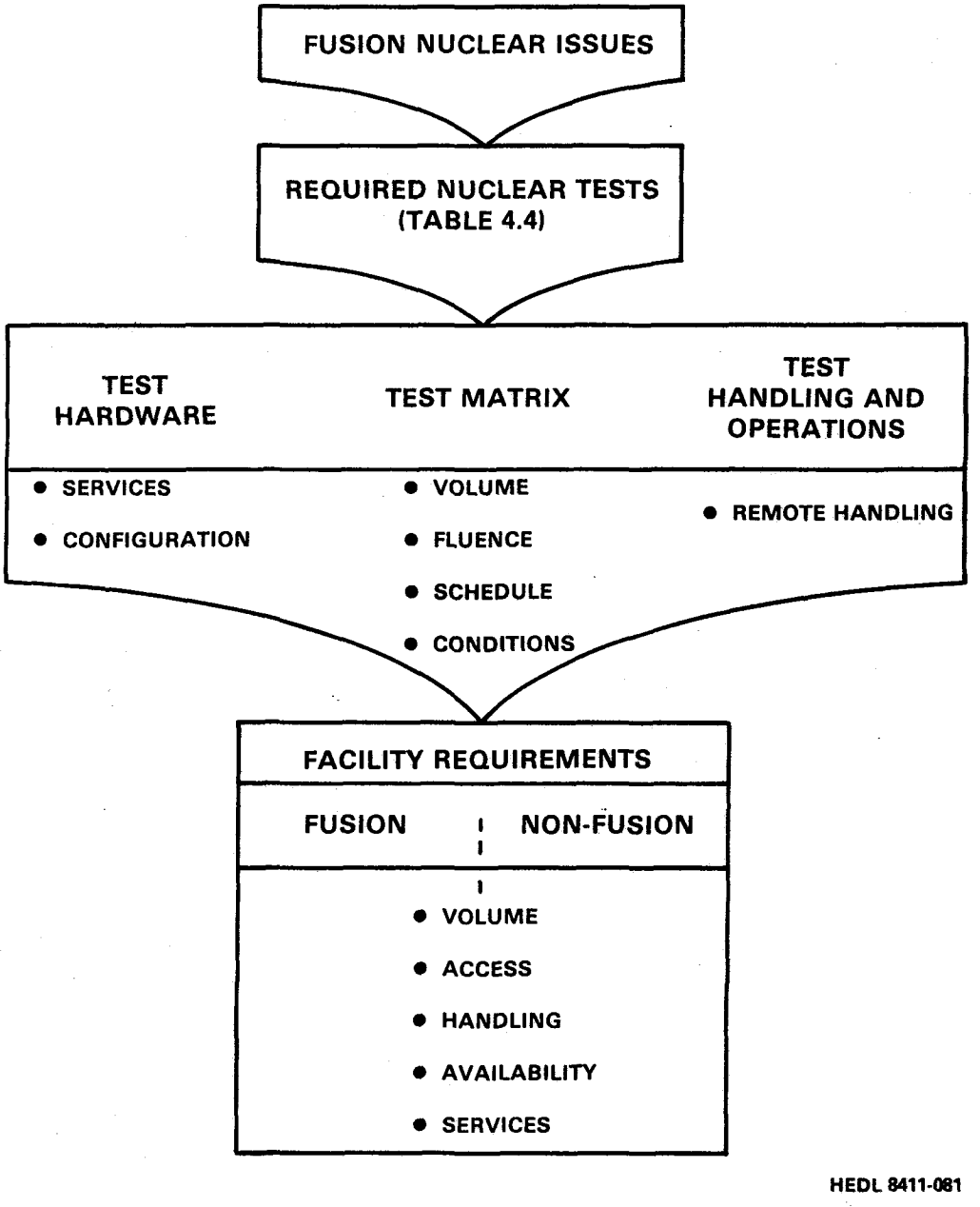


Figure 9.2-1. Relationship between the test matrix and key aspects of nuclear testing.

test designs cannot be completed for each of the tests listed in Chapter 4; however, tests representative of the various broad test categories will be designed.

Having a knowledge of the test matrix and the test hardware and operations, the impacts on the irradiation facility can be determined. For example, a test consisting of a stainless steel specimen-filled module with instrumentation, active cooling and temperature control will impose a number of requirements on the irradiation facility. If the test is irradiated in a high neutron flux field, the structure will become activated and will require remote handling and shielded cask transport from the facility to a hot cell disassembly station. If the coolant is circulated through the irradiation zone, it too will become activated and pose special handling and shielding problems external to the reactor. The overall safe and efficient operation of the test therefore requires that the irradiation facility be carefully designed and be sufficiently versatile to handle a variety of test types and configurations.

Figure 9.2-1 lists five important and closely related requirements that a facility design must satisfy in order to successfully carry out experimental testing. The first is irradiation volume. The volume must not only be of sufficient magnitude, but must also be configured to accommodate a wide variety of tests with good physical access. Since tests typically are fragile, cumbersome and radioactive, their insertion and removal from the facility requires clear and clean access. Access, the second requirement, is necessary for test insertion/removal, attachment of service and instrumentation leads, radiation monitoring, and interfacing with adjacent tests and biological shielding. Access is particularly important following irradiation when special remote fixturing and handling devices are required to remove the test from the reactor.

Test handling, the third requirement, also has a major impact on the irradiation facility design. If the tests become neutron activated then master-slave or electromechanical manipulators, or an overhead crane will be required for test handling. These special handling tools impose special viewing, structural, and access requirements upon the facility design. If shielded casks are required for test transport within the facility, then floor loadings, ramp and elevator designs, etc., are significantly impacted.

Availability, the fourth requirement, is the fraction of the total time that the facility is available for beam-on operation. The facility availability is closely related to all other requirements. A facility with sufficient volume and good access and handling capabilities will require minimal down times for test change-out, repair and maintenance and therefore will have an optimum availability. To maximize facility availability, test design, test reliability, scheduling, handling and maintenance must be carefully planned and coordinated with the operations required to run the facility.

The final requirement in Figure 9.2-1 is that of services. Services refer to the various leads (electrical, hydraulic, pneumatic, instrumentation, etc.) that need to be routed to and from the tests. This requirement, while seemingly obvious, must be carefully considered in the design of the facility, particularly when a wide variety of tests are anticipated. The routing of service leads from the in-reactor test to the data logging and support equipment, which typically is located away from the reactor, requires significant space with good access. Service leads carrying activated fluids pose special problems external to the reactor shielding and must be considered in the facility design.

### 9.2.1 Single Specimen Test Matrix and Preliminary Results

In this section, we discuss the single specimen test matrix and the manner in which the testing issues and test types of Chapter 4 were analyzed to determine the required irradiation volume and first wall areas. The tests given in Table 4.4 represent a broad list of tests and test parameters and is a very general test matrix. As this list is further studied, more detailed test matrices will be developed to further define and clarify the anticipated types of tests. In previous fusion device design studies,[1-3] single specimen test matrices were developed for structural and special purpose materials. The development of these matrices reflected the relative maturity of single specimen testing that is ongoing in the fusion and breeder reactor materials testing programs. Test matrices for the more complex multiple

interaction, integrated and component tests, etc., will require further definition of both the test type and the associated supporting hardware.

A single specimen test matrix is listed in Table 9.2-1. This table, while preliminary, gives the representative specimen numbers required to test a structural material. The table lists three individual test matrices: an alloy development (D), an engineering scoping (S) and full materials qualification (Q) test matrix. The matrices were written for two different types of stainless steels: ferritic (F) and austenitic (A). The alloy development matrix represents the specimens that would be irradiated to screen a large number of alloys in order to select a few leading candidates. The engineering scoping matrix represents the testing required to understand and characterize a material in sufficient detail to formulate design equations for nuclear facility designers. Lastly, the full materials qualification matrix represents the distribution of specimens that would be tested to thoroughly qualify a material for use in a nuclear facility. Ferritic and austenitic materials were both listed to show the difference that the type of material can have on the selection of test specimens. The evaluation of ferritic steels, for example, involves testing a relatively large number of fracture toughness specimens to address concerns over ductile to brittle transition temperatures.

The items listed across the top of Table 9.2-1 represent the testing variables that currently are considered important. The "material" refers to the number of alloy compositions. "Heat treatment" refers to the number of different thermal heat treatments considered. "Chemistry variations" refers to the number of minor variations in alloying elements within the given alloy. "Duplication" refers to the number of identical or redundant specimens, i.e., same material, heat treatment, chemistry composition, etc. "Irradiation temperature" is simply the number of different temperatures at which the specimens are irradiated and the "fluence levels" are the number of different fluences at which specimens are removed from the reactor for property measurements. The number of fluence levels will be a function of the maximum goal fluence for a particular test. The number of fluence levels

Table 9.2-1. Test Matrices for Fusion Materials Applications

| Test | Material | | # Heat Treatment | | Chemistry Variations | | Duplication of Specimens (or Creep Stress Levels) | | #Irradiation Temperatures | | Fluence Levels | | Post Irr. Conditions | | Total # | | Total # | | Total Volume ($cm^3$) | Total Volume ($cm^3$) |
|---|---|---|---|---|---|---|---|---|---|---|---|---|---|---|---|---|---|---|---|---|
| | A | F | A | F | A | F | A | F | A | F | A | F | A | F | A | F | A | F | A | F |
| **Tensile/Ductility** | | | | | | | | | | | | | | | | | | | | |
| D | 1 | 1 | 5 | 1 | 10 | 1 | 2 | 2 | 4 | 4 | 3 | 3 | 2 | 2 | 2400 | 480 | | | 84 | 17 |
| S | 1 | 1 | 2 | 2 | 2 | 1 | 1 | 2 | 6 | 6 | 3 | 3 | 3 | 4 | 288 | 288 | | | 155 | 155 |
| Q | 1 | 1 | 1 | 1 | 2* | 2* | 3 | 3 | 6 | 6 | 3 | 3 | 4 | 4 | 432 | 432 | | | 233 | 233 |
| | | | | | | | | | | | | | | | | | | | (1995) | (1995) |
| **Creep** | | | | | | | | | | | | | | | | | | | | |
| D | 1 | 1 | 0 | 0 | 0 | 0 | 0 | 0 | 0 | 0 | 0 | 0 | 0 | 0 | 0 | 0 | | | 0 | 0 |
| S | 1 | 1 | 6 | 1 | 6 | 1 | 5 | 5 | 6 | 6 | [6] | [6] | 1 | 1 | 1080 | 30 | | | 1134 | 32 |
| Q | 1 | 1 | 1 | 1 | 6* | 2* | 3 | 5 | 6 | 6 | [6] | [6] | 1 | 1 | 180 | 60 | | | 189 | 64 |
| **Fatigue** | | | | | | | | | | | | | | | | | | | | |
| D | 1 | 1 | 2 | 2 | 2 | 2 | 1 | 1 | 6 | 6 | 2 | 2 | 2 | 2 | 0 | 0 | | | 0 | 0 |
| S | 1 | 1 | 1 | 1 | 6* | 6* | 2 | 2 | 6 | 6 | 4 | 4 | 3 | 3 | 96 | 96 | | | 221 | 221 |
| Q | 1 | 1 | | | | | | | | | | | | | 864 | 864 | | | 1987 | 1987 |
| **Crack Growth** | | | | | | | | | | | | | | | | | | | | |
| D | 1 | 1 | 0 | 0 | 0 | 0 | 0 | 0 | 0 | 0 | 0 | 0 | 0 | 0 | 0 | 0 | | | 0 | 0 |
| S | 1 | 1 | 2 | 2 | 2 | 0 | 1 | 1 | 6 | 6 | 2 | 2 | 2 | 2 | 96 | 96 | | | 173 | 173 |
| Q | 1 | 1 | 1 | 1 | 6* | 6* | 2 | 2 | 6 | 6 | 4 | 4 | 3 | 3 | 864 | 864 | | | 1555 | 1555 |
| **Fracture Tough** | | | | | | | | | | | | | | | | | | | | |
| D | 1 | 1 | 0 | 0 | 0 | 0 | 0 | 0 | 0 | 0 | 0 | 0 | 0 | 0 | 0 | 0 | | | 0 | 0 |
| S | 1 | 1 | 1 | 1 | 1 | 2 | 1 | 1 | 6 | 6 | 2 | 2 | 10 | 10 | 120 | 480 | | | 420 | 1680 |
| Q | 1 | 1 | 1 | 1 | 1 | 4* | 1 | 1 | 6 | 6 | 2 | 2 | 10 | 10 | 120 | 480 | | | 420 | 1680 |
| **Swelling/Microstructure** | | | | | | | | | | | | | | | | | | | | |
| D | 1 | 1 | 2 | 2 | 10 | 5 | 3 | 3 | 8 | 8 | 7 | 7 | 1 | 1 | 3360 | 1680 | | | 118 | 59 |
| S | 1 | 1 | 4 | 3 | 3 | 2 | 3 | 3 | 8 | 8 | 7 | 7 | 1 | 1 | 2016 | 1008 | | | 71 | 35 |
| Q | 1 | 1 | 1 | 1 | 6* | 2* | 3 | 3 | 10 | 10 | 7 | 7 | 1 | 1 | 1260 | 420 | | | 44 | 15 |
| **Creep Rupture** | | | | | | | | | | | | | | | | | | | | |
| D | 1 | 1 | 0 | 0 | 0 | 0 | 0 | 0 | 0 | 0 | 0 | 0 | 0 | 0 | 0 | 0 | | | 0 | 0 |
| S | 1 | 1 | 1 | 1 | 1 | 1 | 1 | 1 | 1 | 1 | 1 | 1 | 1 | 1 | 10 | 10 | | | 21 | 21 |
| Q | 1 | 1 | 1 | 1 | 1 | 1 | 5 | 5 | 1 | 1 | 1 | 1 | 1 | 1 | 25 | 25 | | | 53 | 53 |

D = Alloy Development Matrix
S = Engineering Scoping Matrix
Q = Full Materials Qualification
* = Heats

() = Larger round specimen
[ ] = Creep capsules reused after interim examination
F = Ferritic Stainless Steel
A = Austenitic Stainless Steel

shown in the table are representative of a test carried out to 50 to 80 displacements per atom (dpa). "Postirradiation conditions" refers to the number of specimens required in hot cell tests that are carried out following irradiation.

The total number of specimens is simply the product of each of the individual columns in Table 9.2-1. The matrix reveals why a relatively small number of testing variables can lead to large numbers of specimens. The irradiation volume that the total number of specimens occupy is given in the last column. These volumes are based on the specimen dimensions and the packing allowances listed in Table 9.2-2. The specimen sizes and packing factors are the same as those used in the INTOR study.[1]

Table 9.2-2. Single Specimen Volumes

| Specimen | Specimen Volume ($cm^3$) | Packing Factor | Effective Volume per Specimen ($cm^3$) |
|---|---|---|---|
| Tensile (Scoping) | 0.18 | 3 | 0.54 |
| Tensile (Qualification) | 1.54 | 3 | 4.62 |
| Creep | 0.35 | 3 | 1.05 |
| Fatigue | 0.76 | 3 | 2.3 |
| Crack Growth | 1.2 | 2 | 2.4 |
| Fracture Toughness (Compact Tension) | 2.3 | 2 | 4.6 |
| Swelling/Microstructure | 0.014 | 5/2 | 0.035 |
| Creep Rupture | 0.35 | 6 | 2.1 |

Preliminary Test Volume and First Wall Area Results

A summary of the test volume and first wall area needed to carry out the tests listed in Table 4.4 were given in Chapter 2.4.5. In this section, we will describe in more detail the way in which those volume and area values were determined.

The volume and area required for testing are of primary importance in assessing the facility requirements. If the required volume is small, then the facility can be correspondingly small, and if the volume is large, then the facility must be appropriately designed or multiple facilities utilized. The volume of a single test (Table 4.4) was calculated by taking the product of the test area and its depth. The total test volume was then simply determined by multiplying the single test volume by the total number of tests. The total volume, therefore, represents the volume that the tests will occupy over the period of time required to complete the testing. A summary of the test areas and volumes is given in Table 9.2-3. The table lists the tests having a high priority for fusion-like neutrons and those having a lower priority for fusion neutrons. The table also lists the appropriate facilities in which the testing will likely take place. Fission reactors, point neutron sources, test stands and a future fusion device were considered.

Table 9.2-3 Summary of Testing Space and Facility Utilization (Units $M^2$, $M^3$)

| | Point Neutron and Fission Reactors | | Test Stands | | Fusion Test Device | | Total | |
|---|---|---|---|---|---|---|---|---|
| | Area | Vol. | Area | Vol. | Area | Vol. | Area | Vol. |
| High Priority | 5-9 | 1-4 | --- | --- | 57-117 | 60-91 | 62-91 | 61-95 |
| Lower Priority | 10-17 | 2-6 | 80-120 | 60-80 | 30-45 | 13-27 | 120-182 | 75-113 |
| | | | | | | TOTAL | 182-308 | 136-208 |

The total area and volume values for the high priority neutron tests listed in the Table 9.2-3 are significant and exceed the testing space available in large fusion devices such as the INTOR.[1] The instantaneous volume will be determined by studying the way in which the tests are sequenced into and out of the irradiation facility. Based on previous studies, the irradiation space required at a given time is typically less than half of the total volume required.

The values in Table 9.2-3 may increase slightly as testing statistics are considered. When the number of tests were listed in Table 4.4, consideration was given to "all necessary test variations that are considered for an adequate test matrix (materials, grain size, impurity content, temperature, chemistry, flux, fluence, etc.)". The number of specimens or tests required to ensure good statistical data was not, however, directly included in the test numbers. For example, ceramic mechanical property tests require a large number of specimens in order to determine a statistically averaged property value. Structural metal and alloy tests typically include a sufficient matrix of test variables (see Table 9.7-1) that extra specimens are not specifically included for statistical reasons.

The larger and more complex integrated and component tests are difficult to assess from a statistical stand point. If one looks today at the manner in which large test devices and fission reactor components are developed for irradiation service, we find that a relatively small number of actual full sized in-reactor tests are carried out prior to final component design. Due to the stringent fabrication, quality assurance, and safety requirements imposed on irradiated components, it is typically too costly to build more units than is absolutely necessary. A strong emphasis is therefore placed on the design and rigorous mockup and prototype bench testing of large reactor component prior to irradiation. Data from irradiation tests of single specimens are used as a basis for larger component design.

Components being developed for fusion are however at an embryonic stage when compared to the more advanced fission reactor components. The testing

of first-of-its-kind fusion reactor components will likely require significantly more basic testing in a prototypic irradiation environment than do fission components today. Statistical considerations do not really apply to the large components developed early in development sequences since the results from one test will almost always lead to a redesigned or upgraded second generation test. Overall, the consideration of testing statistics is not expected to significantly increase the overall testing volume required during the initial years of fusion development.

## References for Section 9.2


1. "US INTOR Conceptual Design Report," USA INTOR/81-1, 1981.

2. "TASKA - Tandem Spiegelmaschine Karlsruhe A Tandem Mirror Fusion Engineering Test Facility," KFK 3311/2 and UWFDM-500, June 1982.

3. E. K. Opperman, "Fusion Materials Irradiation Test Facility - Experimental Capabilities and Test Matrix," HEDL-TME 81-45, January 1982.

# CHAPTER 10

# NON-NEUTRON TEST STANDS

TABLE OF CONTENTS

Page

10.1 Usefulness of Non-Nuclear Tests..... 10-2

10.2 Test Stands for Single Effects, Interactive and Partially Integrated Testing..... 10-4

10.2.1 Test Stands for Limiters and First Walls.....10-10

10.2.2 Test Stands for Solid Breeder Blankets.....10-11

10.2.3 Test Stands for Liquid Metal Blankets.....10-13

10.3 Existing Test Stands and Future Needs.....10-14

10.3.1 Test Stands for Blankets.....10-14

10.3.2 Test Stands for High Heat Flux Components.....10-16

References.....10-20

# 10. NON-NEUTRON TEST STANDS

During its first year the effort in FINESSE has been focused primarily on neutron-producing non-fusion and fusion facilities. This emphasis is appropriate due to the large cost and complex technical and programmatic issues associated with performing irradiation experiments with significant neutron flux.

There is also a clear recognition that in the immediate future non-neutron test facilities can and should serve an important role in the development of fusion nuclear technology. Many types of tests that do not require neutron irradiation were identified in Chapter 4.

The use of single effects tests, for example, for data on mechanical properties, is fairly well understood. Less clear is the role of non-neutron multiple effects tests. This chapter will emphasize the potential usefulness of non-neutron test stands for partially integrated tests.

Information from experimental programs on fusion technology contributes in many ways to the ultimate decision to build a specific fusion device. The basic concepts and issues involved are refined through design studies that often utilize rather limited data. These exercises clarify issues and identify needs for additional data and provide input to guide programmatic decisions.

Generally tests that address these needs may be broad in scope with little depth, e.g. many materials and general trends in behavior. These "phenomenological tests" provide sufficient data to shed light on the nature of critical issues, on the expectations of success in addressing them and on the most productive directions and least harmful limitations in scope for the program.

In advance of the construction of advanced fusion devices, programs to develop hardware must be implemented and supported by design specific testing, e.g. qualification tests on a selected vendor's cladding for a limiter. Sometime in the next decade we anticipate commitment to a D-T device that will employ advanced nuclear systems perhaps including a full breeding blanket. The need for data to support detailed design and construction will justify various developmental tasks and related "design support tests" for specific components.

Integrated tests in a nuclear environment will be sufficiently expensive that design specific non-neutron tests will, in support of these integrated tests, be warranted as a cost effective measure to reduce the risk of inappropriate results from the integrated test. For example, if an integrated test on a solid breeder module with a sphere-pac assembly were planned, then a sphere-pac assembly using solid breeders produced by a prototypic method for large scale production is a probable prerequisite. Fabrication development and tests on heat transfer of the product from the developed technique would form a part of the overall plan to develop an integrated test.

Any credible scenario for the development of fusion nuclear technology will include the roles of testing in providing general information on programmatic aspect and the construction-oriented aspect of testing. For example, the development of one or more workable blankets is a challenging goal in fusion technology and will most likely require fairly sophisticated partially integrated tests in support of concept development to judge the feasibility of the basic engineering to operate the leading candidate blankets (exclusive of their breeding potential). Subsequently the successful performance of a (full scale) integrated test is a probable requisite for commitment to the construction of a full breeding blanket on an advanced fusion reactor.

The important point here is not a specific strategy but the overall programmatic problem of reaching a workable strategy within a limited budget. The fusion program will of necessity have to build test facilities. The ideal role for non-neutron tests is to permit sufficient breadth of scope and sophistication in testing so that the fundamental problems are recognized and overcome and the number of integrated tests, which may be costly in both money and time, can be restricted to a few productive confirmations of successful performance.

## 10.1 Usefulness of Non-Nuclear Tests

A practical criterion for usefulness must blend two types of information. The first is a judgment of technical merit based on (a) the technical need for the data and (b) the appropriateness of the test or facility to meet this need. Second is a judgment of the anticipated programmatic effectiveness based on priorities of technical need tempered by realistic budget constraints. The element of risk (in degraded performance of a large experiment

or of a fusion reactor) due to lack of data is an important factor in determining priorities among technical needs.

Extensive investigation and development of scenarios and definitions of useful non-neutron tests are beyond the scope of this brief commentary. However some qualitative comments about test stands are presented.

Test stands for multiple effects tests are of particular interest because tests to resolve many critical issues in fusion nuclear technology require simulation of multiple effects and because exploitation of the potential of non-neutron tests in combination with nuclear tests where necessary is perceived as the most cost effective program. Several options for combinations of features for multiple effects tests stands are presented later.

The usefulness of non-neutron tests for baseline data is fairly obvious. Mechanical properties and corrosion of unirradiated structural materials, liquid metal MHD and surface erosion of plasma-side materials are examples of areas where the fusion program has already justified ongoing programs with non-neutron tests.

When the objective is to simulate several effects simultaneously or to demonstrate the performance of a component under reactor-like conditions, non-neutron tests may be incomplete simulations for several reasons. Some typical sources of such incompleteness are given below.

A. Production of tritium in breeders.

B. Activation products.

C. Fluence-dependent changes in the physical or mechanical properties of the material affect the phenomena of interest, e.g. radiation damage in solid breeders affects tritium release and heat transfer.

D. Thermal gradients from nuclear heating affect the phenomena of interest, e.g. thermal stresses in blanket structure.

E. Fluence-dependent changes in the physical or mechanical properties of the material affect the probable failure mode of the test article, e.g. loss of ductility.

These sources of incompleteness in simulations generally impose one of the following two limitations on how non-neutron tests can be used. (1) A desired test cannot reasonably be conducted because one or more elements essential to the phenomenology (e.g. tritium breeding in a solid breeder module) are missing. This limitation relates primarily to items A-C above. (2) The objective of determining failure modes is severely compromised without fluence-dependent changes in materials properties (e.g. stress relaxation due to radiation creep). This limitation relates primarily to items D and E above.

Rather than reviewing a list of candidate tests to gain insight into the usefulness of non-neutron test stands, several reasonable combinations of possible major features of non-neutron test stands will be briefly evaluated.

## 10.2 Test Stands for Single Effects, Interactive, and Partially Integrated Testing

The environment of the nuclear system in a fusion reactor can be simulated by supplying the basic features listed in Table 10.2-1. "Neutrons" are listed for completeness but would not be part of a non-neutron test stand, although some provisions for specimens with radiation damage or activation might be included, for example, to trace activation products in a corrosion loop. It is likely that not all of the features could be combined in any facility other than a fusion-based test facility; however there are sensible combinations of these features that would lend themselves readily to less complete but nevertheless potentially useful test stands.

A fairly limited list of options for non-neutron test stands may be developed by first considering the basic requirements for different components -- (1) in-vessel components such as limiters, divertor-collectors or first walls, (2) solid breeding blankets, and (3) liquid breeding blankets -- and second, noting any mutually exclusive or difficult combinations of features. Guidance on parameters for test stands can be derived from basic fusion parameters. Some examples are given in Table 10.2-2. Typical values for fusion parameters are given in parentheses in the left column of the table. The other columns in the table give scaled values of these parameters for test modules of three sizes with volumes of 10 $\ell$, 100 $\ell$ and 500 $\ell$.

Table 10.2-1. Features of Test Facilities

| Basic Features | Fusion Reference | Methods/Features for Simulation* |
|---|---|---|
| Coolant | First Wall and Blanket Coolant<br>Water (High P,T)<br>Helium (High P,T)<br>Liquid Metal (High P,T)<br>Molten Salt (Low P, High T) | Pumps, Heat Rejections, Flow Control<br>Circulating Water System<br>Circulating Helium System<br>Liquid Metal Loop<br>Molten Salt Loop |
| Purge Gas | Tritium Recovery System<br>Helium | Low Pressure Helium Loop |
| Static Magnetic Field | Steady State Confinement | Large Coils, External Envelope |
| Pulsed Magnetic Field | Eddy Currents from Disruptions | Large Pulsed Coils |
| Surface Heat | First Wall Heating | Power Supply System<br>Particle Beams/Plasma<br>Resistive Surface Heaters<br>Arc Lamps |
| Particle Bombardment | First Wall Environment | Low Energy Plasma Source |
| Bulk Heat | $^{6}$Li Transmutation, Neutron and Gamma Heating | Power Supply System<br>Resistive Elements<br>RF System |
| Distortion/Stress | Mechanical and Hydraulic Loads | Mechanical Displacement<br>Hydraulic Loads, Pressurization |
| Vacuum | Plasma Chamber, Plenum | Vacuum Chamber or Plenum |
| Neutrons | Radiation Damage | None in Non-nuclear Stands |
| Neutrons | Tritium Production | None in Non-nuclear Stands |
| Neutrons | Activation | Activated Samples |

* Simulation in a non-neutron test stand.

Table 10.2-2. Examples of Parameters Requirements for Non-Neutron Test Stand

| Module Size ("First Wall" Area & Thickness) | 10 ℓ .1 $m^2$ x .1 m | 100 ℓ .25 $m^2$ x .4 m | 500 ℓ 1 $m^2$ x .5 m |
|---|---|---|---|
| Surface Heat (10 $MW/m^2$) | 1 MW | — | -- |
| Surface Heat (0.5 $MW/m^2$) | .05 MW | .13 MW | 0.5 MW |
| Bulk Heat (3 $MW/m^2$) | .2 MW** | .6 MW | 2.4 MW |
| Water Flow* (300°C, 15 MPa, 40°C ΔT) | 1.6 ℓ/s | 4.8 ℓ/s | 19 ℓ/s |
| Helium Flow* (500°C, 5 MPa, 250°C ΔT) | 60 ℓ/s | 180 ℓ/s | 700 ℓ/s |
| Lithium or Li-Pb (500°C)* | 7 ℓ/s | 40 ℓ/s | 100 ℓ/s |
| Liquid Metal Loop - Volume | 500 ℓ | 3000 ℓ | 10,000 ℓ |
| - Flow Rate | 9 ℓ/s | 60 ℓ/s | 150 ℓ/s |
| Magnet Strength | > 2 T | > 2 T | > 2 T |
| Magnet Bore (l x w x h) | 2 x .5 x .2 m | 4 x .7 x .6 m | 6 x 1.2 x .7 m |

* Flow rates for water and helium are based on combined heat load of the first wall and bulk heating divided by the heat capacity times the temperature rise. For liquid metal, the volumetric flow rate shown is based simply on a linear flow velocity of 0.2 m/s.

** Heating rates equivalent to volume-averaged heating with neutron wall load of 3 $MW/m^2$.

Of the two values of surface heat flux in Table 10.2-2, the higher value (10 $MW/m^2$) and smaller size (10 ℓ) might be suitable for testing heat sinks (e.g., limiter section) and the lower value (0.5 $MW/m^2$) represents first wall heating in tokamaks. The available sources for surface heating (described in the next section) cover the range of surface heating power given in Table 10.2-2. Intense heat sources to simulate vaporization and melting during disruptions are not included here.

The average volumetric heating rates decrease with the thickness of the blanket. In Table 10.2-2 the volumetric heating is equivalent to a volume-averaged value (over thickness is indicated in the table) for the near-first-wall portion of a STARFIRE-type blanket with a neutron wall loading of 3 $MW/m^2$. For water and helium, test modules would include the full temperature rise in this flow path and the flow rates are simply the total heating divided by $\rho C_p \Delta T$. The flow rates for liquid metal are based on a fractional temperature rise as indicated in the footnote of the table. The linear flow rates are generally consistent with the bulk velocity in the BCSS of 0.3 m/s and in the MARS blanket of 0.2 m/s. For tests on heat transfer and MHD effects lower flow velocities will be preferred to increase both the rise in temperature and the magnetic interaction parameter.

The sizes of both the magnets and the liquid metal loops reflect requirements for simulating MHD effects in liquid metals, which is the primary purpose for including magnets in a blanket test stand. The test articles for flowing liquid metal blankets are larger than their solid breeder counterparts because they require long inlet and outlet manifolds for flow development. The assumption used here is that these manifolds are each four hydraulic diameters* in length. We assume the test articles will also have flow straighteners outside the magnetic field. The test articles are envisioned as a linear flow sequence as in currently envisioned blankets (e.g. MARS) rather than "U" shaped. The latter configuration would reduce the length of the magnet but introduce unwanted complications in the test article. The overall length plus clearance width and height determines the working volume of the

* Hydraulic diameter is equal to four times the cross sectional area of flow divided by the length of the wetted perimeter.

magnet bore. The volume of fluid in the test articles and the pumping requirements establish the size of the liquid metal loops.

The information above is based on continuing efforts in the U.S. Blanket Technology Program[1] to assess requirements for experiments. As part of this program a liquid metal MHD loop is currently being readied at Argonne National Laboratory and is about the size indicated in the first column (10 ℓ). By comparison, the Experimental Lithium System (3800 ℓ inventory, 38 ℓ/s) at HEDL, is roughly equivalent to the second column (100 ℓ).

The previous descriptions give some feel for sizes and test parameters in test stand concepts for development of fusion nuclear components. There are also mutually exclusive or difficult combinations of features that limit the choices for non-neutron test stands.

A high flux of neutrons, bombardment by charged particles and a strong magnetic field (parallel to the first wall) for most practical purposes are mutually exclusive features except in a fusion-based device. For example, one might imagine installing a large magnet in the pool of a reactor such as ORR to combine the leakage spectrum with a strong magnetic field. However the field vector would be normal to rather than parallel to the neutron source (i.e. surface of constant neutron flux) as in a fusion device. Also the adverse impact on the reactor structure and instrumentation from the operation or potential failure of the magnet as well as the installation itself present formidable obstacles. Similarly, there is probably a conceptual basis for simultaneous irradiation and plasma bombardment. However, the engineering of such a feat, especially with high enough flux of particles at the appropriate energies is far from straightforward.

The limitation of charged particle bombardment across magnetic fields is fairly obvious from plasma confinement in fusion reactors. The orbiting diameter of a 10 keV deuterium atom in six tesla field is about the size of a pencil (0.6 cm). However, a mirror-like test stand (discussed later) with the plasma born within the field lines has been proposed.

Now let us consider several combinations of features that might be of interest as separate test stands for nuclear components. Table 10.2-3 gives several combinations (A-E) of features that might reasonably be proposed for non-neutron test stands. The numbers at the bottom are a judgment about their

Table 10.2-3. Combinations of Features for Test Stands

| Combinations of Features* | A. Surface Heat, Pulsed Field | B. Plasma, Mag. Field | C. Surface Heat, Magnet | D. Surface & Bulk Heat, Magnet | E. Surface & Bulk Heat |
|---|---|---|---|---|---|
| **Test Stand Features** | | | | | |
| Coolant | | | | | |
| Water or Helium | X | X | - | - | X |
| Liquid Metal | - | - | X | X | - |
| Salt | - | - | - | or X | - |
| Purge Gas | - | - | - | - | X |
| Steady Magnetic Field | - | X | X | X | - |
| Pulsed Field | X | - | - | X | - |
| Surface Heat | X | X | X | X | X |
| Plasma Bombardment | - | X | - | - | X |
| Bulk Heat | - | - | - | X | X |
| Distortion/Stress | X | X | - | - | X |
| Vacuum | X | X | X | X | X |
| **Usefulness of Test Stand Options** | | | | | |
| **Multiple Interactions Tests** | | | | | |
| First Wall/Limiter | 2 | 1 | 2 | - | - |
| Blanket - Liq. Met. Circ. | - | - | 2 | 1 | - |
| Blanket - Solid Breeder | - | - | - | - | 2 |
| Blanket - Salt Cooled | - | - | - | 1 | - |
| **Partially Integrated Tests** | | | | | |
| Integrated FW&B Liq. Met. | - | - | 2 | 2 | - |
| Integrated FW&B Solid | - | - | - | - | 3 |

1. Most needs fulfilled.
2. Many needs fulfilled - significant omissions.
3. Major shortcomings.

* X's in columns indicate those particular features included in combination A, B, C, D or E.

usefulness for multiple interaction tests and for integrated tests. Subsequent sections discuss test stands for limiters and first walls, solid breeder blankets and liquid metal blankets.

### 10.2.1 Test Stands for Limiters and First Walls

For limiters, divertor collector panels and first walls, the primary concerns for a test environment are thermal loads, particle fluxes, transient magnetic loads, neutron radiation and for liquid-metal-cooled limiters, a steady-state magnetic field. Reasonable combinations for non-neutron test stands include: (a) combined thermal and charged particle loads and (b) magnetic field and surface heating. The introduction of transient electromagnetic effects is possible for large test articles by using surface heating in an electromagnetic test stand (e.g. FELIX, see later discussion). Studying the motion of material melted by plasma disruptions seems possible on a small scale (10 $cm^2$) by simulations where material is melted and eddy currents are then induced by a pulsed field.

Combinations A and B in Table 10.2-3 are appropriate for testing plasma-side heat sinks but not for integrated blanket tests. A (He or $H_2O$ coolant, surface heat, pulsed magnetic field) offers simultaneous surface heating and magnetic loads and would be useful for thermal fatigue with loads from intermittent electromagnetic transients and, with an appropriate heating source, for short term tests on melt layer motion. B (He or $H_2O$ coolant plus plasma bombardment) offers the capability to do erosion and redeposition studies using fusion-based source but excludes the possibility of transient electromagnetic loads. Mechanical loads, for example helium overpressure, or supports that oppose bending produced by temperature gradients could be added to the heating and magnetic field for A and B.

For liquid-metal-cooled limiters (or first walls), the presence of a strong magnetic field is mandatory because of the pronounced effects of MHD on heat transfer. The magnetic field in combination C (liquid metal coolant, surface heat and magnetic field) provides the appropriate MHD effects but probably precludes the use of plasma sources for simulating plasma materials interaction except in a fusion device.

The U.S. program has utilized several test stands for surface heating and has supported various single effects tests (radiation effects, sputtering,

etc.). Table 10.2-4 lists the features for the surface heating test stands. Work in ESURF and ASURF, Westinghouse facilities located near Pittsburgh[2,3] has been terminated. Completion of the PMTF, the Plasma Materials Test Facility located at Sandia-Albuquerque[4] is expected in mid-1985.

Although the PMTF will utilize an ion beam source, its primary function will be high power for surface heating over relatively large areas. Its high ion energies and beam impurities are not appropriate for studies of erosion and surface related behavior. Another ion source PISCES[5] at UCLA is also operated for the fusion program. Its primary mission is simulations of particle removal (pumping) rather than surface heating.

A working concept for a test stand combining a magnetic field and ion bombardment (B in Table 10.2-3) has been developed by Argonne National Laboratory.[6] The facility is based on a mirror with RF stabilized end cells and can produce temperatures and densities of ions and electrons representative of edge conditions expected in tokamak reactors and produce both erosion and redeposition.

### 10.2.2 Test Stands for Solid Breeder Blankets

Primary concerns for a test environment relate in large part to tritium production and release from the solid breeder. For thermomechanical testing of a solid breeder module, bulk heating of the breeder and surface heating of the first wall are required. For some configurations (e.g. breeder-out-of-tube) bulk heating may be possible using RF power. Preliminary investigations of this heating technique have been performed at Argonne National Laboratory and a bench test is in preparation.

Various basic and single effects tests on solid breeders have been performed as part of the U.S. program, including mechanical, physical properties, the effectives of radiation and equilibrium thermodynamics. TRIO, an in-reactor tritium recovery test[7] was in miniature a multiple effects test although temperature gradients and radiation damage were relatively low.

A thermomechanical test[8] representing a unit cell (coolant tube surrounded by breeder) in a STARFIRE-type blanket was designed as a possible predecessor to an in-reactor multiple effects test. The work was part of the Blanket Technology Program, however this test was never realized.

Table 10.2-4* High Heat Flux Test Facilities

| Features | ESURF | ASURF | SANDIA e-Beam | PMTF |
|---|---|---|---|---|
| Heat Source | e-beam<br>150 kV<br>5-330 mA | e-beam<br>16 kV<br>6 A | e-beam<br>30 kV<br>1 A | H-ion beam RF<br>40 kV @ 40 A<br>or 20 kV @ 80 A<br>30 sec pulses |
| Power Output | 50 kW peak<br>36 kW cont. | 100 kW peak<br>64 kW cont. | 30 kW cont. | 1600 kW |
| Target Area | .01 - 500 $cm^2$ | .01 - 10,000 $cm^2$ | .01 - 100 $cm^2$ | 380 $cm^2$ |
| Heat Flux | .1 - 5000 $kW/cm^2$ | .01 - 10,000 $kW/cm^2$ | .3 - 3000 $kW/cm^2$ | 2 $kW/cm^2$ |
| Heater Life | 40 hours | 1000 hours | 40 hours cont.<br>400 hours pulsed | unknown |
| Coolant | water | water | water | water |
| Pressure | 1000 psi | 2200 psi | 300 psi | 1000 psi |
| Flow Rate | 20 gpm | 60 gpm | 50 gpm | 500 gpm |
| Heat Removal | 100 kW | 2000 kW | 30 kW | 10,000 kW |
| Vacuum Size | $10^{-4}$ Torr | $10^{-5}$ Torr | $10^{-5}$ - $10^{-7}$ Torr | $10^{-4}$ - $10^{-6}$ Torr |
| Tank Size | 28 $ft^3$ | 226 $ft^3$ | 9 $ft^3$ | 55 $ft^3$ |

* Table from Reference 5.

The generation of bulk heating is important for simulating thermomechanical performance. Experiments are in preparation at Argonne National Laboratory to demonstrate the use of RF heating to produce bulk heating in a test article with nine unit cells (coolant pipes surrounded by $LiAlO_2$). The decrease in nuclear heating with depth into the blanket can also be simulated with this method. The use of RF bulk heating with surface heating, as in E (Table 10.2-3), would offer thermo-mechanical simulation for example, for the study of heat transfer and thermal fatigue (cracking of breeder) in an assembly where the coolant is contained in tubes. The application of RF heating to breeder-in-can concepts has not yet been investigated.

### 10.2.3 Test Stands for Liquid Metal Blankets

Magneto-hydrodynamics (MHD) will drastically affect heat transfer and may also affect corrosion in circulating (self-cooled) liquid metal blankets. The primary concerns for a test environment are a strong magnetic field, sufficiently long flow paths to obtain fully developed flow and surface heat (first wall). The influence of temperature profiles in the coolant as a result of bulk heating may be important in full scale (act alike) simulations. This point is discussed in Chapter 6 in Sections 6.2.2 and 6.2.3.

A combination of non-neutron multiple effects tests appears to offer substantial benefit as support of a full scale demonstration of a liquid metal blanket. Four possibilities are suggested below.

Table 10.2-5. Liquid Metal Blanket Multiple Effects Tests

| Test Label | Magnetic Field | Surface Heating | Bulk Heating | Corrosion (Time/Temp) |
|---|---|---|---|---|
| MS | X | X | - | - |
| MSB | X | X | X | - |
| MC | X | - | - | X |
| MSC | X | X | X | X |

The two more basic multiple effects tests, MHD effects on heat transfer (MS) and on corrosion (MC), in addition to single effects tests can probably provide most of the data to support a full scale integrated test (e.g. large module or sector in a fusion engineering experimental reactor.) If thermo-mechanical simulations required bulk heating of the liquid, then bulk heating could be imperfectly simulated with upstream heaters. The temperature profiles created would persist for fairly long periods (> 1 minute). However the dominant issue governing heat transfer in liquid metal blankets is removing heat from the first wall.

Although the basic requirements of a loop and large magnet are similar, the experimental requirements for corrosion versus thermal-hydraulics are vastly different. Corrosion tests require long times, thousands of hours, high temperature operation with the fluid of interest and extreme care in controlling and monitoring temperature and impurity levels (O, N, etc.). Thermal-hydraulics tests using NaK simulate well the effect of MHD on heat transfer and the relatively low temperature operation permits the use of hot film probes to measure velocity profiles that could not be used with lithium or lithium-lead.

An analytical and experimental program[9] on liquid metal MHD was started in FY84 as part of the U.S. Blanket Technology Program. A liquid metal loop (340 ℓ. Nak, 22 ℓ/s) with a 2.5 tesla magnet (.76 x 1.8 m pole face) at Argonne National Laboratory (ANL) will have been completed by the end of 1984. These parameters will permit experiments with magnetic interaction parameters and Hartmann numbers above 1000; values above 1000 are deemed necessary for satisfactory simulation of effects in a fusion blanket where these parameters are of the order of $10^4$ - $10^5$. Small loops for corrosion studies with lithium and lithium lead are in operation also at ANL. The only large lithium loop in operation is the Experimental Lithium Loop (3800 ℓ Li, 38 ℓ/s) constructed at the Hanford Engineering and Development Laboratory as a prototype for the Fusion Materials Irradiation Test Facility.[10]

## 10.3 Existing Test Stands and Future Needs

### 10.3.1 Test Stands for Blankets

Various facilities around the U.S. have basic elements for test stands

Table 10.3-1. Examples of Institutions With Existing Capabilities

| Basic Elements | Some Existing Facilities* |
|---|---|
| Coolant/Heat Rejection | |
| Pressurized Water | ANL, BW, CE, CU, EGG, HEDL, LANL, PNL, WEC |
| Helium | EGG, GA, HEDL, ORNL, PNL |
| Li or Li-Pb | HEDL (Li), (small loops ANL, ETEC, WEC) |
| (Na or NaK) | ANL, EGG, ETEC, HEDL, WEC |
| Salt | SNL |
| Surface Heating | LLNL, MDAC, ORNL, SNL, WEC |
| Bulk Heating | -- |
| Magnet | AEDC, ANL, AVCO, CDIF |

* Abbreviations for host institutions.

AEDC -- Arnold Engineering and Development Center (TN)
ANL -- Argonne National Laboratory (IL)
AVCO -- AVCO-Everett Research Laboratory (MA)
BW -- Babcock & Wilcox (VA)
CDIF -- Components Development and Integration Facility (MT)
CE -- Combustion Engineering Inc. (CT)
CU -- Columbia University (NY)
EGG -- EG&G Idaho (ID)
ETEC -- Energy Technology Engineering Center (CA)
GA -- General Atomic Technologies (CA)
HEDL -- Hanford Engineering Development Laboratory (WA)
LANL -- Los Alamos National Laboratory (NM)
LLNL -- Lawrence Livermore National Laboratory (CA)
MDAC -- McDonnell Douglas Astronautics Company (MO)
NASA -- NASA Lewis Research Center (OH)
ORNL -- Oak Ridge National Laboratory (TN)
PNL -- Battelle Pacific Northwest Laboratories (WA)
SNL -- Sandia National Laboratory (NM)
WEC -- Westinghouse Electric Corporation (PA)

but, as might be expected, multiple effects test stands appropriate for fusion are not a forthcoming legacy from other technologies. Table 10.3-1 gives examples of large test stands that exist at various locations and have a basic element relevant to fusion needs. The list is not intended to be comprehensive and is based in part on a survey[11] done by EG&G Idaho for the Blanket Technology Program.

The important point here is that a fairly extensive survey of major institutions with experimental facilities uncovered no test stands that would be suitable for integrated tests, although some are suitable for single and multiple effects tests. This result is not unexpected because of the rather unique environment of fusion nuclear components.

The development of appropriate technology for fusion nuclear systems will involve explorations into basic scientific phenomena such as liquid metal MHD and radiation effects in materials and engineering-oriented testing for empirical verification that the complex and interacting phenomena are sufficiently well understood to proceed with the construction of advanced fusion devices. It is important to recognize that the wide range of possible tests on single effects and multiple effects, partially integrated and fully integrated tests, is not really a continuum of possibilities. The use of non-neutron tests will be attractive and cost effective insofar as they can provide data that will support the development of feasible fusion concepts. Some partially integrated non-neutron tests may provide very useful simulations of operating behavior, for example in circulating liquid metal blankets. However, if testing must provide simulation of failure modes, then fully integrated testing is the only possible answer. For example, non-neutron tests for liquid metal blankets may be able to simulate well the liquid metal flow and heat transfer at the first wall; however effects such as stress relaxation due to irradiation creep of the structure cannot be simulated without neutrons.

The need for several future test stands for the development of fusion nuclear technology seems clear even now. The exact mix between non-neutron and neutron test stands will become more evident through studies like FINESSE as we move into a generation of tritium breeding fusion devices.

### 10.3.2 Test Stands for High Heat Flux Components

There are several facilities in operation or under construction that can

be used for testing plasma interactive materials that are subjected to high heat fluxes. The key question is how well these facilities simulate the actual environment and operating conditions. A summary of facilities that are past the planning stage is presented in Table 10.3.2-1. A more detailed characterization is presented in Reference 12.

These facilities can be grouped by bombarding particle type and energy. The electron beam facilities have similar characteristics. All are scanned, either raster or line scan. Thus, very high heat fluxes may be obtained by a preprogrammed scan pattern that limits the target area. In this way, disruption heat fluxes can be simulated. The facilities are generally capable of steady state operation. The principal objection to electron beam testing is that most components are subject primarily to ion damage; thus, the true environment is not being simulated. The main differences are depth of penetration of the energy deposition, energy imparted to and amount of material leaving a surface in a disruption event and material loss by sputtering. The HEDL electron beam facility will be coupled to a hot cell. Components may be first irradiated in a nuclear reactor and then subjected to high heat fluxes and stresses. This sequential technique is as close as we can come to the synergistic effects of nuclear radiation and the plasma operational environment.

The ion beam facilities can be separated into two groups by the energy of the incident particles. The PMTF and the neutral beam test stands at LBL and ORNL use high energy ions to obtain high heat fluxes over moderate size areas. Because ions are used, the environment is close to that of a fusion device. The high ion energy provides a good simulation of neutral beamline components, beam dumps, regions of high charge exchange flux from neutral beams, and mirror end cell components. However, the particle energies are significantly higher than the particle energies at plasma edge of a tokamak. These facilities are limited to moderate pulse lengths of about 30 seconds. The PISCES, TRW and ISURF facilities use low energy ions. They are principally to perform physics, materials and engineering experiments such as sputtering, blistering, gas conductances and pumping efficiencies. The low energy facilities can generally run steady state.

All of the electron and ion beam facilities listed in Table 10.3.2-1 are essentially accelerators. Another approach to high heat flux component

Table 10.3.2-1. High Heat Flux Test Facilities

| Facility Name/Laboratory | Particle (keV) | Energy (keV) | Power (kW) | Area ($cm^2$) | Heat Flux ($kW/cm^2$) | Status |
|---|---|---|---|---|---|---|
| ESURF/Westinghouse | $e^-$ | 150 | 36 | 0.01-500 | < 5000 | Operational |
| ASURF/Westinghouse | $e^-$ | 16 | 64 | 100-10,000 | < 2000 | Operational |
| /Sandia | $e^-$ | 30 | 30 | 0.01-100 | 0.3-3000 | Operational |
| /HEDL | $e^-$ | 12-25 | 60 | 1-200 | 0.3-60 | Construction[a] |
| PMTF/Sandia | H ions | 40-80 | 1600 | 100-200 | 8 | Construction |
| PISCES/UCLA | H,D,He ions | 0.05-0.5 | 25 | 50 | 0.05-0.25 | Operational |
| /TRW | Gas ions | 0.05-2 | 20 | 100 | 0.005-0.2 | Operational |
| /LLNL | H,He ions | 50-100 | 10 | 10-100 | 0.1-1 | Operational |
| ISURF/Westinghouse | H to Xe ions | 0.05-0.5 | | 1 | $6 \times 10^{-4}$ | Operational |
| /LBL | H,D ions | 40-120 | 2000 | ~ 1000 | ~ 2 | Operational |
| METF/ORNL | H ions | 80 | 4800 | 1000 | < 30 | Operational |
| HETF/ORNL | H ions | 120 | 3600 | 100 | < 50 | Operational |

[a] e-beam operational.

testing is to use a simple confinement device. This allows testing in a mixed spectrum of ions, electrons and neutrals and in the presence of a magnetic field. Ion redeposition and sheath effects can best be studied in such a device. The most promising approach is to use an open confinement system such as a tandem mirror. The particle energy can be adjusted by supplemental heating. There have been several scoping design studies of devices of this type but no confinement device has been used primarily for high heat flux component testing.

In summary several facilities are operational or under construction to test plasma interactive components. One of these, the HEDL e-beam facility, will be in a hot cell to allow testing of activated components. However, none of these facilities yet provide an adequate simulation of the expected plasma operational environment.

## References for Chapter 10


1. R. E. Nygren, "Recent Progress in the First Wall/Blanket/Shield Program," 10th Symposium on Fusion Engineering, Philadelphia, PA, December 1983, IEEE Cat. No. 83-CH1916-6.

2. J. R. Easoz, R. Bajaj, R. E. Gold and J. W. H. Chi, "Thermo-mechanical Testing of First Wall Test Pieces in ESURF," Supplement to Nuclear Technology/Fusion 4, (2) Sept. 1983, p. 780.

3. H. D. Michael, J. Lempert, J. W. H. Chi and R. P. Rose, "Large Area Surface Heating Facility (ASURF) & Test Program for First Wall Design Concepts," ibid. p. 785.

4. W. B. Gauster, J. A. Koski and R. D. Watson, "Materials Requirements for High Heat Flux Components," Journal of Nuclear Material 122&123, 1984, p. 80.

5. D. M. Goebel and R. W. Conn, "Observations of Advanced Particle Removal Rates in Pump Limiter Simulation Experiments," to be published in Proceedings of 6th Int'l Conf. on Plamsa Surface Interactions in Fusion Devices, Nagoya, Japan (May 1984).

6. J. N. Brooks, R. F. Mattas, D. A. Ehst, C. D. Boley and N. Hershkowitz, "An Impurity Control Test Facility (ICTF) for the Study of Fusion Reactor Plasma/Edge Materials Interactions," Argonne National Laboratory, ANL/FPP/TM-188, May 1984.

7. R. G. Clemmer, et al., "The TRIO-01: In-Situ Tritium Recovery Results," Journal of Nuclear Material, 122&123, 1984, p. 890.

8. G. A. Deis, "Pre-test Analysis of the Solid Breeder Integral Simulation Test for PE-II," Supplement to Nuclear Technology/Fusion 4 (2), Sept. 1983, p. 791.

9. B. Picologlou, C. B. Reed, R. Nygren and J. Roberts, "Magneto-fluid-dynamic Issues for Fusion First Wall and Blanket Systems," Fourth Beer-Sheva International Seminar on Magnetohydrodynamic Flow and Turbulence, Beer Sheva, Israel (Feb. 1984).

10. J. M. Atwood, J. D. Berg, R. Kolowith and W. C. Miller, "Experimental Lithium System Experience," Third International Conference on Liquid Metal and Technology in Energy Production, Oxford, England (April 1984).

11. A. G. Ware and G. R. Longhurst, "Test Program Element II Blanket and Shield Thermal-hydraulic and Thermomechanical Testing, Experimental Facility Survey," published by EG&G Idaho in 1981 (undated report).

12. M. A. Abdou, et al., "Magnetic Fusion Energy Plasma Interactive and High heat Flux Components, Volume II, Technical Assessment of the Critical Issues and Problem Areas in High Heat Flux Materials & Component Development," PPG-815, UCLA-ENG-84-25, June 1984.

# CHAPTER 11

# ACCELERATOR-BASED POINT NEUTRON SOURCES

TABLE OF CONTENTS


| | | Page |
|---|---|---|
| 11.1 | Introduction | 11-1 |
| 11.2 | Point Neutron Sources for Fusion Experiments | 11-1 |
| | 11.2.1 Rotating Target Neutron Source (RTNS-II) at LLNL | 11-2 |
| | 11.2.2 Intense Neutron Source (INS) at LANL | 11-2 |
| | 11.2.3 LAMPF A-6 Target Station at LLNL | 11-2 |
| | 11.2.4 Fusion Materials Irradiation Test (FMIT) Facility at HEDL | 11-3 |
| 11.3 | Point Source Potential | 11-3 |
| 11.4 | Conclusion | 11-4 |
| References | | 11-6 |

# 11. ACCELERATOR-BASED POINT NEUTRON SOURCES

## 11.1 Introduction

Point neutron sources are attractive for irradiation testing because of their promise of easy access, simplicity, and relatively low cost. In reality, point sources often suffer from limited neutron intensity, inappropriate neutron spectra, and difficulties associated with operating very high technology machines. It should also be noted that as neutron exposures approach levels of interest to fusion reactor technology, the costs associated with utilization of point sources increase dramatically. The increased costs are associated primarily with shielding and remote handling. Still, total testing costs are generally much less than for comparable tests conducted in fission reactors.

This chapter will concentrate on the various neutron sources proposed over the recent past for testing fusion materials. Prior to this writing, no point source with sufficient flux for blanket or first wall experiments has been formally advanced. However, use of an advanced FMIT type machine capable of large scale testing will be discussed as an "upper limit" on point neutron source application.

## 11.2 Point Neutron Sources for Fusion Experiments

A number of point neutron sources have been suggested for fusion materials testing. Only the RTNS-II at Livermore is actually in operation. In the mid-70's the INS was pursued at LANL as a somewhat larger test volume than RTNS-II, but it was eventually supplanted by FMIT which had sufficient flux and testing volume to fulfill the materials testing needs for the U.S. fusion program. Recently, construction of FMIT was postponed indefinitely such that only the RTNS-II will be available for testing in the foreseeable future. It has been suggested that a large volume of relatively high neutron flux will be available at LAMPF in the near future. The potential for fusion testing in LAMPF has been clouded by concerns over the appropriateness of the neutron spectra to blanket and first wall experimental objectives.

### 11.2.1 Rotating Target Neutron Source (RTNS-II)[1] at LLNL

RTNS-II generates neutrons by bombarding a tritium-containing target with 400 KeV deuterons. Neutrons are produced by the DT fusion reaction which produces a nearly monoenergetic 14 MeV neutron spectra. The tritium is held in a target in the form of zirconium hydride which is coated on a water cooled copper disk. The deuteron beam is focused as a 1 $cm^2$ spot on the target. Rotation is used to reduce heat loads to levels which allow the tritium to be retained on the target. A maximum flux level of about 5 x $10^{12}$ $n/cm^2$-sec is attained in a test volume of less than 0.1 $cm^3$. While this is adequate for low fluence testing of miniature material specimens, RTNS-II is much too small for nuclear experimentation supporting first wall and blanket multiple effects tests.

A proposal to upgrade RTNS-II capabilities by about 16-fold has been made. While this could significantly improve material test capabilities, RTNS would still be too small for multiple effects.

### 11.2.2 Intense Neutron Source (INS)[2] at LANL

The intense neutron source (INS) was intended to generate neutrons by injecting a 1.1 amp 300 KeV tritium beam into a gas target consisting of a supersonic deuterium jet. The deuterium density in the jet provides for sufficient (d,t) reaction to yield a neutron source of about $10^{15}$ n/sec. The limiting feature of this arrangement is the ability of the gas target to remove the heat generated by the beam. Since the neutron source is more or less cylindrical in shape, testing is conducted in an annulus around the target. A peak flux of 1 x $10^{14}$ $n/cm^2$-sec 14 MeV neutrons was predicted for a few tenths of a centimeter next to the target. Since flux drops off as $1/r^2$, the volume of test space at $10^{13}$ $n/cm^2$-sec or better was expected to be about 1 $cm^3$. Again as with RTNS-II, this space would have been useful for the limited material testing but is not large enough for multiple effects experimentation.

### 11.2.3 LAMPF A-6 Target Station[3] at LANL

The Los Alamos Meson Physics Facility (LAMPF) is an 800 MeV 1 mA proton accelerator. The A-6 target station at LAMPF offers the potential for testing at relatively low neutron flux with test volume approaching levels practical

for integrated experimentation. At the A-6 target position, spallation neutrons from the LAMPF beam stop provides a flux of about 1 x $10^{13}$ n/$cm^2$-sec at a volume of 0.02 $m^3$. The neutron spectra is much different than for fusion with most having energies below 1 MeV but a significant portion having energies reaching almost to $10^3$ MeV. The combination of flux, spectrum and duty factor are sufficient to provide about a displacement level of 1 dpa/year in copper. While of interest to materials science, the flux/spectrum/duty factor combination is probably too small for multiple effects testing for high exposure materials testing.

### 11.2.4 Fusion Materials Irradiation Test (FMIT) Facility[4] at HEDL

The Fusion Materials Irradiation Test Facility was specifically designed to meet the needs of the U.S. fusion program for a "fusion like" materials neutron irradiation facility. In FMIT, neutrons would be produced by bombarding a flowing lithium target with 35 MeV deuterons. The (d,Li) reaction would provide a broad neutron energy spectra averageing around 14 MeV. Damage calculations indicated that the spectra from 35 MeV deuterons on lithium was appropriate for fusion materials evaluation.

FMIT would provide 10 $cm^2$ of test space with a neutron flux of 1 x $10^{15}$ n/$cm^3$-sec or greater. approximately 500 $cm^3$ would be available at 1 x $10^{14}$ n/$cm^2$-sec or greater. While peak neutron flux levels and volume were expected to be excellent for small specimen testing, the steep flux gradients and source characteristics are inappropriate for multiple effects experiments. It should be noted that FMIT construction has been postponed pending the outcome of negotiations with the EEC and Japan concerning joint sponsorship.

## 11.3 Point Source Potential

In an effort to explore the potential of point sources for multiple effects testing, a device for producing a fusion-like neutron environment in a 23x23x23 cm cube was scoped. The approximately 10-inch cube was assumed to be the smallest size of interest to integrated experiments; however, depending on the results of the FINESSE study, a different lower limit may emerge.

The approach taken was to scale-up the FMIT accelerator to the maximum possible using relatively small extrapolations of existing technology. The result yielded a neutron flux of about 5 x $10^{13}$ n/$cm^2$ at the front face of the

ten by ten inch cube. Gradients from front to back of the cube can be adjusted over a reliably wide range. While it cannot be stated that gradients will match the precise requirements for "act-alike" tests of reduced size, there is considerably more flexibility than in other neutron generating machines.

For lack of a better designation, we call this source "Super-FMIT." In Super-FMIT, 14 MeV average energy neutrons are produced by interaction of a 70 MeV beam of $D_2^+$ ions with a flowing lithium target. The accelerator consists of a radio frequency quadrupole of the zero-mode type[5] that supports four accelerating channels, and an Alvarez Linac in which the drift tubes accommodate four beams. The multiple beam lines are contained in a single RF tank. Using the multiple beams and $D_2^+$ instead of $D^+$ as in FMIT, a 1 amp beam can be obtained. The beam interacts with a large flowing lithium target which dissipates less energy per unit area than FMIT and, therefore, should be easier to engineer and operate. Separate aiming of the beams gives flexibility that may be used to achieve the desired flux shaping and gradients.

## 11.4 Conclusion

The primary point source for fusion materials testing in use in the United States in the RTNS-II. Other more powerful sources are needed for materials testing but have been canceled or deferred. The small test space of point sources considered to date precludes their use in integrated testing, however a scale-up of the FMIT concept could produce a point source of interest to nuclear component testing activities.

Table 11-1 Point Neutron Sources for Fusion Multiple Effects Testing

| Facility | | Peak Flux | Testing Volume | Applicable to Multiple Effects |
|---|---|---|---|---|
| RTNS-II | In-Use for Materials Testing | $\sim 5 \times 10^{12}$ n/cm$^2$-sec | $\sim 0.1$ cm$^3$ | No |
| INS | Conceptual Design Completed - Project Terminated | $1 \times 10^{14}$ n/cm$^2$-sec | $\sim 1$ cm$^3$ | No |
| LAMPF A-6 | Operational | $1 \times 10^{13}$ n/cm$^2$-sec | $\sim 0.02$ m$^3$ | No |
| FMIT | Design Completed Project Deferred | $1 \times 10^{15}$ n/cm$^2$-sec | $\sim 10$ cm$^3$ | No |
| SUPER-FMIT | Scoping Study | $5 \times 10^{13}$ n/cm$^2$-sec | $\sim 0.016$ m$^3$ | Yes |

## References for Chapter 11


1. Anonymous Experimenters Guide, Rotating Target Neutron Source II Facility LLL, M-094 (July 1978).

2. Armstrong, Dale D., Emigh, Robert C., Meier, Karl I., Meyer, Earl A., and Schneider, David J., "An Intense Neutron Source Facility," Nucl. Inst. and Methods, 145, 127 (1977).

3. Wechsler, M.S., Sommer, W.F., "Spallation Radiation Damage and the Radiation Damage Facility at the LAMPF A-6 Target Position," J. Nucl. Mat., 122, 1078 (1984).

4. Trego, A.L., Hagan, J.W., Opperman, E.K., Burke, R.J., "Fusion Materials Irradiation Test Facility for Fusion Materials Qualification," Nucl. Tech./Fusion, 4, 695 (1983).

5. A. Schempp, et al., "Status of the Frankfurt Zero-Mode Proton RFQ," IEEE Trans. on Nuclear Science, Vol. NS-30, 4, p. 3536 (August 1983).

# CHAPTER 12

# UTILIZATION OF FISSION REACTORS

TABLE OF CONTENTS


Page

12.1 Key Issues for Fission Utilization ..... 12-2
12.1.1 Radiation Damage ..... 12-2
12.1.2 Power Density ..... 12-3
12.1.3 Lithium Burnup Rate ..... 12-4
12.1.4 Test Volume ..... 12-4
12.1.5 Non-Nuclear Conditions ..... 12-5
12.1.6 Reactivity Considerations ..... 12-5
12.1.7 Availability for Testing ..... 12-5
12.1.8 Cost ..... 12-6

12.2 Technical Approach ..... 12-6
12.2.1 Facility Survey ..... 12-7
12.2.2 One-Dimensional Criticality Study ..... 12-12
12.2.3 Two-Dimensional Parameter Study ..... 12-13
12.2.4 Test Development/Analysis ..... 12-15
12.2.5 Summary of Technical Approach ..... 12-20

12.3 Analysis of Key Issues ..... 12-21
12.3.1 Radiation Damage ..... 12-21
12.3.2 Power Density/Lithium Burnup Rate ..... 12-23
12.3.3 Test Volume ..... 12-35
12.3.4 Non-Nuclear Conditions ..... 12-37
12.3.5 Reactivity Considerations ..... 12-39
12.3.6 Availability for Testing ..... 12-41
12.3.7 Cost ..... 12-41

12.4 Conclusions on Technical Usefulness of Fission Testing ..... 12-42

12.5 Overall Conclusions on Utilization of Fission Reactors ..... 12-43

References ..... 12-44

# 12. UTILIZATION OF FISSION REACTORS

One option for performing the nuclear engineering testing needed for fusion development is utilization of fission reactors. Fission testing capabilities have been investigated, to some degree, in previous efforts, and some unique advantages have been found. Typically, previous efforts investigated the use of specific reactors for specific tests, such as those mentioned in Appendix F (a discussion of the utilization of fast reactors). Although this type of real facility-specific information is extremely important in identifying particular advantages and disadvantages for the purposes of the FINESSE study, it is also necessary to determine how large a role fission testing can play in the overall fusion engineering development effort, and in what particular areas it can best be used. It is important to note that the degree to which fission testing is used in fusion development depends somewhat on the overall fusion development strategy; that is, scenarios can be envisioned which do not involve fusion engineering test devices until late in the development of a DEMO. In such cases, fission testing would probably be applied to a greater degree than in other scenarios in which fusion test devices are available early in the program. Conversely, the technical capabilities and programmatic considerations related to fission testing will impact decisions about the development strategy to be adopted. For instance, if fission testing could solve most of the critical issues of fusion development and if there were no restrictions on its use, the need for fusion engineering test devices might be somewhat reduced. For these reasons, it is difficult to specify how fission testing should be utilized in fusion engineering development without considering the strategy as a whole; this is one of the objectives of FINESSE. It is important, however, to examine the technical and programmatic constraints on the use of fission testing, in order to clarify the advantages and disadvantages, and thereby further define the role of fission testing in fusion development.

In this connection, the discussions which follow focus only on engineering testing issues. Fission reactors are currently being used in the fusion program for materials testing, and the continued use of fission testing in this capacity is assumed. The focus of this effort is on the

performance (or failure) of engineered blanket components or systems, rather than on the specific properties of the materials involved. This will require tests of various sizes and configurations, from the smallest blanket subunit up to and including full modules. In addition, greater emphasis is placed, in the following discussion, on multiple-effects and integrated testing than on single-effects testing. While the environmental requirements for single-effects testing are generally less severe, more complex tests can have stringent requirements which imply more costly test devices and greater impact on program strategy. Thus, higher-level tests are of more interest (initially) to the FINESSE program, and are suitably emphasized in the remainder of this chapter.

## 12.1 Key Issues for Fission Utilization

There are a number of issues which are typically mentioned as technical or programmatic restrictions which limit the usefulness of fission-based testing for fusion engineering development. These are listed in Table 12.1-1, and explained below. The concern over some of these individual issues (such as power density, lithium burnup, etc.) can be reduced to a limited extent, whereas for others (such as test volume and availability for testing) it cannot. However, even if individual issues can be eliminated by test design, for multiple effects tests, this typically results in degraded performance in other areas. Thus, these issues must be considered as a coupled set which together may restrict the usefulness of fission testing. They have only been used here to focus the analyses and discussion, and conclusions are presented on the importance of each.

### 12.1.1 Radiation Damage

One of the obvious differences between the "fusion environment" and the "fission environment" is the neutron spectrum. This is typically cited as a fundamental problem with fission testing. One of the primary areas where the spectrum is known to be extremely important is in radiation damage in materials. There are three main considerations. First, is the type of damage produced in the test the same as is expected in the actual

Table 12.1-1. Key Issues for Utilization of Fission Reactors

| | | |
|---|---|---|
| 1. | Radiation Damage | - types and rates |
| 2. | Power Density | - magnitude spatial profile |
| 3. | Lithium Burnup Rate | - magnitude spatial profile |
| 4. | Test Volume | - total of existing test locations |
| 5. | Non-Nuclear Conditions | - magnetic field surface heat particle flux mechanical forces |
| 6. | Reactivity Considerations | |
| 7. | Availability for Testing | |
| 8. | Cost | |

component operating on a fusion device? For instance, are there important threshold reactions which would occur in the fusion spectrum and not in the fission spectrum. Second, is the rate of damage production in the fission test close enough to that expected in actual operation? Third, can sufficient total damage be accumulated in a fission test to reveal important failure mechanisms and/or synergisms? These considerations apply primarily to structural materials, since radiation is predicted to play an important role in structural failure in most cases. Radiation damage is also important in solid breeders and multipliers.

### 12.1.2 Power Density

For many of the issues outlined in Section 3, the local power density, or its distribution over some volume, is an important factor. With regard to fission testing, there is concern over whether or not sufficient power density can be attained, given the neutron fluxes in current fission test reactors. If prototypical power densities cannot be attained, scaling will be required, and this will introduce the limitations and uncertainties discussed in Sections 5 and 6. There is also concern over the effect of the spectrum difference between fusion and fission on the power density profile in fission tests. Because of the higher thermal flux fraction in the fission spectrum, and the high $^{6}Li$ thermal cross section, high local

power density and higher power density gradients are expected near the fission core. This might require design of specific act-alike test modules to be compatible with the altered power density profile.

### 12.1.3 Lithium Burnup Rate

The issue of lithium burnup rate is closely related to the power density issue, since lithium reactions are typically responsible for a large fraction of the power density in blankets. There are two concerns here: the lithium burnup rate which can be attained in fission reactors, and the spatial profile. The overall burnup rate is important, since it is likely that some failure modes for ceramic breeders will be driven by lithium burnup, and thus realistic total burnup in tests is desirable. The profile is important for much the same reason, except that the objective in some tests may be to observe possible failure modes associated with the burnup gradient, such as differential swelling of the breeder.

### 12.1.4 Test Volume

The test volume available in fission reactors has been an area of some concern. In previous discussions in this area, considerable effort has been devoted to the packaging of fusion blanket tests so that they will physically fit into the fission reactor, while satisfying the requirements for test containment. Largely because of the containment requirements (resulting from the reactive materials, high temperatures, and high pressures), fusion blanket tests typically require rather large test space even for tests of simple configuration such as unit-cell tests. Tests of larger components, such as full-scale modules, obviously have space concerns, since the volume of the test assembly can be as large as the core itself. Thus, the question of whether or not acceptably-large test locations exist for fusion blanket tests of interest is not at all trivial. There is also a second related concern which has not been addressed extensively in the past; i.e., the question of whether or not a sufficient number of acceptable test locations exist to satisfy the needs of the fusion engineering program. From the testing needs defined in Section 4, it is apparent that hundreds of fission-based engineering tests

could be of interest. Presumably, if there were no restriction on the number of tests which could be run in fission reactors, the need for a fusion engineering test device might be reduced or delayed to some degree. Thus, the question of how many acceptable test locations exist (or could exist) is important to any considerations regarding engineering testing strategy.

### 12.1.5 Non-Nuclear Conditions

Considering all testing issues, neutrons are probably the single most important environmental factor. Nevertheless, other non-nuclear factors can be equally or more important for many individual issues. For instance, first-wall issues are driven as much or more by heat/particle flux as they are by neutron-related effects. The strength of fission-based testing is in the availability of neutrons, and an obvious question, therefore, is to what extent can other important effects be incorporated in fission-based tests. Particular effects of concern include particle flux, heat flux, magnetic field, and mechanical forces. The extent to which these effects can be included in fission-based tests will determine to a large degree the technical usefulness of the tests.

### 12.1.6 Reactivity Considerations

In considering any specific test to be performed in a fission reactor, core physics issues must be addressed early on. One important consideration in this area is the question of whether or not the reactor will be able to attain criticality with the test in place, given the usual conditions of excess reactivity, etc. This is important for fusion-blanket tests because they will involve test assemblies which will have large negative reactivities, and may, in addition, be physically large compared to the core. These considerations will limit the choice of test reactors and test locations.

### 12.1.7 Availability for Testing

Although there are many fission reactors which could be considered for use in fusion engineering testing, some may not actually be available

because of programmatic priorities or lifetime issues. This could limit the use of fission-based testing simply by limiting the number of facilities which could be accessed.

### 12.1.8 Cost

One aspect of fission testing which has not been investigated in detail is the cost compared to alternate approaches. This is generally believed to be an important advantage of fission testing with respect to fusion testing, simply because fission facilities currently exist.

## 12.2 Technical Approach

By examining the testing needs outlined in Section 4, the need for two general types of fission-based engineering tests can be defined. First, some tests require a rather large volume with a planar neutron source on one side. This type of test, which is referred to as slab module or core-side testing, is typified by a test of a full solid-breeder blanket module; this module is conceptually placed against the side of a fission-reactor core, which supplies neutrons in much the same geometry as the plasma in an actual reactor (Fig. 12.2-1). The general idea of such testing is to simulate nuclear conditions over a full-module area. The second general type of test which can be defined is the in-core or submodule experiment, which would fit entirely within the fission core. This type of experiment is smaller in size and less complex than a slab module test, and attempts to simulate nuclear conditions in some subassembly of the blanket module. In this case, the neutron source completely surrounds the test assembly. These two general types of tests are not the only types of fission-based tests which will be of interest; note in particular that capsule-type materials tests have not been mentioned since the focus in this section is on engineering testing. However, a combination of slab-type and submodule-type fission tests can resolve many of the issues discussed in Section 3, and this classification is useful in discussing the requirements for and differences between each type of test.

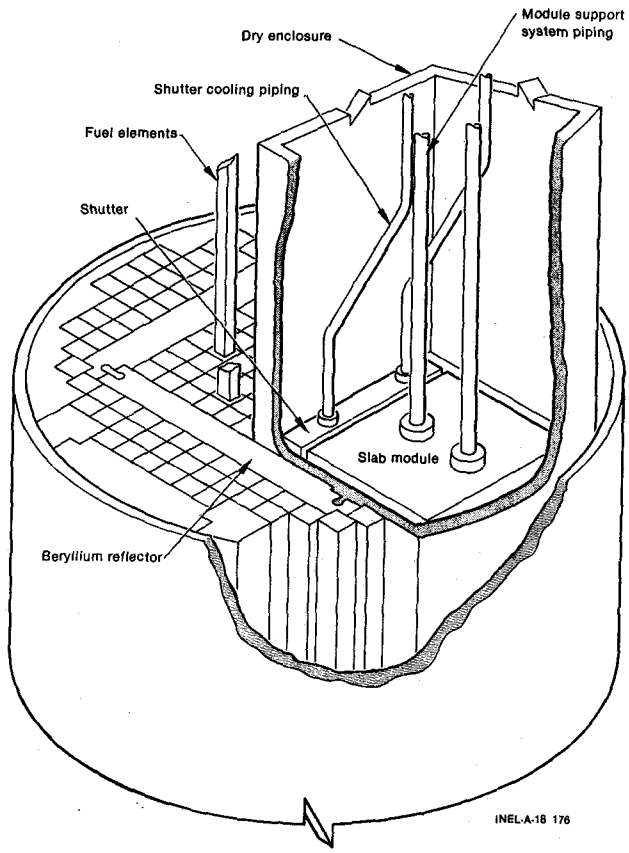


Figure 12.2-1. Cutaway view of slab module fission test configuration.

In order to address the key issues discussed in the previous section, four primary tasks have been defined. Each of these tasks has produced information on a number of key issues for slab and/or submodule test concepts. Several of the tasks are also interrelated, in that calculations performed for one task also yield output of interest in other tasks. Because of the tight interrelationships between these tasks, and the manner in which they relate to the key issues for fission testing, it is useful to discuss each task individually before detailing the results; the results are then discussed as they relate to the key issues.

### 12.2.1 Facility Survey

Most of the key issues depend to some extent on the particular characteristics of individual fission reactors. For instance, the fluxes attainable and the test volumes available will be different for each facility. Thus, in order to develop a clear picture in each of the key

areas, it is necessary to know what types of capabilities exist (or could reasonably exist) in the nation's (or world's) fission reactors. To develop this understanding, two related efforts were undertaken: first, a review of published specifications of test reactors, and second, a survey of a number of the "best" United States test reactors.

The purpose of the review of published specifications was twofold: first, to help in selecting fission reactor facilities to receive the survey, and second, to develop some idea of the total capabilities which exist today in fission reactors. Of particular interest is the number of test locations as a function of physical size, neutron flux, and configuration. This information can then be coupled with results from the other tasks, which give essentially the technical capabilities of tests as functions of size, flux, etc., to give an overall picture of the capabilities of fission testing. The review of published specifications used information available in standard manuals on U.S.[1] and foreign[2,3,4] test reactors. This information included the size of test locations, the neutron flux in each, as well as general information on the reactor such as power, core size, peak flux, etc.

The purpose of the survey of reactor facility capabilities was also twofold: first, to gain additional information on those fission reactors which appeared to be most suitable for fusion blanket engineering testing, and second, to develop some idea of the relationship between the published specifications and the true capabilities and potential for use in fusion testing. The first step in this effort was to select a number of reactor facilities to receive the survey. To accomplish this, the criteria shown in Table 12.2.1-1 were employed. The specifications of each reactor facility in the U.S.[1] were screened through these criteria to generate the list shown in Table 12.2.1-2. When the same criteria were applied to foreign reactor specifications, the list in Table 12.2.1-3 resulted. Note, however, that these lists are not intended to represent all of the acceptable reactor facilities. However, the lists do contain the largest and highest-flux thermal and fast reactors, and thus should yield a good sampling of the best capabilities for fusion testing. The next step in the survey was to distribute it to the facilities listed in Table 12.2.1-2.

Table 12.2.1-1. Test Reactor Selection Criteria

| | |
|---|---|
| 1. | Material/engineering type test reactor |
| 2. | Currently not decommissioned |
| 3. | Allows lead experiments (not just capsules) |
| 4. | Capable of steady-state operation |
| 5. | Test volume: |
| | (a) In-core test position >7 cm ID |
| | OR |
| | (b) Core-side test position >50 cm x 50 cm x 50 cm |
| 6. | Unperturbed fast flux (E > 0.1 MeV) in test location $\geq 5 \times 10^{13}$ $cm^{-2}s^{-1}$ |

The survey consisted of a cover letter describing the general purpose of the effort, a questionnaire with specific questions to be answered, and an attachment with additional information on the types of tests which would be of interest in fusion engineering. This format was chosen so that well-focused, specific, answers could be obtained while providing enough background information to allow some creativity in considering possible test characteristics (i.e., each facility operator could consider facility-specific modifications to increase the usefulness or capability of the reactor). The questionnaire consisted of four main sections: (a) one on overall current and projected facility status and availability; (b) one on existing technical capabilities for submodule-type tests; (c) one on existing technical capabilities of slab-type tests; and (d) one on possible modifications to the facility to provide additional or improved capabilities. To date, responses have been received from all facilities except NBSR, but detailed analysis of the responses has not been completed. Thus, for this interim report, discussion of the results of this task will be limited to information obtained from the review of published specifications.

Table 12.2.1-2. Capabilities of Selected U.S. Test Reactors

| Reactor | Location | Power (MW) | Exp. Neutron Flux $n/cm^2/sec$ | Exp. Size (cm) | Test Position Exp. Vol. (L) | Notes | Core Side Facility Dim. |
|---|---|---|---|---|---|---|---|
| ATR | Idaho | 250 | $1.5 \times 10^{15}$F | 7.6 Dia x 122 | 5.6 | 9 Flux Traps | None |
| EBRII | Idaho | 62.2 | $2 \times 10^{15}$F | 7.4 Dia x 36 | 1.5 | Na Cooled | None |
| FFTF | Washington | 400 | 3-7 x $10^{15}$F<br>6-7 x $10^{15}$F | 6.35 Dia x 91<br>10.92 Dia x 91 | 2.9<br>8.5 | 6 closed and open loops<br>3 open loops | None |
| HFIR | Tennessee | 100 | 1.3 x $10^{15}$F<br>1.5 x $10^{14}$Th | 13 Dia x 51<br>7 Dia x 51 | 6.8<br>2.0 | Flux Trap<br>2 ref. pos. | None |
| ORR | Tennessee | 30 | $4.5 \times 10^{14}$F | 7.8 Dia x 38.4 | 0.5 | Any core pos. | Pool Side<br>71 x 76 cm<br>5 x $10^{13}$ |
| PBF | Idaho | 28 | 8 x $10^{13}$Th<br>2 x $10^{13}$F | 15.5 Dia x 91 | 17.2 | | Possible<br>61 x 91 cm<br>? |
| NBSR | Maryland | 10 | 1 x $10^{14}$Th | 10.3 Dia x 74 | 6.2 | Vert. Thimbles | None |

Table 12.2.1-3. Capabilities of Selected U.S. Test Reactors

| Reactor | Location | Power (MW) | Exp. Neutron Flux $n/cm^2/sec$ | Exp. Size (cm) | Test Position Exp. Vol. (L) | Notes | Core Side Facility Dim. |
|---|---|---|---|---|---|---|---|
| DR-3 | Denmark | 10 | $1 \times 10^{14}$Th<br>$5 \times 10^{11}$F | 17.8 Dia x 61 | 15.2 | | None |
| HFR | Netherlands | 20 | $5 \times 10^{14}$1F | 14.5 Dia x 60 | 9.9 | Thru loop | Pool side<br>$0.8 \times 10^{14}$1F<br>77.5 x 72 cm |
| HFR | France | 57 | $1.5 \times 10^{15}$ | ? | ? | $D_2O$ Mod. | ? |
| MIR | USSR | 100 | $3 \times 10^{14}$F | 7.8 x 100 | 4.8 | In-core positions | ? |
| NRU | Canada | 200 | $1 \times 10^{14}$Th | 12 Dia x 300 | 33.9 | 3 loops | Possible<br>240 x 240<br>5 s $10^{13}$ |
| PLUTO | England | 25.5 | $1 \times 10^{14}$Th | 17.9 Dia x 61 | 15.1 | In $D_2O$ | None |
| SAFARI-I | So. Africa | 20 | $1 \times 10^{14}$Th<br>$2 \times 10^{14}$Th | 7.6 Dia x 61<br>15.2 Dia x 61 | 2.8<br>11.2<br>$1 \times 10^{14}$ | | Pool side<br>70 x 61 |
| SILOE | France | 15 | ? | ? | ? | ? | Possible<br>48 x 63<br>? |
| SM-1 | USSR | 75 | $5 \times 10^{14}$F | 10 Dia x 35 | 2.8 | Loop | None |

### 12.2.2 One-Dimensional Criticality Study

Currently, there is no experience in conducting large fusion engineering tests on the side of a reactor core. There are concerns over the requirements such tests would place on the facility, in terms of test volume, neutron flux, and excess reactivity. A serious consideration is: can a fission core be critical with a large negative reactivity on one or more faces of the core. This obviously affects the choice of reactors for such testing. One parameter which will be extremely important is the size of the reactor core; larger cores will be affected less by the presence of the test module. The main purpose of the 1-D Criticality Study is to examine the reactivity effect of the slab test module as a function of fission core thickness, with the hope of determining a core thickness below which criticality probably cannot be attained.

The basic approach employed for this task was to perform neutron physics calculations using the model shown in Figure 12.2.2-1, for varying core thickness.[5] The model in Figure 12.2.2-1 represents a slab module test of a $Li_2O$/He/HT-9 blanket module in a light-water test reactor. The neutronic model of the module itself is identical to that used in calculations for the reference $Li_2O$/He/HT-9 design with a fusion plasma source. The core model which was employed[5] used material fractions from a model of the Engineering Test Reactor (ETR), which are considered typical of most high-flux light-water test reactors, including ORR, ATR, MURR, OWR, etc. The thickness of the core model was varied from approximately 23 cm to 53 cm, corresponding to fission cores with thicknesses of three to seven standard 3-in.-square fuel elements. Between the core and blanket models are two additional regions. One is a 2-cm thickness of 316-ss, which represents the containment structure that will surround the module during the test. The other region is initially a void, intended to allow space in the model for the addition of a neutron filter; previous experiences in studying fission-based blanket tests have shown that the addition of a Cd filter improves the power density profile in the test assembly. Thus, two cases were examined as a part of this task: one with a 0.15-cm thick Cd filter in front of the test module, and one without. In all cases, the model was considered infinite in the two directions transverse to the core thickness.

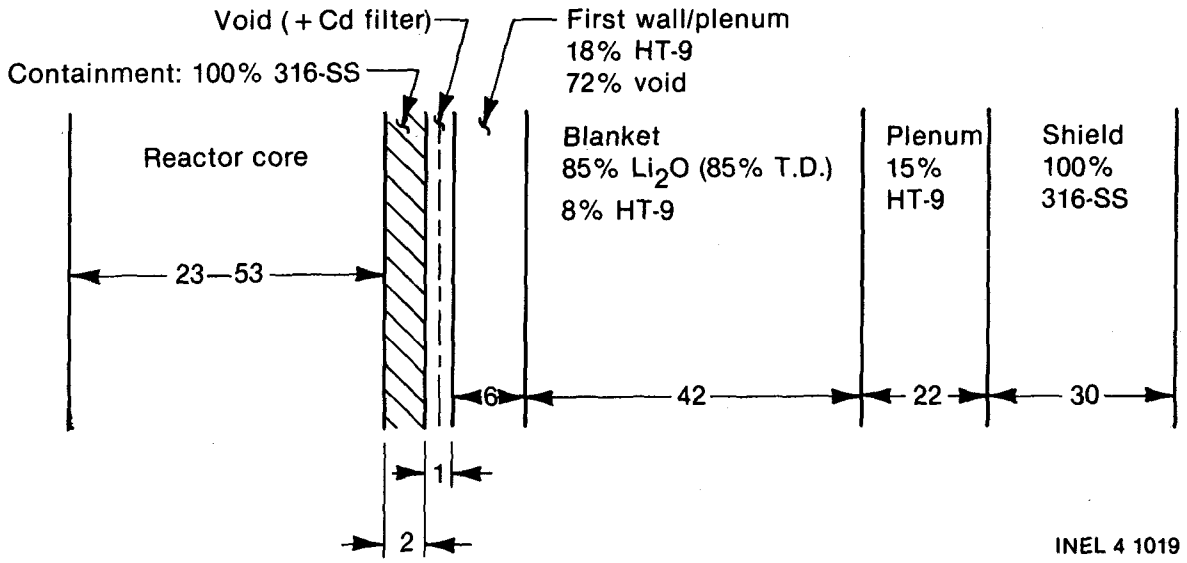


Figure 12.2.2-1. Neutronic model used for 1-D criticality study (not to scale; all dimensions in cm).

A number of results were obtained from these calculations, the details of which are presented in the sections on the key issues they affect. In general, results were obtained on the net reactivity effect of the test module as a function of core thickness (see Section 12.3.5), and the fast and thermal flux depression as a function of core thickness (Section 12.3.2) on the test module performance. In addition, other blanket models were examined using the same core model (at the 53-cm core thickness) as part of the Test Development Task.

### 12.2.3 Two-Dimensional Parameter Study

Another area of uncertainty regarding slab-type tests is the useful test volume available when the spatial distribution of the flux in the reactor core is considered. Typically, values of flux are quoted for positions at the center of the core or at the center of a test location. In a slab module test, the source flux from the core will be at a maximum at the center of the front face of the test module (the face nearest the core) and will decrease on that face with distance from the center. Since flux directly influences test performance, it is clear that some sections of the test module (near the outside) may perform poorly. This effectively reduces the useful test volume. Since test volume is felt to be critical, this consideration could be quite important.

The purpose of this task, therefore, is to evaluate the importance of core width on the performance of slab-type tests. To accomplish this, a simple 2-D neutronics model (Figure 12.2.3-1) was developed. As in the 1-D Criticality Study, the $Li_2O$/He/HT-9 reference blanket concept was chosen for this analysis, and a planar neutron source with the same spectrum as at the test module face in the 1-D criticality study was used. In this analysis the core thickness was fixed at 53 cm (seven rows of 3-in. elements), and the core width was varied from 45 to 75 cm. The test assembly width is assumed to be the same as the core width, and the actual test module is assumed to be 30 cm wide. The remaining space (15 to 45 cm) is assumed to be filled by dummy modules with the same composition as the test module. The test conditions (flux, spectrum, power density, etc.) along the test module centerline are compared with those at the edge of the test module (15 cm away from centerline) to determine if there is an acceptable volume (module-size) and if test conditions remain fairly uniform. These calculations are currently in progress and results will be included in the final report.

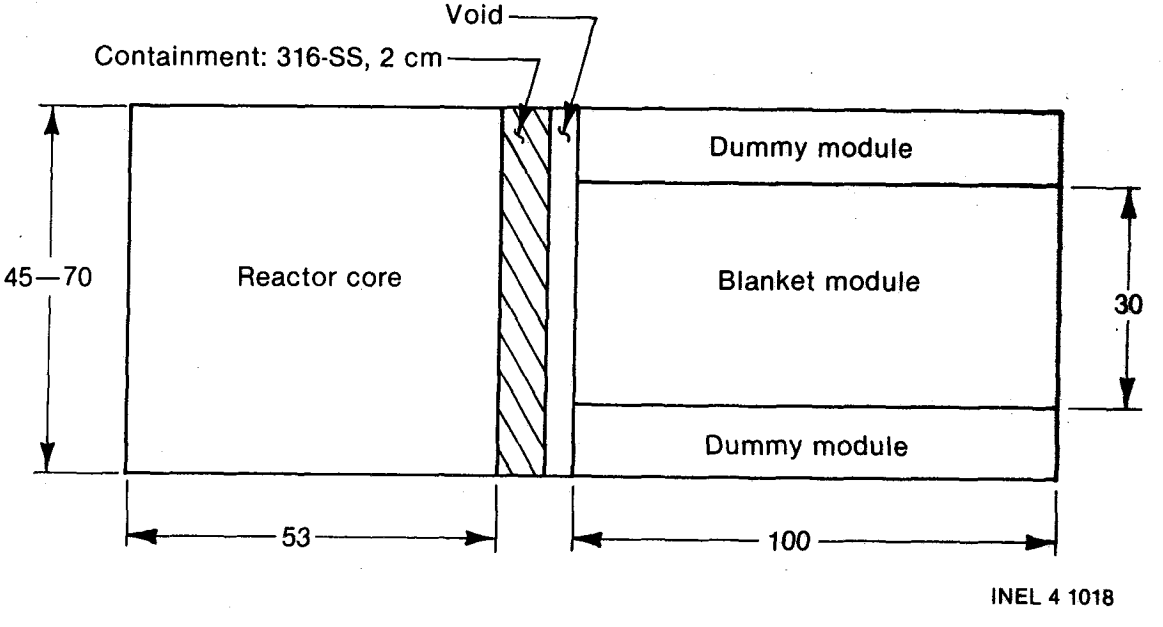


Figure 12.2.3-1. Neutronics model for two-dimensional parameter study (all dimensions in cm).

### 12.2.4 Test Development/Analysis

One of the most important issues in considering fission testing is the projected performance of the tests themselves, as this determines the technical desirability of the test. In order to address this concern, which relates to a number of key issues, it is necessary to actually conceptualize experiments and then analyze their performance. It is important to include as much detail as possible in the concept, since the neutronics depends strongly on the amount of parasitic material, such as steel containment. In addition, it is useful to determine the performance variables as functions of reactor characteristics (particularly flux), so that the published reactor specifications can be understood in terms of test performance.

A number of different tests have been studied as part of the task: two solid breeder submodule tests and three (solid and liquid breeder) slab-type tests. These are discussed below.

The first submodule test studied is of a unit cell of a $LiAlO_2/Be/H_2O$/PCA blanket, consisting of a central coolant tube surrounded by $LiAlO_2$ breeder. The outer diameter of the unit cell (which corresponds to the tube-to-tube spacing in the actual blanket) was selected to be the same as the minimum size in the STARFIRE blanket[6]: 3.2 cm. The containment, insulation, and support required for this test then led to the test assembly concept shown in Figure 12.2.4-1. This test assembly, based on a unit cell in the front of a blanket, was felt to be the smallest test assembly conceivable.

The second submodule test concept developed relates to the $Li_2O$/He/HT-9 blanket concept. The heart of test assembly (Figure 12.2.4-2) is a series of eight prototypical clad $Li_2O$ plates.

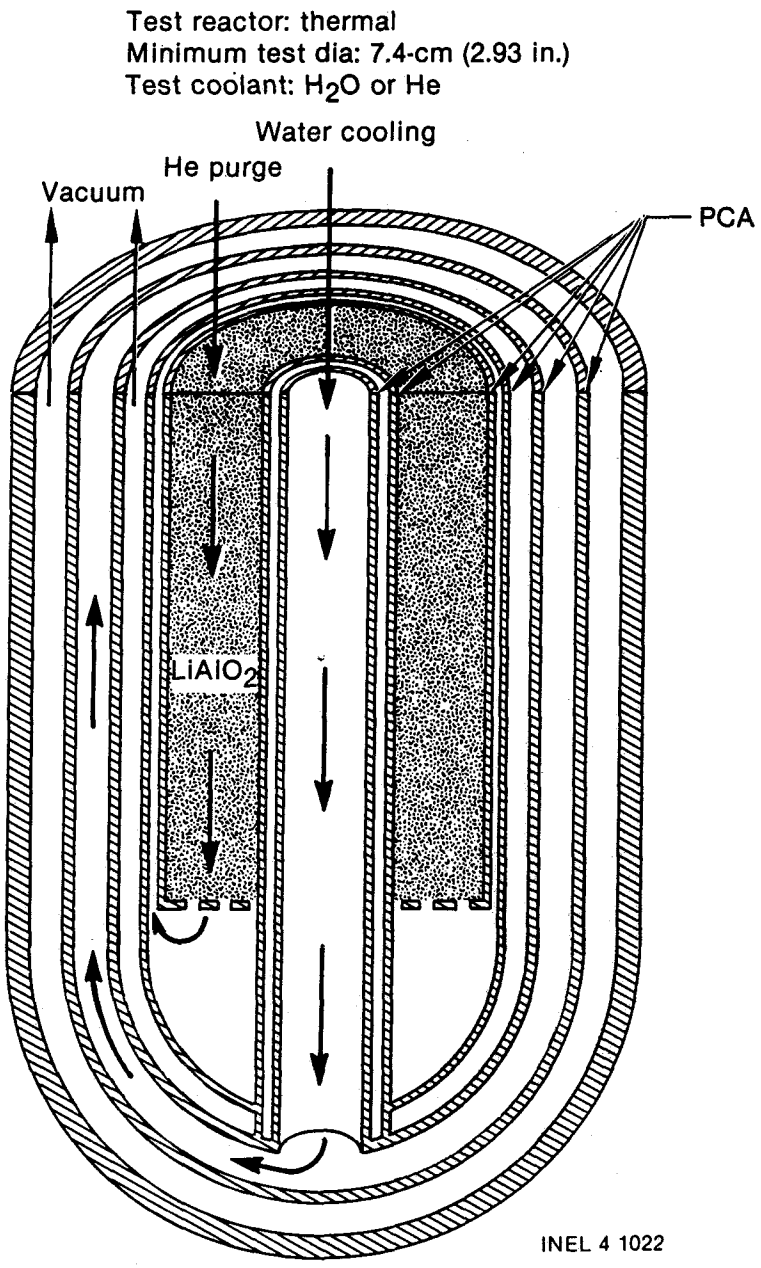


Figure 12.2.4-1. Submodule test concept for $LiAlO_2$/Be/$H_2O$/PCA blanket.

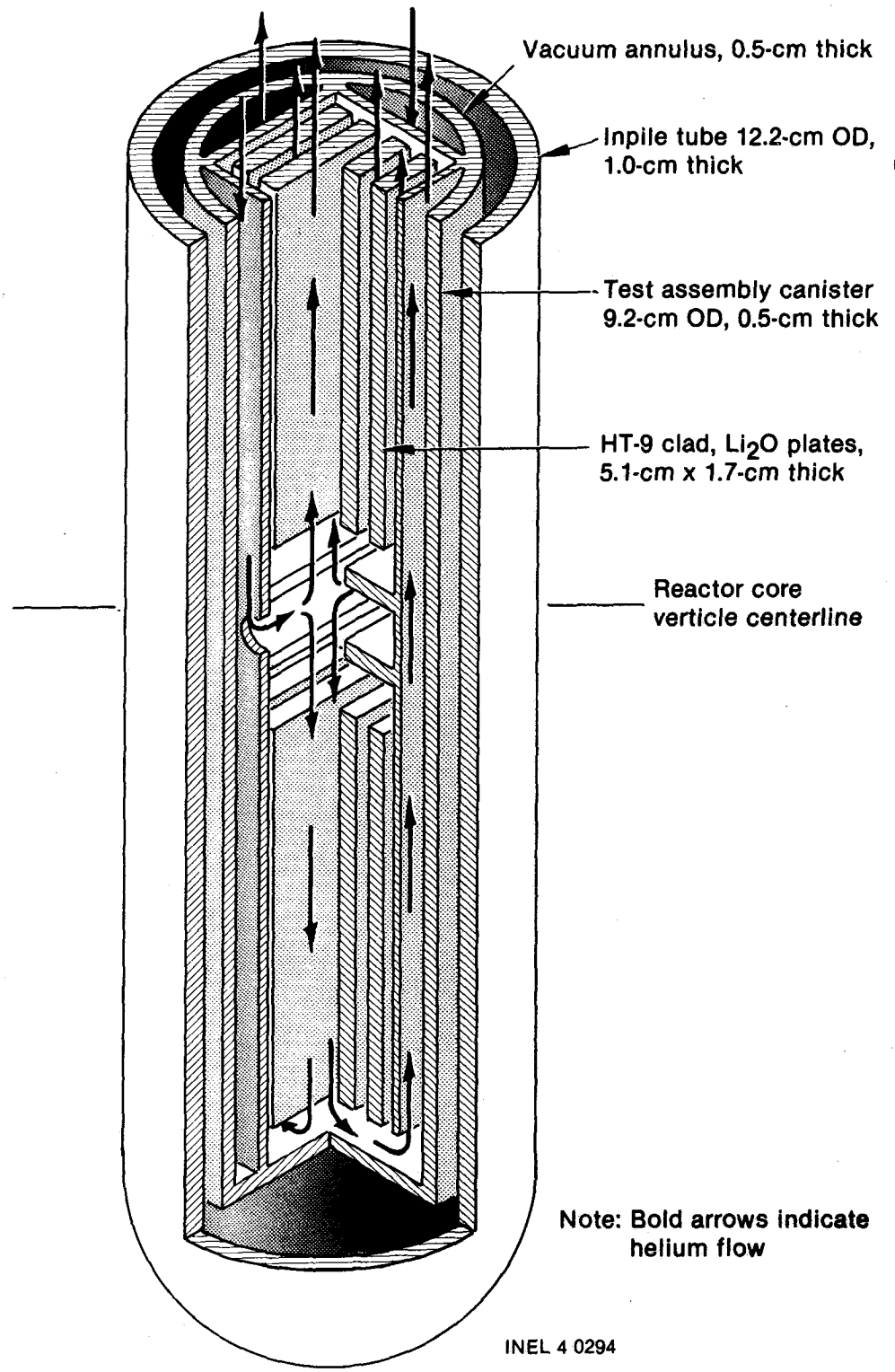


Figure 12.2.4-2. Submodule test concept for $Li_2O$/He/HT-9 blanket.

These plates are arranged with four above and four below the core centerline. Helium coolant enters at the core centerline, dividing to flow up through the top set of plates and down through the bottom set of plates. The principle behind this test concept is to use the vertical power variations in the core to simulate the power variation with depth into the blanket. Thus, the two sets of plates represent two separate tests; the area near the core centerline simulates the front of the blanket and the areas near the top and bottom of the core represent the rear of the blanket. The plates themselves are assumed to be the same size and geometry as in the blanket concept; the overall dimensions of each of the plate assemblies is 5 cm wide x 1.15 cm thick x 42 cm deep. The containment, insulation and support requirements lead to the concept shown in Figure 12.2.4-2.

For each of these submodule test concepts, one-dimensional (radial) physics calculations were performed to determine pertinent test conditions. These calculations assumed an annular, light water reactor core, of the same composition as that used in both the 1-D and 2-D calculations performed under other tasks (Section 12.2.2 and 3); the material fractions used correspond directly to the composition of the ETR core, and are typical of many high flux light water reactors. In both calculations, a minimum critical core configuration was first developed for the cases in which the test assemblies are absent and the resulting space is voided. This minimum critical configuration is established by adjusting the outer diameter of the annular core. Next, calculations are performed using the critical configuration with the test assembly model at the center. These calculations yield data on test power density and tritium production profiles, radiation damage rates, flux depression, net reactivity worth of test assembly, etc. Detailed results are presented as part of the discussions of key issues.

In the initial development of the submodule test concepts, some effort was put into developing one or more liquid-breeder tests which would be roughly analogues to the solid breeder concepts discussed above. Many submodule tests can be envisioned for liquid-breeder concepts, but the emphasis in most such tests is less on integrated issues than for the solid

breeder tests. This is because of a mismatch between the capabilities of fission testing and the currently perceived technical issues for liquid metal blankets. The most critical issues for liquid metal blankets (as discussed in Section 5) that might be addressed at the submodule scale are MHD effects (hot spots, pressure drop, etc.), material compatibility, and tritium permeation. While the general capabilities of fission testing, (bulk heating and in situ tritium production) are perhaps of interest in investigating these issues, they are felt to be of less importance than other factors (such as surface heating and magnetic field). In contrast, for solid breeder blankets, the most critical issues (tritium release and thermal performance) depend fundamentally on bulk heating and in situ tritium production. These considerations affect the desirability of multiple-interaction and more complex tests in which it is important to have all of the major environmental effects present. Investigation of individual issues, such as neutron irradiation effects on corrosion rates, or the generation of helium bubbles in liquid metals from the tritium-breeding reaction are ideal situations for fission testing. For the purposes of FINESSE, however, the capabilities of more complex tests are of particular interest, as discussed in Section 12.0. Therefore, no liquid-metal submodule test concepts are pursued.

Three basic slab module test concepts have been considered, one each for the following reference blanket concepts: $Li_2O$/He/HT-9, $LiAlO_2$/Be/$H_2O$/PCA, and Li/Li/V. The general principle behind each of these tests is to employ a full-scale module or section of a module, placed in a containment box, next to a face of the reactor core. For the two solid-breeder blanket concepts, which both have pod-type geometries, an entire module of truncated length is assumed, and dummy modules are placed alongside to improve the test performance, as discussed earlier. For the Li/Li/V concept, a small section of a full module is used. In all cases, service lines would probably be routed through the back of the test module as in the actual blanket. It is assumed that because of the temperatures, pressures, and materials involved, a containment box is required, adding 2 cm of 316-ss between the core and test module. These assumptions were used to develop neutron physics models for each of the tests. This core model was the same as that used for the 1-D criticality study; the

calculations performed for that study are also used for the $Li_2O$/He/HT-9 test module performance results in this task. As with that concept, cases were run for the other blankets with and without a 0.15-cm thick Cd neutron filter to reduce the local power density peaking due to $^6Li$ self-shielding. The calculations produced data on power density and tritium breeding profiles, radiation damage rates, flux depression, and net reactivity effect. These results are discussed in the following sections with the key issues to which they apply.

### 12.2.5 Summary of Technical Approach

Four interrelated technical tasks were undertaken to develop information on the key issues. These tasks focused on engineering tests of two types: submodule tests which could be conducted within a fission core, and slab-type tests which would be positioned against an external face of the core to simulate the plasma neutron source. More emphasis was placed on the slab tests, since the environmental requirements are more strict and since they have not been investigated in great detail in the past. Two of the four tasks address slab tests specifically. The four tasks are:

A. 1-D Criticality Study--Intended to examine the effects of fission core thickness on test operation. Of particular interest is the reactivity effect of the test assembly as a function of core thickness, as this could influence which reactors could be used for slab tests.

B. 2-D Parameter Study--Examines the effect of the face dimensions of the core, particularly in determining the effective useful test volume in a slab test.

C. Test Development Task--Addresses both submodule and slab tests and examines test performance parameters (power density, tritium breeding, etc.) to indicate areas of usefulness as well as areas of deficiency.

D. Facility Survey--Develops a picture of what parameters are available in existing fission test reactors, and gives some consideration to what might be attainable with modifications.

The first three tasks, taken together, will essentially indicate the technical usefulness of fission testing as a function of reactor parameters (peak flux, size, etc.). The fourth task adds to our understanding of the usefulness of fission testing by indicating the reactor parameters attainable.

## 12.3 Analysis of Key Issues

In this section, the results of the analysis performed for the four tasks discussed above are presented. In order to focus the discussions as much as possible, the results are presented by key issues rather than by technical tasks, since each task can produce information relating to a number of key issues.

### 12.3.1 Radiation Damage

The central issue here is the radiation damage produced in structural materials in fission tests compared to fusion operation. This includes the types and rates of damage production, and the total amount which can be accumulated. These considerations are discussed here only as they apply to structural materials; damage to solid breeders is discussed under the lithium burnup issue.

There are two primary irradiation damage mechanisms which can result in changes in material properties: atomic displacements and helium production. While displacement damage occurs over a wide range of incident neutron energy, helium production depends upon particular (n, $\alpha$) reaction cross sections which generally have high energy thresholds. Since typical fusion spectra at the first wall contain a greater fraction of high-energy neutrons than typical fission spectra, fission tests are expected to produce less helium for equivalent displacement rates. The effect of this increased helium production is currently a major uncertainty in fusion

engineering, and motivates the need for 14 MeV neutron sources. In engineering tests, such as those being considered here, the main interest in radiation damage is in observing life-limiting failure modes in a multimaterial, multiple-effect test assembly. In order to examine the prospects of accomplishing this objective, structural radiation damage rates for the two fission-based submodule tests were calculated. These damage rates are based on the assumption that the fission test is operated so that the power density in the blanket is roughly equivalent to that in the reference blanket operating at 5 $MW/m^2$ wall loading. The results which are compared to the damage rates at the first wall in the STARFIRE reactor are shown in Table 12.3.1-1.[6] The immediate conclusions from the table are that for equivalent blanket power density, higher damage rates are expected in the fusion spectrum, as well as much more helium production per atomic displacement. These conclusions duplicate the current understanding of fusion vs. fission radiation damage.

There are several additional points which can be made. First, it is important to note that other materials, such as solid breeders or beryllium are much less sensitive to the differences between fusion and fission spectra, and therefore excellent information on their performance can be obtained from fission reactor tests. Second, a number of innovative techniques have been developed in the past to overcome the lower helium production rates expected in fission tests. These include use of the $^{58}Ni(n,\alpha)$ reactions in nickel-bearing materials or doping with trace amounts of boron or lithium to increase the rate of helium production in the fission spectrum. Third, since the neutron flux in a fusion blanket decreases with distance from the first wall, so must the damage rates. It is also known that the spectrum can change considerably, due to moderation in the blanket. These factors (particularly the change in spectrum) will alter the He/DPA ratio as well as the damage rates, with distance from the first wall. It is therefore reasonable to expect that fission tests would provide a better simulation of damage in structure deeper in the blanket, rather than at the first wall. Calculations are currently in progress to determine damage rates as functions of depth in the blanket for both the reference fusion designs and fission test cases, so that direct comparisons can be made.

Table 12.3.1-1. Comparison of Fusion First Wall and Fission Radiation Damage in Structure

| | $\frac{Disp}{cm^3 \cdot s} \times 10^{-16}$ | | $\frac{He}{cm^3 \cdot s} \times 10^{-10}$ | | $\frac{He}{Disp} \times 10^{7}$ | |
|---|---|---|---|---|---|---|
| Material | Fusion[a] | Fission[b] | Fusion | Fission | Fusion | Fission |
| PCA[c] | 15 | 2.5 | 190 | 1.7 | 130 | 6.6 |
| HT-9[d] | 14 | 5.4 | 140 | 1.1 | 99 | 2.0 |

a. Starfire first wall conditions at 5 $MW/m^2$.

b. Same power density in test as in blanket near first wall.

c. Fission results based on $LiAlO_2/Be/H_2O$/PCA test module.

d. Fission results based on $Li_2O$/He/Ht-9 test module.

It is possible to draw some useful interim conclusions. First, fission testing can produce the same types of damage (atomic displacement and helium production) in a complex, multiple-effect test as in the actual fusion environment, although the rates are different. Second, fission testing may be better suited to simulation of damage at the rear of the blanket, rather than at the front where helium production is more important. Overall, this implies that fission testing is better suited for beginning-of-life (BOL) testing, where there is less emphasis on material damage, than for middle or end-of-life (MOL/EOL) testing, where radiation damage may influence blanket failure mechanisms. Nevertheless, the capability of fission testing to provide various other test conditions simultaneously, with some radiation damage testing possibilities, is unique and potentially useful.

### 12.3.2 Power Density/Lithium Burnup Rate

The ability to produce volumetric heating and tritium in situ are the two outstanding capabilities of fission testing. It is important to note that no other approach (except neutron/gamma heating) can bulk heat virtually all materials (metals, ceramics, etc.) simultaneously, which is

required for complex engineering tests. Furthermore, true volumetric heating is sometimes mandatory in simulating fusion operation, such as in studying the thermal performance of solid-breeder blankets. The in situ production of tritium is also important and difficult to obtain without a fission or fusion neutron environment. It is important to note that tritium production is felt to be the dominant cause of material damage in solid breeders, and thus in situ tritium production introduces the possibility of examining MOL/EOL issues for solid breeders. The capability of providing both bulk heating and tritium production opens a wide range of test possibilities unique to fission testing.

The main concerns regarding power density and lithium burnup in fission-based tests are the magnitudes and spatial profiles attainable; these concerns have been addressed for both slab and submodule test geometries.

For the $LiALO_2/Be/H_2O/PCA$ submodule (unit cell) test, a flat spatial distribution of both power density and tritium production is desired, since the test assembly simulates a relatively small portion of the blanket, over which conditions do not change drastically. Within the test assembly, the power density and the dimensions of the $LiALO_2$ annulus must be related in a manner that simulates the breeder maximum and minimum temperatures correctly. Since a small unit cell was used in the test configuration, high power density is required. Thermal calculations, using $K_{LiA102} = 1.8 \frac{W}{mK}$ and minimum and maximum temperatures of 350°C and 1000°C, indicate the power density required for proper operation is approximately 100 $W/cm^3$. The neutron physics calculations performed for this test show that 100 $W/cm^3$ is attained for a total neutron flux of $9.1 \times 10^{14}$ $n/cm^2$-s at the outer edge of the $LiA10_2$ annulus. For the particular core model used, this corresponds to a peak flux (in core) of $1.1 \times 10^5$ $n/cm^2$ s. This peak flux value, however, could easily be reduced by modifying the hypothetical core loading (assumed uniform) with more fuel near the test assembly. Nevertheless, the magnitude of the flux required at the outer surface of the annulus indicates the general range needed to attain such high power densities, and this may limit the choice of reactors where such tests can be performed. However, as mentioned

previously, test power density and size are related, and if the test assembly outer diameter could be increased, the power density would decrease. This scaling could therefore be used to adapt the test to large, lower-flux reactors, if necessary. For the 100 $W/cm^3$ power density operation, the average tritium production rate is $1.1 \times 10^{14}$ $T/cm^3$ s, or approximately 13% burnup per year, which is typical for high-power-density areas in the blanket. Actual reference case calculations and more complete information on spatial profiles are currently in progress, and will be included in the final report.

For the $Li_2O$ submodule test described earlier, the objective is to take advantage of the axial power variation in an inpile tube-type test to simulate the power variations with depth into a fusion blanket. For this reason, it is desired that radial variation within the test be minimized. The inclusion of four breeder plates in the test concept itself is an attempt to minimize these radial effects. The outer two plates are subject to higher-than-average power density due to $^6Li$ self-shielding; they act as thermal neutron filters, improving the conditions in the center two plates. In addition, the width of the plates was chosen to be sufficient to eliminate thermal end effects over a region near the middle of the plates. One-dimensional (radial) neutron physics calculations were performed to determine the power density and tritium production profiles. These calculations used a cylindrical homogenized model for the area containing the breeder plates. The resulting power density and tritium breeding radial profiles are shown in Figure 12.3.2-1. Since the plate thickness is 1.15 cm, it is apparent that the center two plates will experience nearly uniform bulk heating, while the outer two will experience strong variations. Perpendicular to the test axis the plates are 5 cm wide, and thus power peaking will occur in the end 5 mm of the middle plates. However, in this case, the higher-than-normal power density is an advantage, since it supplies additional heat at a cooled end; this will help to eliminate or further localize the thermal end effects in the center two plates. Thus, these two plates will experience a minimum of radial effects.

In the Reference $Li_2O$/He/HT-9 blanket, the maximum power density in the $Li_2O$ is 43 $W/cm^3$ and the minimum is 3.3 $W/cm^3$. Table 12.3.2-1

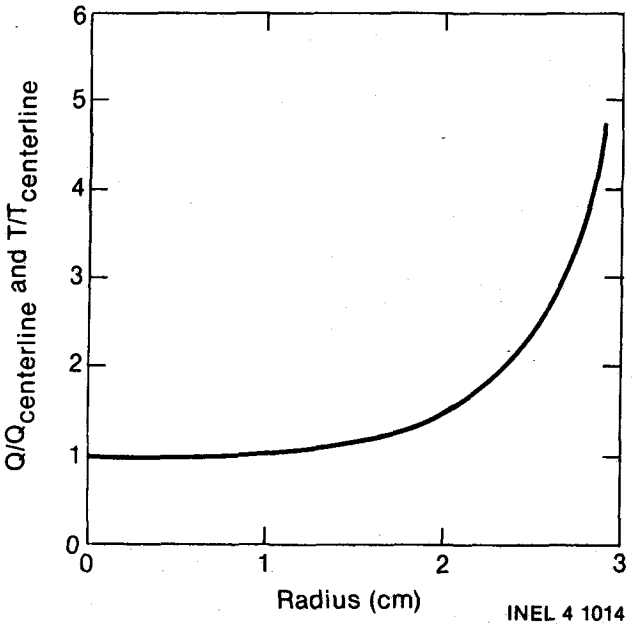


Figure 12.3.2-1. Normalized power density and tritium production profile in $Li_2O$/He/HT-9 submodule test.

shows the total neutron flux required at the edge of the test to duplicate these values. For the particular core model used in the calculation, Table 12.3.2-1 also shows the peak flux in the core. Again, these values will change with core loading. Finally, Table 12.3.2-1 shows the comparison between the tritium production rates in the fission and fusion cases, where the power density is matched at 43 and 3.3 $W/cm^2$. For this test configuration and at equivalent power density, tritium production rate is higher by a factor of two at the front of the blanket than the fusion case. Tritium production is equivalent to the fusion case at the rear of the blanket. The increased tritium production at the front of the plates is probably an advantage, since it implies accelerated damage in the ceramic. However, it could also change the chemistry or thermodynamics of tritium recovery, and therefore its effect must be studied closely.

The axial power density profile in the fission test is shown in Figure 12.3.2-2 and compared with the profile expected in an actual fusion blanket. It is apparent that the decrease in power with distance is much more rapid in the fusion case (roughly exponential) than in the fission case (roughly cosine). There are several options which can be considered

Table 12.3.2-1. $Li_2O$/He Submodule Performance Parameters

| Location in Blanket to be Simulated | Fusion and Fission Power Density[a] ($w/cm^3$) | Tritium Production ($T/s \cdot cm^3$) | | Test Flux ($n/cm^2 \cdot s$) | |
|---|---|---|---|---|---|
| | | Fusion | Fission | Edge of Test | Peak In Core |
| Front | 43 | $1.6 \times 10^{13}$ | $3.1 \times 10^{13}$ | $2.1 \times 10^{15}$ | $2.8 \times 10^{15}$ |
| Rear | 3.3 | $2.4 \times 10^{12}$ | $2.4 \times 10^{12}$ | $1.6 \times 10^{14}$ | $2.2 \times 10^{14}$ |

a. All results for fission test normalized to same power density as fusion case. All calculations based on "uniform conditions" which exist within center 4 cm diameter of test ($^6Li$ self-shielding peak ignored).

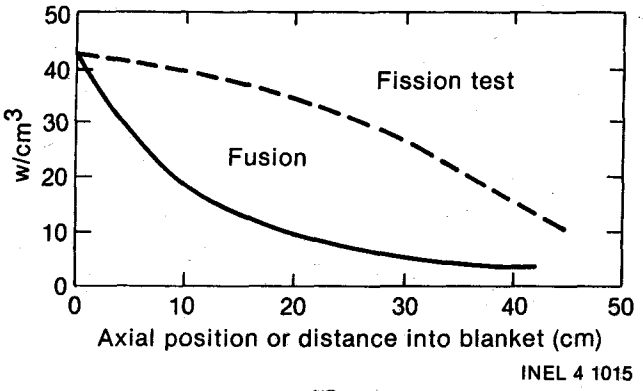


Figure 12.3.2-2. Axial power density profile in fission test compared with power density variation with depth in fusion blanket.

(conceptually) to bring these into closer agreement. First, the plates could be positioned with their ends near the edge of the core and extending outward. In this region, the neutron flux in the fission reactors falls off exponentially, and the simulation could be quite good. The difficulty with this approach lies in getting sufficient total flux to attain the desired power density. However, this could be possible at several facilities. A second approach would be not to attempt a simulation of the initial 5 to 10 cm of the plates where the power density varies most rapidly. This would have the desirable effects of improving the simulation and also of reducing the required test flux (since the region of highest power density is removed from the test). Unfortunately, this region is probably of most interest because of high power density. A third approach would be to match the maximum fusion power density with the plates aligned on the center of the core, and incorporate a neutron absorber which varies in transmittance with axial position, thus reducing the power to that desired at each axial location. Finally, a fourth option would be to incorporate a neutron moderator at the center of the test assembly, to reflect moderated neutrons up and down to the plate assemblies, for the purpose of inducing power peaking by $^{6}Li$ self-shielding. Although this is somewhat speculative, it would have the advantages of improving the profile and reducing the maximum flux required.

Three slab module test concepts have been investigated: one each for the $Li_2O$/He/HT-9, $LiAlO_2$/Be/$H_2O$/PCA, and Li/Li/V concepts. As discussed previously, it is assumed that these core-side tests would include double walled containment. Thus, for the neutron physics calculations, 2 cm of 316-ss was modeled between the core and the test module. The models used for the test modules themselves correspond exactly to those used for reference design calculations. Cases were run with and without a 0.15 Cd filter for each concept. The power density and tritium production profile calculated for the $Li_2O$/He/HT-9 concept compared to reference calculations for a 1 $MW/m^2$ fusion neutron source are shown in Figure 12.3.2-3; the general similarity between the profiles is clear. However, the effect of the lower-energy fission spectrum is also obvious in the initial peaks in both power density and tritium production, as well as in the slightly steeper slope farther into the blanket. These effects are slightly less prominent in the power density profile due to heating from

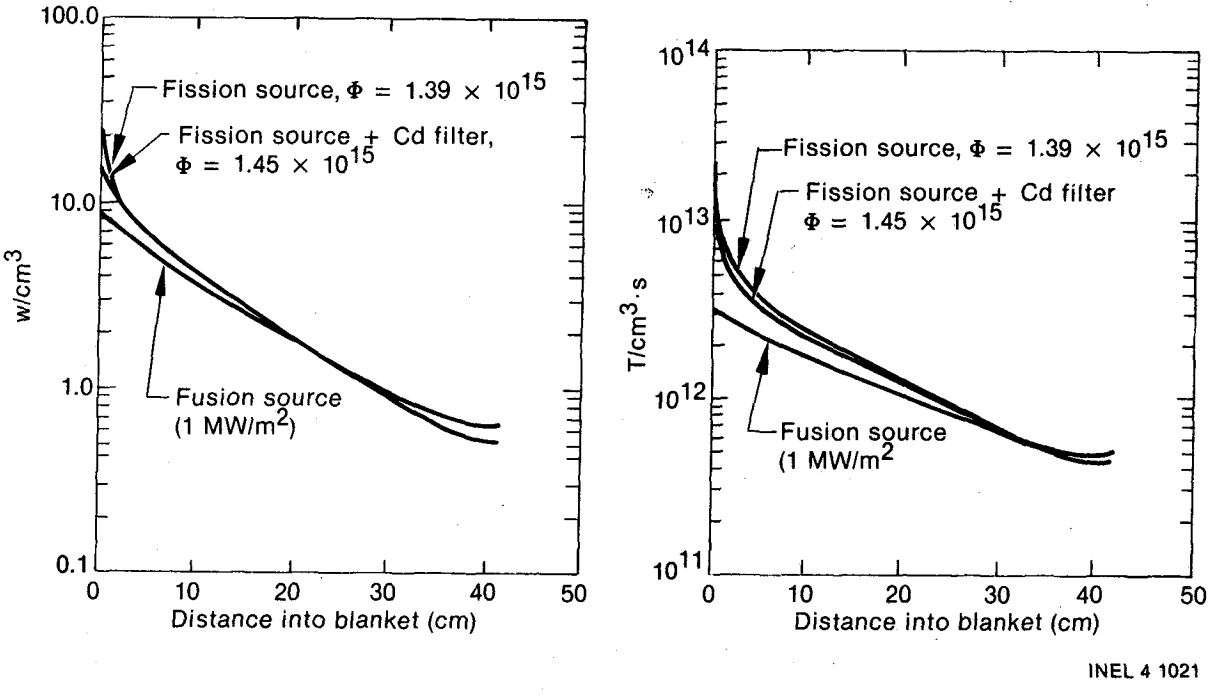


Figure 12.3.2-3. Power density (left) and tritium production (right) profiles in fission slab module test for $Li_2O$/He/HT-9 blanket.

fission gammas, which decays more slowly with distance into the blanket. The effect of the cadmium filter is more noticeable in the tritium breeding profiles for the same reason. In order to provide a better simulation (if this is felt necessary), a 1/v absorber such as boron, $^{6}Li$, or $^{3}He$ will probably be required, in order to remove neutrons with energies above the cadmium cutoff energy.

The results of calculations for the $LiAlO_2/Be/H_2O$/PCA slab module test are shown in Figure 12.3.2-4; no reference fusion-case calculation is available for this concept at present. In this case, the addition of the Cd filter makes virtually no difference past the initial thin layer of $LiAlO_2$ (in front of the beryllium multiplier). This is due to the relatively high moderation by water at the front of the blanket. In addition, the spectrum in most of the blanket is softened considerably by the water fraction throughout. This will cause the fusion spectrum to resemble the fission spectrum much more quickly than in the $Li_2O$/He/HT-9 concept. It is therefore likely that the power density and tritium breeding profiles in the fission test will simulate those in actual fusion operation quite closely.

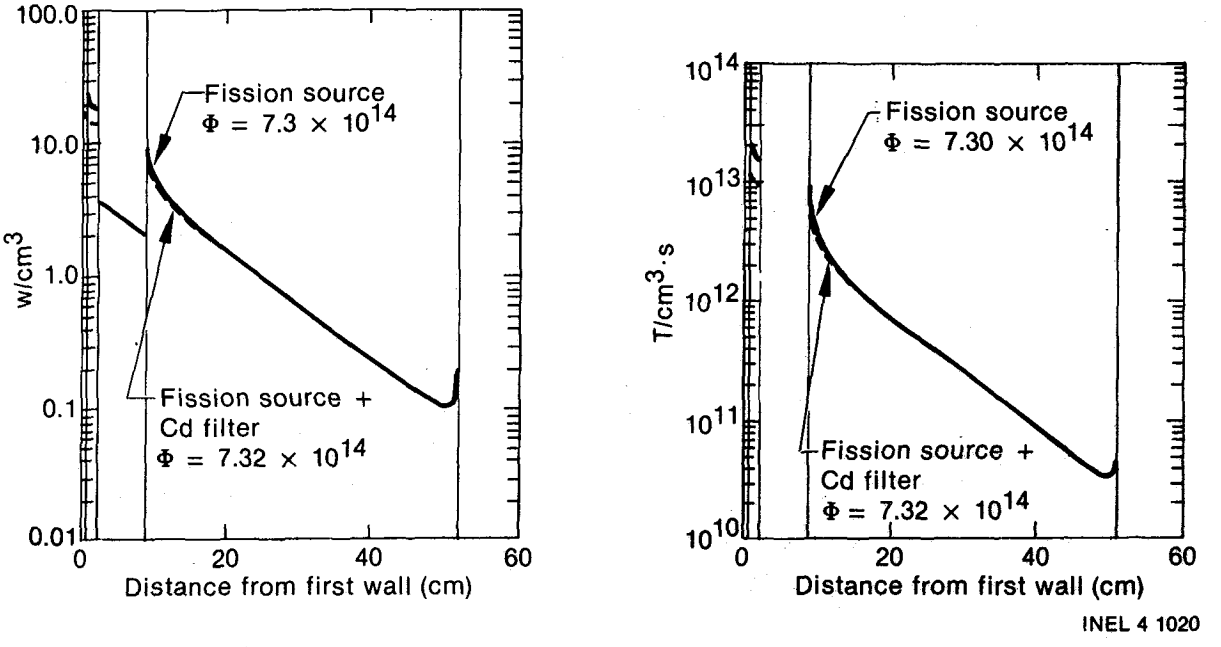


Figure 12.3.2-4. Power density (left) and tritium production (right) profiles in fission slab module test for $LiAlO_2/Be/H_2O$/PCA blanket.

The results of neutron physics calculations for the Li/Li/V slab module test are shown in Figure 12.3.2-5, with a reference 1 $MW/m^2$ fusion case for comparison. Again, the general similarity in profiles is apparent, especially in the poloidal manifolds, and peaking is observed in the forward lithium channel (the toroidal channel). Although this additional bulk heating in the liquid lithium is not prototypical, it could be beneficial by supplying extra power to simulate surface heating (or augment it) at the first wall. It may also be useful in simulating higher average power density in the channel. In a good thermal conductor such as lithium, bulk heating is more important than the power density profile, and thus a peaked profile such as that in Figure 12.3.2-5 may be acceptable. In this case, the average power density could be higher for a given source flux, since neutrons are not being lost to filters. If the peaking in power density and tritium breeding is felt to be a problem, a solution is indicated by the lack of peaking in the poloidal channel; a $^6Li$ filter placed in front of the entire module should have roughly the same effect as the toroidal channel in the unfiltered case. Presumably, any 1/v absorber should also be acceptable. This would bring the power density and tritium breeding profiles into good agreement. Another discrepancy between the power density profiles is apparent in the reflector region, where the power density for fission is much higher initially, but falls off rapidly. This effect is due to gamma heating in the high-density region. This would be improved by the addition of a gamma filter (such as lead) in front of the module. Gamma heating is not a large contributor in the lower-density regions in front of the reflector, so conditions in these areas will be only slightly changed.

Overall, the conclusion reached from the foregoing discussion is: fusion-relevant spatial profiles of power density and tritium production can be produced in both submodule and slab-type fission-based tests. In most cases, local peaking due to $^6Li$ self-shielding can be expected. This condition can, in many instances, be used to advantage. In cases where it cannot be used constructively, neutron spectrum filtering can be used to remove the lowest-energy portion of the spectrum and thereby reduce peaking. This may increase the total flux required for prototypical operation.

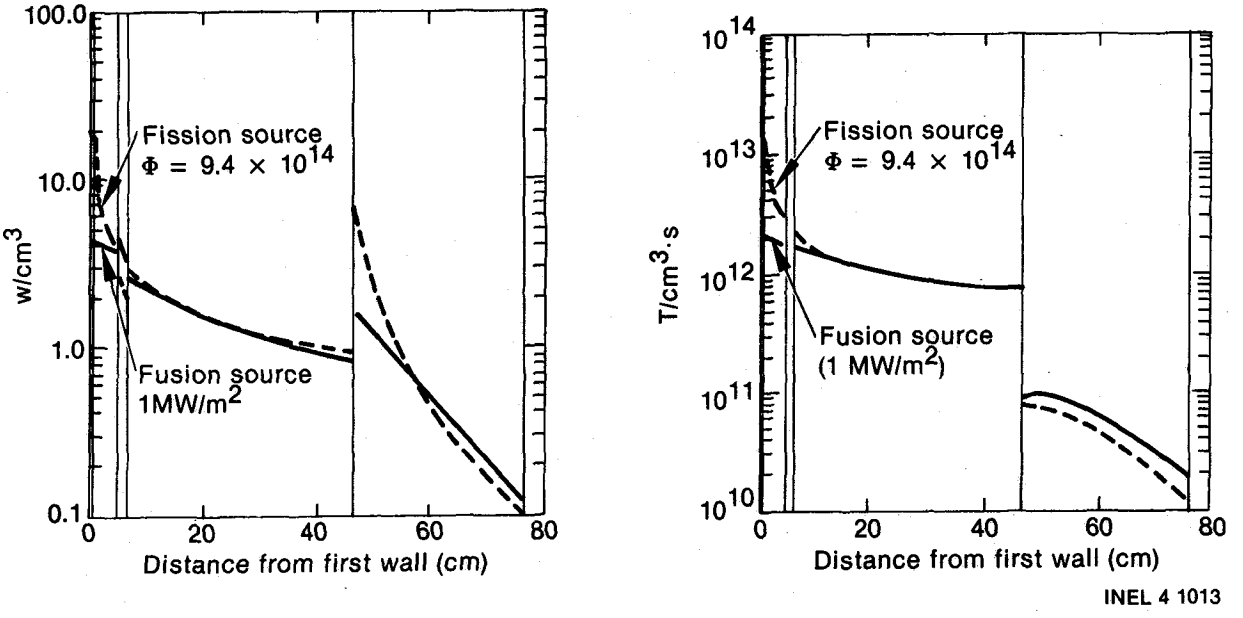


Figure 12.3.2-5. Power density (left) and tritium production (right) profiles in fission slab module test for the Li/Li/V blanket.

The primary remaining uncertainty is in the magnitudes attainable in power density and tritium production. In the data presented previously, all calculations for fission tests were normalized to produce power densities similar to 1 $MW/m^2$ fusion operation. Note that the tritium production profiles were normalized by the same factor to maintain consistency. The issue, then, is: can the required source fluxes be attained. Table 12.3.2-2 summarizes the fluxes required for both submodule and slab-type tests. The values shown are for the total flux at the surface of the test assembly. These values, though high, are probably attainable in most cases, as indicated in Section 12.3.3. An important point to consider is the difference between the usual flux in the test location (unperturbed) and the flux there when the test assembly is in place. Figure 12.3.2-6 shows this flux depression effect for slab module tests as a function of core thickness. The plotted values are equal to the fraction of the unperturbed flux that is lost when the test module is installed. Although the flux depression is not a strong function of reactor core thicknesses, the overall magnitudes are quite high. This leaves a concern that the required fluxes may be difficult to attain when flux depression is taken into account. This is also indicated by

Table 12.3.2-2. Flux Required at Face of Test Assembly to Simulate Power Density at Front of Fusion Blanket at 1 $MW/m^2$

| Test Type | Blanket Concept | Neutron Filter | Flux[a] ($cm^{-2}$ $s^{-1}$) |
|---|---|---|---|
| Slab[b] | $Li_2O$/He/HT-9 | -- | $1.4 \times 10^{15}$ |
| | | Cd | $1.5 \times 10^{15}$ |
| Slab | Li/Li/V | -- | $9.4 \times 10^{14}$ |
| | | Cd | $9.8 \times 10^{14}$ |
| Slab | $LiAlO_2$/Be/$H_2O$/PCA | -- | $6.2 \times 10^{14}$ |
| Slab | | Cd | $8.7 \times 10^{14}$ |
| Submodule[c] | $Li_2O$/He/HT-9 | -- | $5.1 \times 10^{14}$ |
| Submodule | $LiAlO_2$/Be/$H_2O$/PCA | -- | $2.1 \times 10^{14}$ |

a. Water-moderated, plate-fueled fission reactor assumed.
b. Core-side.
c. In-core.

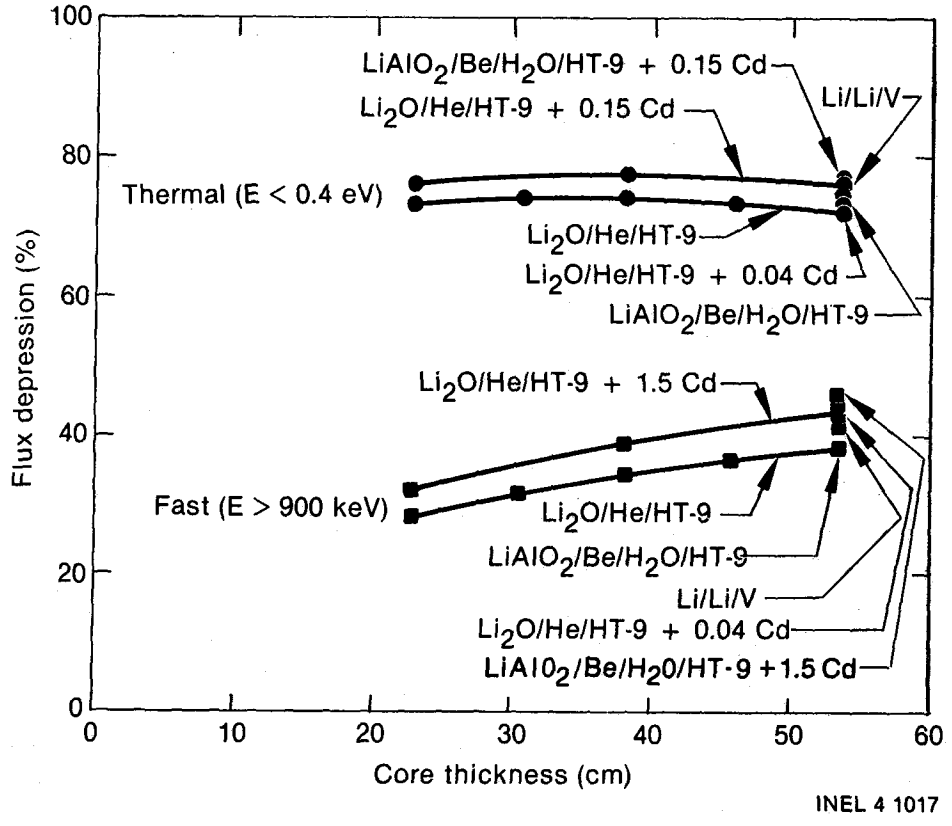


Figure 12.3.2-6. Flux depression as a function of core thickness for slab-type fusion blanket tests.

Table 12.3.2-3, which shows the peak flux in the core for each of the test calculations performed, normalized to 1 $MW/m^2$ equivalent power density. These values are near the limits of fission reactor heat transfer technology. It is extremely important to observe, however, that both the peak fluxes in Table 12.3.2-3 and the flux depression values in Figure 12.3.2-6 depend upon the fission core configuration. In the case of the submodule calculations, the core was assumed to be of uniform composition; the core configuration for the slab tests was nearly uniform[5]. Actually, it is likely that elements with higher fuel loadings would be used near the test modules to help flatten the flux profile in the core edge. This would reduce the flux depression effect and thereby the peak flux required. Therefore, the information in Table 12.3.2-3 and Figure 12.3.2-6 probably represents upper-limit values; both peak flux and flux depression in real tests will be less than indicated.

Table 12.3.2-3. Peak Flux in Core Required to Simulate Power Density at Front of Blanket at 1 $MW/m^2$

| Test Type | Blanket Concept | Filter | Peak Flux in Core[a] ($n/cm^2 \cdot s$) |
|---|---|---|---|
| Slab[b] | $Li_2O$/He/HT-9 | -- | $2.9 \times 10^{15}$ |
| | | Cd | $3.4 \times 10^{15}$ |
| Slab | Li/Li/V | -- | $2.1 \times 10^{15}$ |
| | | Cd | $2.5 \times 10^{15}$ |
| Slab | $LiAlO_2$/Be/$H_2O$/PCA | -- | $1.4 \times 10^{15}$ |
| | | Cd | $2.2 \times 10^{15}$ |
| Submodule[c] | $Li_2O$/He/HT-9 | -- | $5.6 \times 10^{14}$ |
| Submodule | $LiAlO_2$/Be/$H_2O$/PCA | -- | $3.0 \times 10^{14}$ |

a. Water-moderated, plate-fueled fission reactor assumed.

b. Core-side.

c. In-core.

Overall, it appears that adequate (1 $MW/m^2$ equivalent) power densities and tritium production rates can be attained in fission based tests, although the required fluxes (Table 12.3.2-2) are high. Considering the flux depression effect even higher unperturbed flux will be required in the test location. Though attainable, this will impact the number of reactors which can be used for fission-based testing.

### 12.3.3 Test Volume

The issue of test volume is closely interrelated with power density, tritium production, etc., since in order to be useful, a test location must also be able to produce reasonable test conditions. The main consideration here is how many useful test locations exist. To address this, as a part of the Facility Survey Task, the published specifications of U.S. reactors[1] and some foreign reactors[2,3,4] were reviewed to determine how many test locations exist which have a given physical size and total flux. In order to narrow the scope of this review, reactors were considered only if they met the following criteria: (a) power greater than or equal to 1 MW; (b) test area flux greater than or equal to $10^{13}$ $n/cm^2$ $s$; (c) test location minimum diameter greater than or equal to 5 cm. The data obtained for submodule tests in U.S. reactors (and for U.S. plus foreign reactors) are summarized in Table 12.3.3-1. Each entry is the number of test locations which could be used to conduct a test of a given size at a given flux; the entries also include larger and higher-flux locations, since, for instance, a small test could be conducted in a large hole. In developing submodule tests for FINESSE, the smallest test size devised was 7.4 cm OD; this is probably the minimum credible size for any engineering-type test. In addition, neutron fluxes in the range of $10^{14}$ $n/cm^2 \cdot s$ are required; this is typical of the flux required for any engineering test. These two considerations will limit the total number of test locations to less than 100 for U.S. and foreign reactors combined. Larger test assembly size and especially higher required flux will further limit the possibilities.

Table 12.3.3-1. Numbers of Existing Acceptable In-Core Test Locations in U.S. (U.S. and Foreign) Reactors

| Minimum Required Flux ($n/cm^2 \cdot sec$) | Test Assembly Maximum Dimension (cm) | | | | |
|---|---|---|---|---|---|
| | 5 | 7.5 | 10 | 12.5 | 15 |
| $5 \times 10^{12}$ | 180(315)[a] | 119(168) | 33(79) | 16(45) | 2(27) |
| $5 \times 10^{13}$ | 167(292) | 106(145) | 30(66) | 15(44) | 1(26) |
| $5 \times 10^{14}$ | 49(69) | 13(30) | 13(30) | 10(27) | 0(16) |
| $5 \times 10^{15}$ | 40(40) | 4(4) | 4(4) | 1(1) | 0(0) |

a. Numbers in parentheses are for U.S. and foreign reactors.

For slab-type tests, the situation is somewhat clearer, due to the scarcity of such locations. Table 12.3.3-2 shows the pertinent data. It appears that with current reactors, reasonable slab module tests at prototypical conditions are not possible without modifications.

All of these considerations, however, are based on the published specifications of existing reactors. It is vital to understand that if reactor modifications are considered, the situation can be changed. For instance, one reason for the lack of slab-type test locations is the general lack of need for such locations in the past. Some possible

Table 12.3.3-2. Numbers of Existing Acceptable Slab Test Locations in U.S. (U.S. and Foreign) Reactors

| Minimum Required Flux ($n/cm^2 \cdot sec$) | Test Assembly Maximum Dimension (cm) | | | | |
|---|---|---|---|---|---|
| | 25 | 50 | 75 | 100 | 150 |
| $5 \times 10^{13}$ | 7(11)[a] | 1(4) | 0(2) | 0(1) | 0(1) |

a. Numbers in parentheses are for U.S. and foreign reactors.

locations have been converted to other uses, such as thermal columns. Relatively minor modifications could serve to increase the availability of larger test locations (both core-side and in-core). Modifications could also improve the test fluxes obtainable, although not as much as the physical size. As discussed previously, modified core loadings with higher fuel densities near the test will decrease the flux depression and improve the test performance. These considerations are extremely facility-specific and also somewhat speculative (in terms of quantitative impact). However, one specific example of particular interest concerns the possibility of conducting slab tests in the Oak Ridge Research Reactor (ORR). Currently, slab tests approximately 68 x 75 cm could be operated at total fluxes up to $3 \times 10^{14}$ $n/cm^2$-s. With an increase in allowable reactor power (which could entail additional plant equipment such as heat exchangers) and careful management of the core loading, the test area flux could be more than doubled, which would probably permit acceptable test conditions in the module. Furthermore, since these types of tests will be of interest a number of years in the future, sufficient time exists to accomplish necessary modifications and thereby make the required test locations available.

In summary, it is fair to conclude that the number of useful test locations in fission reactors is somewhat limited. There may be an adequate number of in-core positions, particularly if reactor modifications are considered. There are few truly useful existing slab test locations, primarily due to flux (as opposed to geometry) requirements. However, modifications could improve the situation, and in fact, it appears that at least one acceptable location could be produced at the ORR.

### 12.3.4 Non-Nuclear Conditions

When considering any test in a fission reactor, the initial requirement is that the test must not impact reactor safety in any way. In addition, impact on reactor operation, outside of normal limits, is generally prohibited. These guidelines directly affect the conditions which can be incorporated in a fission test. It is also important to keep in mind that test volume is often at a premium, so all components in the

test assembly must be considered carefully. In the context of these guidelines, the various non-nuclear conditions of interest are discussed below.

Mechanical Forces. The application of mechanical forces during irradiation is standard practice in many in-reactor tests such as irradiation-creep tests. It is usually accomplished by small gas cylinders with leads routed outside the reactor where the pressure can be controlled. This allows time-variable loadings.

Surface Heating. Fundamentally, there is no problem in supplying a surface heat flux. Many in-reactor experiments incorporate some type of electrical heater to maintain temperature control. Conceptually, electrical resistance heaters could easily be used to simulate the first wall heat flux. Another approach would be to use the volumetric heat generated in the neutron filter which is normally part of the test; if temperature limits allow, the heat could be conducted to the first wall of the test module. Both approaches would be relatively compact and neither would affect reactor safety or operation.

Magnetic Field. In order to produce magnetic fields of high enough intensity and in large enough volume (1 Tesla or more) to be of interest, large magnets are usually required. Incorporating these into a test assembly to fit a small test location will be rather difficult. In addition, it will be difficult to ensure that the stray field (or return flux) will not exert transient or steady-state forces on reactor components. A stray field could slow the drop of a control rod during a scram by simple eddy-current braking. Implementing magnetic fields within fission tests may be difficult.

Particle Flux. To date, no acceptable method of producing a first wall-like particle flux in the fission reactor environment has been developed. Use of a $^{3}He$ layer would produce some ions and heat, but at levels below those of interest in engineering testing.

### 12.3.5 Reactivity Considerations

Since test assemblies for fusion blanket engineering will be extremely efficient neutron absorbers, the effect of the test on the ability of the fission reactor to remain critical is of interest. By comparing the physics calculations performed for the Test Development and 1-D Criticality Study Tasks, with similar calculations for the reactor alone (without the test assembly in place), it is possible to assess the net reactivity effect of the test.

For the submodule tests, the base case without the test in place was run to establish a minimum critical reactor configuration; the outer diameter of the core was varied (for each case) until criticality was achieved. Then the test assembly model was included and the net reactivity effect was determined. The results for the two submodule tests are summarized in Table 12.3.5-1. As might be expected, a thicker core is required to maintain criticality for a larger test location. As a point of reference, an average control rod with fuel follower for the type of core modeled is worth approximately +2.50$. Thus, the negative reactivity effect of the test modules is not a serious problem (less than three rod worths).

Table 12.3.5-1. Reactivity Effect of Submodule Tests

| Concept | Test OD (cm) | Minimum Annular Core Thickness (cm)[a] | Test Reactivity Worth[b] |
|---|---|---|---|
| $LiAlO_2/Be/H_2O/PCA$ | 7.5 | 15.3 | -6.2 $ |
| $Li_2O/He/HT-9$ | 12.2 | 22.3 | -7.1 $ |

a. Thickness needed to achieve criticality without test in place, using standard MTR-type fuel composition.

b. One average control rod with fuel follower equals ∿ +2.50 $.

For the slab test modules, the 1-D Criticality Study Calculations were used to investigate the net reactivity worth of the test module and the test performance parameters as functions of core thickness. In this study, the base case which was used included a beryllium reflector where the test module is normally installed; in addition, the 2-cm 316-ss containment was not included in the base case. The core thickness was found to make no difference in the operation of the test (power density profiles, etc.) for a given source flux level. The results of all the reactivity calculations for slab tests are shown in Figure 12.3.5-1. Again, an average control rod with fuel follower is worth approximately +2.50$. The data points shown correspond to fission reactor cores which are 3, 4, 5, 6, and 7 elements thick (where a standard fuel element is 3 in. square). The implication of Figure 12.3.5-1 is that small cores (less than approximately 30 cm thick) will have serious difficulty in supplying necessary reactivity. Large cores, greater than 50 cm thick, can certainly accommodate tests. Medium cores (30 to 50-cm thick) can probably accommodate slab tests, but it is likely that some modifications (such as higher fuel loading or rearrangement of control rods) will be necessary.

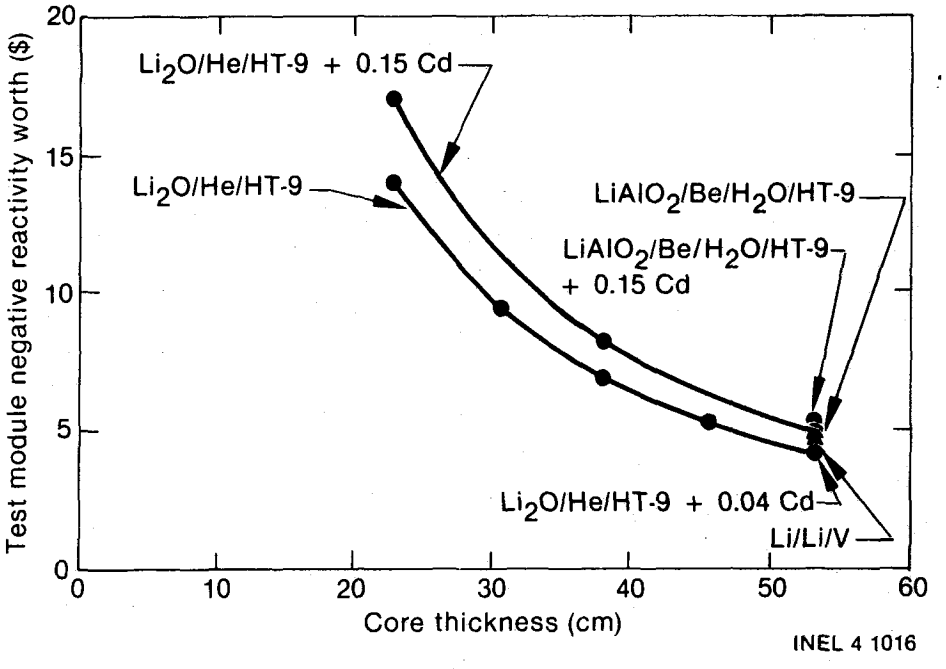


Figure 12.3.5-1. Slab test module negative reactivity worth as a function of fission core thickness.

In summary, reactivity (criticality) considerations do not seem to be a serious problem for submodule tests. For slab tests, reactivity requirements will probably restrict the choice of useful reactors to those with core thicknesses greater than 30 cm. Some modification of this conclusion is conceivable if extreme reactor modifications are considered.

### 12.3.6 Availability for Testing

The availability of facilities is essentially a programmatic issue, and information on it has been obtained from a cursory examination of the responses received from the facility survey. In all responses, facility operators indicated that their reactors either were available or could be available given proper programmatic priority. In addition, current plans for most facilities are to continue operation for the indefinite future; the exceptions to this are: EBR-II, projecting only 10 years' operation, and PBF, projecting only one year. Note also that ETR was mothballed several years ago. There are currently no indications that any new, large, high flux test reactors are being planned. Taken together, all this information seems to indicate a slow downward trend in the availability of fission reactors for testing. This trend appears to be slow enough that it could be reversible if programmatic issues would so dictate.

### 12.3.7 Cost

Although no specific effort has been put on comparisons of the cost of fission tests with that of fusion tests, three main points can be made. First, equivalent test hardware for fission and fusion tests will have equivalent cost, since the design requirements for both will be similar. Second, the cost of facility operation will be much higher for a fusion test device than for a fission test reactor. Early fusion test reactors may be driven machines, which require large amounts of input electrical power. Third, fission test capabilities, some highly developed, exist and are available now; the construction of a new facility may not be necessary. Consideration of these points leads to the conclusion that fission testing will be less costly than fusion testing. However, each experiment needs to be considered on a cost/benefit basis.

## 12.4 Conclusions on Technical Usefulness of Fission Testing

On the basis of discussions in the previous sections, a number of conclusions can be drawn on the technical aspects of fission testing and how they relate to fusion engineering testing. These conclusions are somewhat relative, since the final decision on technical usefulness of fission reactors depends to some extent on the cost and benefit of the other testing options (point neutron sources, fusion test devices, etc.). Nevertheless, general technical guidelines will be required in considering credible development strategies.

From the preceding information, it appears that fission testing will be most useful in conducting "multiple effects" as opposed to "component" tests. Although fission testing can produce several important elements of the fusion environment, in many cases true act-alike component tests will be impossible because of environmental differences. This may also hold true even for testing on fusion devices, due to limitations on test size, neutron wall loading, etc. In general, true component testing will probably be extremely limited. Instead, multiple effects tests will be used extensively, with results integrated via analysis and modeling to yield the desired engineering data base. In this context, there is less need for true act-alike tests, and more need for a varied program of multiple-effects tests. Fission testing is uniquely qualified for conducting these types of tests. In particular it appears that the primary role of fission testing in fusion engineering will be in conducting submodule tests. There are a number of reasons for this conclusion. First, the technical requirements for submodule tests are somewhat less strict than for more complex full module tests. The neutron flux required is somewhat lower, and the test area can be small. The quality of simulation will be better, since it is easier to simulate conditions over a smaller physical extent. Many locations also exist which could be used for such tests.

Fission experiments will also have some role in full-module testing and can be extremely useful for examining beginning of life performance of large modules for three main reasons. First, fission tests can provide a

good simulation of a fusion environment for beginning of life issues. Second, test sites can be available as soon as required, with modification of existing reactors. Third, fission experiments will be cost-effective compared to fusion testing since no new facility construction will be necessary. Fission testing may also allow identification of some radiation-related synergisms, since most components of the fusion environment will be present. Use of large testing is limited mainly by the availability of suitable test locations, which require large size and high flux.

Fission-based multiple effects tests, such as those investigated here, will probably be more useful for solid breeder blanket concepts than for liquid metal blankets. Most liquid metal blanket issues must be addressed at both smaller (single-channel) and larger scales. Fission testing will certainly be useful for smaller scale liquid-metal tests; larger tests have requirements somewhat incompatible with fission testing. The critical issues for solid breeder blankets (tritium release and thermal performance) are a much better match to the inherent capabilities of fission testing.

## 12.5 Overall Conclusions on Utilization of Fission Reactors

In order to specify how and why fission testing should be used, it is necessary to examine its identified limitations, and the programmatic considerations involved.

Fission testing is limited in three main areas. First, it is difficult to provide a complete simulation of the "integrated fusion environment." While fission reactors are excellent bulk neutron-providers, it is difficult to incorporate particle fluxes and magnetic fields in tests. The second main limitation is often loosely referred to as the "spectral difference." From studies of the actual effects of this difference, it was shown earlier that in two main areas (power density and tritium production), spectral differences do not represent a serious limitation. However, in the area of radiation damage to structure, the spectrum is quite significant and fission reactors will provide a poor simulation. In addition, the spectral difference will always lead to

lingering doubts about spectrum-related synergisms which might not be visible in fission tests, but would appear in actual operation; this is one of the strongest arguments that some fusion testing is mandatory. The third main limitation in fission testing is in the total number of acceptable test locations available. While up to 100 locations may be suitable for submodule tests, no acceptable slab module test locations currently exist, and relatively few could be generated via modifications to existing facilities. This limitation could be eased by constructing new reactors, optimized for fusion testing, but such high-cost options have not been considered in this effort.

These limitations apply primarily to component testing, where complete act-alike behavior is required. They are of much less concern for multiple-effects testing, where the emphasis is on incorporating a number of different effects (rather than all effects) in a given test. Since it is likely that single and multiple-effects tests (which are well suited for fission reactors) will constitute the bulk of the fusion engineering testing program, fission testing can and should be an integral, useful part of the fusion engineering program. Although it cannot reasonably replace or eliminate the need for fusion testing (except for extremely high-risk development scenarios), it can address many critical testing needs to some degree. The advantages will be timeliness (it is available now) and cost-effectiveness (no new facility construction required). In the final analysis, each fission experiment must be evaluated on a cost/risk/benefit basis. In this context, fission testing is less costly and lower risk than fusion testing. The attractiveness of acquiring considerable data on critical issues for fusion, by testing early and in existing facilities should not be underestimated.

## REFERENCES FOR CHAPTER 12


1. American Nuclear Society, Research, Training, Test, and Production Reactor Directory, September 1979.

2. International Atomic Energy Agency, Directory of Nuclear Reactors, 1959-1976.

3. International Atomic Energy Agency, Research Reactors in Member States, 1980 Edition.

4. Commission of the European Communities, Handbook of Materials Testing Reactors and Associated Hot Laboratories in the European Community, 1981.

5. D. A. Struttmann, Preliminary Calculations for Testing of $Li_2O$, $LiAlO_2$, and V/Cs/Ti Fusion Blankets in an ETR Configuration, EG&G Idaho, Inc., EGG-FSP-6667, July 1984.

6. C. C. Baker, et al., STARFIRE--A Commercial Tokamak Fusion Power Plant Study, Argonne National Laboratory, ANL/FPP-20-1, September 1980.

# CHAPTER 13

# TANDEM MIRROR TEST FACILITIES

TABLE OF CONTENTS


Page

13.1 Background and Introduction..... 13-1

13.2 The Technology Demonstration Facility..... 13-5
13.2.1 TDF Design Objectives..... 13-6
13.2.2 Physical Description..... 13-7
13.2.3 Operating Description..... 13-8
13.2.4 Engineering Description..... 13-15
13.2.5 Critical Engineering Issues.....13-20
13.2.5.1 Magnets.....13-20
13.2.5.2 Neutral Beams.....13-21
13.2.5.3 Shielding.....13-22
13.2.5.4 Tritium.....13-23
13.2.5.5 Test Facilities.....13-24
13.2.5.6 Maintenance.....13-24

13.3 The MFTF-α+T Upgrade of MFTF-B.....13-27
13.3.1 MFTF-α+T Design Objectives.....13-27
13.3.2 Physical Description and Configuration.....13-28
13.3.3 Physics Mode.....13-32
13.3.4 Engineering Description.....13-34
13.3.4.1 Magnet System.....13-34
13.3.4.2 Heating, Fueling and Drift Pumping.....13-36
13.3.4.3 Halo Scraper, Direct Converter and Vacuum Pumping.....13-38
13.3.4.4 Tritium Systems.....13-41
13.3.4.5 Maintenance.....13-41
13.3.5 Consideration of a More Ambitious Test Cell.....13-45
13.3.5.1 Parametric Analysis.....13-46
13.3.5.2 Optimized Cases.....13-49
13.3.5.3 Conclusions for MFTF-α+T Physics Modeling.....13-50

TABLE OF CONTENTS (contd.)


Page

13.4 Resolving the FINESSE Nuclear Issues in a Tandem Mirror Nuclear Test Facility....13-53

13.4.1 General Considerations....13-53

13.4.2 Assessment of Tandem Mirror Nuclear Experimentation/ Testing vis-a-vis FINESSE Nuclear Issues List....13-60

13.4.2.1 Methodology....13-60

13.4.2.2 Results....13-63

References....13-84

# 13. TANDEM MIRROR TEST FACILITIES

## 13.1 Background and Introduction

Tandem mirrors offer a unique capability among fusion devices for carrying out nuclear experiment/test programs and for demonstrating the operation of nuclear technologies. This capability derives from an ability to produce high fusion power densities by injecting high energy D-T neutral beams into a magnetic mirror test cell which is inserted within the central cell of a tandem mirror. The volume of plasma can be kept arbitrarily small by selecting the length of the cell, with the result that low-cost test areas can be designed. The physics of ion confinement in the mirror cell is essentially the physics of single cell mirrors, for which there is a long experimental history. That history shows that well understood classical predictions of ion-ion scattering (i.e., confinement times proportional to $T_i^{3/2}/n$) and ion-electron drag (i.e., confinement times proportional to $T_e^{3/2}/n$) account for losses from the cell. Thus, it appears possible to design the test cell with considerable confidence in the essential physics.

It was recognized more than 10 years ago that single cell mirrors might be attractive as nuclear research test facilities. A device which was designed for that purpose in 1974 was the Fusion Engineering Research Facility (FERF)[1]. With the invention of the tandem mirror, the idea was adapted to the evolved confinement configuration by beam driving the entire center cell of a tandem mirror as a test cell. Such a facility would operate in the "Kelley mode" with the large majority of ions being magnetically trapped and the minority fraction being electrostatically confined in the tandem mirror end plugs.

To this end, Fowler and Logan[2] proposed a Tandem Mirror Technology Demonstration Facility (TDF) which would use beam-driven axicell plugs and quadrupole anchors, similar to the present TARA machine at MIT but without thermal barriers. The original TDF configuration is shown schematically in Fig. 13.1-1. The end plugs of TDF were to be stream-stabilized by the plasma outflow from the central cell, while the anchors were to provide MHD stability through electron conduction between the high density plug and the low density

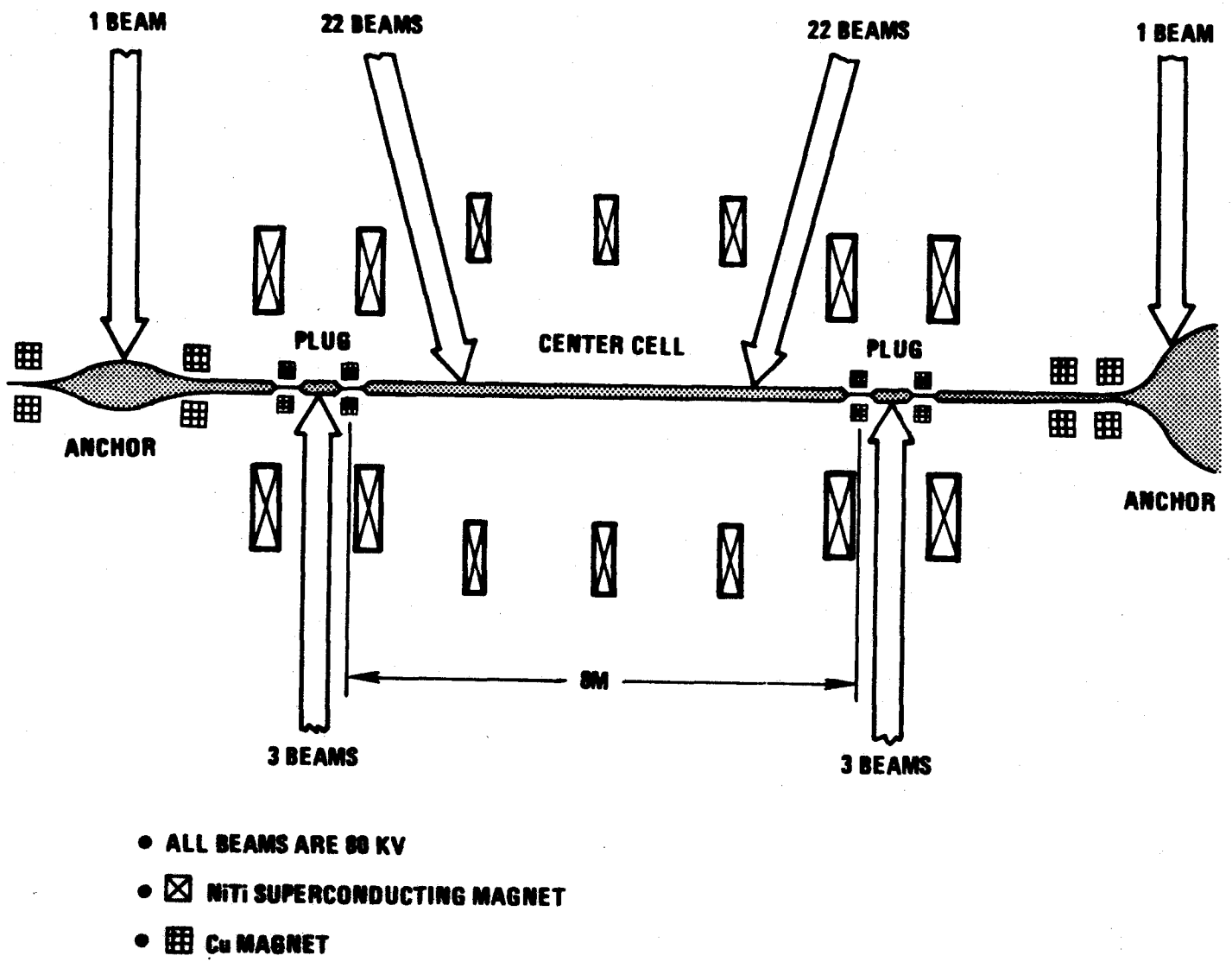


Figure 13.1-1. Original Technology Demonstration Facility (TDF) configuration.

anchors. With 68 MW of 80 kV beams, Fowler and Logan predicted that 15 MW of fusion power would be produced in the 8 m central cell. Because the energetic ion lifetime was assumed to be only one collision time, the physics basis was believed to be conservative. A major advantage of this 1981 neutron test facility proposal was that the physics could largely be verified from standard tandem mirror operation of the LLNL TMX facility. A thermal barrier version, with double the power output (and wall loading) for the same beam power, was also proposed at that time.

The initial suggestion of using tandem mirrors as technology facilities led to a larger TDF study, led by the Lawrence Livermore National Laboratory, and involving many fusion organizations. The TDF design which emerged from the latter study[3] differed from that suggested by Fowler and Logan in its physics configuration. This change was made necessary by the discovery of trapped particle modes in tandem mirror reactors. These modes are unstable when the quadrupole anchor regions are not well connected to the electrostatic plugging regions. To address this problem in the TDF design of reference 3, the electrostatic plugs were moved outwards, from an axisymmetric "axicell," to the quadrupole cell. At the same time, a simple choke coil would replace the axicell and a thermal barrier would be formed in the anchor. The TDF configuration would, therefore, be essentially the same as the current MFTF-B configuration.

Two different options for achieving microstability in TDF were considered. With the first, stream stabilization[4], low electron temperatures and confinement times lead to a wall loading of 1.4 $MW/m^2$ from 20 MW of fusion power (65 MW of 80 kV beams). The second option, based on stability by sloshing ions, has potential to provide improved performance[5] with the stream gas removed. In this case, the electron temperature and lifetime doubles, fusion power increases to 35 MW (with 51 MW of 55 KeV beams), and the wall loading increases to 2.1 $MW/m^2$.

Less expensive (than TDF) approaches to test facilities have been proposed as novel upgrades to MFTF-B. The first of these, designated MFTF-B+T[6], was designed using a short axisymmetric mirror cell for the central cell of the machine. The design featured 12 T copper coils and a 4 m long test cell. When driven with 16 MW of beams (80 kV), this test cell is expected to produce 13 MW of fusion power (1.3 $MW/m^2$ wall flux). Designed for

10-hour runs with only 1% availability, MFTF-B+T was proposed as an inexpensive technology test facility whose configuration would be only a minor adaptation to MFTF-B as constructed. The largest modification to the existing facility would be long-pulse upgrades to the heating systems. The low design availability results because MFTF-B was not designed for full remote maintenance.

A different direction for mirror test facilities was taken with the design of a more recent MFTF-B upgrade option, MFTF-$\varepsilon$+T[7]. With MFTF-B+T there was concern that the only major tandem mirror facility in the program would be devoted exclusively to fusion technology and would not be available to take the next physics step. The MFTF-$\alpha$+T option addresses this problem. Importantly, the $\alpha$+T upgrade is intended to be a DT-burning machine with significant $\alpha$-power deposition in the central cell. It would incorporate many recent ideas which are expected to result in tandem mirror concept improvement (i.e., MARS end plugs with additional anchoring, drift pumping, halo pumping) and would also feature several next-step technolgies (e.g., 200 keV negative ion beams, 18 T choke coils, direct conversion). A second phase of MFTF-$\alpha$+T operation would focus upon technology development and nuclear testing with a beam driven test cell insert. The insert could be built at the outset or later. With the insert, the machine would be operated in a different lower confinement mode to provide a relatively high ($\sim$ 2 MW/m$^2$) neutron wall loading. As in MFTF-B+T, the insert would be embedded in the central cell.

Another design study, TASKA-M, was recently completed by the Kernforschungszentrum, Karlsruhe, Federal Republic of Germany, in conjunction with Fusion Power Associates/University of Wisconsin[8]. The TASKA-M mission was to identify "the smallest and least costly tandem mirror test facility possible which still retains a considerable degree of reactor relevance." The TASKA-M design was based upon near-term physics assumptions and mid-1980's level technological capabilities. TASKA-M would produce 6.8 MW of fusion power to provide a peak neutron fluence of $\sim$ 80 dpa in a 0.17 m$^3$ test area. The facility would also accommodate two small blanket component test modules, however, the neutron wall loading varies greatly in the axial direction. Nevertheless, TASKA-M with a projected direct cost of less than 400 \$M (1983 dollars), serves as an excellent example of a starting point in the spectrum

of capabilities for low power but intermediate fluence, tandem mirror test facilities.

With TDF, MFTF-$\alpha$+T and TASKA-M, the design of test facilities has matured and the unique value of using tandem mirrors with driven test cells to address technology issues has been shown. Further steps in the design of test facilities will surely be taken, but in some sense these will only be variations of the TDF (full central cell test section, dedicated machine) or the MFTF-$\alpha$+T (insert section, shared physics and technology missions).

For example, the use of octupole end plugs has already been proposed for MHD stabilization in tandems. Successful use of these octupole designs would permit much shorter end plugs and, therefore, much shorter central cells for a given performance level (in $n\tau$ or Q). In fact, with octupole plugs, it is projected that central cell ignition could be achieved in a machine length comparable to the present MFTF-B. Such a device would have wall loadings of $\sim$ 1 MW/m$^2$, but if operated in a lower confinement mode, with a beam driven test cell insert, the wall loading could be raised to 2-3 MW/m$^2$.

Whatever the best technique for MHD stabilization turns out to be (octupoles, TARA anchors, wall stabilization, or electron rings), a nuclear technology facility could be built using any of these end region schemes, with thermal barriers for efficient plugging. Whether or not the existing designs, using quadrupole end plugs prevail, is only a matter of program timing. As the program develops, options will expand as new end plug schemes are tested experimentally.

In Sections 13.2 and 13.3, brief overviews of the TDF and MFTF-$\alpha$+T tandem mirror facility designs are provided. Section 13.3 also presents recent results relating to MFTF-$\alpha$+T modifications which would be required to provide a greater neutron wall loading and/or a larger test cell area. In Section 13.5 of this chapter, a discussion of how the FINESSE nuclear issues might be resolved using a tandem mirror technology facility and complementary facilities is provided.

## 13.2 The Technology Demonstration Facility (TDF)

This section provides a brief review of the 1982 Technology Demonstration Facility (TDF) design study performed by LLNL with support from several fusion

organizations.* This design has been documented in a detailed LLNL report[9] as well as in two review articles[4,5]. It should be noted that the original "stream-stabilized", TDF design[9] would operate at a fusion power of 20 MW with a neutron wall loading of 1.4 $MW/m^2$. Recent experimental results from the TMX-upgrade experiment at LLNL confirm that the deisign can be improved to achieve a fusion power of 36 MW and a wall loading of 2.1 $MW/m^2$ without major changes in the configuration or its engineering difficulty. Updated parameters for the "beam-fueled", higher wall loading mode of operation are, therefore, provided in this section.

### 13.2.1 TDF Design Objectives

The primary objective defined for the TDF was to generate engineering data on the nuclear technologies needed to build an engineering test reactor (ETR). To accomplish the objective outlined above, the following mission guidelines were adopted:

- Demonstrate the steady-state operation of plasma heating systems, vacuum pumping, tritium handling systems, and superconducting magnets in a high flux neutron environment.

- Provide a steady-state neutron environment sufficient to test blankets that are designed to address power/tritium fuel cycle issues for fusion.

- Develop and demonstrate instrumentation, control, and maintenance methods to show the safety and viability of operating fusion power devices.

The plasma production and containment components of TDF would be required to function at the MFTF-B level of difficulty and magnets, neutral beams, and electron-cyclotron resonant heating (ECRH) systems would differ little in

---

* Major participants were TRW, GD Convair, and the FEDC at Oak Ridge. Additional participation from Argonne, MIT, LASL, UCLA, SAI, Bechtel, and the University of Wisconsin.

their parameters from those in MFTF-B. Even the steady-state operation requirement was considered to be only a modest extension of the 30 s capability of MFTF-B.

D-T operation, with the attendant shielding, tritium permeation, design constraints to accommodate maintenance, and the required reliability to extend the engineering data base was considered to be the major challenge in the TDF mission. In particular, a major goal of this device would be an intermediate flux/fluence capability which would enable significant testing of power and fuel cycle components and systems. Blanket operation at a first-wall flux $> 1$ MW/m$^2$, for periods of time sufficient to discover failure modes that might occur well beyond any initial (first-operation type) failure, but short of its expected operating life was a key mission requirement. Such a test program was believed to require $10^3$ to $10^4$ hours of test time per blanket module. The facility was designed to accommodate an ultimate test cell fluence of about 10 MW-yr/m$^2$, so that an ambitious test program might be accomplished.

An important aspect of the mission concerned the safe operation and maintenance of the device and the role of this facility in generating a data base that would be required to site and construct an ETR. One would expect to develop the necessary instrumentation and control for safe operation; establish operations and maintenance procedures based on experience in running the facility; and demonstrate the adequacy of systems for emergency events such as loss of flow or coolant, tritium release to secondary containment, and other such off-normal events. Experience gained here would be invaluable in establishing the safety of fusion power plants.

### 13.2.2 Physical Description

By limiting the central cell to the shortest length consistent with a minimal test area in the center of the machine, TDF can be comparable in size to present generation tandem mirror experiments. The magnet set would be about as long as the Tandem Mirror Experiment-Upgrade (TMX-U) magnet set, while the overall length would be slightly less than the length of MFTF-B. Fig. 13.2-1 shows the general layout of the magnets, vessel, beams, fueling and vacuum systems, and shielded central cell.

All magnets would be superconducting except for the two copper alloy choke coils that would product 12 T of the 15 T mirror in the central cell.

The three large central cell coils would have a 4 m bore, and the smallest of them would store 342 MJ of energy. The two outboard coils would store 700 MJ, and all would use niobium-titanium (NbTi) conductors. Each yin-yang anchor and transition coil would have a 1.25 m major radius, half of the radius of MFTF-B yin-yangs.

The testing space for blankets would be located in the 8-m-long central cell, with provision for two modules that are each 1 m wide and 0.25 m in minimum first wall radius. An uncollided neutron flux of 2.1 $MW/m^2$ at the 30-cm first wall radius is generated by fusion reactions in the 15-cm radius plasma. A total of 13.6 $m^2$ of surface is irradiated at this flux and about half of it is readily accessible between the solenoid coils. This central portion of the machine is shown in Fig. 13.2-2.

Maintaining the high temperature and density of the central cell plasma would require the absorption of 51 MW of 55 kV beam power. There would be four azimuthally spaced beamlines on each end of the central cell, and each beamline would house four sources. If each source puts 50 A incident on the plasma, one of every four sources is not needed and can be installed as a spare to improve the availability. Shielding of these beamlines and central cell to permit contact maintenance, access for maintenance of short life components, accessibility and rapid change-out for test modules were important requirements to be met in designing the machine.

The end cells are 16 m in diameter and nearly 20 m long. These end cells are well isolated geometrically from the neutron "line source," which is the 8 m long plasma column in the central cell. Only modest shadow shielding of the transition and anchor (superconducting) coils is required because the copper choke coils at the ends of the central solenoid provide considerable axial shielding.

### 13.2.3 Operating Description

The 8-m long simple mirror cell (Fig. 13.2-2) would be the heart of TDF. This 4.5-T field cell, with its 15-T copper choke coils, would be beam-driven with 1244 A (incident) of 55 kV beams with a species mix of 80:15:5. With 94% of the beam trapped by the 15-cm radius plasma at a density of $5.8 \times 10^{14}$ $cm^{-3}$, about 36 MW of fusion power would be produced (29 MW in neutrons).

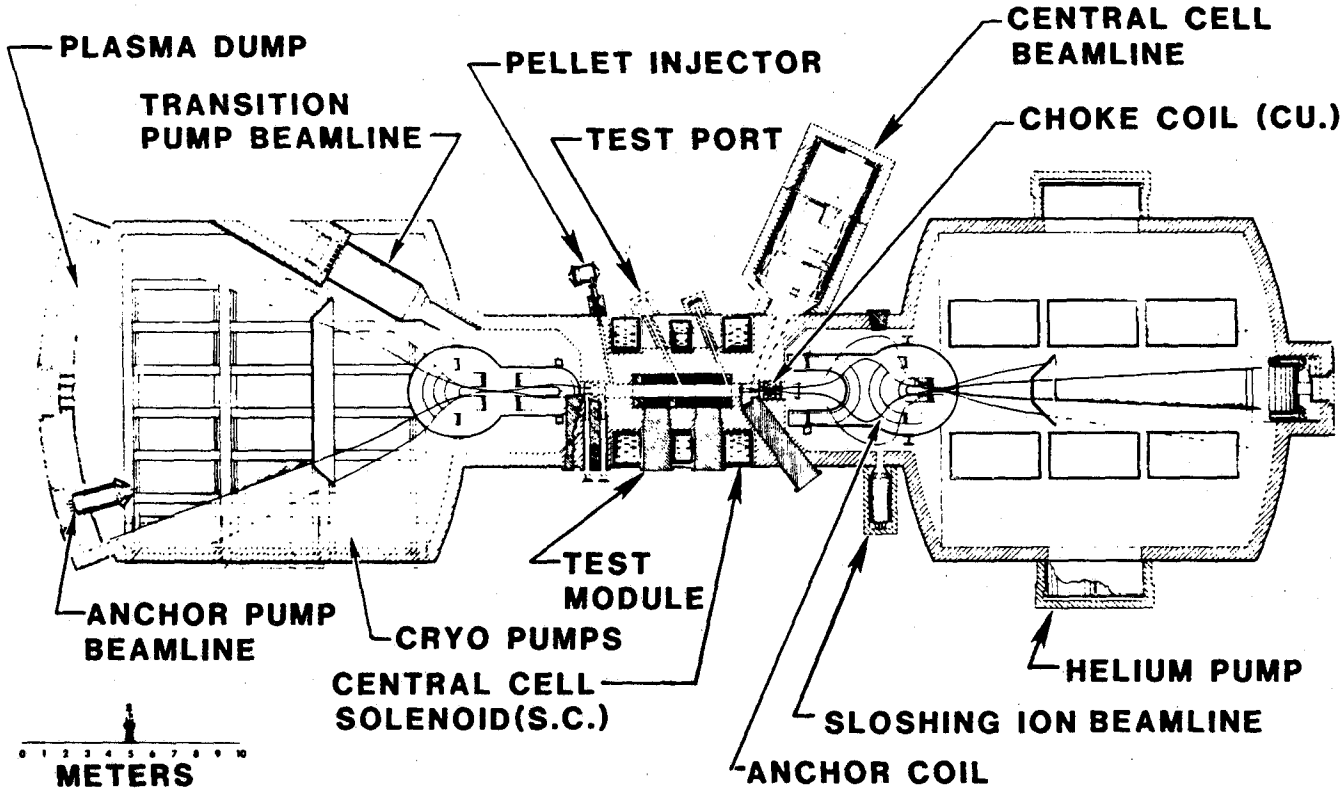


Figure 13.2-1. Cross-section of TDF machine. (Some components are shown rotated out of plane for clarity, and only one of the eight center cell beamlines is shown.)

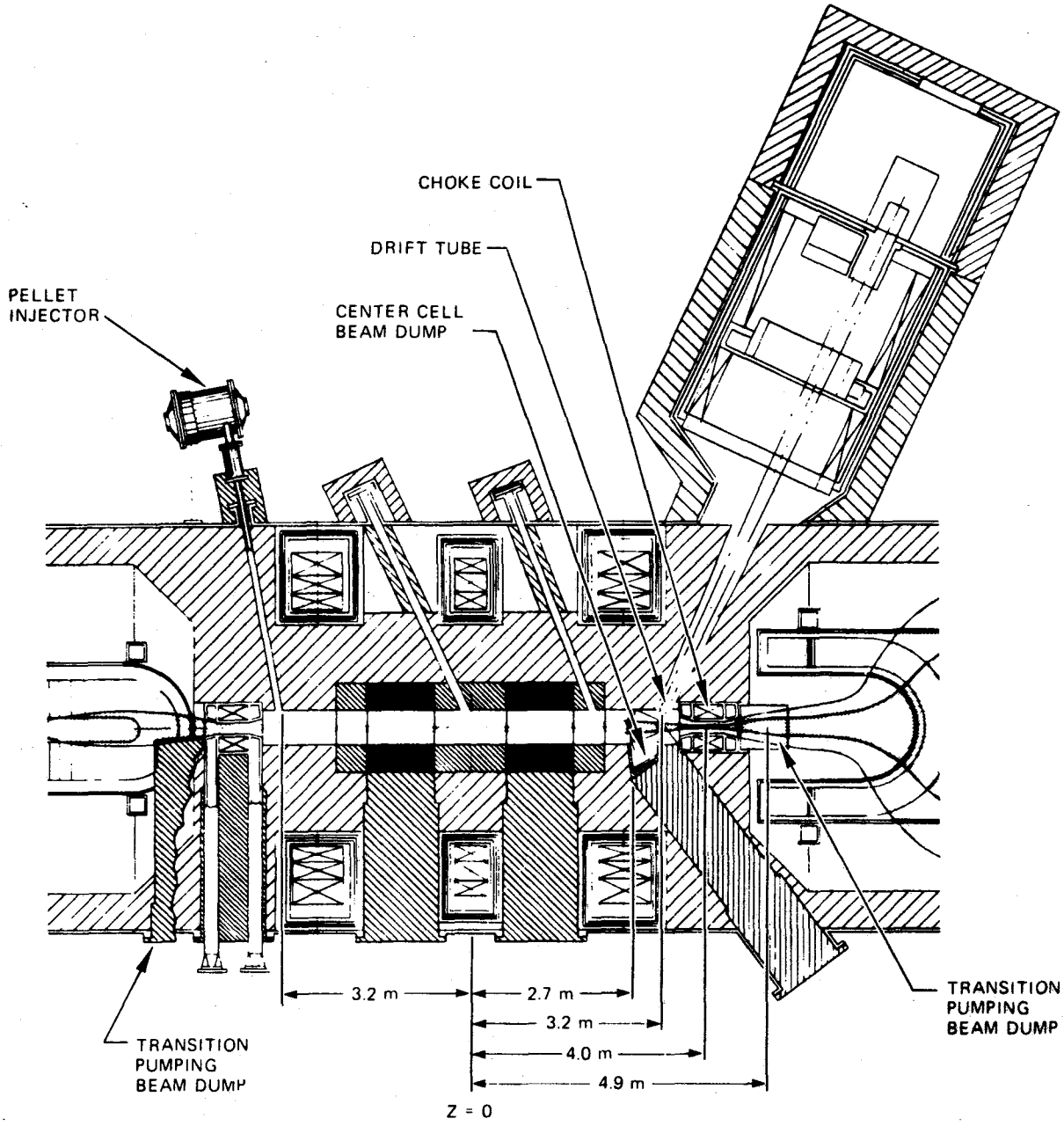


Figure 13.2-2. Central portion of TDF. (Shows the two blanket module test locations, scheme for removing choke coils, beamline penetration through shielding, and beam dump access for repair. Also shown is the access to the high flux test area under the superconducting coils, which allows for inserting material samples for radiation damage studies.)

The TDF density, field, and potential profiles are shown in Fig. 13.2.3. In arriving at this operating point, an MHD central cell $\beta_c$ limit (to m = 1 ballooning modes) of 40% peak for a 50% $\beta_a$ peak in the anchor is observed. While the density profile of the higher performance, beam fueled TDF version discussed here would be nearly the same as would be achieved in the lower performance, stream-stabilized version, the potentials would be significantly higher. The peak potential would be 37 kV, and the central cell potential would be 25 kV.

A thermal barrier and a confining potential peak, or plug, would be created in a 3:1 mirror that joins the central cell through a 1-T transition region. To create the thermal barrier, a 5.7 A (incident) beam at 80 kV with a 90:7:3 species mix would be injected at the inside sloshing peak shown in Fig. 13.2-3. With a total of 1 MW of 35 GHz power absorbed at both ends, the thermal barrier would be formed. The confining potentials would then be erected by applying 560 kW of 60 GHz power to the end plug regions.

Table 13.2-1 lists the key physics and machine parameters for both the original stream-stabilized and the improved beam-fueled versions of TDF. A key difference is the factor of 2 increase in central cell electron temperature. Although the mean hot ion energy (37 keV) would be the same in each case, the mean beam energies of 60 keV and 41 keV, respectively, would be very different for the 80 and 55 kV systems. In the beam-fueled version, the beam voltage was reduced to maintain the average hot ion energy so as not to exceed the MHD beta limit. However, with an improved magnetic configuration, the beta limit could be raised, and the reduction of beam energy could be less drastic, or possibly eliminated. At higher energy and fixed density, the fusion power would further increase, achieving near optimum performance at beam energies $\sim$ 80 keV.

It should be stressed that the transition design is crucial in tandem mirrors, and that the TDF study occurred prior to the extensive work done for MFTF-B and its upgrades. Consequently, issues of MHD stability, radial transport, and equilibrium, all of which are influenced by geodesic and normal curvature in properly designed transitions, need to be reexamined in any further study of this class of machines. Nevertheless, the beam-fueled

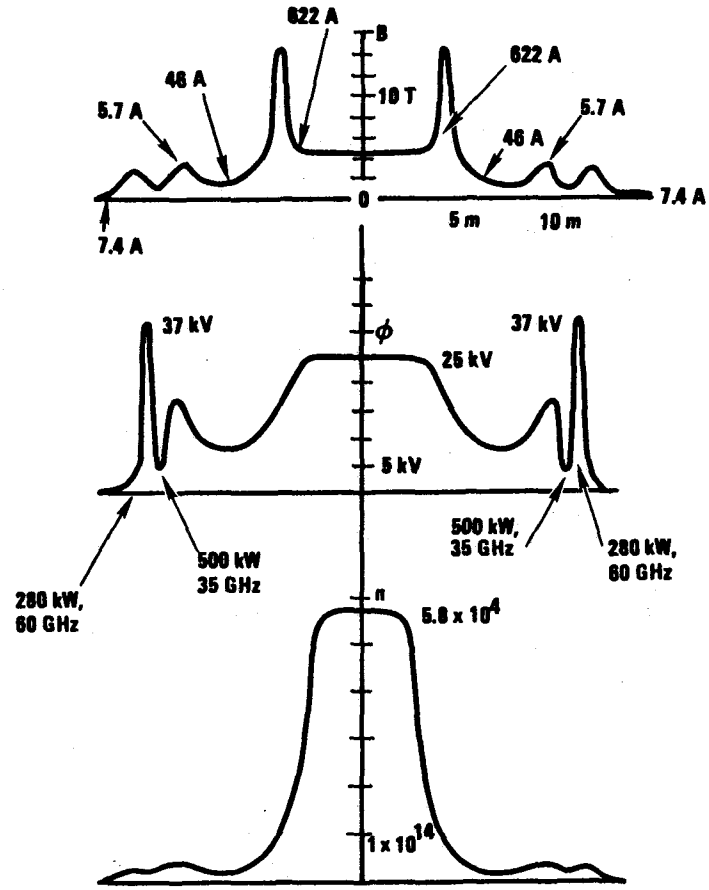


Figure 13.2-3. Profiles of the TDF magnetic field, potential, and density along the machine axis. (The central cell population is nearly all magnetically trapped, and those ions that escape are confined by the 4 kV confining potential.)

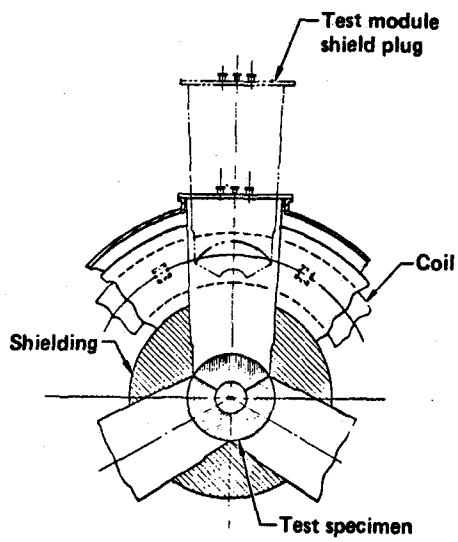


Figure 13.2-4. Details of the TDF blanket test area. (Showing how modules could be readily removed.)

Table 13.2-1(a). TDF Central Cell Parameters

| Parameter | Stream-Stabilized | Beam-Fueled |
|---|---|---|
| Plasma length (m) | 8 | 8 |
| Plasma radius (cm) | 10 | 15 |
| Magnetic field (T) | 4.5 | 4.5 |
| Peak beta (%) | 40 | 40 |
| Electron temperature (keV) | 2.1 | 4.1 |
| Mean hot ion energy (keV) | 37 | 37 |
| Hot ion lifetime (ms) | 11 | 26 |
| Hot ion density ($cm^{-3}$) | $6 \times 10^{14}$ | $5.3 \times 10^{14}$ |
| Warm ion temperature (keV) | 5.3 | 10 |
| Warm ion density ($cm^{-3}$) | $5 \times 10^{13}$ | $5.3 \times 10^{13}$ |
| Beam voltage* (kV) | 80 | 55 |
| Beam power (MW) | 65 | 51 |
| Incident current (A) | 1080 | 1244 |
| Trapped current (A) | 853 | 1169 |
| Pellet gas feed (A) | 800 | 0 |
| Fusion power (MW) | 20 | 35.6 |
| Wall flux at $r_w$ = 25 cm ($MW/m^2$) | 1.4 | 2.1 |
| Central cell potential (kV) | 13 | 25 |
| Confining potential | 4 | 12 |

* Neutral beams have an 80:15:5 species mix. Average beam energy is 60 and 41 keV for the two cases.

Table 13.2-1(b). TDF End Region Parameters

| Parameter | Stream-Stabilized* | Beam-Fueled* |
|---|---|---|
| Transition pump incident current (A) | 59 | 92 |
| Transition pump voltage (kV) | 80 | 80 |
| Transition density ($cm^{-3}$) | $3 \times 10^{12}$ | $4.3 \times 10^{12}$ |
| Plug density ($cm^{-3}$) | $5 \times 10^{12}$ | $8 \times 10^{12}$ |
| Barrier potential (kV) | 12 | 20 |
| Plug potential (kV) | 17 | 37 |
| Barrier ECRH power (kW) | 500 | 1000 |
| Plug ECRH power (kW) | 667 | 560 |
| Sloshing beam (80 kV) incident current (A) | 4.2 | 11.3 |
| Barrier pump incident current (A) | 2.9 | 14.8 |
| Barrier pump voltage (kV) | 80 | 40 |
| Hot electron temperature (keV) | 396 | 466 |
| Plug electron temperature (keV) | 6.5 | 21.2 |

* Values given are totals for both ends. Neutral beams have a 90:7:3 species mix. Average beam energy is 70 keV (80 kV beams) and 35 keV (40 kV beams).

version of TDF is based on rather conservative physics. The millisecond confinement times needed for Kelley* mode operation are very short[11], and most of the fundamentals have been demonstrated experimentally. TMX-U is addressing the issues of thermal barrier formation while TMX-S (S for symmetric, denoting planned modifications to add a throttle coil) and TARA (an axicell tandem at MIT) should discover whatever constraints the trapped particle modes will impose.

### 13.2.4 Engineering Description

The engineering philosophy used in the TDF study was to provide a high reliability device for engineering demonstration and testing. Technology that was either in-hand or scheduled to be demonstrated in programs presently in place was specified. This approach, coupled with the conservative physics assumptions that were used, was expected to produce a machine with a high probability of fulfilling its mission in a timely manner. The goal of the design effort was to describe each of the required subsystems in sufficient detail to allow one to do credible cost estimating and establish a configuration that meets interface requirements and points out critical technology issues. The results of the 10 man-year TDF design study[9] can be summarized by saying that the beam-fueled version of the TDF design would produce 36 MW of fusion power, developing an uncollided neutron flux of 2.1 $MW/m^2$ on an area of $\sim$ 8 $m^2$, while consuming about 0.2 g of tritium per hour and 250 MW of line power, for an estimated cost of about $1000 M (1983 dollars). A summary of the major engineering parameters is given in Table 13.2-2.

---

* Kelley mode refers to the two-component ion distribution in the central cell, with the majority species being the hot, magnetically trapped ions. This differs from the "two-component" or "wetwood burner" operation proposed in various tokamaks, which have the hot component as the minority species. The mode is named after Dr. G. Kelley, formerly at ORNL, for his work on different modes of operation in mirror devices.

Table 13.2-2. TDF Engineering Parameters

| System | Units | Quantity |
|---|---|---|
| OVERALL MACHINE | | |
| Full power run length | h | 100 |
| Availability | percent (life average) | 30 |
| Design life | Full power years | 5.4 |
| Total Capital cost | $M (1982 dollars) | ~ 1000 |
| PLASMA | | |
| Length (central cell) | m | 8.0 |
| Radius | m | 0.15 |
| Peak beta | | 0.4 |
| TEST ZONE | | |
| First wall radius | m | 0.30 |
| Neutron wall load | $MW/m^2$ | 2.1 |
| Test Module area | $m^2$ | 3.6 |
| Total area | $m^2$ | ~ 8 |
| Heat load | $W/cm^2$ (average) | 50 |
| Fusion power | MW | 36 |
| TRITIUM | | |
| Consumption rate | g/h | 0.23 |
| Inventory | kg | ~ 0.3 |
| VACUUM | | |
| Base pressure | Torr | 5.0E-06 |
| Total pump speed | L/s | 1.3E08 |
| MAGNETS | | |
| Superconducting | | |
| Material | | Nb-Ti |
| Peak cond. field | T | 8 |
| Peak center field | T | 4.5 |
| Resistive | | |
| Material | | Cu alloy |
| Peak center field | T | 15 |

Table 13.2-2. TDF Engineering Parameters (cont'd)

| System | Units | Quantity |
|---|---|---|
| NEUTRAL BEAMS | | |
| Mode | | Continuous |
| Energy (max) | keV | 80 |
| Power | | |
| Central cell | MW | 51 |
| Pumping | MW | 7.0 |
| Sloshing | MW | 0.8 |
| RADIO FREQUENCY SOURCES | | |
| Type | | ECRH |
| Frequency | GHz | 35/60 |
| Power | MW | 1.0/0.6 |

The engineering description of TDF begins with the central cell region where virtually all of the neutrons are produced. An axial magnetic field of 4.5 T would be provided by three Nb-Ti superconducting magnets spaced to allow the insertion of test modules up to 1 m in axial dimension. The ends of the central cell provide access for the central cell beams that drive the fusion reactions. The main design considerations in this area are shielding for the solenoid magnets in the area adjacent to the beam ducts and the desire to keep the 15-T resistive choke coil close to the solenoids for field reinforcement. A detailed trade study between beam shielding and magnet requirements in this area largely set the parameters for the rest of the design.

The principal nuclear experiment/test area would be the 8 $m^2$ wall of the central cell between the central cell beam ducts (see Fig. 13.2-2). There would be direct access to two full-diameter test zones between the solenoid magnets, each capable of accommodating a 1-m-long test module (1.6 $m^2$ wall area). Fig. 13.2-4 (shown on page 13-12) shows how TDF test modules might be inserted in this test area. Access to the areas inside the coil boundaries would also be available to test smaller specimens, either as long-term resident samples for fluence testing or as short-term samples inserted in "rabbit tubes."

To generate the high-wall flux in TDF, 51 MW of neutral beams must be provided in the central cell. Figs. 13.2-5 and 13.2-6 show how four beamlines would be arrranged at each end of the machine, with four sources in each beamline. The beams are designed to operate in a relatively high radiation environment for several hundreds of hours. The beamlines would be located in an area where the background magnetic fields are as high as 2000 G. Superconducting magnetic shielding would be employed to get the local fields down to a few gauss level needed for neutral beam source operations.

Because the TDF plasma would be small in diameter, about 15% of the incident beam power would pass through to beam dumps. These dumps, designed for a peak power density of 1000 $W/cm^2$ would be well within the state of the art for two-phase heat transfer in the sub-cooled nucleate boiling regime. The dumps, like the choke coils, would not be a lifetime elements. Both would be built into shielded modules designed for convenient removal and replacement.

Beyond the central cell would be the transition and anchor regions, which would stabilize the central-cell plasma. The fusion power in this region would be small, and only minimal shielding would be required. The magnets would be C-shaped with a Nb-Ti conductor and would be housed in an independent vacuum vessel. Three neutral beam systems would deliver particles to this area: two pump beams that enter at shallow angles; and another beam which would provide sloshing ions normal to the axis. The relatively complex magnet geometry, coupled with rigorous beam geometrical requirments, control the design in this area. Elimination of the pump beams in a more advanced design with RF magnetic field drift pumping, will substantially relax design constraints in this region.

The end cell would be the outboard part of the system, and its principal functions would be to house the primary vaccum pumping and provide a dump for the plasma-leakage power. Vacuum pumping in the baseline design would be provided by cycling cryopumps located above and below the plasma leakage fan. Pumps of the type called for here have been developed and tested by Batzer[13]. There is redundant pumping capacity so that some of the pumps would always be off-line being degassed. The internal tritium inventory can be controlled by the amount of excess capacity specified.

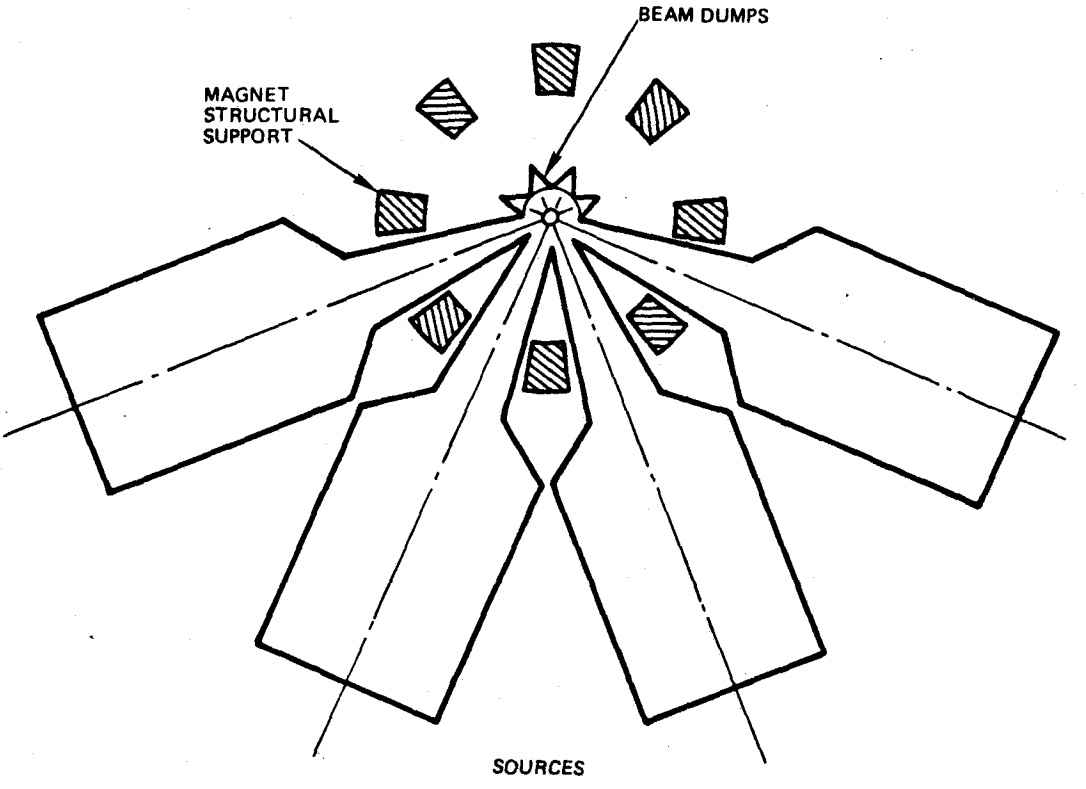


Figure 13.2-5. Azimuthal view of the four beamlines at each end of the TDF central cell.

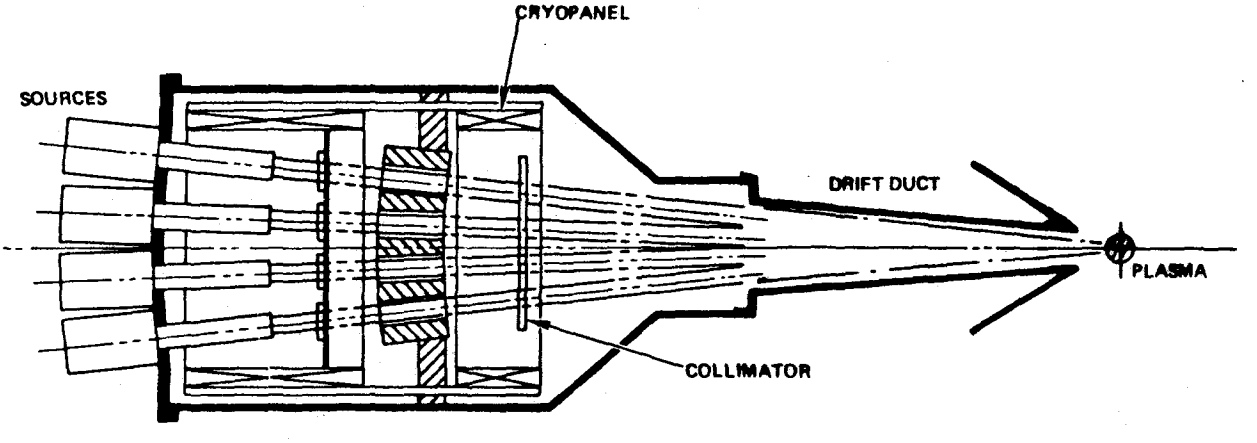


Figure 13.2-6. An individual TDF beamline with four sources, one a spare to improve reliability. (The duct design and source optics are chosen to minimize neutron streaming without incurring beam blockage by high gas pressure in the duct.)

A more advanced design would replace cryopumping with the halo pumping scheme recently developed (in concept) by Logan and Barr at LLNL. Halo pumps, similar to pumped limiters in tokamaks would remove plasma edge ions in a high pressure plenum ($\sim 10^{-3}$ Torr) separated from the main plasma ($\sim 10^{-6}$ Torr). Using this scheme, it will also be possible to recircularize the plasma, dramatically reducing the size of the end tanks.

The TDF is designed for maximum contact maintenance. Specialized tooling would be provided for scheduled maintenance tasks, and general-purpose tooling would be used for random failure repair. Therefore, contact operations would be performed in the vault during regular work schedules after a short cooldown with the magnets de-energized and the tritium removed. In this way, all the major connections can be made and broken in a contact mode, but components would be removed with remote tooling because of the high flux of gamma rays coming from unshielded machine ports. Because the components were designed for high reliability, and because most maintenance tasks would be performed in an efficient contact mode, there is confidence that the TDF would be a high-reliability device with a specified availability of 40-50% in the last half of its 15-yr life.

### 13.2.5 Critical Engineering Issues

The critical engineering issues for TDF are discussed in detail in references 5 and 9. These issues, some of which are briefly highlighted below, are considered critical either because they represent very large components of the overall cost, or because their technology has not been demonstrated under the conditions required by this application.

#### 13.2.5.1 Magnets

Of the various coil types incorporated in the design, the high field choke coils represent the most advanced technology. Although coils of higher field have been successfully built and operated, they are much smaller, were operated for short lifetimes, and were not exposed to high fluxes of neutron irradiation.

The choke coils are of composite design with an insert of normal conductor backed up by the field contribution from the NbTi superconducting solenoids. The inner normal conducting coil is subject to very high magnetic

forces, high heat loads, and high levels of neutron irradiation. The magnetic forces require that the coil be constructed of a copper alloy, such as AMZIRC, which is 0.13 to 0.2% zirconium, with the balance copper. AMZIRC has a higher resistivity than pure copper, which increases the power consumption for the same number of ampere turns. The heat load continues to increase over the life of the coil because of the transmutation of copper to more resistive materials by neutron capture. In the TDF design, the coil is capable of dissipating 26 MW of resistive heating power, 20% of which is caused by resistivity changes in the material over 1 full power year (FPY) of operation.

The coil was designed to minimize cost by reducing volume consistent with electrical efficiency. The conductor operates at a specific current of 4800 $A/cm^2$, which results in a peak magnetically-induced stress of ~ 18 Ksi. This is well within the capability of AMZIRC. Cooling is accomplished by flowing water around the conductors. This approach maximizes heat transfer, but requires that the coolant be in direct contact with the insulation.

The coil insulation is exposed to the same level of irradiation as the conductors and if conventional organic insulations were used, they would be the limiting elements in the lifetime of the coil. For this reason, the coils incorporate inorganic insulators. Inorganic insulations have the necessary strength and radiation resistance, but are brittle and can be difficult to fabricate in complex shapes. In this design, Spinel ($A\ell 2MgO4$) was selected as the insulation material because it has the required radiation resistance, is fabricable into the required shapes, has adequate mechanical properties and is chemically inert.

### 13.2.5.2 Neutral Beams

The neutral beams on TDF provide the fueling, drive the fusion reactions in the test region, and provide necessary plasma control functions in the end cells. The major application of beams in TDF is the injection of large currents of deuterium and tritium in the central cell to fuel and heat the reacting plasma. The TDF beam system parameters were limited to those of the MFTF-B beams, namely to 80 kV or less positive ion-based sources. The TDF central cell beams would operate at 55 kV.

Each 55-kV ion source would provide 52 A of particles incident on the plasma and 24 sources would be needed to provide the incident 1248 A of

current necessary to trap 48 MW of power. For redundancy and reliability, an extra source would be provided in each beamline. Half of the beamlines would use deuterium gas, while the other half would use tritium.

In each source, gas admitted to the arc chamber would be ionized by a discharge of electrons produced by tungsten filaments. These ions would then be electrostatically accelerated by a grid structure before passing to the neutralizer duct and the separating magnet. The central cell beams are grouped in lots of four into an injector unit, as shown previously in Fig. 13.2-6. The injector unit provides a bending magnet to separate the non-neutralized ions from the neutrals and the necessary vacuum pumping to maintain a duct pressure of $10^{-4}$ Torr. In this system, the vacuum pumping is accomplished with a set of recycling cryopumps.

Eight injector units service the central cell (Fig. 13.2-5). At operating plasma conditions, approximately 6% of the neutrals pass through the plasma and into a dump. The dumps have been limited to a power density of 1.0 kW/cm$^2$, which is lower than the level being incorporated into the MFTF-B dumps. Heat is removed by a high pressure water cooling system common to these and the other particle dumps in the machine.

The principal engineering issues relevant to the beams are the effect of the high flux of uncollided neutrons streaming up the beam duct, the need for highly effective magnetic shielding, the requirement for small beam divergence to minimize the duct size, and the need for high-availability and steady-state operation.

### 13.2.5.3 Shielding

The shielding requirements for TDF are based on: 1) protecting the workers and the general public from excessive radiation doses, and 2) protecting sensitive components, such as superconducting magnets, from damage and heating. The most demanding requirement is to allow efficient maintenance operations by the facility staff. To this end, the machine shielding must hold the post-shutdown dose rate in the vault low enough to allow normal work schedules for maintenance. The vault shielding must also be capable of reducing the dose of gamma rays emanating from open ports and exposed components when the machine is undergoing remote maintenance operations.

The neutral beam injectors are subject to neutrons streaming up the beam duct. Both the internals of the injectors and the nearby superconducting coils are highly sensitive to this flux. The injector shielding would consist of an efficient series of water-cooled steel shadow shields with a tungsten bulk shield in the area close to the first solenoid coil.

Biological shielding is incorporated in the form of 0.5 to 1.0 m of low sodium concrete surrounding the end cells and injectors, with some shielding interposed between the solenoid coils. This shielding will limit the dose rate in the vault 24 hours after shutdown to 2.5 mR/hr, which will allow personnel to enter for maintenance operations. Very few neutrons are born in the end cell and, therefore, the shielding is based on attenuating the streaming radiation from the central cell through the choke coil. Shadow shielding is used to reduce the flux to levels that allow the end cell magnets to be lifetime components.

13.2.5.4 Tritium

The use of tritium is often considered to be the major safety consideration in facilities such as TDF. The TDF system would include both the fueling and cleanup systems and is based upon the design and development work done on the Tritium Systems Test Assembly presently under construction at the Los Alamos National Laboratory.

The total tritium inventory in the TDF system was estimated to be about 300 g, with 80 g of this present in the main vacuum vessel system at any one time. The remainder would be either in storage or in the process loop of the fueling system. Some fraction of the tritium present in the vacuum vessel would be vulnerable to release to the vault under various accident scenarios. In the event of a release, the vault would be maintained at a negative pressure while the discharge air is being processed through a cleanup system. A spill in the tritium process or storage facility would be handled in the same manner. The backup to the cleanup system would be a tall stack discharge system capable of discharging the maximum credible spill in a manner consistent with accepted safety guidelines.

### 13.2.5.5 Test Facilities

The principal test areas in TDF would be located in the central cell between the solenoid magnets. As illustrated in Fig. 13.2-2, the test facilities would include both large, directly accessible modules and smaller thimbles for fluence testing in a controlled environment. The large modules would be capable of act-alike testing of various breeding blankets. The thimbles are for long-term testing of materials and small assemblies.

The blanket test module ports are designed for maximum flexibility and ease of access. The module is a reentrant unit, and it may be divided into 2-4 segments like the three shown in Fig. 13.2-4. The number of segments may be varied from one to four in the final design to suit the test program needs. Each segment is an independent unit, with the piping, wiring, and vacuum seals located in a shielded area to allow contact operations during most of the installation and removal period. The test module can be isolated from the plasma with an independent first wall, and a first wall heat source can be provided to test tokamak blanket concepts at $\sim 50$ w/cm$^2$.

### 13.2.5.6 Maintenance

Maintenance operations run the full range of difficulty from simple hands-on contact to complex, fully remote procedures. As a design philosophy, contact operations would be maximized while providing specialized remote tooling where component lifetimes demand them. A complete set of remote tools would allow repair and replacement on all systems, including those whose design life exceeds that of the overall machine. A list of estimated component lifetimes is shown in Table 13.2-3.

Table 13.2-3. Expected Lifetimes of Components in the Central Cell, Anchor Cells, and End Cells of TDF

| COMPONENT | EXPECTED LIFETIME (Full Power Years) | COMMENTS |
|---|---|---|
| CENTRAL CELL | | |
| S-0 coil | 5.4 | Full lifetime |
| S-1 coil | 5.4 | Full lifetime |
| Test modules | 0.1 to 1 | Weekly, monthly, yearly |
| Beamlines | 0.2 | |
| Dumps | 0.2[a] | System driver |
| Sources | > 0.1[b] | |
| Cryopanels | 0.5 | |
| Magnets | 5.4 | Full lifetime |
| Beam dumps | 0.2 | |
| Choke coil | 1 | Design objective; 0.25 may be actual |
| Pellet injector | 0.2 | |
| ANCHOR CELL | | |
| Transition coil | 5.4 | Full lifetime |
| Anchor coils | 5.4 | Full lifetime |
| Sloshing ion beamline | 0.5 | |
| Dumps | 0.5[a] | System driver |
| Sources | 0.2[b] | |
| Cryopanels | 1.0 | |
| Magnets | 2.0 | |
| Transition pumping beam dump | < 0.2 | |
| Sloshing ion beam dump | < 0.2 | |
| Anchor cell pump beam dump | < 0.2 | |

Table 13.2-3. Expected Lifetimes of Components in the Central Cell, Anchor Cells, and End Cells of TDF (cont'd)

| COMPONENT | EXPECTED LIFETIME (Full Power Years) | COMMENTS |
|---|---|---|
| END CELL | | |
| Particle dump | 0.5 | |
| Cryopanel assemblies | 1.1 | |
| Helium pumps | 1.7 | |
| Transition pumping beamline | 0.2 | |
| Dumps | 0.2[a] | System driver |
| Sources | < 0.1[b] | |
| Cryopanels | 1.0 | |
| Magnets | 2.0 | |
| Anchor cell pumping beamline | 0.5 | |
| Dumps | 0.5[a] | System driver |
| Sources | 0.2[b] | |
| Cryopanels | 1.0 | |
| Magnets | 2.0 | |

a) The system driver is that component with the shortest life, which requires the entire system, or module, to be removed for maintenance.

b) Beamline sources are not system drivers, even though their expected lifetimes are the shortest in the beamlines because they are designated to be replaced as independent submodules within the beamline system.

## 13.3 The MFTF-α+T Upgrade of MFTF-B

This section provides a brief review of the LLNL/FEDC MFTF-α+T upgrade design of 1983. This design has been documented in a detailed LLNL report[14] as well as in a comprehensive review article[7].

During the past year, the physics model of MFTF-α+T has been refined with the result that some parameters reported in Section 13.3 would be updated and slightly modified. The improved models and suggested modifications to the original baseline parameters are described in more detail in Appendix G.

An additional activity performed during the past year has been the development of new test cell operating points for MFTF-α+T which have potential to provide a higher neutron wall loading and/or a higher test area (more test modules). These parametric results are presented in Section 13.3.5 following the presentation of the original baseline design in Sections 13.3.1, 2, 3, and 4.

### 13.3.1 MFTF- α+T Design Objectives

Various tandem mirror designs for dedicated nuclear technology testing devices (e.g., TDF) had been proposed over the past decade, but their high cost and lack of "physics relevance" had discouraged their incorporation into fusion program plans. In response to this criticism, during 1983 Lawrence Livermore National Laboratory (LLNL), with the support of the Fusion Engineering Design Center (FEDC) at Oak Ridge National Laboratory, considered ways to use an MFTF upgrade for conducting nuclear technology testing/ experimentation and for addressing improvements in tandem mirror confinement. The MFTF-α+T upgrade which was proposed would be operated in two phases, the second of which would be devoted to a nuclear technology mission.

To address the nuclear mission, an axisymmetric mirror cell insert would be added at the center of the machine. This insert would be driven with neutral deuterium and tritium beams to produce a high density/temperature plasma. A high fusion power density ($\sim$ 50 W/cm$^3$) and high wall loading ($\sim$ 2 MW/m$^2$) would be achieved in this short section, yet the fusion power would be modest ($\sim$ 11 MW). A 100-hour continuous run time goal was selected for MFTF-α+T, so that the longest transient behaviors (e.g., tritium equili-

brium in solid breeder blankets) could be investigated in the nuclear experimentation program. The overall availability goal for MFTF-α+T was specified to be 10%.

As detailed in reference 14, the cost effectiveness of this approach to integrated testing lies in the relatively low cost of adding the insert and designing for approximately 100-hour runs (compared with, say 100 to 300-second runs for the physics mission alone). Indeed, the initial cost estimate for the entire upgrade is approximately $400,000,000 (1983 dollars). Only a third of this cost is associated with the added nuclear technology mission.

### 13.3.2 Physical Description and Configuration

To improve on the expected performance of MFTF-B, the ion energy and the electrostatic confining potential must be raised by providing a higher beam energy (200 keV in this case) and a higher level of magnetic field. The MFTF-α+T upgrade would also incorporate a MARS-type end plug configuration. This new magnet design is compared in Fig. 13.3-1 with the present MFTF-B magnet set. The differences include the addition of a pair of recircularizing coils on the ends (to be used in conjunction with new end region pumping and direct converter schemes), the use of a yin-yang pair rather than a baseball-type coil in the transition, and the elimination of the axicell in favor of the simple choke coil. Also, as noted earlier, an axisymmetric mirror cell, or insert, is imbedded in the cental cell.

A layout of the MFTF-α+T in the present MFTF-B vault is shown in Fig. 13.3-2. The device has a short central cell (20 m between the 18-T coils) which limits the Q (fusion power/power absorbed by the plasma) to values of the order of unity. The overall length between the final recirculating coils is 50 m; the vessel itself is 65 m long.

Extensive internal shielding would be required to allow contact maintenance at the surface of the vessel. This shielding would also allow access to the vault 24 hours after shutdown. Access to components inside the vessel would be through the six hatches on top of the vessel. These are seen in Fig. 13.3-3, an external view of the upgrade vessel inside the 2-m-thick shielded vault that now houses MFTF-B.

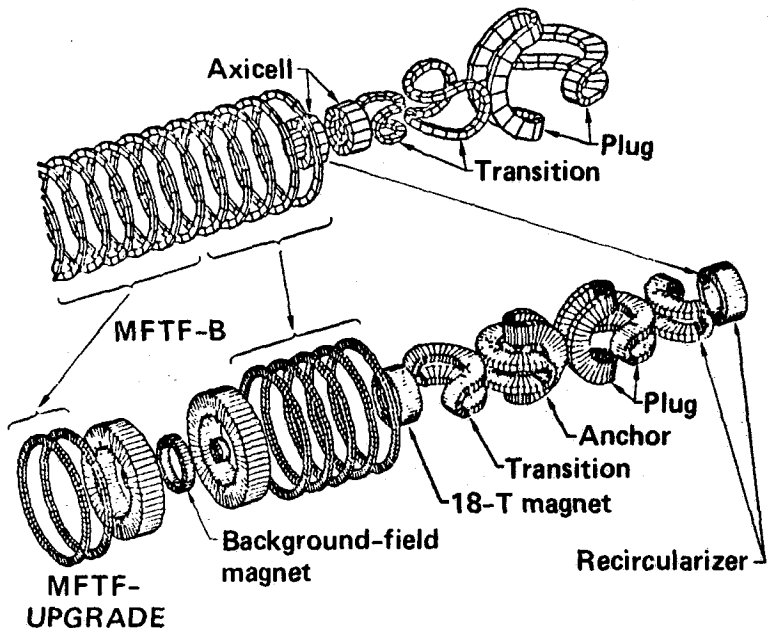


Figure 13.3-1. Comparison of the magnet set for MFTF-B with that for the DT-burning MFTF-α+T upgrade.

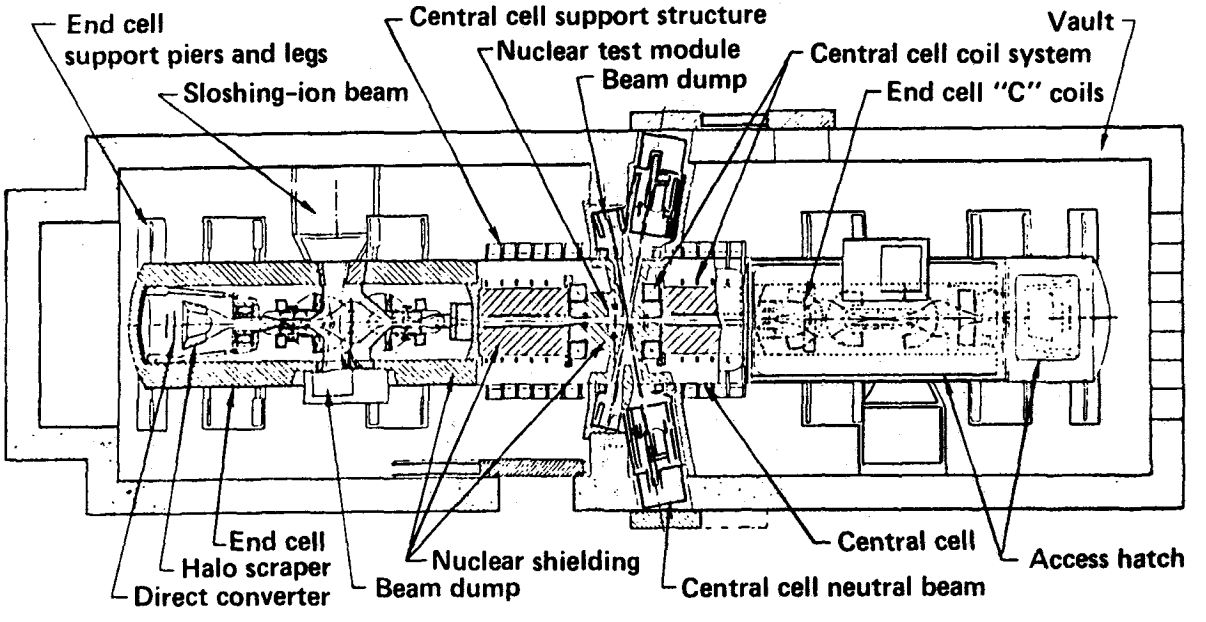


Figure 13.3-2. Cross section of the MFTF-α+T upgrade in the existing MFTF-B vault.

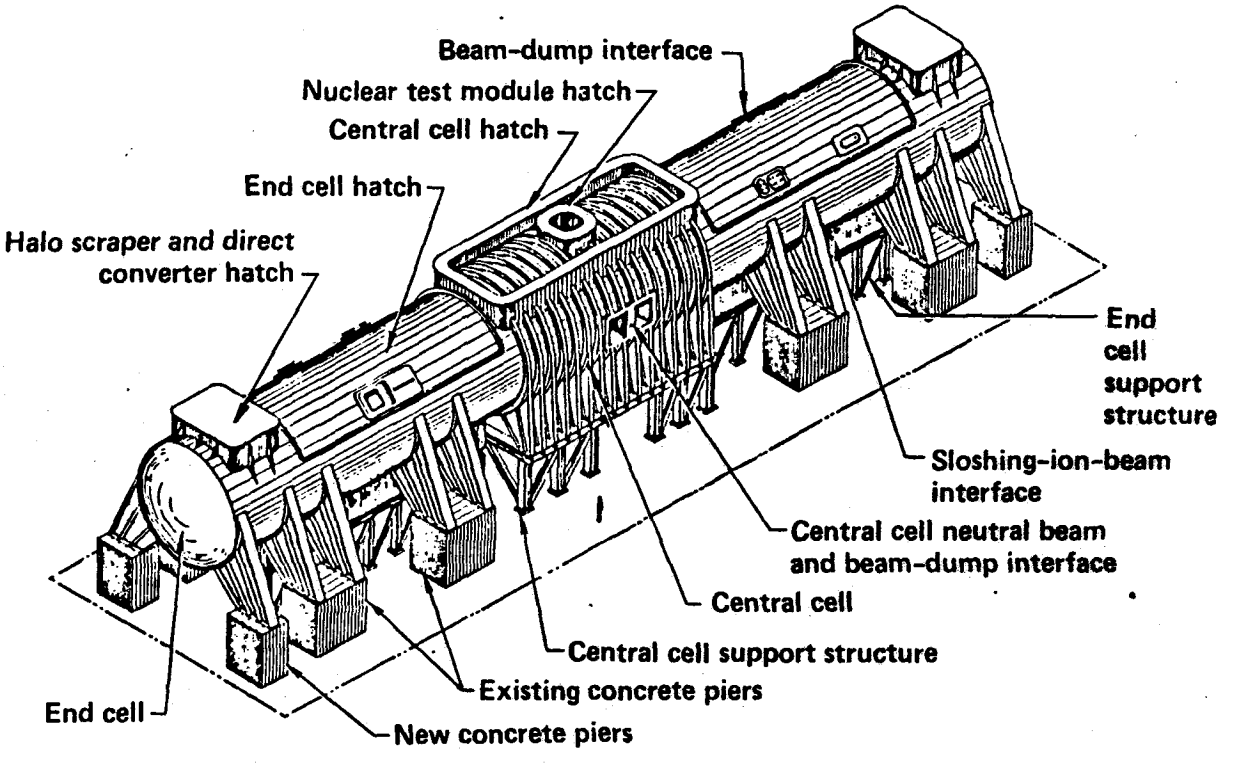


Figure 13.3-3. External view of the MFTF-$\alpha$+T vacuum vessel and support structure.

### 13.3.3 Physics Mode

There would be two modes of operation for the MFTF-$\alpha$+T upgrade, distinguished by their density and potential profiles: high-Q (tandem mirror physics and concept improvement) and high-$\Gamma$ (nuclear testing/experimentation). As shown in Fig. 13.3-4, the high-Q mode would have a 70-kV confining potential and minimal particle feed into the central cell. In this mode, 31 A of the 45 A incident on the plasma would be trapped and the wall loading would be only 0.33 MW/m$^2$ from a fusion power of 2.25 MW in the axicell.

In the high-$\Gamma$ mode ($\Gamma$ = wall loading), the incident current would increase to 240 A, with 190 A trapped. The wall loading would increase to 2 MW/m$^2$ and the fusion power would be 11 MW. An additional 5.9 MW would be produced in the rest of the central cell (at a low wall loading of 0.14 MW/m$^2$). As seen in Fig. 13.3-4, the confining potential would be reduced to 22 kV to allow the high particle flow through the machine (relative to the flow in the high-Q mode).

Control of the plasma potential in the central cell would be essential to reducing radial transport to acceptable levels. By negatively biasing the plasma at the end wall with potential control plates, the radial electric field would be forced to vanish in the central cell. Plasma E x B rotation would then be eliminated, and there would be no resonant particles (those that are 90$^0$ displaced azimuthally in one transit of the central cell). With this bias, the radial electric field would be turned inward in the transition regions, so that the E x B drifts present would be opposite to the field gradient drifts. This is important in controlling radial step sizes for particles that pass through the double-fan transition regions, thereby reducing transport by this (random-walk) mechansim.

Electron heating at the thermal barrier in the high-Q mode would require 320 kW of trapped power at a frequency of 35 GHz and 300 kW at 56 GHz. In the high-$\Gamma$ mode these would become 500 kW and 400 kW, respectively, for each plug. Power at 56 GHz would also be needed to produce the confining potential peak. The machine requires 60 kW and 100 kW, respectively, trapped in each plug for the high-Q and high-$\Gamma$ modes.

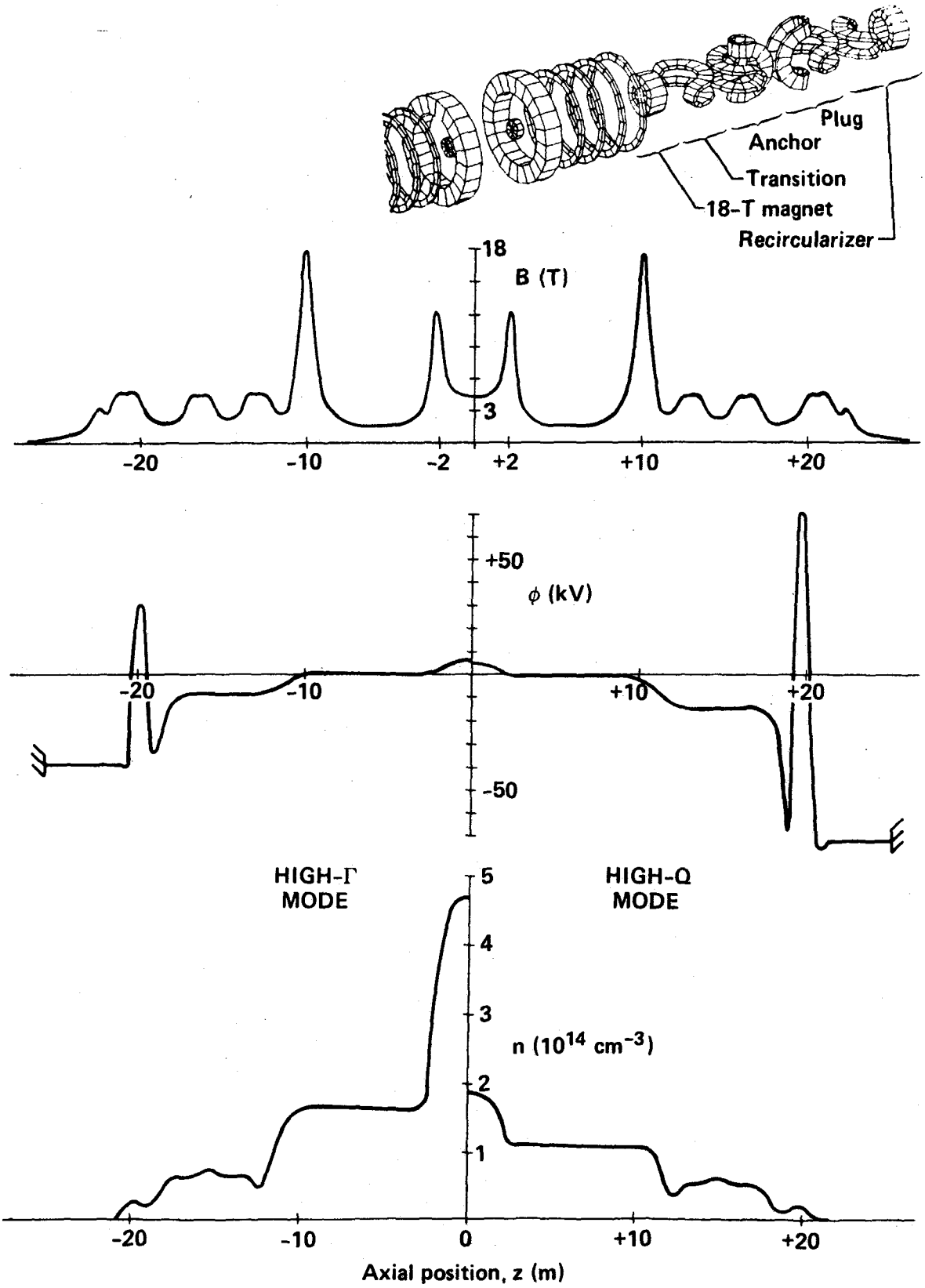


Figure 13.3-4. Profiles of the magnetic field (B), density (n), and potential ($\phi$) for the two different operating modes in the MFTF-$\alpha$+T upgrade: High-$\Gamma$ and high-Q.

Sloshing-beam currents of 4.2 A and 2.2 A incident would be required for the high-Q and high-$\Gamma$ modes, respectively, Drift pumping requirements would also differ for the two modes. In the anchor, the MFTF-$\alpha$+T would require 3 MW of reactive power for the high-$\Gamma$ mode and 0.66 MW for high-Q. In the plugs, 200 kW would be required for either mode. Finally, the ion heating in the anchor would also differ. For the high-Q mode, MFTF-$\alpha$+T would need 350 kW absorbed at 25 MHz and 67 kW at 50 MHz. For the high-$\Gamma$ mode, these become 400 kW and 170 kW, respectively.

### 13.3.4 Engineering Description

The MFTF-$\alpha$+T Upgrade (Fig. 13.3-3) would incorporate existing hardware and would modify existing components wherever possible to maximize the contribution of MFTF-B. The Upgrade would also feature some totally new systems (Table 13.3-1). The most technologically innovative would be the continuous 80 and 200-keV neutral beams[16,17], the high-field unshielded copper coils, and the drift pumping system. However, with aggressive development programs, these items can be available in the early 90's[18]. The new features that will have the greatest impact on operations are the introduction of tritium fuel and the maintenance of an activated machine. A description of each of the major MFTF-$\alpha$+T systems is given below. The reader is also referred to Section 13.2, as much of the MFTF-$\alpha$+T design philosophy and approach is common to TDF.

#### 13.3.4.1 Magnet System

The MFTF-$\alpha$+T magnet system would differ significantly from that of MFTF-B. Major additions would be the MARS-like end cells and the nuclear test module in the central cell. However, the superconducting magnet technology would be extrapolated from MFTF-B, and, as shown in Fig. 13.3-1, 12 of the 24 superconducting coils in the Upgrade would be taken from MFTF-B.

Of the five normal coils, four are inserts to superconducting coils. These coils, which would produce on-axis fields of 12 and 18 T, represent significant extensions of the state of the art. Although small in size, these insert coils would be subject to very large, magnetically induced stresses and heat loads. As in the TDF design, the conductors would be of high-strength copper alloy (Amzirc).

Table 13.3-1. New Engineering Features of the MFTF Upgrade

| COMPONENT/SYSTEM | DEVELOPMENT PLAN/DATA BASE |
|---|---|
| • Negative-ion beams (200 kV)<br>• Hybrid copper superconducting coils (18 T) | • Included in the DOE Fusion Technology Development Plan |
| • rf drift pumping<br>• Direct converter with potential control<br>• End region pumping with halo scraper | • Develop in existing tandem mirror facilities |
| • Full shield for contact maintenance<br>• Remote maintenance for internal components<br>• Tritium processing systems<br>• Safety and monitoring systems for DT operation | • Nuclear technology based on design studies and on TSTA[a] (for tritium) |

a) TSTA = Tritium Systems Test Assembly (at Los Alamos)

There are two designs for the superconducting insert coils which would be used in the 18-T "choke" coil. Both are being studied at LLNL, and one will be chosen for development for the high field magnet program. Specifically, each 18-T coil design uses and 8-T NbTi background coil, but incorporates a different $Nb_3Sn$ insert. Each of these 60-cm-bore inserts would raise the on-axis field to 15.4 T. With the final 25-cm-bore copper-coil insert, the field is raised to 18 T. One $Nb_3Sn$ design would use He-I coolant at 1.8 K, whereas the other would use forced-flow He-II at 4.2 K. A high-field superconducting 18-T insert (to eliminate the copper insert) is being designed by the magnet group a KfK Karlsruhe, West Germany.

### 13.3.4.2 Heating, Fueling, and Drift Pumping

In comparison with MFTF-B, the MFTF-α+T Upgrade calls for steady-state operation with increases in electron-cyclotron resonant heating (ECRH) and ion-cyclotron resonant heating (ICRH) power, the addition of rf drift pumping in each anchor and plug, and a 200-kV sloshing-beam system.

Three options for the 200-kV sloshing ion beam system were considered by Fink[17]. The lowest risk option, a positive-ion beam with a magnetic separator to remove molecular ions, would have a 3.5-m-long neutralizer and would be only 13% efficient. However, it would not require cryopumps and would be 40% gas efficient, introducing 5.7 Torr ℓ/s of gas into the beamline. Very little development is needed for such a system.

The second and third options would utilize negative-ion sources which promise higher efficiency and the third option would also utilize a transverse field focusing (TFF) accelerator to remove the ion sources from the neutron streaming path. These systems will, however, require development. For redundancy, a spare source and transport system would be provided in the sloshing-ion system.

In Fig. 13.3-2, the two central cell beamlines are shown. One beamline would use deuterium gas, the other would use tritium. Each would house four sources, three active azd one spare. Each source would deliver 40 A at an average energy of 60 keV (an 80:15:5 species mix for each 80 kV source). Anticipating a regular schedule for component changeout, either the source or the entire beamline (cryopanels and ion dumps as well as sources) could be removed to a transfer cell from the back end (Fig. 13.3-5). Although these 80-kV beams would be quite similar in their electrical and thermal behavior to those now in MFTF-B, the introduction of neutrons and tritium would complicate the design significantly, An addition, charge exchange heat fluxes near the beam-plasma interaction zone could be large enough to require special attention.

Electron heating in the barrier and plug would be accomplished with 200-kW steady-state gyrotrons. At each barrier, six gyrotron tubes would be needed - three at 35 GHz and three at 56 GHz. The plugging potential would be created with one tube at 56 GHz. Thus, the Upgrade would use 14 tubes, whereas MFTF-B will use 8.

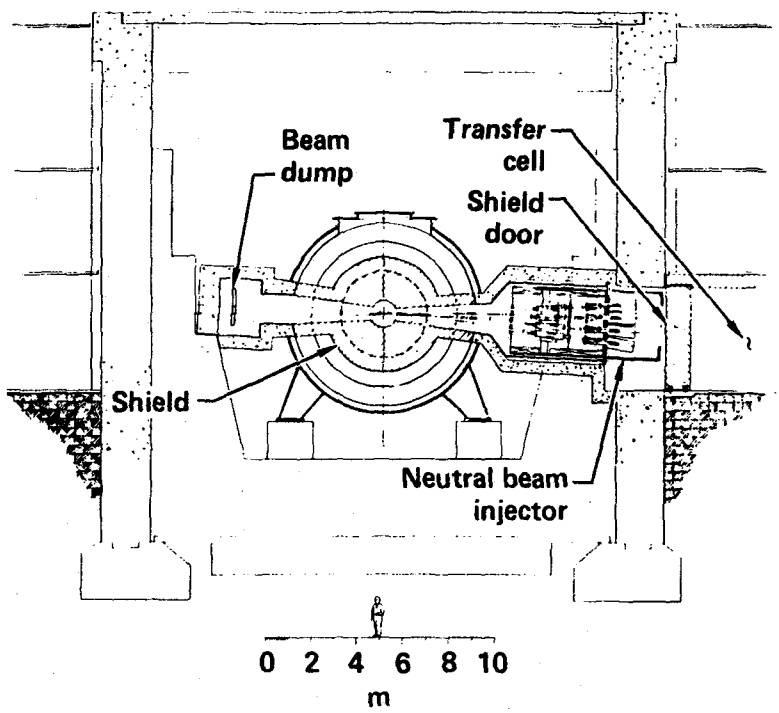


Figure 13.3-5. Arrangement for MFTF-$\alpha$+T neutral beam maintenance. (This job is performed by removing sources or the entire beamline through shielded access doors to the transfer cell.)

In MFTF-B, a 400 kW (absorbed) ICRH system at 6 to 20 MHz will heat ions in the central cell. In the MFTF-α+T, this system would be upgraded to 800 kW and 25 MHz and used in both anchors. To maintain the proper ion velocity distribution, MFTF-α+T would require 170 kW at the second harmonic (50 MHz) in each anchor. Placement of these heating systems in their anchor and plug locations is shown in Fig. 13.3-6.

Figure 13.3-6 also depicts the drift pump coil at the plasma fan between the anchor and choke coils. Drift pumping would be accomplished by applying an rf magnetic field at the trapped-ion bounce or drift frequencies. This field would be applied perpendicular to the broad plasma fan for the region in question. Trapped particles would be pumped radially in steps, the step size determined by the geodesic curvature introduced by the rf field perturbation.

Circuit designs for drift pumping are in a very evolutionary state, and an optimum approach has not been found. Approaches under consideration include individual oscillators to cover the frequency range as well as frequency modulation schemes, including sinusoidal and square-wave modulation of the basic frequency. High-Q circuits will be required if the driving power is to be manageable.

### 13.3.4.3 Halo Scraper, Direct Converter, and Vacuum Pumping

The evolved halo pumping[17] and direct conversion[19] schemes have had a major impact on the end region design of tandem mirrors, simplifying them enormously. These systems are a natural outgrowth of the radial separation of the ions from the plasma in the transition region. This separation directs the ions to the halo scraper and the elctrons to the direct converter. The MFTF-α+T direct converter would be a simple collecting plate instead of the gridded structure that would be needed if the ions were decelerated. Also, relatively simple halo-scraper plates, pumping ducts, and plenum chambers would replace large surface area cryopanels resembling those used in MFTF-B. As a direct result, the MFTF-α+T end vessel would be reduced substantially in size relative to the MFTF-B end vessel.

The MFTF-α+T halo-scraper and direct converter plates are shown in Fig. 13.3-7. The outer plate and duct leading to a pumping plenum have been designed to act in a manner which is similar to that of a pumped limiter in a tokamak. There must be sufficient energy fed to the halo, and it must be

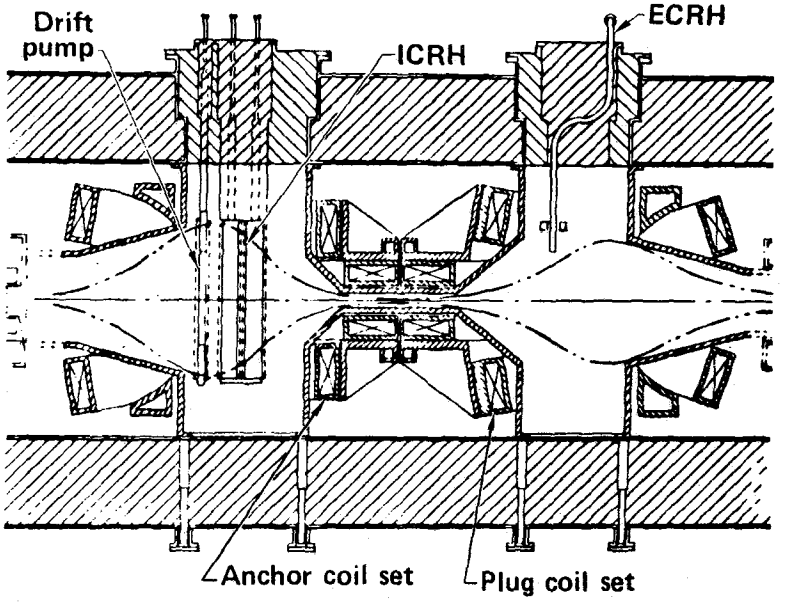


Figure 13.3-6. Heating and pumping systems in The anchor and plug regionsof MFTF-α+T. (Not shown is the sloshing-beam path through the end plug.)

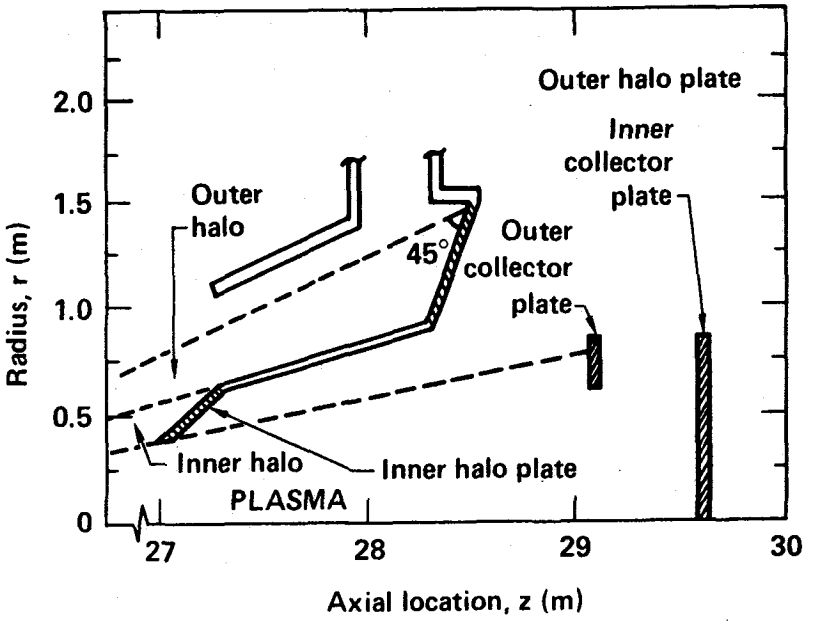


Figure 13.3-7(a). Geometric model of the MFTF-α+T halo scraper and direct converter plates.

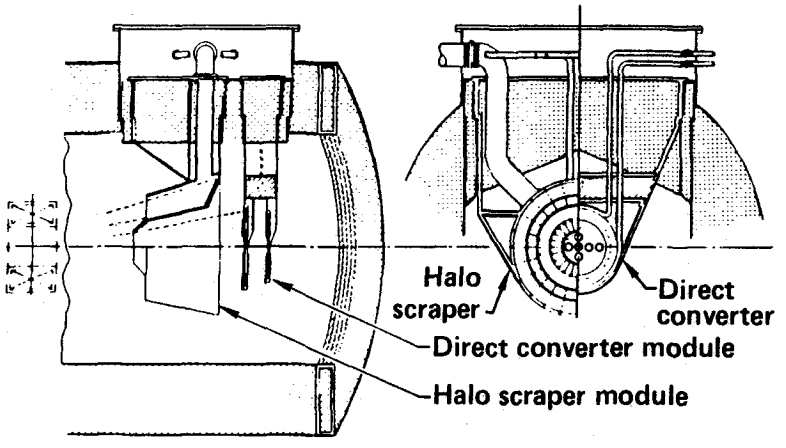


Figure 13.3-7(b). Schematic of the MFTF-α+T halo scraper and direct converter system.

sufficiently dense - to prevent backstreaming of the neutrals formed at the outer plate when the halo impinges on it. It is intended that the MFTF-α+T duct design will allow enough gas recycling at the outer plate to produce the high density halo. Energy for the halo would be supplied by those alpha particles in the central cell with orbits that pass through the halo. Particle energies and heat loads would be higher on the inner plate even though the flux to the outer plate ($10^{23}$ particles/cm$^2$) is 200 times higher than that to the inner plate. Peak heat loads to the inner plate are about 300 W/cm$^2$.

13.3.4.4 Tritium Systems

The MFTF Upgrade would produce 17 MW of fusion power in pulses lasting over 100 hours with a burn fraction of 0.02. These fueling requirements make it imperative to include a tritium recovery/reprocessing system on the plasma side of the first wall. With a complete fuel cycle, only ~ 450 g of tritium inventory will be required. The MFTF-α+T tritium system would include components for processing and storage, secondary containment, atmospheric tritium recovery, waste processing, accountability analysis, and safety. As for TDF, the tritium processing and cleanup system would be based on the developments of the Tritium Systems Test Assembly (TSTA) presently underway at the Los Alamos National Laboratory. Any tritium recovery associated with blanket experimentation would require a separate and dedicated tritium process loop.

13.3.4.5 Maintenance

The maintenance philosophy for the MFTF-α+T Upgrade is a four-fold approach based on designing operational flexibility into this near-term device and on accomplishing numerous maintenance tasks between operating runs. The design addressed the following maintenance requirements:

- Contact operations at the shield boundary to be permitted 24 hours after device shutdown.
- Major maintenance and disassembly operations to be accomplished remotely under both normal and emergency conditions.

- Modularized component installations to be arranged for independent disassembly procedures.

- Proven remote-equipment technology to be specified.

The design of the vacuum vessel and support structure addressed these needs for maintenance and high availability. Hatches and access ports would be provided to allow direct removal of major components where possible. Figure 13.3-8 indicates these access ports and the removal of test cell components.

The Upgrade would make maximum use of the MFTF-B facility itself at LLNL. Building 431 and the reactor vault would be used in their entirety, as would other existing LLNL facilities. However, modifications of the reactor vault would be needed to make it meet the more stringent seismic requirements of a tritium-burning device and to provide remote maintenance facilities (see Fig. 13.3-9). A hot-cell facility and a tritium-processing plant would be added, and some modifications to the power supply and cooling systems would be required.

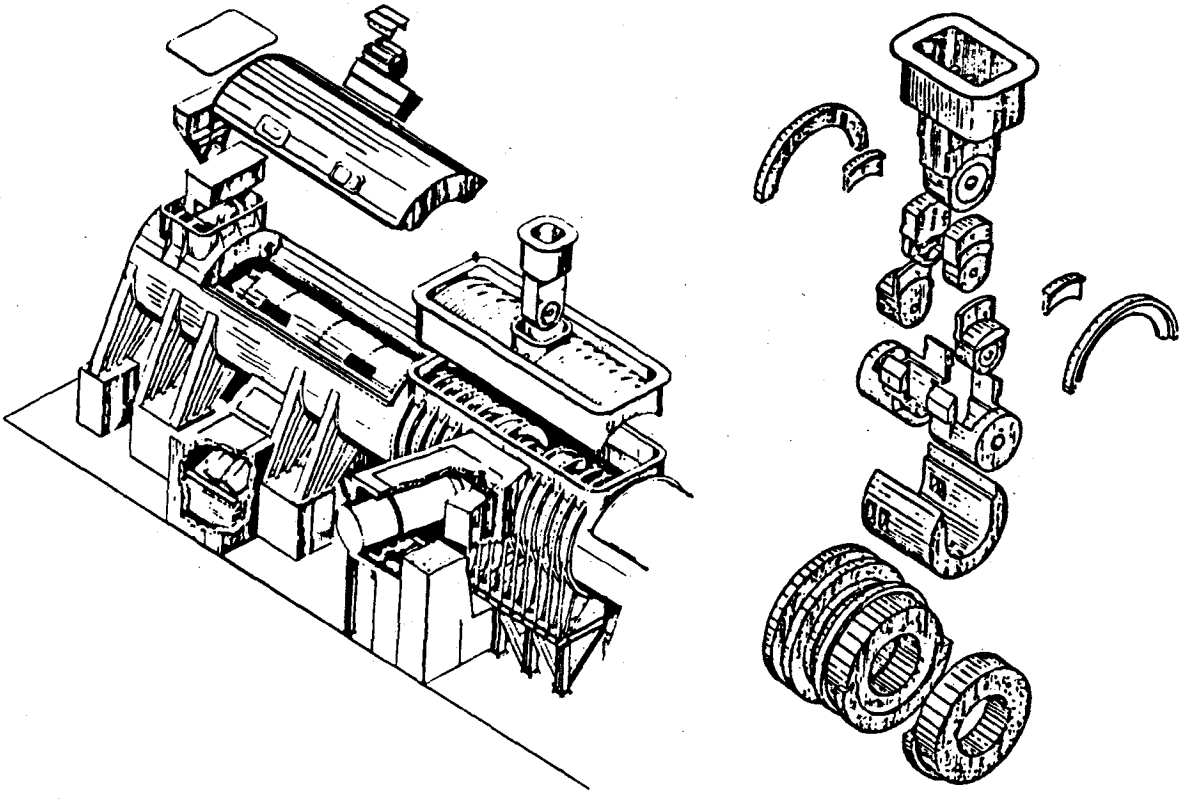

Figure 13.3-8. MFTF-α+T test station assembly and access ports for the major components.

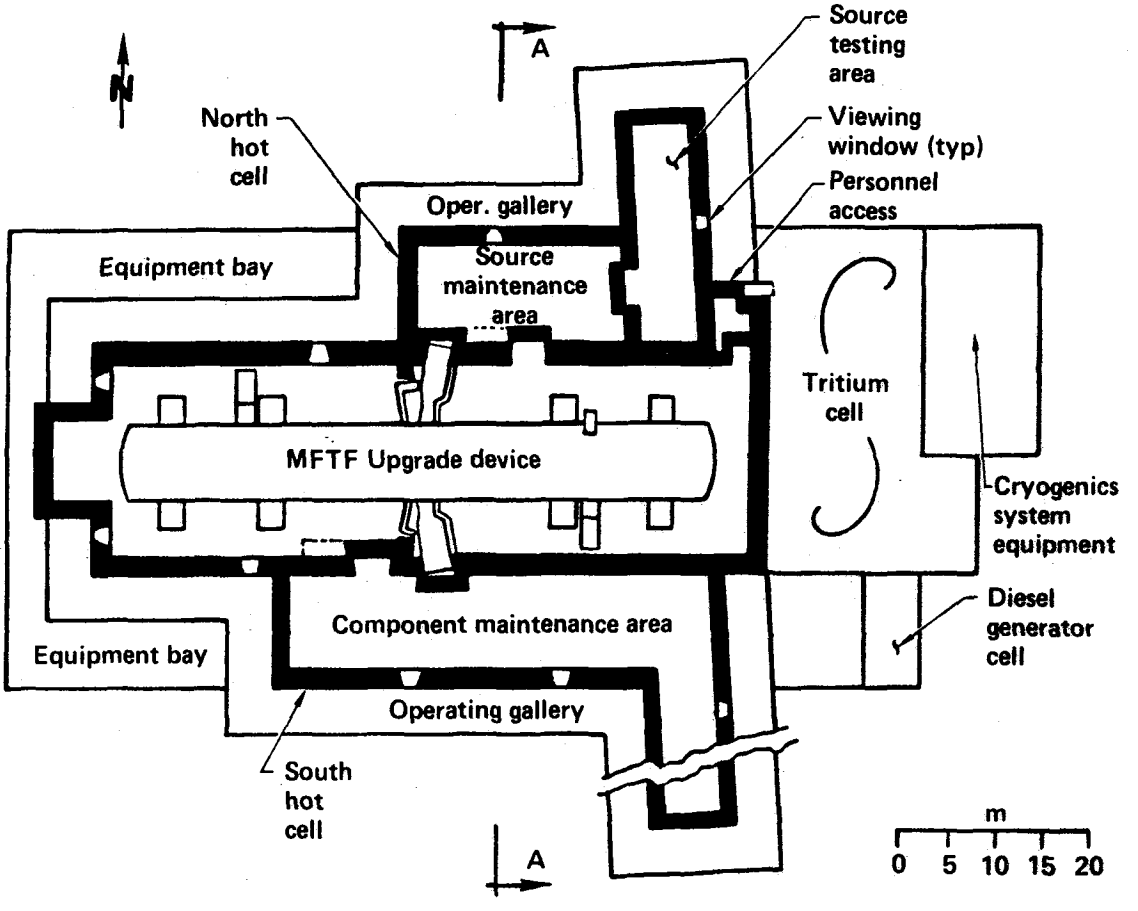


Figure 13.3-9. Use of space for the MFTF-$\alpha$+T upgrade within the existing MFTF-B facility.

### 13.3.5 Consideration of a More Ambitious Test Cell

The goal in this section will be to present attractive options for MFTF-α+T configurations having improved test cell performance over the baseline* configuration. Partially optimized configurations have been obtained by combining design constraints, performance figure-of-merit considerations, physics parametrics and some intuition.

The preliminary design goals and constraints adopted for this investigation were as follows:

- require a test cell length which is sufficient to incorporate two blanket test module ports (including shielding and coolant piping), each of which is the length of the baseline MFTF-α+T test module;
- obtain a test cell wall loading in the range $1.8 \leq \Gamma_{TC} \leq 2.5$ MW/m$^2$ and;
- minimize the neutral beam injection power and current to the test cell and limit the injection energy to 95 keV.

The maximum injection energy is set by projections of the achievable high power neutral beam technology in the MFTF-α+T time frame. Expansion of the test cell to accommodate two blanket test modules is desirable for two reasons. First, additional blanket components could be tested simultaneously in the same environment. Second, the magnitude and uniformity of the neutron flux in the blanket test modules is significantly improved when out-scattering is minimized by increasing the number of test cells.

The physics constraints of MHD stability for the central cell and test cell (beta limits), microstability of the plug sloshing ions, and mirror confinement of the sloshing ions must also be satisfied. All of the results to follow satisfy the requirements of the up-to-date physics understanding of MFTF-α+T as detailed in Appendix E.

---

*The "baseline" case and the other cases discussed in this section reflect the improved models and methods discussed in Appendix E, "Modeling of MFTF-α+T High-Γ Mode Performance".

13.3.5.1 *Parametric Analysis*

Given the design goals and constraints from the previous section, two variables characterizing the test cell region have been chosen for parametric variations: the neutral beam average injection energy and the injection angle. Both of these directly impact the design of the test cell insert and its neutral beam lines.

The sensitivity of test cell performance to changes in the neutral beam injection angle (and the consistent beam energy) is shown in Fig. 13.3-10. At a fixed ion temperature outside of the test cell, these curves represent cases for which the central cell and end cell parameters remain nearly constant and only the performance and design of the test cell changes. The results show that high wall loading and low beam energy are obtained at nearly perpendicular injection angles. Note, however, that with near perpendicular injection, the axial density profile in the test cell is expected to be less uniform. Specifically, the wall loading near the outer edges of the blanket modules may be much lower than the average value given here. In addition, peaked mirror trapped distributions are subject to Alfven ion cyclotron instabilities. Injection at $\theta_{INJ} = 75^{o}$ (proposed in the original work on MFTF-$\alpha$+T) results in an acceptable injection energy and a near-maximum neutron wall load.

Test cell performance, as a function of the neutral beam trapped current, is shown in Fig. 13.3-11. The trend in wall loading is consistent with that obtained from less sophisticated models; higher test cell wall loading is obtained at higher beam power. At a neutron wall loading of 2 $MW/m^2$, the beam current is 297 A compared with 181 A at $\Gamma_{TC} = 1.5$.

Note that the neutron wall loading increases slightly less than linearly with increasing injected power. This can be understood from scaling arguments. For fixed beta (ratio of plasma pressure to magnetic field pressure) in the test cell and central cell, and fixed axial confinement parameter for the central cell ions, the ion temperature must decrease to let the additional particles out of the device as the injection current increases. This results in lower electron temperature and test cell hot ion energy and correspondingly reduced test cell ion confinement and fusion reaction rate as the injection current increases. Combining these effects leads to a less than linear increase of neutron wall loading with injection current.

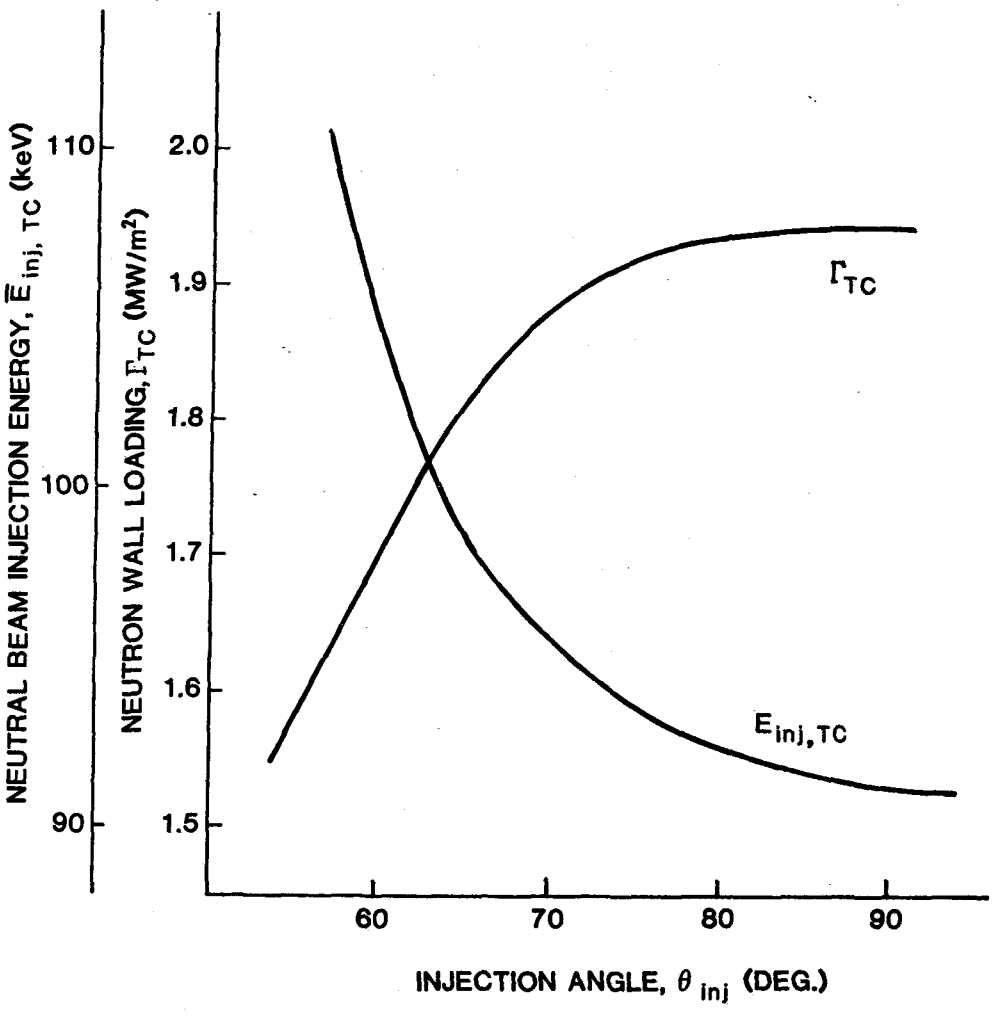


Figure 13.3-10. Updated MFTF-α+T test cell wall loading and average injection energy as a function of beam injection angle.

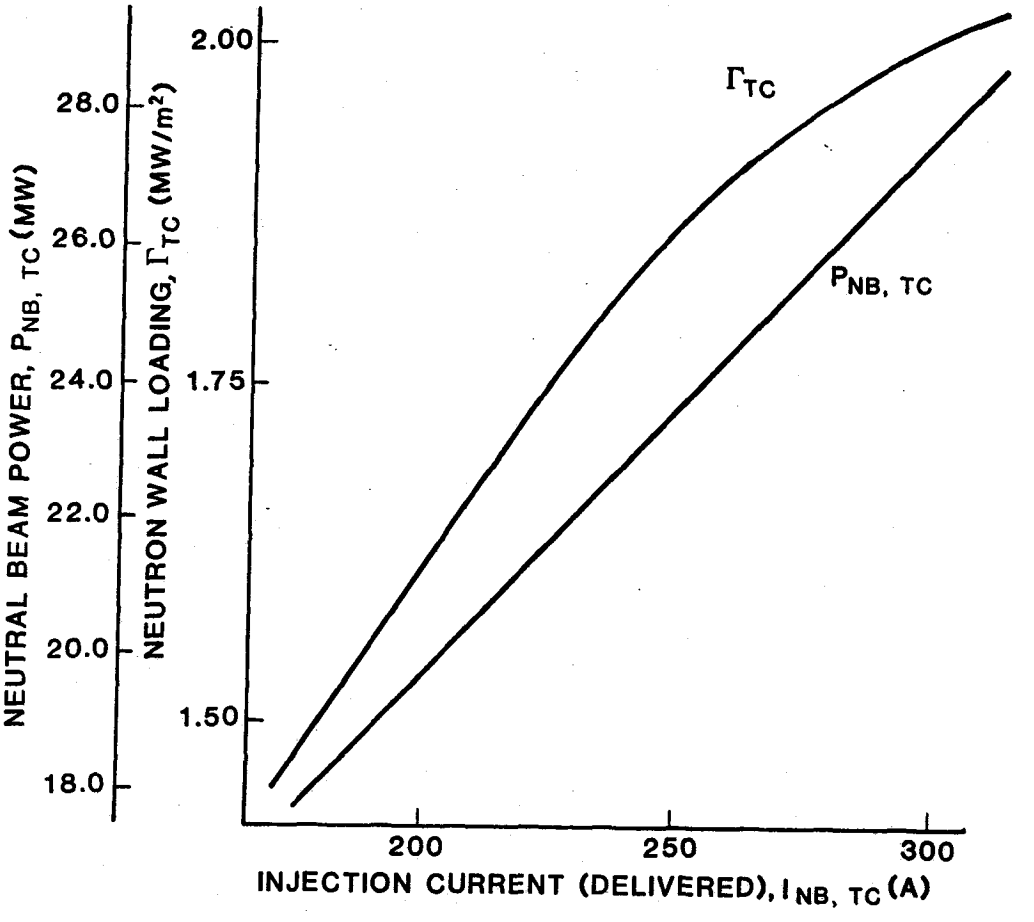


Figure 13.3-11. Updated MFTF-α+T test cell performance versus neutral beam current.

13.3.5.2 Optimized Cases

Partially optimized parameter sets have been developed for particular configurations of MFTF-α+T. In this section, four cases will be presented. In each case, the central cell ion temperature and the central cell and test cell beta were allowed to vary, with the test cell wall loading uniquely determined by the constraint that the average injection energy be nearly constant ($E_{INJ}$ = 94 keV). This procedure leads to a parameter set with better performance than the baseline.

Parameters for the partially optimized MFTF-α+T cases with two blanket test modules in the test cell are compared with those for the baseline case of Appendix E (one test module) in Table 13.3-2. The injection energy, $E_{INJ,TC}$, neutral beam power, $P_{NB,TC}$, and the neutral beam current to the test cell, $I_{NB,TC}$, are nearly constant among these cases. The test cell wall loading increases by 27% from $\Gamma_{TC}$ = 1.92 to 2.44 MW/m$^2$ as the center cell ion temperature and beta values are increased. In addition, the trapping current (drift pump requirement) cold fueling current (pellet injector requirement) and ECRH power at the potential peak (point a) all decrease as the wall loading increases. This indicates more efficient use of the end cell plasma to sustain the test cell. The ECRH power at the barrier (point b) increases 8% (80 KW) over this range of ion temperatures. The final case at $T_c$ = 17 keV requires central cell and test cell beta values which are very near the stability boundary given by MHD analysis of this configuration.

Comparing the performance of CASE 4 with the baseline parameters, the same test cell wall loading is achieved and the required ECRH and ICRH powers in the end cell are lower. In addition, the neutral beam power per unit test cell effective length is 6.21 MW/m in CASE 4 compared with 6.46 MW/m in the original configuration. The increased average energy of the beams results in more efficient use of the beam power. The CASE 4 requirements which are increased over the original configuration are the beam current (277 A delivered compared with 217 A) and the cold fueling current (88.0 A compared with 32.8 A). The cold fueling could be accomplished using pellet injection. Note that the beam current per unit test cell length, important for access considerations, is down to 46 A/m from 62 A/m in the baseline.

Table 13.3-2. Partially Optimized Parameter Sets for MFTF-α+T with a 6.0 m (2 Test Module) Test Cell

| PARAMETER | BASELINE* | CASE 1 | CASE 2 | CASE 3 | CASE 4 |
|---|---|---|---|---|---|
| $\Gamma_{TC}$ (MW/m$^2$) | 2.46 | 1.92 | 2.13 | 2.27 | 2.44 |
| $P_{NB,TC}$(MW) | 18.1 | 24.9 | 25.4 | 25.7 | 26.1 |
| $I_{NB,TC}$(A) | 217 | 266 | 268 | 278 | 277 |
| $E_{INJ,TC}$ (keV) | 83.2 | 93.5 | 94.6 | 92.3 | 94.2 |
| $I_{TRAP}$ (A) | 55 | 12.7 | 9.98 | 8.01 | 6.45 |
| $I_{FUEL,c}$ (A) | 32.8 | 107 | 100.4 | 90.9 | 88.0 |
| $P_{ICRH}$ (MW) | .583 | .676 | .600 | .550 | .490 |
| $P_{ECRH,a}$ (MW) | .060 | .022 | .019 | .017 | .014 |
| $P_{ECRH,b}$ (MW) | 1.56 | .92 | .94 | .97 | 1.00 |
| $T_c$ (keV) | 15.0 | 14.0 | 15.0 | 16.0 | 17.0 |
| $T_{ec}$ (keV) | 6.36 | 5.63 | 5.90 | 6.07 | 6.34 |
| $\beta_c$ | .60 | .49 | .52 | .55 | .58 |
| $\beta_{TC}$ | .46 | .40 | .43 | .45 | .48 |

* One module. See Appendix E.

13.3.5.3 Conclusions for MFTF-α+T Physics Modeling

The modeling and optimization of MFTF-α+T High-Γ mode operation have been reexamined using the original proposal[14] as a starting point. Improvements in the physics modeling of this type of tandem mirror facility, which have occurred in the interim between these studies, have been incorporated in the current study.

Benchmarking the results of the present study against the original baseline parameters (see Appendix E for details) shows that similar physics parameters can be achieved when improved physics models are included. However, these results indicate that, for the same test cell trapped beam current, the average beam injection energy must be increased from 60 keV to 83 keV. This increase is consistent with the inclusion of hot ion drag on the cold ion species (which has been modeled in the present study). Another difference between our current understanding and the baseline is that the need for supplemental fueling of the central cell Maxwellian population is indicated by the present model. This is consistent with the direct axial loss of the hot mirror trapped population occupying the central cell. Other differences between the results of the two studies can be traced to improvements in the physics understanding of the device.

Partial optimization of MFTF-$\alpha$+T in the High-$\Gamma$ operating mode has been performed using an expanded version of the LLNL TMRBAR tandem mirror physics code which includes the test cell plasma models. A set of operating parameters was found which features a 2.4 $MW/m^2$ wall loading over a 4.2 m test cell plasma effective length (two test module parts) with a test cell neutral beam power of 26 MW, a delivered current of 277 A, and an average injection energy of 94 keV. In comparison with the baseline, this set of parameters represents some improvement in the beam power per unit test cell effective length and results in lower requirements on the other systems of the tandem mirror central cell and end cell. An exception is the higher required cold fueling current in the central cell.

Further optimization may be possible using the present models and will be an area for future work. Specifically, a cost and power flow optimization has not been performed. Nevertheless, it is clear that the cost impact of an $\sim$ 2 m increase in the test cell length combined with an $\sim$ 10 MW increase in neutral beam power will be tolerable - especially considering an ability to double the component test area while increasing the neutron flux and its uniformity (see Section 13.4).

Finally, it should be noted that the models of the test cell ion particle and energy balances use essentially the same Logan-Rensink analytical form as in the previous study. Consequently, no new information on the interaction of these ions with the ions passing through the test cell has been obtained.

Calibration of the model ($n\tau$) value at a single parameter point using multi-region Fokker-Planck code results has been done. However, to calibrate the model over a wide range of electron temperatures and passing ion densities requires further Fokker-Plank analysis. This represents the most important area for future work on the performance of tandem mirror devices with test cell inserts, because it directly impacts the performance of the test cell plasma.

## 13.4 Resolving the FINESSE Nuclear Issues in a Tandem Mirror Nuclear Test Facility

This section provides a preliminary assessment of the ability of an MFTF-α+T or TDF class Fusion Engineering Research Facility (FERF) to resolve FINESSE nuclear issues. Importantly, this assessment focuses on the ability of tandem mirror FERF options, in conjunction with complementary fusion and non-fusion facilities, to play a role in tokamak development. This activity represents a first attempt within FINESSE to resolve nuclear technology issues and testing needs (Chapters 3 and 4) in test facilities (Chapters 9, 10, 11, 12) subject to an implied development scenario (Chapter 16). This type of activity will be expanded in 1985 to cover more cases and to provide a more detailed consideration of the amount of testing required (e.g., number of experiments/tests, required test period, test article size, etc.).

### 13.4.1 General Considerations

As indicated in Fig. 13.4-1, any fusion engineering research facility (FERF), operating in a nuclear environment with tritium breeding, will be required by its design and operation alone, to resolve technology issues in several areas. As a result, it can be argued that a steady-state, or quasi-steady state capability to explore the nuclear environment, even to the level of understanding only the beginning-of-life performance of act-alike component test modules, would be the single largest contribution to resolving fusion nuclear issues that a FERF could make. Beyond this, other FERF attributes, such as wall area, average availability, pulse length, and fluence are also quite important as these determine the number of tests and the test objectives (e.g., end-of-life testing) which can be addressed.

In considering tandem mirror FERF options, we note that the ability of tandem mirror FERFs to provide an act-alike environment for tokamak blanket test modules was a key concern entering the FINESSE program. Specifically, it was known that the tokamak and tandem mirror geometries, magnetic field profiles, and plasma-side conditions (i.e., heat flux and erosion) were quite different. These issues were addressed, to some extent, during the first year of FINESSE and it appears that many act-alike aspects of tokamak blanket performance can be achieved in scaled-down tandem mirror test module (such

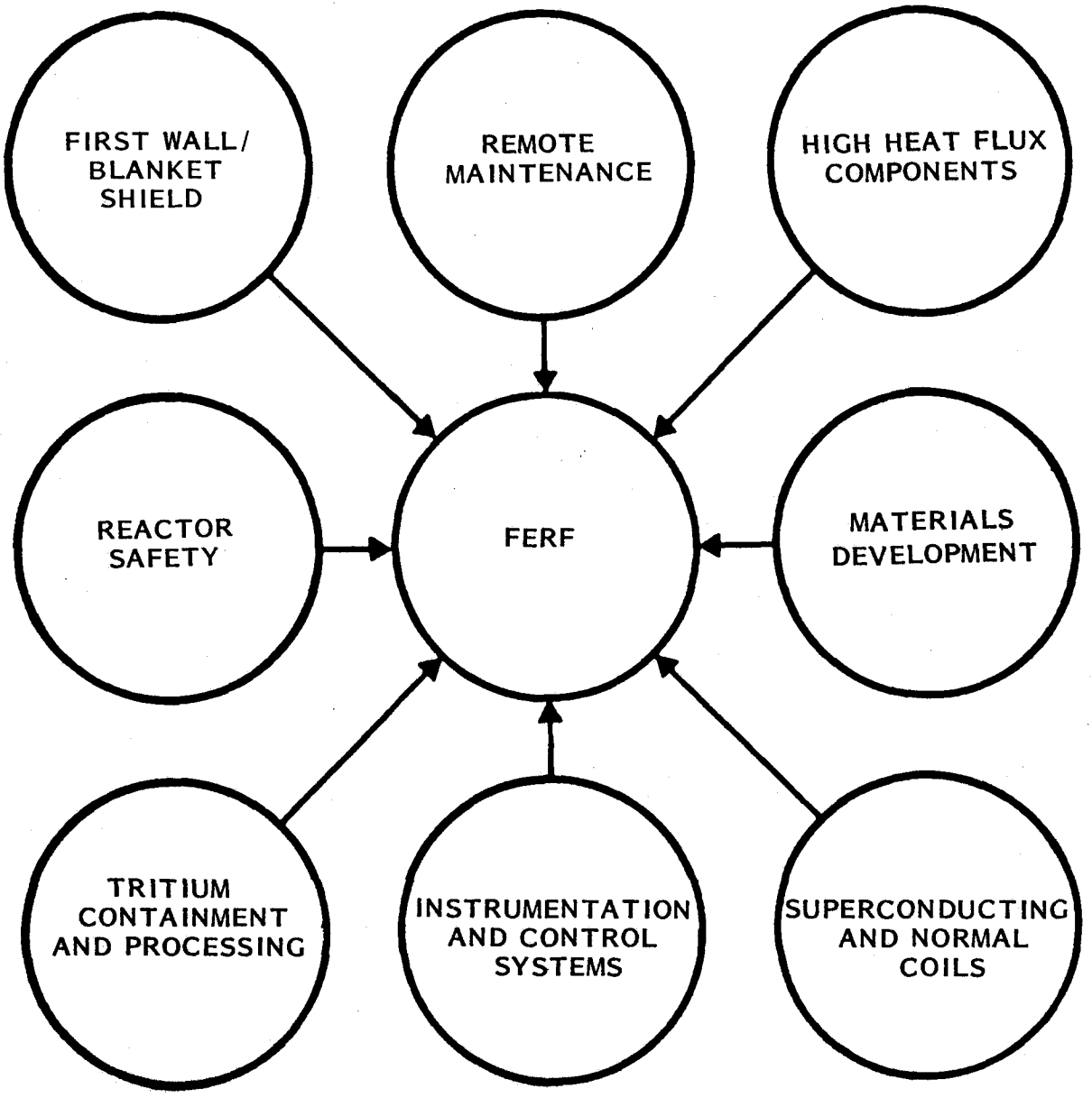


Figure 13.4-1. Requisite technology areas for a tandem mirror FERF.

as the module shown in Fig. 13.4-2) if a radiant heat flux can be applied to the test module first wall to simulate particle and radiation losses from the tokamak plasma. The preliminary design of a tungsten filament resistive heater, to provide 50-100 $W/cm^2$ of surface heat flux on the 25 cm radius first wall of a tandem mirror test module, has been performed and results for several operating points are shown in Table 13.4-1. Such a capability is clearly possible.

Differences between the capabilities of an MFTF-α+T class facility and those of a TDF class facility are indicated in Table 13.4-2. Both MFTF-α+T and TDF appear to be attractive candidates to perform thermal-hydraulics and thermal-mechanical testing of act-alike fusion nuclear components. Also, both facilities can, and would be used to investigate and resolve early failure modes. However, a TDF class FERF (ultimate fluence 5-10 $MW-yr/m^2$) would provide much greater operating time than an MFTF-α+T class FERF (ultimate fluence $\sim$ 1 $MW-yr/m^2$) and, consequently, is more attractive for tests which involve extended fluence effects ($\gtrsim$ 4 $MW-yr/m^2$).

In considering tandem mirror test cells for nuclear component testing, it should be noted that axial neutron leakage can reduce the flux relative to the apparent neutron source strength. For example, Fig. 13.4-3 depicts a typical 2-D test cell model which is applicable to MFTF-α+T. As shown, the displacement ($E > 1.0$ MeV) flux level near the axial center line of the self-cooled MARS-type lead-lithium blanket test module is reduced by about 25% relative to the usual "infinite geometry" situation in which the length of both the blanket and source are very long in comparison with the first wall bore. Thus, to provide a damage rate equivalent to an infinite source of 1.5 $MW/m^2$, a 2.0 $MW/m^2$ finite source must be provided. This correction becomes less important for a two test port tandem mirror FERF such as TDF and the MFTF-α+T varients described in Section 13.3.5.

Given the above perspective on capabilities, it is of interest to compare the performance and cost of MFTF-α+T and TDF with those of recent tokamak test facility designs, the FED-R design[20] and the INTOR design[21]. Such a comparison is presented in Tables 13.4-3(a) and 13.4-3(b). The reader is advised that the assumptions required to construct this table are uniform and consistent, but do not, in all cases, reflect the published values. Nevertheless, the trends are expected to be relatively valid.

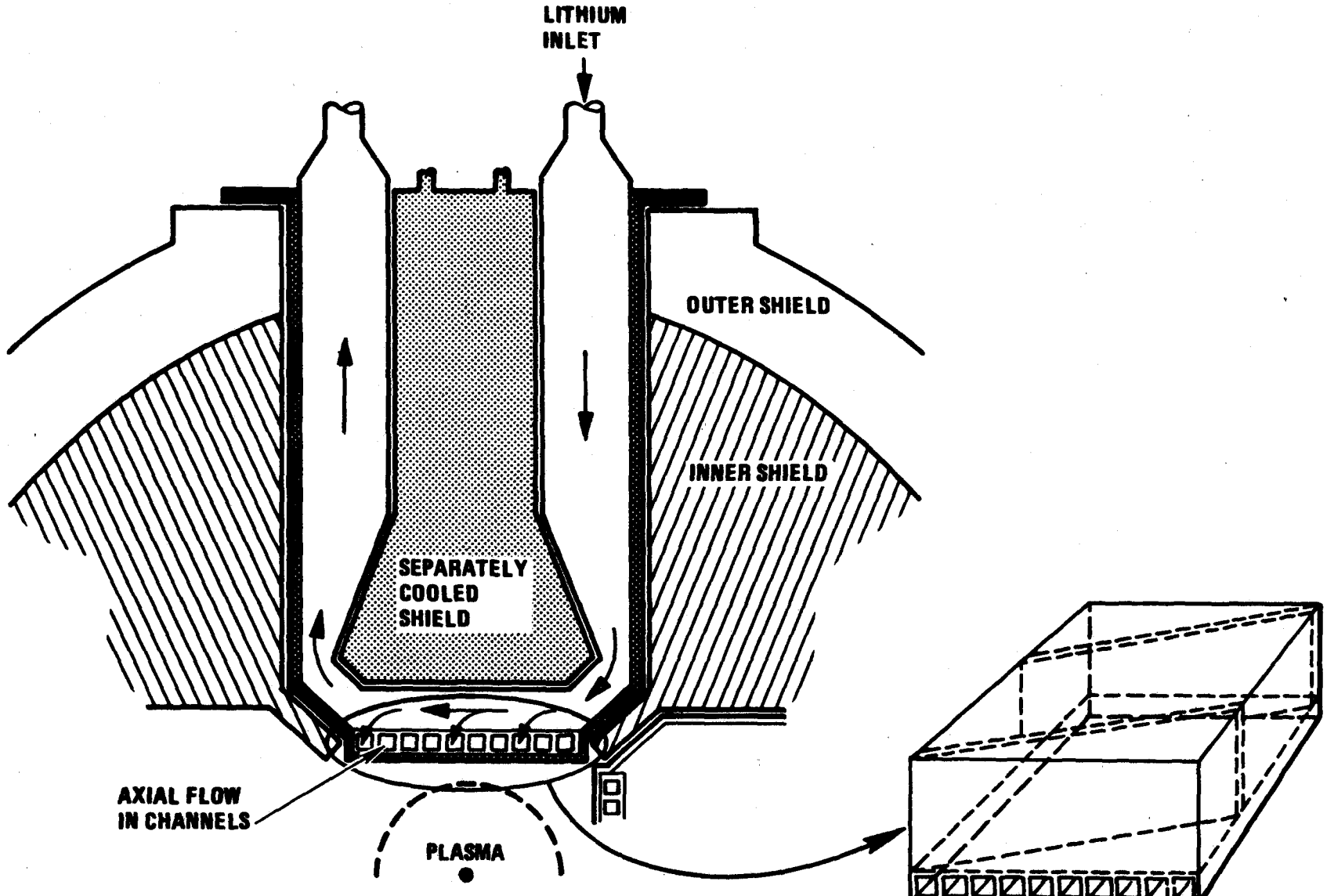


Figure 13.4-2. Lithium cooled vanadium tokamak blanket test module for tandem mirror testing.

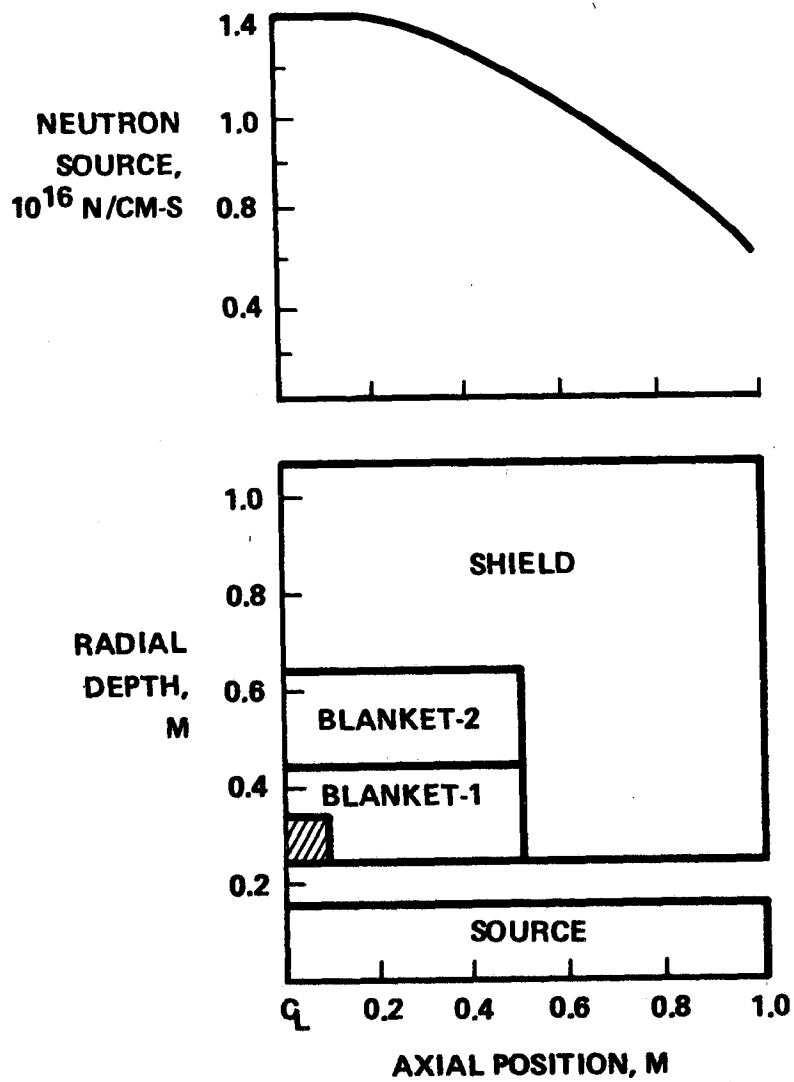


| | INFINITE | FINITE UNIFORM SOURCE | FINITE SHAPED SOURCE |
|---|---|---|---|
| Normalized Neutron Flux at Centerline | | | |
| E > 10.0 MeV | 1.0 | 0.98 | 0.93 |
| E > 1.0 MeV | 1.0 | 0.85 | 0.76 |
| E > 0.1 MeV | 1.0 | 0.90 | 0.69 |
| TOTAL | 1.0 | 0.74 | 0.68 |
| Normalized Heating Rate at Centerline | | | |
| TOTAL | 1.0 | 0.85 | 0.85 |

Figure 13.4-3. Typical tandem mirror test module neutronics.

Table 13.4-1. Performance of a Tungsten Filament Resistive Heater in a Tandem Mirror Test Module

| Filament Radius (mm) | Mesh Transmission Fraction | Net Absorption Efficiency | Average Mesh Thickness (mm) | Surface Heat Flux ($W/cm^2$) | Filament Power (KW) | Filament Voltage (Volts) | Filament Current (Amps) |
|---|---|---|---|---|---|---|---|
| 0.25 | 0.886 | 0.846 | 0.05 | 32 | 5.69 | 311 | 18.1 |
| 0.50 | 0.772 | 0.725 | 0.18 | 55 | 9.70 | 204 | 47.5 |
| 1.0 | 0.544 | 0.536 | 0.72 | ~ 80 | 14.3 | 124 | 115 |
| 2.0 | 0.084 | 0.287 | 2.90 | ~ 60 | 15.3 | 64 | 239 |

Number of tungsten filaments = 90
Filament length - 4 m
Filament temp. = $2760^0$ C K

Filament resistivity = $8.4 \cdot 10^{-7} \Omega \cdot m$
Filament emissivity = 0.323
Unoxidized steel wall emissivity = 0.25

Table 13.4-2. General Applicability of Tandem Mirror FERFs to Various Nuclear Experiment/Test Categories

| | Hybrid Experiment/ Test Category | Low Fluence (e.g, MFTF-$\alpha$+T) | Intermediate Fluence (e.g., TDF) | Key Nuclear Facility |
|---|---|---|---|---|
| I. | Neutronics | Attractive | Attractive | Point D-T source |
| II. | Tritium breeding/ extraction | Attractive | Attractive | Fission Test Reactor |
| III. | Irradiation chemistry | Not suitable | Attractive | Fission Test Reactor |
| IV. | Irradiation damage/ basic data | Not suitable | Marginal | Accelerator Neutron Source |
| V. | Thermal - hydraulics Thermal - mechanical | Attractive | Attractive | Fusion Test Reactor |
| VI. | Early failure modes | Adequate | Attractive | Fusion Test Reactor |
| VII. | Extended fluence testing for blanket structure | Not suitable | Adequate | Fusion Test Reactor |

Table 13.4-3(a). Performance Comparisons of Various Fusion Engineering Facility Candidates

| | MFTF-α+T | TDF[a] | FED-R(II) | INTOR |
|---|---|---|---|---|
| Fusion power, MW | 17 | 36 | 250 | 620 |
| Neutron wall loading, $MW/m^2$ | 2.0 | 2.1 | 1.3 | 1.3 |
| First wall radius, m | 0.25 | 0.30 | 1.05 | 1.2 |
| Component test area, $m^2$ | 1.6[b] | 3.8 | 60 | 380 |
| Ultimate availability, % | 10 | 40 | 40 | 35 |
| Lifetime at ultimate availability, yr | 10 | 10 | 10 | 10 |
| Lifetime fluence, $MW-yr/m^2$ | 2.0 | 8.0 | 5.2 | 4.6 |

a) beam fueled version
b) can be increased to 3.2 $m^2$ as described in Section 13.3.5

Table 13.4-3(b). Cost Comparison of Various Fusion Engineering Facility Candidates

| | MFTF-α+T | TDF | FED-R(II) | INTOR |
|---|---|---|---|---|
| Total capital cost, $M | 400 | 1300 | 2100 | 2600 |
| Electrical consumption, $MW_e$ | 150 | 250 | 600 | 300 |
| Annual Electrical Cost, $M/yr[a] | 7 | 44 | 105 | 46 |
| Tritium consumption, Kg/yr | 0.10 | 0.8 | 5.7 | 6.2[b] |
| Annual tritium cost, $M/yr[c] | 2 | 16 | 115 | 124 |
| Annual operating cost, $M/yr[d] | 41 | 67 | 105 | 130 |
| Total Annual Cost, $M/yr | 50 | 127 | 325 | 300 |
| Total cumulative cost, $M | ~ 1000 | ~ 2800 | ~5700 | ~6000 |

a) at 50 mil/$KW_eH$
b) assumes INTOR TBR and blanket coverage of 50%.
c) at 20,000 $/g
d) estimate

As shown, the tandem mirror facilities have potential to produce neutron wall loadings comparable to, or in excess of those of the tokamak facilities. This would be done over a much smaller test area, at a fusion power which is reduced by an order of magnitude or more. The tandem mirror component test area can be increased (Section 13.5.5), but it will, in any case, be small in comparison with that of the tokamaks. Although the limited test area is a major concern for tandem mirrors with driver test cells, the virtually steady-state operation of tandem mirrors is believed to be a substantial advantage in the conduct of several types of experiments; most notably those that involve the dynamics of tritium recovery from solid breeder blankets.

The rough cost comparisons of Table 13.4-3(b) can be used to demonstrate that MFTF-$\alpha$+T, TDF, and the tokamak alternatives represent distinct cost categories. The MFTF-$\alpha$+T upgrade would have a low capital cost and an annual operating cost which is expected to be dominated by personnel costs. As a result, the cumulative (i.e., life cycle) cost is expected to be on the order of 1 \$B. In comparison, the initial TDF cost is 3 times higher and the total cumulative (i.e., life cycle) cost is also 3 times higher; primarily due to purchased electricity. These differences are compounded by the tokamaks which cost 60-100% more than TDF and require more than double its total cumulative cost despite the fact that the INTOR class facility is assumed to breed half of its own tritium. The FED-R facility is especially costly in electrical consumption because its copper TF coils would require a large electrical input.

Thus, the cost differential between MFTF-$\alpha$+T and a large tokamak engineering test reactor is 5-6 fold and their respective capabilities should be viewed in this light. The key challenge will be to demonstrate that tandem mirrors and complementary fusion and non-fusion facilities can address a sufficient number of tokamak nuclear issues.

### 13.4.2 Assessment of Tandem Mirror Nuclear Experimentation/Testing Vis-a-Vis FINESSE Nuclear Issues List

#### 13.4.2.1 Methodology

Each issue and sub-issue of the preliminary list of FINESSE nuclear issues (129 total issues) was subject to a preliminary assessment of the contribution to issue resolution which could be made in an MFTF-$\alpha$+T or TDF class

facility. Four figures-of-merit which were used to categorize different aspects of tandem mirrors as experiment/test platforms are defined in Table 13.4-4. A fifth figure-of-merit was used to integrate and rank the combination of the first four. This integrated measure of the overall value of a tandem mirror test capability in resolving a given issue is defined as follows:

| Test Value | Tandem Mirror Testing Contribution |
|---|---|
| a) | Sufficiently resolves issue independent of other major test facilities. |
| b) | Sufficiently resolves issue in conjunction with existing fusion and/or potential non-fusion facilities. |
| c) | Confirms performance/reliability goals (developed from non-fusion testing) to mid-life conditions. |
| d) | Establishes an early life performance confirmation/model benchmark and/or explores early failure modes. |
| e) | No significant benefit due to insufficient or previously existing capability. |

with the test values assigned according to the criteria described in Table 13.4-5.

It is important to note that the achievement of an "a" test value is extremely difficult as it requires full scale testing to end-of-life conditions. Test value "b" implies an important new contribution to the data base, while test values "c" and "d" imply confirming and/or early failure mode data. Only test value "e" implies that a significant benefit would not be obtained with tandem mirror testing. A particular nuclear issue cannot receive a test value for tandem mirror testing greater than "c" if no more than a fusion confirmation is required (i.e., sufficiency of non-fusion testing $\geq$ 4). The non-fusion testing facilities do include existing fusion facilities (e.g., TFTR, MFTF-B, JET), but do not assume the existence of a high fluence acceleration-driven neutron source (e.g., FMIT).

Table 13.4-4. Four Figures of Merit Used to Categorize Tandem Mirrors as Test Platforms to Address the FINESSE Nuclear Issue

| Sufficiency of Testing in Facilities Other Than an Integrated Fusion Nuclear Test Facility[a] | Adequacy of Tandem Mirror Fusion Test Environment[b] | Relative Scale of Tandem Mission Fusion Test Article | Tandem Mirror Fusion Test Duration |
|---|---|---|---|
| 1 Fusion test environment clearly essential to successful resolution of issue. | 1 Full simulation possible. for full simulation. | 1 Full scale or sufficiently large | 1 Complete or end-of-life. |
| 2 Aspects of fusion environment are among those expected to dominate resolution of the issue | 2 Simulates major features of environment | 2 Subscale or submodule. | 2 Extended or mid-life simulation. |
| 3 Some resolution, but fusion testing require for sufficient issue resolution. | 3 Limited simulation of dominant aspect of nuclear issue. | 3 Unit cell or specimen. | 3 Early performance/ failure mode simulation. |
| 4 Fusion confirmation desirable. | 4 Not adequate. | 4 Not applicable. | 4 Design benchmark/ verification. |
| 5 Sufficient issue resolution without fusion testing. | | | 5 Not applicable. |

a) Includes existing fusion facilities (e.g., TFTR, MFTF-B, JET), but not FMIT.

b) Does not consider fluence (which is considered in the Fusion Test Duration Category).

Table 13.4-5. Integrated Tandem Mirror Test Value Assignment Criteria

| Test Value | Sufficiency of Non-Fusion Testing | Adequacy of Tandem Mirror Environment | Tandem Mirror Test Scale | Tandem Mirror Test Duration |
|---|---|---|---|---|
| a | ≤2 | ≤2 | ≤1 | ≤1 |
| b | ≤3 | ≤2 | ≤2 | ≤2 |
| c | ≤4 | ≤3 | ≤3 | ≤2 |
| d | ≤4 | ≤3 | ≤3 | ≤4 |
| | e | all other combinations | | |

13.4.2.2 Results

An issue-by-issue evaluation of the potential value of tandem mirror testing is shown in Table 13.4-6. In addition to the figures-of-merit described above, the table also shows the "level of concern" for each issue (see Chapter 3). The second through fourth columns apply equally well to MFTF-α+T and TDF while the fifth and sixth apply to MFTF-α+T only and the seventh and eighth apply to TDF only. In this evaluation, no attention was paid to the available test area and/or scheduling. Each issue was considered individually.

Statistics condensing the results of Table 13.4-6 are shown in Figs. 13.4-4, 5, 6, and 7. These statistics are further summarized in Table 13.4-7. As shown in Fig. 13.4-4, MFTF-α+T resolves only one blanket/first wall issue independent of other major facilities (test value "a"). Adding those issues which can be addressed with a "b" value (i.e., those which can be resolved using a tandem mirror in conjuntion with other facilities), it appears that 44% of all critical and high concern issues for the blanket/first wall can be addressed in MFTF-α+T (see Table 13.4-7). Adding those issues whose tandem mirror test values are "c" and "d", the number of critical and high concern blanket/first wall issues which can be addressed in MFTF-α+T rise to 69% and 92%, respectively.

Table 13.4-6. Issue-by-Issue Evaluation of Potential Tandem Mirror Test Values

| Issue/Technical Area | Level of Concern | Testing Adequacy Without Fusion NTF | Adequacy of NTF Fusion Test Environ. | Adequacy of NTF Fusion Test Scale | MFTF-α + T Fusion Test Duration | MFTF-α + T Fusion Test Value | TDF Fusion Test Duration | TDF Fusion Test Value |
|---|---|---|---|---|---|---|---|---|
| I. BLANKET/FIRST WALL ISSUES | | | | | | | | |
| A. STRUCTURE | | | | | | | | |
| 1. Irradiation Damage | | | | | | | | |
| a. Changes in Properties and Behavior of Materials | Critical | 3 | 1 | 1 | 3 | d | 2 | b |
| b. Prediction of Radiation Damage Indicators | High | 3 | 1 | 1 | 3 | d | 1 | b |
| 2. Distortion and/or Breach of Components | | | | | | | | |
| a. Effect of First Wall Heat Flux and Cycling on Fatigue or Crack Growth Related Failure | Critical | 3 | 2 | 2 | 4 | d | 2 | b |
| b. Premature Failure at Welds and Discontinuities | High | 2 | 2 | 2 | 2 | b | 1 | b |
| c. Failures due to Hot Spots | High | 3 | 1 | 1 | 1 | b | 1 | b |
| d. Interaction of Primary and Secondary Stresses and Deformation | High | 3 | 2 | 2 | 1 | b | 1 | b |
| e. Effect of Swelling, Creep, and Thermal Gradients on Stress Concentrations | Medium | 2 | 2 | 2 | 4 | d | 2 | b |
| f. Failure due to Shutdown Residual Stress Effects | Medium | 2 | 3 | 2 | 2 | c | 2 | c |
| g. Interaction between Surface Effects and First Wall Failures | Medium | 3 | 4 | 4 | 5 | e | 5 | e |
| h. Magnetic Field Interactions within the Structure | | | | | | | | |
| 1) Magnetically Induced Stresses in Ferritic Steel | Low | 4 | 3 | 2 | 1 | c | 1 | c |
| 2) Magnetic Forces due to Disruptions and Magnetic Transients | Critical | 3 | 4 | 4 | 5 | e | 5 | e |

Table 13.4-6. Issue-by-Issue Evaluation of Potential Tandem Mirror Test Values (con't)

| Issue/Technical Area | Level of Concern | Testing Adequacy Without Fusion NTF | Adequacy of NTF Fusion Test Environ. | Adequacy of NTF Fusion Test Scale | MFTF-α + T Fusion Test Duration | MFTF-α + T Fusion Test Value | TDF Fusion Test Duration | TDF Fusion Test Value |
|---|---|---|---|---|---|---|---|---|
| i. Environmentally Assisted Cracking | Low | 4 | 1 | 2 | 2 | d | 1 | d |
| j. Self-Welding of Similar and Dissimilar Metals | Low | 4 | 1 | 1 | 1 | c | 1 | c |
| 3. Tritium Permeation through the Structure | | | | | | | | |
| a. Effectiveness of Tritium Permeation Barriers | Critical | 2 | 1 | 1 | 1 | a | 1 | a |
| b. Effect of Radiation on Tritium Permeation | Medium | 3 | 1 | 1 | 3 | d | 1 | b |
| 4. Structural Activation Product Inventory | | | | | | | | |
| a. Long-Lived Isotopes | Low | 4 | 1 | 1 | 1 | c | 1 | c |
| b. Contribution of Materials Impurities | Low | 4 | 1 | 1 | 1 | c | 1 | c |
| B. COOLANT | | | | | | | | |
| 1. MHD Pressure Drop and Pressure Stresses | Critical | 4 | 2 | 2 | 1 | c | 1 | c |
| 2. MHD and Geometric Effects on Flow Distributions | High | 3 | 2 | 2 | 1 | b | 1 | b |
| 3. Coolant Flow Stability | High | 3 | 1 | 2 | 1 | b | 1 | b |
| 4. Stability/Kinetics of Tritium Oxidation in the Coolant | He:H<br>Li-He:M<br>Salt:M | 3 | 2 | 1 | 1 | b | 1 | b |
| 5. Helium Bubble Formation Leading to Hot Spots | Low | 3 | 1 | 1 | 1 | b | 1 | b |
| C. BREEDER, MULTIPLIER AND PURGE | | | | | | | | |
| 1. Tritium Recovery and Inventory in Solid Breeder Materials | | | | | | | | |
| a. Intergranular Tritium Diffusivity and Solubility | Critical | 3 | 1 | 1 | 2 | b | 1 | b |

Table 13.4-6. Issue-by-Issue Evaluation of Potential Tandem Mirror Test Values (con't)

| Issue/Technical Area | Level of Concern | Testing Adequacy Without Fusion NTF | Adequacy of NTF Fusion Test Environ. | Adequacy of NTF Fusion Test Scale | MFTF-α + T Fusion Test Duration | MFTF-α + T Fusion Test Value | TDF Fusion Test Duration | TDF Fusion Test Value |
|---|---|---|---|---|---|---|---|---|
| b. Tritium Surface Migration and Desorption | High | 4 | 1 | 1 | 1 | b | 1 | b |
| c. Porosity, Purge Flow Distribution, and Tritium Transport | High | 3 | 1 | 2 | 1 | b | 1 | b |
| 2. Liquid Breeder Tritium Extraction | Li:M LiPb:H | 4 | 1 | 1 | 1 | c | 1 | c |
| 3. Mechanical Interactions in Solid Breeder Materials | | | | | | | | |
| a. Thermal Expansion Driving Force | Medium | 4 | 2 | 2 | 1 | c | 1 | c |
| b. Swelling Driving Force | $Li_2O$:C TC:L | 3 | 2 | 2 | 5 | e | 2 | b |
| c. Stress Concentrations at Cracks and Discontinuities | High | 3 | 2 | 2 | 3 | d | 2 | b |
| d. Strain Accommodation by Creep and Plastic Flow | $Li_2O$:C TC:M | 2 | 2 | 2 | 5 | e | 2 | b |
| 4. Temperature Limits and Variability in Solid Breeder Materials | | | | | | | | |
| a. Temperature Limits | Critical | 3 | 1 | 1 | 1 | b | 1 | b |
| b. Thermal Conductivity Changes under Irradiation | High | 3 | 1 | 1 | 3 | d | 2 | b |
| c. Effect of Cracking | High | 4 | 1 | 2 | 3 | d | 2 | c |
| d. Effect of LiOT Mass Transfer | High | 3 | 1 | 2 | 1 | b | 1 | b |
| 5. Neutron Multiplier Mechanical Interactions | | | | | | | | |
| a. Swelling Driving Force in Beryllium | High | 4 | 1 | 1 | 3 | d | 2 | c |
| b. Strain Accommodation by Creep in Beryllium | Medium | 4 | 1 | 1 | 3 | d | 1 | c |
| c. Mechanical Integrity of Unclad Beryllium | Low | 4 | 1 | 1 | 2 | c | 1 | c |

Table 13.4-6. Issue-by-Issue Evaluation of Potential Tandem Mirror Test Values (con't)

| Issue/Technical Area | Level of Concern | Testing Adequacy Without Fusion NTF | Adequacy of NTF Fusion Test Environ. | Adequacy of NTF Fusion Test Scale | MFTF-α + T Fusion Test Duration | MFTF-α + T Fusion Test Value | TDF Fusion Test Duration | TDF Fusion Test Value |
|---|---|---|---|---|---|---|---|---|
| 6. Tritium Transport | | | | | | | | |
| a. Tritium Release Form from Solid Breeder | High | 4 | 1 | 1 | 1 | c | 1 | c |
| b. Stability/Kinetics of Tritium Oxidation in the Helium Purge | High | 4 | 2 | 1 | 1 | c | 1 | c |
| D. COOLANT-STRUCTURE INTERACTIONS | | | | | | | | |
| 1. Thermal Interactions | | | | | | | | |
| a. MHD Effects on First Wall Cooling and Hot Spots | Critical | 4 | 2 | 2 | 1 | c | 1 | c |
| b. Response to Cooling System Transients | LM and DS:C,$H_2O$ and He:L | 3 | 2 | 1 | 1 | b | 1 | b |
| c. Flow Sensitivity to Dimensional Changes (Thermal Instability) | Medium | 3 | 2 | 2 | 3 | d | 2 | b |
| 2. Mechanical and Materials Interactions | | | | | | | | |
| a. Mass Transport Rates and Consequences due to Corrosion and Sputtering | Critical | 3 | 2 | 2 | 2 | b | 1 | b |
| b. Mechanical Wear and Fatigue from Flow-Induced Vibrations | Medium | 3 | 1 | 2 | 1 | b | 1 | b |
| c. Failure of Coolant Wall due to Stress Corrosion Cracking | Low | 3 | 1 | 2 | 3 | c | 2 | b |
| d. Failure of Coolant Wall due to Liquid Metal Embrittlement | Low | 4 | 1 | 2 | 2 | c | 1 | c |
| E. SOLID BREEDER-STRUCTURE INTERACTIONS | | | | | | | | |
| 1. Mechanical and Materials Interactions | | | | | | | | |
| a. Clad Corrosion from Breeder Burnup Products | Critical | 4 | 1 | 1 | 2 | c | 1 | c |

Table 13.4-6. Issue-by-Issue Evaluation of Potential Tandem Mirror Test Values (con't)

| Issue/Technical Area | Level of Concern | Testing Adequacy Without Fusion NTF | Adequacy of NTF Fusion Test Environ. | Adequacy of NTF Fusion Test Scale | MFTF-α + T Fusion Test Duration | MFTF-α + T Fusion Test Value | TDF Fusion Test Duration | TDF Fusion Test Value |
|---|---|---|---|---|---|---|---|---|
| b. Breach of Structure | High | 2 | 2 | 2 | 2 | b | 1 | b |
| c. Distortion of Components | Medium | 2 | 2 | 2 | 2 | b | 1 | b |
| d. Material Compatibility with Lithium Burnup | Medium | 4 | 1 | 1 | 1 | c | 1 | c |
| 2. Thermal Interactions | | | | | | | | |
| a. Breeder/Structure Interface Heat Transfer (Gap Conductance) | Critical | 3 | 1 | 2 | 2 | b | 1 | b |
| F. GENERAL BLANKET | | | | | | | | |
| 1. Adequate Tritium Breeding | | | | | | | | |
| a. Uncertainties in Doubling Time Margin and Predictive Capabilities | Critical | 4 | 2 | 2 | 2 | c | 2 | c |
| b. Lithium Burnout Effects | Medium | 4 | 1 | 1 | 3 | d | 2 | c |
| 2. Tritium Inventory Behavior during Transients | SB:H others:L | 3 | 2 | 2 | 3 | d | 2 | b |
| 3. Chemical Reactivity of Lithium | Medium | 5 | 1 | 1 | 1 | e | 1 | e |
| 4. Tritium Permeation: | | | | | | | | |
| a. From Breeder to Blanket Coolant | SB:H LiPb:H Li:M | 4 | 1 | 2 | 1 | c | 1 | c |
| b. Characteristics at Low Pressure | High | 4 | 3 | 2 | 4 | d | 4 | d |
| 5. Assembly and Fabrication of Solid Breeder Blankets | Medium | 5 | 1 | 2 | 1 | e | 1 | e |
| 6. Recyling of Irradiated Lithium and Beryllium | Low | 4 | 1 | 1 | 2 | c | 1 | c |
| 7. Nuclear Heating Rate Predictions | High | 4 | 2 | 2 | 1 | c | 1 | c |
| 8. Chemical Toxicity Inventory | Low | 5 | 2 | 1 | 1 | e | 1 | e |
| 9. Blanket Response to Near Blanket Failures | High | 4 | 2 | 2 | 3 | d | 2 | c |
| 10. Uncertainties in Failure Frequencies and Failure Modes | Critical | 2 | 2 | 2 | 2 | b | 2 | b |

Table 13.4-6. Issue-by-Issue Evaluation of Potential Tandem Mirror Test Values (con't)

| Issue/Technical Area | Level of Concern | Testing Adequacy Without Fusion NTF | Adequacy of NTF Fusion Test Environ. | Adequacy of NTF Fusion Test Scale | MFTF-α + T Fusion Test Duration | MFTF-α + T Fusion Test Value | TDF Fusion Test Duration | TDF Fusion Test Value |
|---|---|---|---|---|---|---|---|---|
| II. PLASMA INTERACTIVE COMPONENTS | | | | | | | | |
| A. GENERAL CONCERNS | | | | | | | | |
| 1. Materials Data Base Devel. | High | 3 | 2 | 1 | 2 | b | 1 | b |
| 2. HHFC Surface Damage Mechanisms | | | | | | | | |
| a. Physical Sputtering and Re-desposition | Critical | 2 | 3 | 3 | 4 | d | 4 | d |
| b. Arcing and Related Erosion | High | 3 | 4 | 4 | 5 | e | 5 | e |
| c. Chemical Erosion | Medium | 4 | 3 | 3 | 4 | d | 4 | d |
| d. Surface Damamge due to Helium Implantation (Blistering) | Medium | 4 | 3 | 3 | 4 | d | 4 | d |
| e. Disruption-Induced Surface Melting and Erosion | Medium | 3 | 3 | 3 | 4 | d | 4 | d |
| 3. HHFC Thermomechanical Response | | | | | | | | |
| a. Leading Edge Design | High | 2 | 4 | 4 | 5 | e | 5 | e |
| b. Thermal Hydraulic Techniques | Critical | 4 | 2 | 2 | 3 | d | 3 | d |
| c. HHFC Structural Integrity | High | 2 | 3 | 2 | 4 | d | 4 | d |
| d. Plasma Side Hot Spots due to Plasma | Critical | 2 | 4 | 4 | 5 | e | 5 | e |
| e. Distruptions Shock Loading | Tok:H Mirror:L | 3 | 3 | 3 | 4 | d | 4 | d |
| 4. Plasma Edge Conditions and Exhaust | | | | | | | | |
| a. Plasma Edge Temperature and Density Control | Critical | 2 | 4 | 4 | 5 | e | 5 | e |
| b. Helium and Impurity Exhaust | High | 3 | 3 | 2 | 4 | d | 4 | d |
| c. Plasma Exhaust Stream Pressure and Composition | Medium | 3 | 4 | 4 | 5 | e | 5 | e |
| d. Surface Conditioning Effectiveness | Medium | 4 | 3 | 2 | 4 | d | 4 | d |

Table 13.4-6. Issue-by-Issue Evaluation of Potential Tandem Mirror Test Values (con't)

| Issue/Technical Area | Level of Concern | Testing Adequacy Without Fusion NTF | Adequacy of NTF Fusion Test Environ. | Adequacy of NTF Fusion Test Scale | MFTF-α + T Fusion Test Duration | MFTF-α + T Fusion Test Value | TDF Fusion Test Duration | TDF Fusion Test Value |
|---|---|---|---|---|---|---|---|---|
| 5. Safety | | | | | | | | |
| a. Tritium Permeation and Inventory with Implantation | Critical | 3 | 2 | 2 | 2 | b | 1 | b |
| b. Tritium Inventory Behavior during Maintenance* | High | 3 | 2 | 2 | 2 | b | 1 | b |
| c. Eroded Activation Product Behavior in the Vacuum Chamber | Medium | 3 | 3 | 2 | 4 | d | 4 | d |
| d. Oxidation/Volatility Energy Release during Transients | High | 4 | 3 | 3 | 4 | d | 4 | d |
| B. LIMITER/DIVERTOR SPECIFIC ISSUES | | | | | | | | |
| 1. Alignment | Medium | 2 | 4 | 4 | 5 | e | 5 | e |
| 2. Maintenance and Replacement | High | 2 | 4 | 4 | 5 | e | 5 | e |
| 3. Choice of Limiter vs Divertor | High | 3 | 4 | 4 | 5 | e | 5 | e |
| C. VACUUM SYSTEMS | | | | | | | | |
| 1. Compound Cryopump Helium Pumping and Regeneration Lifetime | Medium | 3 | 2 | 1 | 1 | b | 1 | b |
| 2. Large-Diameter Vacuum Valve Reliability | Low | 4 | 1 | 1 | 1 | c | 1 | c |
| 3. Vacuum Pump Operation under Thermal/Pressure Transients | Low | 4 | 1 | 1 | 1 | c | 1 | c |
| 4. Vacuum Chamber Outgassing and Leak Rates | Medium | 3 | 3 | 2 | 1 | c | 1 | c |
| D. RF COMPONENTS | | | | | | | | |
| 1. RF Launcher Technology and Performance | Critical | 2 | 3 | 2 | 2 | c | 1 | c |

* (Surface Re-emission and Effectiveness of Baking)

Table 13.4-6. Issue-by-Issue Evaluation of Potential Tandem Mirror Test Values (con't)

| Issue/Technical Area | Level of Concern | Testing Adequacy Without Fusion NTF | Adequacy of NTF Fusion Test Environ. | Adequacy of NTF Fusion Test Scale | MFTF-α + T Fusion Test Duration | MFTF-α + T Fusion Test Value | TDF Fusion Test Duration | TDF Fusion Test Value |
|---|---|---|---|---|---|---|---|---|
| 2. Windows and Feedthrough Technology and Performance | Critical | 3 | 1 | 1 | 2 | b | 1 | b |
| 3. RF Transmission System Technology and Performance | Medium | 3 | 1 | 1 | 1 | b | 1 | b |
| III. SHIELD | | | | | | | | |
| 1. Shield Optimization in Complex and Varied Geometries | | | | | | | | |
| a. Thickness of Deep Penetration or Bulk Shield | High | 4 | 1 | 1 | 1 | c | 1 | c |
| b. Neutron Streaming Through Access Ports and Ducts | High | 4 | 2 | 1 | 1 | c | 1 | c |
| c. Local Shielding of Highly Sensitive Components | High | 3 | 2 | 2 | 1 | b | 1 | b |
| d. Biological Dose During Operation and Maintenance | High | 4 | 3 | 1 | 1 | c | 1 | c |
| e. Analytical Techniques and Data Base | High | 4 | 2 | 1 | 1 | c | 1 | c |
| 2. Shield Compatibility with Blanket including Assembly and Disassembly | High | 4 | 2 | 2 | 3 | d | 2 | c |
| 3. Time Constant of Magnetic Field Penetration for Plasma Control | Medium | 3 | 4 | 4 | 5 | e | 5 | e |
| 4. Shield Compatibility with the Vacuum Boundary and One Turn Resistance | Low | 3 | 4 | 4 | 5 | e | 5 | e |
| IV. TRITIUM PROCESSING SYSTEM | | | | | | | | |
| 1. Impurity Removal in the Fuel Cleanup Process | High | 3 | 2 | 1 | 1 | b | 1 | b |

Table 13.4-6. Issue-by-Issue Evaluation of Potential Tandem Mirror Test Values (con't)

| Issue/Technical Area | Level of Concern | Testing Adequacy Without Fusion NTF | Adequacy of NTF Fusion Test Environ. | Adequacy of NTF Fusion Test Scale | MFTF-α + T Fusion Test Duration | MFTF-α + T Fusion Test Value | TDF Fusion Test Duration | TDF Fusion Test Value |
|---|---|---|---|---|---|---|---|---|
| 2. Tritium Monitoring and Accountability | High | 3 | 2 | 1 | 1 | b | 1 | b |
| 3. Tritium Losses in Solid Waste | High | 4 | 1 | 1 | 1 | c | 1 | c |
| 4. Tritium Extraction from Water Coolant | High | 5 | 1 | 1 | 1 | e | 1 | e |
| 5. Tritium Processing System Integration | High | 3 | 2 | 1 | 1 | b | 1 | b |
| 6. Atmospheric Cleanup Process | Medium | 4 | 1 | 1 | 1 | c | 1 | c |
| 7. Breeder Tritium Extraction Stream Characteristics | Low | 4 | 1 | 1 | 1 | c | 1 | c |
| V. MAGNETS | | | | | | | | |
| 1. Structural Overloading and Quenching due to Plasma Disruptions | High | 3 | 4 | 4 | 5 | e | 5 | e |
| 2. Nuclear Heat Removal within Cryostability Limits | High | 3 | 1 | 2 | 1 | b | 1 | b |
| 3. Maximum Levels of Radiation Damage and Recovery Process for Magnet Components | | | | | | | | |
| a. Critical Current Reduction | High | 3 | 2 | 1 | 1 | b | 1 | b |
| b. Electrical Resistivity of the Stabilizer | High | 4 | 2 | 1 | 2 | b | 1 | b |
| c. Insulator Structural Degradation | High | 4 | 2 | 2 | 1 | b | 1 | b |
| d. Annealing of Radiation Damage | High | 4 | 2 | 1 | 2 | b | 1 | b |
| e. Consequences of Magnet Failures | High | 3 | 3 | 2 | 3 | d | 2 | c |

Table 13.4-6. Issue-by-Issue Evaluation of Potential Tandem Mirror Test Values (con't)

| Issue/Technical Area | Level of Concern | Testing Adequacy Without Fusion NTF | Adequacy of NTF Fusion Test Environ. | Adequacy of NTF Fusion Test Scale | MFTF-α + T Fusion Test Duration | MFTF-α + T Fusion Test Value | TDF Fusion Test Duration | TDF Fusion Test Value |
|---|---|---|---|---|---|---|---|---|
| VI. INSTRUMENTATION AND CONTROL | | | | | | | | |
| 1. Definition of Transducer Lifetimes and Hardening Reqmts. | High | 3 | 1 | 1 | 2 | b | 1 | b |
| 2. Breakdown of Insulation Resistance | High | 3 | 2 | 1 | 2 | b | 1 | b |
| 3. Decalibration of Transducer through Transmutation | Medium | 3 | 2 | 1 | 2 | b | 1 | b |
| 4. Ceramic Insulator/Substrate Seal Integrity | Medium | 3 | 1 | 1 | 1 | b | 1 | b |
| 5. RF Transmission Losses in Horns, Antennae, Wave Guides, and Windows | Medium | 4 | 2 | 2 | 2 | c | 1 | c |
| 6. Optical Window, Lens, and Prism Darkening and Distortion | Medium | 3 | 1 | 1 | 2 | b | 1 | b |
| 7. Shielding of Instrument Penetrations | Low | 4 | 2 | 2 | 1 | c | 1 | c |
| 8. Radiation Effects on Electrical Components beyond the First Wall and Shield | Low | 5 | 2 | 1 | 3 | e | 2 | e |
| 9. Cable Noise from RF, Magnetic Fields, Charges Particles, etc. | Low | 3 | 2 | 2 | 1 | b | 1 | b |
| VII. BALANCE OF PLANT | | | | | | | | |
| 1. Tritium Contamination of the Reactor Room | Medium | 3 | 2 | 1 | 2 | b | 2 | b |
| 2. Atmospheric Cleanup Process | Low | 4 | 2 | 1 | 2 | c | 2 | c |

Table 13.4-6. Issue-by-Issue Evaluation of Potential Tandem Mirror Test Values (con't)

| Issue/Technical Area | Level of Concern | Testing Adequacy Without Fusion NTF | Adequacy of NTF Fusion Test Environ. | Adequacy of NTF Fusion Test Scale | MFTF-α + T Fusion Test Duration | MFTF-α + T Fusion Test Value | TDF Fusion Test Duration | TDF Fusion Test Value |
|---|---|---|---|---|---|---|---|---|
| 3. Cryogenic System Failure | Low | 4 | 2 | 1 | 1 | c | 1 | c |
| 4. Remote Maintenance System Failure | Critical | 3 | 3 | 2 | 2 | c | 1 | c |
| 5. Inert Gas System Failure | Low | 4 | 2 | 2 | 2 | c | 2 | c |
| 6. Liquid Metal Pumps | Medium | 4 | 2 | 2 | 3 | d | 2 | c |
| 7. Adequacy of I&C for Safe Plant Operation | Critical | 1 | 2 | 1 | 2 | b | 2 | b |

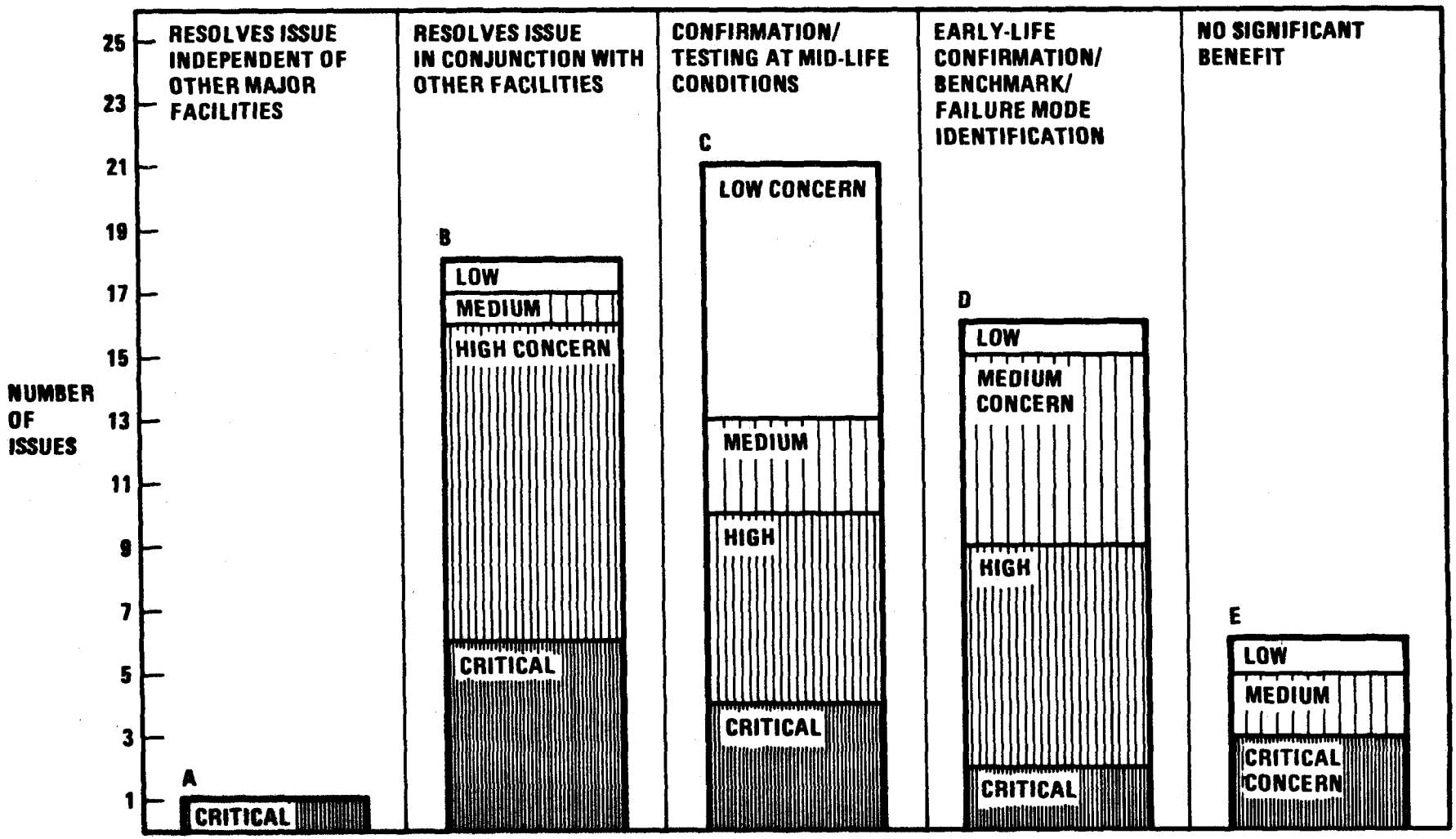


Figure 13.4-4. Blanket/first wall issues resolution in MFTF-$\alpha$+T.

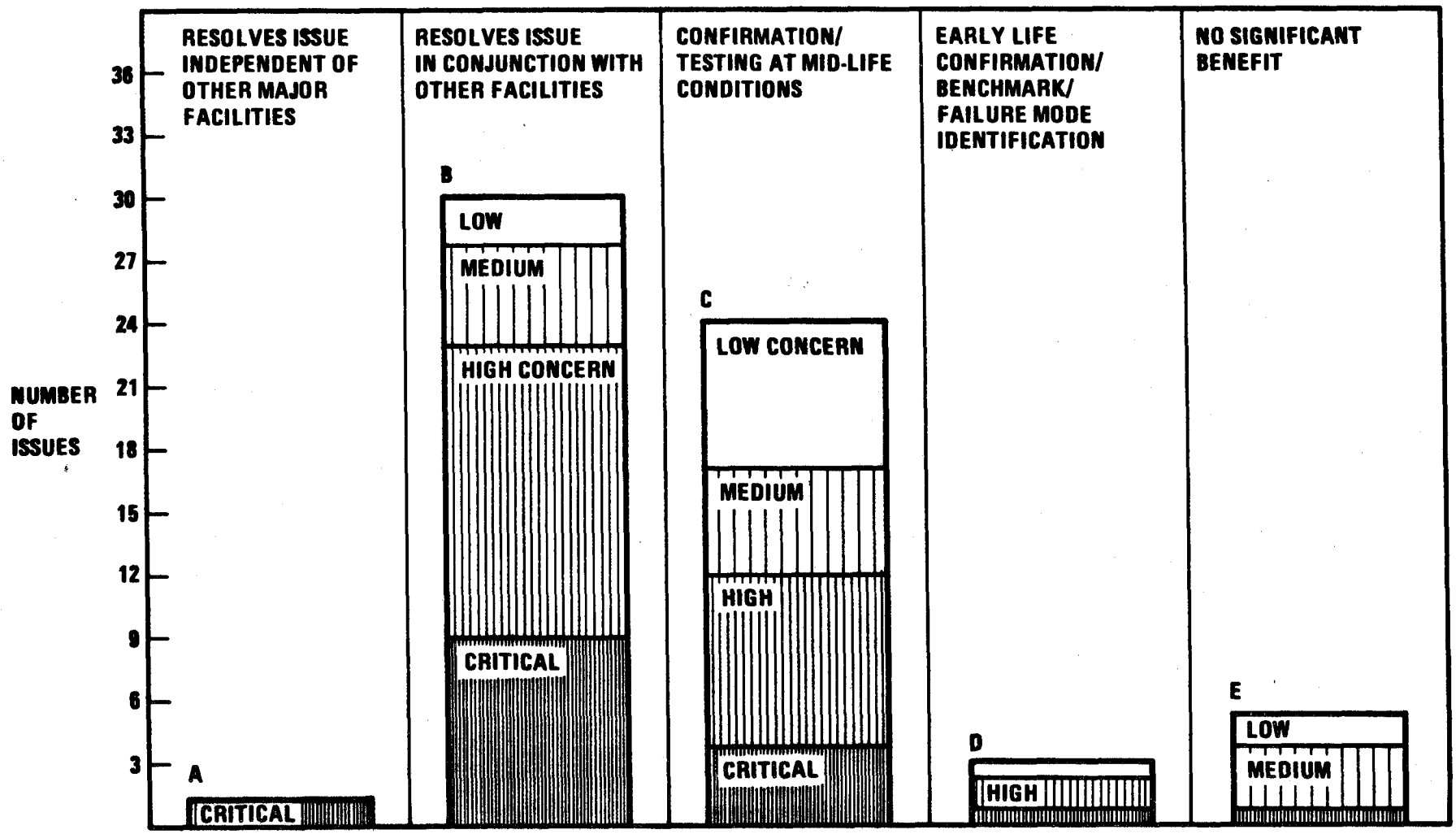


Figure 13.4-5. Blanket/first wall issues resolution in TDF.

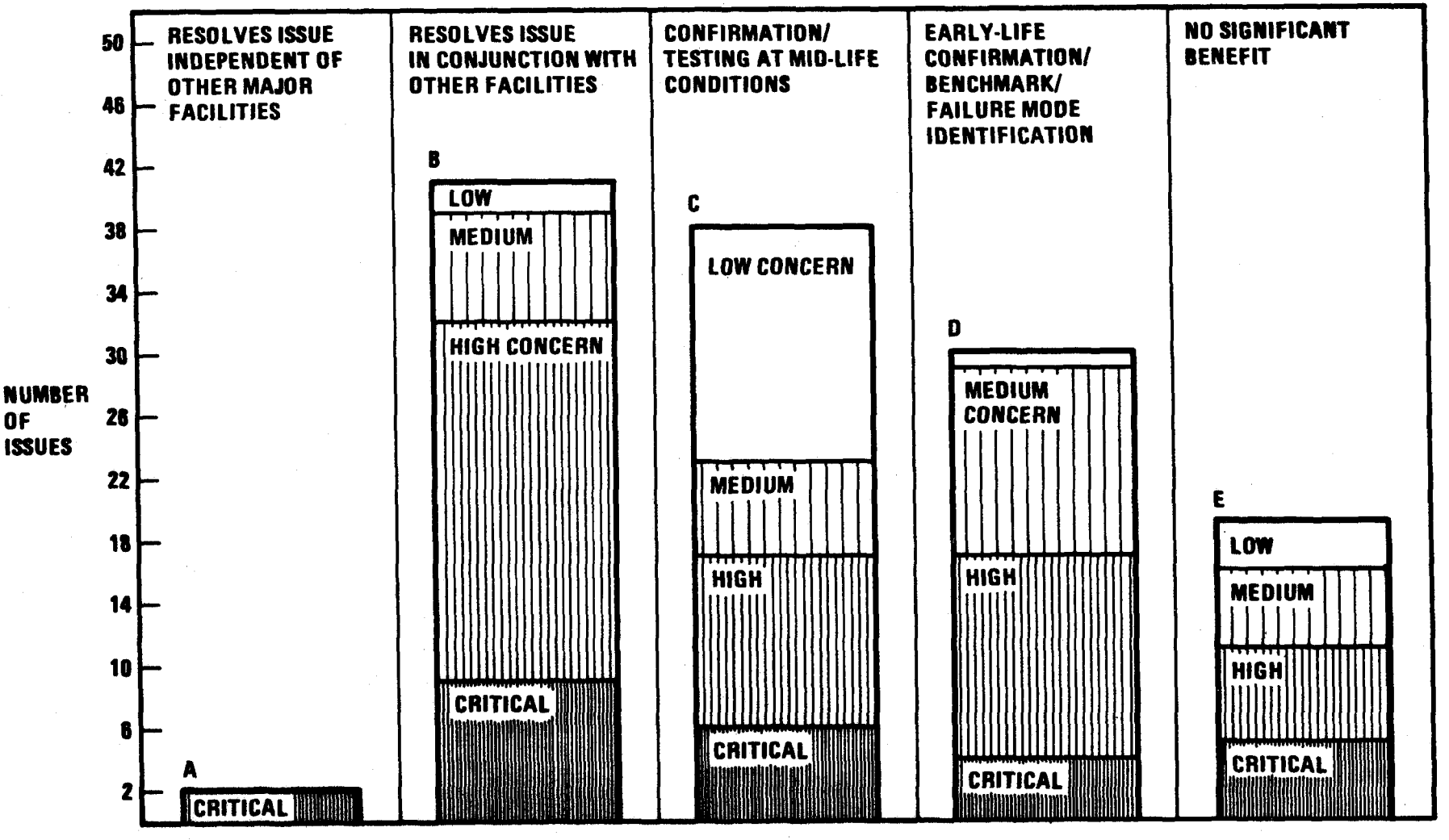


Figure 13.4-6. Overall tokamak nuclear issues resolution in MFTF-α+T.

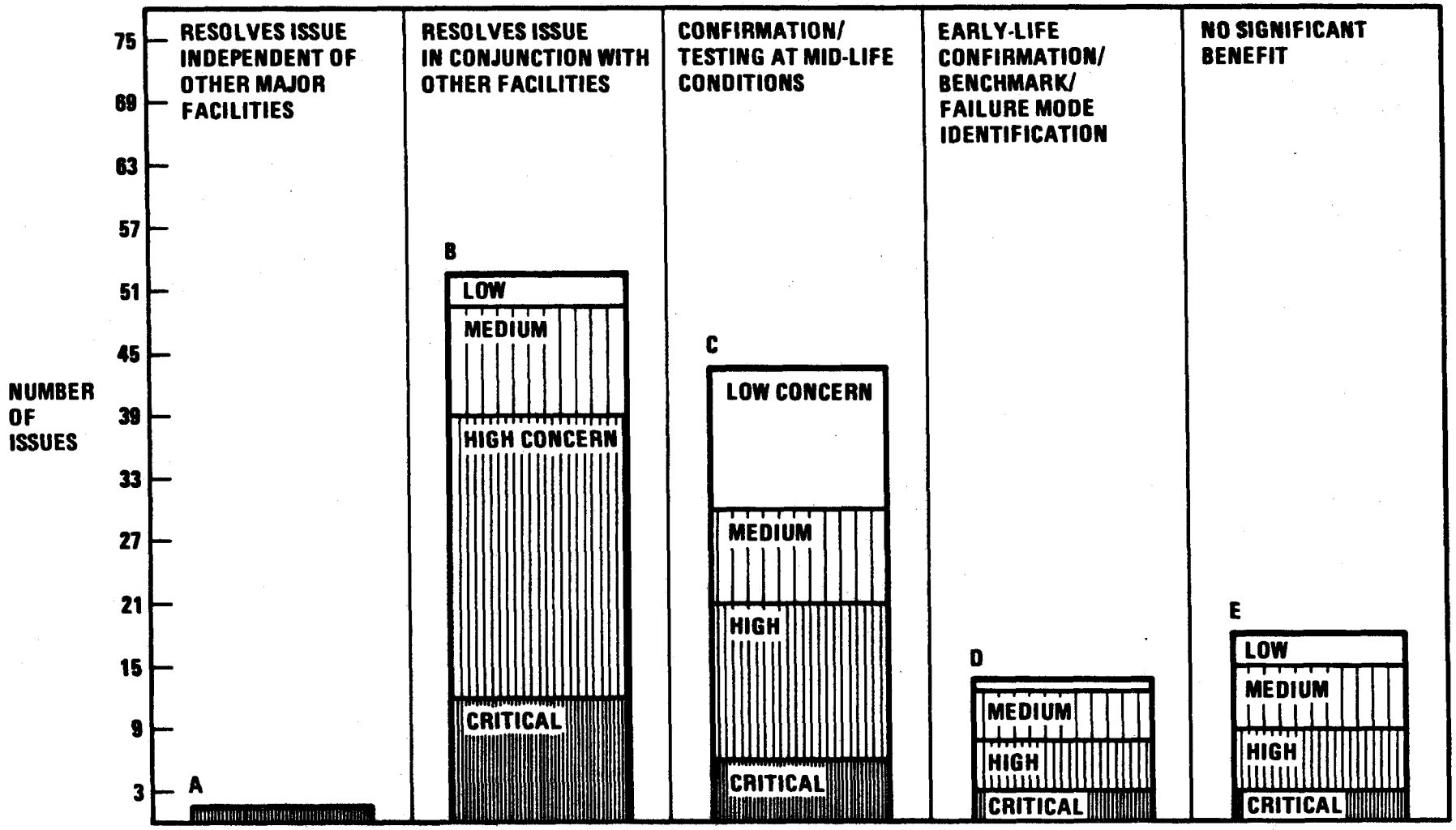


Figure 13.4-7. Overall tokamak nuclear issues resolution in TDF.

Table 13.4-7. Tandem Mirror Fusion Engineering Research Facility Test Value Statistics Summary

| Blanket/First Wall Testing | | |
|---|---|---|
| | Percentage of Critical + High Concern Issues Addressed | |
| Test Values | MFTF-α+T | TDF |
| a or b | 44% | 62% |
| a or b or c | 69% | 92% |
| a or b or c or d | 92% | 97% |
| **Overall Tokamak Testing** | | |
| | Percentage of Critical + High Concern Issues Addressed | |
| Test Values | MFTF-α+T | TDF |
| a or b | 42% | 53% |
| a or b or c | 64% | 78% |
| a or b or c or d | 86% | 88% |

In comparison with MFTF-α+T, TDF (Fig. 13.4-5) operation to intermediate fluence levels (~ 4 MW-yr/m2) would transfer the tandem mirror test values for several first wall/blanket issues from "d" to "b." As a result, it appears that TDF can address 62% of the critical and high concern blanket/first wall issues at the "a" or "b" level and 97% of the critical and high concern issues at the "a", "b", "c", or "d" level.

When the number of issues is expanded beyond blanket/first wall components to include those associated with tokamak plasma interactive components, nuclear shielding, tritium processing systems, magnets, instrumentation/control systems, and balance of plant systems, the fraction of critical and high concern issues which can be addressed in MFTF-α+T (Fig. 13.4-6) or TDF

(Fig. 13.4-7) decreases, but the number of issues which an be addressed increases and the fraction remains high. MFTF-$\alpha$+T and TDF can achieve "a" or "b" values for 42% and 53%, respectively, of all high and critical priority nuclear issues for tokamaks. Similarly, it appears that they can achieve an "a", "b", "c", or "d" test value for 86% and 88% of the high and critical priority issues for tokamaks.

The MFTF-B test value statistics for tokamak nuclear issues are summarized slightly differently in Fig. 13.4-8. As shown, 28 of the 77 critical and high priority issues cannot be addressed in MFTF-$\alpha$+T with a value of "c" or better. However, candidates to fill these "holes" exist among complementary fusion and non-fusion facilities which might join an MFTF-$\alpha$+T class facility in the development pathway. For example, when the 28 remaining issues are evaluated in this context, it appears that an additional 21-23 issues might be resolved as follows:

- For 7 of the 28 remaining issues, test values of "d" or "e" were assigned because of a non-fusion testing figure-of-merit of 4 or 5. In these cases, fusion testing was not required in the first place.
- Four of the 28 remaining issues could be addressed if a high fluence ($\gtrsim$ 8 MW-yr/m$^2$) accelerator neutron source (e.g., FMIT class) were to exist.
- An additional 10-12 tokamak nuclear issues could be addressed if a long pulse ignition tokamak experiment (e.g., TFCX class) were to exist. The higher value requires superconducting TF and OH coils.

Thus, although all of the issues are not equally important, it appears likely that a combination of facilities, including a TFCX-class facility and an MFTF-B class facility, can address the great majority of tokamak nuclear issues to the extent that a tokamak ETF/EDF (see Chapter 16) could follow at reasonable risk.

These results are summarized in Fig. 13.4-9. Starting with existing fusion and non-fusion facilities, it appears that 21 of 77 high and critical priority issues can be resolved. Other issues are addressed in these facilities, but are not resolved. An FMIT class facility would resolve an additional 4 important issues. Adding MFTF-$\alpha$+T, an additional 36 issues can be resolved in conjunction with FMIT and the existing fusion and non-fusion

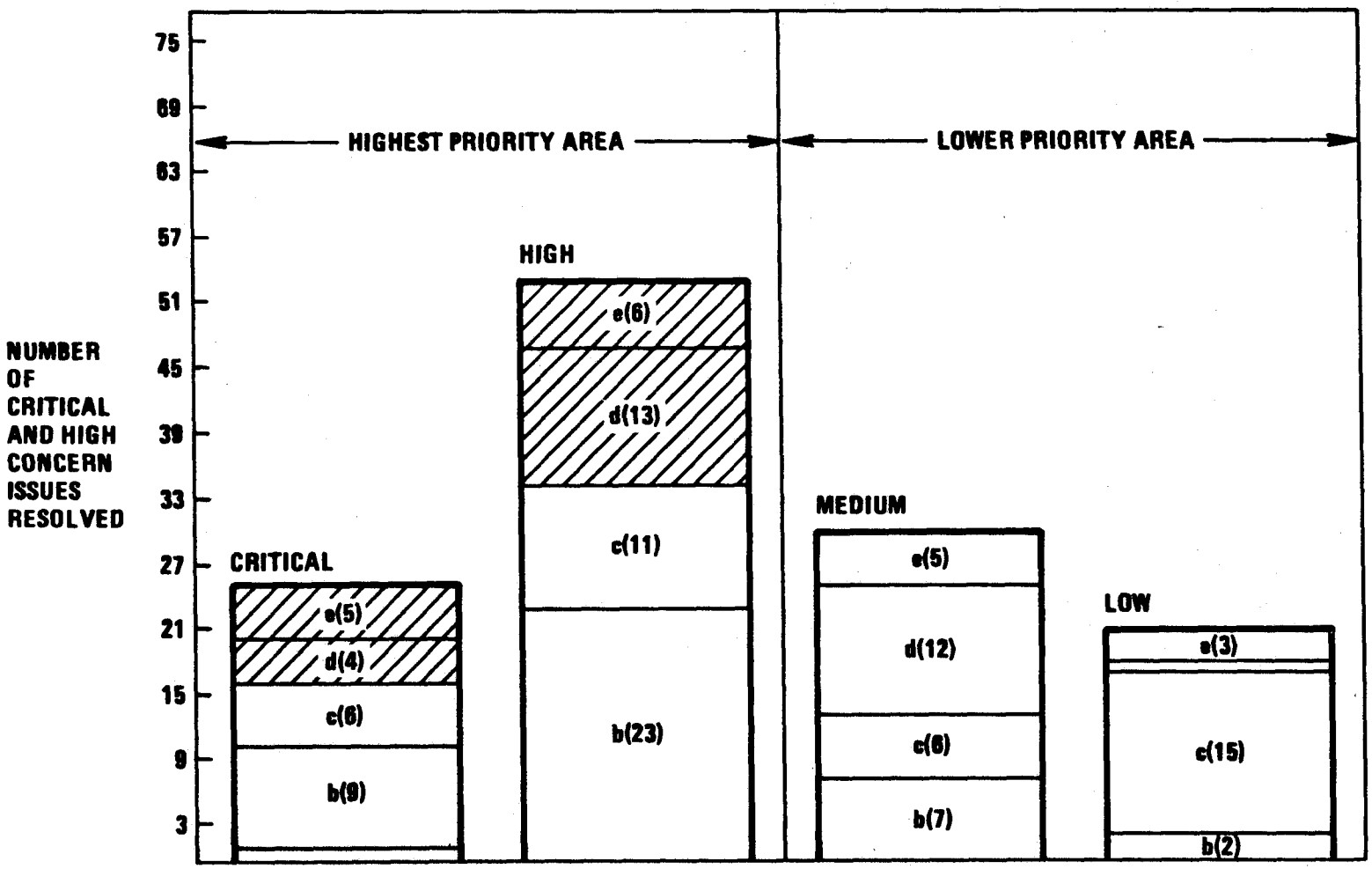


Figure 13.4-8. High priority holes in MFTF-α+T test capabilities

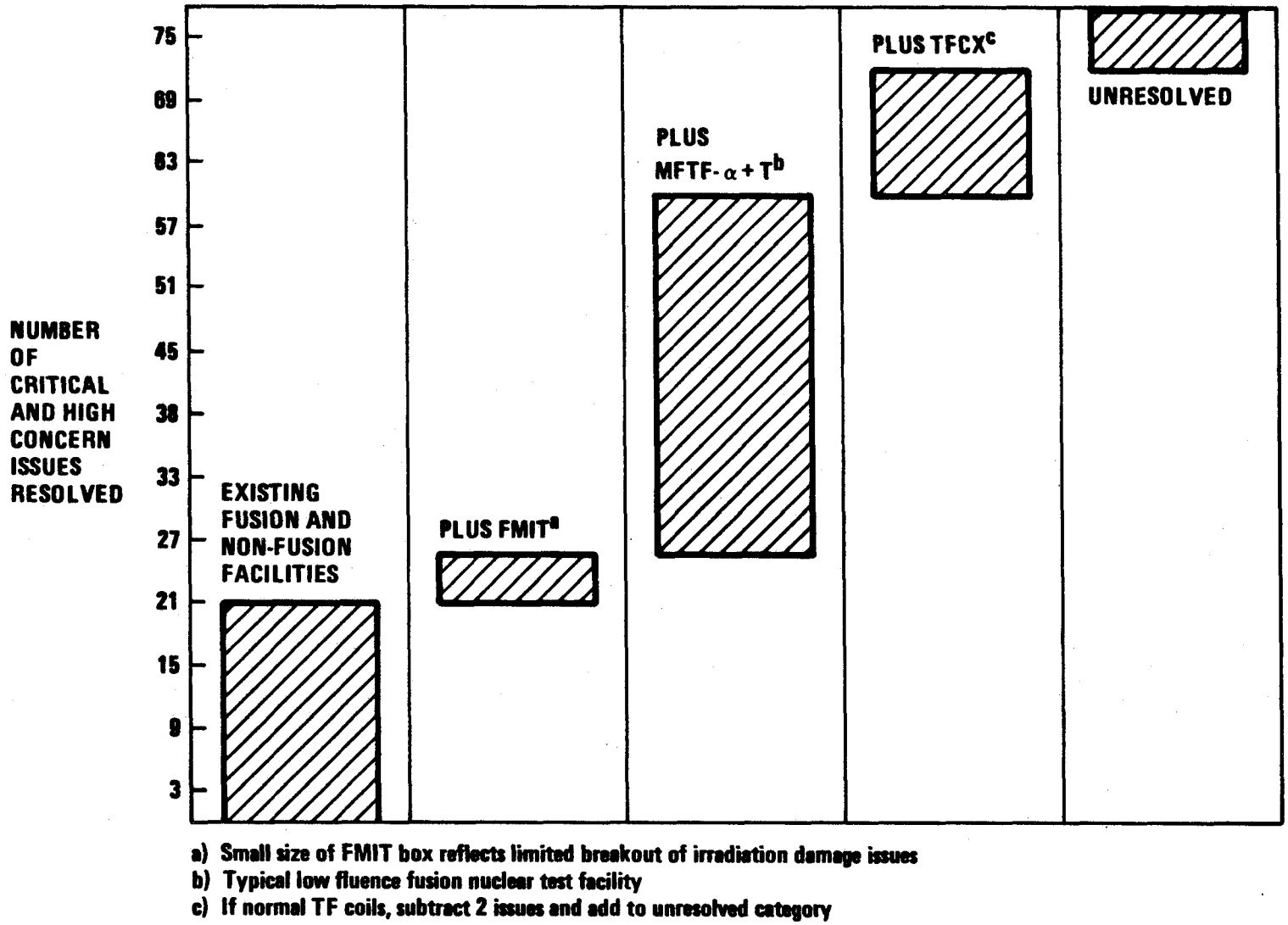


Figure 13.4-9. MFTF-α+T issue resolution in the context of a multi-facility development plan.

facilities. Adding a TFCX class facility, an additional 12 issues can be resolved, leaving 6 unresolved issues which are all associated with intermediate-to-high fluence testing of components which are too large for an FMIT class facility. These unresolved issues are listed below:

| Issue | Issue Number | Remaining Level of Concern |
|---|---|---|
| • Fluence effects on large scale, complex, stressed components<br>• first wall<br>• solid breeder structure/ clad<br>• high heat flux components | I.A.2.a, I.C.3.b, I.C.3.c, I.C.3.d, III.A.3.c | • Medium - benefits from low fluence stress mapping/ development from MFTF-α+T and from properties data |
| • Burnup/transmutation effects<br>• solid breeder tritium release at high burnup<br>• solid breeder tritium inventory during transients | 1.F.2 | • Low-to-medium - benefits from low fluence experience from MFTF-α+T and from high fluence irradiation in fission reactors and FMIT |

Note that, although these 6 issues are not fully resolved in the Fig. 13.4-9 pathway, they are addressed to some extent, and the remaining level of concern may be tolerable. Also note that a TDF class facility, costing about twice as much, could resolve the remaining issues.

## References for Chapter 13


1. T.H. Batzer, et al., "Conceptual Design of a Mirror Reactor for a Fusion Engineering Research Facility (FERF)," UCRL-51617, August 1974.

2. T.K. Fowler and B.G. Logan, "Tandem Mirror Technology Demonstration Facility," UCID-19193, September 1981.

3. "A Tandem Mirror Technology Demonstration Facility," UCID 19328, October 1983.

4. K.I. Thomassen and J.N. Doggett, "A Technology Demonstration Facility," J. Fusion Energy 3:109 (1983).

5. J.N. Doggett, B.G. Logan, J.E. Osher, K.I. Thomassen, "A Fusion Technology Demonstration Facility (TDF)," UCRL-90824 (preprint), Lawrence Livermore National Laboratory (1984).

6. K.I. Thomassen, J.N. Doggett, B.G. Logan, "An MFTF-B Upgrade for Blanket Technology Testing," UCID-19570, October 1982.

7. K.I. Thomassen, J.N. Doggett, B.G. Logan, W.D. Nelson, "An Upgrade to MFTF-B for Fusion Technology," UCRL-90825, Lawrence Livermore National Laboratory (1984).

8. B. Badger, et al., "TASKA-M, A Low Cost, Near-Term, Tandem Mirror Device For Fusion Technology Testing," KfK-3680/FPA-83-7/UWFDM-600, Kerforschungszentrum Karlsruhe/Fusion Power Associates/University Wisconsin (1983).

9. J.N. Doggett, et al., "A Tandem Mirror Technology Demonstration Facility," UCID-19328, Lawrence Livermore National Laboratory (1983).

10. D.L. Correll, et al., "Production of Large-radius, High-beta Confined Mirror Plasmas," Nucl. Fusion 20:655 (1980).

11. R.P. Drake, et al., "The Effect of End-Cell Stability on the Confinement of the Center Cell Plasma in TMX," Nucl. Fusion 20:359 (1981).

12. T.C. Simonen, et al., "TMX-Upgrade (TMX-U) Operation in the Sloshing-ion Mode," Lawrence Livermore National Laboratory, Livermore, CA, UCID-19568 (September 1982).

13. T.H. Batzer and W.R. Call, "A Continuous Cryopump for Steady-State Mirror Fusion Reactors," Lawrence Livermore National Laboratory, Livermore, CA, UCRL-87732 (September 1982). (Also given at the 29th National Vacuum Symposium, Baltimore, MD, November 16-19, 1982.)

14. K.I. Thomassen and J.N. Doggett, "Options to Upgrade the Mirror Fusion Test Facility," Lawrence Livermore National Laboratory Report, Livermore, CA, UCID-19743 (1983).

15. C.D. Henning, et al., Mirror Advanced Reactor Study Final Report, Lawrence Livermore National Laboratory, Livermore, CA, UCRL-53480; to appear.
16. W.S. Cooper and R.V. Pyle, The National Negative-Ion-Based Neutral Beam Development Plan, Lawrence Berkeley Laboratory Report, Berkeley, CA, PUB-464 (1983).

17. J.H. Fink, "Neutral Beams for Mirrors," Lawrence Livermore National Laboratory Report, Livermore, CA, UCRL-89166 (1983); submitted to J. Vac. Sci. Tech.

18. D.H. Berwald, et al., "Alternative Technological Pathways for Fusion," TRW-FRE-003, TRW Energy Development Group (1984).

19. W.L. Barr and B.G. Logan, Lawrence Livermore National Laboratory, Livermore, CA, private communication (April 1984); see also Ref. 5 above.

20. D.L. Jassby and S.S. Kalsi (editors), "FED-R - A Fusion Engineering Device Utilizing Resistive Magnets," ORNL/FEDC-82/1, Fusion Engineering Design Center (1983).

21. W.M. Stacy, et al., "U.S. FED-INTER Activity - Critical Issues," FED-INTOR/TEST/82-2, Georgia Institute of Technology (1982).

# CHAPTER 14

# TOKAMAK FUSION TEST FACILITIES

TABLE OF CONTENTS


| | | Page |
|---|---|---|
| 14.1 | Objectives and Requirements | 14-1 |
| | 14.1.1 Introduction | 14-1 |
| | 14.1.2 Study Objective | 14-1 |
| | 14.1.3 Facility Requirements | 14-1 |
| 14.2 | Design Approach | 14-4 |
| | 14.2.1 Introduction | 14-4 |
| | 14.2.2 Principal Features | 14-5 |
| 14.3 | Design Description | 14-6 |
| | 14.3.1 Quasi-Ohmic Heating to Ignition | 14-6 |
| | 14.3.2 Device Operation | 14-10 |
| | 14.3.3 Magnet Considerations | 14-10 |
| | 14.3.4 Power Consumption and Cost | 14-11 |
| 14.4 | Risks and Uncertainties of the Reference Approach | 14-13 |
| | 14.4.1 Areas of Uncertainty | 14-13 |
| | 14.4.2 Alternative Startup Method | 14-14 |
| | 14.4.3 Comparison with Existing Tokamaks | 14-14 |
| 14.5 | Conclusions | 14-16 |
| Explanation of Symbols | | 14-17 |

# 14. TOKAMAK FUSION TEST FACILITIES

## 14.1 Objectives and Requirements

### 14.1.1 Introduction

Interest in the tokamak as a nuclear technology test facility stems mainly from its position as the most advanced laboratory fusion device. Only the tokamak is likely to be capable of providing a feasible large-area fusion-neutron source in the next decade, if one is required on that time scale. The traditional pulsed operation of the tokamak can even be circumvented with newly demonstrated current-drive techniques, although there is a heavy price to pay in electrical power consumption to realize that feature. In fact the principal obstacles to the implementation of the tokamak as a suitable nuclear test facility are probably not fundamental technical ones, but rather very high capital and operating costs that are difficult to avoid.

### 14.1.2 Study Objective

The objective of this study was to identify a tokamak device configuration and operational mode that would best utilize the tokamak concept for meeting specific nuclear testing requirements while minimizing capital and operating costs.

### 14.1.3 Facility Requirements

The principal test requirements, which are explained in other chapters of this report, are the following:

Nuclear Performance

1. Test volume at least 0.5 m in depth with frontal area of at least 10 $m^2$ exposed to the fusion neutron current.

2. Neutron wall loading at least 1 $MW/m^2$ and preferably 3 $MW/m^2$.

3. Lifetime fluence capability = 1 to 10 MW-yr/$m^2$.

4. Surface heat load > 20 W/$cm^2$.

5. Ease of test module installation and replacement.

Duty Factor

6. Burn time at least several hundred seconds (preferably steady state).

7. Dwell time between pulses < 100 s.

8. Continuous operating period > 1 week.

Cost Constraints

9. Capital cost < $1,000 million for the complete facility.

10. Minimum operating cost- ie, electrical power consumption < 200 MWe and tritium consumption < 5 kg/a. The last constraint implies a fusion power < 200 MW, assuming a capacity factor near 0.5.

In a nutshell, the ideal machine is a tokamak that can deliver 2 MW/$m^2$ to a substantial outboard testing region at 95% duty factor, with fusion power $\lesssim$ 100 MW and circulating power < 200 MWe.

Various device configurations and operational modes that could potentially satisfy the above requirements were examined. These candidates included the numerous toroidal concepts that have been proposed since the mid-1970s (Table 14.1-1), as well as new variations made plausible by recent theoretical and experimental plasma physics results. Previous concepts delivering more than 1 MW/$m^2$ wall loading resulted in values of fusion power and circulating power that were unacceptably large.

Table 14.1-1. Previous Tokamak Nuclear Technology Test Facility Concepts

| PROPERTY | T E T R [1] (U. Wisc. 1976) | T E T F [2] (ANL, 1976) | F E D - R [3] (FEDC, 1982) |
|---|---|---|---|
| TF Coil Mat'l | Superconducting | Superconducting | Copper, demountable |
| EF Coil Mat'l | In-bore, copper | Ex-bore, copper | Ex-bore, supercond & in-bore, copper |
| OH System Size | Major | Moderate | Modest |
| Major Radius | 3.25 m | 3.0 m | 3.5 m |
| Plasma Current | 2.5 MA | 1.4 MA | 4.4 MA |
| Beta | 6.6% | 5% | 5% |
| Operating Mode | Beam-driven, Q = 1.8 | Beam-driven, Q = 0.7 | Beam-driven, Q = 2.5 |
| Burn Pulse | 60-200 s | 40-100 s | Steady-state, with current drive |
| Fusion Power | 265 MW | 21 MW | 250 MW |
| Neutron Wall Load | 1.4 $MW/m^2$ | 0.15 $MW/m^2$ | 1.3 $MW/m^2$ |
| Test Area | 20 $m^2$ | 5 $m^2$ | 60 $m^2$ |
| Circulating Power | 355 MW | 110 MW | 505 MW |


[1] G.L. Kulcinski, et al., in Proc. 2nd Topical Meeting on the Technology of Controlled Nuclear Fusion (NTIS, 1976), Vol. 1 (1976), 73-93.

[2] W.M. Stacey, et al., in Proc. 2nd Topical Meeting on the Technology of Controlled Nuclear Fusion (NTIS, 1976), Vol. 1 (1976), 95-105.

[3] D.L. Jassby and S.S. Kalsi, Nuclear Technology/Fusion, Vol. 4, No. 2 (1983), 1052-57.

## 14.2 Design Approach

### 14.2.1 Introduction

The requirements of small capital cost and small fusion power result in small physical size. The following trade-offs were considered from the points of view of achieving the required nuclear performance and duty factor in a relatively compact device while minimizing capital cost, operating cost, and risk:

* Copper vs superconducting toroidal-field (TF) coils
* Steady-state low-Q vs pulsed ignited plasma operation
* Low-beta vs high-beta plasmas
* Neutral-beam injection heating vs radiofrequency (RF) heating
* Maximizing ohmic heating vs maximizing auxiliary heating
* Magnetic divertor vs pumped limiter
* In-bore vs centrally located ohmic-heating (OH) coils.

From the point of view of maintenance, the best location for the OH primary coils is in the tokamak throat, where they can escape neutron irradiation and are readily accessible. However, in that location the magnetic flux swing is very limited, so that significant RF power would be required for assisting startup of the plasma current, and the pulse length would be limited to a few tens of seconds. On the other hand, if the coils are located in the TF coil bore, their in-situ maintenance is impossible, but the available magnetic flux swing can be very large. The benefits are that no RF power is required to assist in current startup, and the pulse length can be up to 1000 s.

### 14.2.2 Principal Features

The following selections resulted from the above trade-offs:

1. Water-cooled copper TF coils, principally because of the inability to shield superconducting coils in a compact device, but also because of the greater tolerance of copper coils for pulsed operation, and the elimination of warmup/cooldown times.

2. Ignited operation, to minimize the electrical power required during the burn. The size penalty for an ignited device was found to be small.

3. RF heating (ion cyclotron waves), because of the difficulty of operating neutral-beam injectors in a reactor environment, as well as uncertainty in the development of injectors of the required energy and efficiency.

4. Quasi-ohmic heating to ignition, to minimize the capital cost for auxiliary heating power, and to minimize degradation of plasma confinement.

5. Steady-state current drive was rejected because of its high electrical power cost. (If required at some future date, steady-state current drive could be implemented by installing RF power antennas.)

6. Location of the OH coils in the TF coil bore, to maximize the magnetic flux swing available for current startup and for driving 1,000-s pulses.

7. High-beta operation during the burn (beta = plasma pressure/magnetic pressure), to minimize TF-coil power loss. This choice requires an elongated bean-shaped plasma with an elaborate system of auxiliary coils.

8. Pumped limiters, to avoid the additional size and complexity of magnetic divertors.

## 14.3 Design Description

Once the above choices are made, it is still necessary to examine the trade-offs among neutron wall loading, fusion power, device size, and electrical power dissipation in the various magnet sets. Table 14.3-1 gives the principal device geometric parameters and performance characteristics for a facility providing 1.3 $MW/m^2$ at the outboard midplane. Figure 14.3-1 shows an elevation view schematic, and Fig. 14.3-2 shows how the device sectors are utilized.

### 14.3.1 Quasi-Ohmic Heating to Ignition

An important assumption for minimizing reactor size is that the confinement parameter n*tauE will not degrade significantly from its value in the ohmic-heated regime; this assumption should be valid if the externally injected power does not significantly exceed the ohmic power, and the plasma density does not exceed about $5 \times 10^{14}$ $cm^{-3}$.

To achieve ignition mainly by ohmic heating ("quasi-OH ignition"), very high magnetic field and current are required during startup, but the auxiliary RF power is relatively low. An analysis using typical radial profiles shows that it is possible to reach ignition in a dee-shaped tokamak plasma with B = 12 T at the TF coils and major radius Rp > 2.2 m, when the RF power is comparable with the ohmic power (4-5 MW). This range of Rp is larger than has previously been associated with proposals for ohmic-heated ignition devices; the reason is the empirical strong increase in tauE with Rp that has only recently been well documented.

(To maximize current density in the plasma, the dee-shaped plasma must have an elongation of 2.0-2.1. The vertical bore of the vacuum vessel and the TF coils must be increased somewhat beyond the levels shown in Fig.

Table 14.3-1

Illustrative Tokamak Nuclear Technology Test Facility

| PARAMETER | UNIT | START-UP PHASE | BURN PHASE |
|---|---|---|---|
| **GEOMETRY** | | | |
| Major Radius | m | 2.55 | 2.55 |
| Minor Radius | m | 0.75 | 0.75 |
| Aspect Ratio | | 3.40 | 3.40 |
| Plasma Shape | | dee | bean |
| Elongation | | 2.0 | 2.0 |
| Vessel Horz Bore | m | 1.75 | 1.75 |
| Vessel Vert Bore | m | 3.5 | 3.5 |
| Inboard Bl/Shld | m | 0.50 | 0.50 |
| Max. B at Coils | T | 12 | 6.0 |
| **PLASMA** | | | |
| B at Plasma Axis | T | 5.6 | 2.8 |
| Avg Beta | | .04 | .23 |
| Peak Temperat | keV | 6.5 | 35 |
| Avg Temperat | keV | 2.2 | 15 |
| Avg Density | $10^{14}/cm^{-3}$ | 4.5 | 1.4 |
| Plasma Current | MA | 7.0 | 5.4 |
| n*tauE,neoAlc | $10^{14}s/cm^{-3}$ | 14 | 2.1 |
| Zeff | | 1.2 | 1.2 |
| Ohmic Power | MW | 4.9 | < 1 |
| RF Power | MW | 5.0 | 0 |
| Loop Voltage | V | 0.65 | 0.015 |
| Solenoid Flux | Wb | 32 | 18 |
| Pulse Length | s | 20 | 1000 |
| **MAGNETS** | | | |
| TF Horiz. Bore | m | 3.5 | 3.5 |
| TF Vert. Bore | m | 4.8 | 4.8 |
| TF Coil Mat'l | | Cu | Cu |
| Max. J, TF Coil | $kA/cm^2$ | .93 | .47 |
| TF Coil Loss | MW | 490 | 122 |
| PF Coil Loss | MW | 60 | 45 |
| **POWER PROD'N** | | | |
| Fusion Power | MW | 60 | 185 |
| First Wall Area | $m^2$ | 129 | 129 |
| <Neut Wall Load> | $MW/m^2$ | | 1.15 |
| at Outboard | $MW/m^2$ | | 1.3 |
| Surf Heat Flux | $W/cm^2$ | | 30 |
| Circul. Power | MW | 590 | 190 |

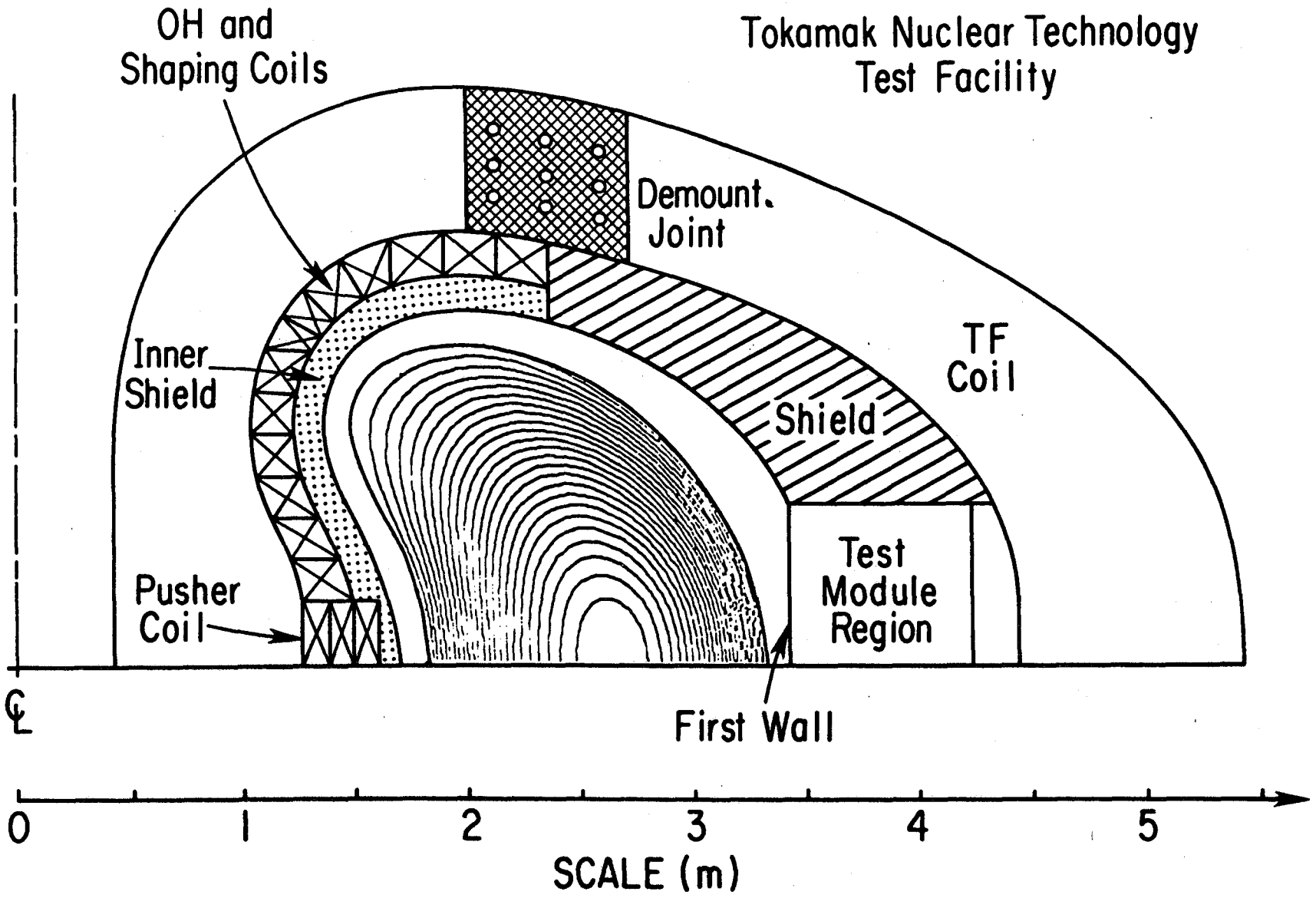


Figure 14.3-1. Partial elevation view of tokamak facility.

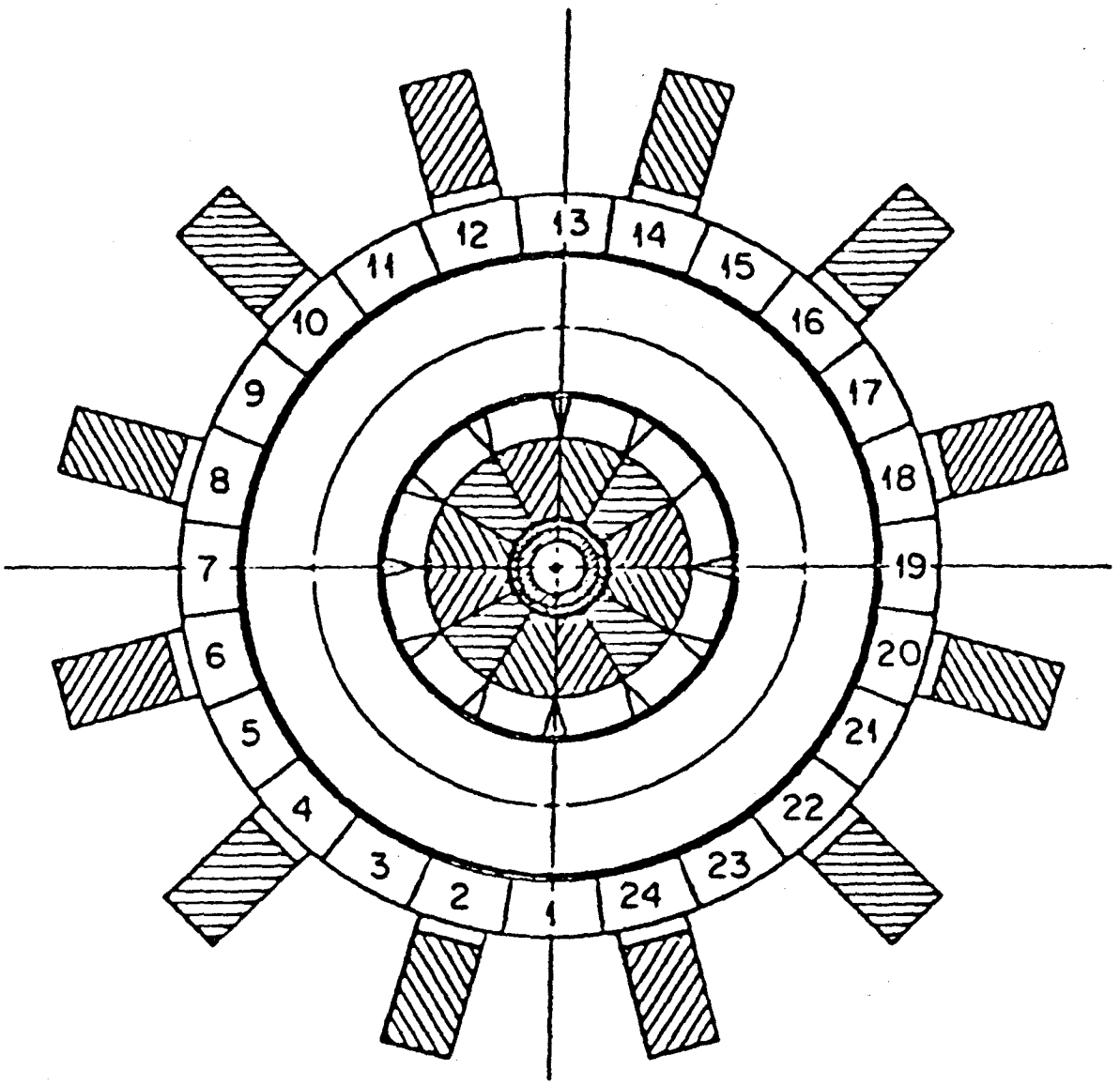


| FUNCTION | TOKAMAK NUCLEAR TEST FACILITY<br>SECTORS DEDICATED TO EACH FUNCTION |
|---|---|
| HEATING | 11, 15 |
| FUELING | 13, 19 |
| PUMPING | 9, 23 |
| DIAGNOSTICS | 1, 2, 3 |
| MODULE TESTING | 4, 5 6, 7, 8 AND 17, 18, 20, 21, 22 |

Figure 14.3-2. Plan view showing utilization of sectors.

14.3-1 in order to accommodate the taller dee-shaped plasma during startup.)

### 14.3.2 Device Operation

Almost 600 MW of electrical power is required in the 20-s start-up phase. However, the duration of this phase is very short compared with the burn period, so that the time-averaged coil dissipative loss is acceptable. The excess power required during startup would probably be obtained from motor-generator sets.

When ignition is reached, the magnetic field can be reduced by a factor of 2, and beta is increased to 0.23 while the plasma assumes the bean shape needed for high-beta operation. The length of the burn can be of the order of 1000 s. Less than 100 s is required to lower the plasma current, reset the transformer, and re-ignite the plasma, so that the duty factor would exceed 0.9.

### 14.3.3 Magnet Considerations

The copper "pusher coil" required for indenting the bean plasma is located in the inboard shield region and dissipates about 20 MW of power. The current-driving OH solenoid is also located in the bore of the TF coils, along with the "shaping coils" needed to maintain the plasma shape during startup and burn. These in-bore coils are referred to collectively as the PF (poloidal-field) coils. Minimal neutron shielding is provided for the PF coils, all of which use SPINEL (magnesium aluminate) insulation. The TF coils, which are constructed of copper plates insulated by sprayed-on SPINEL, are relatively well shielded, in part by the PF coils. SPINEL has a radiation dose limit of $10^{13}$ rads, corresponding to 5 MW-yr/$m^2$ of fusion neutron flux. Thus even with modest shielding, the lifetime of the PF coils against radiation damage would exceed the specified lifetime fluence capability of the facility (10 MW-yr/$m^2$).

Redundant coils must be included among the sets of in-bore PF coils, as repair of these coils in the event of electrical or thermal damage is probably impossible. The TF coils are demountable to permit periodic

replacement of the inboard TF coil trunk on which are wound the PF coils, but the downtime for this procedure would be many months.

### 14.3.4 Power Consumption and Cost

Figure 14.3-3 shows the power-flow diagram for the tokamak test facility. With the configuration described herein, both the fusion power and the time-averaged circulating electric power are slightly under 200 MW. For a capacity factor of 0.5, the annual operating costs would be approximately $35 million for electricity (at 40 mills/kWh) and $75 million for tritium (at $15,000/g). A significantly different (and still unidentified) design approach would be required to reduce the fusion power and circulating power to the 100 MW level, while maintaining or increasing neutron wall loading.

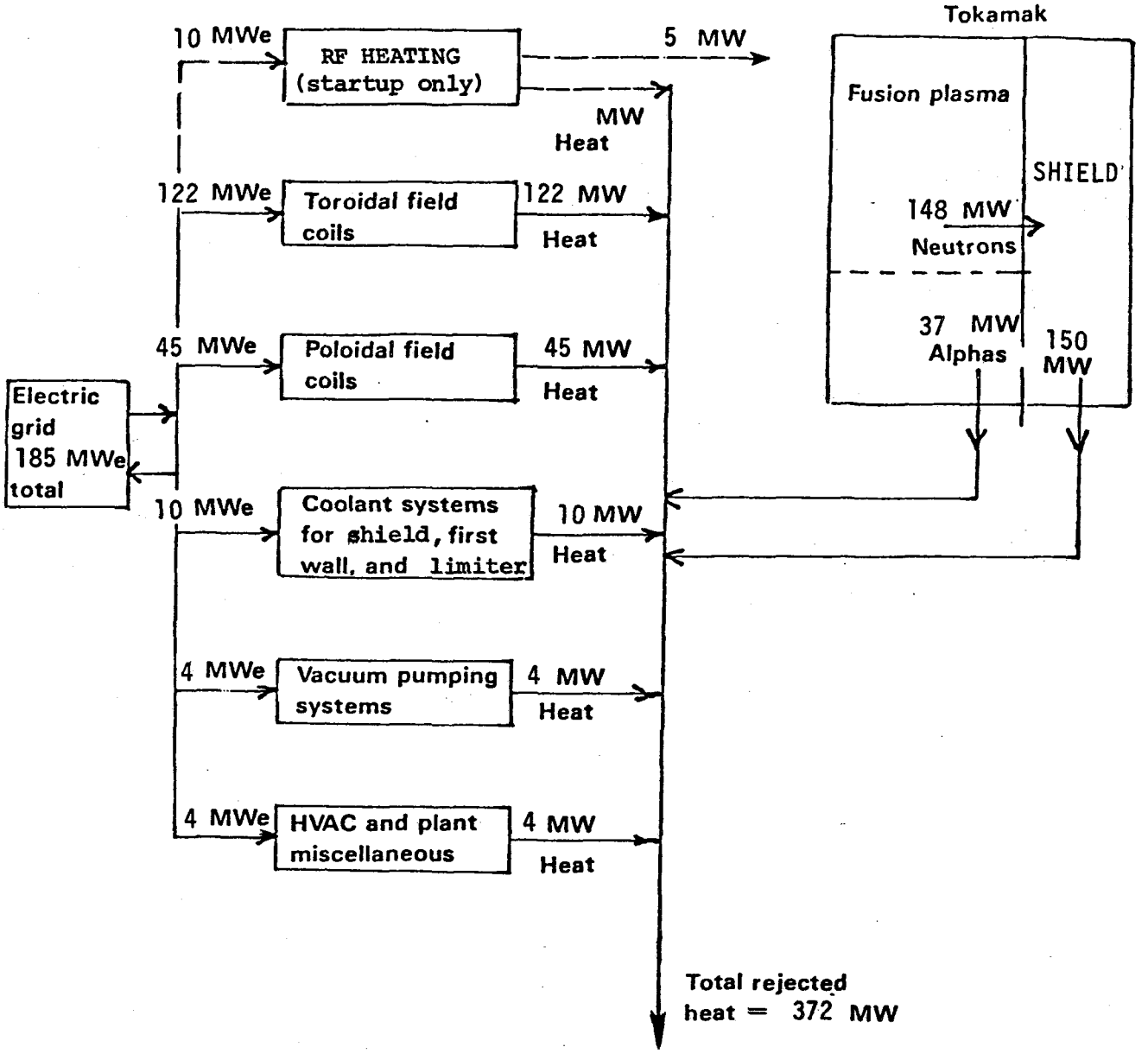


Figure 14.3-3. Power flow diagram of tokamak test facility.

## 14.4 Risks and Uncertainties of the Reference Approach

### 14.4.1 Areas of Uncertainty

The following are the physics and technology areas of greatest uncertainty for the proposed approach.

1. While bean-shaped plasmas have been operated in the PBX device with <beta> up to 0.04 for short periods, the feasibility of achieving and maintaining <beta> = 0.20-0.25 in tokamaks has not been demonstrated.

2. The favorable scaling of tauE observed in the purely ohmic-heating regime is assumed to be maintained in the fusion-alpha-heated burn phase. The basis of this assumption is that in both regimes the heat input to the plasma has toroidal and poloidal symmetry.

3. The integrity of SPINEL insulation when subjected to the stresses expected in tokamak magnets, including cycling, needs to be verified.

4. The lifetime of the first wall under plasma erosion can be estimated only crudely.

5. Maintenance of the inboard OH and shaping coils is impossible, so that their reliability (including the provision of redundancy) must be adequate to insure operation for several years. In general, remote maintenance methods for tokamak devices, including expeditious replacement of the first wall, are in a primitive stage of development.

6. Feasibility of the TF coil demountable joints, particularly in coils that are repetitively pulsed to very high field.

7. The use of liquid metals in the test modules may be problematical during startup, because of the much larger magnetic field required in

that phase. However, the field in the outboard test modules would never exceed 4.5 T.

### 14.4.2 Alternative Start-Up Method

The reference startup technique could be replaced by a method that depended largely on RF heating (ion cyclotron waves). The advantages of this 2nd approach are (1) the magnetic field could be kept at a steady and relatively low value throughout the burn cycle, thereby enabling considerable cost savings in structural material and power supplies; (2) the maximum current that has to be generated by the OH system would be considerably reduced, also leading to cost savings. These cost reductions would have to be weighed against the cost of providing approximately 30 MW of additional RF heating power. Another advantage of continuous low magnetic field is the alleviation of liquid metal flow problems.

The principal argument against the alternative startup method is that present-day tokamak experiments show significant reduction in tauE upon the application of appreciable RF or neutral-beam power. Such reduction could not be tolerated in the present design concept, which has only a small margin for reaching ignition.

### 14.4.3 Comparison With Existing Tokamaks

Experimental tokamak devices have demonstrated reactor-level n*tauE in the near-ohmic-heated regime, reactor-level temperatures at smaller n*tauE, the effectiveness of ion cyclotron heating, and the stability of bean-shaped plasmas (albeit at relatively low beta to date). Table 14.4-1 compares the parameters of the present concept with those of TFTR and JET. The major plasma physics and engineering advances required relative to the expected performances of TFTR, JET, JT-60 and DIII Upgrade are associated with achieving and sustaining ignited, high-beta operation over pulse lengths of the order of 1,000 s. Within the next few years, existing tokamaks are expected to demonstrate very high beta and pulse lengths of tens of seconds, but no existing machine is likely to achieve ignition.

Table 14.4-1. Comparison With Existing Large Tokamaks

| PARAMETER | UNIT | Test Facility Concept | TFTR (operating | JET (operating) |
|---|---|---|---|---|
| **GEOMETRY** | | | | |
| Major Radius | m | 2.55 | 2.50 | 2.95 |
| Minor Radius | m | 0.75 | 0.85 | 1.25 |
| Aspect Ratio | | 3.4 | 2.9 | 2.35 |
| Elongation | | 1.4 | 1.0 | 1.6 |
| Inb'd Shield | m | 0.5 | 0.1 | 0.1 |
| **PLASMA** | | | | |
| <beta> | | 0.23 | 0.03 | 0.06 |
| Plasma Current | MA | 5.4 | 3.0 | 6.0 |
| RF or Beam Power | MW | 5 | 30 | 25 |
| Peak Temperat | keV | 35 | 15 | 15 |
| Plasma Heat Removal | | Pumped Limiter | Simple Limiter | Simple Limiter |
| **MAGNETS** | | | | |
| TF Horiz. Bore | m | 3.5 | 2.8 | 3.1 |
| TF Vert. Bore | m | 4.8 | 2.8 | 4.9 |
| TF Coil Mat'l | | Cu plates | Cu, wound | Cu, wound |
| Max. B at Coils | T | 12 [a] | 9.2 | 7.0 |
| PF Coil Mat'l | | Cu | Cu | Cu |
| **POWER FLOW** | | | | |
| Fusion Power | MW | 185 | 30 | >25 |
| Neut Wall Load | $MW/m^2$ | 1.3 | 0.2 | 0.2 |
| Burn length | s | 1000 | 2 | 10 |
| Duty Factor | | >0.9 | 0.002 | 0.01 |

[a] Startup Phase only; 6.0 T during burn

## 14.5 Conclusions

The tokamak approach outlined herein can meet the neutron wall loading, fluence and burn cycle requirements for a nuclear technology test facility, although the wall loading is at the lower end of the range of interest. The electrical power and annual tritium consumption are at the higher ends of acceptable ranges, and the capital cost would probably exceed $1 billion. Thus further efforts are needed to reduce the physical size and fusion power level while increasing neutron wall loading. The proposed approach also has significant technological uncertainties which are likely to be present in any alternative toroidal concept. These issues can be resolved only through extensive development programs.

## Explanation of Symbols

| | |
|---|---|
| a | plasma minor radius in mid-plane |
| beta | ratio of plasma pressure to magnetic pressure |
| <beta> | spatially averaged beta |
| JET | Joint European Torus (largest European tokamak) |
| n | plasma temperature |
| NTF | Nuclear Test Facility |
| OH | Ohmic Heating |
| PF | Poloidal Field (magnetic) |
| Q | fusion power/plasma heating power |
| RF | RadioFrequency |
| Rp | plasma major radius (center) |
| tauE | plasma energy confinement time |
| TF | Toroidal Field (magnetic) |
| TFTR | Tokamak Fusion Test Reactor (largest U.S. tokamak) |

# CHAPTER 15

# RELIABILITY DEVELOPMENT TESTING IMPACTS ON FUSION REACTOR AVAILABILITY

TABLE OF CONTENTS

Page

15.1 Introduction..... 15-1

15.2 Confidence Levels in Component Performance..... 15-2

15.3 The NAVAIR Approach to Development Testing..... 15-9
15.3.1 Description of Method.....15-13
15.3.2 Fusion Reactor Development Pathways.....15-14
15.3.3 Availability Models.....15-16
15.3.4 Baseline Analysis.....15-20
15.3.5 Parametric Studies.....15-30
15.3.6 Conclusions.....15-36

15.4 Summary and Conclusions.....15-37

References.....15-38

# 15. RELIABILITY DEVELOPMENT TESTING IMPACTS ON FUSION REACTOR AVAILABILITY

## 15.1 Introduction

A key observation relating to the reliability of fusion nuclear components is that many components intended for the first fusion facilities will represent new design applications without engineering precedence. This will be particularly true of nuclear components because a representative nuclear environment can not be provided prior to the operation of such a facility. Despite the best efforts in the design, fabrication, and pre-fusion testing phases of development, the nuclear components will, at best, suffer from a lack of confidence in their estimated reliabilities. More likely, the fusion engineering facility would be used to implement an iterative design/test/fix sequence aimed at improving component reliabilities.

An apparent paradox results because those nuclear components which would be targeted in a reliability improvement program depend upon the reliable performance of other nuclear components in the system. One example of this would be the development of reliable blanket test modules in a high fusion power facility (e.g., INTOR) which must also breed its own tritium in myriad (perhaps 60) tritium breeding modules. Although the latter components would be designed for the highest possible reliability, they would be complex in both design and operating environment. Consequently, their impact upon plant availability can negatively influence the blanket test module development program by reducing the available test time.

This chapter provides a quantitative perspective relating to the reliability/availability aspects of development testing in fusion facilities. Two studies will be presented. First, blanket module testing times which provide a given statistical level of confidence as a function of blanket availability goals are presented. Second, neglecting arguments relating to statistical confidence, a study of reliability improvement resulting from an iterative design/test/fix sequence is presented. Both studies are based upon Department of Defense guidance[1,2] relating to the management of component reliability testing/development programs.

## 15.2 Confidence Levels in Component Performance

Unproven component reliabilities can be estimated from the proven reliabilities of components of similar design and application, if such designs and applications exist. However, high confidence in component performance in entirely new applications must result from testing in relevant environments. In the case of components which must be extremely reliable, reliability proof testing is difficult because testing periods must be very long. The INTOR critical issues study[2] concluded that the achievement of 80 percent confidence in a given component mean time between failures (MTBF) in the constant failure rate regime of operation (i.e., random failure probability) would typically require a cumulative test period of 3.5 times the MTBF. This estimated test time was based on a study of specific MIL-STD-781 test plans. It is intended to provide a 20 percent risk that the actual MTBF is less than the specified MTBF.

Some components, such as the superconducting toroidal field (TF) coils, are not expected to fail during the lifetime of the facility (a design basis), and have required MTBF periods which are orders of magnitude in excess of the facility lifetime. For example, a tokamak engineering demonstration facility (EDF) might have 10 TF coils and might require a TF coil system reliability of 80 percent over a 10 full power year operational lifetime. This implies that a single coil must have a reliability of $(0.80)^{1/10} = 0.978$, or 97.8 percent, during the same period. Since a random failure probability is assumed, the reliability, R, is related to the component MTBF by $R = e^{-\tau/MTBF}$, where $\tau$ is the operational period (10 years in this case). It follows that for $R = 0.978$, the individual TF coil MTBF must be 450 operating years. For 80 percent confidence in this MTBF, a $3.5 \times 450 = 1575$ year test might be required. Although this requirement might be reduced 10-fold because there might be 10 TF coils in an early engineering facility which precedes the EDF, it is clear that such components would not be amenable to the prior development of a high confidence reliability data base.

For blanket modules, the overall reliability requirements would be somewhat relaxed. With the possible exception of catastrophic failures such as a severe breach of the primary pressure boundary (resulting in a gross deformation) or a non-routine radioactive spill, blanket removal is expected to be a relatively routine maintenance operation. In this case, a minimal EDF blanket

system availability goal might be a 60%. Since an EDF might have 6 blanket modules per TF coil sector (60 total), the required availability for individual components might be $(0.6)^{1/60} = .9915$, or 99.15%. Since the component availabilty is given by the MTBF/(MTBF + MTTR), where the MTTR is the mean time to repair or replace (whichever is quickest), a typical MTTR of 1 month results in a required MTBF of $8.5 \cdot 10^4$ hours, or about 10 years. This implies a typical test period of $3.5 \times 8.5 \cdot 10^4$ hours, or 34 years. Again, an early engineering facility, preceding the EDF, would test several modules in parallel, resulting in a reduced test period. For 6 modules, tested in parallel, the required test period would be reduced to about 5 full power years (~ 15 years at 30 percent availability). If 60 blanket modules were tested in parallel, a 0.5 full power year test period would be required.

These results are illustrated in Table 15.2-1 and in Fig. 15.2-1, where the individual blanket module availability is shown as a function of the overall blanket (60 modules) availability. Note that the required module availability exceeds 99 percent for blanket availability goals exceeding 50 percent. Typical required test times to provide an 80 percent confidence in the required module availability, for different values of the MTTR (which imply different MTBF requirements), are also shown in the figure. Figure 15.2-1 also shows that a substantial reduction in module MTTR to about 1 day has the potential to reduce the required testing time by factors as large as 25. Such replacement times would be more difficult and expensive to engineer than longer times. For this reason, designers will have the option to trade testing requirements against the requirements for facility maintenance.

In a more rigorous sense, the Poisson distribution can be used to relate the number of testing failures, the confidence level, the testing time and the estimated MTBF. Typically, availability goals, such as those shown in Table 15.2-1, would be used to establish blanket module availability requirements, and subsequent testing would be used to confirm the achievement of such requirements to a specified level of statistical confidence. Figure 15.2-2 shows the upper statistical confidence level is a function of the test time in MTBF multiples and the number of failures which have occurred during the test.

Table 15.2-1. Module Availability Requirements as a Function of Blanket Availability Goals

| Blanket Goal Availability | Module Availability |
|---|---|
| 0.99 | 0.9998 |
| 0.90 | 0.998 |
| 0.80 | 0.996 |
| 0.70 | 0.994 |
| 0.60 | 0.992 |
| 0.50 | 0.989 |
| 0.40 | 0.985 |
| 0.30 | 0.980 |
| 0.20 | 0.974 |
| 0.10 | 0.962 |
| 0.01 | 0.926 |

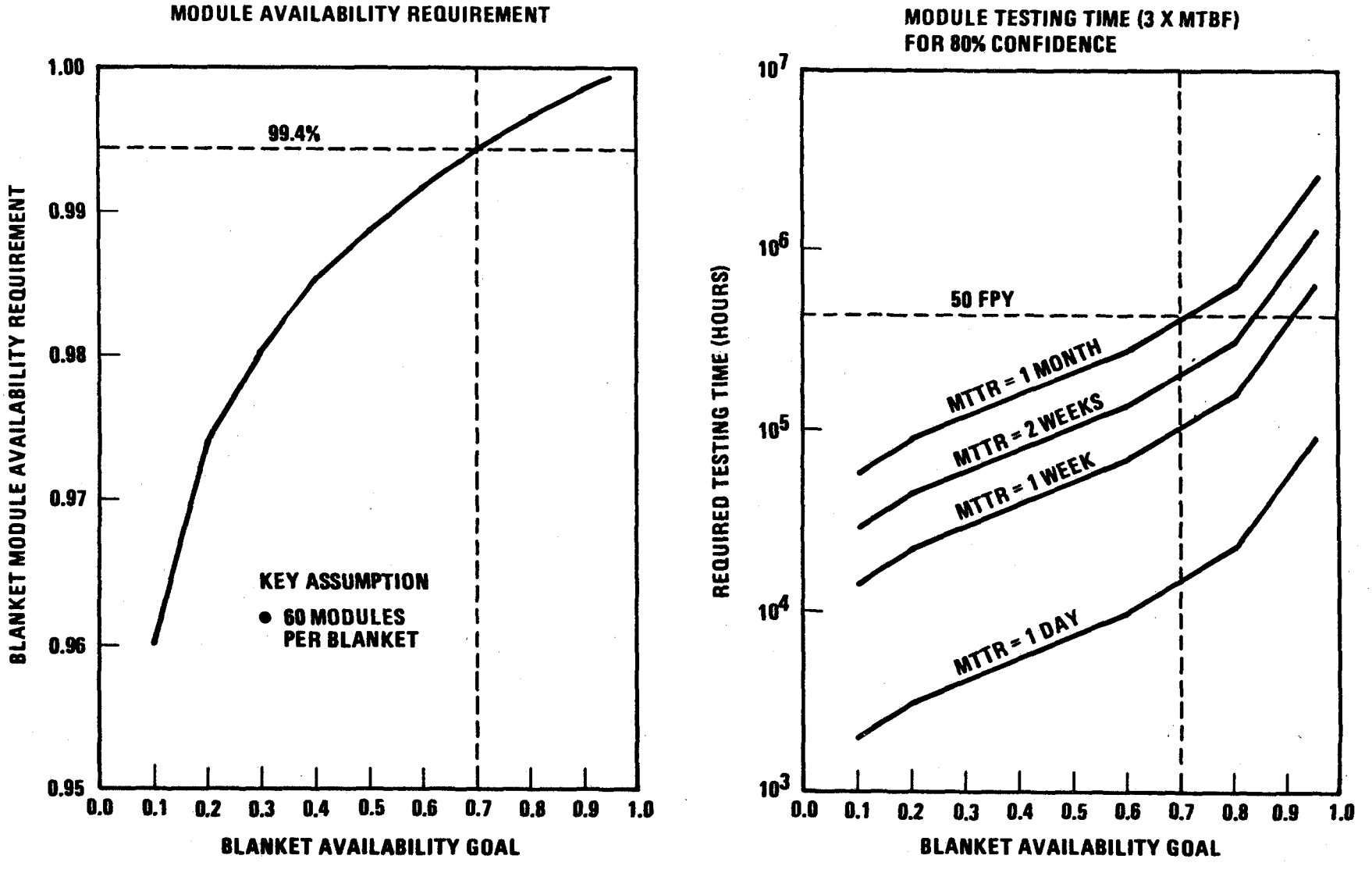


Figure 15.2-1. Blanket module availability and typical test time (3 x MTBF) requirements for 80 percent confidence as a function of the blanket availability goal.

For example, if an initial MTBF is assumed (or estimated) and a test is conducted for two times the MTBF with the result of two failures, then the confidence level (i.e., the probability that the actual MTBF is greater than or equal to the estimated value) for the assumed MTBF would be only about 30 percent. If larger numbers of failures occur, then very much longer test times are required to give high confidence that the actual MTBF is greater than or equal to the estimated MTBF. Conversely, if very few failures occur during the test period, high confidence levels can be provided with relatively short test periods. This implies that quick reliability confirmations might be obtained if the "as demonstrated" (i.e., tested) availabilities of components (i.e., as developed) are higher than their required availabilities.

Figure 15.2-3 and Table 15.2-2 show the MTBF which must be demonstrated to achieve an 80 percent confidence level in a relatively low MTBF of 29,000 hours as a function of the integrated testing time. From the figure, it is evident that for limited testing times, the inherent module MTBF must be higher than the design requirement by some demonstrated safety margin (see table) in order to insure an 80 percent confidence in its performance. Longer testing times reduce this margin significantly. For example, a comparison of Figs 15.2-1 and 15.2-3 reveals that the more simplistic 3.5 x MTBF method discussed earlier would require a safety margin of about 1.45.

In summary, to confirm the reliability of high MTBF components such as blanket modules, the following test program features are highly desirable:

- Reliability safety margins in the demonstratable versus required MTBF in the range of 1.2-1.6
- A capability to perform several parallel tests

However, safety margins will be difficult to determine when the component is entirely lacking in engineering precedence and a test history. Also, as discussed in Section 15.3, the parallel development of several blanket modules at one time can severely penalize the overall availability of the facility. Finally, reductions in component MTTR will reduce MTBF goal values and testing time requirements.

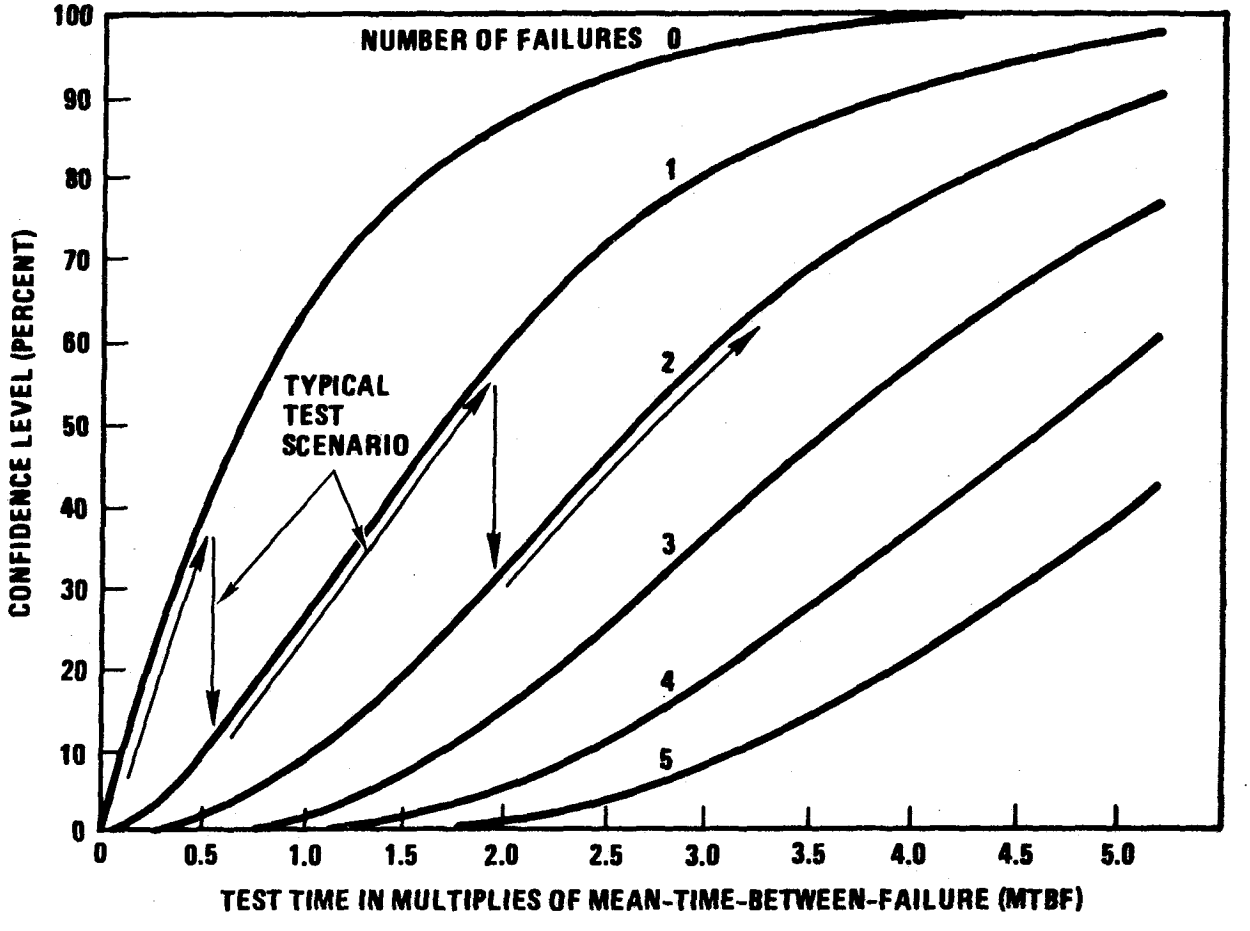


Figure 15.2-2. Confidence level for a Poisson distribution time terminated test.(4)

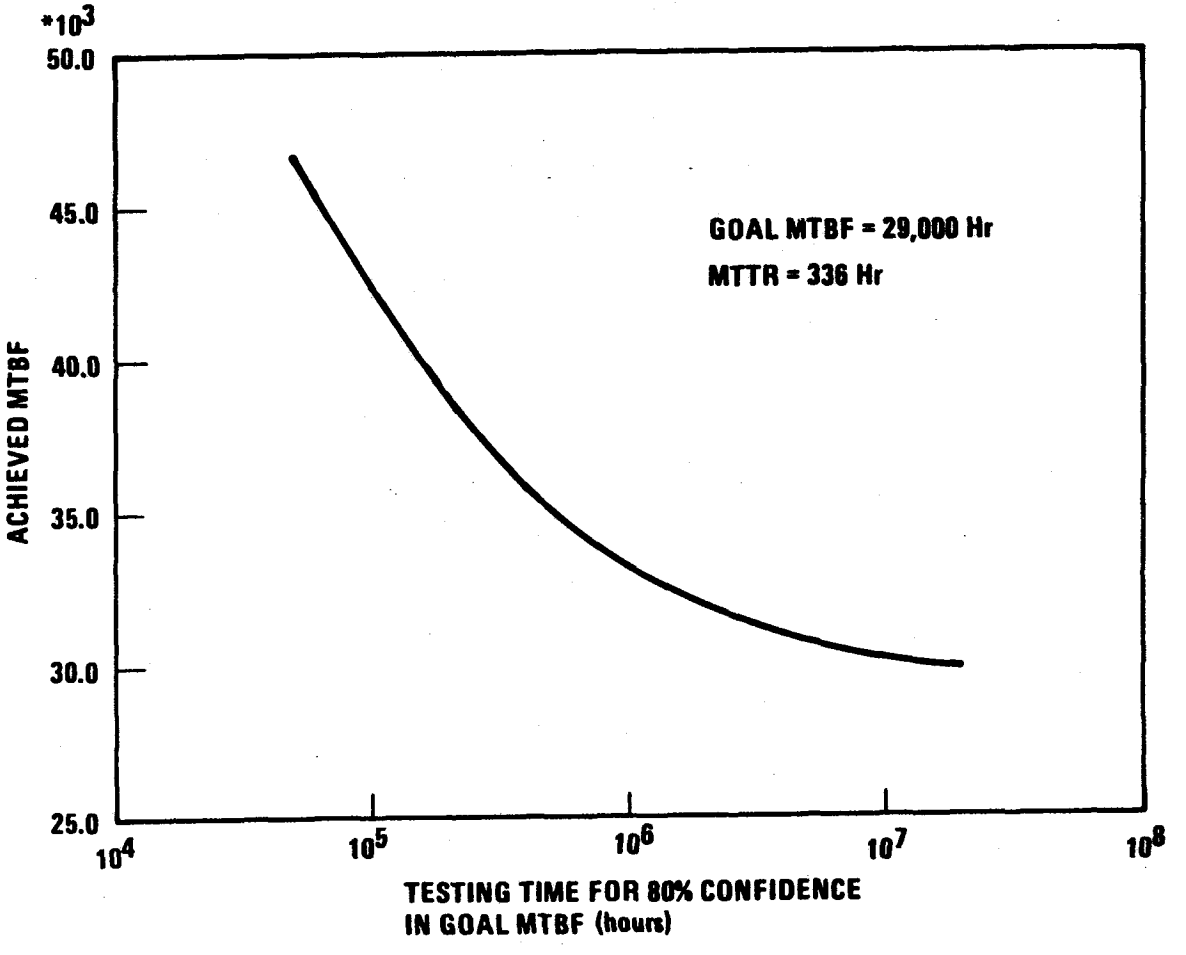


Figure 15.2-3. Achieved MTBF required for 80 percent confidence in the goal MTBF (29,000 hours with 336 hours MTTR) versus the integrated testing time.

Table 15.2-2. Blanket Module MTBF, Margins at the 80 Percent Confidence Level As a Function of Testing Time

| Total Integrated Testing Time (Full Power Years) | Integrated Testing Time with a 6 Module Parallel Test (Full Power Years) | Integrated Testing Time with a 60 Module Parallel Test (Full Power) Years) | Module MTBF Safety Margin: Demonstrated MTBF/Goal MTBF* |
|---|---|---|---|
| 5 | 0.83 | 0.083 | 1.61 |
| 11 | 1.8 | 0.18 | 1.49 |
| 34 | 5.7 | 0.57 | 1.28 |
| 114 | 19.0 | 1.9 | 1.15 |
| 228 | 38.0 | 3.8 | 1.10 |
| 570 | 95.0 | 9.5 | 1.07 |
| 1140 | 190.0 | 19.0 | 1.05 |
| 2280 | 380.0 | 38.0 | 1.03 |

* Goal MTBF = 29,000 hours, MTTR = 336 hours.
Module availability = $a_m$ = 0.9885.
Blanket availability = $a_m^{60}$ = 0.50

## 15.3. The NAVAIR Approach To Developmental Testing

In the previous section, it was found that confirming a high level of statistical confidence in the reliability of blanket modules and other components will be difficult and time consuming under the best of circumstances. Nevertheless, reliable designs might be developed, though not necessarily confirmed in a statistical sense, through a reliability development testing program. This will be assumed in order to examine the implications of a reliability improvement program in downline facility availability.

The central thesis of this work and the NAVAIR[1] approach to reliability development is that an iterative design/test/fix sequence can reduce component failure rates. Component failures can be generally described by a "bathtub" curve, shown in Fig. 15.3-1. In this figure, the impact of testing is shown

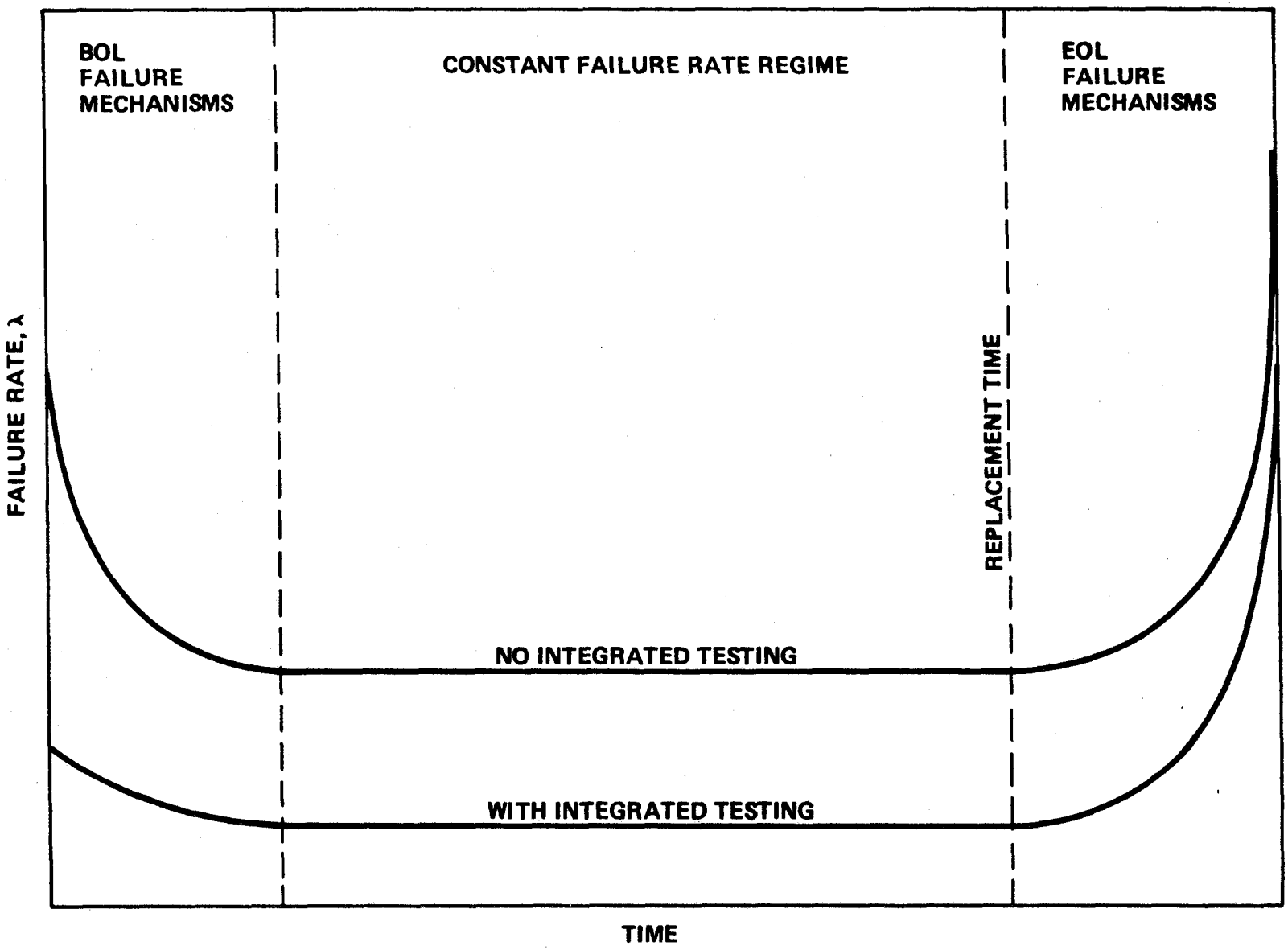


Figure 15.3-1. A key objective of a fusion nuclear test facility will be to reduce the failure rate to a tolerable level.

as a lowering of the failure rate during three phases of component life. Any developmental application will tend to reduce failures in all phases of life. Beginning of life (BOL) mechanisms are the easiest to address because the failure rate is higher. End of life (EOL) mechanisms are generally determined by systematic effects such as irradiation damage. Design changes are typically required to lengthen the desired lifetime. Improvements during the constant failure rate regime, often called the operational lifetime, are sometimes elusive because the failure rate may be very small. These failures will be difficult to see in reasonable test times. The NAVAIR approach is a method for quantifying improvements in the constant failure probability regime, assuming that a testing program can be designed to meet failure rate goals and improvement rates.

The basis for the work presented here is described in reference 2 and contained in reference 1, a NAVAIR publication about managing reliability development programs. NAVAIR specifies a reliability growth model and the planning and management structure which should be implemented in order to follow the growth curve. Typical reliability growth curves are shown in Fig. 15.3-2. The model is intended to specify attainable goals for reliability escalation under reliability development programs of varying intensity. A high growth rate, using an exponent of 0.6, applies to an aggressive program of reliability development where failures are thoroughly analyzed and design changes immediately applied to all deployed components. The lowest growth rate, which uses an escalation exponent of 0.1, applies to an unaggressive reliability development program where only failed components are repaired or replaced. Persistent failures are eventually analyzed and spare components are replaced and/or modified. Other growth exponents span these two development approaches.

In the application of the NAVAIR method, the growth curve represents a program goal which requires planning so that it can be achieved. It also requires that the component MTBF be monitored. This can be done according to reference 1 by recording 1) the cumulative MTBF, 2) instantaneous MTBF, or 3) the moving average MTBF. The cumulative MTBF is the total test time divided by the cumulative number of failures. The instantaneous MTBF can be estimated from the cumulative MTBF and local slope of the MTBF growth curve. The moving average MTBF is calculated by looking at some past time period or by

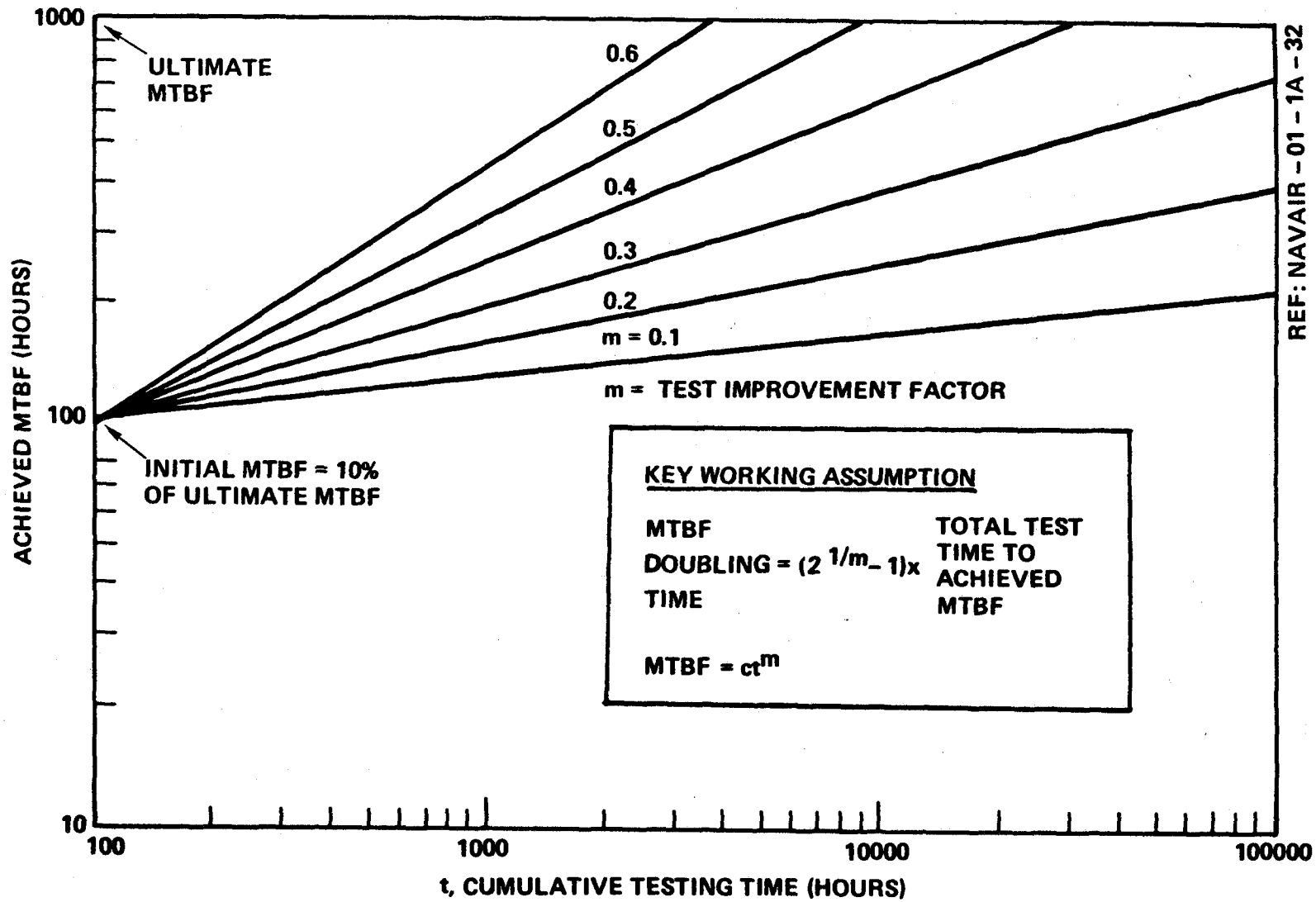


Figure 15.3-2. NAVAIR reliability improvement model.

considering some number of past failures and their occurrence times. None of these apparent MTBFs will guarantee the high confidence levels discussed in the previous section.

The MTBF improvement curves have the following form

$$T_m(t) = ct^m \qquad (15\text{-}1)$$

where m is the improvement factor. The constant c is determined by the initial conditions, $t_o$, the initial testing time, and $T_m(t_o)$, the starting component MTBF:

$$c = T_m(t_o)/t_o^m \qquad (15\text{-}2)$$

$T_m(t_o)$ can be estimated from similar first deployed components or can be the result of previous testing. For avionic systems $T_m(t_o)$ is said to be between 10 percent and 30 percent of the ultimate MTBF.[1] Thus, three variables will determine the availability escalation curve: the improvement factor, m, the initial test time, $t_o$, and the initial MTBF, $T_m(t_o)$.

### 15.3.1 Description of Method

The fusion component of interest in these studies is a tritium breeding blanket which would be developed for use in a tokamak engineering demonstration facility (EDF). Typically, each EDF blanket contain 10 sectors, and each sector would contain six modules. There would be a total of 60 modules per blanket. Application of the reliability growth curves to fusion tritium breeding modules was done in four steps.

1) Identification of three fusion reactor development paths. These fusion technology development pathways would use different test facilities.

2) Development of facility availability models corresponding to the pathways mentioned in step 1. These models quantify availability as a function of the availability of the components and/or the blanket test modules.

3) Definition of blanket module reliability improvement models based on the NAVAIR escalation curves and likely starting MTBFs, initial test times for blanket modules, and improvement factors. Reasonable

parameter ranges were also developed for the purpose of sensitivity studies.

4) Quantification of the impact of blanket module availability on test facility availability. This determines how rapidly blanket module MTBF goals might be attained. It also models the availability impact of blanket modules on EDF availability as a function of the testing time in a precursor facility (e.g., INTOR or TDF).

### 15.3.2 Fusion Reactor Development Pathways

Three fusion reactor development pathways were considered, and, following the notation of Chapter 16, they are:

1) TFTR/TFTR-U → INTOR → STARFIRE DEMO

2) $$\text{TFTR} \rightarrow \left.\begin{matrix}\text{TFCX}\\ \text{TDF}\end{matrix}\right] \rightarrow \text{TF/EDF}$$

3) $$\text{TFTR} \rightarrow \left.\begin{matrix}\text{TFCX}\\ \text{MFTF-}\alpha\text{+T}\end{matrix}\right] \rightarrow \text{ETF/EDF}$$

These pathways are also shown in Fig. 15.3-3. The first pathway leads from scientific feasibility experiments, TFTR and TFTR-U, to a sophisticated engineering test facility (ETF), INTOR. INTOR, as modeled here, has a tritium breeding ratio greater than 1.0 and a full complement of 60 blanket modules. Of these, 54 are dedicated tritium breeding modules and 6 are the more advanced blanket test modules being developed for later use in the EDF to follow. The engineering development facility (EDF), STARFIRE DEMO, is prototypical of future commercial applications. In the second pathway, TFTR leads to two facilities, TFCX and TDF, whose purpose is to test fusion components in a smaller, less costly facility compared to INTOR. In the jargon of Chapter 16, TFCX is a plasma burning experiment (PBX) and TDF (see Chapter 13) is a fusion engineering research facility (FERF). These facilities would be followed by an ETF which would, eventually, be upgraded to a full EDF. The third pathway substitutes a less ambitious FERF facility, MFTF-$\alpha$+T. MFTF-$\alpha$+T is less ambitious because it is not anticipated to have the capability of high fluence neutron effects testing which TDF can accomplish. In this third scenario, the PBX and FERF will be followed by an ETF/EDF whose initial goals will include the necessary fluence testing.

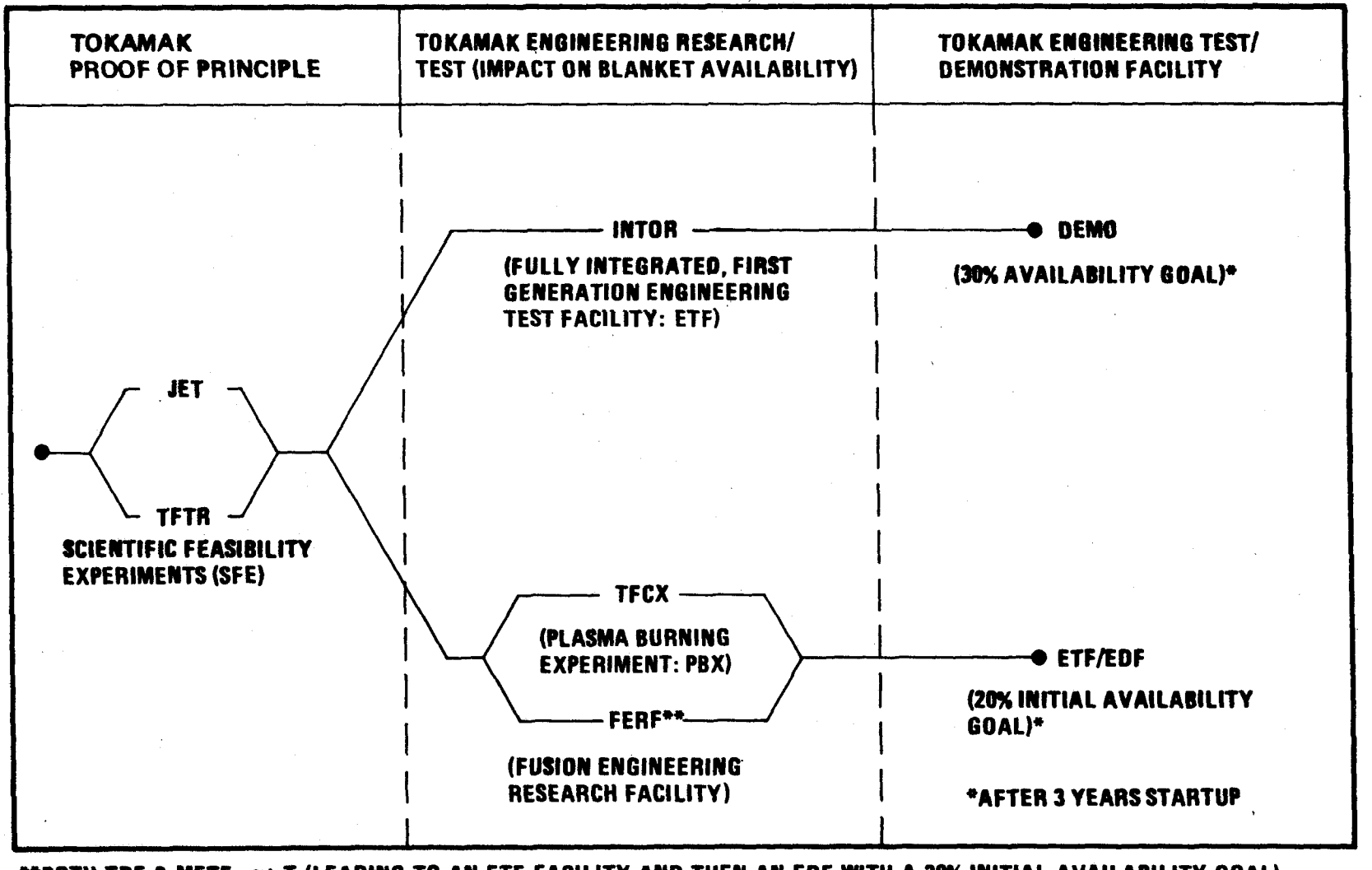


Figure 15.3-3. Tokamak development pathways.

In both the second and third pathways, the low fusion power FERF facilities will not have a tritium breeding requirement or dedicated tritium breeding modules. Only the blanket test modules will be included because the purpose of the FERF is component development. The ETF facilities (e.g. INTOR) would operate at a fusion power level which is an order of magnitude higher and would breed substantial amounts of tritium (see Chapter 16). Consequently ETFs are expected to suffer from lower overall availability.

### 15.3.3 Availability Models

The availability models describe how the availability of the second step fusion test facilities (ETF and FERF) and the downline facilities (DEMO and ETF/EDF) are affected by the availability of the blanket modules (both the tritium breeding modules and the test modules). Figure 15.3-4 shows the ETF availability model for INTOR. This model assumes that the balance of plant (BOP) and all blanket modules must function for the reactor to function. For simplicity, the BOP availability is assumed to be constant, and it is based on a facility goal availability which is achieved if the tritium breeding modules and the test modules meet their goal availability. This model also describes the ETF phase of the ETF/EDF which follows TFCX and MFTF-$\alpha$+T in pathway 3. The 54 dedicated tritium breeding modules will dominate all contributions to unavailability in this configuration.

Figure 15.3-5 describes the FERFs used in pathways 2 and 3. This configuration is inherently more reliable because there are no tritium breeding modules. In addition, the test modules are designed to be more easily removed and replaced (lower MTTR) than the tritium breeding modules. This also helps to improve facility availability. BOP availability is calculated, as described above, based on some overall plant availability goal at the test module goal availability.

The final step in all of the pathways is a DEMO or an ETF/EDF, prototypical commercial facilities. In the ETF/EDF, component development work will be carried out to make up for the lack of a fully integrated facility like INTOR. DEMO's initial availability will, therefore, be higher because of the experience in INTOR. For the same reason, DEMO initial BOP availability is assumed to be better than that of an ETF/EDF. Figure 15.3-6 contains this availability model. The overall availability will depend on the level of

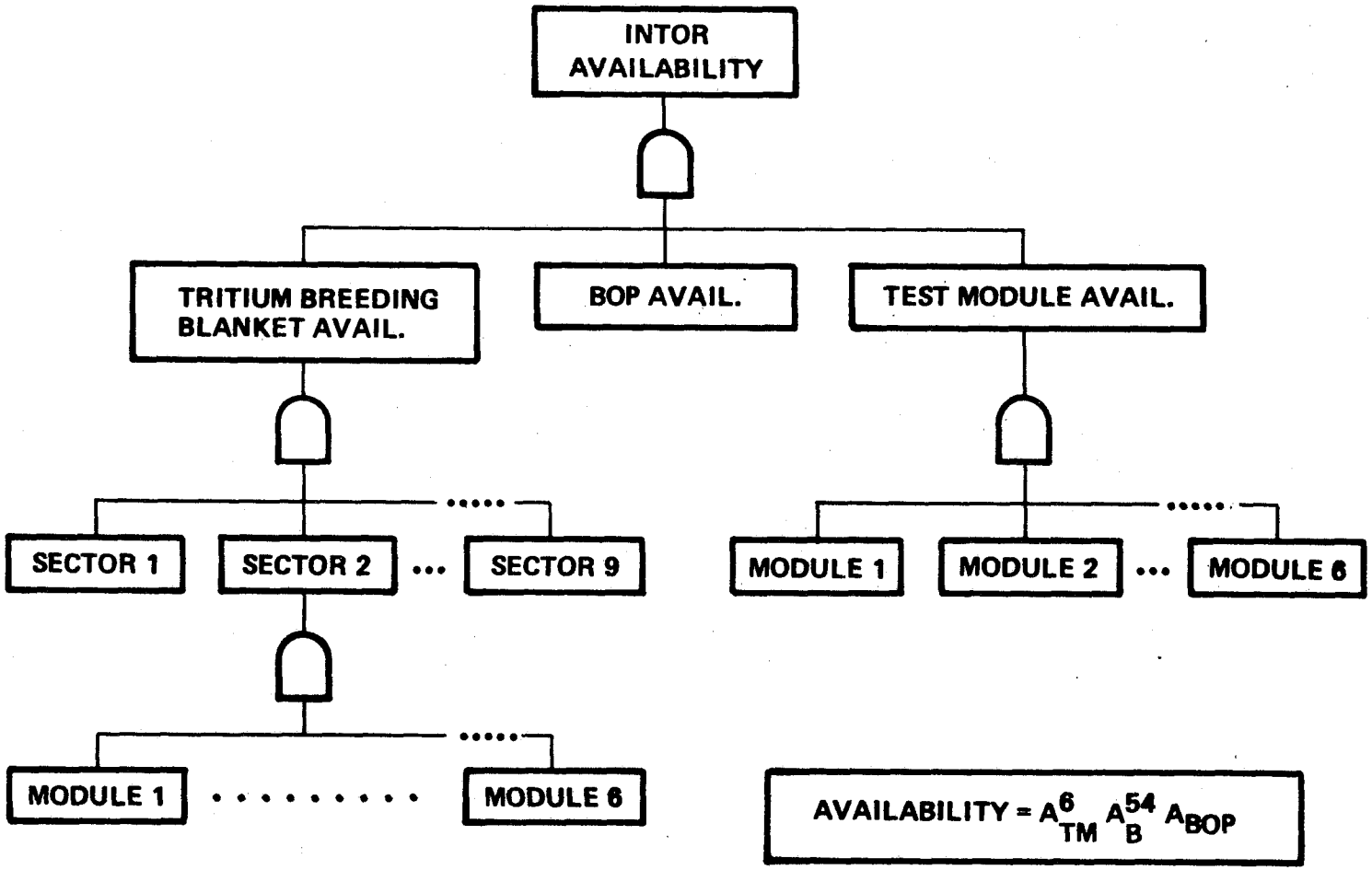


Figure 15.3-4. INTOR availability growth is dominated by reliability growth in the tritium breeding blanket modules. This model is also used for the ETF/EDF following TFCX and MFTF-α+T.

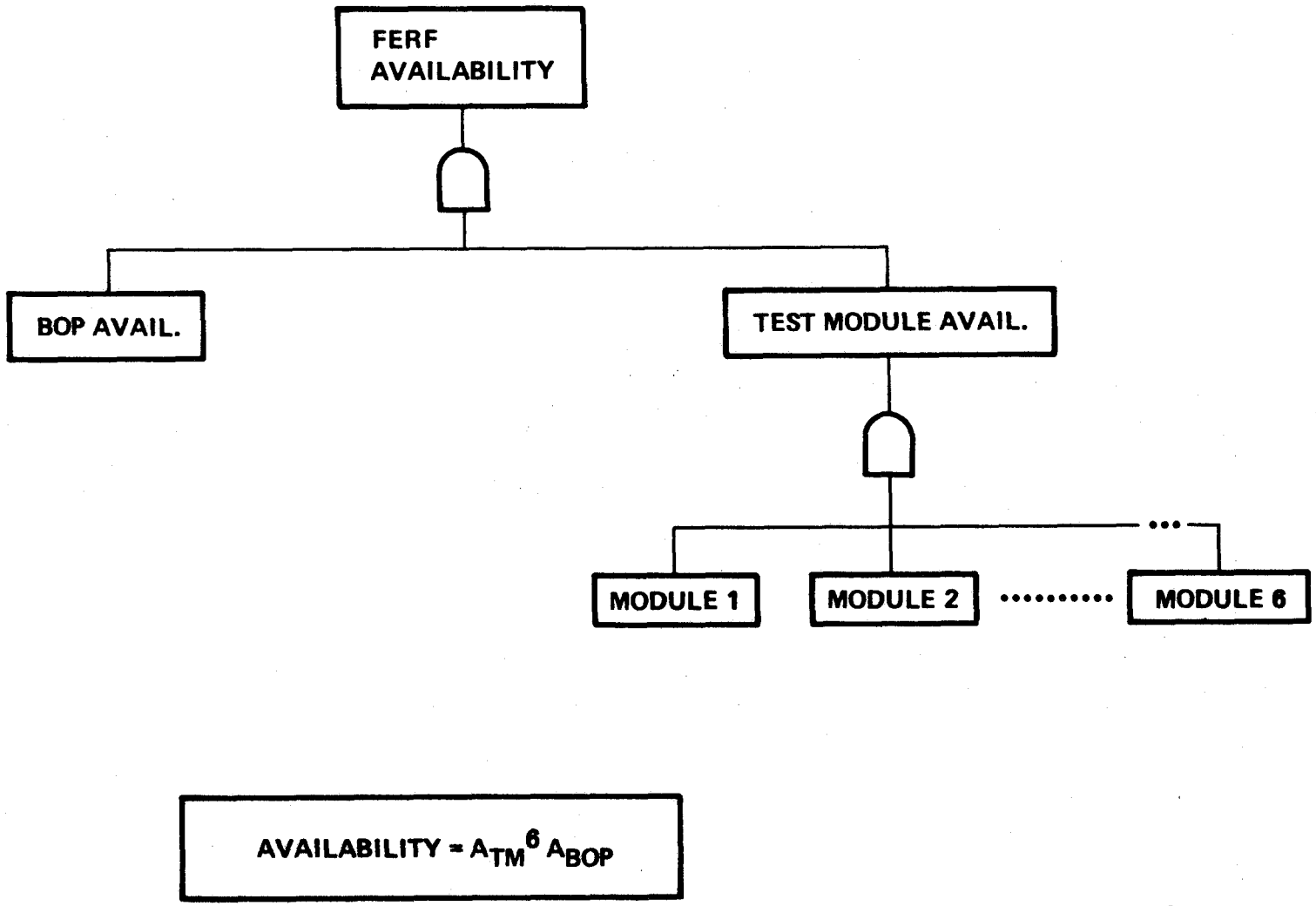


Figure 15.3-5. Fusion Engineering Research Facility (FERF) availability growth is quicker because the tritium breeding blanket modules are eliminated.

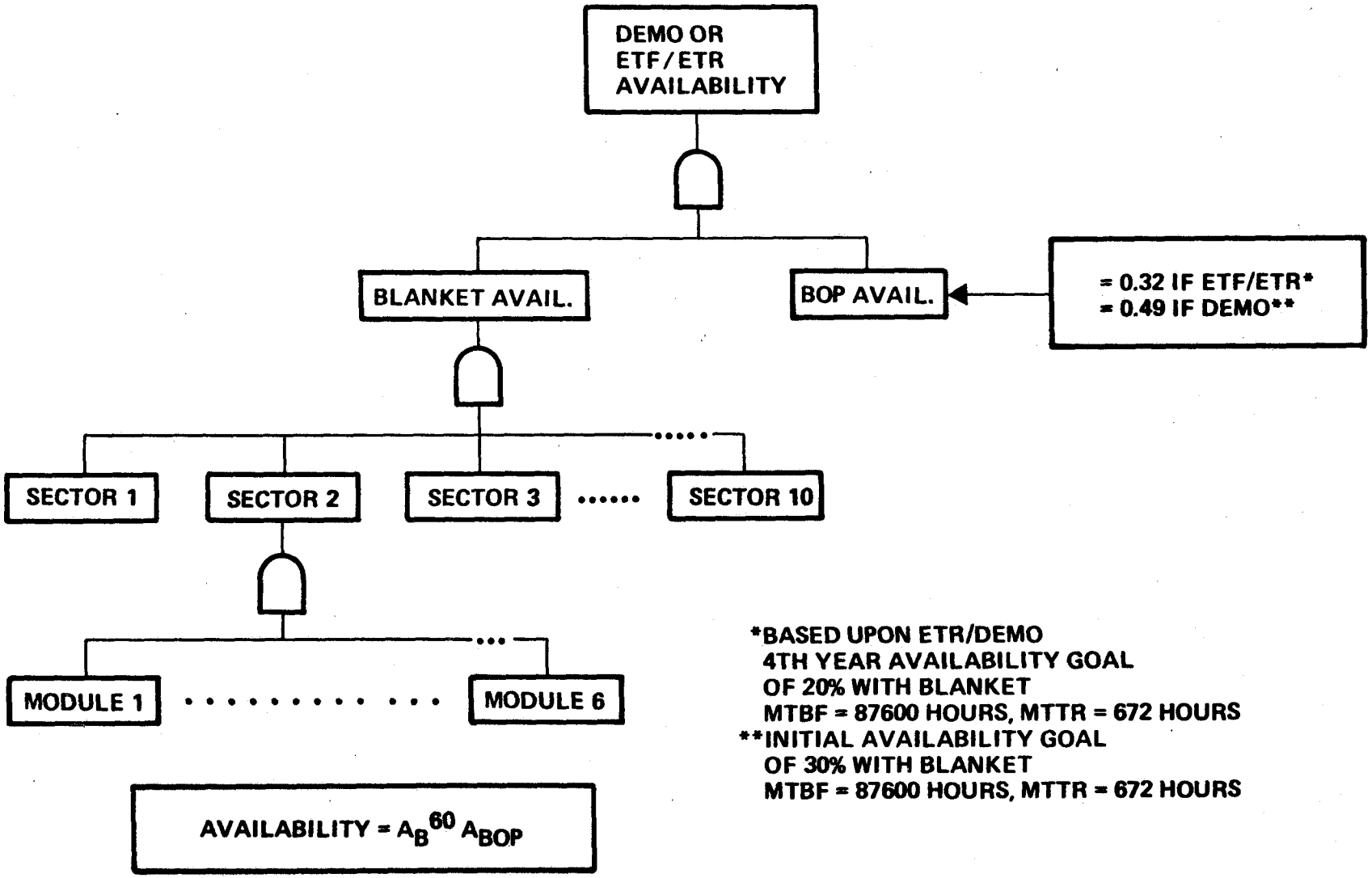


Figure 15.3-6. The DEMO and ETF/EDF initial availabilities depend upon blanket module and BOP development in earlier facilities.

blanket module perfomance which has been achieved in the test facilities. If the test facilities have achieved their blanket development goal, then the initial DEMO or ETF/ETR availability goal will also be achieved. If the developmental testing time is limited, however, the DEMO or ETF/ETR initial availability will be lower.

### 15.3.4 Baseline Analysis

Using the availability models and the NAVAIR reliability improvement model, the three fusion development scenarios were analyzed. The objective was to see how long each of the three fusion component development pathways would take to achieve various blanket availabilities. Achievable testing time in terms of calendar time is a function of the availability of the testing facility during testing. The testing facility may be unavailable for various reasons including scheduled outage and component failures.

The NAVAIR escalation model is a means of specifying the component MTBF, $T_m(t)$, as a function of testing time, t:

$$MTBF(t) = T_m(t) = ct^m \qquad (15\text{-}3)$$

The incremental calendar time, $dt_c$, for a small time interval of full power operation, dt, is given by

$$dt_c = \frac{dt}{a(t)}, \qquad (15\text{-}4)$$

where the instantaneous availability, a, is given by

$$a(t) = f(MTBF(t), MTTR) \qquad (15\text{-}5)$$

At some final testing time, T, the corresponding calendar time, $t_c$, is given by

$$t_c = \int_0^T \frac{dt'}{a(t')} \qquad (15\text{-}6)$$

Equation (5) is specified by the availability models in section 15.3.3 and the analysis consists of integrating Equation (6).

For the baseline analysis, a reasonable set of parameters was defined which described the three developmental pathways including the tritium breeding modules, the test modules, and the MTBF escalation. These are shown in Table 15.3-1 for the test modules and Table 15.3-2 for the tritium breeding modules. These tables show parameter ranges for parametric studies, which will be discussed later. They also have a brief discussion of the logic behind most of the values. Table 15.3-3 contains a summary of various availability goals and their relationship to BOP availabilities.

Of particular note in Tables 15.3-1 and 15.3-2 is the application of experience factors to determine how much test credit is given to each module in a parallel test. A classical parallel test of duration T with N components is equivalent to a single component test for time NT. The experience factor reduces this by the factor $N^{n-1}$. This is meant to account for the fact that similar failure causes may be seen in different blanket modules. Redesign and replacement of several failed modules may only address this single failure cause rather than several separate causes. In other cases, separate failures will be caused by separate phenomena. The experience factor is used to express the intuitive feeling that in a parallel blanket module test the total testing experience is actually something between T and NT rather than NT.

Figure 15.3-7 shows the results of this analysis for development pathway 1, testing in INTOR. Three curves are shown. The first is the test facility availability as a function of calendar time. The second is the blanket test module MTBF growth from its initial value to its goal value. The third curve gives the cumulative test time in the test facility. This is multiplied by $N^n$ and used in Equation (1) to calculate the new MTBF. Including a three year startup, when some early failure mode testing can be done, the model predicts 24.5 years of calendar time may be required to reach the blanket module MTBF goal (87,600 hours) in INTOR.

These same curves are presented in Fig. 15.3-8 for the FERF (TDF) in development pathway 2. From the first curve, the higher testing plant availability can be seen. This higher availability allows the blanket module MTBF goal to be reached in 10.3 years, including 3 years of preoperational testing.

Table 15.3-1 Blanket Test Module Key Assumptions
for the Availability Analysis

| | Baseline (Plausible Range) |
|---|---|
| Initial MTBF (hrs) | 8760[a] (2190, 35040) |
| Initial test experience (hrs) | 758[b] (200, 7000) |
| MTTR (hrs) | 336[c] (168, 1240) |
| Goal MTBF (hrs) | 87600[d] (31595, 207857) |
| Test improvement factor | 0.50[e] (0.30 - 0.70) |
| Experience factor | 0.50[f] (0.20 - 0.80) |
| Initial module availability | 0.920 (0.638 - 0.995) |
| Goal module availability | 0.996 (0.962 - 0.999) |

a. Beyond infant mortality testing, 10 percent of goal MTBF, reference FED/INTOR/TEST (1)
b. 36 months x 4.3 wk/mo x 2 hr test/wk x $(6 \text{ modules})^{0.5}$, where 0.5 is the test experience factor
c. 2 weeks
d. Gives module reliability of 78% at 2.5 FPY in DEMO (21,900 hours)
e. Vigorous development program for test modules in a test facility
f. (Credit for N modules/credit for 1 module) = $N^n$ where n is the experience factor, $0 \leq n \leq 1$.

Table 15.3-2. Tritium Breeding Module Key Assumptions for the Availability Analysis

| | Baseline (Plausible Range) |
|---|---|
| Initial MTBF (hrs) | 25263[a] (12638, 60900) |
| Initial test experience (hrs) | 2374[b] (700, 20000) |
| MTTR (hrs) | 672[c] (336, 1344) |
| Goal MTBF (hrs) | 87600[d] (31595, 207857) |
| Test improvement factor | 0.10[e] (0.05 - 0.30) |
| Experience factor | 0.50[f] (0.20 - 0.80) |
| Initial module availability | 0.974 (0.904 - 0.995) |
| Goal module availability | 0.992 (0.959 - 0.998) |

a. For 17520 hr full power life (2.0 FPY in INTOR, 2.0 $MW/m^2$, 4 $MW\text{-}yr/m^2$) gives 50% reliability
b. Assumes 3 x test module experience
c. 1 month
d. Gives module reliability of 78% at 2.5 FPY in DEMO (21900 hours)
e. Low level improvement program. Not set up as a testing/development facility
f. (Credit for N modules/credit for 1 module) = $N^n$, where n is the experience factor, $0 \leq n \leq 1$.

Table 15.3-3. Key Assumptions About Plant Availability Goals

Testing facility ultimate availability following achievement of test module goal reliability

| | Plant | BOP |
|---|---|---|
| FERF* | 0.50 | 0.512 |
| INTOR | 0.30 | 0.486 |

DEMO and ETF/EDF facility initial goal availabilities following achievement of test module goal reliability

| | Plant | BOP |
|---|---|---|
| ETF/ETR | 0.20 | 0.324 |
| DEMO | 0.30 | 0.486 |

* Note: MFTF-$\alpha$+T is assumed to have a testing availability of 0.10.

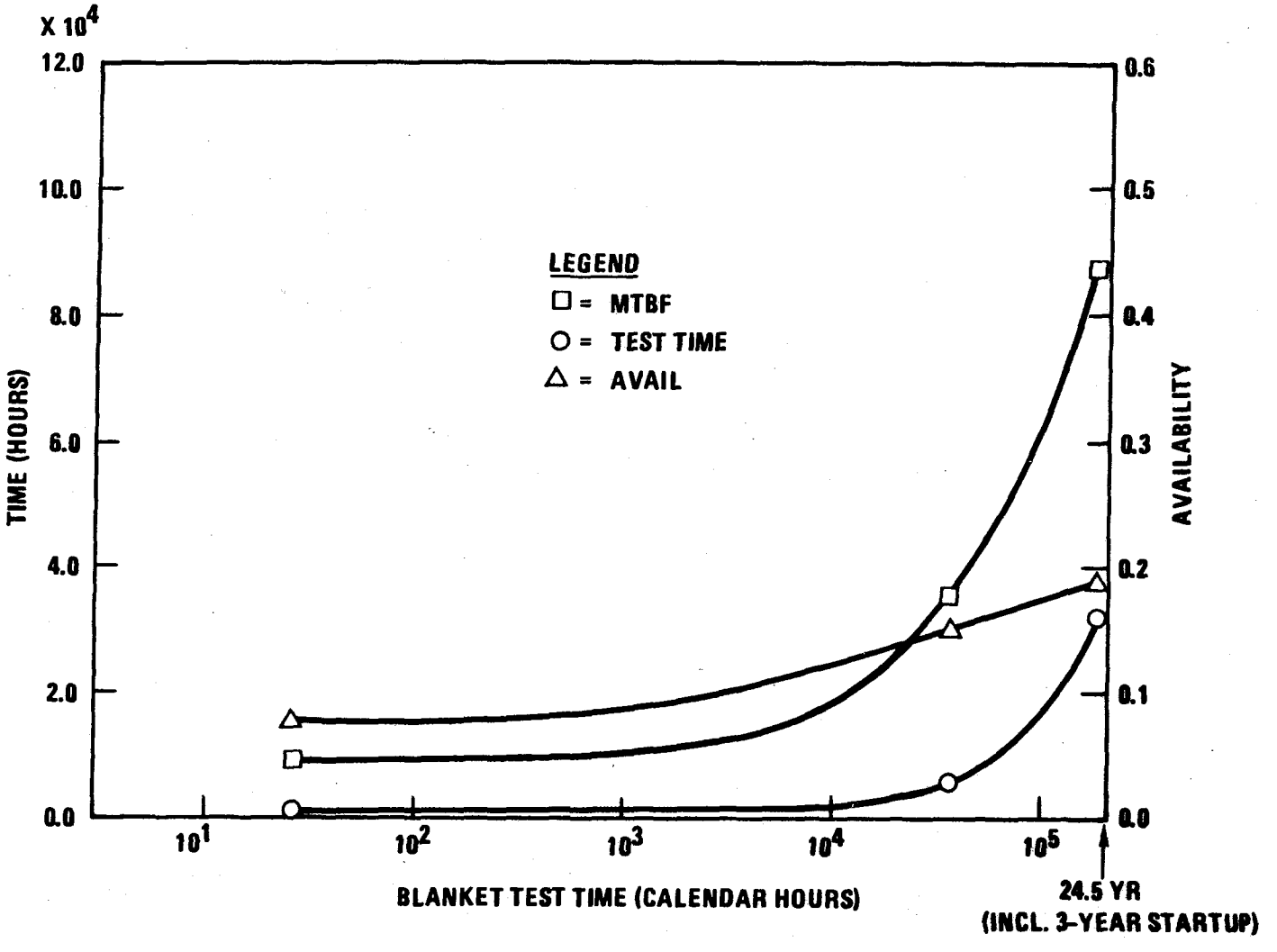


Figure 15.3-7. Because the INTOR availability growth is slow, the test time is limited and the test module MTBF growth is slow.

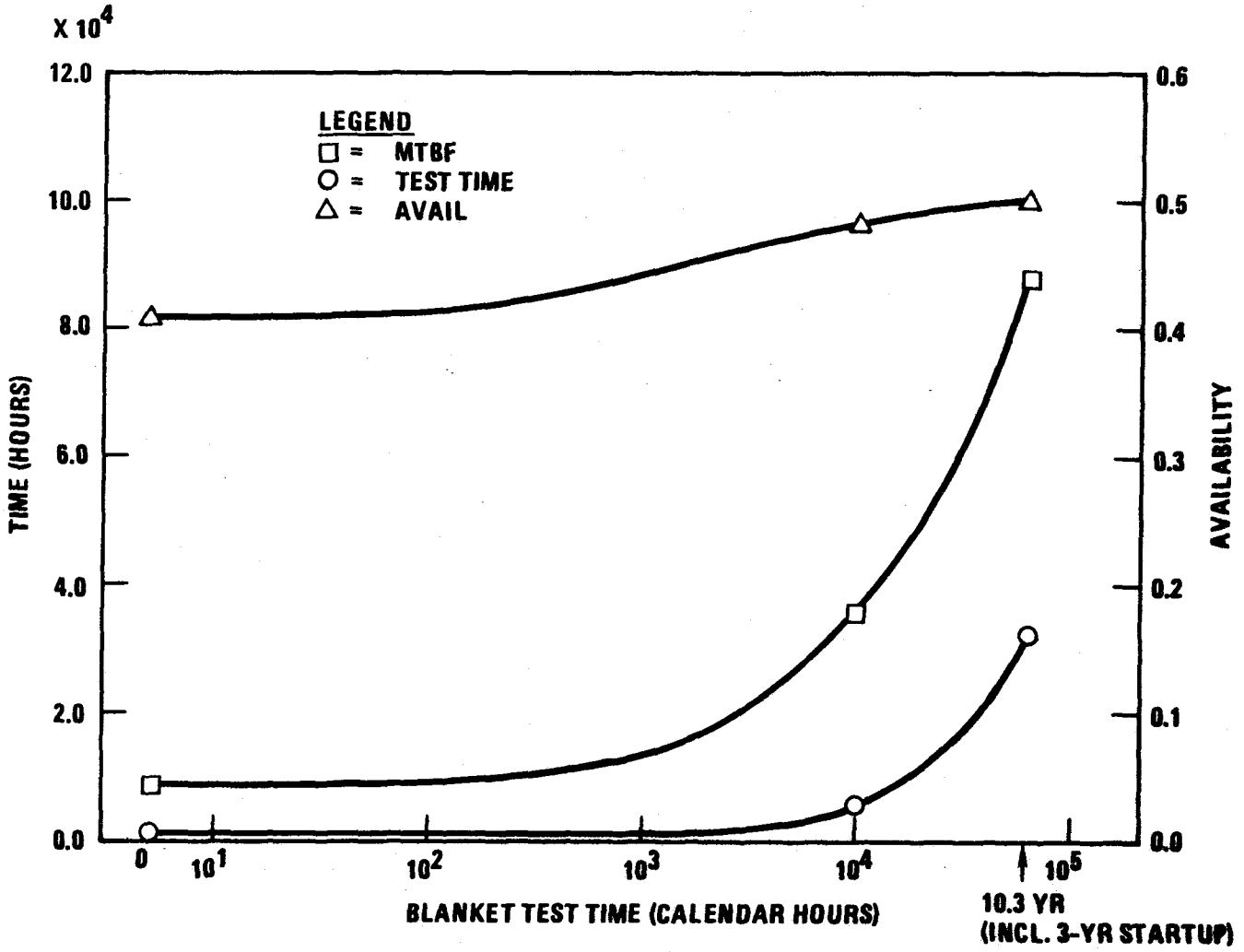


Figure 15.3-8. Higher FERF availability leads to more test time and faster MTBF growth.

Pathways 1 and 2 lead to a DEMO and an ETF/EDF respectively. These downline reactors have similar configurations but different availability goals because DEMO reflects INTOR developmental experience with a higher BOP initial availability. Thus, if the blanket module goals are met in the INTOR or TDF precursors, it is assumed that DEMO can operate initially at 0.30 availability and ETF/EDF at 0.20 availability. Lower levels of performance in INTOR or TDF will result in lower initial availabilities in DEMO or ETF/EDF. The effect of this in a comparison of the two developmental pathways can be seen in Fig. 15.3-9 where the achievable downline facility availabaility is shown as a function of calendar time in the testing facility. At the end of each testing scenario, blanket module performances are the same, the goal of 87600 having been reached, although the downline facility availabilities are different.

The third developmental pathway leads from TFTR to the parallel operation of TFCX and MFTF-$\alpha$+T. This is followed closely by ETF/EDF where the ETF phase is operated like INTOR and is required to continue with the testing started in MFTF-$\alpha$+T. The EDF phase is operated like DEMO. This pathway is equivalent to providing INTOR of pathway 1 with partially developed blanket models out of the low availability facility, MFTF-$\alpha$+T. In the operation of MFTF-$\alpha$+T, 3 years of startup early failure mode testing are assumed. This is assumed to be followed by the equivalent of 7 years operation of TDF (pathway 2) at 0.10 availability. This gives (from a starting MTBF of 8760 hours) an MTBF of $4.2 \times 10^4$ hours, equivalent to 1.6 years operation in TDF with an average availability of 0.45. Starting with an MTBF of $4.2 \times 10^4$ hours, an INTOR-like ETF achieves the blanket module goal (87600 hours) in 10.8 calendar years. The total pathway 3 time leading to EDF phase (like DEMO) operation at 0.30 availability is 20.8 years.

All three blanket module development pathways are compared in Table 15.3-4. For this baseline set of parameters, pathway 2 reaches its goal much quicker than either of the other two options. Pathway 3, the MFTF-$\alpha$+T option is comparable to pathway 1, because even at an availability of 0.10 the test configuration is more available than that of INTOR. It is also important to point out that the operational mission of the ETF phase of ETF/EDF would probably include operation for something like 10 years to achieve its fluence goals. The 10.8 year blanket development time requirement in pathway 3 may not, therefore, be an unreasonable requirement.

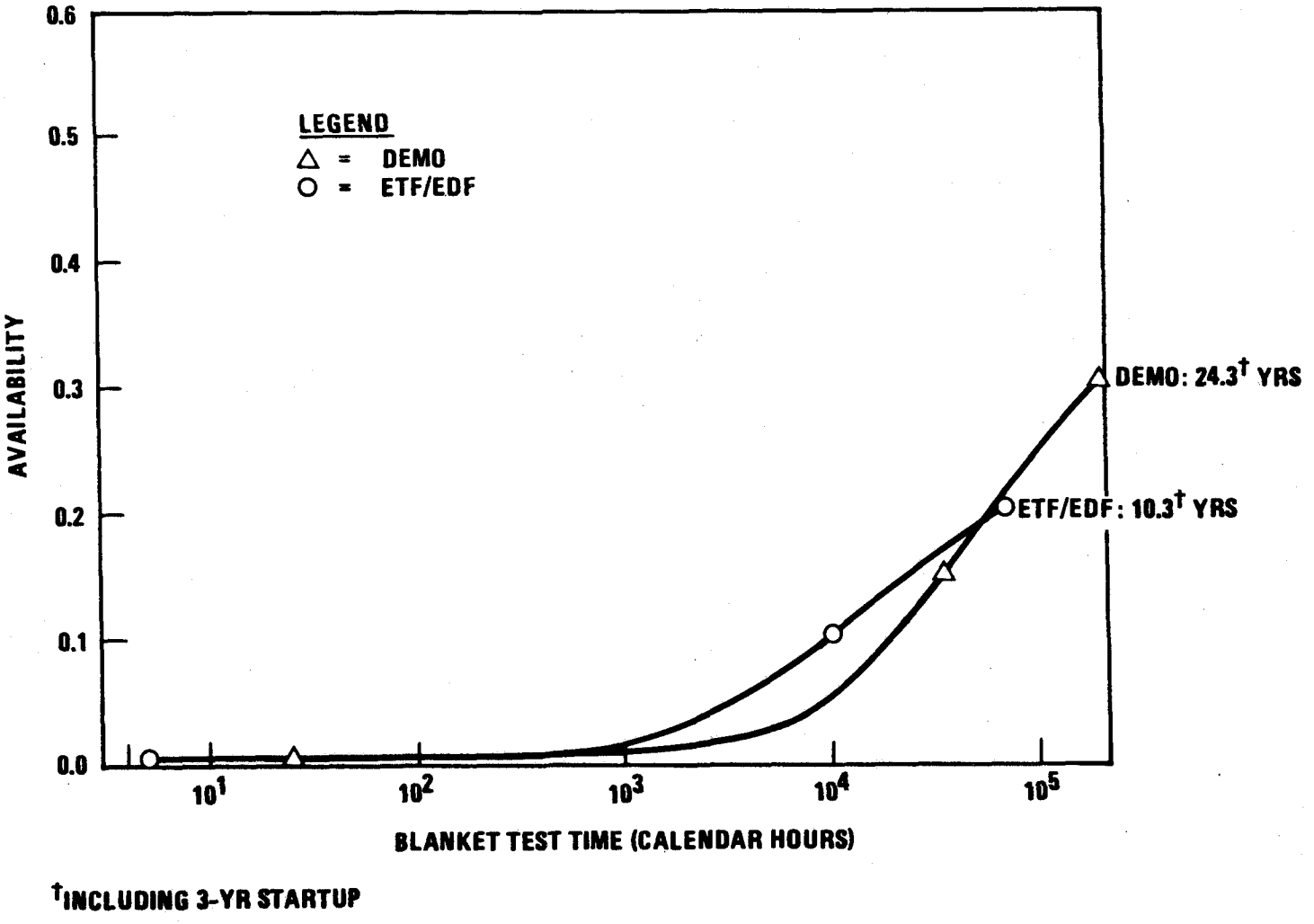


Figure 15.3-9. As a result, the FERF could lead to an earlier achievement of the goal availability in the subsequent facility.

Table 15.3-4. Three Blanket Module Developmental Pathways

| Blanket Module Test Pathway | Goal Facility | Goal Facility Initial Availability Facility | Goal | Time to Goal |
|---|---|---|---|---|
| 1) TFTR/TFTR-U → INTOR → DEMO → INTOR | DEMO | | 0.30 | 25 years[3] |
| 2) TFTR → TFCX / TDF → ETF/EDF | TDF | ETF/EDF | 0.20 | 10 years[3] |
| 3) TFTR → TFCX / MFTF-α+T → ETF/EDF | MFTF-α+T<br>ETF[1] | → EDF[2] | 0.30 | 21 years[4] |

1. Phase 1 of ETF/EDF and similar to INTOR.
2. Phase 2 of ETF/EDF and similar to DEMO.
3. Includes 3 years early failure mode testing.
4. Includes 3 years early failure mode testing, 7 years MFTF-α+T operation, 10.8 years ETF operation

### 15.3.5 Parametric Studies

Table 15.3-5 presents the independent variables in the analysis and the sensitivity of the time to goal achievement to +10% changes in the variables. Column 1 shows the relative time to achieve the module goal MTBF along development (TDF → ETF/EDF) pathway 2. Column 3 shows the relative time to achieve the module goal MTBF along pathway 1 (INTOR → DEMO). Column 2 shows the relative time to achieve a module availability which would give the pathway 2 goal availability (0.20) while using pathway 1. Column 2 was pursued because the times were more comparable in magnitude to column 1 than was column 3. In most cases, a +10% change results in effects less than or equal to 10% in the time to goal achievement. Four variables effect larger changes: test module initial MTBF, tritium breeding module MTTR, module goal MTBF, and test module MTBF improvement factor. Studies over the variable values shown in Tables 15.3-1 and 15.3-2 confirm these conclusions. The results of these studies for the four most critical parameters are presented in Figs. 15.3-10 through 15.3-13.

The initial test module MTBF, Fig. 15.3-10 is a critical parameter for all pathways. In Fig. 15.3-11, tritium breeding module MTTR is an important parameter for both of the INTOR based results. In the case of the upper curve of Fig. 15.3-11, shorter tritium breeding module MTTRs result in the test module availability determining the development pace. In the case of the second INTOR curve (related to the ETF/EDF goal), the lowest MTTR shown is not small enough to produce an asymptotic effect. In Fig. 15.3-12 a longer or shorter MTBF goal results in longer or shorter times to the goal as expected. Figure 15.3-13 contains the most important independent variable, the test module NAVAIR test improvement factor. A decrease to about 0.35 gives development times greater than 10 million hours (~ 1000 years), an obviously impossible situation.

The parametric studies reveal, in order of importance, the four most critical independent variables:

- Test module MTBF improvement exponent
- Goal MTBF
- Test module initial MTBF
- Tritium breeding module MTTR

Table 15.3-5. Goal Achievement Sensitivity to 10 Percent Increases in Independent Variables

| Independent Variable Changed by 10% | Relative Time to Achieve | | |
|---|---|---|---|
| | ETF/ETR Goal Availablity Following FERF | ETF/ETR Goal Availablity in DEMO Following INTOR | DEMO Goal Availablity Following INTOR |
| 1.a. Test module initial MTBF | 0.84 | 0.84 | 0.85 |
| 1.b. Tritium breeding module initial MTBF | 1.0 | 1.0 | 0.91 |
| 2.a. Initial test module test experience | 1.09 | 1.09 | 1.09 |
| 2.b. Initial tritium breeding module test experience | 1.0 | 1.01 | 1.01 |
| 3.a. Test module MTTR | 1.002 | 1.008 | 1.005 |
| 3.b. Tritium breeding module MTTR | 1.0 | 1.15 | 1.05 |
| 4. Goal MTBF | 1.19 | 1.23 | 1.22 |
| 5.a. Test module MTBF improvement exponent | 0.65 | 0.75 | 0.68 |
| 5.b. Tritium breeding module MTBF improvement exponent | 1.0 | 0.98 | 0.97 |
| 6.a. Test module experience factor | 0.90 | 0.91 | 0.91 |
| 6.b. Tritium breeding module experience factor | 1.0 | 0.99 | 0.99 |
| 7. Test plant ultimate availability at goal MTBF | 0.91 | 0.91 | 0.91 |

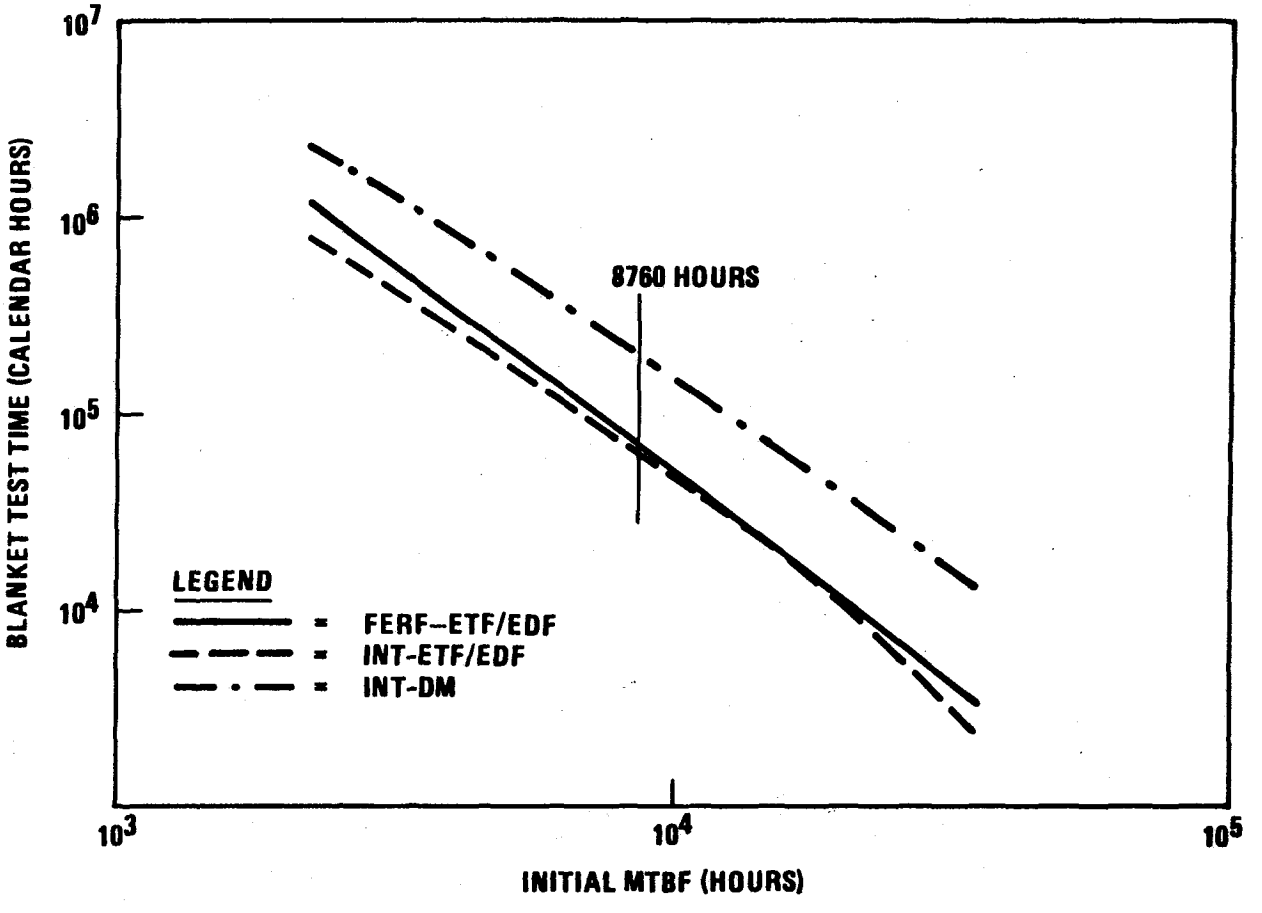


Figure 15.3-10. Required blanket test time to goal availability versus initial test module MTBF.

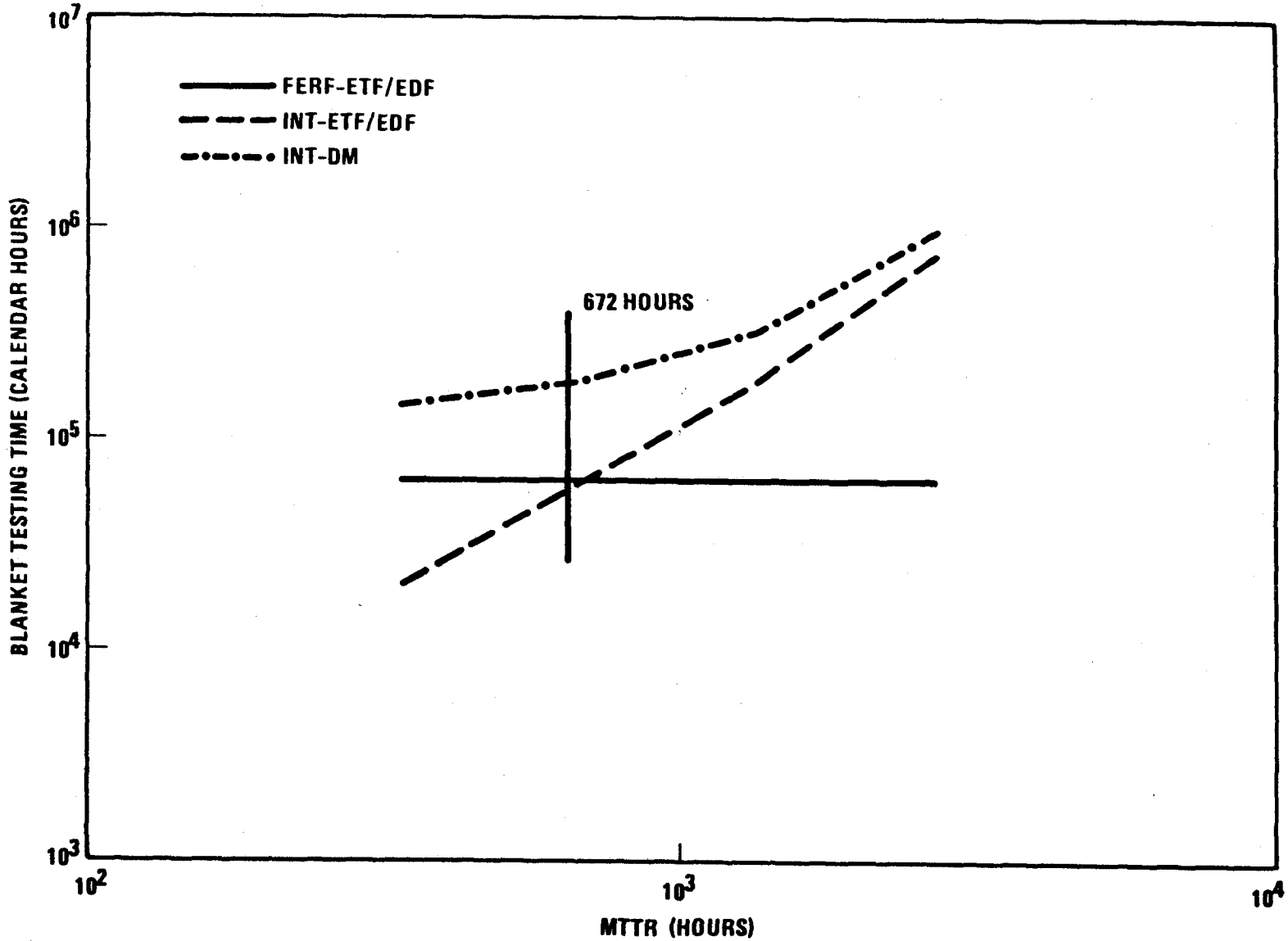


Figure 15.3-11. Required blanket test time to goal availability versus tritium breeding module MTTR.

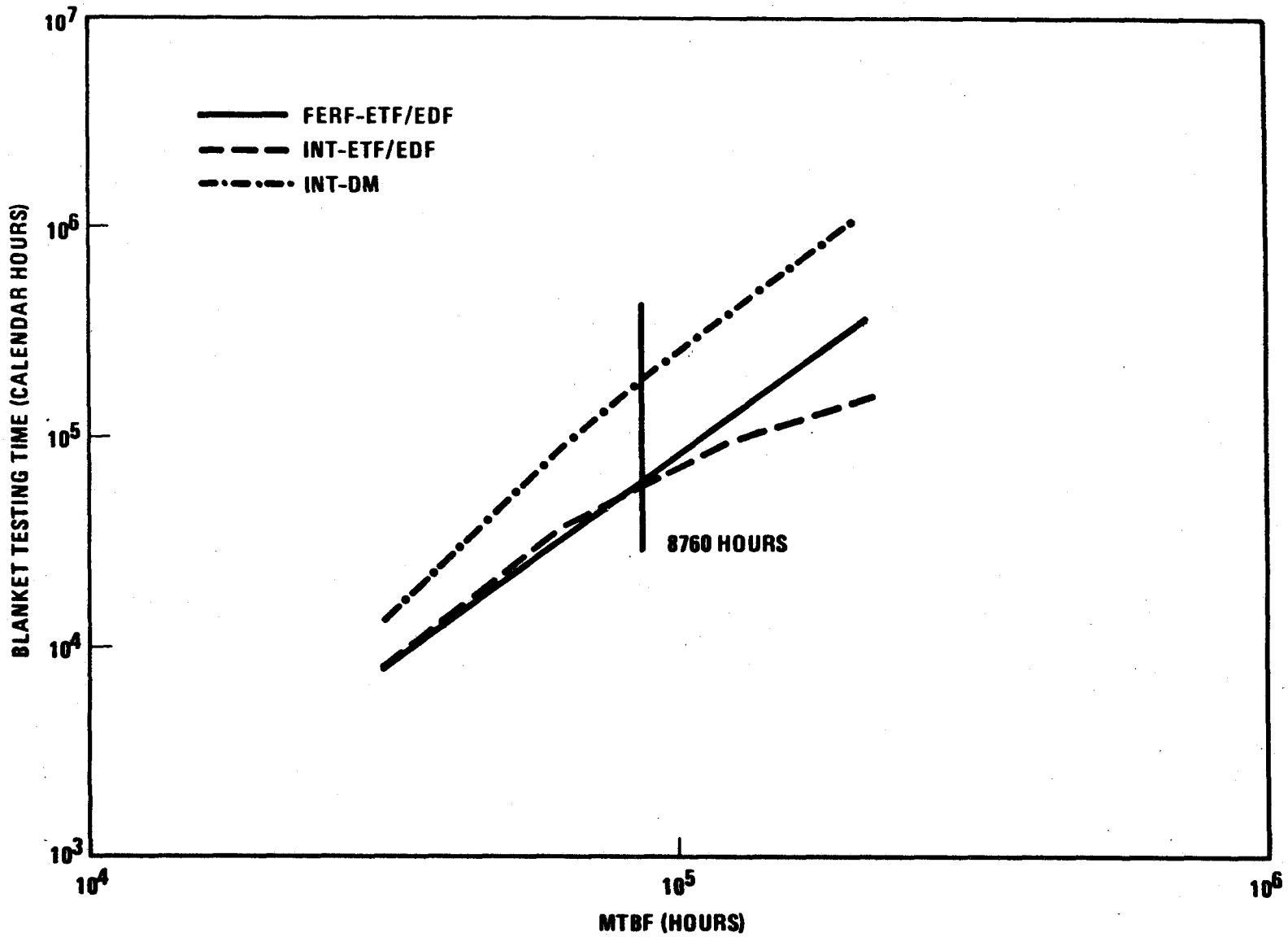


Figure 15.3-12. Required blanket test time to goal availability versus goal MTBF for test and/or tritium breeding module.

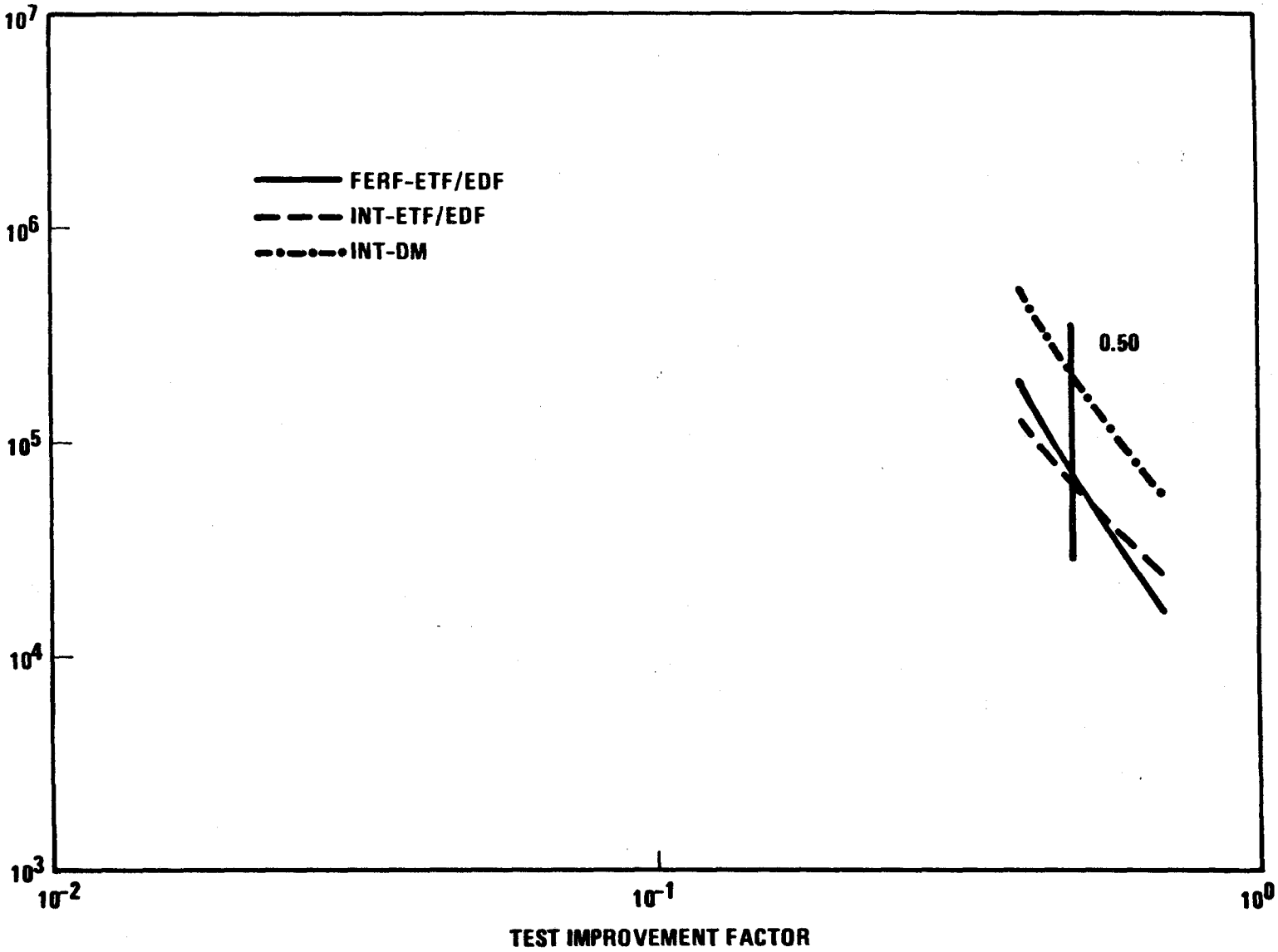


Figure 15.3-13. Required test time to goal availability versus test module test improvement factor.

It should be noted that the goal MTBF, of second most importance, depends to a large extent on the anticipated downline facility requirements. These include the availability requirement and the module MTTR. If the MTTR can be reduced, then the goal MTBF can be relaxed at the same time. A final choice of module goal MTBF and MTTR would require trade studies which examine the economic impact of module development costs versus module replacement costs. Of course, safety implications might also be of paramount importance. Also notable from the parametric studies is the fact that the variations shown do not change the relative performance of the FERF and INTOR options except that in some cases the times to module development become so short or so long that it does not make much sense to discriminate between the two options.

### 15.3.6 Conclusions

The application of the NAVAIR reliability improvement model has shown that reasonable values of the independent parameters produce blanket module development times on the order of 10 years. Substantial advantages are demonstrated for the fusion development pathway which relies on blanket module test facilities specifically tailored to develop blanket modules (TDF and MFTF-$\alpha$+T) without the complication of unproven and potentially unreliable tritium breeding modules (INTOR). Parametric studies do not substantially change the relative performance of the development pathways. However, in any case, some variables can result in extremely long blanket module development times. Especially critical is the test module improvement factor. This places emphasis on the choice and justification of any improvement factor and its relationship to achieveable improvements in MTBFs. In the NAVAIR approach, major emphasis is placed on the development of testing programs capable of tracking a reliability escalation curve. These programs are the heart of the efforts to achieve MTBF improvements. It should be stressed that this study tries to show the implications of certain reliability development pathways and test machine configurations. The specification of test programs and the understanding of complex test and fusion issues is a future task barely begun.

## 15.4. Summary and Conclusions

This two part study looked at two issues in reliability developmental testing:

- The statistical significance of blanket module test times relative to module availability goals
- The implications of reliability testing on different fusion technology development pathways.

In the first study, it was found that high statistical confidence in blanket module designs will, at best, be difficult to develop based on reasonably achievable test times and anticipated module goal MTBFs and MTTRs. If the MTTR can be substantially reduced (to 1 day), however, lower MTBFs would be acceptable lead to reduced test time requirements and give high confidence in reactor performance.

In the second study, the NAVAIR reliability improvement models were applied to fusion blanket module development using reasonable, but not unique, assumptions. It was found that smaller, less complex, test facilities without tritium breeding requirements could give reasonable module development times. Fully integrated facilities without the benefit of substantial preoperational testing would require much longer times to do the same task. These conclusions are based on the NAVAIR hypothesis is that reliability testing management programs can be developed which can achieve the ambitious reliability improvements described by the improvement curves.

## References for Chapter 15


1. Reliability Engineering Handbook, Volume II (Management Manual), NAVAIR 01-1A-32, July 1, 1977.

2. M. Abdou et. al., FED-INTOR/TEST/82-4, Chapter XII, "Engineering Testing", pp 38-52, 1982.

3. A.E. Green and A.J. Bourne, Reliability Technology, John Wiley and Sons, 1972.

4. A. Coppola, "Bayesian Reliability Tests are Practical", RADC-TR-81-106, July 1981.

# CHAPTER 16

# FUSION DEVELOPMENT SCENARIOS

TABLE OF CONTENTS


Page

16.1 Introduction and Motivation..... 16-1

16.2 Planning Considerations..... 16-2
16.2.1 Reactor Relevance..... 16-3
16.2.2 Tritium Production..... 16-3
16.2.3 Number of Blanket Options..... 16-6
16.2.4 Test Objectives..... 16-6
16.2.5 High Fluence..... 16-8

16.3 Use of Existing Fusion and Non-Fusion Experimental and Test Facilities.....16-9

16.4 Fusion Experimental and Test Facilities.....16-11
16.4.1 Plasma Burning Experiment (PBX).....16-11
16.4.2 Fusion Engineering Research Facility (FERF).....16-13
16.4.3 Engineering Test Facility (ETF).....16-14
16.4.4 Engineering Demonstration Facility (EDF).....16-14
16.4.5 Other Facilities and Combinations.....16-15

16.5 Preliminary Fusion Development Scenario Evaluation.....16-15
16.5.1 Fusion Development Pathways.....16-15
16.5.2 Pathway Evaluation Guidelines.....16-18
16.5.3 Pathway Evaluations.....16-22

16.6 Summary and Conclusions.....16-32
16.6.1 Near-Term Experimental Program.....16-32
16.6.2 Preliminary Pathway Evaluations.....16-32
16.6.3 International Implications.....16-34

References.....16-36

# 16. FUSION DEVELOPMENT SCENARIOS

## 16.1 Introduction and Motivation

A principal objective of the FINESSE program will be the development of a recommendation regarding the types and sequences of experimental and test facilities which are expected to be best suited to furthering the development of fusion nuclear technologies. As a first step towards fulfilling this objective, a preliminary screening evaluation of many possible technology development pathways was performed and is reviewed in this chapter. A limited number of pathways (perhaps 4) will be developed in more detail during the second year of the FINESSE program. A discussion of the many considerations which must be taken into account in the development scenarios is also presented in this chapter.

The construction of detailed development pathway scenarios will, ultimately, provide a framework for the integration of the following FINESSE activities into a consistent program of experimentation, development, and testing:

- The identification of nuclear technology issues (see Chapter 3).
- The design of act-alike nuclear tests and experiments (Chapters 5, 6, 9).
- The assessments of candidate non-nuclear, fission accelerator, and fusion experimental and test facilities (Chapters 10, 11, 12, 13, 14).
- The development of experiment/test plans (see Chapter 9).
- The study of availability/reliability considerations in fusion development (Chapter 15).

However, it is important to emphasize that these FINESSE activities will be on-going into the second year of the program and will continue to impact the scenario development task as the results evolve. Also, we recognize that the development scenarios task must, necessarily, have a larger scope than that of other FINESSE activities. Specifically, a successful development scenario must address all of the principal physics and technology areas, not only the nuclear technologies. It must provide a blueprint for advancing the state of fusion science and technology at a pace which is timely, yet consistent with an acceptable level of risk as well as budget constraints.

Because the available funding for fusion research and development is limited, and because any increases to support a sustained and aggressive fusion development scenario will require externally motivated incentives, it is important that the development scenarios that are created fully utilize existing, non-fusion facilities, beginning with a near-term focus on novel, small-scale experiments. A clear perception that the introduction of alternatives to fossil and fission electricity will be required during the first decades of the next century might constitute a motivating incentive for fusion research and development. A recognition that fusion research and development can be used to explore new areas of science and technology that may have important scientific and technological applications beyond electricity generation might provide an additional motivating incentive.

## 16.2 Planning Considerations

In constructing a "roll-forward" logic for fusion development, the planner must strive for a uniformity of assumptions and a consistency of logic to the maximum extent possible. For example, the following four questions can be pivotal in determining the cost, risk, and schedule of fusion development pathways:

- Can a near-term, D-T burning fusion facility operate in a physics mode which is not presently perceived to be extrapolable to a reactor-relevant "strategic goal" of the program? For example, will a non-ignited, beam driven, physics mode be acceptable for an early technology facility if it results in a lower cost and/or risk?
- Will early experimental fusion technology facilities be required to provide much or all of the tritium fuel required to sustain their own operation?
- Will the number of blanket structure/coolant combinations be reduced to one or a few principal options prior to large scale testing in a fusion facility?
- Will the objective of testing in the fusion environment be screening for early failure modes, extended testing to achieve a reliability data base with a high statistical confidence, or a design/test/fix sequence for reliability improvement? How will these objectives be modified in consideration of available facilities?

- Will a high fluence, 14 MeV, irradiation damage data base be available from point neutron sources prior to the extended operation of structural and breeding materials in a fusion environment? How will the availability (or unavailability) of such a facility affect development risks and planning.

As discussed below, these questions do not have simple or uniform answers, but must be considered for each specific scenario.

### 16.2.1 Reactor Relevance

It is important to note that several of the preliminary FINESSE development pathway scenarios will not require that early technology facilities operate in a reactor relevant physics mode. For example, pathways which include Fusion Engineering Research Facilities (FERF) which do not necessarily feature reactor relevant fusion physics, but operate in parallel with reactor relevant Burning Plasma Experiments (PBX), can receive favorable evaluations as FINESSE scenarios. In such cases, a favorable evaluation will require that the two fusion facilities and any complementary facilities address nearly all of the critical and high priority issues such that the level of risk in progressing to an ambitious and reactor relevant (i.e., integrated) next step is reasonably low. In this context, the next step is typically an ambitious Engineering Test Facility (ETF) which may be upgraded to an Engineering Demonstration Facility (EDF).* It should be noted that FERF operation in a non-reactor relevant physics mode does not, in all cases, imply that the FERF plasma physics regime would be "uninteresting." Rather, such a facility could provide unique opportunities to study high density, high temperature, fusioning plasmas.

### 16.2.2 Tritium Production

The issue of tritium production in the first experimental technology facilities is most important when the facility has a high fusion power level. For example, an INTOR class facility[1], with a 500 MW fusion power

---

* These facilities are defined in more detail in Section 6.3.

level and an ultimate capacity factor of 40% would burn about 12 kg of tritium per year. As shown in Fig. 16.1-1[2], a steady supply of 2.8 kg/yr tritium from the Canadian nuclear program[2], starting in 1988, would sustain this level of operation only if an internal tritium breeding ratio (TBR) of about 0.8 could be achieved. If the fusion power were reduced to 200 MW, a 0.5 TBR would still be required. Conversely, even if the tritium were available for purchase (e.g., from a U.S. military stockpile), the cost might be prohibitive. If all of the tritium required to sustain a 500 $MW_f$ fusion power level were available at a cost of 10,000-20,000 $/g, the annual operating cost for tritium alone would be in the range of 120-240 $M/yr.

Any requirement for in situ tritium breeding impacts the cost of the facility, but more importantly it impacts its operational risk. That is, it is not clear that an operational tritium breeding blanket which is reliable enough to enable a 30-40% overall facility availability can be developed for this application if no prior testing and/or development in an operating fusion environment is available. The apparent paradox of not being able to develop a reliable blanket until such a blanket exists has been explored in some detail (Chapter 15 of this report) with the result that it appears prudent to penalize any first generation fusion facility which requires a large insitu tritium breeding ratio. During 1985, a small effort will be aimed at exploring whether a credible option exists a "low-tech" tritium breeder blanket which does not extrapolate to reactor relevant applications, but does promise high reliability without requiring an extensive prior development effort.

If such a blanket can not be identified, low power fusion technology facilities, with low tritium requirements, might be most acceptable for early blanket testing and development to an adequate level of reliability. Note that the fusion nuclear technology development requirements in Chapter 4 can be met with only about 20 to 50 MW of fusion power. Therefore, higher power is only a limitation of the physics of particular confinement concepts (e.g., in tokamaks, the device power, power density, and wall load are strongly coupled).

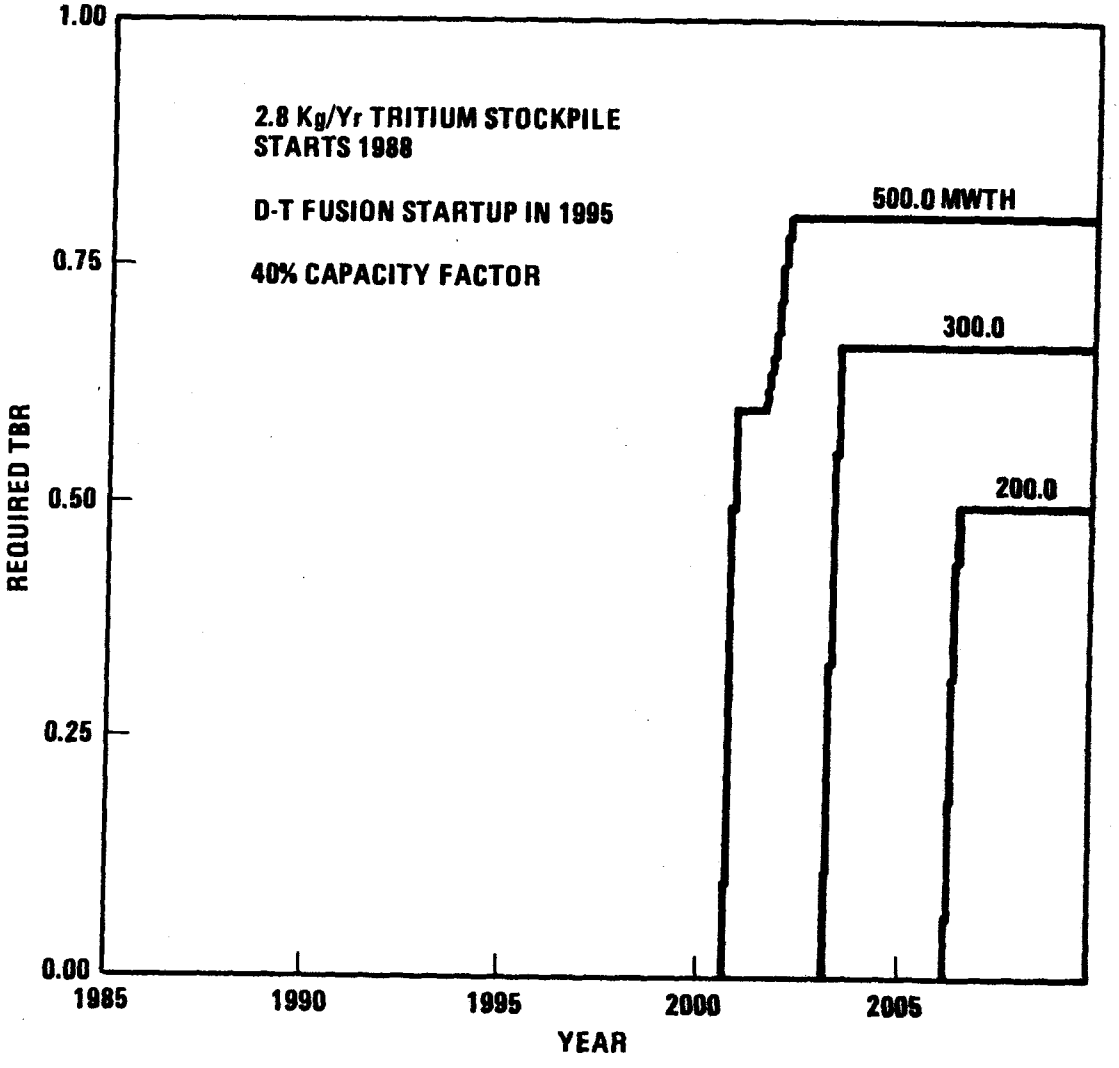


Figure 16.1-1. Tritium breeding ratio needs for 2.8 kg/yr tritium supply rate (starting 1988) with startup of fusion device delayed until 1995.

### 16.2.3 Number of Blanket Options

The number of combinations of blanket coolants, tritium breeding materials, and structural materials presently being considered by the fusion community is enormous although attempts at narrowing down the options via the Blanket Comparison and Selection Study (BCSS) have recently begun[3]. The cost impact of continuing to carry several options will increase as the program progresses to operating blankets on fusion technology facilities. Each type of blanket will require many experiments and tests (see Section 16.2.4) and can have unique and far reaching requirements regarding safety systems, tritium release, power conversion, and remote maintenance. Therefore, as the scope of development issues and the number of required experiments and tests for any given blanket concept become further enumerated, it is expected that a dramatic reduction in the number of blanket concepts will be required so that a development program of reasonable scope and cost can be conducted.

The FINESSE development scenarios anticipate a vigorous activity, early in the technology development program, which is aimed at performing the low-to-modest cost experiments which are required to compare competing blanket concepts and eliminate non-viable concepts while establishing sufficient physical data such that one generic blanket design can be pursued with a high confidence in its ability to be developed for attractive performance and reliability. Such a generic design would not be expected to be specified in its ultimate design detail, but choices such as the coolant, structure, and breeder (preferably in that order) would be defined. It is likely that one or more backups would also be defined and pursued at a substantially lower level of effort.

### 16.2.4 Test Objectives

It is important that the various objectives of experiments and tests to be conducted in fusion facilities are clearly defined as the technology development scenarios are developed. Specifically, some possible experiment/test objectives are as follows:

- Obtain required data points by conducting experiments for fixed and predetermined periods of time. Such data would include any information necessary for gaining sufficient understanding of new phenomena such

that an evaluation and comparison of the feasibility and attractiveness of candidate concepts can be conducted.

- Identify design flaws and early failure modes by conducting beginning-of-life screening tests.
- Implement a reliability improvement goals in addition to the identification of early design flaws and failure modes by conducting iterative design/test/fix/test sequences.
- Generate sufficient data to support a high statistical confidence in the reliability of components by conducting long term operation/test programs.

Among these, the first type of experiment/test can apply to any type of test (e.g., specimen unit cell, submodule, component), while the second is most applicable to submodule and component testing, and the latter two objectives are most applicable to component testing in a fully integrated environment. The amount of time required to conduct the second type of experiment/test depends upon the particular design feature, but is typically measured in hours or days. In contrast, the time required to perform the first, third, or fourth type of experiment/test can be much longer.

For example, the amount of time required to conduct an iterative design/test/fix/test sequence to achieve a given reliability goal is highly uncertain due to the novelty and complexity of fusion nuclear components. Although the required time to implement such a sequence for blanket modules is being considered in FINESSE (using data generated in the Department of Defense NAVAIR program[4,5]), the preliminary results which have been generated (Chapter 15) indicate that relatively long periods testing time ($\gtrsim$ 10 yrs) may be required to achieve high reliability via an iterative design/test/fix/test sequence. These results have not, as yet, been factored into the construction of the development scenarios.

Chapter 15 also discusses the implementation of an operation/test program to develop high statistical confidence in a reliability data base prior to an engineering demonstration. Such a program is clearly a desirable goal, but can be difficult to implement due to the requirement for an extended test period and because such a program would logically follow a relatively long design/test/fix/test sequence (i.e., one should achieve high reliability prior to confirming it).

A key determinate in the size (as opposed to the time duration) of a test program is the number of identical test articles in the test matrix which are required to provide acceptable test statistics. Clearly, it will become increasingly difficult and expensive to accommodate a large number identical test articles. This concern will be especially valid as the test articles become larger (e.g., for component testing) and as longer test times are required (e.g., for fluence testing). The problem will be compounded by a need to test for off-normal and transient conditions as well as a need to perform destructive testing in developing a fluence data base. For example, to establish data to N MW-yr/$M^2$, NM test articles could be required where M would be the number of identical test articles required to achieve adequate test statistics. Although such considerations have not, as yet, been incorporated into the scenario development work, some reasonable observations about the value of M follow:

- M = 1 is the minimum, but can lead to misleading results if a spurious materials or manufacturing defects (e.g., bad welds) are present in the test article.
- M = 2,3 should be sufficient to eliminate some of the above concerns.
- $(M)^{-0.5} << 1$ will provide good test statistics, but can result in a large number of test articles.

These arguments will be further developed during the 1985 program.

### 16.2.5 High Fluence

A final consideration in the creation of development scenarios is the possible future availability of a facility to generate a data base for high fluence irradiation damage due to high energy neutrons. Candidate facilities include accelerator-based neutron source experiments (e.g., FMIT class, but possibly more modest) which would be operated prior to, or in parallel with, fluence testing in fusion technology facilities. The data provided by such experiments would be used to calibrate the more available, but softer neutron spectrum, fission reactor damage data which could be developed in a similar timeframe.

In the absence of a high energy, high fluence calibration, there is a significant possibility of experiencing unanticipated damage phenomena which could result in a premature and systematic failure of the blanket structure

and/or other structural components. Consequently, fusion development scenarios which proceed to an engineering demonstration facility stage without either a high energy, high fluence, irradiation damage calibration or actual fusion component testing in the intermediate to high fluence regime (which would be best) will suffer from an increased level of risk. With a high fluence calibration, it will be possible to consider a program of act-alike, but low fluence, fusion testing as a reasonable compromise to provide a basis for proceeding to the minimum acceptable demonstration facility. The logic which has been incorporated into the preliminary development scenarios assumes that a high fluence calibration (e.g., FMIT class) will exist prior to the construction of a high fluence fusion engineering demonstration facility (EDF).

## 16.3 Use of Existing Fusion and Non-Fusion Experimental and Test Facilities

As mentioned earlier, a successful fusion technology development pathway will incorporate the maximum utilization of both existing experimental facilities and any new facilities that can provide a substantial risk reduction or long range cost savings. To provide the greatest leverage with available funding, it is reasonable that experimentation in such precursor facilities should initially concentrate upon the investigation of critical feasibility issues for which an unfavorable resolution might lead to the unacceptability of a given design option (e.g., MHD flow effects in self cooled liquid metal blankets might prove to be excessive). A second priority would be the identification of poorly understood physical phenomena (e.g., tritium recovery from solid breeders). Beyond this, the test program should be programmed to develop key engineering data bases and to qualify components and subsystems for use in first generation of fusion facilities.

The many types of experiments which can be performed in precursor experimental and test facilities can be distinguished by the type of the experiment and the type of the facility as follows:

- Basic property data experiments performed in non-nuclear facilities (e.g., liquid metal capsule corrosion experiments).
- Basic property data experiments performed in fission reactors (e.g., beryllium swelling experiments).

- Basic property data experiments performed in accelerator neutron sources (e.g., structural swelling at high dpa levels).
- Multiple effects experiments performed in non-nuclear facilities (e.g., high heat flux test assemblies and/or disruption response experiments).
- Multiple effects experiments performed in fission reactors (e.g., solid breeder tritium recovery experiments).
- Multiple effects experiments performed in accelerator neutron sources (e.g., neutron transport benchmarks for simulated blanket/shield configurations).
- Multiple effects experiments performed in existing fusion physics experimental facilities (e.g., limiter/divertor edge physics studies using existing tokamaks).
- Partially integrated tests performed in non-nuclear facilities (e.g., a full-scale, self-cooled liquid metal blanket simulation with a full-scale surface heat flux and a full-scale magnetic field).
- Partially integrated tests performed in fission reactors (e.g., an act-alike simulation of a solid breeker sub-module tritium loop).

These experiment types and their suitabilities for resolving the fusion nuclear issues identified in Chapter 3 have been discussed in varying detail in Chapters 4, 7, 9, 10, 11, and 12 of this report and will not be reviewed in detail. The examples given above are only a small sub-set of those which might be considered.

It is important to recognize that a "basic property data experiment" generally implies a less complex, less costly, less time consuming, or less important endeavor than a "partially integrated test." There are, however, some exceptions. For example, if the development of high neutron fluence irradiation damage requires the construction of an FMIT-class facility, then it is expected that such data would be obtained at a higher level of cost than a full-scale, partially integrated simulation of a self-cooled liquid metal blanket utilizing a high heat flux source and existing magnetic field coils (such as those developed for the international large coil program). The value of a given body of data or test (which is very high in both of the above cases) must be weighed against its cost and fit to the facility sequence of a given development scenario. Subjective judgement will, of necessity, play a large role in this determination.

In the preliminary scenario development which follows, we have assumed that existing and/or small-scale test facilities (including a delayed FMIT class facility) can be made available to support experimentation and testing as they are required. The specific precursor facilities included in each scenario will be better defined during the 1985 FINESSE program.

## 16.4 Fusion Experimental and Test Facilities

As a first step towards the evaluation of fusion technology development scenarios, a set of generic definitions for major fusion facilities were developed. These definitions, summarized in Table 16.4-1, apply to both tokamaks and tandem mirrors (as well as other confinement concepts) and were used as guidelines in the construction of the various development pathway scenarios. It is not required that each pathway include each type of facility. For example, several of the candidate pathways which have been included in the preliminary evaluation move directly from a plasma burning experiment (PBX) to an engineering test facility (ETF). Others include an early fusion engineering research facility (FERF), but eliminate the first generation ETF and replace it with a more advanced engineering test facility which can be upgraded to a first generation engineering demonstration facility (EDF). Such a facility is designated as an ETF/EDF and is considered to be about 1/2 step beyond the first generation ETF of Table 16.4-1.

### 16.4.1 Plasma Burning Experiment (PBX)

The primary mission of the plasma burning experiment is to develop an understanding of the scaling and physics optimization of burning plasmas. This generally requires a regime of operation such that the plasma is heated by its alpha debris (i.e., very high plasma gain or ignited operation). A second requirement, long pulse operation, is intended to ensure that the plasma operates in a stable equilibrium and that impurities can be controlled. For a given confinement concept, the configuration should be reactor relevant enough to resolve all of the major plasma physics issues associated with that concept.

Table 16.4-1. Descriptions of Major Fusion Development Pathway Facilities

| | PLASMA BURNING EXPERIMENT (PBX) | FUSION ENGINEERING RESEARCH FACILITY (FERF) | ENGINEERING TEST FACILITY (ETF) | ENGINEERING DEMONSTRATION FACILITY (EDF) |
|---|---|---|---|---|
| Mission | Develop understanding of burning plasma operation and optimization. | Investigate operation of fusion components in a high duty cycle nuclear environment. | Optimize and test fusion technologies using a reactor relevant mode of operation. | Provide an engineering demonstration of the technology at reasonable availability |
| Description | Configuration relevant to resolve major plasma physics issues. | Configuration relevant to nuclear experimentation. Capability for several experiments. | Fully integrated environment suitable for testing majority of interactive effects. | Nearly all systems prototypical, but smaller than full scale commercial. |
| Minimum Flux/ Fluence Goals | Negligible | ~ 1 MW-yr/$m^2$ at ~ 1 MW/$m^2$ | ~ 4 MW-yr/$m^2$ at ~ 1.5 MW/$m^2$ | ~ 8 MW-yr/$m^2$ at ~ 3 MW/$m^2$ |
| Minimum Availability Goal | Negligible | Tens of runs per year | Ultimately ~ 30% | Ultimately ~ 50% |
| Risk/Schedule | Risk can be high. Should be first facility in path. | Risk as a neutron provider must be low. Experimental risk can be higher | Only test articles can be high risk. | Only higher fluence tests ($\gtrsim$4 MW-yr/$m^2$) can be risky. |
| Facility Examples | TFCX,[7] LITE,[8] MFTF-$\alpha$[9] | MFTF-$\alpha$ + T,[9] TDF[6], FED-R[10] | INTOR,[1] FPD,[11] | STARFIRE DEMO[12] |

The PBX facility is not required to develop nuclear components. Its fluence and availability goals must be sufficient to satisfy the physics experimental program. These are not expected to be very demanding. As the first long pulse fusion facility in the pathway, the risk associated with this facility can be high, but its operational flexibility should also be high such that significant reconfigurations would be possible should they be required to better optimize the physics mode and/or plasma engineering.

### 16.4.2 Fusion Engineering Research Facility (FERF)

The primary mission of the fusion engineering research facility is to explore scientific and engineering phenomena involving the operation of fusion components in a fusion environment. The tritium breeding blanket is typical of components which would be the focus of the FERF experimental program, but other components which would be investigated include plasma interactive components, instrumentation/control systems, remote maintenance systems, tritium control systems, safety systems, radiation tolerant magnetic coils, and environmental control systems.

The most important operational requirements for a FERF include steady state plasma operation or long burn with a high duty cycle, an ability to simulate act-alike performance for blanket modules (and other components), and the inclusion of a sufficiently large test cell area. A minimum neutron wall loading of about 1 $MW/m^2$ is required and a high fluence capability is desirable if the facility capital cost, tritium requirements, electricity costs, and other operating costs are reasonable in an overall budget context. The minimum fluence requirement of 1 $MW\text{-}yr/m^2$ reflects a modest minimum goal of performing early-life experiments and early failure mode identification as a precursor to an ETF/EDF class facility. This requirement would, most likely, be increased for a new FERF, but is consistent with the proposed upgrade of MFTF-B[9] to achieve a low fluence FERF capability. The FERF must have sufficient availability to meet its fluence goal and must have a low physics risk as a neutron provider. Specifically, the FERF does not require an ignited mode of plasma operation, but would most likely operate in a subignition, driven mode. The risk in screening blankets and other components (a primary mission) can be higher than the physics risk.

### 16.4.3 Engineering Test Facility (ETF)

The principal mission of an engineering test facility would be to test and optimize fusion components in a facility which operates in a reactor relevant physics and engineering mode. The facility itself would be fully integrated and suitable for testing a majority of interactive effects. Thus, in some proposed development pathways, the ETF would incorporate the missions of both the PBX and the FERF in a single, fully integrated facility.

The ETF is the first type of facility in the pathway that has a reasonably high minimum fluence goal. The minimum goal of 4 MW-yr/$m^2$ is sufficient to qualify components for intermediate fluence conditions in an engineering demonstration facility (EDF) if the later facility operates with a neutron wall loading of 3 MW/$m^2$, an average availability of 50%, and a structural lifetime goal of 4-5 years. If the ETF achieves its minimum flux and ultimate availability* goals of 1.5 MW/$m^2$ and 30%, then the annual fluence accumulation is 0.45 MW-yr/$m^2$ per year and it will require about 9 years operation at full availability to achieve the minimum fluence goal.

Although the ETF mission is attractive, it can be difficult to achieve in a single, early facility without being preceded by PBX and/or FERF type facilities. The ETF must have a low physics risk because of its ambitious technology mission. To support the fluence test goal, its technology must also provide a low risk. As discussed in Chapter 15, a requirement for tritium breeding compounds the difficulty in achieving such a goal for an INTOR class facility.

### 16.4.4 Engineering Demonstration Facility (EDF)

The primary mission of an engineering demonstration facility would be to provide a "classical" demonstration of fusion physics and technology, operating with prototypical and near-commercial-scale components at a high level of plant availability. The EDF is not required to produce economical power, but

---

* In this discussion, the facility availability is defined as the fraction of time that it operates. This quantity is usually designated as the overall average capacity factor.

should provide a basis to estimate the cost of power from a commercial-scale plant. An EDF is assumed to exist in every development pathway scenario.

The EDF minimum fluence goal of 8 MW-yr/$m^2$ reflects a minimum fluence requirement to qualify structural components for a first generation, commercial-scale fusion plant. That is, with a neutron wall load of 3 MW/$m^2$ and a plant availability of 60%, structural components in a commercial-scale plant would survive for 4.5 calendar years prior to being replaced. The EDF minimum fluence goal would require about 5 years operation at an ultimate availability of 50% and a 3 MW/$m^2$ neutron wall loading. The only high risk aspect of EDF operation would be the extension from 4 to 8 MW-yr/$m^2$.

### 16.4.5 Other Facilities and Combinations

The ETF/EDF facility combination was described earlier in Section 16.4. Other facilities and facility combinations, which reflect possible upgrades are defined as follows:

- SFE/SFE-U - Scientific Feasibility Experiments (SFE) such as TFTR and MFTF-B might be upgraded for scenarios which proceed directly from the SFE to an ETF. The SFE-U mission would be less ambitious than that of the PBX due to the limitations of existing facilities.
- PBX/FERF - An upgrade of a burning core experiment during a second phase to perform experimentation/testing in a fusion nuclear environment is a reasonable option for consideration, but is expected to substantially increase the initial cost of the PBX.

## 16.5 Preliminary Fusion Development Scenario Evaluations

### 16.5.1 Fusion Development Pathways

A list of generic fusion development pathways is provided in Table 16.5-1. Typical example cases for tokamak and tandem mirror development (designated T and M) are also shown. In some cases, a useful and analogous pathway for tandem mirror development was not identified.

Table 16.5-1. Generic Fusion Development Pathways and Typical Examples

A) SFE/SFE-U → ETF → EDF

1) T: TFTR/TFTR-U → INTOR → STARFIRE DEMO

2) M: MFTF-B/MFTF-U → FPD → EDF

B) SFE → PBX → ETF → EDF

1) T: TFTR → TFCX → ETF → EDF

2) M: MFTF-B → MFTF-α → FPD → EDF

C) SFE → PBX/FERF → ETF/EDF

1) T: TFTR → TFCX/TFCX-U → ETF/EDF

2) M: MFTF-B → MFTF-α+T → ETF/EDF

D) SFE/SFE-U, FERF → ETF → EDF

1) T: TFTR/TFTR-U, MFTF-α+T → ETF → EDF

2) T: TFTR/TFTR-U, TDF → ETF → EDF

3) M: NONE

E) SFE → PBX, FERF → ETF → EDF

1) T: TFTR → TFCX, MFTF-α+T → ETF → EDF

2) T: TFTR → TFCX, TDF → ETF → EDF

3) M: NONE

Table 16.5-1. Generic Fusion Development Pathways and Typical Examples (Cont'd)

F) SFE → PBX, FERF → ETF/EDF

1) T: TFTR → TFCX, MFTF-α+T → ETF/EDF

2) T: TFTR → TFCX, TDF → ETF/EDF

3) T: TFTR → TFCX, FERF (TOKAMAK) → ETF/EDF

4) M: MFTF-B → MFTF-α, TDF → ETF/EDF

G) SFE → PBX, FERF → EDF

1) T: TFTR → TFCX, FERF(TOKAMAK) → EDF

2) M: MFTF-B → MFTF-α, TDF → EDF

It is important to note that both major confinement schemes can contribute to a given development pathway. For example, both tokamak development pathways of generic pathway D (see Table) include FERF class facilities which would be small, neutral beam driven, tandem mirror test facilities (i.e., MFTF-α+T and TDF). Such facilities can be very attractive in the tokamak development pathways because they promise low fusion power at high power density with low capital cost, tritium and electrical power requirements. Also note that the major facilities in the examples are often generic rather than specific examples (e.g., the ETF facility for tokamaks in pathway B). In many cases, design studies have not yet defined a candidate facility close enough to the implied mission to be specified. This does not imply that

pathways which include generics are less valid than those which do not. Note also that we have not explored the possibility of alternative confinement concepts serving a role either as a FERF or as a primary development path.

### 16.5.2 Pathway Evaluation Guidelines

Preliminary evaluations hav been performed for a number of the pathways shown in Table 16.5-1. To perform the evaluations, a standard format, shown in Table 16.5-2, was developed. The top half of the form is an evaluation of the risk associated with each facility, while the bottom half is an evaluation of the milestone dates, professional resource utilization, and funding requirements for the overall pathway. With the exception of the milestone dates, the evaluation is performed on a subjective basis consistent with the discussion of the preceeding sections of this chapter.

Before discussing the individual evaluations, some discussion of the risk categories and the rules used to estimate the milestone dates will be useful. The various risk types shown in Table 16.5-2 are categorized as follows:

- Physics Risk - risk in providing plasma at the predicted performance.
- Nuclear Operational Risk - risk in providing nuclear systems reliability to support a testing/development program.
- Integration Risk - risk in integrating various interactive systems in a fusion reactor.
- Flexibility - ability to accommodate physics and/or technology failures and/or changes in mission.
- Nuclear Testing/Development Risk - risk in providing an adequate combination of flux, test area, etc. to assure a successful step to the next facility.

where the first four risk types are operational risks (i.e., those which affect the ability of a facility to reach its availability goal) and the fifth risk type relates to the risk in conducting an experimental program to test and develop nuclear components. Nuclear components are defined to include those components whose design is substantially impacted by operation in the nuclear/tritium environment.

Table 16.5-2. Common Form for Pathway Evaluations

| PATHWAY | | | | | |
|---|---|---|---|---|---|
| DESCRIPTION | | Facility #1 | Facility #2 | Facility #3 | Facility #4 |
| Class (example (op. date) | | | | | |
| OPERATIONAL RISK (Reliability) | Physics | | | | |
| | Nuclear | | | | |
| | Integration | | | | |
| | Flexibility | | | | |
| NUCLEAR TESTING/DEVELOPMENT RISK | | | | | |
| MILESTONE DATES | Engineering Feasibility | | | | |
| | Technology Demonstration | | | | |
| PROFESSIONAL RESOURCE UTILIZATION | Scientists | | | | |
| | Technologists | | | | |
| FUNDING REQUIREMENTS | Near Term | | | | |
| | Overall | | | | |

Three pathway milestones, which define a uniform set of development pathway goals, have been defined. These are designated according to the accumulated neutron fluence and overall facility availability as follows:

- Engineering Feasibility Milestone - the achievement of a 2 MW-yr/$m^2$ neutron fluence over several tests and test articles in a Fusion Engineering Research Facility (FERF) or an Engineering Test Facility (ETF).
- Intermediate Fluence and Availability Milestones - an accumulated neutron fluence of 4 MW-yr/$m^2$ on a sufficient number of act-alike component tests and/or test modules to resolve key development issues for the operation of an Engineering Demonstration Facility (EDF) at an average availability of ~30%.
- Engineering Demonstration Milestones - an accumulated neutron fluence of 8 MW-yr/$m^2$ on nuclear components and an average availability of ~50% in the near-prototypical Engineering Demonstration Facility (EDF).

The first of these, "engineering feasibility" is intended to be analogous to the "scientific feasibility" milestone for fusion plasma physics experiments. That is, an engineering system which reaches a neutron fluence goal of 2 MW-yr/$m^2$ is clearly operational in the sense that it has achieved a substantial overall operational availability (perhaps 25-35%) with operational tritium breeding/recovery/control systems, heat removal systems, remote maintenance systems, impurity control systems, RF heating systems, magnetics systems, and instrumentation/control systems.

The second milestone, "intermediate fluence and availability," is the first fluence goal in the pathway. As discussed in Section 16.4.3, the 4 MW-yr/$m^2$ fluence goal would be sufficient to qualify components for intermediate life conditions in an EDF. The "engineering demonstration" milestones correspond to the minimum fluence and availability which might be sufficient to qualify components for end-of-life conditions in the first commercial-scale fusion reactor.

The years in which these milestones are achieved depend upon assumptions regarding when the first facilities in each of the respective pathways might operate, the operating availabilities of those and subsequent facilities,

their respective neutron wall loadings (to achieve fixed fluence goals), and various interface assumptions.

The earliest operation dates which are assumed are as follows:

- PBX - 1992
- FERF - 1995
- ETF - 1997
- EDF - three years after intermediate fluence milestone.

In the case of PBX, the 1992 date is intended to be consistent with a 1988 construction start. The 1995 date for the FERF assumes a 1990 construction start (5-year construction). The 1997 operation date for the ETF assumes a 1991 construction start, corresponding to a six year construction period, and an additional one year delay in planning and design. The above dates are intended to represent the earliest possible dates. In pathways, which feature an ETF as a follow-on facility, construction of the ETF is delayed until one of the following events occur (as applicable to the Table 6.5-1 pathway being considered):

- The PBX facility operates for 2 years (Pathway Type B)
- The FERF facility operates for 4 years (Pathway Types C and D)
- Both of the above (Pathways E and F)

Additional assumptions are required for pathways which feature ETF/EDF type facility upgrades. To reduce risk, construction of an ETF/EDF is assumed to begin after the experimental program on the preceding facility has been completed. An 8-year construction period is assumed because the ETF phase must anticipate the EDF phase plant requirements. If the intermediate fluence milestones is achieved in a FERF prior to the ETF/EDF, it is assumed that the ETF/EDF mission will be to accumulate the demonstration milestone fluence as an initial mission beyond a 4-year facility startup (see below). If the intermediate fluence milestone is not achieved prior to the ETF/EDF, it is assumed that both milestones will be achieved in that facility, in a two-phase program. In this case, a 3-year retrofit between achievement of the intermediate fluence milestone and the beginning of operations towards the demonstration milestone is assumed.

Table 16.5-3. Neutron Wall Loading, Facility Availability, and Startup Assumptions for Development Pathways

| Facility | Neutron Wall Load | Average Availability | Startup Delay |
|---|---|---|---|
| FERF | 1.5 MW-yr/$m^2$ | 40%* | 4 yr** |
| ETF | 1.5 MW-yr/$m^2$ | 30% | 4 yr |
| EDF | 3.0 MW-yr/$m^2$ | 50% | 2 yr |
| ETF/EDF | 3.0 W-yr/$m^2$ | 30/50% | 4/3 yr |

* Reduce to 10% for special case of MFTF-$\alpha$ + T Upgrade.
** For FERF, startup delay includes initial experiment/test program at low fluence.

Neutron wall loading, average availability, and startup delay assumptions for the three nuclear facilities are given in Table 16.5-3. Note that the neutron wall loadings and availabilities for the FERF are significantly higher than the minimum acceptable values given in Table 16.4-1.

The final two categories of Table 16.5-2 describe funding requirements. The near-term funding requirement describes the level of funding through 1992 with a low funding level being consistent with funding less-than-or-equal to the current DOE budget (~ 440 $M in 1985), a moderate funding level being roughly consistent with a 40-50% funding increase, and a high funding level being consistent with an increase greater than 50%. The overall funding requirement is primarily influenced by the length of the program (e.g., the technology demonstration date) and the number of facilities.

### 16.5.3 Pathway Evaluations

The following tokamak development pathways were subjected to a preliminary evaluation during the first year of FINESSE: A1, B1, D2, E2, and F2. Pathways A1 and B1 are "conventional" pathways which have received a large amount of consideration during the past decade. Pathways D2, E2, and F2 are of particular interest because they attempt to utilize a tandem mirror FERF in a tokamak development pathway. For the preliminary evaluation, it is assumed that all pathways include an FMIT-class (but possibly more modest) irradiation

damage calibration prior to construction of the EDF. Pathways not considered in the preliminary evaluation will be considered during the first part of the second year of FINESSE.

16.5.3.1 Evaluation of Pathway A1

The Pathway A1 evaluation is summarized in Table 16.5-4. In this scenario, a physics upgrade of TFTR is assumed to operate in the 1990-1994 time frame and an ETF class facility (e.g., INTOR) is assumed to begin operation in 1997. After a 4-year startup, 4 more years are required to achieve the engineering feasibility milestone. The ETF characteristics of Table 16.5-3 enable it to reach the intermediate fluence milestone in 4.5 more years (i.e., 2010). The EDF (e.g., STARFIRE DEMO) begins operation in 2013. After a 2-year startup, the engineering demonstration milestone is attempted and, assuming success, it is achieved in 2020.

In this scenario, the ETF class facility is considered to be high risk for three reasons. First, it would represent the first facility to combine very long pulse and ignited plasma operation. Particular concerns include plasma equilibria and scaling, the efficiency of impurity control, and the response to, and control of, plasma disruptions. Second, because a large tritium breeding ratio will be required, such a facility will require many tritium breeding blanket modules. The difficulties of achieving a reasonably high overall availability, discussed earlier in this chapter (and in Chapter 15), may well be intolerable. Third, the number of interacting systems in an ETF class facility is very large. The integration risk is expected to be large because many of the reactor systems would operate in harsh environments together for the first time. Because the facility would be large and complex, the flexibility to implement major modifications and address fundamental design faults may not exist.

Scenario A1 makes good use of professional resources by providing challenging scientific and techological goals in the development of a relatively near-term ETF. The required funding is relatively low until about 1990 increases greatly during ETF construction, (1991-1997), and is low overall because the total number of major facilities is low.

Table 16.5-4. Evaluations of Pathway A1

| PATHWAY A1 | | | | | |
|---|---|---|---|---|---|
| DESCRIPTION | | Facility #1 | Facility #2 | Facility #3 | Facility #4 |
| Class (example (op. date)) | | SFE-U (TFTR-U (1990)) | ETF (INTOR (1997)) | EDF (STARFIRE DEMO (2013)) | |
| OPERATIONAL RISK (Reliability) | Physics | Moderate - physics test bed | Moderate-to-high - first very long pulse ignited operation | Low - done in ETF | |
| | Nuclear | Moderate - remote maintenance required | High - tritium breeding prior to fusion testing | Low - blankets previously tested to 5 MW-yr/$m^2$ | |
| | Integration | Low | High - first time many reactor systems together | Low-to-moderate - few new systems, but large scale | |
| | Flexibility | High | Low-to-moderate | Low | |
| NUCLEAR TESTING/DEVELOPMENT RISK | | No significant nuclear program | High - prospects for unanticipated failures/ low availability | Low-to-moderate - primary fluence accumulation | |
| MILESTONE DATES | Engineering Feasibility | 2005 | | | |
| | Technology Demonstration | 2020 | | | |
| PROFESSIONAL RESOURCE UTILIZATION | Scientists | Good | | | |
| | Technologists | Good | | | |
| FUNDING REQUIREMENTS | Near Term | Low-to-moderate | | | |
| | Overall | Low - few facilities | | | |

### 16.5.3.2 Evaluation of Pathway B1

The Pathway B1 evaluation is summarized in Table 16.5-5. In this pathway, a PBX class facility (e.g., one of the TFCX options currently under consideration) is inserted into the pathway prior to the ETF class facility. In this case, the PBX class facility provides a dramatic reduction in the physics risk of the ETF and can also reduce the integration risk and the need for ETF configurational flexibility. The latter observation will be especially valid for PBX options which tend towards reactor relevance (e.g., very long pulse options with reactor relevant plasma interactive components). It is, however, recognized that reactor relevant PBX options will be the most costly. The nuclear risk for the ETF of Pathway B1 is not reduced relative to the previous case.

In this scenario, a PBX is assumed to begin operation in 1992. After 2 years of PBX operation, ETF construction starts. ETF operation begins in 2000 with an initial test phase which terminates in 2004. The ETF is assumed to reach the engineering feasibility milestone in 2008 and its intermediate fluence milestone in 2013. The EDF begins operation in 2016 and is assumed to reach the engineering demonstration milestone in 2023.

This scenario makes good use of scientific expertise and manpower, but does not include a major techology facility early on and could contribute to a loss of interest among career fusion technologists. The required funding requires a significant increase in the near-term fusion budget, but appears to be moderate in an overall sense.

### 16.5.3.3 Evaluation of Pathway D2

The Pathway D2 evaluation is summarized in Table 16.5-6. In this pathway, an early FERF class facility (e.g., the tandem mirror TDF) is included, but a PBX class facility is not included. Instead, it is assumed that several of the plasma physics issues (e.g., long pulse, current startup, disruptions) can be usefully (but not completely) pursued in an SFE-U facility (e.g., a TFTR upgrade). The highest risk areas for this pathway are associated with the ETF class facility. Specifically, the physics risk is expected to be moderate-to-high because an SFE-U facility would not be able to fully explore

Table 16.5-5. Evaluation of Pathway B1

| PATHWAY B1 | | | | | |
|---|---|---|---|---|---|
| DESCRIPTION | | Facility #1 | Facility #2 | Facility #3 | Facility #4 |
| Class (example (op. date)) | | PBX (TFCX (1992)) | ETF (2000) | EDF ( 2016) | |
| OPERATIONAL RISK (Reliability) | Physics | Moderate - ignition/long pulse test bed | Low - done in BCX | Low | |
| | Nuclear | Moderate - remote maintenance | High - tritium breeding prior to fusion testing | Low - previous testing to 5 MW-yr/$m^2$ | |
| | Integration | Moderate - many near steady-state systems | Low-to-moderate - depends on PBX reactor relevance | Low-to-moderate - large scale | |
| | Flexibility | Moderate | Low-to-moderate | Low | |
| NUCLEAR TESTING/DEVELOPMENT RISK | | No significant nuclear program | Moderate-to-high - prospects for low nuclear system reliability | Low-to-moderate - primarily fluence accumulation | |
| MILESTONE DATES | Engineering Feasibility | 2008 | | | |
| | Technology Demonstration | 2023 | | | |
| PROFESSIONAL RESOURCE UTILIZATION | Scientists | Good | | | |
| | Technologists | Poor - distant goals | | | |
| FUNDING REQUIREMENTS | Near Term | Moderate | | | |
| | Overall | Moderate | | | |

Table 16.5-6. Evaluation of Pathway D2

| PATHWAY D2 | | | | | |
|---|---|---|---|---|---|
| DESCRIPTION | | Facility #1 | Facility #2 | Facility #3 | Facility #4 |
| Class (example (op. date)) | | SFE-U (TFTR-U (1990)) | FERF (TDF (1995)) | ETF (2005) | EDF (2021) |
| OPERATIONAL RISK (Reliability) | Physics | Moderate | Low - presuming success on existing experiments | Moderate-to-high - first very long pulse ignited operation | Low |
| | Nuclear | Moderate | Low - only limited high flux area | Low-to-moderate - FERF experience | Low |
| | Integration | Low | Moderate - first time many reactor systems introduced | Moderate-to-high - TFTR-U not reactor relevant | Low - lots of experience |
| | Flexibility | High | Moderate - small, but not facility | Low-to-moderate | Low |
| NUCLEAR TESTING/DEVELOPMENT RISK | | No significant nuclear program | Moderate - possibly test area limited | Low-to-moderate - $\sim$ 8 MW-yr/m$^2$ fluence goal | Low - assuming fluence goal achieved in ETF |
| MILESTONE DATES | Engineering Feasibility | 2002 | | | |
| | Technology Demonstration | 2028 | | | |
| PROFESSIONAL RESOURCE UTILIZATION | Scientists | Good | | | |
| | Technologists | Good | | | |
| FUNDING REQUIREMENTS | Near Term | Moderate | | | |
| | Overall | Moderate-to-High | | | |

burning plasma operation. The integration risk would fall into the same category because, although the tandem mirror FERF would provide nuclear testing and experience to the intermediate fluence regime, the ETF would be the first reactor relevant tokamak with many new systems (e.g., high duty cycle impurity control, complex remote maintenance).

In this scenario, the FERF is assumed to begin operation in 1995. After an initial test phase of 4 years, the engineering feasibility milestone is reached during 2002, and the intermediate fluence goal is reached during 2007. The ETF construction phase begins 4 years after initial operation of the FERF and the ETF begins operation in 2005. After a 4-year startup, the intermediate fluence goal is achieved for the second time in 2018. The EDF begins operation in 2021 and achieves the technology demonstration milestone in 2028.

This scenario makes good use of engineering manpower resources throughout, but does not fully utilize scientific manpower in the late 80's and early 90's. The required near-term funding is moderate, increasing in the 1990 time frame. Nevertheless, the relatively large total number of major facilities and the duration of the program (~45 years) are expected to result in a moderate-to-high overall funding requirement.

#### 16.5.3.4 Evaluation of Pathway E2

The Pathway E2 evaluation is summarized in Table 16.5-7. In this pathway, an early PBX (e.g., a TFCX option) is substituted for the SFE-U facility of Pathway D2. The primary advantage of this pathway is that the physics risk associated with the ETF is dramatically reduced because the PBX can be used to explore plasma physics scaling and long pulse operation in a regime which is also relevant (albeit somewhat scaled down in size and power) to ETF operation. To the extent that the PBX addresses and incorporates new issues and component technologies that are relevant to the ETF, the integration risk for the ETF will also be reduced. Recognizing that a FERF (e.g., the tandem mirror TDF) is also in the pathway, it is especially important to the success of this pathway that the tokamak PBX begin to address those ETF issues and technologies which are unique to tokamaks. The three highest priority items are considered to be disruption control, plasma interactive component (e.g., limiter/divertor) lifetime, instrumentation control systems, remote maintenance systems, and superconducting coil structural interactions.

Table 16.5-7. Evaluation of Pathway E2

| PATHWAY E2 | | | | | |
|---|---|---|---|---|---|
| DESCRIPTION | | Facility #1 | Facility #2 | Facility #3 | Facility #4 |
| Class (example (op. date)) | | PBX (TFCX (1992)) | FERF (TDF (1995)) | ETF (2005) | EDF (2021) |
| OPERATIONAL RISK (Reliability) | Physics | Moderate | Low | Low - due to TFCX | Low |
| | Nuclear | Moderate | Low | Low-to-moderate | Low |
| | Integration | Moderate | Moderate | Moderate - adding TFCX + TDF experiences | Low |
| | Flexibility | Moderate | Moderate | Low-to-moderate | Low |
| NUCLEAR TESTING/DEVELOPMENT RISK | | No significant nuclear program | Moderate | Low-to-moderate | Low |
| MILESTONE DATES | Engineering Feasibility | 2002 | | | |
| | Technology Demonstration | 2028 | | | |
| PROFESSIONAL RESOURCE UTILIZATION | Scientists | Good | | | |
| | Technologists | Good | | | |
| FUNDING REQUIREMENTS | Near Term | High | | | |
| | Overall | High | | | |

In this scenario, a PBX is assumed to begin operation in 1992 and a FERF is assumed to begin operation in 1995. The engineering feasibility milestone is achieved in 2002 and the intermediate fluence goal is achieved in the tandem mirror FERF during 2005. The ETF begins operation in 2005 (similar to Pathway D2) and repeats the intermediate fluence goal in 2018. The EDF operates in 2021 and achieves the engineering demonstration milestone in 2028.

This scenario makes good use of scientific and engineering manpower, especially in the near term. The required near-term funding level is, however, considered to be high due to the specification of two major facilities for completion prior to 1995. Overall, the relatively large total number of major facilities, and the duration of the program result in a high long range funding level. It should be noted, however, that the lower risk associated with this path may, in practice, result in a lower overall cost than for higher risk pathways which may be prone to major failures. Thus, risk and cost must both be considered in the overall evaluation.

#### 16.5.3.5 Evaluation of Pathway F2

The Pathway F2 evaluation is summarized in Table 16.5-8. In comparison with the previous pathway, this pathway combines the ETF and EDF into a single upgrade facility, the ETF/EDF. In so doing, it is expected that a more ambitious program, with fewer major facilities, can be implemented to save cost while maintaining a reasonable level of risk. In this scenario, the physics risk remains low, while the integration risk and the operational risk for nuclear systems are expected to increase slightly because the EDF phase of operation will require that the ETF nuclear systems function adequately enough that only minor retrofits, if any, would be required in ensure reliable operation.

In this scenario, the PBX and FERF are assumed to follow the same schedule as in Pathway E2. The FERF achieves the engineering feasibility milestone in 2002 and the intermediate fluence milestone in 2005. Construction of the ETF/EDF is assumed to start in the same year (i.e., sequential), and operation is assumed to begin during 2013. The technology demonstration milestone for this facility might be achieved in 2023, after a 4-year ETF (startup) phase and about 5 years operation at a neutron wall loading of 3 $MW/m^2$ and a 50% average availability.

Table 16.5-8. Evaluation of Pathway F2

| PATHWAY F2 | | | | | |
|---|---|---|---|---|---|
| DESCRIPTION | | Facility #1 | Facility #2 | Facility #3 | Facility #4 |
| Class (example (op. date)) | | PBX (TFCX (1992)) | FERF (TDF (1995)) | ETF/EDF (2013) | |
| OPERATIONAL RISK (Reliability) | Physics | Moderate | Low | Low | |
| | Nuclear | Moderate | Low | Moderate | |
| | Integration | Moderate | Moderate | Moderate-to-high | |
| | Flexibility | Moderate | Moderate | Low | |
| NUCLEAR TESTING/DEVELOPMENT RISK | | No significant nuclear program | Moderate | Low | |
| MILESTONE DATES | Engineering Feasibility | 2002 | | | |
| | Technology Demonstration | 2023 | | | |
| PROFESSIONAL RESOURCE UTILIZATION | Scientists | Good | | | |
| | Technologists | Good | | | |
| FUNDING REQUIREMENTS | Near Term | High | | | |
| | Overall | Moderate | | | |

Professional resource utilization for this scenario is well balanced with respect to both scientists and technologists. Although the near term costs are high, the long range costs are moderate because a separate ETF is eliminated from the pathway.

## 16.6 Summary and Conclusions

A framework for considering and evaluating fusion development pathway scenarios has been proposed and exercised for several cases among a larger list of potential pathways which have been identified. This work will be expanded in both scope and detail during 1985, and it is emphasized that the results reported in Section 16.5 are of a preliminary nature.

### 16.6.1 Near Term Experimental Progam

As a general trend, it is clear that all technology development pathways would utilize existing experimental facilities to the greatest extent possible during the next 10 to 15 years. Importantly, fision reactors can be especially useful in investigating tritium recovery/transport phenomena in solid breeder blankets, while non-nuclear partially integrated test facilities (PITF) can be especially useful in investigating MHD and surface heart flux related issues for liquid metal blankets.

The use of accelerator-based neutron sources for neutronics experiments is clearly desirable. The use of accelerator-based neutron sources for irradiation damage experiments is also desirable, but will be expensive (i.e, hundreds of millions of dollars) relative to other near-term tests. If lower cost neutron damage sources cannot be identified, the fusion program might omit such facilities and accept a higher level of risk through an engineering demonstration facility (EDF). A preferred alternative would be to delay operation of an FMIT class facility such that it operates later in the program, in parallel with an engineering test facility (ETF) or a fusion engineering research facility (FERF).

### 16.6.2 Preliminary Pathway Evaluations

Comparing development pathways A1, B1, D2, E2, and F2 of Section 16.5, our preliminary ranking would be in reverse order of the above list (i.e, F2 ranks highest). As shown in Table 16.6-1, pathway A1, featuring a scientific

feasibility experiment upgrade (SFE-U) followed by an engineering test facility (ETF), is expected to result in a high level of risk despite impressive cost and schedule attributes. In our judgment this level of risk is unacceptable. Pathway B1 reduces the level of risk by providing a plasma burning experiment (PBX) prior to the ETF. Nevertheless, the risk in integrating and testing nuclear components in the ETF remains high.

Table 16.6-1. Summary of Preliminary Evaluations

| Pathway | A1 | B1 | D2 | E2 | F2 |
|---|---|---|---|---|---|
| Fusion Facilities | SFE-U<br>ETF<br>EDF | PBX<br>ETF<br>EDF | SFE-U<br>FERF<br>ETF<br>EDF | PBX<br>FERF<br>ETF<br>EDF | PBX<br>FERF<br>ETF/EDF |
| Overall Operational Risk | High | Mod-to-High | Mod-to-High | Low | Low |
| Nuclear Testing/ Development Risk | High | High | Low-to-Mod | Low-to-Mod | Low-to-Mod |
| Engineering Feasibility Milestone Date | 2005 | 2008 | 2002 | 2002 | 2002 |
| Engineering Demonstration Milestone Date | 2020 | 2023 | 2028 | 2028 | 2023 |
| Near-Term Funding Required | Low-to-Mod | Mod | Mod | High | High |
| Overall Funding Required | Low | Mod | Mod-to-High | High | Mod |
| Rank (No. 1 = Best) | 5 | 4 | 3 | 2 | 1 |

Pathway D2 removes the PBX, but adds a fusion engineering research facility (FERF). In this case, the nuclear risk is reduced, but the physics risk is increased relative to pathway B1. The time required to achieve the demonstration milestone is extended by about 5 years, increasing the overall funding requirements.

Pathway E2 features both a PBX and a FERF. In this case, the risk is acceptable, but the near-term and overall costs are large due to the large number of major facilities. Some apparent advantage is provided by combining the engineering test facility and the engineering demonstration facility in pathway F2. In the later case, the risk is increased, but the overall cost and schedule are improved. Consequently pathway F2 appears to be the most attractive of those considered in the preliminary evaluation.

Additional pathways which appear to be promising include those which feature a PBX and a low fluence FERF (e.g., MFTF-$\alpha$+T upgrade of Chapter 13) leading to an ETF or an ETF/EDF. Comparing the latter cases (i.e., pathways E1 and F1) with pathways E2 and F2, the risk would increase somewhat, but the engineering demonstration milestone would be achieved more quickly and the near-term funding requirement would be more moderate. The inclusion of an FMIT class facility in such a pathway would help to ameliorate the risk.

### 16.6.3 International Implications

Clearly, pathways E and F, featuring PBX and FERF facilities in parallel, imply a near-term funding requirement which is in excess of current fusion funding levels of any of the large national and multinational programs in the U.S., Europe, or Japan. Consequently, international cooperation might prove to be the most effective means of achieving a well balanced and aggressive fusion development program. Although the FINESSE program has made no serious attempt at defining an international strategy which resolves the myriad institutional difficulties which would be sure to arise, some reasonable observations regarding possible frameworks for such a venture follow.

First, it is observed that many facilities could be involved in an international strategy. These might include (but would not be limited to) non-nuclear test stands, partially integrated test facilities, point accelerator neutronics facilities, fission test reactors, accelerator based irradiation damage facilities, scientific feasibility experiments for advanced confinement

concepts, plasma burning experiments for established confinement concepts, fusion engineering research facilities, and fusion engineering demonstration facilities. Consequently, many opportunities for international cooperation can be available.

Second, it is observed that the time to develop fusion will be long and that no nation is likely to derive an early economic advantage. Consequently, the philosophical basis for a long range developmental agreement exists.

Third, three cooperative mechanisms are apparent candidates for an international participation:

- Several nations could jointly sponsor the same, shared facilities and experimental programs
- Individual nations could construct and operate separate, but complementary facilities
- Several nations could jointly sponsor one or more "user facilities" (e.g., a FERF) and maintain their autonomy by conducting separate experimental programs.

The first of these would be the most efficient, but the most difficult to arrange. The second option, although efficient, would be costly for the individual participants. The third option has attractive attributes, but the operational implications (e.g., number of required test ports) could prove to be excessive. These options will be more fully explored during the second year of FINESSE.

## References for Chapter 16


1. "International Tokamak Reactor," Phase Two, Part I, International Atomic Energy Agency, Vienna, Austria (1983).

2. P.J. Gierszewski, CFFTP/UCLA, personal communication, April, 1984.

3. M.A. Abdou, et al, "Blanket Comparison and Selection Study - Interim Report," ANL/FPP-83-1, Argone National Laboratory (1983). Final Report in preparation at ANL.

4. "Reliability and Maintainability Management Handbook," NAVAIR 01-1A-31, U.S. Naval Air Systems Command (1977).

5. W.M. Stacy, et al, "U.S. FED-INTOR Activity...Critical Issues," FED-INTOR/TEST/82-2, Georgia Institute of Technology (1982).

6. J.N. Doggett, et al, "A Tandem Mirror Technology Demonstration Facility," UCID-19328, Lawrence Livermore Laboratory (1983).

7. Papers presented at the Tokamak Fusion Core Experiment Design Review, Princeton Plasma Physics Laboratory, June 6-8, 1984.

8. L. Bromberg, et al, "A Long Pulse Ignited Test Experiment - (LITE)," Nucl. Tech./Fusion, 4, 2, 1013 (1983.

9. K.I. Thomassen and J.N. Doggett (editors), "Options to Upgrade the Mirror Fusion Test Facility," UCID-19743, Lawrence Livermore National Laboratory (1983).

10. D.L. Jassby and S.S. Kalsi (editors), "FED-R-A Fusion Engineering Device Utilizing Resistive Magnets," ORNL/FEDC-82/1, Fusion Engineering Design Center (1983).

11. C.D. Henning, et al, "Fusion Power Demonstration: Baseline Report," UCID-19975, Lawrence Livermore National Laboratory (1984).

12. M.A. Abdou, et al, "A Demonstration Tokamak Power Plant Study (DEMO)," ANL/FPP/82-1, Argonne National Laboratory (1982).

# APPENDIX A

# EVALUATION OF EXPERIENCE FROM FAST BREEDER REACTORS

TABLE OF CONTENTS


| | | Page |
|---|---|---|
| A.1 | Introduction | A-1 |
| A.2 | History of LMFBR Development | A-4 |
| | A.2.1 Genesis | A-4 |
| | A.2.2 The National Laboratories and Early U.S. Fast Reactors | A-5 |
| | A.2.3 Early Industry Initiatives | A-11 |
| | A.2.4 Establishment of a Priority Breeder Program | A-14 |
| | A.2.5 LMFBR Program Planning | A-16 |
| | A.2.6 Fast Flux Test Facility | A-17 |
| | A.2.7 Developments Leading to LMFBR Commercialization | A-19 |
| | A.2.8 Institutional Constraints on LMFBR Development | A-24 |
| | A.2.9 Overview of Foreign Fast Reactor Program | A-27 |
| A.3 | Technical Program Developments and Problems | A-29 |
| | A.3.1 Fuels and Materials | A-29 |
| | A.3.2 Components Development | A-35 |
| | A.3.3 Safety | A-45 |
| | A.3.4 Experimental Reactors and Plant Design | A-57 |
| A.4 | Summary Observations and Conclusions | A-64 |
| | References | A-72 |

# APPENDIX A. EVALUATION OF EXPERIENCE FROM FAST BREEDER REACTORS

## A.1 Introduction

The attempt to develop the fusion process as a useful power source has brought to light many questions regarding the engineering feasibility of such a source once it has been proven feasible from a scientific point of view. Beyond the fundamental questions of initiating and maintaining the nuclear reactions in the system, one must consider the mechanisms for extracting the energy, fueling the reaction, and maintaining the integrity of the system over a period long enough to make the system economically attractive. These problems in total constitute the increasingly important field of fusion technology. As with any developing technology, it will be built on an extensive experiment and testing program that not only provides data for detailed model construction and calibration, but eventually must provide proof tests for many of the integrated systems prior to the contruction of a meaningful, working pilot plant.

Without question, a testing program is required to advance any technology. In most complex engineering systems, the interactions among numerous phenomena arising in design, construction, and operation are far too complicated to predict with confidence, even if the interactions could be properly enumerated. And simply listing the possible interactions is, in itself, a task that introduces uncertainty. A properly planned program of separate-effects (phenomenological) testing and integral testing can resolve many of these uncertainties, permitting more effective use of a full-scale machine. Obviously, such a program is an essential part of developing the technology necessary to make the fusion reaction a useful source of energy.

In defining and developing a fusion testing program, there is a benefit to examining the programs of other technologies. Such an examination might produce a better understanding of the role of testing, the advantages and costs, the process by which testing technology itself develops, and the manner in which a working system evolves from a testing program. Particular benefit is derived from a study of the testing program in the development of fast breeder reactors - an effort that parallels the fusion program in at least two important areas: the use of liquid metals as a heat transfer agent, and the fact that a neutron field is formed by the nuclear reaction. It is clear from

fusion systems now being studied that these parallels may not persist (that is, not all fusion systems under consideration produce large amounts of neutrons or use liquid metals); but the fact that these parallels exist, and that both programs will result in large nuclear/mechanical systems for energy production, makes the study particularly interesting and significant.

On an international scale, the technology of liquid-metal-cooled breeder reactors is rapidly approaching maturity. The development began in the U.S. in 1946 with the construction of the small Clementine reactor (discussed later) and is currently reaching commercial scale with the construction of the 1200 MWe Super-Phoenix reactor in France. Reaching this point of maturity required development in all areas of breeder reactor technology: physics, materials, components, safety, and system design. Because of the markedly different missions in each area, there were equally different testing requirements, testing approaches, data requirements, and decision processes in the respective programs. In some cases scale models were useful only in a separate-effects test; in others, integral scale models immediately preceded prototype testing. Some efforts required simulant materials, others used only real materials. Some efforts required a neutron-radiation environment, others avoided it. Some tests could be run only on a full-scale operating plant; others could be isolated and examined under more controlled conditions. But in spite of their diversity, there are some common experiences that not only cross technical areas in breeder research, but also may extend to other technologies such as fusion power. We will attempt to elaborate on some of these experiences in the following report.

We begin with a brief history of breeder reactor development to establish a chronological framework for the discussions that follow and to illustrate the progress of this major technological effort. (Figure A-1 summarizes the major decisions and events in the development of the breeder.) We will then briefly describe some of the planning that was an important part of the testing program for the maturing technology, and the impact of more recent developments in breeder reactor research. Following that, we discuss some of the highlights of the testing programs in several areas of breeder research, with elaborations on selected examples. From these examples and the summarizing observations, it is hoped that the reader will derive an understanding of the role of testing and need for testing in technology development. Our

# PANORAMA OF LMFBR PROGRAM EVENTS

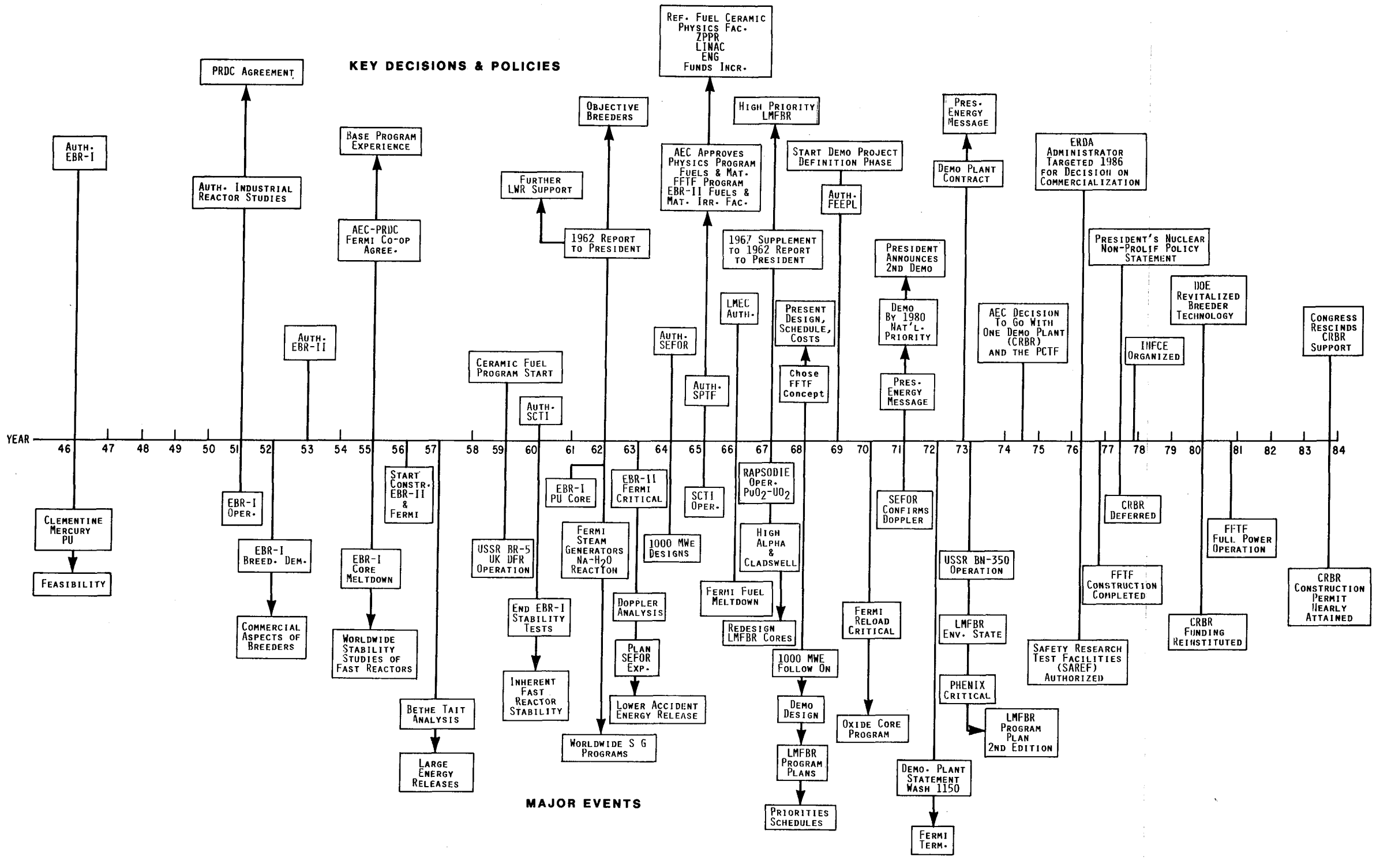


Figure A-1.

purpose is not to give a broad overview of breeder reactor testing, but rather to describe a few specific experiences that seem to demonstrate the overall approach to testing and the problems typically encountered in the program. With such a background of breeder experiences, the worker in fusion technology can then extrapolate the experiences to his or her own program and possibly direct a more efficient effort in the use of testing for fusion reactor development.

## A.2 History of LMFBR Development

### A.2.1 Genesis

The unique characteristics and potential of fast breeder reactors were recognized early. In fact, the birth of fast breeder reactor technology may be traced to the years during World War II when extensive efforts were devoted to the subject of nuclear fission. Obvious, even then, was the possibility of fuel breeding, but little of a tangible nature emerged during this period to demonstrate the validity of the concept.

In the period following World War II, the understanding, equipment and techniques developed in the wartime nuclear programs were turned to peaceful applications of nuclear technology. On August 1, 1946, the President signed into law the Atomic Energy Act which became the first vehicle for developing nuclear power. Shortly thereafter, the President announced the appointment of a five-member commission to administer all aspects of the nation's nuclear affairs. One month after its formation, the U.S. Atomic Energy Commission (AEC) became the custodian for extensive research and development facilities situated throughout the United States.

Subsequently the AEC became part of the U.S. Energy Research and Development Administration (ERDA), in January, 1975 (at which time the Nucleear Regulatory Commission, NRC, absorbed the functions of the AEC,s Regulatory Division). And later still, the ERDA was transformed into the Department of Energy (DOE). The jurisdiction over all research and development in the U.S. associated with the Liquid Metal-Cooled Fast Breeder Reactor (LMFBR) resided in each of these organizations, in turn, and involved direction of the work through National Laboratories, private industry, utilities, and universities.

### A.2.2 The National Laboratories and Early U.S. Fast Reactors

To hasten and promote the peaceful applications of nuclear technology, the system of Federally-supported National Laboratories was instituted in the late 1940's. Of these, Los Alamos Scientific Laboratory (LASL) and Argonne National Laboratory were assigned the principal responsibilities for pioneering early LMFBR technologies. Four facilities built and operated by these laboratories merit discussion for their contribution to LMFBR technology: Clementine; Experimental Breeder Reactor-I (EBR-I); the Los Alamos Molten Plutonium Reactor Experiment (LAMPRE); and Experimental Breeder Reactor-II.

#### A.2.2.1 Clementine

Clementine was the world's first liquid metal-cooled fast reactor. It was designed, built, and operated by Los Alamos Scientific Laboratory to: serve as a critical facility for investigating the effects of fuel configuration on criticality; provide a copious source of undermoderated neutrons for physics studies; study and evaluate the feasibility of controlling fast neutron systems; and provide information concerned with the breeding of plutonium as a fuel for larger LMFBR's.

The concept of Clementine, like EBR-I, originated during the war years. As the war years came to a close, realization of the potential of breeding systems, spurred on initiation of conceptual design studies on a modest facility that would demonstrate the feasibility of operating a plutonium-fueled fast neutron system capable of producing power. The construction of Clementine was formally proposed in November 1945, approval was given the following month, and design work begun immediately. Construction began in September 1946, and criticality experiments were performed as early as November 21, 1946, even though the facility was technically still under construction. Construction resumed during February 1947, and continued intermittently until January 1949. In March 1949, the system was brought to full operating power at 25 kWt.

The fuel material consisted of delta-phase plutonium machined into rods 0.647 in. in diameter and 5.5 in. long, surrounded by tubes of Type 1020 steel, 0.020 in. thick, as cladding. Reflector rods containing natural uranium were fabricated to the same dimensions and used the same cladding. Fuel and reflector rods were fixed on a hexagonal pitch between a system of

upper and lower positioning plates which allowed for the flow of coolant. When fully assembled for operation the core consisted of 35 fuel and 20 reflector rods arranged in a cylindrical bundle about 5.9 in. in diameter. The core assembly was contained in a 46-in. long, 6.2 in. outside diameter, mild steel cylinder, 0.10 in. thick. Immediately above the core, and extending to the top of the containment cylinder was a removable relector and shield plug. The containment cylinder, or pot, was surrounded by a 6-inch steel reflector and four inches of lead. Additional shielding consisted principally of layers of borated plastic, steel and, finally, concrete.

Coarse reactivity control was effected by a large block of uranium located directly under the core. Raising the uranium block increased reactivity through increased relectivity. Dropping the block under gravity provided scram capability. Fine control of reactivity was provided by two uranium rods which moved vertically outside the pot in the radial reflector. Two safety rods, composed of sections of uranium and boron-10, were also located in the radial reflector. When operating, the uranium section was inserted in the reflector. During shutdown the rods were lowered and reduced reactivity even further by the insertion of boron.

Criticality at one watt was reached on November 21, 1946. Several low power tests (at one watt) were completed in the following months, including: a measurement of critical mass; an evaluation of control problems; and measurements of the isothermal temperature coefficient, neutron spectrum and delayed neutron fraction.

After work on the biological shield was completed, by December 1947, additional measurements were made with the shield installed, including the effects of alpha-phase plutonium on reactivity, neutron distributions in the core and reflector, danger coefficients, and activation croos-sections.

Final assembly and closure with the mercury system operating was achieved in February 1949. Shortly thereafter, the system was brought to full power. From March 1949 until December 1952, Clementine served as a valuable, highly intense source of undermoderated fisson neutrons for a variety of experiments, which led to refinements in cross-section data and neutron parameters. In addition, the operation of Clementine at power demonstrated the ease of control action for plutonium-fueled systems.

In December 1952, a fuel rod ruptured and plutonium entered the coolant system. Since all original objectives had been met, Clementine was shut down and dismantled.

### A.2.2.2 Experimental Breeder Reactor-I (EBR-I)

At the urging of Enrico Fermi, ANL undertook, in late 1944, to plan a small-scale proof-test facility for proving the validity of the breeding principle and to evaluate the feasibility of using a liquid metal as coolant. General plans for the facility, which eventually became EBR-I, were reasonably complete by late 1945. This design was planned to employ fast neutron fissioning to minimize parasitic meutron capture loses.

The years 1945 to 1949 were spent firming up the nuclear and engineering design. In addition to the paucity of fast neutron physics data, little was known about liquid metal pumping, sodium and potassium corrosion, NaK-to-water heat exchangers, and the behavior of fuel, cladding and structural materials under the hostile environments of radiation and temperature. Nevertheless, design parameters were fixed, sometimes on the basis of the best information available, and sometimes as a matter of intuition and judgement.

Construction began at the National Reactor Testing Station (NRTS) in Idaho in October 1949. Criticality was achieved in August 1951, and full power operation at 1.1 MWt was reached on December 19,1951. On December 20, 1951, useful electric power was generated from nuclear fission for the first time.

In the course of its useful life, EBR-I operated with four different fuel loadings. The first of these, Mark I, was fueled with cylindrical slugs of fully enriched uranium metal contained in Type 347 stainless steel tubes. NaK in the annulus between the slugs and the tubes provided an adequate heat transfer medium. The Mark I fuel diminished in reactivity beyond that expected from burnup; this was attributed, correctly as it turned out, to axial fuel growth and after 3.5 x 10 6 T kW-hr of energy output, operations with this fuel were concluded. However, a breeding ratio of 1.01 ± 0.05, was achieved and it was clear that higher values for breeding could be achieved by reducing the pronounced neutron leakage and by fueling with Pu-239.

The operation with the Mark I loading also confirmed the theoretical prediction that the neutronic behavior of both fast and thermal systems below prompt critical should be identical. Other significant contributions appeared in the forms of realistic tests of fast reactor instrumentation, the production of "super-pure" plutonium in the outer blankets, and the confirmation that the liquid metal, NaK, could be pumped both centrifugally and electromagnetically.

A second loading, Mark II, consisting of uranium-2w/o zirconium was installed in February 1954, to study the effects of alloying on radiation resistance. The inclusion of zirconium significantly increased the integrity of the fuel; reactivity losses from axial growth were eliminated and became consistent with burnup predictions.

After it suffered an unintentional partial core meltdown during a planned transient test, the Mark II core loading was terminated. As a consequence of the meltdown incident, concern arose over the safe operation of future fast breeder reactors. To prove otherwise, the damaged core was replaced with a third one measurably responsive to fuel, coolant and structural expansions. As a result of an extensive experimental program, it was concluded that the instability noted in earlier core loadings could be eliminated by rather elementary changes in mechanical design.

The fourth and final loading in EBR-I was fueled entirely with metallic plutonium with 1.25 w/o of aluminum. Benefits derived from the operation of EBR-I with plutonium included:

(1) Assurance that there is nothing inherently hazardous in the operation of a plutonium-fueled system.

(2) Proof that the breeding ratio of a plutonium-fueled system can exceed that of a system fueled with U-235. Foil-activation experiment yielded a value of 1.27 + 0.08.

Following completion of the Mark IV tests in 1965, EBR-I was shut down, decommissioned, and in 1966 was declared a national historic landmark.

### A.2.2.3 Los Alamos Molten Plutonium Reactor Experiment (LAMPRE)

LAMPRE was designed, built and operated by the Los Alamos Scientific Laboratory to: demonstrate the feasibility of using molten plutonium alloys

as a fuel material for fast reactors; evaluate the relative merits of various binary and ternary plutonium alloys; and investigate the compatability of molten plutonium alloys with various containment materials. Among the four early LMFBR's discussed here, LAMPRE was in a sense the most visionary.

Research and development activities including criticality studies began in 1957; installation effort was completed in 1959. Wet criticality was reached during March 1961 and the system was operated at its design power level of 1 MWt shortly thereafter. After about 60 h of full-power operation a pronounced accumulated reactivity loss was noted. This was identified to be a result of a fission-product gas accumulation that tended to form bubbles. In April 1962, the system was reloaded with a fuel mixture without the carbide and plutonium carbide additives previously used. Operation with this fuel mixture continued uneventfully until September 1962, when a capsule failure released approximately 75 grams of fuel into the coolant. A few months later two additional releases were noted. In all three cases fuel was releaed rapidly under pressure. Although the coolant system was contaminated no evidence of gaseous fission products in the operating area was indicated. In all cases defective capsules were identified and removed.

A second loading, without the additives, reached criticality in April 1962. Operation with the second core continued until July 1963. The second core was unloaded in April 1964. Subsequent experiments with ternary plutonium alloys were conducted, until operations were concluded upon program cancellation in 1965.

Aside from the problems of fuel-frothing, bubble accumulation, reactivity loss, and capsule failure the operation of LAMPRE was characterized by extreme stability. At no time was there any evidence of control problems originating from frothing and bubble accumulation. The principal problem in the development of LAMPRE was the design and construction of a capsule that could provide adequate containment of the molten fuel. Material choices were eventually narrowed to various tantalum alloys or to "super-pure" tantalum.

### A.2.2.4 Experimental Breeder Reactor-II (EBR-II)

The initial success of EBR-I in the early 1950's encouraged further plans for the exploitation of the fast breeding principle. At the request of the then-AEC, ANL in 1953 submitted a proposal for a second and larger liquid

metal-cooled fast reactor. This system, later known as EBR-II, was conceived as a pilot plant and as an intermediate step toward a full-scale commercial fast breeder. Although much useful information was derived from EBR-I, additional information was clearly needed for the design of much larger systems.

The initial design of EBR-II embodied higher power densities to evaluate the performance of fuel, cladding, and structural materials under higher fluence and temperature; to develop performance information on pumps, heat exchangers, valves, flowmeters, control rod drives, and kinetic stability; and to demonstrate the feasibility of metal-fueled fast reactors for central station power-plant use. Another important objective was to establish the feasibility of "closing the fuel cycle" through on-site fuel reprocessing by means of a contiguous and integrated facility for reprocessing spent fuel.

Site preparation began in October 1957, and formal construction began in December 1957. By May 1961, installation and construction effort was sufficiently near completion to permit planning of dry critical experiments (without sodium coolant), which were then carried out in late 1961. Measurements of the dry critical mass when compared with the wet critical mass, later determined, allowed for a measure of the overall sodium coefficient. The approach to wet criticality began on October 30, 1963, and criticality was reached on November 11, 1963, with a fuel loading of 181.2 kg U-235.

By June 1964, all systems including the secondary sodium, steam, and turbine generator were ready for operation. The approach to power was begun on July 16, 1964, and a power level of 37.5 MWt was reached on October 13, 1964. Reactor power was then raised in several sucessive steps to 62.5 MWt, the design level, in September 1969.

During the initial ascent to power in July 1964, measurements of the transfer functions were made. The results demonstrated conclusively the kinetic stability of the system for all credible reactivity insertions. As predicted from the lower power kinetic information, the neutronic performance of the system at 62.5 MWt was stable. Since that time EBR-II has continued to operate at 62.5 MWt with no evidence of anomalous reactivity effects.

Aside from problems of a relatively trivial nature, all major systems and subsystems have performed well. The following systems have been particularly trouble free: primary sodium, secondary sodium, steam, power plant, and plant

instrumentation (flow, temperature,pressure, etc.). Many dificulties have been experienced with the fuel handling and rotating plug systems, but even these were correctible by relatively simple modifications. Many years of operating experience have demonstrated the feasibility of conducting routine and special maintenance on FBR systems and components.

Since 1965, EBR-II has served as the nation's only facility for irradiation-testing of fuels, structural materials, absorbers, and sensors under conditions similar to those expected for more advanced FBR's. To date, EBR-II has generated over 1.5 billion kilowatt-hours of electricity.

### A.2.3 Early Industry Initiatives

In the private sector two fast reactor facilities deserve particular recognition. One of these, the Enrico Fermi Fast Breeder Reactor (EFFBR), was funded, designed, built, and operated at Laguna Beach, Michigan, by a consortium of two nonprofit organizations (Atomic Power Development Associates and the Power Reactor Development Company), with the principal member in each consortium being the Detroit Edison Company, a private stockholder-owned utility.

The other venture in the private sector was SEFOR (Southwest Experimental Fast Oxide Reactor), a highly specialized experimental facility that was designed, built, and operated as a joint venture of the Southwest Atomic Energy Associates, the Karlsruhe Laboratory of West Germany, Euratom, and the General Electric Company. Research and development effort was supported by the U.S. AEC.

#### A.2.3.1 Enrico Fermi Fast Breeder Reactor (EFFBR)

Interest in the construction and operation of a commercial size fast breeder reactor power plant began in the early 1950s when industrial groups were invited by the AEC to consider the economic and technical feasibility of generating electric power at a commercial level with nuclear-fueled systems. As a result APDA, a nonprofit research group, was organized in March 1955 to formulate the conceptual development of promising systems. In August 1955, a second nonprofit organization, PRDC, was formed to design, build, and operate a plant which was eventually named the EFFBR. The intent was to evaluate the economics of operating a commercial size sodium-cooled fast reactor for gener-

ating salable amounts of electricity, establish licensing and regulatory criteria for follow-on reactors, and evaluate the performance of large-scale plant systems.

A provisional construction permit was issued by the USAEC in August 1956 and work began immediately. For the next five years vigorous attempts were made by intervenors to halt construction activities. Despite such attempts, construction continued and in June 1961, the U.S. Supreme Court cleared the way for plant completion and ultimate operation. Nuclear operation at low power (about 1 MWt) began in August 1963 and continued through 1965, pending licensing for operation at 200 MWt. A provisional license to operate at 200 MWt was granted in December 1965.

The first nine months of 1966 were devoted to the testing of plant systems under 100 MWt operating conditions. During this period two difficulties were encountered. The once-through sodium-water steam generators developed leaks at the tube-to-tube sheet weld joints. A much more severe problem, however, was a flow blockage condition which became apparent on October 5, 1966, during a planned power-increase to 67 MWt. The initial evidence of difficulty appeared in two forms: an inconsistency between predicted and measured reactivity, and the presence of abnormal radiation levels as sensed by a gaseous fission product monitor. Upon such evidence the plant was shut down without further incident for investigative action.

As a result of intensive investigation the origin of the flow blockage was traced to a wedge-shaped zirconium piece which had dislodged from a conical flow guide, moved to a position which partially blocked the entrance flow to four fueled subassemblies, and caused fuel melting. As a result of fuel melting, gaseous fission products were released and the reactivity balance was upset by fuel rearrangement.

A formal report of the flow-blockage incident was submitted to the AEC in January 1969. Petition was made to continue with the ascent to power, and permission was granted in February 1970. Criticality was achieved in July 1970 and in October 1970 the plant was again operated at 100 MWt. Full licensed power of 200 MWt was reached on October 26, 1970. Operations continued with no evidence of previous difficulties. The subsequent test program under 200 MWt operating conditions verified the stability and performance of the reactor and plant systems.

At that time fuel supply was limited. Fuel discharged as the result of the 1966 flow blockage was awaiting requalification. Plans were made for reloading the core with uranium oxide fuel and increasing the power level to the original design level of 430 MWt. However, there arose difficulties in funding.

On November 27, 1972, the PRDC Executive Committee made the difficult decision to decommission the plant since it was evident that funding for a $50,000,000 uranium-oxide fuel-upgrade program could not be arranged. Of the total sum needed, $30,000,000 was pledged by American utilities and Japanese and Western European industrial groups. Had the requisite funding been realized, the EFFBR might very well be operating today.

### A.2.3.2 Southwest Experimental Fast Oxide Reactor (SEFOR)

The design, construction and operation of SEFOR was prompted principally by the need to demonstrate the safety characteristics of oxide-fueled fast reactors. SEFOR was a 20 MWt sodium-cooled, $PuO_2$-$UO_2$ fueled, experimental reactor constructed and operated in an international cooperative program involving Southwest Atomic Energy Associates (SAEA-a group of U.S. electrical utilities), General Electric Company, Gesellschaft fur Kernforschung (GfK), of Karlsruhe, West Germany, and the U.S. AEC. Design of the reactor began in 1966, and construction at the Fayetteville, Arkansas site was completed in 1968. The experimental program was completed in early 1972. The main objective of the project was to convincingly demonstrate the inherent safety of the LMFBR provided by the Doppler coefficient and to obtain an accurate measurement of the coefficient for application to large LMFBRs. An additional objective was to obtain further practical experience in the design, construction, licensing, and operation of a sodium-cooled fast reactor.

The need for experimental verification of the Doppler coefficient to make the LMFBR a viable reactor concept was recognized in the early 1960's, shortly after discovery of the existence of a substantial Doppler coefficient in fast reactors. This need was simultaneously recognized by scientists in the Federal Republic of Germany, who proposed to their government the construction of an experimental facility having objectives similar to the SEFOR project. In 1962, GE responded to the request for proposals from SAEA who were interested in contributing to the development of long-range, low-cost nuclear

energy and suggested the SAEA, together with GfK, GE, and AEC, embark on the SEFOR program.

The SEFOR experimental program, which began with core loading in April 1969, was successfuly completed in January 1972. The program consisted of a series of static, oscillation, and transient tests (both sub-prompt and super-prompt critical) with a core that had the characteristics of large LMFBRs. The super-prompt critical tests, in particular, provided a most convincing demonstration of the effectiveness of the Doppler coefficient in limiting the enrgy release in a fast reactor power excursion.

### A.2.4 Establishment of a Priority Breeder Program

In 1962, the AEC issued a report to the President on civilian nuclear power, which indicated that the use of nuclear breeder power plants could solve the problem of an adequate and economic energy supply for the future. The report concluded that nuclear power could and should make an essential contribution toward meeting the Nation's long-term energy requirements and that economic breeders were basic to achieving this goal.

During the early and mid-1960's, rapid advances were taking place in the development of light water reactor plants, and nuclear power moved towards commercial acceptance as a new competitive source of electrical energy. It was also recognized that the plutonium produced in the light water reactors could be most efficiently used in fast breeder reactors and that the advent of breeders would significantly reduce uranium ore requirements and demands placed upon the diffusion plants for uranium enrichments. The breeder development program was thus vested with a sense of mission and urgency which had been lacking earlier.

Early in 1965, the AEC initiated a series of technical reviews, aimed at evaluating the future course to be taken by the U.S. breeder reactor development program. These reviews indicated the need for additional engineering information, the construction of facilities, and the expenditure of other resources. There was clear evidence of the need for strengthening the engineering capabilities of the laboratories and industry and to assemble the necessary resources for achieving the development of safe, reliable, and economical breeder power plants suitable for operation in the utility environment. These early reviews also called for an in-depth review of the technical

elements of the breeder program and initiation of detailed plans for each of these elements (about which more will be said shortly).

In early 1967, the AEC issued the "1967 Supplement to the 1962 Report to the President on Civilian Nuclear Power." The supplement set forth the changes that had occurred since 1962 and considered the ongoing AEC reactor programs in relation to the recommendations of the 1962 report. The supplement reaffirmed the promise of the breeder for meeting the Nation's long-term energy needs. The report also took account of the results and implications of the worldwide LMFBR research and development effort.

In view of the priority established as the result of the civilian power program review that culminated in the 1967 Supplement to the 1962 Report to the President, the level of activity on the breeder reactor was substantially increased. The buildup to bring together the required resources, including manpower, facilities, and funds, for an effective overall research and development program continued within the AEC, the AEC laboratories, and other sectors of the nuclear community.

Several potential coolants that could be used in breeder reactors were evaluated, and sodium was selected because it offers the best combination of characteristics for a breeder reactor including: excellent heat transfer properties; low pumping power requirements; low system pressure requirements; the ability to absorb considerable energy under emergency conditions (due to its operation well below the boiling point); a tendency to retain many fission products within the sodium in the event of a release of fission products to the coolant system due to any fuel element failure; and excellent neutronic properties. The technology and related experience in its use as a coolant were considerable, while the negative aspects of sodium (such as its chemical reactivity with air and water, activation under irradiation, and opacity) were outweighed by its advantages.

The LMFBR was considered more promising than the other breeder concepts principally because of predicted performance, a broad base of technological experience, and proven basic feasibility. These advantages contributed to the expectation that this reactor system could be brought to a stage of commercial application in a relatively short time period.

### A.2.5 LMFBR Program Planning

In the middle to late 1960's, there came an increased awareness that careful and systematic planning and high standards in every phase of development, design, construction, inspection, test, and operation of nuclear power plants were essential to provide the safety, reliability, and economics needed for commercial operation. In recognition of these various programmatic and technical needs, the AEC initiated the preparation of the LMFBR Program Plan in 1966. In developing the plan, experiences from other large-scale nuclear power development programs were used in identifying relationships between program scope, technical management, available resources, and implementation of priorities.

It was recognized that a major reactor development program consists of the following three phases:

(1) Research and development phase--to confirm technical aspects of the concept, by: (a) Developing fuels and materials technology, (b) designing control instrumentation, (c) determining physics and heat transfer data, (d) providing engineering data for component design, and (e) constructing and operating facilities to provide design and component and system performance information.

(2) Engineering and manufacturing phase--to provide a broad industrial base, by: (a) Manufacturing and testing fuel, clad, and core hardware; (b) designing, building, and testing large components and systems; (c) building and testing reliable instrumentation; (d) conducting and developing overall prooftesting and quality assurance programs; and (e) developing and applying codes and standards.

(3) Utility commitment phase--to purchase, build, and operate commercial reactor plants: (a) Based on experience gained through the construction and operation of one or more demonstration plants.

To move successfully through these three phases and accomplish the overall goal of developing and demonstrating a technology that industry and utilities could apply at their option, the LMFBR Program Plan was formulated with the following objectives:

(1) To identify the technology required for design, constructing, testing, and operating commercially practicable LMFBR power plants.

(2) To evaluate the status of the existing technology and compare it with the identified technological requirements.

(3) To describe tasks that must be carried out to advance from the present technology to meet the unfulfilled requirements.

(4) To provide key input for a management system that would focus on key milestones, schedules, costs, status, and projections.

The first edition of the LMFBR Program Plan was issued in 1968 and reflected extensive reviews, judgments, and suggestions from essentially every segment of the technical community. This document which consists of ten volumes (USAEC Report WASH-1101-1110) was then implemented through more detailed work plans, and has proven to be highly successful in identifying and establishing for each element of the program the research and development efforts needed to meet the LMFBR program objectives.

A second edition of the LMFBR Program Plan was prepared and issued in 1973 (USAEC Report WASH 1101-1110, 2nd Edition), and which reflected the experience gained in the interim period, including consideration of the progress that had been made as well as the problems which had been encountered. With the prospect of the overall program moving into the large-scale engineering and demonstration phase, increased attention was given to those elements of the program crucial to the success of the demonstration and commercial LMFBR central station power plants.

### A.2.6 Fast Flux Test Facility

As part of the process that led to initiation of a formalized LMFBR program planning effort, a review of the status of the fuels and materials information then available revealed a significant lack of data from in-pile performance. At this same juncture, ceramic fuels, though lacking significant fast flux and sodium environment data, were selected as having the best potential to reach LMFBR objectives. Plutonium-uranium oxide was chosen as the reference fuel, with the carbide as an alternative. Simultaneously, increased emphasis was placed on the development of fuel cladding materials since reliable containment of fuels in an adequate cladding material in the LMFBR environment was a major problem.

While the testing of fuels and materials in the then exising facilities (EBR-II, FERMI, and some thermal reactors) was accentuated, it was proposed to meet the need for a facility capable of providing ample space in a prototypical fast-flux spectrum by building a new facility, called the Fast Flux Test Facility. The AEC decided in 1965 to undertake the construction of the FFTF, and work was initiated in 1966. Excavation work at the site near Richland, Washington began in December 1970, construction was largely completed by the end of 1977, and beneficial use attained early in 1980.

The FFTF is a nuclear complex consisting of a sodium-cooled fast flux test reactor and associated heat removal loops, coolant servicing systems, fuel handling systems, control systems, and facilities for waste disposal, post-irradiation examination, and maintenance. It is a loop-type plant with three primary sodium loops transporting heat from the reactor to intermediate heat exchangers (IHX). The IHXs in turn transfer the heat to three secondary sodium loops. Ultimate heat rejection is by sodium-air dump heat exchangers to ambient air. The overall cooling capability is 400 MWt.

Irradiation testing is accomplished in FFTF through use of driver fuel assemblies and special test assemblies located in the reactor core region. The special test assemblies fall into two categories: open test assemblies which are cooled by the reactor cooling system, and closed-loop assemblies which are cooled by independent sodium heat transport systems isolated from the reactor sodium environment. This isolation permits the achievement of temperature, pressure, and flow conditions beyond normal plant limits for fuel testing contained within the closed-loop cooling system, and limits possible radioactive contamination to the closed-loop cooling system.

Experience gained from the FFTF design and construction activity revealed some of the difficulties that arise in an undertaking of this complexity. In particular, the cost of the project increased considerably over original and successively revised estimates. Part of these difficulties stemmed from the general inflationary trends, part stemmed from the changing requirements imposed during design and construction, due to evolving environmental and safety considerations, and part from the stretch out in schedule.

### A.2.7 Developments Leading to LMFBR Commercialization

The methodology in the development of a technological base adequate for the realization of commercial LMFBR power plants has been the construction of a succession of fast breeder reactor facilities, each a conservative but significant extrapolation in size and engineering technology over its predecessor. This succession began with the Experimental Breeder Reactor-I, continued through the Experimental Breeder Reactor-II and the Enrico Fermi Atomic Power Plant, to the more recent Fast Flux Test Facility (FFTF), which, in addition to providing a facility in which to perform fuels and materials testing, also serves to add to the experience in design, construction and operation of an LMFBR plant at a significantly increased scale. The next step toward commercial plant construction has been embodied in the Demonstration Plant Program.

All of the LMFBR facilities — experimental and test — built to date, have been used in turn, first as the focus for development of technology and then as a vehicle for the application of current technology as well as the identification and development of the further technology required for the next facility. The experience gained in the development, design and construction of FFTF has been serving to identify the additional technology needed for the LMFBR demonstration plants, the next step in the succession. The demonstration plants will serve the same purposes in the design and construction of the initial commercial LMFBR plants.

The methodology described above was viewed as instrumental in achieving the government's objective of fostering a viable, self-sustaining LMFBR industry. The EBR-I, EBR-II, and FFTF facilities were entirely government funded, and the development leading to their construction was for the most part AEC-sponsored, (although signifcant contributions were made by the privately-funded FERMI and SEFOR, which was only partially funded by the AEC). In subsequent years, an increasing amount of development work has been funded by the utilities, in preparation for their roles in the LMFBR demonstration plant program. It has always been the intent that the later commercial plants be independent of government support and competitive in their own right with other commercial sources of electrical energy.

### A.2.7.1 Plant Studies Program

One of the early steps taken toward achieving the government's policy of ultimately atttaining a competitive LMFBR nuclear industry in a commercial market, to define the technology that must be developed, was the formation of the AEC Plant Study program. In 1963, the AEC sponsored a two year study effort on 1000 MWe LMFBR plant designs, in which four industrial contractors, or groups of contractors, participated. These first studies were limited to the reactor core, the reactor vessel, core instrumentation, control and safety systems, and fuel-handling mechanisms.

In 1967, a second set of studies, the so-called 1000 MWe Follow-on Studies, were initiated, in which the scope was expanded to include the total plant concept. The primary objective of these expanded studies was to identify the research and development needed. However, this objective was to be met through the development of plant design concepts which are optimized through detailed trade-off evaluations and parametric studies.

In the follow-on studies, five industrial contractors participated. Their work was divided into four major tasks, structured on the principle that before one can define the research and development needs, one must define the plant toward which the research and development is to lead. Therefore, the first three tasks defined various aspects of each contractors plant, and the fourth defined the research and development program. Task I comprised a concept-selection task, in which, through preliminary trade-off studies and analysis, each contractor arrived at a selection of his own company-favored preliminary reference concept of a plant that could be marketed commercially in the 1975 to 1985 time frame, and be in commercial operation in 1980 to 1990 time period. The second task was one of more detailed engineering leading to a fairly well-defined design and the preparation of System Design Descriptions on the major plant systems. The third task was then to evaluate and optimize the concept by performing detailed trade-off evaluations on various plant features leading to plant optimization, and the preparation of capital and operating cost estimates to define the economics.

The results of these plant design studies helped define a reference design concept for a 1000 MWe LMFBR plant which could then be factored into the design of the first demonstration plants.

### A.2.7.2 LMFBR Demonstration Plant(s)

The demonstration plant, along with the related industrial engineering efforts, was viewed as an important step in effecting the transition of the fast breeder program from the technology development stage to the point of large-scale commercial utilization.

The demonstration plant is the first point at which utility companies become deeply involved in the demonstration of the LMFBR concept. Each utility involved evaluates the technology in terms of its own needs and methods of operation, factoring its requirements into the program. At the same time, the utility develops its capability to maintain and operate power plants of this type. The demonstration plant stage also constitutes a step increase in the involvement of industrial suppliers, inasmuch as it entails a utility-related power plant designed to demonstrate commercial application rather than a government-owned facility. Therefore, this stage of evolution entails the development of a broadend industrial base so that the utilities will eventually have a number of vendors and reliable components from which to choose.

The construction and operation of an LMFBR demonstration plant is expected to provide practical experience on the functioning of essential plant components. More importantly, it is expected to provide data and experience on operation of a large-scale power plant system and the interaction of that system with its associated supporting facilities and with the local environment.

Until mid-1974, the AEC had stressed this progressive development of successively larger demonstration and "early commercial" plants, using these plants as test beds for component development. It had been the view that three deomonstration plants and three early commercial plants would be required to show the reliability, safety, licensability, and environmental acceptability of the LMFBR concept, and provide private industry with a reliable basis on which to build an LMFBR energy economy. It was recognized that this approach would require considerable government support for developing larger sodium components for each successive domonstration plant.

As a result of a reassessment of the LMFBR program made in mid-1974, the AEC--along with industry, AEC national laboratories, and utilities--identified a severe program imbalance. It was realized that building a number of successively larger demonstration plants placed too much emphasis on developing plant components for each successive plant. This approach would have required

development of several generations of large components--a costly and time consuming process.

Consequently, in July 1974, the AEC made a major redirection to the LMFBR program, which called for terminating plans for multiple demonstration plants and going with one demonstration plant--the Clinch River Breeder Reactor (CRBR). Instead of follow-on demonstration and early commercial plants, a large component test facility--the Plant Component Test Facility--was planned to test full commercial-sized sodium components. Early plant experience was expected to be gained by operating FFTF and CRBR in the U.S. as well as from foreign LMFBR programs. One near commercial plant (with full-size commercial plant components and features, but likely at a lower power level than a commercial plant) was planned to cover any further needs in the plant experience area.

With this revised program, CRBR was placed in an even more important position, since it would now be depended upon to demonstrate the reliability, safety, licensability, and environmental acceptability of the LMFBR concept, and to serve as a focal point for developing components and systems. At the time of the program reorientation, CRBR was planned to become operational in the early 1980s.

### A.2.7.3 Clinch River Breeder Reactor

As a result of the project definition phase activities for the LMFBR demonstration plant, the financial and technical implications of the plant were shown in early 1971 to be such that they could not be handled by a single utility or even a small group of utilities. Such a project had to have the full support and backing of essentially the entire utility industry--including both the investor-owned amd publicly-owned sectors. Accordingly, to obtain this assistance the AEC established in April 1971 two advisory committees: the Senior Utility Steering Committee and Senior Utility Technical Advisory Panel.

The primary purpose of the Steering Committee was to advise the AEC of the extent to which the Nation's electric utilities could participate in the LMFBR demonstraton plant, to identify the specific participation that utilities might appropriately consider, and to advise the AEC of alternative means by which the resources of the electric utilities, in cooperation with the AEC

and the nuclear equipment suppliers, could be effectively applied to the demonstration plant. The scope of the Advisory Panel was to review and evaluate the plans for the AEC demonstration plant, and to advise on the optimal means for effectively achieving the recommended utility participation in, and support of, the technical aspects of the LMFBR demonstration plant.

On June 4, 1971, President Nixon sent an Energy Message to the Congress establishing as a national goal the successful demonstration of the LMFBR by 1980. As a result, Congress provided additional funding for the demonstration plant and for supporting programs. Shortly thereafter, the utility industry pledged about $250 million for the demonstration plant.

In late 1971, proposals were received by the AEC from three groups of utility companies for the construction of a plant. The proposal from the Commonwealth Edison-Tennessee Valley Authority group was accepted on January 14, 1972, as a basis for negotiation.

Two new major corporations were formed in March 1972 as nonprofit, tax-exempt organizations: the Breeder Reactor Corporation (BRC), as the coordinating point for financial and other aspects of participation by the electric utilies; and the Project Management Corporation (PMC), as the central management and contracting organization for all aspects of the project. It was also established that the AEC was to provide technical direction and administration of all aspects of the Nuclear Steam Supply System activities, as well as to provide support from the LMFBR development program. Various supporting and staffing services were apportioned among Commonwealth Edison and TVA as the principal participants, with TVA providing the site for the plant on the Clinch River in Tennessee, and committed to operate and maintain the plant, and to buy the electrical output.

On August 7, 1972, a Memorandum of Understanding among the parties was signed, which set forth the basis of the cooperative AEC-industry arrangement. On November 22, 1972, Westinghouse was selected as the lead reactor manufacturer; on December 19, 1972, Burns and Roe, Inc. was selected to serve as architect engineer. On July 25, 1973, the AEC and the other major participants in the project signed basic agreements outlining the key responsibilities of each organization.

The size of the CRBR plant, as the sole demonstration plant, was determined by an optimization among competing technical and programmatic factors. Chief among these factors was the need to make the plant large enough to minimize the extent of extrapolation of systems and components to a commercial size plant without too large an extrapolation from the existing technological base. Previous plant optimization studies by a number of reactor designers resulted in a consensus that the range of plant size should be 300-500 MWe, and the Senior Utility Technical Advisory Panel corroborated this conclusion. Later design effort, including optimization of the plant heat balances resulted in a 380 MWe-gross, 350 MWe-net rating based on a 975 MWt core power rating.

The CRBR demonstration plant, as an integrated electrical plant, was to include a liquid-sodium-cooled reactor and steam generation system, a heat rejection system, an electrical switchyard, and related auxiliaries and supporting structures and facilities. The design called for fuel assemblies containing mixed plutonium-uranium oxide fuel clad in stainless steel, surrounded by fertile U-238 blanket assemblies.

The demonstration plant was conservatively designed, making maximum use of existing technology to reduce technical risks and assure safe, reliable operation with a minimum of environmental effects. The design effort was supported by a strong research and development program with significant emphasis on prooftesting of components.

### A.2.8 Institutional Constraints on LMFBR Development

A growing national and international concern with weapons proliferation manifested itself in the October 28, 1976, "Statement by the President on Nuclear Policy" which deferred Light Water Reactor (LWR) spent fuel reprocessing and the recycle of plutonium in the United States. The Carter Administration reiterated this policy and extended it further in the April 7, 1977, "Statement by the President on Nuclear Power Policy," deferring LWR reprocessing and plutonium recycle and de-emphasizing the breeder program. The National Enery Plan, April 29, 1977, elaborated on this policy position, proposing to cancel construction of the Clinch River Breeder Reactor Demonstration Project and all component construction, licensing, and commercialization efforts, while sustaining a base level program, including the Fast Flux Test Facility.

It was the expressed hopes of the U.S. that these actions would encourage other nations to pause in their development of plutonium-based technology and to examine alternative methods of meeting their future energy needs. In particular, the administration emphasized alternative approaches to the liquid-metal cooled reactor with its associated uranium-plutonium fuel cycle. The uranium-plutonium cycle, the basis of the CRBR design, had been the cornerstone of the breeder program both in the U.S. and throughout the industrialized world. The objective of the program change was then the development of a breeder fuel cycle that would be more resistant to the diversion of nuclear material for weapons purposes.

As a result, the International Fuel Cycle Evaluation (INFCE) was organized at a conference in Washington, D.C., October 19-21, 1977. The INFCE involved 53 countries and four international organizations. In addition, the U.S. initiated a domestic investigation of alternative nuclear fuel cycles known as the Non-Proliferation Alternative Systems Assessment Program (NASAP), which was also intended to provide input to the U.S. contribution to INFCE.

The Administration's hope that its actions would influence other nations to delay development of breeder reactors until more "proliferation resistant" breeder technologies and fuel cycles and more effective institutional arrangements could be made, was not realized. While there was agreement that the prevention of weapons proliferation was desirable and despite the urgings of the U.S. Government, breeder programs continued in other nations. Several countries continued to make significant advancements in their breeder technology. Great Britain, France, and the Soviet Union were soon operating demonstration reactors, and experimental breeder reactors were soon operating in Germany and Japan. And today the Russians and French have progressed to commercial-size reactors. These nations are convinced that expeditious development of the breeder reactor is necessary to meet their future energy needs. With the exception of the Soviet Union, all of them have more limited domestic energy resources, including uranium, than does the United States.

With the advent of the Reagan Adminstration, yet another major change occurred in the U.S. nuclear energy policy. It became a goal of his administration to stabilize nuclear policy for periods of time commensurate with the long leadtimes characteristic of nuclear technology. The goals of the Department of Energy's programs became:

- To proceed deliberately but swiftly to fulfill the Federal governments responsibility to safely dispose of high-level wastes.
- To remove institutional and regulatory impediments constraining the continued deployment of commercial nuclear power reactors.
- To stabilize Government policy concerning reprocessing of light water reactor spent fuel and to attract renewed commercial interest in this technology.
- To proceed to scale up breeder technology to unit sizes of commercial applicability, to move agressively toward the completion of CRBR, and to establish a framework for con structing a large scale demonstration facility.
- To restore U.S. credibility and strength in international nuclear commerce.

This policy change projected nuclear power to be one of the best potential sources of new electrical energy supplies in the coming decades and not a "technology of last resort." The Department of Energy fostered the return to development of the breeder technology through the classical strategy of plant scaleup to commercial size, as well as reprocessing as part of the overall breeder R&D program. Construction of CRBR was reinstituted, and the project was fast-tracked and the licensing accelerated.

This new phase also provided assurances of government support and encouragement to industrial activities to define the design, cost, schedule, and implementation plans for a large development plant whose construction would be principally funded by the private sector. It also reiterated interest in developing international cooperation.

Escalating costs for CRBR construction soon placed great stress on the Administration's desire to go forward with the project. Opponents of CRBR in Congress pressed for the utilities to vastly increase their financial support. The utilities set forth a proposal that was not considered acceptable. Congressional support, which had become increasingly marginal, faded, and CRBR funding was narrowly voted down, and the project terminated. Almost simultaneously it became evident that approval of a Constuction Permit seemed assured in the Nuclear Regulatory Commission.

The future direction of the LMFBR program is at present clouded. DOE has decided to halt the design effort for the large developmental plant which was intended to be the follow-on to CRBR. Instead, DOE is considering an initiative to fund industry development of innovative advanced design concepts for LMFBRs. Funding for the base technology development is continuing, although at a reduced level. However, that level of funding is vulnerable in the eyes of many, because the immediacy of the mission is no longer there.

### A.2.9 Overview of Foreign Fast Reactor Programs

A brief discussion of worldwide fast breeder reactor programs is provided to round out the historical perspective. The LMFBR is being developed by the majority of the industrially advanced countries of the world, and in some, particularly in France, on a high priority basis. There have been extensive fast breeder reactor research and development programs in the United Kingdom, France, and the U.S.S.R. since the early 1950's and in Germany and Japan since the early 1960's. These countries are proceeding to introduce commercial fast breeder reactors on a large scale into their electric power systems by the mid-1980's or early 1990's. Table A-1 summarizes the status of the fast breeders plants operating or projected in these foreign countries.

Presently the Europeon countries are moving aggressively toward establishing a collaborative approach to further breeder reactor development and construction. This includes France, Britain, Italy, West Germany, and Belgium, thus far, with the likelihood that the Dutch will also sign soon. The intent, apparently, is to optimize the schecule for deployment of breeders in Europe.

Table A-1. Foreign LMFBR Programs

| Name | Country | Power MWt | Power MWe | Full Power Operation |
|---|---|---|---|---|
| BR-5 | USSR | 10 | — | 1959 |
| Dounreay Fast Reactor | United Kingdom | 60 | 15 | 1963 |
| Rapsodie | France | 40 | 16 | 1967 |
| BOR-60 | USSR | 60 | 12 | 1971 |
| BN-350 | USSR | 1000 | 350 | 1972 |
| KNK-2 | West Germany | 58 | 21 | 1972 |
| Phenix | France | 563 | 250 | 1974 |
| Prototype Fast Reactor | United Kingdom | 600 | 200 | 1977 |
| BN-600 | USSR | 1500 | 600 | 1980 |
| Joyo | Japan | 100 | — | 1983 |
| Super Phenix | France | 3000 | 1240 | 1984[a] |
| SNR-300 | West Germany | 762 | 327 | 1987[b] |
| Monju | Japan | 714 | 280 | 1990[b] |
| Commercial Demo Fast Reactor | United Kingdom | 3125 | 1320 | 2000[b] |
| SNR-2 | West Germany | 3420 | 1360 | 1990[b] |

[a]Expected

[b]Projected

## A.3. Technical Program Developments and Problems

In the following sections, four major elements of the fast-reactor development program are discussed in some detail. In each of these sections there are general comments regarding the role of testing and the need for test data, and specific examples to illustrate and highlight a few important points. Also in each section is a summary in the form of a list of observations. These observation emphasize the points that seem to have particular significance for a testing program supporting the development of a large-scale nuclear/mechanical system for energy production.

The four elements discussed below are: 1) fuels and materials, 2) components development, 3) safety, and 4) experimental reactors and plant design.

### A.3.1 Fuels and Materials

#### A.3.1.1 Use and Need for Testing Data

The primary importance of materials development for use in neutron producing facilities has been recognized since the early days of nuclear reactor design and operation. Even in the design stage of EBR-I in the late forties it was suspected that the hostile environment of neutron radiation, high temperature, and sodium exposure might limit the usefulness of a liquid-metal-cooled fast reactor. With little basic data regarding these effects, the designers moved forward at times on the basis of little more than informed intuition. The fuel selected for EBR-I was metallic uranium clad in Type 347 stainless steel; both materials were readily available, easily produced, and had familiar mechanical and chemical properties. However, during irradiation the fuel reactivity dropped significantly below that expected from fuel burnup alone, and after $3.5 \times 10^6$ kWh of output (~ 100 full power days), operations with that core were terminated.

A subsequent examination revealed that the reactivity drop was the result of axial fuel elongation caused by preferred grain orientation. (The Los Alamos Molten Plutonium Reactor Experiment, LAMPRE, was a novel attempt to avoid these dimensional instability problems by operating with molten fuel inside a solid cladding material, but the cladding itself proved to be a limiting factor.) Later, loadings in EBR-I used alloys to limit the anisotropic growth.

Of course, it was recognized that more frequent reprocessing of the fuel could circumvent the swelling problem, but the economics of frequent refueling and reprocessing were not attractive on a large-scale. Then, partly because of an increased emphasis on fast-reactor fuel economics, and partly because the developing light-water-reactor technology was demanding a more reliable fuel, an interest in ceramic fuels began to develop in the late fifties. By 1961 General Electric had begun making mixed (U-Pu) oxide fuel for study and irradiation in a fast reactor. Little was known about the combined effects of radiation and high temperature on oxide fuel, and it was believed that the easiest method of discovery was to simply put the pins in a reactor.

Many of the early investigations with on oxide fuels were efforts to merely observe and understand the material behavior in the fast reactor environment. Initial testing led to enough of an understanding of the phenomenology that calculations became more reliable. This increase in reliability came not only from a better understanding of the basic mechanisms, but also from a better understanding of the interactions among the mechanisms under the influence of high temperature, high temperature gradient, and high neutron flux. For example, much of the detailed chemistry of the fuel constituents was known or could be measured in the lab; but the interactions among these constituents and between the constituents and the fission products in the radiation environment were not obvious. Testing demonstrated the dominant chemical reactions and their result. Testing also demonstrated mechanical phenomena such as crack formation, bubble formation and migration, pore migration, grain growth, and solid fission-product migration; all of which were suspected but not well understood before testing. The integral tests (tests with an entire pin including cladding) could even yield separate effects such as an effective thermal conductivity of the fuel (inferred from the measured power-to-melt and the known melting temperature) or the rate of early restructuring.

An illustrative example of the value of testing can be seen in the history of the phenomenology of cesium. Early in the investigations of fission physics it was recognized that this volatile, chemically active element was produced in significant quantities as a decay product of a xenon isotope. Its volatility, chemical activity, and high yield made the element particularly interesting, but also made predictions uncertain. The chemistry

and movement of elemental cesium, and the chemistry of its various compounds were studied extensively. It was found that Cs could change the oxygen balance of oxide fuel, could combine with iodine (a fission product having particular biological hazard) and inhibit its release in an accident, and could cause swelling in the oxide if it remained in the fuel matrix. By the late sixties, it was believed that the behavior of cesium was reasonably well understood.

Then in 1969 workers began to find that the global behavior of cesium in the fuel pin was not necessarily a simple combination of the local phenomenology; i.e. axial variations in the local environment resulted in global changes in the cesium behavior. Most notably, workers found that the volitile cesium metal or metal vapor would migrate preferentially to cooler axial locations. Thus the local chemistry had to be balanced against this tendency to migrate. Moreover, at about the same time investigators began to suspect cesium oxide as one of the principal corrosive agents attacking the stainless steel cladding. Because the attack was known to be temperature and burnup dependent, and because cesium formation and migration were also temperature and burnup dependent, the interaction between the cladding and cesium oxide was expected to be complex and unpredictable without additional data. Further testing was necessary not only to better characterize this interaction, but also to verify predictions and test the effects of various other materials on the interaction. Quite obviously, the discovery and investigation of these interacting phenomena not only required a prototypic radiation environment, but also required the prototypic temperature field produced by the flowing coolant. It was necessary to build and operate a reactor before the integral cesium behavior could be seen and understood.

Irradiation testing also played an important role in the selection and design of the fuel cladding and structural material. Even in the design stages of EBR-I, it was expected that neutron irradiation would change the mechanical characteristics of the cladding and structural material. Irradiation experience demonstrated that stainless steel did indeed sustain damage and become more brittle in the irradiation field. After numerous studies of irradiated steel, many people felt that the material problems were at least qualitatively understood and manageable with the use of Type 304 stainless steel and with careful design. Then in late 1966 (reported in 1967) British

scientists found that stainless steel irradiated to high fluences in a fast-neutron flux exhibited a dramatic density decrease. Engineers quickly recognized that this swelling would have a profound effect on the design of fast reactors; and the reference structural material was changed to 20% cold-worked Type 316 stainless steel, although experience with this material was also limited. The U.S. then began a success-oriented effort to prove that this new material was satisfactory, but produced only a qualified success: irradiation testing demonstrated that the Type 316 stainless also swelled, although not as severely as 304 at selected temperatures. (The U.S. is currently exploring the use of the ferritic steel HT-9 for use in the cans that surround the bundle of pins and possibly for use as cladding material.) Thus, the initial discovery of the swelling phenomenon and the testing that followed the discovery required extensive irradiation under prototypic conditions; the phenomenon was not seen or expected prior to long-term irradiation. As in the case of cesium migration and numerous other examples in nuclear materials, the integral tests themselves produced basic data on phenomenology and led to important changes in design and materials selection.

One final example of integral testing for phenomenological data is noteworthy because of the usefulness of the data in current reactor proposals. In the early cores for EBR-II, it was found that the burnup was limited by unanticipated cladding weakness at a relatively low fluence. Examination of the fuel showed a gas-drivel fuel swelling that had not been previously observed. Cladding failures were caused by the fuel material swelling out to the cladding, producing metallurgical changes in the cladding and stressing the cladding. This interaction, the so-called fuel-cladding mechanical interaction, occurred at low burnup because of the small amount of space allowed between the fuel material and the cladding--a space necessarily small to maintain a high fuel density and thus a high breeding ratio. As the mission of EBR-II changed from that of a pilot plant to an irradiation facility, greater attention was given to increasing burnup and thus the economics of the EBR-II core. With this changed emphasis, there was more freedom to modify the fuel pins to accommodate the swelling. At about the same time (mid- and late-sixties), it was discovered from irradiation data that when swelling from fission-gas bubble growth was allowed to approach ~ 30%, the bubbles began to touch, connect, and release any additional gas to the surface. (This phenomenon had been predicted as early as 1964 but was not observed until 1968.)

Designers of a modified EBR-II driver pin (the Mark-II pins) used this information in increasing the gap by 67% to permit the fuel to swell 30% before contacting the cladding. With this simple change and with a few other modifications made obvious by test irradiations, it has been shown that Mark-II elements can routinely attain a burnup of 10 at.% and in many cases have reached burnups as high as 16 at.% without cladding breach (compared to ~3 at.% with the earlier design).

These results are particularly important because of a renewed interest in metal fuels for uses beyond the needs of EBR-II. The ease with which spent metal fuels can be remotely processed and refabricated in a local facility makes them extremely diversion-resistant, a characteristic that has become increasingly important in recent years. With a high burnup potential, a good breeding performance, and a demonstrated refabrication technique, the metal fuels are again being seriously considered. Thus, the testing that led to simple observation of bubble phenomenology may have a significant impact on breeder strategy in the future.

The integral tests were not the only tests required for materials data and phenomenology. For example, out-of-pile and separate-effects tests were particularly important in measuring changes in steel mechanical properties. One important parameter of the cladding material was its strength as a function of irradiation damage. Initially, these tests involved pressurizing an irradiated tube, held at a high temperature, to the point of failure while measuring failure strength, ductility, and deformation. However, in the early seventies it was recognized that the static high temperature behavior of these materials was not necessarily the same as the transient behavior during heating, and a considerable effort was needed to produce transient heating while pressurizing the tubes. When specific transients were considered, the number of parameters in a test matrix involving irradiation history, temperature transients, and pressure transients quickly became unmanageable, and analysts were forced to limit the experiments and use judgement in extrapolating the results to other conditions. Nevertheless, the tests did yield and continue to yield important information on the transient behavior of steel cladding. But even these out-of-pile tests required irradiation facilities to produce the materials to be studied.

The above examples highlight the development of important phenomenological data from irradiation testing, but the uses of testing are not limited to separate effects alone. Statistical information on fuel failures can be obtained to establish failure probabilities that are necessary for design changes and economic calculations. The times at which fuel failures occur are often randomly distributed about some mean, so very early or very late failures are always possible. To investigate this distribution large numbers of pins with the same design must be irradiated under near-identical conditions for extended periods. Such testing requires dedicated facilities - a role served since 1967 by EBR-II and since late-1980 by both EBR-II and the Fast Flux Test Facility. Both facilities not only provide exposure for experimental materials, but also act as experimental reactors themselves by irradiating large numbers of driver pins. The data from these driver pins and from test bundles thus provide a broad phenomenological and operation base for fuels and materials development.

### A.3.1.2 Observations

The emphasis of this section on fuels and materials has been to demonstrate the value of prototypic testing in discovery and development. This value was highlighted by several examples that brought out the following points.

(1) Unanticipated or previously unobserved phenomena are likely when exposing well-characterized materials to new environments. The phenomena are often seen only when the material is placed in prototypic conditions.

(2) As demonstrated by the cladding embrittlement, the effect of the new environment can be anticipated but not quantifiable without testing. Without quantitative information, such anticipation is of little value.

(3) Some phenomena can be slow in developing, but can have profound impact on material use. The swelling tendency of stainless steels in fast reactors was not seen until 1967 even though these steels had been used since the early fifties. Up until the mid-sixties the fluence on samples under investigation had not been high enough to see the swelling.

(4) Phenomenological data on materials is not only useful in constructing and calibrating models, but is also directly useful in design work. This

is abundantly clear in the manner in which the fuel and steel swelling data were used.

(5) For any system where the randomness of failures becomes important (e.g. for cores with thousands of fuel pins, or for heat exchangers or steam generators with thousands of tubes) statistical data on these failures are necessary to establish probabilities and to permit economic calculations.

### A.3.2 Components Development

Because of the rapid pace of breeder reactor development in the U.S., particularly liquid-metal-cooled breeder reactors, an intense components program continues to thrive. Throughout their history in the U.S., metal-cooled reactors have been considered to be in a developmental stage - either as a feasibility study such as EBR-I, a pilot plant such as EBR-II, or a demonstration plant such as the recently-cancelled CRBR. This developmental process naturally carries over into the design, testing, and operation of system components. The principal focus of the breeder reactor components program has been on the large single-function units such as steam generators, heat exchangers, pumps, sodium-purification systems, and valves. These units may, however, have common problems such as corrosion, weld integrity, or seal degradation and often require common programs addressing separate effects. Thus, the current components development program is a combination of large-scale testing of prototype units and smaller laboratory-scale experiments.

If one were to examine the history of a particular component, it would be seen that an adequate design at one point in the program may not have been adequate at a later date in a more advanced system. Even if a unit worked properly in a system, changes other than mere scale up often were necessary to keep pace with the development of the entire reactor. Commonly in any developmental program, this process can be assisted first by providing a proof test for a particular design or component and then by pushing the component beyond the design limits. In exercising the component in this manner, the design limits themselves can be examined and failure modes can be investigated. (Obviously, one can do this only if the tested unit is not costly to repair or replace, or the if loss of the unit is not disastrous.) The momentum in a program of proof-testing, operating, and eventually pushing beyond design limits, can lead to a rapid evolution of component design.

The U.S. breeder program has not followed this evolutionary process in every case. It will be shown in a later section on plant design that the U.S. decided to build an early experimental reactor in the pool configuration and developed components to fit into such a system. But for numerous reason that appeared to be both political and technical, the US program chose the markedly different loop configuration for the large FFTF and CRBR plants, thus seeming to lose the early momentum generated by EBR-II. One can contrast these decisions with the ambitious French program in which many of the important components appear to be a simple scale-up with improvements of a preceding unit. One finds, for example, that the tube configuration, wall thickness and tube spacing in intermediate heat exchangers are very similar between the various plants even though the plants have grown significantly larger and more complex. Obviously, the success of the French program in components has not been due solely to their design approach, but their relatively consistent use of evolutionary development has resulted in several notable success. More will be written on the pool/loop contrasts and other choices in a later section.

The U.S. components program has had its own dramatic successes in developing the necessary technology for a large-scale demonstration plant. The discussion below focuses on this program and the testing included as a necessary part of the effort. General issues will be outlined first, and then a detailed discussion follows giving a view of the issues and development of two large components necessary for a metal-cooled power plant.

### A.3.2.1 Representative issues

Generally, the problem in components design and testing is to prove the component will simply work as expected. That is, a components test program must eventually demonstrate that the new pump or heat exchanger functions properly and economically under the design conditions or must explore the reason for improper functions or failures. Commonly, a testing program on a prototypic component begins with exploratory testing at conditions less severe than nominal. If the equipment performs properly, the conditions are raised to nominal for an extended period. Finally, as a test of the limitations of the component the conditions may be raised to an abnormally severe point or even to force failure. In following the test through this procedure the

experimenter can establish both the proper design limits and the inherent margin to failure. Such data can then be used either in accepting the component, in redesigning the component, or in redesigning other parts of the system to accomodate the newly established operating conditions of the component.

The specific problems in components testing include not only the engineering of the equipment, but also its construction and operation. In breeder reactor development it was necessary to address such details as the survival of seals and bearings in the sodium environment, and such integral issues as the manufacturing and performance of very large pumps and steam generators. In the reactor itself questions arose regarding the effect of thermal transients on the core and supporting structures, the selection of control rod materials, the design and lifetime of fuel elements, and the core thermal-hydraulics. This last issue particularly required the development of analytical methods as well as experimental data because of the changing conditions in the core as the burnup increased. (Burnup adds neutron absorbers to the fuel rods decreasing the local power in those positions, but builds plutonium in the blanket raising the power there.)

A number of examples can demonstrate the role of testing in component development, but because of the importance of a few large components to the overall system, the experience with these components will be representative of the testing program and will be discussed in detail. These components are the large sodium circulating pumps and the sodium-heated steam generators.

### A.3.2.2 Sodium Pumps

Prior to the development of metal-cooled fission reactors, there had been no large-scale application of sodium, or a sodium-alloy, as a coolant and heat transfer agent. There had been limited experience with other liquid metals such as mercury, but in most cases the unique properties of sodium were not required and other fluids were used. In designing early fast reactors a need arose for a neutronically benign coolant to transfer the heat out of the core for other uses or to be dumped. For the coolant to be acceptable it could not have an appreciable fast neutron absorbtion cross-section, could not degrade the neutron spectrum significantly, and should have a high volumetric heat capacity to cool the compact fast reactor core without a large penalty in

pumping cost and pumping pressure. Although both sodium and potassium were known to be chemically active with water and air and were presumed to be incompatible with many other materials, a sodium-potassium alloy was selected as a suitable coolant for a liquid-cooled fast reactor. (Other coolants in the breeder reactor program have been helium, mercury, and steam.)

In spite of the fact that little was known about pumping this alloy, commonly called NaK, an entire power plant was designed on the basis of experience with other fluids and at times on mere educated intuition and judgement. The plant, designated Experimental Breeder Reactor-I (EBR-I), reached full power in late 1951 and produced history's first useful electricity from nuclear power. The pumps in this plant, as well as many of the other components, were small integral experiments in themselves, because of their first-of-a-kind nature.

The world's first metal-cooled fast reactor had actually been the Clementine reactor, which went critical in 1946 and reached full power in 1949. This facility was built primarily for physics studies and had only a low-volume, highly inefficient induction pump, and dumped the fission heat to air. Early design studies of other fast reactors had also considered using induction pumps because of their high reliability and the ease with which they could be sealed, but experience with these pumps, including the Clementine experience, showed that the pumps could not effeciently generate the heads that larger plants would eventually require. EBR-I showed that even a crude centrifugal pump could be operated with some reliability in the hostile environment, and most metal-cooled fast reactor systems since then have used the more standard centrifugal pump in the primary system.

The pumps for EBR-II were based on the knowledge gained from experience in EBR-I and other sodium systems and incorporated many of the features of those earlier pumps. The pumps for the Enrico Fermi plant, particularly the primary pumps, were somewhat different from the EBR-II pumps, because of the hydraulic requirements of the larger, loop-type plant design (a marked variation from the pool or pot-like construction of the parallel EBR-II plant.) Again, as in EBR-I, the plant designs of EBR-II and Fermi were virtually fixed before the pumps had been built and tested.

It is significant to note that in these early reactor plants, which included the entire system for converting fission energy to electrical energy,

the pumps as well as other major components were a significant part of the experiment and were not fully tested before being placed in the system. Such an integral approach to testing components should be undertaken when the components are a major reason for the integral test and when the remainder of the system is not prohibitively expensive. (That is, if the component failed, it should not be a major financial burden to temporarily shut down the entire system.) This was not the case in the large metal-cooled Fast Flux Test Facility and the Clinch River Breeder Reactor. Here the pumps were large and expensive, but the entire system was larger and more expensive, and a complete testing program was undertaken before the pumps were used.

The testing program for these large components included scale models, partially-scaled models, and full-size prototypes. The scale models were used to test pump parts rather than a entire scale pump and often used water as a test fluid. Useful information on flow patterns and hydraulics in such parts as the impeller, the entrance and exit regions, and the bearings were gained from such models. Detailed but important, sub-components such as seals and bearings occasionally were also tested with scale models in sodium. One of the more innovative parts in the large CRBR pumps - a combination seal, bearing, and internal oil pump - required extensive testing in sodium before it could even be used in a prototype. Similarly, partially-scaled models were used to test parts of a pump but in a more integral configuration. In these tests the part was usually contained in a complete pump, but no attempt was made to scale the entire unit, only the sub-component of interest. The test thus comprised an actual working pump, but useful data was taken from only one portion of the systems. Full-size prototypes were also tested with water to avoid the obvious safety, cleaning, and operational hazards with sodium. These water tests on the prototypes are the near-final proof test of the component, and they are used to demonstrate that the equipment indeed functions as expected with water.

In addition to hydraulic performance data, these water tests provided important mechanical data to show that the pumps had been manufactured properly. One important concern in the development of very large pumps was the symmetry of the large impeller and the ability of the shaft bearing to keep the shaft centered. A water test for such a pump is thus a test of both an engineering and a manufacturing problem. To understand the magnitude of the

problem one must understand that the prototype primary pumps built for the Large Scale Prototype Breeder Reactor are the largest sodium pumps ever built, with an overall length of 35 feet (pump alone, excluding the motor) and a net output of 85000 gpm, while the radial clearance in the hydrostatic bearing for the impeller is only .030 inches. If the impeller distorts or is misaligned the pump would rapidly fail. However, water tests with these pumps have shown that the orbital radius of the shaft in this bearing is only .003 inches, well within the design limit.

To avoid putting these large components into service before being tested under prototypic conditions, a large sodium loop was built principally to test sodium pumps. This Sodium Pump Test Facility included provisions for testing values, piping, coolers, and other components, as well as a position for the test pump, a heat removal system, and a pressure reducing region. The FFTF centrifugal and electromagnetic pumps and the CRBR prototype pumps were tested in this facility, and there are plans to test the LSPB primary pump there.

Thus a combination of increased size and complexity of the pumps along with a marked increase in the complexity and cost of the rest of the system caused a change in the approach to the testing of these large components. In the early years of metal-cooled reactor development, the pumps along with other large components were a major uncertainty in the system and a substantial fraction of the cost of the system; and the integrated reactor system provided a reasonable test bed for these components. But as the size, complexity, and cost of the reactor increased it became obvious that using the reactor itself as a test bed was not appropriate, and separate loops and testing programs were built solely for components testing prior to actual use in the reactor.

The final step in any component test program, however, is the use of the component in an operating system. It is here that the practical problems of manufacturing, assembling, and installation are seen, as well as the gathering of operational experience. For the smaller sodium pumps, this step was a majority of the test program, but for the large sodium pumps this is the final test in a lengthy test program. FFTF pumps are currently operating and yielding useful experience, but the very large CRBR and LSPB pumps may be set aside indefinitely because of basic changes in the LFMBR program.

### A.3.2.3 Steam Generators

Like the sodium (or sodium-potassium alloy) pumps, the liquid-metal-heated steam generators for the early plants were one of the major uncertainties. When NaK was selected as the coolant in EBR-I it was known that a leak in one of the numerous steam generator tubes or welds would produce a severe chemical reaction releasing hydrogen and a caustic liquid. Also, EBR-I was merely to be a proof-of-principle experiment, not a demonstration that breeder reactors were an economical source of useful power. For these reasons, the EBR-I steam generators were built with a highly conservative design - a triple-wall construction in which each steam/water tube was surrounded by two additional tubes which were then surrounded by the hot sodium. This redundancy was further enhanced by using separate welds for the inner and outer tubes, with the outer tubes welded to a tube-sheet, and the inner tubes welded to a water header. This complex design, with its inherent high cost, was used to minimize the possibility of the metal-water reaction, which could occur only with a failure in both welded attachments or in both inner and outer walls. Operational experience in EBR-I showed that the design could indeed maintain the separation of sodium and water, but the design was not without faults. The mechanical redundancy (two welds for each end of the triple-walled tube) increased the probability of a single weld failure. Moreover, the use of a double attachment complicated the task of repairing a leak in the tube-to-tubesheet attachment. Finally, the triple-tube design degraded the performance of the system and was obviously costly.

These positive and negative contributions of the triple-wall design are highlighted because they draw attention to a particular decision in the early sodium-heated steam generator program - a decision to test a component design that was not expected to become a standard. The decision was based on the need for steam-generator engineering data, along with the need to have some assurance that the component would function long enough to gather data. Later experimental reactor systems used a slightly-less complicated design; EBR-II, the Sodium Reactor Experiment (an experimental sodium-cooled, graphite moderated, thermal reactor) and the Hallam Nuclear Power Facility (a commercial scale-up of the SRE) all used double tubesheets with adequate results. But for large-scale applications, it was generally believed that a more conventional single-wall design would be needed.

And indeed an attempt was made to use the more simple design in an operating steam generator. The Enrico Fermi Power Plant, a privately-owned 65 MWe plant, had three single-wall units that were built with technology that was thought to be adequate at the time. With hindsight it is easy to see that these units would quickly become a limiting feature in obtaining full-power operation. Early failures were numerous and all three units eventually required major repairs. One unit required complete retubing; in another, a severe sodium-water reaction occurred causing a rupture disc to burst; and all three units required complete rewelding of the tube-to-tubesheet attachments. The failures that required complete retubing were attributed to stress-corrosion cracking. (The corrosion agent was found to be the fluids used for cleaning and hydrostatic testing - a striking example of the value of an integral test in which all procedures are included.) Other failures were due to flow-induced vibrations, weld porosity, and undetected micro-cracks. Moreover, once the steam generators were brought to a significant power level (33 MWt) large temperature oscillations were observed at the sodium outlet requiring modifications on the water/steam side. Eventually, the plant reached full power, but additional small leaks continued to occur demonstrating the need for design changes.

From the Fermi experience it became obvious that an extensive development and testing program solely for steam genators would be necessary. Once EBR-I proved the feasibility of producing steam with sodium, it was no longer reasonable to built an entire plant to test a steam generator, nor to limit the operation of the plant with an untested unit. The steam generator test program that has evolved to date has been a combination of scale model testing, phenomenological testing, sub-component testing, and full-scale prototype testing in flowing sodium loops. Scale-model testing has been used principally for hydraulic information such as flow distributions and pressure drops in models of both complete steam generators and parts of the steam generator. Sub-component tests, the so-called few-tube tests, provide data on both hydraulics and heat transfer. In these tests a sub-section, either a single tube or a few tubes, from the full-size unit are run under prototypic conditions to measure the performance characteristics, and the data is used in calculational extrapolations to the full unit. Single tube tests have been performed in the Steam Generator Test Facility at Argonne National Laboratory. Few-tube tests and full-scale prototype tests have been performed by General

Electric and Westinghouse, and at the Energy Technology Evaluation Center in California.

Phenomenological testing on steam generators and heat exchangers have addressed a variety of issues, but one of these programs has raised a point that is particularly noteworthy. The flow-induced vibration test program has considered the effects of the sodium cross-flow on the steam generator (or heat exchanger) tubes. Research has shown that not only are vibrations self-induced in a single tube by vortex shedding from the tube, but also that the tubes can couple hydraulically and set up vibrational states that would not exist in a single tube. This observation itself is useful and emphasizes the importance of expanding separate-effects tests into integral tests; but a more interesting point arose in the application of the data. The data had been developed using a measurable flow across the modeled steam-generator/heat-exchanger tubes, and because of this use the flow was a necessary parameter in the application. But when the data was translated from the laboratory experiment to a full-scale system it became obvious that the necessary flow parameter itself was not well known in the larger system. That is, the geometry of the full-scale system so confounded the flow data that the translation of the flow parameter from laboratory to prototype was difficult. Simply establishing a relation between the flow parameters in the two systems required additional testing data and additional analytical work. The separate-effects data eventually was quite useful; but the task could not be satisfied by the clean laboratory environment alone, and required additional information from a prototype facility.

The steam-generator developmental effort therefore obtained data from a testing program that ranged in complexity from small separate-effects tests to full-scale prototype tests. Data was also obtained from other technologies that effectively acted as full-size test beds. Because the hydraulic characteristics of sodium are not too different than those of water, many of the hydraulic problems seen in sodium-heated steam generators were also seen in more conventional heat exchangers and steam generators (except leaks and tube failures had much less serious consequences in the latter, for obvious reasons). Observations, operating experience, and data collected from selective other facilities proved to be useful in the steam-generator test program, particularly in the area of flow-induced vibrations.

The current steam-generator program is centered on a prototype unit intended for the CRBR and on two other units developed for the Large Scale Prototype Breeder. The program to design and test these units has cost on the order of $100 million, and has been developed to the point of successful operation of a prototype steam generator in the Sodium Component Test Installation. Although the program to develop these units has been both impressively large and impressively successful, other less visible contributions have been important. A particularly important program, costing on the order of $10 million, has been an effort to develop reliable and rapid leak detection instrumentation. Such instruments are necessary to quickly quench the type of destructive sodium-water reaction that destroyed one of the Fermi units. Quite obviously, a components-testing program requires the development of a prototype component, but one cannot neglect the possibility that peripheral issues may be costly and time consuming.

A.3.2.4 Observations

A summary of significant points in the discussion on plant components is given below.

(1) The U.S. breeder reactor program to date has been developmental in nature, and as such, has required an extensive program to design and test components that, prior to the emergence of metal-cooled reactors, had little industrial application.

(2) In the early development of many components, small integral systems were often used as experimental test beds, but as the sophistication of both the components and the remainder of the system grew, the integral tests were in part replaced by stand-alone tests of individual units. The integral tests with the entire reactor system assembled were then to be used mostly as performance checks and to gain operating experience.

(3) Early components were often conservatively designed to insure that they would operate and would not be the limiting unit in the integral test. Such designs indeed resulted in the successful operation of early plants, but did not provide a true test of the concepts that they represented.

(4) Premature expansion of some of the early technology beyond its limits (e.g. the single-wall steam generator in the Fermi power plant)

resulted in costly failures and caused delays in obtaining more valuable information on plant performance.

(5) Scale-model testing was useful in components testing, particularly in obtaining hydraulic data. Tests were carried out not only on models of entire units, but also on models of parts of the units. Few-tube tests, a form of scaled testing, was also particularly useful in obtaining thermal/hydraulic data on heat exchangers and steam generators.

(6) A variety of issues was studied with phenomenological experiments, but the application of the data from at least one of these test series was confounded by the difficulty in translating laboratory parameters to measurable parameters in the prototype.

### A.3.3 Safety

The role of safety research in LMFBR development in many respects follows the role of research in the other elements considered in this report. In studies that are not specifically directed at safety, the objective is to produce a system that operates adequately and economically under normal operating conditions and successfully withstands off-normal, but expected, conditions. In safety studies the objective is again to prove that the system is capable of withstanding certain off-normal conditions. However, in this case the off-normal conditions range from expected minor accidents to hypothetical accidents which, while having extremely low probability, can cause significant damage in the system. Moreover, in estimating the outcome of these events the safety analyst must maintain a conservative approach. That is, if an uncertainty exists in a chosen parameter or in the outcome of an intermediate event in the accident sequence, then the analyst can effectively prove the safety of the system only by choosing the limit of the uncertainty that leads to a more severe outcome. This constant emphasis on a conservative approach differs somewhat from the approach taken in other aspects of the system research and development in which a balance was made between performance and cost. In safety research, the public safety, rather than economics, is the principal motivation for focusing on the consequences of a bounding severe accident. Economic considerations are certainly a part of the design or operational solutions to safety problems, but the safety problems themselves arise because of a concern not directly related to economics.

Early calculation of a severe accident in which there was widespread core melting - the so-called core-disruptive accident (CDA) - so emphasized this conservative approach that no attempt was even made to argue the physical possibility of the initial conditions. In one of these calculations, by Bethe and Tait, the assumptions were so extreme (but not considered impossible at the time) that the calculation predicted an energetic nuclear excursion - a nuclear explosion. It was readily admitted that the assumptions and initial conditions were overly conservative, but without more information about the detailed mechanics of a CDA, the safety analyst was obiged to chose such assumptions and conditions.

The demand for detail was not limited, however, to the analysis of core disruptive accidents. Early investigations had suggested that more common small-scale events could lead to significant core damage. And to avoid uneconomical restrictions on operations or costly design changes that would maintain a calculated safety margin, the analyst needed more information on some of these event. Thus, a safety testing program arose, not to prove a particular component would work or to discover problems with a given material, but rather to generate information on the details of accidents and thereby reduce the calculated maximum theoretical consequences of the accident.

### A.3.3.1 Early Representative Issues

The early issues in fast reactor safety generally fell into two broad categories: (1) highly improbable, but highly destructive, core disruptive accidents, and (2) accidents that begin with a localized problem that could propagate and cause extensive damage. The CDA's had the greatest potential for environmental damage because of the possibility of an energetic excursion in the course of the accident. This possibility was believed to be possible because the fuel in a fast reactor is not in its most reactive configuration. That is, by rearranging the fuel inventory, in particular by compacting the fuel, the neutron multiplication factor could be raised significantly causing the power to rise rapidly. The fuel melting and collapse that leads to this fuel compaction was believed to follow from several postulated accident initiators such as a core-wide loss of coolant flow without shutdown, a main pipe break, a reactivity insertion without shutdown, a loss of heat sink, and others. The purpose of the testing program was to provide a mechanistic

description of the events following such initiators and to establish the possibility of large-scale fuel compaction. Such a description was the very thing Bethe and Tait avoided by making grossly conservative assumptions regarding the initial conditions of the core. As noted before, the details were avoided by chosing the conditions leading to the most severe outcome.

The early testing program for CDA's was guided by the safety analysts' expectation of the accident sequence following a given initiator. It was quite obvious, for example, that sodium boiling would follow a core-wide loss of coolant flow, but uncertainties existed in estimates of coolant superheat before boiling, coolant hydrodynamics after boiling, and heat transfer from the fuel pin during boiling. Moreover, once the coolant flow over the fuel had been stopped, it was not clear how the fuel would behave as it melted. A conservative estimate had been that the fuel would collapse toward the core midplane raising the reactivity; but possible dispersive mechanisms were seen, and testing was necessary to discover the effectiveness of these mechanisms. Testing was also necessary to reduce the upper limits on the efficiency of vapor explosions that might occur if the liquid sodium coolant were to reenter the core containing molten fuel (principally a concern for ceramic fuels with a very high melting point). It is seen then, that the early testing program addressing CDA's arose mainly from the informed imagination of the safety analyst, rather than from a wealth of experience in the area.

Similarly, the imaginative analysts had forseen problems with small, local faults propagating to adjacent areas and eventually causing substantial damage. Indeed, some workers had estimated that propagation could occur so rapidly that the fault would effectively be another initiator for a core disruptive accident which would then follow the expected course of wide-spread sodium boiling, sodium expulsion and fuel melting and compaction. However, even if the faults were to propagate slowly, the damage could still be extensive before the fault was detected. Examples of the initial faults were fuel cladding rupture and pin depressurization, small coolant blockages in the fuel bundle, and improperly over-enriched fuel pins.

As expected, many of the early issues were resolved, or the uncertainties were reduced, by the initial testing program. For example, sodium superheat and rapid, coherent core collapse have been all but eliminated as dominant issues. Also, as expected, the testing program itself has shown that mecha-

nisms other than those initially considered, can be important, raising additional issues that required tests to resolve. Moreover, by eliminating or reducing some of the early issues, the importance of some of the lesser issues was increased, and the uncertainties introduced by these lesser issues appeared as an attractive target for testing. Finally, the CRBR licensing effort generated additional questions (from a new group of imaginative analysts). Thus, the testing program in this area continues at a significant level in spite of the substantial progress made toward establishing the inherent safety of LMFBR's.

### A.3.3.2 Testing Compromises in Safety Research

As the early issues became more clearly defined, the requirements for safety tests were more evident, and the compromises that must be made in any testing program became more obvious. One of the first divisions that must be considered in the approach to an issue was whether the tests required a neutron field or simply an out-of-pile study. Some of the trade-offs considered in making a decision were:

Cost: In general in-reactor tests are more costly because of the expense in operating a reactor facility; however, attempts to simulate aspects of the reactor environment that influence the outcome of the out-of-reactor experiment can quickly raise the cost of such tests

Induced Activity and Contamination: Materials placed in a reactor for relatively long-term irradiation become activated by the neutron field and require special procedures and equipment for handling. In addition, when the experiments are disassembled in a hot cell facility they become contaminated with other hazardous materials (often plutonium in reactor research) and disposal costs go up significantly. However, it should be noted that many experiments begin with pre-irradiated fuel and additional irradiation or contamination adds little additional burden.

Location of Energy Source: Fission energy is deposited very close to the original site of the fissioning nucleus (~80% of the energy is carried as fission-frament kinetic energy which is deposited within $\sim 10^{-2}$ mm). It is possible to simulate this energy deposition with a variety of techniques when the materials in the experiment are well separated; but if the materials are mixed, a simulation method usually results in energy deposits in non-fuel as

well as fuel components and may confound the data. Moreover, when the materials are moving many of the heating methods fail completely or become less predictable.

Limits on the Achievable Range of Parameters: Fission energy can provide an intense energy source that is, under certain circumstances, difficult if not impossible to reproduce in out-of-reactor experiments - particularly when one is considering the effects of a rapid power burst. Most heating techniques (ohmic, microwaye, RF) are limited in the maximum power available. On the other hand, in-reactor experiments are not without constraints. Some of the experiments can be quite energetic and the experimenter must protect the reactor facility from damage by the experiment. Such a protection requirement has at times limited the in-reactor test parameters.

Limits on Space in Reactors: Because of restrictions imposed by neutron economy, the available experiment space in a test facility is relatively small. In an experiment program, the early experiments are usually tailored to fit in the existing positions, but as instrumentation requirements expand and as a bigger tests are considered, the size limitations become important. In safety testing it was often found that size limitations did not preclude an in-reactor program, but that the program outgrew the reactor and larger facilities were sought. (This size-factor will be discussed in more detail in a section below.)

With considerations such as these, some of the experiments obviously fell into the in-reactor or out-of-reactor categories; there was no question that experiments on sodium superheating could more readily be done, at least initially, in the laboratory, while a neutron radiation environment was definitely necessary to produce heat in the experiments examining pin-to-pin failure propagation. Others less clearly required in-reactor testing; for example, the dynamics of sodium boiling could be examined in the laboratory with well instrumented, electrically heated pin bundles, but the interaction between the actual fuel pellets and the cladding (which affects the heat transfer characteristics into the sodium) could be properly simulated only in an in-reactor experiment.

(It should be noted that in most of the early safety programs the requirement for an in-reactor experiment was based mainly on the need for a prototypic heat source. The effects of radiation damage and fuel restructur-

ing could be included in the experiments by preirradiating the fuel in a separate facility or by attempting to mechanically simulate a few of the important property changes of the material. This separation of preirradiation and destructive experiment has appeared to be successful, but the concept has never been clearly tested.)

Out-of-reactor tests could be further broken down into tests with prototypic materials and tests with simulant materials. The latter selection was often made for ease in handling (using water in place of sodium), for transparency (again, water rather than sodium), or to avoid unmanageable extremes in experiment conditions (using Woods' metal to simulate cladding in a test of molten cladding motion). But such simulant tests were not always definitive. Using simulants involves further compromises in heat transfer rates, fluid-mechanical effects, material thermodynamics, and possible effects from chemical reactions, any of which can significantly change the outcome of the experiment. To resolve these compromises it is often necessary to run confirming experiments with prototypic material or components.

A notable example of a successful program using simulants has been the study of the potential for vapor explosions resulting from the mixing of molten fuel and sodium. In this case it was possible to get useful data from experiments using prototypic materials; but the theory that was being tested could also predict that the dynamics of the interaction for parameters (temperature, pressure, heat-transfer characteristics) not obtainable with these materials. To further test the theory, experiments were run with Freon and water, Freon and mineral oil, and other combinations, and a useful theory was confirmed by these tests. Note however that at some point in the program the actual materials were used.

Thus simulant tests are useful, but not always definitive. The degree of certainty needed in safety experiments often requires that at some point the data taken from a simulant test be confirmed with prototypic materials in a relatively prototypic environment. If this final step is not taken in safety research, the theory derived from the data is subject to scientific and political challenges that may not be possible to refute with certainty. Simulant tests are useful, however, in developing theories, extending parameters, and providing guides for further experiments; and the relative low cost of such tests usually makes them cost effective.

### A.3.3.3 Demonstration Plant Requirements for Safety Testing

Even without a detailed analysis, one can quickly conclude that a large-scale demonstration plant is inappropriate as a safety test. Such a plant is certainly needed to provide a focal point for the tests; that is, to provide a basis for selecting materials, conditions, test geometry and test conduct. But to operate a prototype plant as a safety experiment is an undeniably costly method of generating a single, or at most a few data points, particularly when the test deliberately results in extensive damage in the core. Exceptions can be found, however, particularly when an existing facility approaches obsolescense as a system test either through age or because better system test facilities have been built. Examples are found in reactor development, both in the water-reactor program and the metal-cooled reactor programs. The BORAX-I destructive experiment in 1954 is a typical example of forcing a violent transient in a reactor approaching the end of its usefulness, in this case a rather simple swimming-pool reactor, to generate limited data. (Actually, the quantity of data derived from the experiment was much less than the experimenters had envisioned because the transient, which they purposely initiated by attempting to eject a transient rod entirely out of the core, was unexpectedly destructive and spoiled much of the data.)

Fewer large metal-cooled reactor facilities have been built, so examples are more limited. But the current mission of the EBR-II reactor, a reactor that historically has been a combination of system test and irradiation facility, has been moving more toward safety tests. Although the safety experiments in EBR-II are far from being a threat to the integrity of the core, it can be seen that the potential for contamination of the coolant system has increased. Indeed, one of the purposes of the experiments is to examine the release of contamination from failed fuel pins and to determine both the mechanisms involved in the release and the length of time the reactor can safely operate with a given number of failures. These are obviously not experiments that one would undertake with a reactor system that was built to check steam-generator performance, fuel-cycle problems, or plant effeciency. But as EBR-II contributions in system-performance areas such as these have been either reduced by time or supplanted by newer facilities such as the Fast Flux Test Facility, the value of EBR-II as a safety test bed has risen significantly. However, in neither the BORAX-I case nor the EBR-II case was an

operating reactor built specifically for a single distructive safety test. The idea is appealing because of its simplicity, but the costs far outweigh the benefits.

### A.3.3.4 Other Facility Requirements for Safety Testing

The testing sequence in LMFBR safety followed a general progression from small, separate-effects tests, to small integrated tests, and eventually to large integrated tests. The early safety calculations - for example, the calculation by Bethe and Tait mentioned above - were overly conservative in order to accomodate uncertainties in a few general events, but as more detailed mechanistic computer models were developed some of the general uncertainties disappeared, only to be replaced by numerous uncertainties in the details of the mechanics. Bethe and Tait began with the general assumption that the fuel in the core was completely molten and able to collapse under the force of gravity; they made no arguments about how the core comes to that condition or about the available mechanisms that might mitigate or prevent the collapse. But by including the approach to melting and the collapse-preventing (dispersive) mechanism the modeler was forced to write equations for phenomena that were not well understood. Thus many of the early experiments were guided by uncertainties in the models: was there an appreciable sodium superheat before boiling; did the sodium leave a liquid film on the fuel pins as the liquid coolant was forced from the bundle; what were the proper criteria for cladding failure during an accident; how did the fuel pellets behave under the rapid heating conditions caused by an accident. These questions and many others were points for investigation in the early safety program, and some continue to demand additional attention.

A common hazard in building a testing program around the predetermined models in a code is the possibility that the models do not fully contain the mechanisms affecting the outcome or that the mechanisms interact in an unexpected manner. For this reason it is necessary to compare the calculations to integral tests. Moreover, some of the key safety issues were too complex and involved too many mechanisms to model with any reliability, so integral tests were needed for data on these phenomena. Thus the models often guided the phenomenological tests, but the integral tests were justified as producing data that was directly useful in the mission of the safety research

program; the integral tests not only demonstrated what the calculations predicted, but also could demonstrate mechanisms for which models did not exist.

The early demands, therefore, were for facilities to accomodate both phenomenological and integral tests. The out-of-reactor phenomenological experiments were accomodated by facilities built on an ad hoc basis, with the only extraordinary requirements coming from the need to handle pre-irradiated material, a need that could be satisfied by existing hot-cell facilities. Similarly, existing reactor facilities were available for material irradiation for the tests. But adequate reactor facilities were not available for the experiments themselves. Because of the need to drive experiments through severe transients, to easily accomodate experiments on a routine basis, and to reduce the possible cost of damage from even a low-probability experiment accident, a reactor facility was built specifically for fast reactor safety experiments. This reactor, the Transient Reactor Test Facility (TREAT), a graphite moderated, pulsed thermal reactor, was designed and constructed in the late 1950's and experiments began in 1959.

TREAT was first used as a dedicated facility to examine fuel motion under transient heating conditions. As discussed in a section above, the initial conservative safety calculations readily showed that the rate of core compaction was an important parameter in the estimates of accident energetics. The TREAT experiment program addressed this issue using both fresh and irradiated pins in a variety of capsule tests. The program, although highly successful in producing data, raised many questions about the influence of other core materials on the fuel motion and led to the development of experiments containing flowing sodium coolant. The improved tests began to take on the appearance of integral tests even though they were addressing only fuel failure and fuel motion and contained at most three fuel pins. Later improvements in the experiment apparatus allowed the use of more pins (up to a maximum of seven), longer pins (a full length FFTF pin is ~2.4 m long), and pins containing substantial quantities of plutonium. Other improvements allowed a more accurate simulation of the hydraulics of a prototype reactor. Thus the phenomenological program on core compaction progressed smoothly into a series of integral tests, rather than evolving separately from the integral series.

On the other hand there were other issues such as pin-to-pin failure propagation for which larger integral tests alone were thought to be neces-

sary. Indeed, the issue of failure propagation was the basis for an expensive effort to design and construct a large flowing-sodium loop to be placed in the Engineering Test Reactor in Idaho. The self-contained loop had a sodium-to-helium heat exchanger and an induction pump for circulating coolant, as well as extensive instrumentation and a wide containment margin to safety. These features, which required both numerous modifications to the ETR and several new support systems, allowed the fuel to be irradiated at steady-state for extended periods (up to ~20 days at full power) and to continue safe operations even with extensive fuel failures. It is interesting to note that none of the seven experiments in this large, sophisticated loop addressed the very issue of pin-to-pin failure propagation for which the loop was originally intended. That issue, which even as late as the early 1970's was a still major concern in fast reactor safety, has been addressed through detailed analysis of failure-propagation mechanisms that pointed to the improbability of such propagation. The loop, however, was however adapted for fuel motion studies and studies of the effects of a flow blockage within a fuel bundle.

TREAT and the ETR provided the main in-reactor testing facilities for safety research. Three other large facilities that were used by the safety program were the EBR-II for extended fuel irradiation in a fast flux (with limitations on the length of the irradiated pin), the General Electric Test Reactor (GETR) for irradiation of longer pins in a thermal neutron field, and the Hot Fuels Examination Facility-North for remote experiment assembly and disassembly. Although these facilities were not built or operated solely for the safety program, their existence and funding were certainly made more secure because of their significant contributions to that program.

One final large facility that should be mentioned is the Safety Research Experiment Facility (SAREF). The success of the TREAT fuel-motion experiments was in large part due to the successful development of a fuel imaging method that used fission neutrons generated in the experiment itself to quantitatively indicate the presence of fuel. This method was able to produce a time-dependent image of the fuel mass in the experiment even though the pin was sealed in a steel container at the center of the reactor and was in many cases cooled by flowing sodium. A limitation of the TREAT reactor, however, was the inability to drive experiments with more than seven pins through a meaningful transient. On the other hand, the ETR system could drive up to thirty-seven

pins, but only at steady-state or on slow transients, and had no fuel motion monitor. For these reasons it was argued that the safety program needed a new dedicated facility to drive large bundles through transients, while also accommodating a fuel imaging device (which required a slot in the reactor core and reflector). The large SAREF project was organized to design a new test reactor for such experiments and to upgrade TREAT for additional complementary experiments. In late 1976 the SAREF funding was approved by Congress as a line-item for FY1978, but political forces and economic program constraints curtailed the effort. The project scope was reduced, leaving the TREAT upgrade intact, but eliminating the new reactor. The final steps in the TREAT upgrade construction are scheduled to begin in late 1984, and the reactor will be available in late 1985 for experiments. The upgrade is being made principally to handle longer experiments (requiring changes in the building dimensions) and bigger bundles (requiring changes in the core design), but it will not have the flexibility envisioned for the new reactor.

### A.3.3.5 Scaling in Safety Experiments

The requirements for large in-reactor facilities have been outlined, but the use of scaled experiments in either in-reactor or laboratory safety experiments has purposely not been given much attention in the preceding discussion. In a sense, experiments with simulant materials are scaled experiments because of the planned, consistent change in temperatures, boiling point, pressures, etc.; but true scale experiments in safety research, in which geometries as well as conditions are scaled, are not common. Rather, one finds more frequently that safety experiments use a full-size subset of the system - a small bundle of full-size pins, a small fuel-steel pool, or even a small piece of fuel pin. In some of the structural-mechanics safety experiments true scale models have been useful, but in efforts addressing such phenomena as the movement of molten fuel or molten cladding during an accident the value of scale models is limited. In the main, the limitations arise because of the number of mechanisms that affect the outcome and because of the difficulty in insuring that each effect is properly scaled. For example, one could easily scale the cladding motion resulting from sodium vapor streaming but the change in materials and pressure would affect the boiling point of the simulated cladding resulting in improper scaling of steel-vapor effects on fuel motion. Moreover, and perhaps most importantly, the principal use of a

true scale model would probably be to estimate the interaction between those full-size subsets that are used in experiments; but it is believed these interactions can be calculated more accurately than they can be measured with scale models. When there has been concern that bundle-size related effects are not understood well enough to be calculated, the approach has been to increase the size of the subset used in the experiments rather than resorting to scaling. Thus, the movement from small integral tests such as single-pin and seven-pin tests) to larger, more sophisticated tests (up to thirty-seven pins in in-reactor experiments and larger out-of-reactor) represents a meaningful examination of many size-related interactions without resorting to scaled experiments.

A.3.3.6 Observations

A summary of significant points in the above discussion and a few related observations that were not specifically discussed are given below.

(1) Conservative safety calculations (that is, calculations that give an upper bound on the damage produced by an accident) are possible with only a very limited knowledge of the mechanisms involved in the course of the accident, but the usefulness of such calculations is questionable because the uncertainties result in a very loose upper bound. A principal value of such calculations has been to stimulate experiments and testing to reduce the uncertainties.

(2) Experiments with simulant materials are useful for examining phenomenology, for extending parameters, and for guiding experiments with prototypic materials; and simulant-material tests are usually less costly. But these tests often are not sufficient for safety applications where uncertainties can lead to difficulties.

(3) Issues can be resolved with or without experiments. There are instances in fast reactor safety where issues disappeared before the completion of expensive facilities that were being built specifically for that issue. Elaborate and expensive experiment facilities should be flexible enough to change mission.

(4) Issues not only can disappear without additional data, but they can also appear without prior observations. Issues in safety research often arise

from sheer conjecture. Although the number of surprises in the safety program has been reduced by planning and careful early analysis, it is probable that issues will arise that will require new tests and new models.

(5) Although early program planning may differentiate between phenomenological (separate-effects) tests and integral test, it was seen that frequently the small-scale tests that address separate effects evolve into large integral tests. In other cases however, a distinct division exists between the two groups of experiments even to the point of requiring different in-reactor facilities.

(6) As shown by the cancellation of the new reactor test facility to be built by the SAREF project, changes in national policy and economics can cause an immediate and strong perturbation in long-term research programs.

### A.3.4 Experimental Reactors and Plant Design

#### A.3.4.1 Need for Integral Experimental Systems

Up to this point, the report has addressed the testing programs that focus on specific aspects or sub-systems of the overall fast reactor plant. But clearly, the ultimate test of a reactor system is to build and operate a plant. One must build a plant to find problems, and one must expect problems in operating the plant that were not previously considered. In fast reactor development, developmental plants were always built for a specific primary mission -- for example, EBR-I was built to demonstrate breeding and feasibility of extracting useful energy from fission; EBR-II was built as a pilot power plant and to demonstrate a self-contained fuel cycle; Fermi addressed the commercial viability of the technology — but in all cases problems unrelated to the primary mission were expected and encountered and many lessons were learned. These problems and lessons often arose from the interaction of the parts of the system and may not have been seen in a test of an isolated part. A few examples have already been noted: the corrosion of the Fermi steam generators due to the choice of cleaning fluid, or the fission-product bubbles formed in the LAMPRE molten-metal fuel; and other examples are numerous in the testing and operation of all the breeder reactor systems. In each case, the problem or lesson was not seen until construction on the actual system began, or until the system was operated in a prototypic manner.

Three examples are of particular interest; two because they resulted in the only unintentional fuel melting in a fast reactor, and the third because of its similarity to one of the others. The first to be considered is the EBR-I incident, often referred to in the now-ominous terms as the EBR-I core meltdown. (One commonly thinks of a core meltdown as producing vast quantities of molten fuel; but it is necessary to keep in mind the football-size dimensions of the EBR-I core, and the fact that only a fraction of the fuel melted.) The fuel melting resulted from the improper execution of an experiment to measure core-kinetics parameters, and by itself is not a particularly significant contribution to this report; but the reasons for the kinetics experiment are significant. Early in the high power (1 Mwt) operation of EBR-I, it was noted that the reactor power coefficient of reactivity had a relatively large positive component which was believed to exist under all conditions, but which could be observed only when power-to-coolant-flow ratio was high and when the rate of change of power was high. That is, when these conditions existed, neutron multiplication (reactivity) seemed to increase as power increased. A slow negative coefficient of larger magnitude was also observed. Both reactivity coefficients could be seen when sudden changes in either power or flow were made. As late as 1955, four years after the reactor was first operational, the source of these coefficients was still not fully understood.

Prior to 1955 a series of power run-ups had been executed to examine these reactivity coefficients, but the instrumentation was poor, and in November 1955 it was decided that the tests should be ran again. Because of a poorly detailed procedure, a reactor operator failed to properly terminate an experiment, and the power rose nearly exponentially to a level high enough to cause some of the fuel to melt. The direct cause of the accident (improper experiment planning) and the direct result (fuel melting and motion) produced numerous lessons for the reactor safety community, but for the purposes of this report the important point is the cause of the reactivity changes reflected in the measured coefficients. After considerable analysis of the accident, of the reactor behavior prior to the accident, and of the reactor behavior with a new core after the accident, it was determined with confidence that the initial prompt power coefficient was caused by fuel rod deformation due to the thermal gradient across the core. That is, the side of the fuel rod nearer the center, a region of higher power, was hotter and expanded more

than the side away from the center. Thus, the 14 inch fuel rod bowed inward toward the center of the core. This inward bowing increased the effective fuel density in the core, raising the reactivity.

On the other hand, explanations for the negative power coefficient are less widely accepted. One of the most plausible explanations, although not without its doubters, is one in which a 4 inch thick steel plate, tightly supporting the upper ends of the fuel rods, also bows under a thermal gradient. Only in this case, the bowing is said to bend the fuel rods back out, eventually reducing the fuel density a point below that at which it started before the fuel deformed in either direction. Such dynamic interaction between the power level, the flow rate, the temperature gradient, fuel-rod bowing, and shield plate deformation would be very difficult to foresee and even more difficult to predict. Quite obviously, the plant had to be built before the effect could be observed or studied.

To further emphasize the dynamic nature of such interactions, one can cite an incident in the EBR-II system much like that seen in EBR-I, but this time the incident had a safe resolution. In the mid-1960's it was decided that EBR-II had successfully achieved its primary goal of demonstrating both the feasibility of local fuel recycle and the practicality of power production with a fast reactor; and the mission of the facility was changed to one of fuel irradiation. Without a primary interest in fuel breeding, the radial blankets were found to be somewhat detrimental to the new mission of the reactor, and they were replaced with steel reflector bundles. After various neutronic calculations, and various tests, it was believed that the effect of the new "blanket" material was well known, and the reactor was raised to full power. In the course of raising the power, a distinct and unexpected positive contribution to the power coefficient was noted. Argonne physicists were notified of the possiblity that the core could have melted - an over-reaction that was perhaps due to the EBR-I experience more than ten years earlier - but an examination of the instruments quickly ruled this out. Additional study and some innovative experiments with the reactor eventually proved that the positive contribution was again due to core deformation, even though in EBR-II the deformation was expected.

The original design of the core had in fact made use of this expected deformation. The design called for the base of hexagonal cans containing the

pins to be firmly clamped while the upper portion of the cans was relatively free to move. Thus, in the original core the temperature gradient bowed the can; but when the cans deformed, the base stayed fixed and the upper regions moved away from the core centerline, resulting in a net decrease in fuel density in the core. However, when the uranium blankets were replaced with steel rods, the rigidity of the new bundles was not fully considered. With these steel rods surrounding the core, the tops of the fuel cans were not as mobile as they had been in the prior configuration. Thus, the bowing can could not move the top away from the centerline, so it moved the middle toward the centerline, adding reactivity similar to EBR-I. In this EBR-II example it is found that the interaction had initially been anticipated and even used in a beneficial manner, yet a small change in the system caused the interaction to completely change its net effect, further demonstrating the need to build and operate an entire system as an integral test for both expected and unexpected phenomena.

A final example of this need is found in the fuel melting incident in the Enrico Fermi plant. In this case, an attempt to improve the safety of the system actually led to a costly accident. The original design of the reactor had called for a large region below the core to contain the material from a core meltdown without recompressing the material into a critical mass. To prevent, or at least delay, the molten metal fuel from eating through the lower boundary of this container, the container was lined with zirconium metal. Should the core undergo an accident that melted the fuel, the molten material from the core region was to flow down the open center portion of the bottom axial blanket and onto a conical flow guide located just above this zirconium lined region. The flow guide, which in normal operation redirected the sodium coolant at the inlet, was to deflect the downward flowing molten material onto the zirconium liner preventing a local recriticality.

The original design for this portion of the system called for a bare steel conical flow guide, but during the construction of the reactor it was decided that this component also should be lined with zirconium. These liner pieces were pre-formed and spot-welded to the flow guide, and later became the classic example of too many safety features making the system less safe. The hydraulic forces from the inlet sodium flow eventually caused the welded attachment to fail, two of six liner pieces broke lose, and at least one piece

blocked the inlet flow to a bundle leading to fuel overheating and melting. This incident clearly shows both the importance of proper engineering analysis and testing, and the fact that the interactions among components are not always forseeable. Without building and operating the system, one can never be certain the system will work as planned.

### A.3.4.2 Criteria for Design of Experimental Reactors and In-Reactor Experiment Facilities

In sections preceding we have already noted the influence that the primary mission of a system had on the design of certain systems, but it is interesting to examine some of the less obvious choices that were made in the design of both experimental reactors such as EBR-I and II or Fermi, and experiment test beds such as the FFTF. Because EBR-I was to be simply a feasibility study of plutonium breeding and power extraction, and because there was no prior experience with many of the systems that were necessary for the plant, there was no detailed design study to optimize the design. In many cases the design was fixed on little more than an educated intuition. The numerous trade-offs that were eventually to be considered in the design of later plants were not considered for EBR-I, at least in any quantitative manner. The plant was designed with what was considered to be adequate conservatism; and it was satisfactory that the system simply worked, regardless of the efficiency of the design or the scaling problems that might be encountered in attempting to build a bigger plant with the same technology.

By the time EBR-I was operational and had demonstrated the feasiblity of the concept, engineers and physicists had begun thinking about larger plants that would serve either as a small pilot plant (EBR-II) or a larger, commercial-scale plant (Fermi). In designing these plants, more thought was given to the details of the plant and the effect these details might have on the operating characteristics. The goal was no longer mere feasibility, but rather a demonstration of the commercial benefits of the system. Choices were numerous and experience was limited. The decisions included such items as: the choice between sodium and NaK coolant; provisions for decay heat removal; the direction of coolant flow through the core (up or down); the position of the primary pump (hot leg or cold leg); materials selection; provisions for sodium purity monitoring and cleanup; plant layout, maintenance, and accessibility; and many others.

One item that even today continues to receive attention is the choice between a piped primary coolant system (a loop) and a tank- or pot-type primary system (a pool). In a loop system the reactor is contained in a relatively small reactor vessel, and the primary sodium is pumped through vessel penetrations and into piping that leads to the intermediate heat exchangers that are located in vaults external to the reactor. In the pool system the reactor container and all of the main primary heat transfer equipment, including pumps and heat exchangers, are contained within a relatively large tank and submerged in sodium. Nonradioactive sodium is pumped out of the tank through a piped system or steam generator. Historically, the pool system has found support because of its inherent safety features of high heat capacity and readily established natural convection cooling. However, these features can be engineered into a loop system which also has numerous other attractive engineering features. An important feature of the loop design is that most of the components are outside the reactor vessel and can be decoupled. This is a particularly attractive feature for an experimental facility because it facilitates the design, construction, testing, and to some extent the maintenance of the components, and it is a more traditional configuration that in the past was thought to be easier to handle from a structural point of view. This argument of familiarity with a loop, of concerns over construction difficulties with a pool, and of uncertainties in temperature fields in the pool and the resulting structural deformations, led the Fermi designers to choose a loop system for their reactor. Other sizable sodium-cooled loop systems have included the Sodium Reactor Experiment, SEFOR, the FFTF, and the Clinch River Plant, all in the U.S., the Dounreay Fast Reactor (UK), BOR-60 and BN-350 (USSR), JOYO and MONJU (Japan), KNK-2 (Rep. Germany), and Rapsodie (France). Pool systems have included, along with EBR-II, the Prototype Fast Reactor (UK), Phenix and Super Phenix (France), BN-600 (USSR), and Argonne and GE designs for a demonstrtion plant.

The interesting point in the pool/loop choice is not the possibility that one system is intrinsically better than the other, but rather that the choice, which strongly affects the design of many components, is a parameter in the design of an experimental facility, and that this parameter is influenced by the purpose of the facility, the acceptable level of risk in operating the facility, and even the size of the facility. This point is highlighted in a decision by the Atomic Energy Commission concerning the design of a fuel-

irradiation facility. In the late 50's, the fast reactor community had recognized a need for a fuel irradiation facility to gain experience with advanced fuels, particularly carbides and oxides, under prototypic conditions. (EBR-II was not converted to an irradiation facility until 1967.) In 1960 Argonne National Lab. proposed a small (~50 MW) reactor dedicated to operations using advanced fuels. A major feature of this Fast Reactor Test facility (FARET) was that the reactor was critical on the test fuel alone, and did not rely on driver fuel to produce an irradiating neutron field. Criticality was maintained in the small core by raising the enrichment of the uranium component of the fuel over that needed in a larger core. By changing only the isotopic composition of the fuel, prototypic chemical and metallurgical interactions were maintained, although the small, highly enriched core was expected to have a slightly harder flux than a larger reactor.

Construction had started on FARET in the early 60's when the AEC began to consider the possibility of building a large demonstration power plant. To gain construction and operating experience, and to obtain a needed facility, it was proposed that a large irradiation facility could be built, particularly at a Richland, Wash. site, as an intermediate step before a large demonstration plant. Even though both FARET and this new irradiation facility (which was to become FFTF) had a loop configuration, the choice of a loop in place of a pool in the larger plant was not an obvious decision, nor was the loop concept chosen for the same reasons in both FARET and the larger plant. The selection of a loop seemed to be appropriate for FARET because it allowed more rapid access to the test fuel in the core and because the risks accompanying a loop system were acceptable since the reactor was small. On the other hand there was concern that the large costly plant would not be protected adequately by the loop-type primary coolant system and that the plant should be built around the pool design. In this aspect of the FFTF design the risk-weighted economics of the decision had a strong influence on the eventual choice. The problem was that it was difficult to arive at a consensus on the perceived risks and benefits. Some workers saw the FFTF plant as a large and costly reactor that should be protected; others saw the same plant as a pilot plant for larger loop-type plants as well as an irradiation facility, and in any case believed the plant to be adequately protected by the primary system. Eventually, the plans were solidified around the loop design, and the plant was built and is currently the premier fast reactor facility in the U.S.

### A.3.4.3 Observations

(1) The first part of this section gave examples of a fact that is well known to any thoughtful worker in engineering: you never know how, or even if, the system will work until you build and test it. The operation of an integral system that is merely related to the final objective can be valuable in obtaining experience and data, and in highlighting unexpected problems.

(2) A peripheral point that arose in the Fermi incident is that too many safety systems may make the system less safe. Although this is a simplistic summary, it should be recognized that adding defensive devices to a plant may introduce risks that are not always obvious.

(3) In building early experimental facilities (that is, reactors that were themselves experiments), little attempt was made to optimize the design of the facility. With little data or background on which to build, the early designers did not need an optimum facility, just a working facility.

(4) As breeder technology developed, more options and design choices became apparent. However, it was necessary to exercise greater care in making those choices, because later systems were built on the experiences with prior systems. Current choices narrow the path of future development and must be made with increasing care.

## A.4. Summary Observations and Conclusions

In this report we have attempted to give a brief history of breeder reactor development and to highlight aspects of the testing program that accompanied and drove that development. The examples were chosen not only to give a flavor for the scope and purpose of the testing program, but also to illustrate a few observations, or lessons, that seemed to be generic in the development of a large, nuclear/mechanical system for energy production. In each section we have followed the discussion of the examples with a summary of the observations derived from those examples, permitting the readers to extrapolate the lesson to their own existing or proposed testing program. For emphasis it is valuable to assemble and comment further on many of these observations.

We begin with a few general observations based mainly on the history of breeder reactor development and generally supported by the examples detailed in the second part of the report.

- Major technological developments require extremely long lead times for their implementation.

  From the inception of Clementine (proposed in Nov. 1945), which demonstrated the feasibility of operating a plutonium-fueled, metal-cooled system capable of producing power, until the earliest time when a demonstration plant might have been built in the U.S. (setting aside the intervening institutional perturbations experienced), approximately 40-50 years would have elapsed. While foreign experience, notably the French, has been considerably better, this lead time reflects the realities in this country.

- Confirmation of a new, sophisticated technology requires a series of demonstration and prototype plants of progressively larger size, paving the way to a commercial size unit.

  A demonstration plant program provides a bridge between the technology development phase and large-scale commercial utilization. At one stage in the evolution of the LMFBR program the view was held that as many as three demonstration size and three near-commercial size plants would be needed.

- A viable alternative to the progressive plant approach consists of a vigorous component development and testing program in conjunction with selectively fewer demonstration plants.

  Successively larger demonstration plants require the concomitant development of components for each successive plant. The fact that this approach would have entailed the development of several generations of large components - a costly and time consuming process - led to a major LMFBR program redirection. A large component test facility to test full commercial-size sodium components was introduced in the program, along with a single demonstration plant.

- The ultimate test for commercial acceptance, insofar as industry is concerned, will be based on the ability of the system to compete economically with all other sources of electrical energy.

- Early industrial involvement, including the utility industry, is essential to commercial acceptance.

- Public acceptability has less to do with economics, but rather more to do with their perception of the adequacy of safety and environmental considerations.

- Lack of public acceptance can be a major obstacle.

- Test facilities have played an indispensable role in the development of the LMFBR program:

  Clementine served as a proof of principle test facility.

  EBR-I served to further prove the breeding principle, demonstrated the feasibility of using a liquid metal coolant, provided fuel, cladding, and structural material behavior under intense irradiation and at high temperatures. It also demonstrated that there is nothing inherently hazardous in the operation of a Pu-fueled system.

  SEFOR, an example of a very special purpose physics test facility, demonstrated the safety characteristics of the oxide-fueled fast reactor through measurements of the Doppler coefficient, essential to making the concept viable.

  EBR-II, intended as a pilot plant step toward full-scale commercialization, served as a test bed for of major components (pumps, heat exchangers, valves, flowmeters, control rod drives), investigated the performance of fuels and materials, and demonstrated the engineering and performance feasibility of the breeder reactor as a power producing facility.

  Fermi, intended to demonstrate commercial scale-up of a fast breeder power plant, served as an extensive test bed for plant components and systems. Also, as a result of a major flow blockage experienced in the operating reactor, a fundamental design criterion was established for all ensuing plant designs.

Special purpose test facilities have been, or are being used for

- Safety
  - Transient Reactor Test Facility - TREAT;
  - Sodium Loop Safety Facility;
  - EBR-II;
  - Engineering Test Reactor, and others.
- Component Development
  - Sodium Components Test Installation;
  - Steam Generator Test Rig;
  - Sodium Pump Test Facility, and others.
- Fuels and Materials
  - EBR-II
  - FFTF
  - GETR
  - HFEF
  - Hot Cells

Other observations from the detailed discussion of the breeder testing programs are listed below with a few additional comments. Although these observations are more specific to the development of breeder reactors, parallels can be drawn between the points listed below and similar points in the past or future fusion technology program.

Fuels and Materials

- Unanticipated or previously unobserved phenomena are likely when exposing well-characterized materials to new environments. The phenomena are often seen only when the material is placed in prototypic conditions.

- As demonstrated by the cladding embrittlement, the effect of the new environment can be anticipated but not quantifiable without testing. Without quantitative information, such anticipation is of little value.

- Some phenomena can be slow in developing, but can have profound impact on material use. The swelling tendency of stainless steels in fast reactors was not seen until 1967 even though these steels had been used since the

early fifties. Up until the mid-sixties the fluence on samples under investigation had not been high enough to see the swelling.

- Phenomenological data on materials is not only useful in constructing and calibrating models, but is also directly useful in design work. This is abundantly clear in the manner in which the fuel and steel swelling data were used.

- For any system where the randomness of failures becomes important (e.g. for core with thousands of fuel pins, or for heat exchangers or steam generators with thousands of tubes) statistical data on these failures are necessary to establish probabilities and to permit economic calculations.

Components

- The U.S. breeder reactor program to date has been developmental in nature, and as such, has required an extensive program to design and test components that, prior to the emergence of metal-cooled reactors, had little industrial application.

- In the early development of many components, small integral systems were often used as experimental test beds, but as the sophistication of both the components and the remainder of the system grew, the integral tests were in part replaced by stand-alone tests of individual units. The integral tests with the entire reactor system assembled were then used mostly as performance checks and to gain operating experience. In the general comments listed above it was noted that this shift to unit testing was a response to the limitations on resources, and led to a more cost-effective program. The numerous plants needed to test large components, and the risks involved in their operation, made the integral tests with an entire system too expensive to operate as a developmental experiment.

- Early components were often conservatively designed to ensure that they would simply operate and would not be the limiting unit in an integral system test. Such designs indeed resulted in the successful operation of

early plants (with exceptions), but did not provide a true test of the concepts that they represented.

- Premature expansion of some of the early technology beyond its limits resulted in costly failures and caused delays in obtaining more valuable information on plant performance. These delays were caused by using components that had not been thoroughly tested as a separate system. When a single important component failed the entire plant was shut down. Such delays gave further impetus to the move toward more extensive unit testing before integral system operation.

- Scale-model testing was useful in components testing, particularly in obtaining hydraulic data. Tests were carried out not only on models of entire units, but also on models of parts of the units. Few-tube tests, a form of scaled testing, were also particularly useful in obtaining thermal/hydraulic data on heat exchangers and steam generators.

- A variety of issues was studied with phenomenological experiments, but the application of the data from at least one of these test series was confounded by the difficulty in translating laboratory parameters to measurable parameters in the prototype.

- Many factors were considered in the decision to change from the pool concept of EBR-II to the loop design seen in FFTF and CRBR. One view held that an increased risk in a loop plant, a loss of momentum in components development, and an inability to build on past experience, would be significant results of this decision. Clearly, this was not a universally accepted view. At the time a decision was made to build the large loop-type FFTF there did appear to be a greater risk of plant failure in such a design. (This was a perceived <u>economic</u> risk, rather than a risk to public safety.) But as the technology has advanced it appears that the operating experience of loop-type plants compares favorably with pool plants. However, for numerous reasons the demands for large margins of safety recently have increased in importance, and the pool system with its large heat capacity and thermal inertia has again become attractive.

Safety

- Conservative safety calculations (that is, calculations that give an upper bound on the damage produced by an accident) are possible with only a very limited knowledge of the mechanisms involved in the course of the accident, but the usefulness of such calculations is questionable because the uncertainties result in a very loose upper bound. A principal value of such calculations has been to stimulate experiments and testing to reduce the uncertainties.

- Experiments with simulant materials are useful for examining phenomenology, for extending parameters, and for guiding experiments with prototypic materials; and simulant-material tests are usually less costly. But these tests often are not sufficient for safety applications where uncertainties can lead to difficulties.

- Some issues are resolved before planned experiments addressing these issues are executed. There are instances in fast reactor safety where issues disappeared before the completion of expensive facilities that were being built specifically for that issue. Elaborate and expensive experiment facilities should be flexible enough to change mission.

- Issues not only can disappear without additional data, but they can also appear without prior observations. Issues in safety research often arise from sheer conjecture. Although the number of surprises in the safety program has been reduced by planning and careful early analysis, it is probable that issues requiring new tests and new models will continue to arise.

- Although early program planning may differentiate between phenomenological (separate-effects) tests and integral test, it was seen that frequently the small-scale tests that address separate effects evolve into large integral tests. In other cases however, a distinct division exists between the two groups of experiments even to the point of requiring different in-reactor facilities.

- As shown by the cancellation of a large safety facility to be built by the SAREF project, immediate or short-term national economics have a strong effect on long-term research programs. Although this point was raised in the context of the safety testing program, other examples can be found throughout the breeder program. This point is particularly important in planning programs for the development of energy sources to be used in the distant future. Expensive systems are vulnerable to budget pressures.

Systems Design

- In building early experimental facilities (that is, reactors that were themselves experiments), little attempt was made to optimize the design of the facility. With little data or background on which to build, the early designers did not need an optimum facility, just a working facility.

- As breeder technology developed, more options and design choices became apparent, but to limit the scope of the program some had to be eliminated. It was necessary to exercise care in making those choices, because later systems were to be designed and built using on the experiences with the chosen options. Current choices narrow the path of future development; once an option is eliminated, it is difficult to resurrect.

- A peripheral point that arose in the Fermi incident is that too many safety systems may make the system less safe. Although this is a simplistic summary, it should be recognized that adding defensive devices to a plant introduces risks that are not always obvious.

Although certainly not a exhaustive list of interesting observations one might find in the breeder testing program, these points do give a suggestion of the overall course of the program and the decision processes involved. With some thoughtful extrapolation these points should aid the fusion program planner in projecting the course of his program, in foreseeing problems that might be encountered, and in avoiding costly mistakes. Clearly, the parallels between fusion technology and breeder technology will ensure that at least part of the technical history of the breeder is relevant in planning for the development of fusion energy.

## References for Appendix A


Zinn, W. H., Lichtenberger, H. V., Novick, M., Feasibility Report: Fast Neutron Pile for a Test of Conversion, Argonne Natl. Lab. Rep. ANL-4356 (1949).

Zinn, W. H., Proposed Five Year Construction Plant for the Development of Power Reactors (circa 1950).

Levenson, M., Determination of the Conversion Ratio of the EBR-I by Radiochemical Methods, Argonne Natl. Lab. Rep. ANL-5095 (1953).

Jurney, E. T., et al., The Los Alamos Plutonium Reactor, USAEC Rep. TID-10048 (1954).

Joint Committee on Atomic Energy, "Five-Year Reactor Development Program," U. S. Government Printing Office, May 4, 1955.

Bethe, H. A., "Reactor Safety and Oscillator Tests," Atomic Power Development Associates, Inc., Report APDA-117, October 15, 1956.

Koch, L. J., et al., Hazards Summary Report, EBR-II, Argonne Natl. Lab. Rep. ANL-5719 (1957).

Kittel, J. H., Novick, M., Buchanan, R. F., "The EBR-I Meltdown, Physical and Metallurgical Changes in the Core," Nucl. Sci. Eng. 4 (1958) 2.

Joint Committee on Atomic Energy, "Proposed Expanded Civilian Nuclear Power Program," U. S. Government Printing Office, 1958.

U. S. Atomic Energy Commission, "Civilian Power Reactor Program Status Report on Fast Reactors as of 1959," USAEC Publication TID-8518(1), 1960.

Smith, R. R., et al., "An Analysis of the Stability of EBR-I, Marks I to III, and Conclusions Pertinent to the Design of Fast Reactors," Physics of Fast and Intermediate Reactors (Proc. Seminar Vienna, 1961) 3, IAEA, Vienna (1962) 43.

U. S. Atomic Energy Commission, "Civilian Nuclear Power, A Report to the President, 1962," USAEC Report (unnumbered), November 1962.

Thompson, T. J. and Beckerley J. G., (eds.), The Technology of Nuclear Reactor Safety, Vol. 1, The MIT Press, 1964, pp. 625-633.

Smith, R. R., et al., Terminal Report for the Mark-IV (Plutonium) Loading in EBR-I, Argonne Natl. Lab. Rep. ANL-6865 (1965).

Yevick, J. G., Fast Reactor Technology, Plant Design, MIT Press, Cambridge, USA (1966).

Peterson, R. E., Cubitt, R. L., "Operation of the Plutonium Fuelled Fast Reactor LAMPRE," ANS Topical Meeting on Fast Reactors, Trans. Am. Nucl. Soc., San Francisco, April 1967.

Billuris, G., et al., "SEFOR Plant Design," ANS Topical Meeting on Fast Reactors, San Francisco, April 1967.

U. S. Atomic Energy Commission, "Civilian Nuclear Power, The 1967 Supplement to the 1962 Report to the President," USAEC Report (unnumbered), February 1967.

McCarthy W. J. and Jens W. H., "A Review of the Fermi Reactor Damage Incident and a Preliminary Assessment of Its Significance to the Design and Operation of Sodium Cooled Reactors," Proceedings of the International Conference in the Safety of Fast Reactors, Aix-en-Provence, France, September 19-22, 1967.

Ramey, J. T., "Utility Participation in the AEC Fast Breeder Reactor Program," American Power Conference, Chicago, Illinois, April 23, 1968.

LMFBR Program Office, Argonne National Laboratory, "Liquid Metal Fast Breeder Reactor Program Plan," Report WASH-1101 through -1110 10 vols., National Technical Information Service, Springfield, Virginia, August 1968.

U. S. Atomic Energy Commission, "LMFBR Demonstration Plant Program -- Proceedings of Senior Utility Steering Committee and Senior Utility Technical Advisory Panel for the period April 1971 through January 1972," WASH-1201, (March 1972).

Hearings Before the Joint Committee on Atomic Energy, Congress of the United States, "Liquid Metal Fast Breeder Reactor (LMFBR) Demonstration Plant," September 7, 8, and 12, 1972, p. 19.

Hixson J. D., "SEFOR Plant Operating Experience," USAEC Report GEAP-13924, National Technical Information Service, Department of Commerce, Springfield, Virginia, December 1972.

U. S. Atomic Energy Commission, "Liquid Metal Fast Breeder Reactors, Part I: 1948-1961, Part II: 1962-1971," USAEC Report TID-3333, 1972.

Freeman, D. D., "SEFOR Experimental Results and Applciation to LMFBRs," USAEC Report GEAP-13929, National Technical Information Service, Department of Commerce, Springfield, Virginia, January 1973.

AEC Authorizing Legislation Fiscal Year 1974, Hearings Before the Joint Committee on Atomic Energy, Congress of the United States, Civilian Reactor Development, Government Printing Office, March 14, 1973, p. 1814.

Hearings Before the Joint Committee on Atomic Energy, Congress of the United States, "Proposed Changes in Basis for Cooperative Arrangements for the LMFBR," February 28 and May 4, 1973, p. 150.

Hearings Before the Joint Committee on Atomic Energy, Congress of the United States, "Reactor Research and Development; Reactor Safety Research; and Applied Energy Technology," February 26-27, 1974, pp. 826-847.

Alexanderson, E. L., "History, Contributions, and Decommissioning of the EFFBR," US/USSR Seminar in Fast Breeder Reactor Construction and Operating Experience, Obninsk, USSR, June 2-5, 1975.

Billuris, G., Slich, E. E., "SEFOR Construction Experience," US/USSR Seminar in Fast Breeder Construction and Operating Experience, Obninsk, USSR, June 2-5, 1975.

U. S. Energy Policy and Planning, "The National Energy Plan," Executive Office of the President, April, 1977.

U. S. Department of Energy, "National Energy Plan II, A report to Congress", May, 1979.

"International Nuclear Fuel Cycle Evaluation, Summary Volume," IAEA, 1980.

"INFCE, Report of INFCE Working Group 5, Fast Breeders," IAEA, 1980.

Nuclear Enginering International, August 1983 Supplement.

# APPENDIX B

## OBSERVATIONS OF EXPERTS FROM THE FISSION FIELD

TABLE OF CONTENTS


| | | Page |
|---|---|---|
| B.1 | Introduction | B-1 |
| B.2 | Major Problems | B-2 |
| B.3 | Regulations | B-4 |
| B.4 | Setbacks and Failures | B-6 |
| B.5 | Public Acceptance | B-8 |
| B.6 | Power Density | B-10 |
| B.7 | Plant Size | B-11 |
| B.8 | Scaling | B-14 |
| B.9 | Integrated Testing | B-17 |
| B.10 | Personnel and Organizational Structure | B-18 |
| B.11 | Lessons | B-21 |
| B.12 | Reviewers' Comments | B-23 |

## APPENDIX B: OBSERVATIONS OF EXPERTS FROM THE FISSION FIELD

### B.1 Introduction

The development of fission technology is an excellent example of successful and impressive program. As typical in any complex technological development, many unanticipated problems and difficulties were encountered and had to be solved by the developers. We thought that the emerging field of fusion could benefit from examining lessons learned from the fission development experience. Unfortunately, there are no perfect records of experience from such development and published accounts tend to be narrow in scope. Within the resources available to our study, it appeared that an effective approach to learning quickly about the broad fission experience was to interview a number of experts that were directly involved in the fission reactor development.

Two difficulties should be immediately apparent to the reader with this "survey of opinion" approach:

(1) In reflecting on past experience, the opinions of experts will vary depending on their own perspective and areas of expertise. It was not possible to survey a sufficiently large number of experts to show the spectrum of opinions.

(2) The nature of such a survey that attempts to learn from experience is that it tends to paint an overnegative picture because of emphasis on problems rather than success. The reader should remember in reading this section that fission reactors were developed into safe, reliable and economical power sources.

Prof. David Okrent provided advice concerning the kinds of reactor types which had been under development in earlier years and some of the problems that required special attention during development or proved to be signifigant in operation. He also suggested institutions and individuals who were likely sources of good information concerning the above.

The interviews included questions on major design and operational issues that faced the development of each reactor technology, their test facilities

and the environment used in the testing, the need for integrated testing, scaling requirements, failure modes and safety margins used in the tests and things one would have done differently, with hindsight. An attempt was made to take advantage of the experts' intimate knowledge of the subject and their close involvement in the early tests to record information and opinions which are usually absent in published material concerning the tests.

Some of the major fission reactor programs were covered. The people interviewed were:

Dr. Harold Etherington for the PWR program,
Dr. Salomon Levy for the BWR program,
Dr. Spencer Bush on materials issues for both PWR and BWR,
Dr. William Parkins on the Sodium-Graphite program,
Dr. Harold Pearlman on materials issues for the Sodium-Graphite program,
Dr. Alvin Weinberg on the early research at ORNL,
Dr. Herbert McPhearson on the Molten Salt Reactor program,
Dr. Ralph Balent on the SNAP program

The following sections summarize those records of experience and opinions expressed by these experts that we thought would be of interest to reflect upon by the fusion community.

The last section of the report includes comments on the part of some participants within the FINESSE project who reviewed this section. These are comments that we felt will change the spirit of the report and may not truthfully reflect the opinion of the eight persons interviewed if included in the body of the report. However, we thought these comments are important and should be noted.

We wish to thank them all for their cooperation and to say that their assistance is greatly appreciated by all of us in the fusion community.

## B.2 Major Problems

Some of the major problems facing the nuclear industry today have their origin in the early development stages of these nuclear reactors. A hard competition was developing among the different programs and between all of them and the fossil fuel industry. Issues such as stress corrosion of pipes,

metallurgical aspects of the fuel, water chemistry and maintenance were given a lower priority at that point. Getting power out was crucial in the short run to stay competitive while long term potential problems were not receiving enough focus at that time. Any nuclear aspect of the reactor was given a considerable amount of attention as the research was run mainly by nuclear-oriented people while the rest of the plant was neglected somewhat under the assumption that the problems there are mainly of pumps and valves and other conventional components which can be copied from the fossil industry. In some ways a nuclear plant was developed as a fossil fueled plant with a different mechanism for heating a liquid. In the process of getting this plant to be competitive the designers built a compact plant because it should produce a given level of power at a lower initial cost, but this compactness is a drawback in a radioactive environment which severely restricts the normal maintenance process.

When a problem was recognized it was usually adequately solved. For example, the Boiling Water Reactor project focused early on plant stability and critical heat flux and their engineers solved the problems in a satisfactory way proving them to be non-issues. Surprisingly enough, the plant turned out to be considerably more stable than any of the experts and their theoretical models predicted. There was a concern that the big core might decouple, resulting in many local criticalities, but it turned out that even when rods were oscillated and pressure oscillations were applied, no instabilities were recorded. Major problems in the long run were usually areas which did not receive much attention during the plant development stage because they did not seem to be as glamorous or as interesting as other areas.

Another problem related to the competition and time pressures was the issue of long term tests. These tests were usually given lower priority in all programs. The corrosion problems, for example, need time to develop, sometimes up to ten years, and only some fifteen years later, with hindsight, did they learn how to accelerate these tests and perform a ten year test in a few months. There was nothing in the limited literature at that time to indicate that stress corrosion cracking would take longer if low stresses are applied, while large amounts of oxygen in the environment will accelerate the process. Use of oxygen environment would have made these long term tests possible at that time and many of the problems which resulted from the inade-

quate corrosion testing could have been avoided.

The fission industry, being a new development, did not have a comprehensive view of all the problems facing it. Many of them developed long after the design of the first commercial plants was implemented and to deal with these problems an ongoing design process took place. To ensure safe shutdown and adequate heat removal an elaborate network of redundant systems was introduced. Even though the required level of reliability was achieved, the plant nevertheless became cumbersome to some degree and much more difficult to operate and maintain. A good example of this evolution is the seismic load issue. Fission plants are required to ensure that their piping system is able to sustain a given magnitude earthquake without major damage from cracking. Rather than designing their piping system to optimize its durability, industry practice to the present is to introduce snubbers (mechanical devices designed to hold pipes steady in the event of an earthquake) in all the critical pipes. There are now plants where the steel is three to five times thicker around all the places where a primary break was assumed. The problem is that snubber introduction is a costly operation and due to maintenance requirements they have to be removed every three years to a different location for testing. A recent study on PWR plants shows that an adequately performed design can eliminate 50% of these supports. This will reduce plant building costs, reduce the radiation exposure during the snubber testing process and will increase the free space around the pipes which will allow a more thorough search for cracks in the piping system.

## B.3 Regulations

One major feature of the fission industry is the heavy impact the regulatory process had on it. The regulatory system, for the most part, was poorly understood by the plant designers who had to constantly design changes in the plant to adjust to the evolving regulations. Also, in these early days the regulations were not yet firmly established and any new plant was being built at the risk of having to introduce major changes in the future to receive an operating license. For example, some think that one of the reasons for one company's decision to cancel a program to build a plutonium fabrication and reprocessing plant was their uncertainty of the regulations. They did not know what requirements they had to design for and what new regulations would

be posed in the future concerning the allowed ventilation levels, how to treat the wastes and where to store them. The potential supplier believed that these were key issues where the regulator has first to set up the rules before the designing process starts.

The lesson to be learned from this fission experience is that if an industry has to be regulated, the government ought to be given a much larger role in the development stages. The government commitment has to come not only in the basic research stages but also in the long term program itself. Even with the know-how and the adequate funding, such an industry cannot be developed independently without involving and cooperating with the government. A pure commercial approach will not work. Regulators have to come from the ranks of scientists and engineers who are at the forefront of the fusion research and whose knowledge in the field will minimize the process of changing regulations by regulators who are learning and getting familiar in the field.

The fusion industry will have to be regulated because of its neutrons, tritium, radioactive components and the potential of using fusion reactors for the purpose of producing fissionable materials. Even though it may not have to be as heavily regulated as the fission industry, which has a very low potential of releasing large amounts of radioactivity in one single burst, the fusion program should not proceed under the assumption that it will not be regulated. The fact that the fusion industry is to be regulated, should be recognized and the research should be structured differently from a commercial business. That means that fusion will have to employ the best available personnel to build the best possible safety test facilities instead of proceeding along purely competitive programs which are not so helpful in a regulated industry.

The fusion industry should form, early in the development process, a regulatory body which will develop a concise list of regulations to be issued. It is then even advisable to exceed in the application of these regulations so as to have a margin for a possible future toughening of regulations. If regulations are known before the plant design, and key long-term factors like risk level, their application, reliability and cost-benefit are taken into account, a most efficient and safe plant will result.

## B.4 Setbacks and Failures

In the very early days of the fission program, enthusiasm was not lacking and there was a talented group of dedicated people who understood their role as pioneers in a new field. Looking back at some of their achievements, they seem unbelievable. Reactors were built from scratch, licensed and made operational in less than a couple of years. In the process, mistakes were made and programs suffered setbacks which, in general, had no lasting negative effects. Some reactors, for example, did not become critical when assembled and the only effect of this mistake was a delay of a week or two during which a few extra plates of fuel were added to bring the reactor to criticality. This is an extreme example but some lessons can be learned from it. Seeking perfection is not always necessary and sometimes can even have a negative impact. A good example is the Clinch River Breeder Reactor, which generally followed this path. Large sums of money were invested to build a perfect plant in a long term project which was to serve as a model for future plants. When cost overruns were encountered with limited achievements to justify them, the project started being perceived as a white elephant.

This same trend was also responsible in part for the abandoning of the Molten Salt concept in favor of the Liquid Metal Fast Breeder Reactors (LMFBR). The 1962 report to the President which presented the Atomic Energy Commission's justification for the development of breeder reactors was submitted while the Molten Salt Reactor Experiment (MSRE) was under construction. It had proceeded far enough, however, to draw some very favorable comments in the report. As soon as the Report came out, the extant Liquid Metal Cooled Reactor department of the Division of Reactor Development proposed an elaborate and wide ranging program for the development of the LMFBR concept and that program began to gain momentum. On the other hand, the MSRE people adopted a more conservative approach of waiting until the experiment had operated successfully before trying to expand the program. They felt that this was the only prudent thing to do, but at the time they were prepared to develop a larger reactor; the momentum and money needs for the LMFBR program were massive.

It is not necessary to overemphasize perfection as it is essential to have a running system which generates data and allows one to know if the project is on the right track. It is important to set milestones which represent concrete achievements. Successful implementation of each milestone on

time will help build an image of confidence and success around the program long before the final goal is reached.

A few reactor concepts were hurt for not learning this lesson in the late 50's when the Division of Reactor Development of the Atomic Energy Commission realized that they were supporting too many fledgling reactor concepts. While each concept could be researched at the exploratory level with only modest funding, to carry the development of any concept to fruition would require tremendously large expenditures. With funds limited, only a few reactor concepts could survive.

On the other hand, a determined drive towards short term achievements may cause long term problems to be ignored. A very delicate balance has to be sustained and an optimum pace has to be set between the people who will advance only on safe grounds and the ones who are willing to take risks and move ahead.

Another lesson to be learned from the fission industry is just surfacing. They are facing a phenomenon which may well doom the whole industry in the U.S., if taken to the extreme. Three billion dollar plants are being built and then they are required to produce "perfect paper" to prove every detail of the plant was built according to regulations. Documentation of the building of such a plant can hardly be complete when, for example, all an inspector can do at the construction stage is to certify that rebars exist but there is no way their quality and specific location can be inspected after being embedded in the concrete. Requiring X-rays of all reinforced concrete in the plant will be a task that can never be completed. The dilemma is what to do about such a plant if three years later an inspector is accused of signing these documents for tasks which are found to be faulty. Should the plant be stopped at that point?

The extreme of this would be to assume that there is no tolerance for mistakes, that every single recorded value has to be verifiable and verified, that every action of the plant has to be recorded either by television camera or detailed recording and documentation. Building a plant under these conditions will be highly impractical if not impossible. This is one if not the main reason that capital costs of new nuclear plants have risen sharply in recent years and we see a trend to stop construction on plants which are 60% - 90% complete.

Recognition of the fact that plants cannot be built in the above described manner is critical at this stage. The plants have to be built with enough margin of safety to accommodate a reasonable number of mistakes which are certain to occur during construction. Even large safety margins may ultimately be more economical than a requirement for perfection. Building plants more tolerant to mistakes, especially human mistakes, is a sound engineering approach which will allow one to rely on the tolerance of the plants to be confident that even if a mistake is made there will be a way to detect it in time. Such a plant will also have enough safety systems to take care of itself in case of an emergency without any catastrophic effects.

It seems that a fusion plant will be even more complex and costly, but on the other hand regulations may not have to be as severe as the ones on a fission plant. In any case the point can be made that flexibility and tolerance in both the development and the operational stages should not be sacrificed in the pursuit of perfection.

On the other hand, whenever a large and complex system containing extensive circuitry including redundant and diverse systems is built, the probability of failure, in the context of maloperation rather than severe or catastrophic failure, is a very real problem. These maloperations are reflected in the plant capacity factors.

From an economical point of view such problems have and can be solved by control of procedures in great detail, an approach which has not been used in the U.S. in the past. Such maloperation problems are resolvable provided one pays sufficient attention to details. For example, one Japanese PWR has a 99.8% capacity factor over an eight-year period, primarily through a minute attention to details which eliminated many common electrical and instrumentation problems, and by better personnel training to minimize human errors.

## B.5 Public Acceptance

Public acceptance is a growing issue for the U.S. fission industry. It is hard to pinpoint the reason for this public distrust but a few points may be suggested.

It might have been caused in part by the perception the industry promoted in its early days that this new power source is free of problems. The public

willingness to enter the era of nuclear power was high before the problems relating to plant safety were publicized. When the problems became known, parts of the public moved to the other extreme and became disillusioned with the nuclear power idea. Some people in the fusion area today may tend to repeat this mistake by promoting fusion as a problem-free source of power. Problems like radioactivity and maintenance in a radioactive environment tend to be played down. Fusion may avoid part of the fission problem by laying out the potential difficulties early in the development process. This will not solve the public acceptance issue but will raise their credibility in the public eyes. Problems will then be viewed realistically, experts' opinions will be credible and people will not tend to suspect that there is deeper trouble which is being concealed.

Another very important perception subject is the linkage between fusion and fission. If a thorough information drive is not started, very soon people will begin perceiving the fusion process as a kind of fission. There are enough identical components in the two (like neutrons and radioactivity), to confuse many people who are not close to the subject. If this becomes a widespread phenomenon, some of the negative public perception the fission industry has today will spill over to the fusion area. The public has to be educated in a simple but accurate manner of the fundamental differences between the two fields, especially on the subject of radioactive release. This does not mean that the public has to be "educated" that a fusion device is safer than a fission device. The basic differences between the two fields can be pointed out even while stressing the relative merit of both devices from a safety standpoint.

Many people who were convinced that the safety problems of the fission plants are solvable are becoming skeptical about the prospects of nuclear power on economic grounds. In this area, the fusion industry will have even more difficulties. As important as it is to reduce the capital cost of fusion plants through reduction in reactor size for a particular power output, this trend is limited. A minimum size is set by the need to remove the produced heat outside the reacting plasma region by a thick structure of complex design. As important as it was for the fission industry to air their safety problems early in the development stages, it is important for the fusion industry to convince the public that fusion energy can become competitive with

fossil and fission energy sources. Further and detailed engineering studies have to be made available to the public of plant designs and cost estimates for their fabrication and field erection. The public should be informed of the prospects of having a reactor vessel which will have a lifetime to match that of the plant, or if it has to be replaced before, what are the associated costs and shutdown time. Failure to deal with these problems and present them to the public in an honest fashion will most certainly result in major disillusionment on the part of the public if and when problems turn out to be more serious than the experts tend to characterize them today.

The proximity of some of the fission plants to large urban centers is also an issue contributing to their negative public perception. Having large amounts of radioactivity so close to them and the prospect of having one day a major release (as small as the probability of such an event may be) that will affect them, makes these people very uneasy. Some people in the fission industry are today having second thoughts about the wisdom of having built these plants so close to population centers. If fusion plants are to avoid this perception problem they should consider locating plants far from these centers and opt for power transmission instead. Transmission costs can be recovered by having somewhat lower safety related capital cost investment to make this option more attractive. Utilities are at the present transmitting power, anyway, through the country via the electrical grids. Therefore this option should be considered carefully before making the location decisions. Arguments that a fusion plant next to Los Angeles, for example, will not endanger the city residents, may be true; but some people will still choose to believe otherwise, just like the pesticide malathion is thought by experts to be harmless to people, but some still choose to protest in the streets when it is applied on their homes.

## B.6 Power Density

In general, increase in power was achieved by increased size and not so much by increase in power density. The PWR's, for example, increased power by 50% in going from two steam generators to three and then by another 33% in going from three to four steam generators. Power output was generally limited by the size of an economical vessel and the Xe oscillations which are more severe in a large core.

One way to increase moderately the power density was by flattening the

flux profile in the core. Physical mechanisms (like the Departure from Nucleate Boiling-DNB-in the BWR) limit the peak power density. By flattening the flux profile the average power density can be raised without increasing the peak power density in the process.

The early fission plants, like the Yankee PWR and the Dresden 1 BWR, started with relatively low power densities but with "generously" large margins to allow for the lack of knowledge in this area. Dresden 1, for example, at 30 $\frac{kw}{liter}$ was running about 30%-40% below capacity and the Senn plant in Italy ran 50% below capacity. Therefore these plants could later have their power densities raised by about 10%-20% without any adverse effect. By doing so the reactors would be used as testbeds for the next generation of reactors which were designed to operate at the higher power densities. Through step increases, each not larger than 10%-20%, the present day reactors are operating at only about 100% above the early models. GE, for example, built the Big Rock Point reactor in 1964 to test the limit of the power density in its reactors. Densities of 60 $\frac{kw}{liter}$ were achieved but they learned that this value may be too high due to the high flows involved, the vibrations they induce and some control problems. The optimal power density was found to be around 50-55 $\frac{kw}{liter}$ and from the initial value achieved in Dresden 1, this is only a 70% increase.

The BWR 6 operating in Taiwan has the highest power density of the BWR line at 55 $\frac{kw}{liter}$. This increase was achieved by replacing the 7x7 fuel bundles with 8x8 ones thus reducing the heat generation per linear foot of fuel. The latest PWR and BWR plants actually have lowered their power densities and compensate for this reduction by having a refueling period of eighteen months to two years instead of one year.

## B.7 Plant Size

A variety of factors influence the decision on how big a fission plant is to be. One of the main reasons the large plants were developed was to make them competitive with the fossil power plants. Despite creative engineering with regard to high power densities and compactness, the factor that tipped the scale and made them attractive to utilities was the ability to produce large plants. But that was not enough to ensure success to the sodium-graphite plants, for example, because of their inherent low power density. Utilities were interested in a high power output for a limited capital cost

investment and that meant high power density plants.

Some see this trend towards larger units to be wrong. The original design of a 300-500 MWe power plant was in their opinion a better one. Such a small plant would have several advantages such as smaller components and less pressure to keep it online. The economical impacts of shutting down a smaller unit are easier to absorb. A small plant may be easier to operate because of fewer and less complex components. An EPRI (Electric Power Research Institute) study at the present is reviewing the benefits of building smaller plants. This study intends to consider whether a smaller size will have an improved availability during operation to offset the higher capital costs. These costs are higher because due to licensing expenses, shielding requirements, and other factors; building two 500 MWe plants, for example, is more expensive than building one 1000 MWe plant.

Most of the significant economic decisions in the fission industry were made with the emphasis being put mainly on the initial capital cost while the availability was being represented by a rather arbitrary constant factor. This factor was provided by the vendors and was more or less the same for all plants. Some think that canceling out the availability factor and comparing different plant designs based upon their capital cost only, was a mistake. When those considerations are made, credit has to be given for any improved availability factor, less maintenance problems and less exposure of workers to radiation during maintenance. That is the reason why the EPRI study is important. If their conclusion is that plant availability is higher in smaller units, then this might become the trend of the industry in the future.

This would be a subject of interest in the fusion field too. If the tokamak has to be evaluated versus the mirror design, one factor will have to be the potential for building smaller commercial plants. Higher availability of such plants if proven, may offset any additional capital costs.

## B.7 Safety Margins

It is important during the testing stage to provide margins that reflect the state of knowledge. When the state of knowledge is very poor, and the full understanding of all the mechanisms is in question, margins must be emplaced to compensate. Safety margins can be relaxed when the state of knowledge improves.

A typical example of such a process was the Critical Heat Flux (CHF) issue in Boiling Water Reactors. When starting the project, they found a large number of tests described in the literature, dealing with the CHF inside a tube as a function of pressure and flow, but these tests did not apply to the multi-bundle geometry of the reactor. When attempting to plot the CHF versus the exit steam quality, they realized that there was a very large spread in the data but very little understanding of its cause. When they started to generate their own test data it became evident that some of the spread was caused by unreliable data which came from unstable loops, while some came from tests that were run incorrectly. After screening these tests out they started seeing the effects of flow dependence and heat flux distribution. But most importantly, they recognized the effects of the geometry, especially the differences between flow outside a rod as opposed to flow inside a tube. This realization prompted a set of annular tests, in which some 600 points were generated and used to obtain the GE specific CHF curves.

Even with this extensive research they did not have full confidence in this crucial parameter and to be on the safe side they drew a line below the lowest point, added to it a conservative margin of 1.8 to compensate for the lack of knowledge, and used the resulting curve to calculate their CHF. Fortunately, an annulus happens to be a reasonable simulation of a bundle and with the safety margin in place this curve proved to be applicable to the multi-bundle geometry. But to the day Dresden I started operating, some believed that it would only be able to operate no higher than 50% power, partly due to CHF constraints. They proved to be wrong. When additional data on the bundle geometry was obtained, the margin was dropped to 1.5 and only when complete prototype tests were run with full scale bundles, did the team become confident that the experimental data is representative of the CHF and can be used with small margins.

This is a typical process of many other poorly known areas which had to use margins as substitutes for knowledge. Dropping them altogether when enough data is available is, in the opinion of some, not a wise thing to do. They would rather have these margins partially reinstated in the power plants. Running them so close to the limit does not allow the operators the maneuvering grounds before they encounter safety problems. In addition, building back some margins into the power plants will allow for any toughening of regulations in the future or for any unforeseen problems to show up without

having to introduce major changes in the plants. Such margin may also be worthwhile from an economic point of view, making the plant more forgiving as some mistakes will be ignored by the more flexible control systems.

We described how margins are applied when phenomena and mechanisms are not fully understood. The same thing applies for equipment. If it is scaled up, margins have to be provided to make sure it is not operating in its limiting range. For example, if the pump seals are tested at smaller scale and then the data is extrapolated to the operational range, it is advised to use a more conservative seal than the one the extrapolation would indicate for the operating conditions of the larger pump. Therefore margins should be used to represent the state of knowledge and to contribute to a flexible system which will allow in the future for standard toughening and operator mistakes.

## B.8 Scaling

All the programs, except the SNAP (System Nuclear Auxiliary Power) used the concept of scaling down to some degree. The SNAP program did not use it as their purpose was to develop and demonstrate the technological capabilities in a reactor with the least weight per unit of energy. They developed such a small sized reactor, the SNAP10A, and launched it into space.

The other programs used pilot tests, 1/10 to 1/20 of full scale to confirm predictions of analytical calculations or to gain more insight into a particular phenomena. Although this approach worked in many cases and helped the project, some serious notes of caution are being heard about the need to rely too heavily on the data from these tests. There are many examples of problems that were solved only after setting up a full scale test. There are also many examples of problems that surfaced only in the full scale test but did not show in the reduced scale.

Recognizing that the size of a fusion plant, its systems and components, is too large to test at full scale, a modular concept of building the plant should be considered. The fission industry did this when they designed their core so that one fuel rod can be repeated many times. Such a fuel rod or bundle of rods can be tested at full scale for heat transfer and fluid flow. The BWR opted for twenty smaller jet pumps rather than a smaller number of larger pumps because the smaller pumps allowed them to test full scale. Their steam separators were designed also in such a way that they could be tested

full scale. They were even tested two or three at a time to see their interaction.

Other systems or phenomena are not as easy to test full scale. The flow induced vibrations are a good example of such a phenomena. They caused the core and core barrel to shake when the first full scale plants were started. Nobody ran prior tests on this subject and the reactors actually became the first testbed. Some of the vibrations occur from very small leakage flows from seals and they magnify very rapidly. Such vibrations are forceful enough to tear apart a flow channel in a few months. As soon as all the LWR projects discovered the problem, they all built facilities to study the problem. Attempts to build very scaled down facilities were futile as they found that very reduced scale testing never showed the effects seen on full scale. But they were able to eliminate some of the problems when they simulated a slice of the full scale core (30%, for example) while making sure that the end effects are negligible. Due to the large expenses involved in the building of a special full scale facility to test this problem, one vendor decided to instrument the first commercial reactor of this type and thus obtain the data. That was a calculated risk as any problem showing up after delivery to the customer would have required a fortune to solve as the contract obligated the vendor to fix any problem discovered at the plant. To the present, no complete accurate way of scaling down flow vibrations is known.

Another problem which is difficult to scale down in tests is the LOCA (Loss of Coolant Accident). This is because two phase flow is very hard to scale and the researchers who had most successful tests were the ones who used full size models. All ECCS (Emergency Core Cooling Systems) tests of the BWR were on a full scale bundle which when supplied with a small jet pump was used to simulate the core. Tests which tried to predict ECC performance with a shorter rod or annulus could only see the basic mechanisms and phenomena but could not predict the full system behavior.

To this day, one of the biggest problems in fission is the core melt issue and this is because an experiment that gives an accurate description of a large core melt has not yet been devised. An experiment on the melting of a rod is too far to extrapolate to what will happen in a complex core with different temperature distributions. A one half or one quarter scale experiment may give reasonable results but a 1/10 scaling may not provide the needed

results.

On the other hand, there are areas in which full scale testing is not practical. In these areas initial small-scale testing is needed, followed by progressively larger-scale testing, coupled with analytical work to show that the models are working; only then are the models extrapolated. Such a method of scaling up was employed when reactors with higher power densities were designed. The first step was to take an operating reactor and raise its power density to an abnormally high level and record the information regarding those conditions. If the system appeared to be stable, an analytical model was produced to reflect these conditions and if there were no significant discrepancies between the two, the analytical model would be applied to build a new prototype. The prototype would be operated to verify the analytical model. Rod oscillation tests and stability measurements were then used to adjust the model to match the prototype. This process of building a smaller model, pushing it to the limit to learn about the mechanisms which are important at the higher operating regime, and then producing an analytical model of a larger plant, was employed through a succession of models and finally resulted in the commercial plants.

On the other hand, with the increased capacity of the present computers, very detailed models may be employed to simulate full scale plants. The earthquake induced LOCA is being studied at Livermore where the detailed design of a PWR is being laid out in a very large capacity computer, including all piping, supports, vessel, pumps, etc. Using fracture mechanics to simulate crack growth and by simulating a large seismic event the impact on the plant can be evaluated. This program is a key factor in the ACRS and NRC movement toward the relaxation in the seismic design requirements of the double ended pipe break. But even with the new opportunities made possible by these large computers, overconfidence in the results is not widespread as most models are fitted to data and they always cause disagreements among the researchers such as, for example, the debates on the LOCA issue.

The fusion industry should weigh very carefully this point because some of its concepts require extremely large testing facilities. When the size in a particular design concept becomes so big that it makes the building of a prototype impossible, technological problems are due to show up. The building of prototypes was a crucial factor in the success Admiral Rickover had with

the naval reactor program. He always insisted on building a complete prototype of a reactor, testing it and its components full scale. Whenever applicable, the fusion program should consider the modular concept. In addition, any concept which can be implemented as a smaller commercial plant will make the building of a full size prototype easier. This point should be carefully weighed when fusion concepts are compared, as people tend not to give enough credit for such considerations at the start of a development program. Once people embark on a concept and develop it there is generally no return. For example, once the fission industry embarked on the LWR concept it was very hard for them to reverse and consider other thermal reactor concepts. The gas cooled reactors, for example, did not have a fair chance in the U.S. because when they were suggested the utilities and vendors already invested in the LWR and could not allocate research funds to the new concept. The LWR people have invested so much in the development and acquired so much knowledge that they did not perceive any other concept as being able to compete with theirs. That is one lesson the fusion industry ought to learn from the fission.

B.9 Integrated Testing

The fission industry in general had a good record of identifying the problems, setting up separate effects tests, combining them into groups of two or three for partial integrated testing and finally, assembling the full integrated test. As opposed to the fusion area, in-pile facilities in spite of being much more costly than out-of-pile tests, were nevertheless available and all programs utilized them. They were of the philosophy that one never sees the total picture without the integrated test. Among them were in-pile fuel testing, out-of-pile heat transfer and fluid flow facilities, and equipment test facilities including scram systems, control rod drives, seals, etc. Some of the equipment testing was first done in a high pressure environment to record their performance. Then elements like seals, etc. were tested in pressurized loops containing fuel rods to test their performance at different power rates and in-core environments. The same loops were used to record the fuel performance, water chemistry and cladding corrosion. After showing that the loop performs well, attempts were made to find out how defected fuel behaves in the loop. Slits were put in the fuel rods to see what is released. This indicated the degree of contamination produced by failed fuel. When a problem was identified early enough they usually did solve it

adequately.

Sometimes full scale commercial plants were instrumented and used in a sense as test facilities for phenomena that could not be tested otherwise. A reactor which was not designed as an integrated testbed but turned out to be one, is the Heiss Dumpf reactor in Kahl, Germany. After operating for only about 200 hours it experienced a fuel melt and was decommissioned. After clean-up it was turned into a test facility as an analog PWR. This original 300 MWe nuclear plant is now producing, by electrical means, about 100 MWth to heat the coolant passing through the core. To speed up flow velocities to simulate the PWR conditions they use restrictors and a narrower piping system. In that manner, in addition to the temperature and pressure simulation in the core, they also simulate the mass flow per unit of cross section condition.

One problem related to the lack of adequate rigorous integrated testing occurred very often when some piece of equipment would be tested and found to be almost adequate but for a minor point. A change would be made in the equipment and either due to overconfidence, or as a means of trying to perform the tests within budget or time limitations, this change would not be retested before applying it to the plant. There were cases, for example, when following successful testing a minor change would be made on a pump seal, and the same seal would then fail in the field. More often than not, such procedures would cause some unforeseen problem in the plant which proved to be more costly than retesting of the component. The general experience is that even when a change seems to be small enough not to proceed with a retest it has the potential to cause a completely unexpected effect.

## B.10 Personnel and Organizational Structure

The fission research programs typically started with one single project and the members of the research team all worked together as one group. Later when the tasks became much larger, one way to speed up the plant development was to break up the original team into two separate but interactive activities; one for design and construction and the other for research and development. This was the beginning of a functional organization which later could evolve to include a fuel group, a design engineering group, a development group, etc., and above all a project management group.

One problem with having parallel projects is that sometimes there are not enough talented people to run all the groups so there is a shift towards a disciplined hierarchy in which one talented member is heading a team of researchers in what will become a functionalized project. This has its own drawbacks because as people functionalize more and more, they also become more specialized. Experience shows, on the other hand, that frequently the most successful people on a program are the ones that join it in the early stages when all the engineers needed to design a plant are part of the same project group. This is how Bechtel runs their projects, and some see this structure as more effective. The people on such a program are forced to look at the total power plant and they are much better qualified when it comes to the integrating of their area of interest in the overall program. Such a person may start as a heat transfer or fluid flow specialist, and then learn about nuclear fuel, design, safety analysis, etc. People with this kind of broad knowledge about power plants are the most successful in the fission industry.

It may be preferable not to recruit specialists for a new program but rather have people with the kind of knowledge which can balance all of the critical problem areas. The kind of experts most useful to the program are the ones who, for example, not only know all about nuclear fuel but also understand the interaction of the fuel with the rest of the plant, and the effects of the plant environment on the fuel. Understanding the plant environment and what are the factors which determine it is almost as important to a fuel expert as understanding fuel behavior.

System engineers are people with broad knowledge which has to be "created" very early while working on a project so that they can adapt their talents to the specific task. Some of these skills were developed early in the fission program not so much out of insight but more out of necessity as the staffs were often quite limited. This would force them to create a "systems engineer" function in which they would choose the brightest personnel and assign them the task of developing a whole system. Often these people would later surface to the top of the organization. Perhaps the reason for this was their talent, but at least some of their success can be credited to the broad base of knowledge they acquired. When faced with a problem they do not concentrate on the narrow angle only and solve it, but are also able to consider the effects of their solution on other areas. To come up with an efficient,

integrated plant means to develop people with these kinds of qualifications

Another important factor is the general background of the people heading the field. The fission industry started with physicists in the top positions and the fusion area seems to be in the same position now. It may be more desirable to have at least the same weight given to a group of practical engineers who have the knowledge about the hardware and the means to assemble it and deal with its maintenance problems. Tasks may be better accomplished if there is to be one part of the project team who knows how to move things and another part which attempts to hold back, slow down and take a more cautioned approach. In between there has to be a body in charge which responds to both extremes and sets the pace.

Some people are worried to see the fusion industry trend of involving several research groups which specialize each in one narrow subject. If the project is spread around many organizations some think that problems with communications and integration will surface.

When a high volume of tasks is needed there is no other option but to functionalize the program. But in their opinion this is not yet the situation with fusion. They suggest having one group in charge of designing, building and running a model. This group will have to be supported by the national laboratories, each contributing in their own area of expertise, either in research or in equipment development. But there ought to be one large central group of people who are in control, know all details, make things happen and push ahead to stay on schedule. It may be helpful to have a project manager who is an engineer rather than a scientist, as the former tend to better fit the characteristics listed above. In the opinion of some engineers, scientists tend to seek perfection in their designs, having the feeling that things can be further improved and thus often delay decisions or change courses. Sometimes it turns out that making a decision is more important than the nature of the decision itself. This is the case when the options are so close that they are practically equal and hesitation does not contribute much. Once a conclusion is reached that there is no way to generate in a reasonably short time the data which will allow a more intelligent decision, there is no need to spend weeks or months debating pros and cons of each option. A choice has to be made and implemented so that the project can move ahead. Sometimes, good intuition is needed in this class of situation. A program manager with

this quality will usually guide the program to the better options on the basis of this intuition.

A successful program is often characterized by a series of improved prototype model reactors. Ideas which come up during the implementation of one model should not delay the project but rather wait to be incorporated in the next model. These ideas together with the experience gained from the previous prototype, will contribute to an improved next model without delaying the whole program.

Thought should also be given to the employment of smaller, more efficient teams. It takes today 500-600 engineers to build a new power plant and some think that doing the same task with only 100 may be more efficient. A smaller group may be able to work in much closer cooperation with less of the typical differences of opinion which usually center on the overlapping areas and tasks assigned to teams within the project. A smaller group may tend to work in a much higher spirit of cooperation to contribute to the success of the program. The quality of the people is also an asset. Sometimes people may spend large amounts of money looking in vain for an exact solution, while others, on limited funds, may perform a simple test, setting bounds to the solution, and thus allow the rest of the project which needs the output to proceed. Problem solvers are essential to the success of a project, and it is very important to have these kind of people on the team.

To summarize, a project needs a balance of practical engineers and a group of very qualified research and development people who will identify the problems and set up the tests to solve them. Competent management with deep knowledge, broad perspective and insight is essential.

B.11 Lessons

- The less glamorous technologies also require serious attention. This will probably require an early, integrated facility to provide a motivation for such attention.

- Accelerated testing could have been more useful in the fission program.

- Early conceptualization of the entire power plant design will lead

to the best solutions and will avoid band-aid fix solutions.

- Since the fusion industry will have to be regulated it should prepare the grounds by establishing as early as possible its own self-regulatory group to input into the development program.

- When possible, make choices rather than continue studies.

- While developing and operating a plant a balance has to be struck between the pursuit of perfection on the one hand and a built-in flexibility and tolerance to mistakes on the other.

- A major new development program should lay out early in the development process both the promises of the new field and its potential difficulties.

- The fission plant development from low to the current power levels came mainly through increased size and not so much by increase in power density.

- Design safety margins are necessary, but can be more rationally applied if supported by test programs.

- Complex effects require full scale simulation and cannot be addressed prior to the availability of such facilities.

- The history of nuclear technology development suggests that only one major fusion path will be pursued to commercial scale development.

- The commitment to integrated testing has largely been philosophical. It is difficult to anticipate the issues which will arise in development.

- The program direction must eventually transfer from a physics orientation to a systems engineering orientation.

## B.12 Reviewers' Comments

Since the number of experts interviewed was too small to arrive at general conclusions, the material in this appendix was circulated to a number of FINESSE participants who are closely associated with the fission field. The main points from the comments of the reviewers are presented below because we thought they represent a useful supplement to this appendix.

One principal comment can be seen in the following quotation:

> (It should) "Provide sharper identification of the source of opinions cited in the report. In particular, reviewers commented that they could not always tell whether opinions expressed were those of the interviewees or conclusions reached by the authors of the paper from facts furnished by those interviewed."

The views in this report are mostly quotations from recorded interviews. In cases where people were asked to comment on each other's statements the text is not a direct quotation but rather a statement by the author meant to reflect the different nuances of their opinions. To ensure that their views were fairly presented, each was sent an early draft and asked to comment. In general they had no major problems with the report as written and the minor points they raised were all implemented in the final draft.

One group of reviewers felt that in the Major Problem section the following issues should also be included:

- The failure of the fission energy industry in its early stages to fully address its obvious-at-the-time need to retain, collect, treat, and store radioactive wastes, particularly transuranics.

- The industry's failure to identify the specialized technical and administrative expertise required to reliably operate and maintain a nuclear power plant. Note that the U.S. Navy avoided this pitfall.

- Failure to address the need for sufficient human factors, engineering and man-machine interface considerations early in the design of its equipment and facilities. The aircraft industry did a much better job here.

- Reluctance to continually reassess, over the years, the performance and safety of reactor and power plant with the progressively more sensitive and sophisticated instrumentation that developed along the way.

  Given the cost of nuclear power plants, the amount of national dependence upon them, the perceived tendency of the government to overact to non-favorable news, it is easy to understand this attitude. The prevailing philosophy was that the best index of reliability of a nuclear power plant was its continually demonstrated ability to run hour after hour, day after day without shutdown. The nuclear power industry simply did not want, because they felt they could not tolerate, "any more bad news" based solely on data from devices of increasing sensitivity. In the longer run, however, the attitude was counter-productive and late-term diagnostics engendered by crisis contributed to the London-Bridge-is-falling-down view of the nuclear industry by many outsiders

- The section on "Regulations" seems to ascribe the need to back fit modifications as resulting chiefly from poor initial planning and does not address the early needs for in-depth and credible safety research and testing. We believe failure to identify the importance of up-front safety research and testing is a significant deficiency in the current draft. At the present moment, there is little or no test data on fusion component systems to allow specification of safety-related design bases for either normal or off normal operating conditions.

- The authors' discussion on the need for gaining public acceptance is good. It would be strengthened, we believe, if the additional point were made that even "perfect" paper systems are surprisingly vulnerable to attack. Any allegations of poor quality inadequate safety margins, poor construction practices can delay both the construction and licensing processes.

- Based on fission experience, we believe that rigorous control in the selection of construction contractors is one of the most positive steps the fusion industry can take to enhance the public acceptance of fusion energy.

- The discussion of corrosion and other long term effects is good, but the text neglects to point out that this was not a universal experience.

  The MTR was successfully designed, built, and operated in the time period under discussion and lived to achieve an honorable retirement. The ETR had a similar history. The ATR, of course, is still needed and useful today. The MTR achieved nuclear start up early in 1952 and by 1961 construction on the ATR, the newest of the three, had begun. This example also emphasizes that we should look for "lessons to be learned" not only in failure, but in success.

- There is not enough focus upon the pivotal questions which FINESSE must address: "What level of integrated testing of fusion nuclear components is appropriate early in the development program? What risks can we expect if we do not allow for an ambitious program of component and integrated testing prior to deployment of a large ETR or DEMO class fusion reactor?" The current direction of the budget constrained U.S. fusion community is to delay integrated testing in the fusion neutron environment (and also any meaningful separate effects testing program which would support integrated testing) until the operation of the large (~ 600 $MW_{fusion}$) ETR class facility makes such development necessary. TRW's own studies indicate that this direction would seem to be imprudent based upon the fission development history.

  Very early integrated testing at small scales (20-100 MW) has always provided extremely useful results and has often led to the discovery of fundamental concept flaws. The above conclusion was stated in our EPRI (ATP) report and much of the information was developed from case histories in the Loftness book.

# APPENDIX C

## EVALUATION OF EXPERIENCE FROM THE AEROSPACE INDUSTRY

TABLE OF CONTENTS

Page

C.1 Aerospace Approach to Design..... C-1
C.1.1 Establishment of Design Goals..... C-1
C.1.2 Establishment of Design Configuration..... C-2
C.1.3 Testing to Build Confidence in the Design..... C-2

C.2 Example of Aerospace Approach to Design..... C-3

# APPENDIX C. EVALUATION OF EXPERIENCE FROM THE AEROSPACE INDUSTRY

## C.1 Aerospace Approach to Design

To help the fusion community in establishing a viable approach for developing the technology for fusion energy, this appendix briefly reviews and summarizes the approach that an aerospace corporation would take in the design of a component. Aerospace components are typically designed and built to work in environments that have been analytically predicted but not experimentally confirmed. To assure that these components work as planned, large amounts of analyses and testing are performed. To reduce weight and thereby increase performance, aerospace components are typically designed to a low factor of safety. Therefore, because of the low factor of safety and unknown operating environments, testing is used to build confidence in the design.

The typical aerospace approach to design can be broken down basically into three steps. During Step I, design goals and performance requirements of the component to be built are established. In Step II, method of analyses are developed and trade-off studies are performed to the best configuration and materials for optimum overall performance. During Step III, testing is performed to verify analyses and establish material responses. These tests may range in size from simple material specimen tests to testing of full scale components.

These three steps are not necessarily performed in chronological order. For example, material trade-off studies and material specimen tests are usually performed while design concept trade studies are being performed.

### C.1.1 Establishment of Design Goals and Requirements

Typically, the first step in the design process is to establish design goals and performance requirements of the component. These criteria will then be used throughout the program for the design, analysis, and test of subsize, and full-scale components. The requirements not only include the expected environment, but must also address component accessibility, producibility, maintainability, and inspectability requirements, structural configuration with respect to equipment location, deformation requirements, and life requirements. The results of this step are the design criteria for the compo-

nent.

### C.1.2 Establishment of Design Configuration

The next step of the design phase, Step II, is the design of the component. In this phase, trade-off studies are conducted using established analytical methods to determine viable efficient configurations and materials. If appropriate methods of analyses do not exist (e.g., to calculate stresses in the structure for the various types of mechanical loadings and environmental conditions), then methods are developed and then verified through testing and comparing test results with predictions.

Once methods of analyses are established, trade-off studies are conducted to optimize the overall performance and configuration of the component. In these trade-off studies, both the material and the structural arrangement are varied. In addition, weight, producibility, inspectability, reliability, capability for refurbishment, availability of materials, cost and other project requirements are considered. Areas requiring research and development work are identified in these studies. There are generally several design approaches that will do the required job. These must be identified, analyzed and evaluated. Comparing the advantages and disadvantages of the potential candidates, based on the established design requirements, permits a quantitative assessment as opposed to a qualitative judgement. For example, one system may use more material and cost more initially than another, but its additional lifetime and lower development risk may make it a better value.

The primary objective for considering cost in the trade-off studies is to find the least total cost for the system when design, fabrication, operations, maintenance, and repair costs are considered. Performance/cost analyses are conducted at the component subsystem, and system level. At each level, significant cost drivers are identified and estimates are made regarding their influence on cost. Designing to lowest cost is a good way of assuring the maximum performance from a component with the minimum total expenditure over the program lifetime.

### C.1.3 Testing to Build Confidence in the Design

The third step in the design process is the testing to assure structural adequacy and that the component will meet all performance requirements. Tests

will range in size from small material specimen tests to full size component tests. Material specimen tests and subsize tests of viable design configurations will be conducted during the trade-off study phase of the program. Material specimen tests are performed if existing data for the proposed materials in the expected environments is insufficient.

The next step up in complexity of testing is subsize testing. Subsize tests are performed to verify analyses. There are two approaches to subscale component tests. One is "look-alike," using full scale models which duplicate a portion of the actual full scale design. The other is "act-alike," using subscale models which replicate the predicted behavior of the full scale design. Typically, sizes of the test articles are based on test zone capabilities. Once the size and configuration of the subsize test article are determined, detailed analyses are performed for this configuration. Test results are then compared with predictions to verify analysis methods.

Full scale components are then built to verify the manufacturability of the component and tested to demonstrate that performance requirements will be met. For example, in the development of a new aircraft, full size aircraft are tested for structural adequacy and also cycled through the expected flight cycle to determine if the aircraft will meet the design life requirements.

## C.2. Example of Aerospace Approach to Design

A typical example of aerospace design is the evauluation of niobium alloy thermal protection systems (TPS) program conducted by McDonnell Douglas during the conceptual design phase for the NASA space shuttle. The objective of this program was to evaluate coated niobium alloy TPS by a logical sequence of analytical and experimental investigations involving simulated mission and environmental conditions. The typical configuration for the TPS is shown in Figure C.2-1.

To achieve a viable design for the metallic TPS for the space shuttle, a three-phase program was initiated. A three-phase program was used because it separated the design process into logical decision points, allowed for a division of work, and allowed for a better tracking of costs. In Phase I, the design parameters, expected environments, and candidate materials were established. In addition, material specimen tests were conducted to establish a viable materials and material properties for design. At the end of Phase I,

o OBJECTIVE:

EVALUATE COATED COLUMBIUM ALLOY TPS BY A LOGICAL SEQUENCE OF ANALYTICAL AND EXPERIMENTAL INVESTIGATIONS INVOLVING SIMULATED MISSION AND ENVIRONMENTAL CONDITIONS

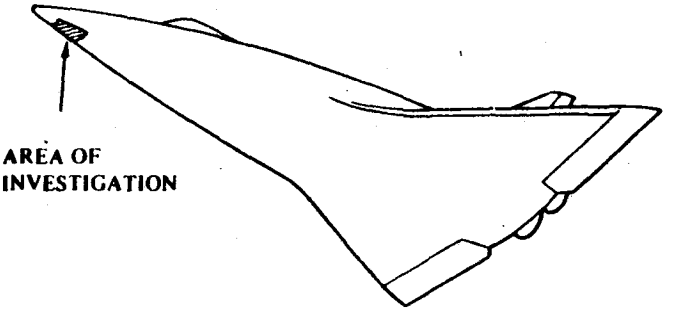


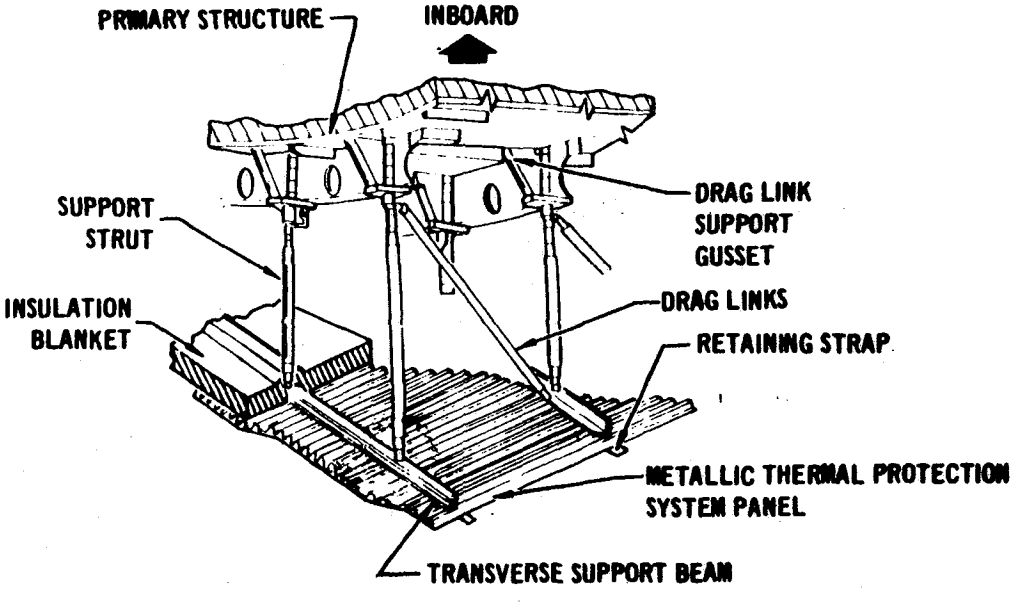


Fig. C.2-1. Example: Evaluation of niobium alloy thermal protection systems (TPS) for the Space Shuttle.

the most likely candidate materials and coatings that would survive the expected environment were selected. In Phase II, analytical trade studies were conducted of several TPS designs were conducted and subscale tests were developed. At the end of Phase II, a design concept for the TPS was selected based on analytical and test results. In Phase III, detailed design of the selected TPS design concept was performed and a full scale component was fabricated and tested.

In Phase I, design parameters, expected environments, and candidate materials were selected. The design criteria and test conditions were established so that a complete analysis and life of the TPS could be predicted. The expected environment that the TPS would see from prelaunch to landing was established. An example of the predicted environment is shown in Figure C.2-2. This figure shows the expected temperatures and loads on the TPS with respect to reentry time of the space shuttle from space.

After the environment and design criteria were selected, candidate niobium alloys and coatings were selected. Elemental candidate material specimens were fabricated and tested through the simulated space shuttle flight profile. Based on results of these material tests, two substrate/coating combinations were selected for further testing in Phase II.

In Phase II, trade studies of seven TPS configurations were conducted. These seven configurations are shown in Figure C.2-3. Five configurations had ribs or corrugations and the other two were honeycomb type structures. This study was directed towards developing a metallic TPS that was efficient and reliable. Since niobium alloys required a coating to resist oxidation and to maintain structural integrity, the designs had to consider potential fabrication problems as well as ease of inspection. In addition, components that are susceptible to wear or damage must be easily removed for repair or replacement.

The trade-off study considered five variables for ranking the seven configurations. These variables were reliability, weight, fabricability, inspectability, and refurbishability. For reliability, the design life goal of 100 flights must be met. Component weight is important and must be kept to a minimum to achieve performance goals. However, all of the other variables will affect weight. Fabrication was based on the amount of time and material. Inspectability was based on time to initially inspect and time to

## Selected Entry History — Lower Surface

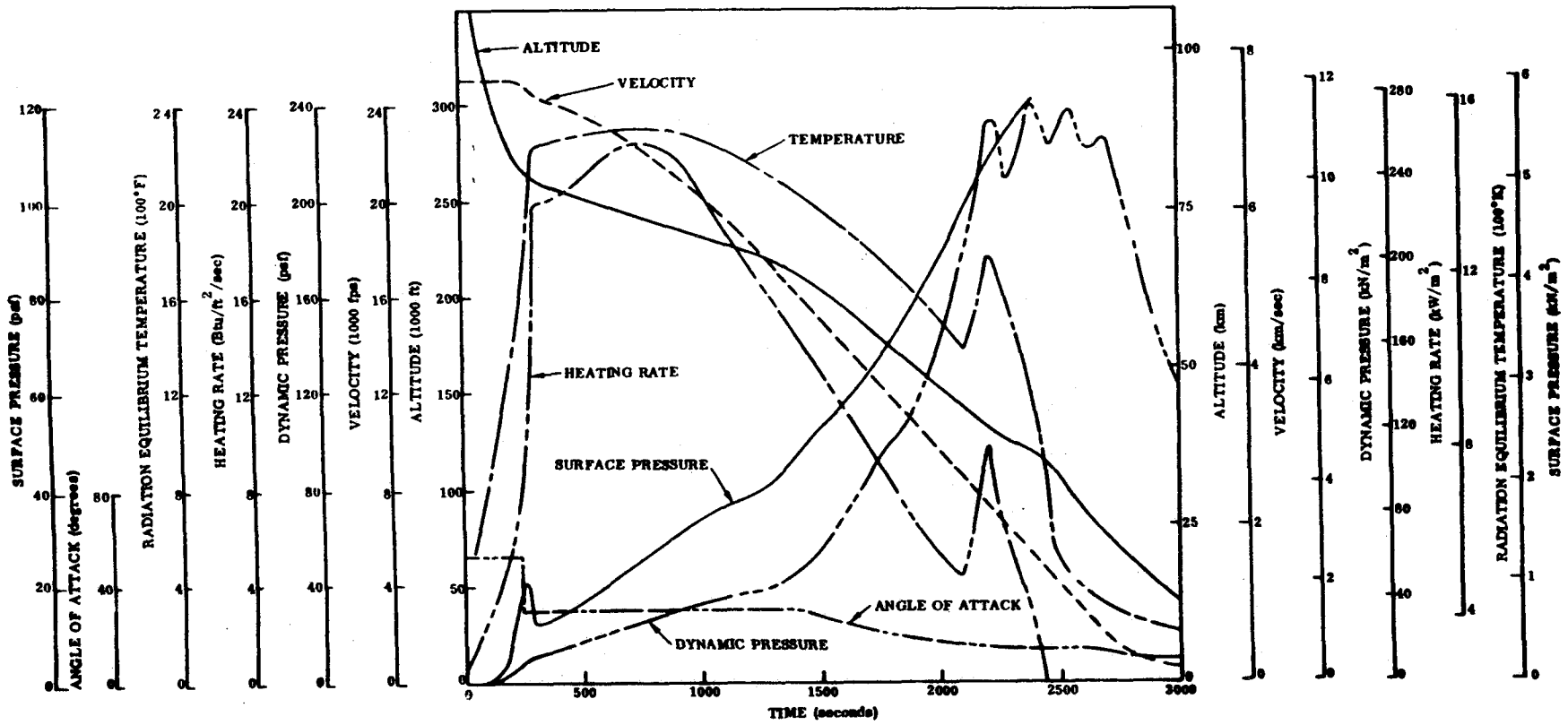


Fig. C.2-2. Predicted environment during entry for the lower surface of the Space Shuttle.

| TPS PANEL CONCEPT | ELEMENTS | Joining (▲Indicates Preferred Process) | | | | | | | | | Coating | | Mfg. | System |
|---|---|---|---|---|---|---|---|---|---|---|---|---|---|---|
| | | Skin/Stiffener Joint ① | | | Beam-Doubler/Stiffener Joint ② | | | Beam-Doubler/Skin Joint ③ | | | Application | Inspection | Complexity | Refurbishment |
| | | Braze | Diff. Bond | Fusion Weld | Braze | Diff. Bond | Fusion Weld | Braze | Diff. Bond | Fusion Weld | (Rankings by Increasing Difficulty) | | | |
| BEADED | 1 SKIN<br>1 BEADED STIFFENER<br>2 | △ | ▲ | — | ← NONE (NO BEAM) → | | | ← NONE (NO BEAM) → | | | 7 | 5 | 1 | 3 |
| TEE STIFFENED | 1 SKIN<br>12 RIBS & CAPS<br>2 BEAM DBLR.<br>15 (MFG. WITH 2 SKINS) | △ | △ | ▲ | △ | — | ▲ | △ | ▲ | — | 4 | 4 | 4 | 2 |
| CORRUGATION STIFFENED | 1 SKIN<br>1 STIFFENER<br>2 BEAM DBLR.<br>4 | △ | ▲ | — | △ | ▲ | — | △ | ▲ | — | 6 | 6 | 5 | 4 |
| HONEYCOMB SANDWICH | 2 SKINS<br>1 CORE<br>4 BEAM DBLR.<br>7 | △ | ▲ | — | △ | ▲ | — | △ | ▲ | — | 1 | 1 | 7 | 5 |
| EGGCRID STIFFENED | 1 SKIN<br>14 RIBBONS<br>4 BEAM DBLR.<br>19 | △ | ▲ | △ | △ | △ | ▲ | △ | ▲ | — | 5 | 7 | 6 | 5 |
| OPEN CORRUGATION | 1 SKIN<br>2 BEAM DBLR.<br>3 | ← NONE (NO STIFFENER) → | | | ← NONE (NO STIFFENER) → | | | △ | ▲ | — | 2 | 2 | 2 | 1 |
| RIB STIFFENED | 1 SKIN<br>12 RIBS<br>2 DOUBLERS<br>15 | △ | △ | ▲ | △ | — | ▲ | △ | ▲ | — | 3 | 3 | 3 | 2 |

Fig. C.2-3. Trade study results for potential TPS configurations.

inspect within a given turnaround time. Refurbishment was based on time to replace or repair within a given turnaround time.

Results from this trade-off study showed that the two most favorable heat shield configurations were the open corrugation and the tee-stiffened configuration. The open design had the advantage of being simple to form, coat and inspect. It also had fewer fasteners and joints than the others. The tee-stiffened panel is also relatively easy to fabricate, but has a large number of parts.

From these analytical studies, subsize panels were made for testing of the two leading candidate TPS configurations. These panels were tested under the same operating conditions as the material element tests. The loading apparatus for the subsize panel is shown in Figure C.2-4 This apparatus, which converts axial load to panel bending load, could be put into a quartz lamp furnace for testing at the expected flight temperatures. A comparison of predicted creep deflections with test results are shown in Figure C.2-5. These results show excellent correlation between the method of analyses used and the test results. Therefore, this testing helped to build confidence in the method of analyses used to predict creep deflections. If the test results did not agree with predictions, then the assumptions used in the analysis and method of analysis would need to be changed to improve predictions. This procedure has also been used in the development of aircraft and missiles.

During Phase III, a full scale nine-panel configuration representative of the shuttle lower surface was designed and fabricated. This configuration was exposed to a total of 100 simulated mission cycles which consisted of combined thermal, mechanical loads and vibration testing. Results of this full scale test demonstrated the structural and thermal adequacy and the manufacturability of a coated niobium alloy TPS. This test also provided data to the project on the performance and cost of the TPS for the space shuttle.

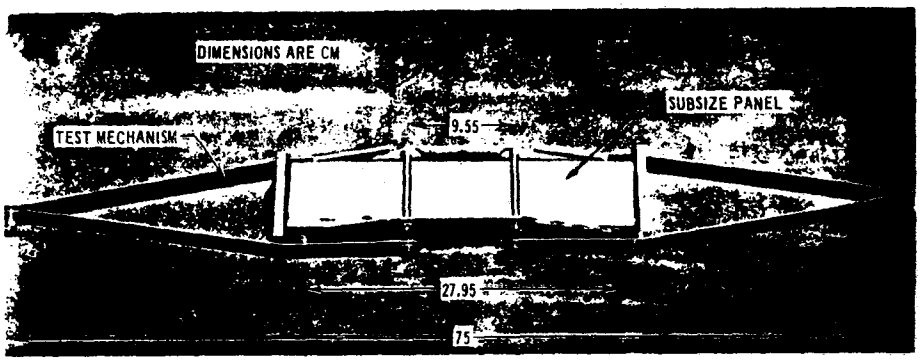


LOAD MECHANISM WITH SUBSIZE PANEL INSTALLED

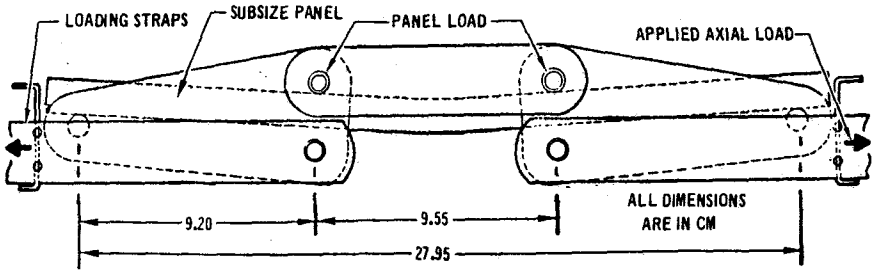


MECHANISM CONVERTS AXIAL LOAD TO PANEL BENDING LOAD

Fig. C.2-4. Loading apparatus for subsize panel testing.

**COMPARISON OF PREDICTED CREEP DEFLECTIONS WITH RESULTS OF CORRUGATION PANEL TESTS L605-21 AND L605-24**

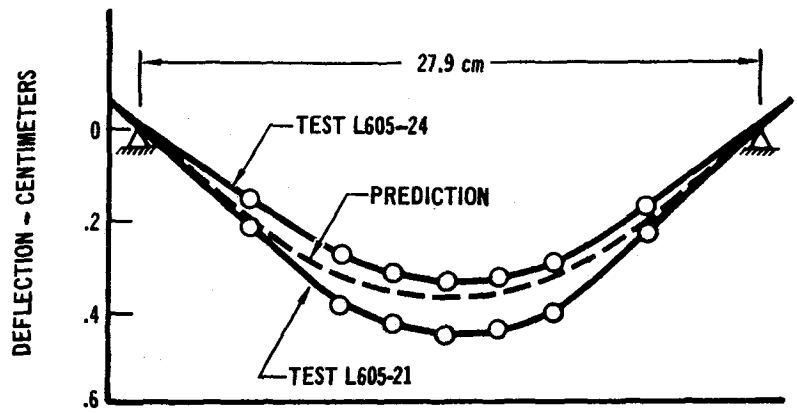


(a) Creep Deflection vs Beam Length at 50 Cycles

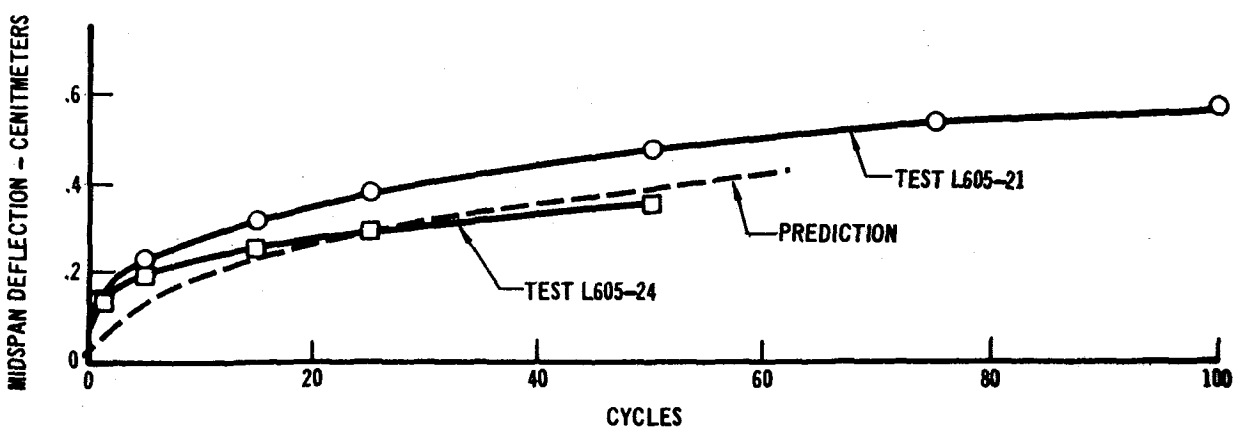


(b) Panel Midspan Creep Deflection

Fig. C.2-5. Comparison of predicted creep deflections with results of corrugation panel tests.

# APPENDIX D

# CHARACTERIZATION OF FUSION NUCLEAR SYSTEMS OPERATING ENVIRONMENT

TABLE OF CONTENTS


Page

D.1 Introduction..... D-1

D.2 Radiation Field..... D-2
D.2.1 Introduction..... D-2
D.2.2 The $Li_2O$ Helium-Cooled Blanket with PCA Structure..... D-5
D.2.3 The $Li_2O$ Helium-Cooled Blanket with Ferritic Steel as Structure..... D-13
D.2.4 The $Li_{17}Pb_{83}$ Self-Cooled Blanket with PCA Structure..... D-20
D.2.5 The Liquid Lithium Self-Cooled Blanket with V15Cr5Ti Structure ..... D-28
D.2.6 The $LiAlO_2$ Water-Cooled Blanket, with Ferritic Steel Structure ..... D-35
D.2.7 Summary Table for the Nuclear Performance..... D-45
D.2.7.1 Tritium Breeeding..... D-45
D.2.7.2 Heat Deposition and Power Multiplication..... D-45
D.2.7.3. Damage Parameters..... D-45
D.2.8 Reference Fluxes at Key Locations..... D-47
References..... D-54
D.3 First Wall Blanket..... D-55
D.3.1 Li/Li/V Concept (Tokamak)..... D-56
D.3.2 $Li_2O$/He/FS Concept (Tokamak)..... D-56
D.3.3 $LiAlO_2/H_2O$/PCA/Be Concept (Tokamak)..... D-57
D.3.4 LiPb/LiPb/V Concept (TMR)..... D-58
References..... D-83
D.4 Plasma-Interactive Components..... D-84
D.4.1 Introduction..... D-84
D.4.2 Plasma Edge Conditions as the Base for Operating Parameters.. D-85
D.4.3 Operating Parameters..... D-86
D.4.3.1 Heat Flux..... D-86
D.4.3.2 Particle Flux and Species..... D-87
D.4.3.3 Neutron Flux and Fluence..... D-87
D.4.3.4 Burn Time and Number of Cycles..... D-88
D.4.3.5 Materials and Operating Temperature..... D-88

D.4.3.6 Manetic Field..... D-90
References..... D-91
D.5 Tritium and Vacuum Systems..... D-92
D.5.1 Fuel Cycle..... D-92
D.5.2 Breeder Cycle..... D-96
D.5.3 Secondary Systems..... D-97
D.5.4 Instrumentation and Control.....D-100
References.....D-102

# APPENDIX D. CHARACTERIZATION OF FUSION NUCLEAR SYSTEMS OPERATING ENVIRONMENT

## D.1 Introduction

The effort on the various tasks of FINESSE required that the operating environment experienced by the nuclear subsystems in a full-scale fusion reactor be characterized. This was particularly important for Task II (see Chapters 5-7), which was concerned with engineering scaling for multiple effect and integral experiments. This appendix documents the results of this characterization. A number of design concepts were selected for the various subsystems for the purpose of covering the range of issues. These concepts should be viewed as representative examples of possible design concepts rather than a preference for specific designs.

## D.2 Radiation Field

### D.2.1 Introduction

In this section, the neutronics performance of several blanket concepts are given. The neutronics performance is characterized by the key parameters listed below:

1. Tritium breeding ratio
2. Heat deposition rate
3. Displacement per atom
4. Hydrogen production rate
5. Helium production rate.

The profiles for these parameters through the blanket concepts under consideration are displayed in graphic form. Tables are also used when necessary. The values shown for each blanket are those calculated in a tokamak fusion machine characterized by a large plasma and first wall radius as compared to those found in a mirror machine. For the latter, the corresponding profiles for the parameters listed above are not given in this section but can be found in the neutronics subsection of Chapters 5 and 6 for the solid breeders and the liquid metal blankets, respectively. More neutronics details pertaining to the $Li_2O$ breeder are discussed in Chapter 7.

The wall load assumed in the calculation is 5 $MW/m^2$ in a tokamak machine, unless otherwise indicated. The tritium breeding ratio (TBR) is expressed in terms of the number of triton (T) atoms produced per D-T source neutron. In some cases, the TBR profile is expressed in terms of the number of T atoms produced per year per unit volume per lithium atom consumed. This particular unit is useful since it indicates the rate at which the lithium atoms are burned in the blanket. Heat deposition rate is expressed in terms of $MW/m^3$ in various zones of the blanket and the profiles are given for the heat deposited from neutrons interactions and gamma-rays interactions, separately. The damage parameters shown are expressed in terms of the number of displacement per atom per year, and the number of hydrogen and helium atoms produced per year per million of atoms of the material under consideration.

The results shown in each of the following subsections have been calculated using a 25n-21$\gamma$ library based on the ENDF/B-IV data. This library was generated from the VITAMIN-C/DLC-41B library[1](171n-36$\gamma$) using the standard

spectrum (evaporation + 1/E + fission + 1/E + Maxwellian) for the neutrons and flat spectrum for gamma-ray cross-section. The energy boundaries for this library are shown in Table D.2.1-1. A cylindrical calculational model was used and the $P_3S_8$ approximation was utilized in the 1-D calculation performed using the ANISN[2] code. A 30% albedo was assumed at the right boundary in each blanket.

In each of the subsections devoted to the characterization field and nuclear performance in a particular blanket concept we give the geometrical arrangement, volumetric fractions, and the atomic densities used in the calculation in each spatial zone. The blankets considered in this section are

1. The $Li_2O$ helium-cooled blanket with PCA as structure ($Li_2O$/He/PCA).
2. The $Li_2O$ helium-cooled blanket, with ferritic steel (FS) as structure ($Li_2O$/He/FS).
3. The $Li_{17}Pb_{83}$ self-cooled blanket with PCA structure (LiPb/LiPb/PCA).
4. The liquid metal self-cooled blanket, with V15Cr5Ti structure (Li/Li/V).
5. The $LiAlO_2$ water-cooled blanket with ferritic steel (FS) structure and beryllium as a neutron multiplier ($LiAlO_2$/$H_2O$/FS/Bc).

A summary table is given in Section D.2.7. In this table, we summarize the total tritium production, heating rate and the damage rates in the five blankets under consideration. Section D.2.8 is devoted to neutron flux characterization at key locations in each blanket. These locations are indicated in the figures displaying the geometrical arrangement for each blanket.

Table D.2.1-1 Energy Boundaries for the 25n-21γ Library

| Neutron | | | | Gamma-ray | | | |
|---|---|---|---|---|---|---|---|
| Group | Upper Energy (ev) | Group | Upper Energy (ev) | Group | Upper Energy (ev) | Group | Upper Energy (ev) |
| 1 | 1.4918+7 | 14 | 3.0119+6 | 1 | 1.4+7 | 14 | 3.0+6 |
| 2 | 1.3499+7 | 15 | 2.4660+6 | 2 | 1.2+7 | 15 | 2.5+6 |
| 3 | 1.2214+7 | 16 | 1.3534+6 | 3 | 1.0+7 | 16 | 2.0+6 |
| 4 | 1.1052+7 | 17 | 7.4274+5 | 4 | 8.0+6 | 17 | 1.5+6 |
| 5 | 1.0000+7 | 18 | 4.0762+5 | 5 | 7.5+6 | 18 | 1.0+6 |
| 6 | 9.0494+6 | 19 | 1.6573+5 | 6 | 7.0+6 | 19 | 4.0+5 |
| 7 | 8.1873+6 | 20 | 3.1878+4 | 7 | 6.5+6 | 20 | 2.0+5 |
| 8 | 7.4082+6 | 21 | 3.3546+3 | 8 | 6.0+6 | 21 | 1.0+5 |
| 9 | 6.7032+6 | 22 | 3.5358+2 | 9 | 5.5+6 | | 1.0+4 |
| 10 | 6.0653+6 | 23 | 3.7267+1 | 10 | 5.0+6 | | |
| 11 | 5.4881+6 | 24 | 3.9279 | 11 | 4.5+6 | | |
| 12 | 4.4933+6 | 25 | 4.1399-1 | 12 | 4.0+6 | | |
| 13 | 3.6788+6 | | 1.000-5 | 13 | 3.5+6 | | |

D.2.2 The $Li_2O$ Helium-Cooled Blanket With PCA Structure ($Li_2O$/He/PCA)

Figure D.2.2-1 shows the geometrical model for the blanket along with the volumetric fractions of the constituents. Natural lithium is used and the neutron spectrum is hard in this blanket since helium is used as a coolant. The atomic densities used in the calculation are given in Table D.2.2-1.

The profiles for the tritium production rate from $^6Li$ and $^7Li$ are shown in Fig. D.2.2-2. Notice that the $T_7$ profile is larger than the $T_6$ profile in the first few centimeter of the breeding zone. However, in the rest of the breeding zone, $T_6$ is dominating especially at the back edge. For a 5 $MW/m^2$ wall load, the maximum tritium production rate is $1.519 \times 10^{13}$ T-atoms/$cm^3$/s which corresponds to $8.64 \times 10^{-3}$ T-atom/yr Li atom$\cdot cm^3$. Note that $T_7$ is appreciable in this blanket and it amounts to ~ 35% of the total tritium production.

Heat deposition profiles are shown in Figs. D.2.2-3 and D.2.2-4 in the breeding zone and entire blanket, respectively. The profiles shown are for the heat deposited in the $Li_2O$ and the PCA structure in the homogenized case as well as for the contribution from heat deposited in $^6Li$ and $^7Li$. The two upper curves are the heat deposition profiles in the $Li_2O$ and the PCA structure when hetrogeneity is considered. These two profiles are obtained by dividing the homogenized profiles value by the volume fraction of the $Li_2O$ and the PCA structure in the breeding zone. Note from the curves that the contribution to the total heating from reactions occuring in $^6Li$ is appreciable. Note that the $^6Li(n,\alpha)t$ is exothermic reaction with a Q-value of 4.78 MeV. The maximum heat deposition rate occurs at the front edge of the breeding zone and reaches the value (homogenized) of ~ 40 $MW/m^3$. The heating profiles for the rest of the blanket are shown in Fig. D.2.2-4 where the contribution from gamma-ray heating is indicated. In the breeding zone, heat deposition rate resulting from neutron interactions are dominant, while the reverse is true in the plenum and the shield where most of the contribution to the total heating comes from gamma-ray interactions. In the first wall, both contributions are almost equal. To arrive at an approximate value for the heat deposition rate in the structure of the first wall, the homogenized values shown in Fig D.2.2-4 for that zone is divided by the 6.6% volume fraction of the structure. The maximum heat deposition rate in the PCA structure of the first wall therefore reaches the value of ~ 53 $MW/m^3$.

The hydrogen production rate (appm/yr), and the helium production rate are shown in Fig D.2.2-5 and Fig D.2.2-6, respectively, for 1 $MW/m^2$ wall load. Note in particular the large values for the hydrogen and helium production rate in nickel. The maximum values occur at the front edge of the first wall and they are 670 and 200 appm/yr for the hydrogen and the helium production rate, respectively, per 1 $MW/m^2$.

Table D.2.2-1 Constituents Atomic Density by Zone (atm/b•cm) in the $Li_2O$ Helium-Cooled Blanket with PCA Structure ($Li_2O$/He/PCA)

| Constituent | First[a] Wall | Breeder Zone | Plenum[b] Zone | Shield |
|---|---|---|---|---|
| Mo | 6.463-5 | 5.876-5 | 9.793-5 | --- |
| Fe | 3.621-3 | 3.292-3 | 5.486-3 | 5.745-2 |
| Cr | 8.356-4 | 7.596-4 | 1.266-3 | 1.599-2 |
| Ni | 8.461-4 | 7.692-4 | 1.282-3 | 1.179-2 |
| Mn | 1.129-4 | 1.026-4 | 1.710-4 | --- |
| Si | 5.533-5 | 5.030-5 | 8.384-5 | --- |
| C | 1.294-5 | 1.177-5 | 1.961-5 | --- |
| Ti | 1.942-5 | 1.765-5 | 2.942-5 | --- |
| N | 2.216-6 | 2.015-6 | 3.358-6 | --- |
| $^6Li$ | --- | 4.115-3 | --- | --- |
| $^7Li$ | --- | 5.134-2 | --- | --- |
| O | --- | 2.773-2 | --- | --- |

[a]Values given are for the constituents of a 100% PCA multiplied by the volume fraction, 6.6%.

[b]Atomic densities for a 100% PCA multiplied by the 10% volume fraction in in that zone.

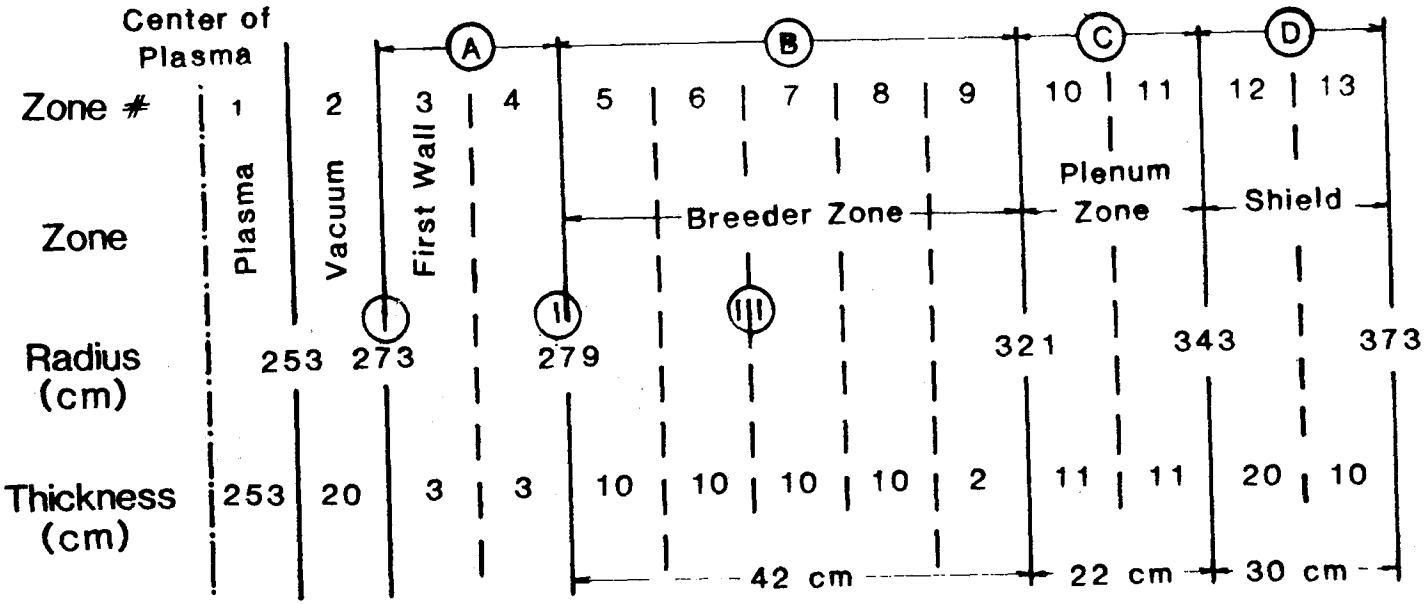


(A) 100% PCA (6.6% dense)

(B) 6% PCA, 85% $Li_2O$ (density factor 0.8), balance Helium

(C) PCA plenum (10% dense)

(D) 100% stainless steel

Figure D.2.2-1 One-dimensional model for $Li_2O$ Helium-cooled blanket with PCA structure ($Li_2O$/He/PCA).

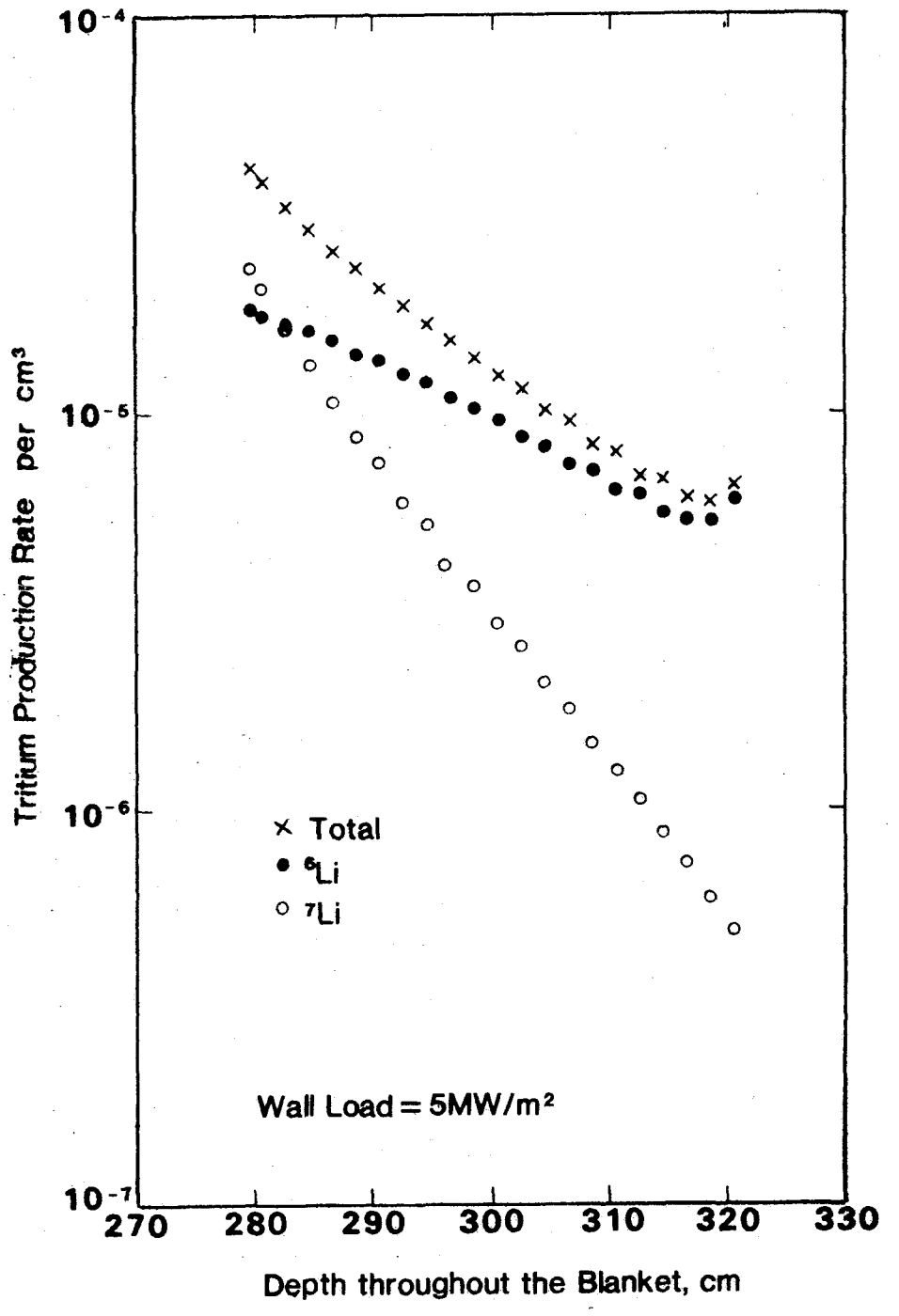


Figure D.2.2-2 The tritium production rate in the $Li_2O$ helium-cooled blanket with PCA structure ($Li_2O$/He/PCA)

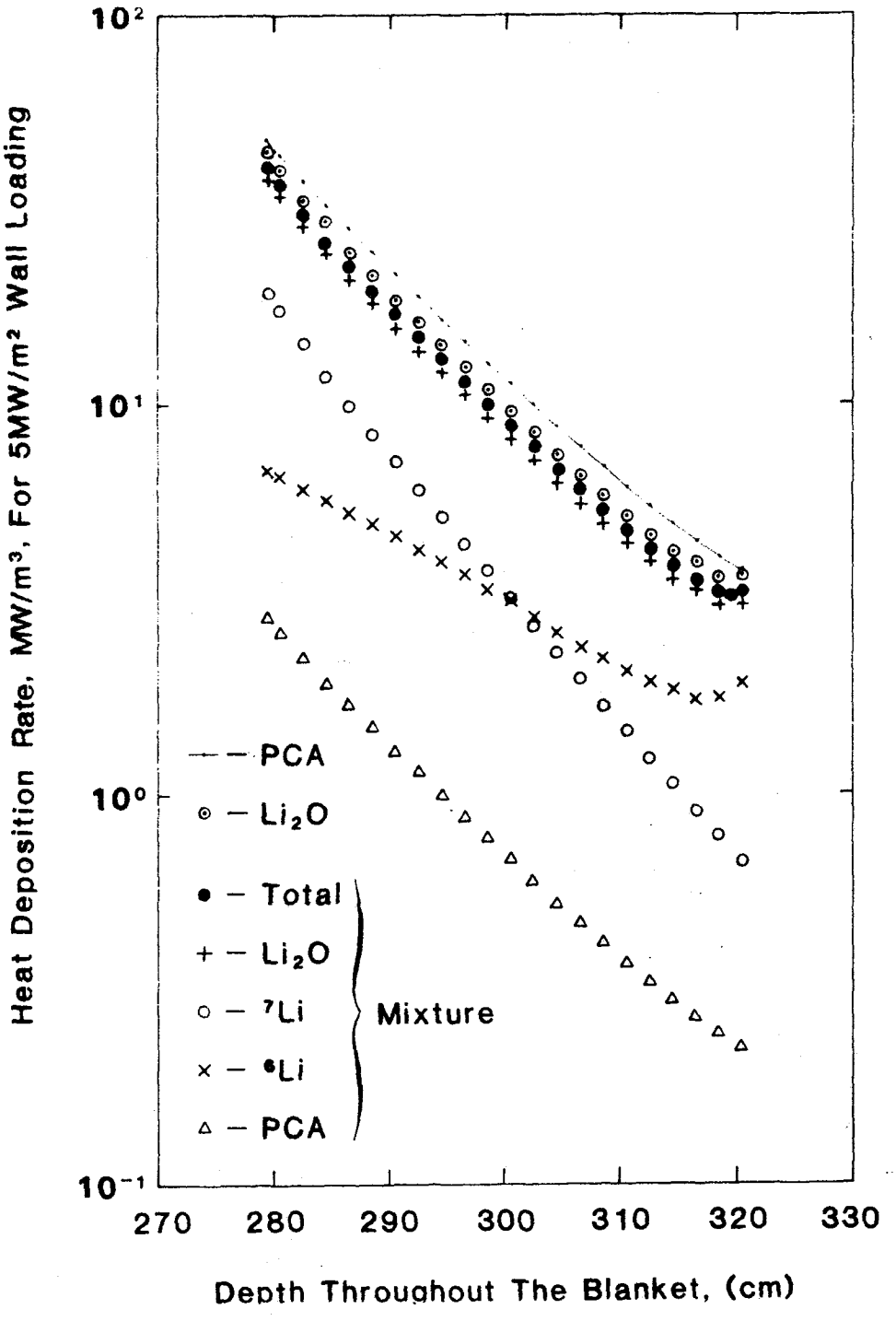


Figure D.2.2-3 Heat deposition rate in the breeding zone of the $Li_2O$/He/PCA blanket.

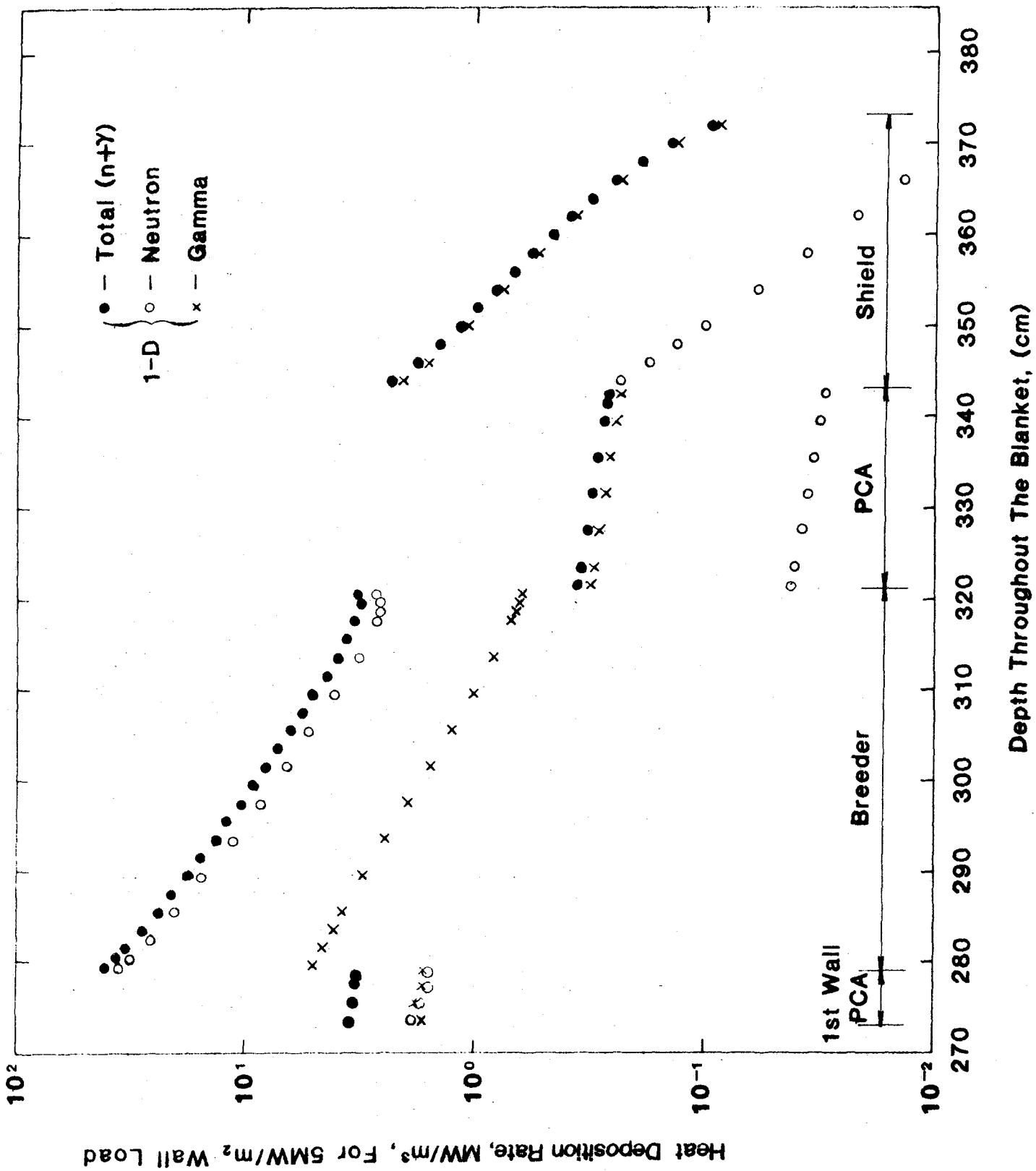


Figure D.2.2-4 Heat deposition rate throughout the $Li_2O$/He/PCA blanket.

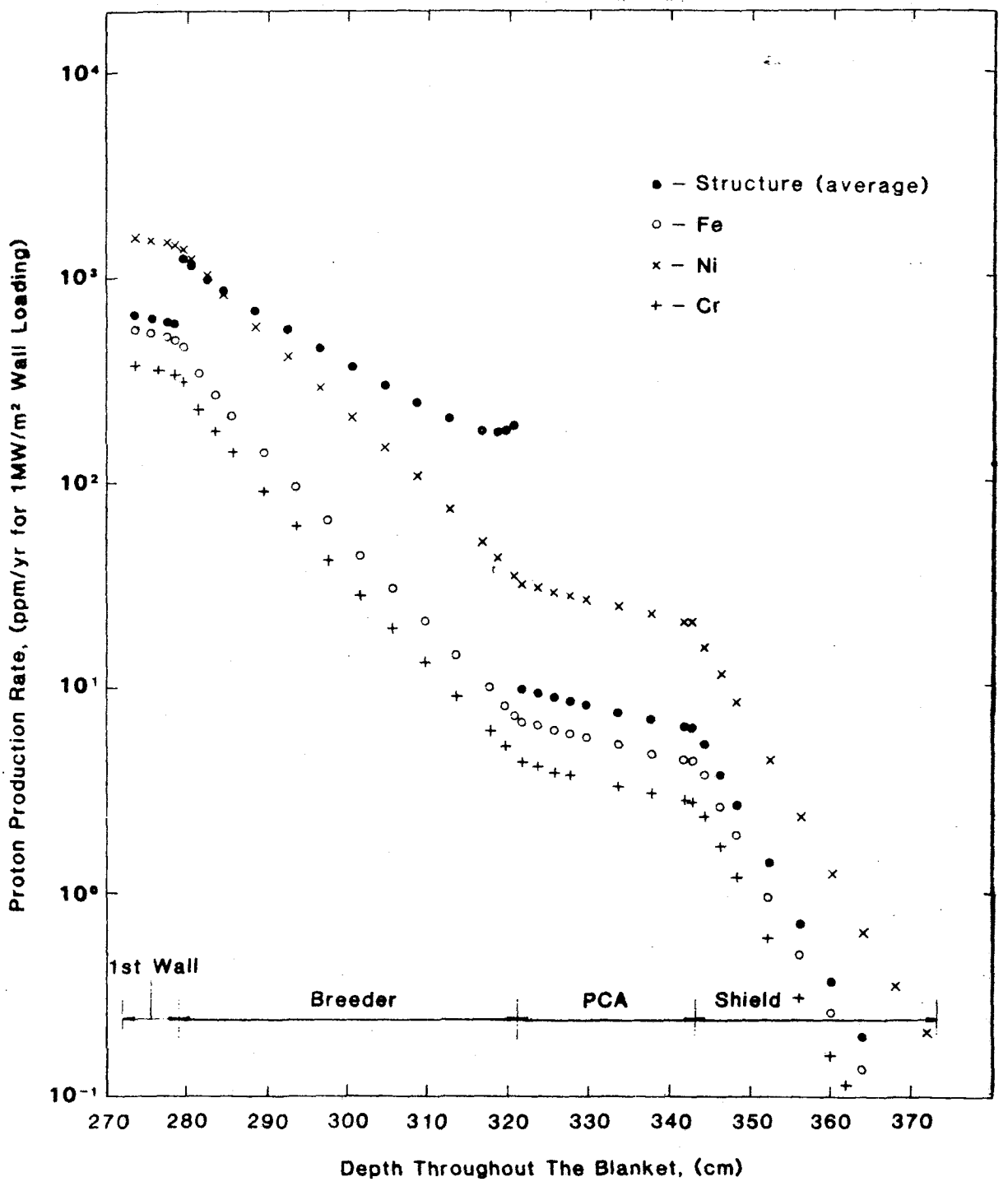


Fig. D.2.2-5 The proton production rate in the $Li_2O$/He/PCA Blanket.

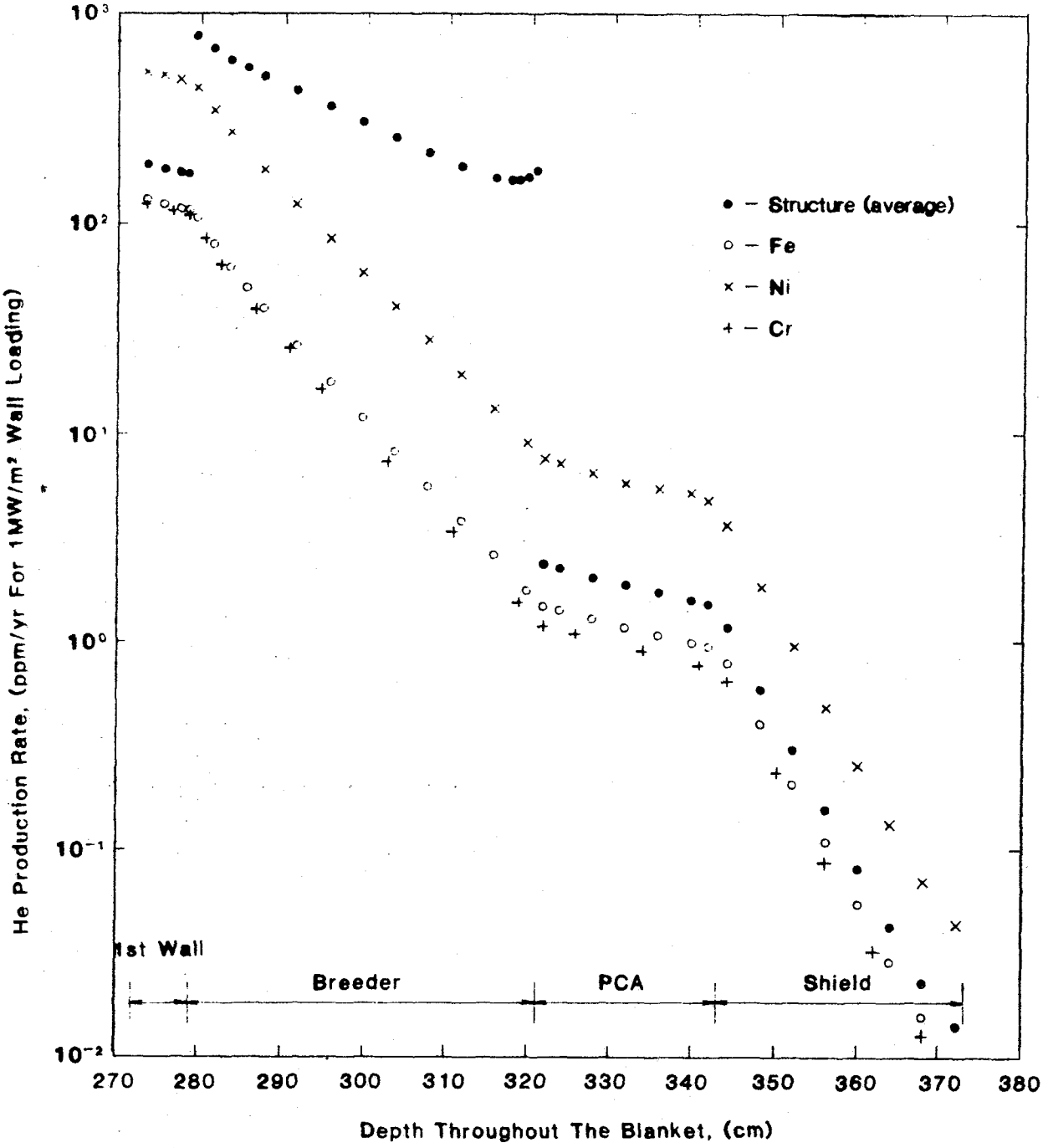


Figure D.2.2-6 The helium production rate in the $Li_2O$/He/PCA blanket.

### D.2.3 The $Li_2O$ Helium-Cooled Blanket with Ferritic Steel as Structure ($Li_2O/H_2O/Fs$)

The geometrical model and material arrangement in this blanket is shown in Fig. D.2.3-1. This arrangement and material choice are the same as in Fig. D.2.2-1 except that ferritic steel replaces the PCA structure with slight changes in the volume fractions and theoretical densities. The model shown in Fig. D.2.3-1 is the one used in the neutronics analysis for solid breeders discussed in Chapter 5. The atomic densities for the blanket constituents which were used in the calculation are given in Table D.2.3-1.

The profiles for the tritium production for $^6Li$, $^7Li$, and the total are shown in Fig. D.2.3-2 for a wall load of 5 $MW/m^2$. The unit used in this figure is in terms of triton atoms produced per year per Li atom per $cm^3$. As mentioned in the introduction, this unit reflects the rate at which $^6Li$ and $^7Li$ atoms are burned due to the $^6Li(N,\alpha)t$ and $^7Li(n,n\alpha)t$ reactions. As shown, and similar to the $Li_2O/He/PCA$ blanket, the contribution from the $^7Li(n,n\alpha)t$ reactions to the total breeding is appreciable (23%) as compared to the other blankets discussed in this section (see Table D.2.7-1). The maximum tritium production rate is $\sim 7.5 \times 10^{-3}$ T/yr Li atom $cm^3$ for a 5 $MW/m^2$ wall load or about $3.69 \times 10^{-5}$ $T/cm^3 \cdot s$ per source neutron. Also shown in Fig. D.2.3-2 is the total tritium production rate for the case where the density factor of the structure in the first wall is ~ 6%. The profile for this case indicates that slight decrease in the total TBR occurs when the structure content of the first wall increases from 6% to 18%.

The heat generation rate profile is shown in Fig. D.2.3-3 throughout the first wall and the breeding zone. Also shown is the contribution to the total heat generation from both neutrons and gamma-rays interactions. Note in particular that gamma-rays heating contributes more than neutrons (a factor of 1.5) to the total heating in the first wall. Furthermore, decreasing the structure contents in the first wall from 18% to 6% results in a more than a factor of four decrease in the total heat deposition in that zone. For the case where the HT-9 structure is 18% in the first wall, the maximum heat deposition rate (homogenized value) for a 5 $MW/m^2$ wall load is $\sim 8.2$ $MW/m^3$. This amounts to $\sim 45.6$ $MW/m^3$ heat deposition rate in the HT-9 structure if we consider its volume fraction (18%) in that zone. The maximum homogenized value for heat deposition rate in the breeding zone is $\sim 50$ $MW/m^3$.

The damage parameters are shown on Fig. D.2.3-4 and Fig. D.2.3-5 for the displacement per atom rate, hydrogen, and helium production rates. The solid curve shown in these figures are for the average value for both iron and chromium. For a 5 $MW/m^2$ wall loading, the maximum dpa rate, hydrogen production, and helium production rates are: 58 dpa/yr, 2000 appm/yr, and 620 appm/yr, respectively.

Table D.2.3-1 Constituents Atomic Density by Zone (atm/b•cm) in the $Li_2O$ Helium-Cooled Blanket with Ferritic Steel Structure ($Li_2O$/He/FS)

| Constituent | First Wall | Breeder | Plenum | Shield |
|---|---|---|---|---|
| Fe | 1.234-2 | 5.484-3 | 1.028-2 | 5.745-2 |
| Cr | 1.787-3 | 7.944-4 | 1.490-3 | 1.600-2 |
| Ni | 6.885-6 | 3.060-6 | 5.734-6 | 1.179-2 |
| Mo | 8.424-5 | 3.744-5 | 7.020-5 | --- |
| Mn | 7.362-5 | 3.272-5 | 6.135-5 | --- |
| Si | 7.200-5 | 3.200-5 | 6.000-5 | --- |
| C | 1.345-4 | 5.984-5 | 1.122-4 | --- |
| $^7Li$ | --- | 5.456-2 | --- | --- |
| $^6Li$ | --- | 4.373-3 | --- | --- |
| O | --- | 2.946-2 | --- | --- |

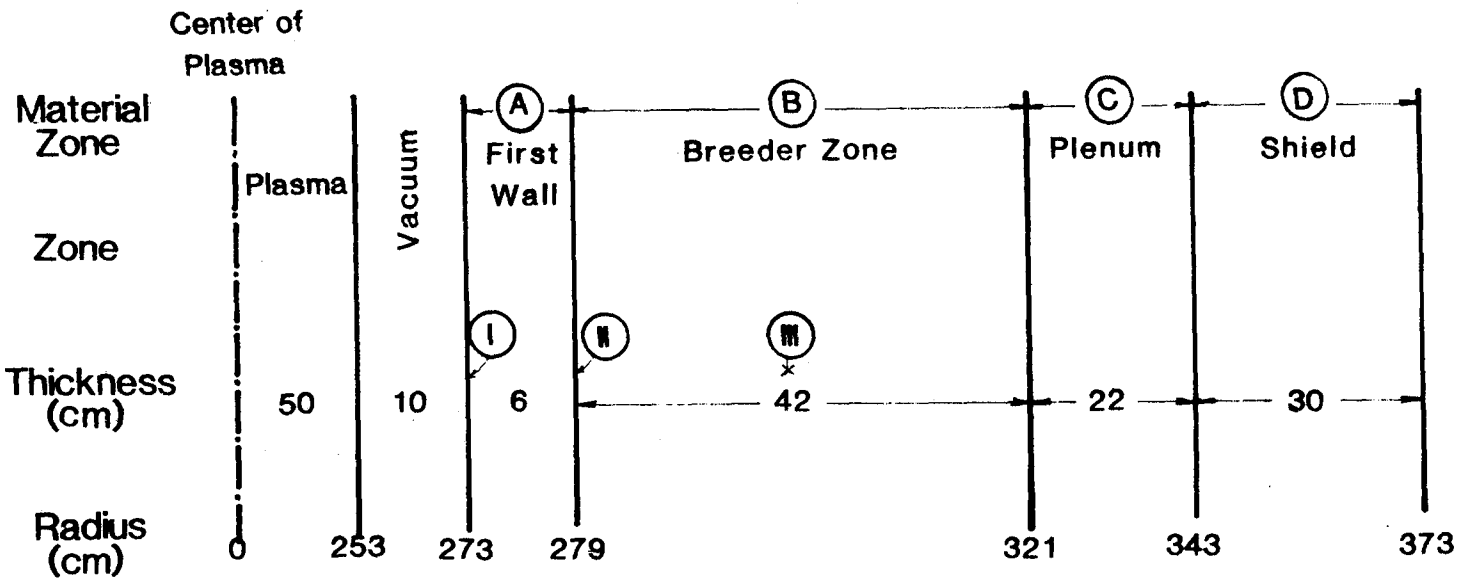


(A) 100% HT-9 (18% dense)

(B) 85% $Li_2O$ (density factor 85%), 8% HT-9, balance helium

(C) 100% HT-9 (15% dense)

(D) 100% stainless steel

Figure D.2.3-1 One-dimensional model for the $Li_2O$ helium-cooled blanket with HT-9 structure ($Li_2O$/He/FS).

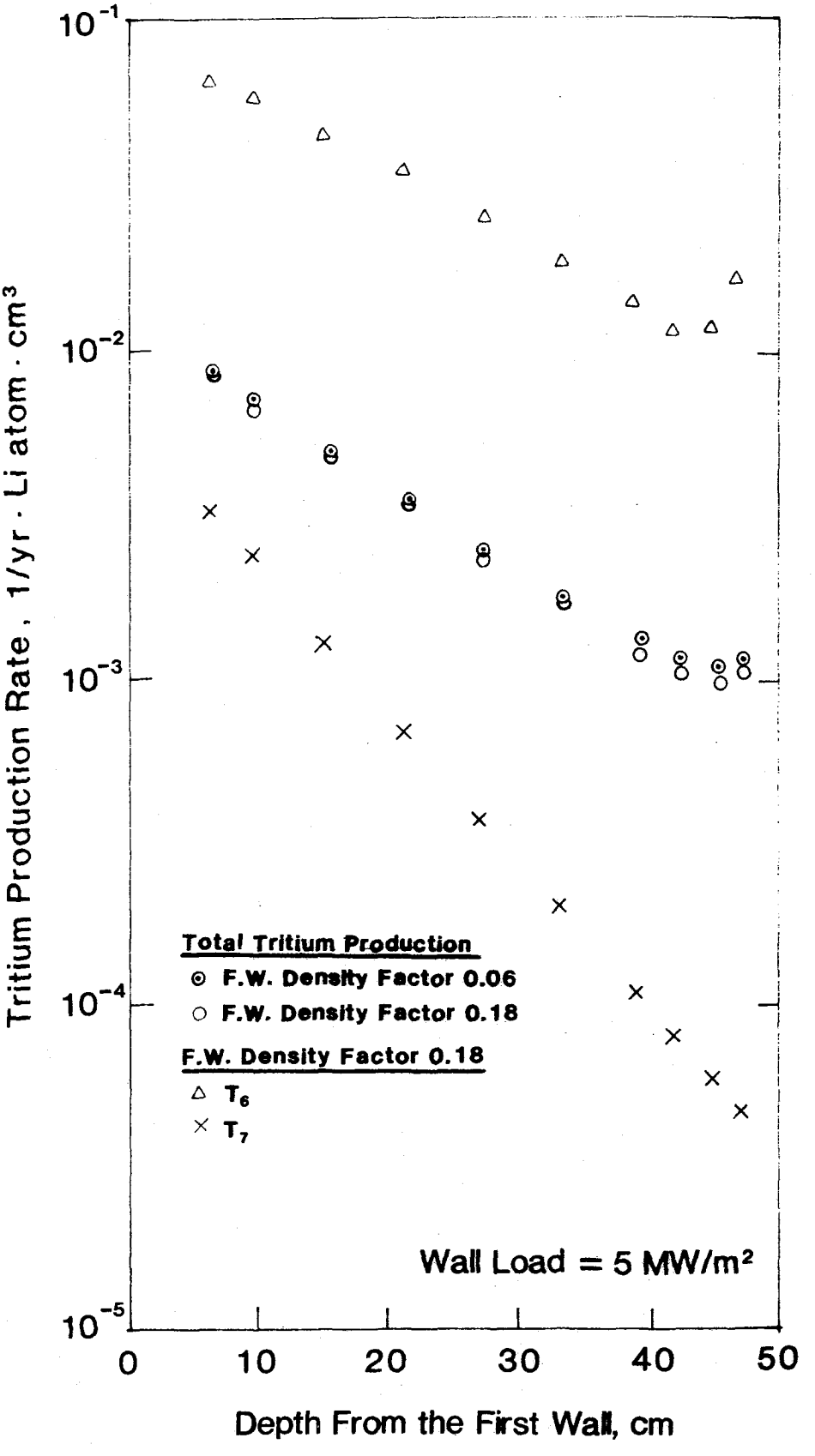


Figure D.2.3-2 The tritium production rate in the $Li_2O$ helium-cooled blanket with ferritic steel structure ($Li_2O$/He/FS).

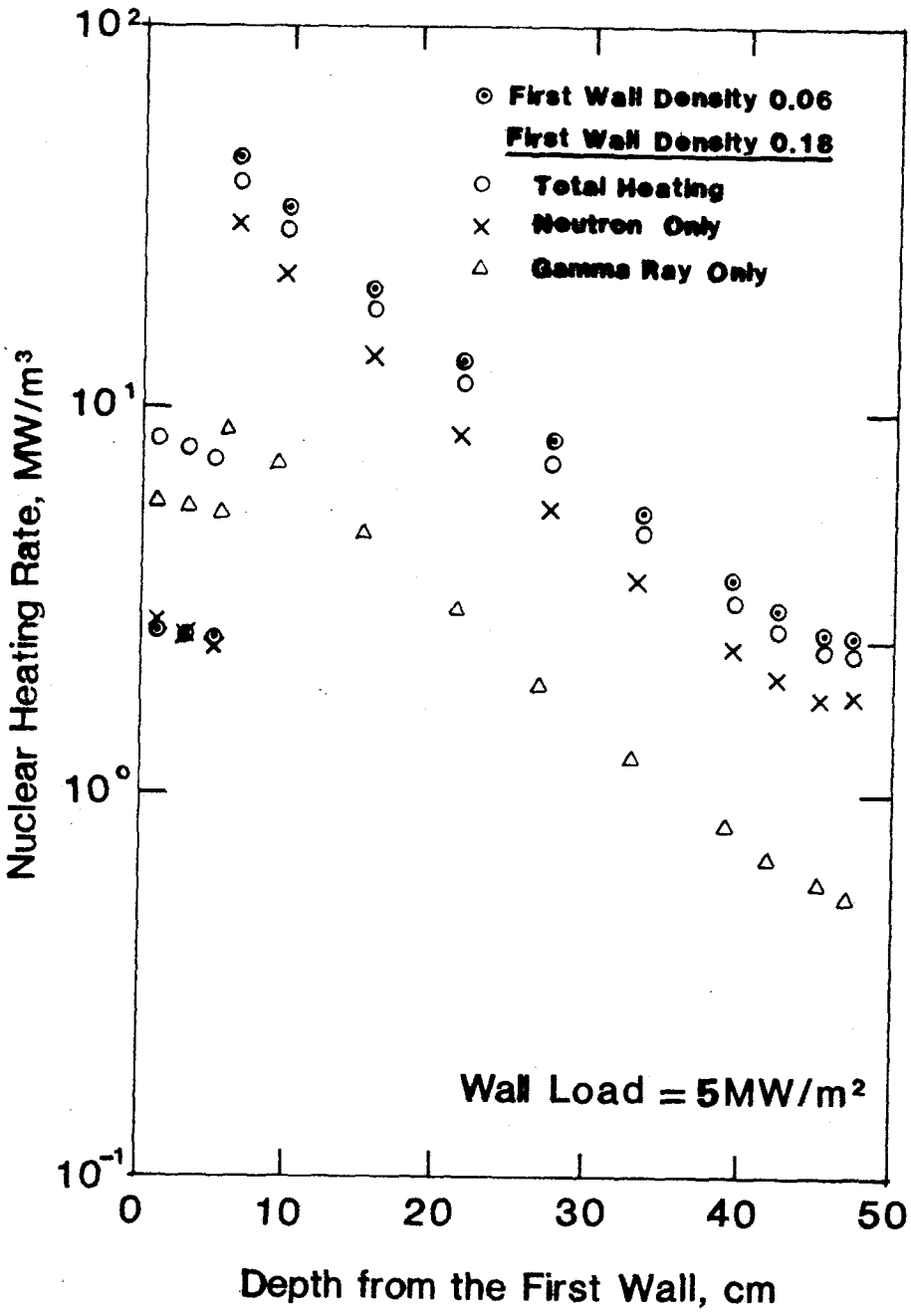


Figure D.2.3-3 Heat deposition rate in the $Li_2O$ helium-cooled blanket with ferritic steel structure ($Li_2O$/He/FS).

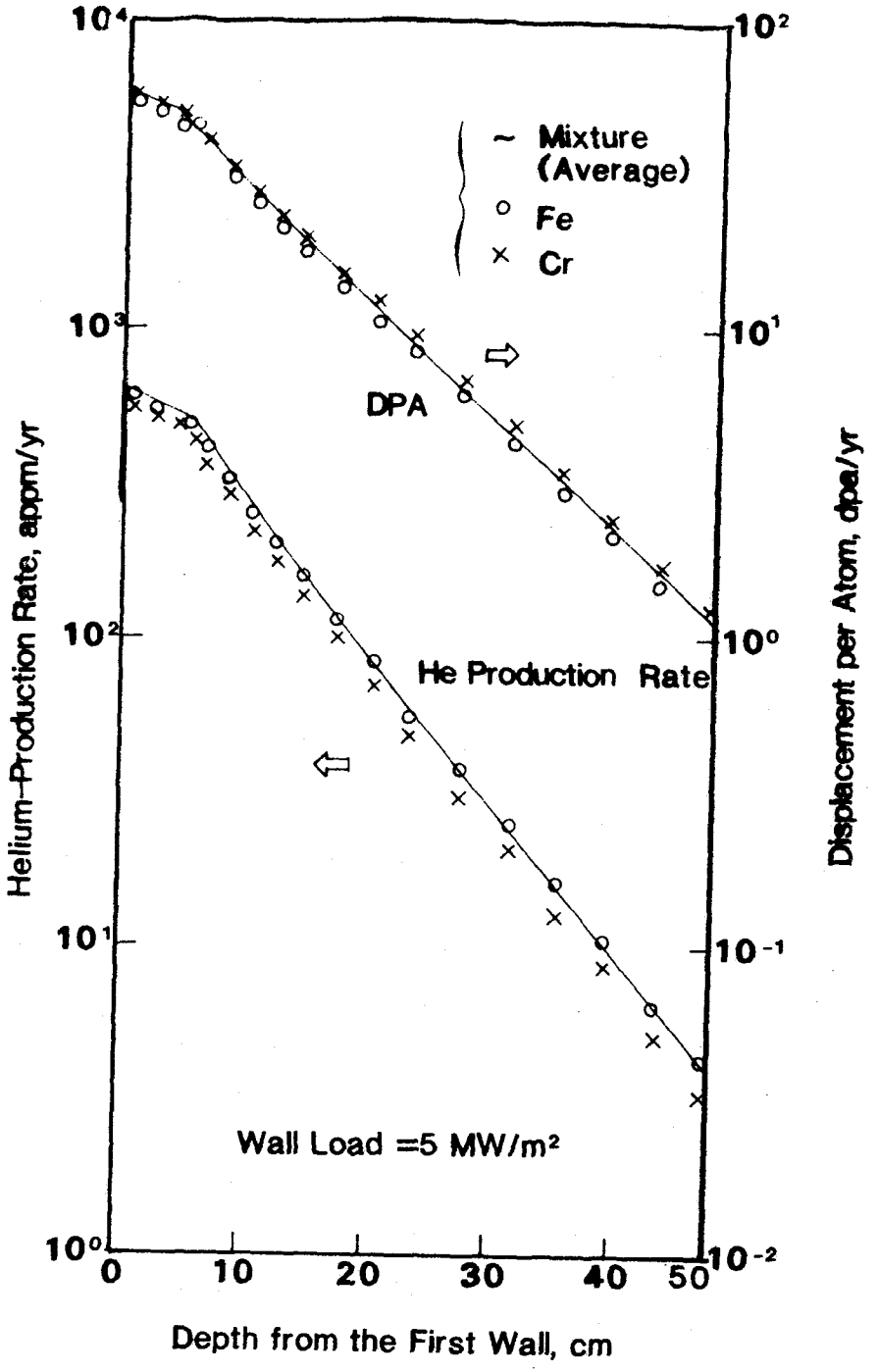


Figure D.2.3-4 Displacement per atom and helium production rates in the $Li_2O$ helium-cooled blanket with ferritic steel structure ($Li_2O$/He/FS).

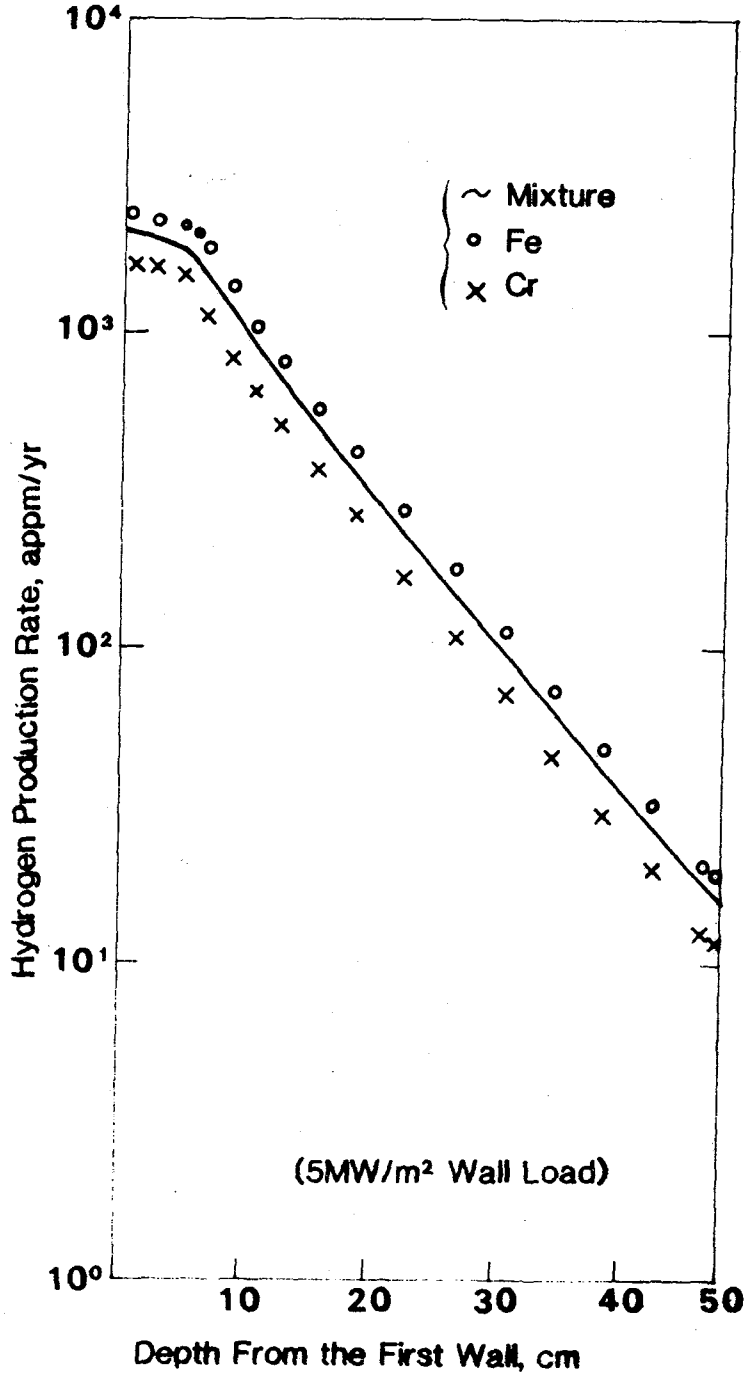


Figure D.2.3-5 Hydrogen production rate in the $Li_2O$ helium cooled blanket with ferritic steel structure ($Li_2O$/He/FS)

D.2.4 The $Li_{17}Pb_{83}$ Self-Cooled Blanket with PCA Structure (LiPb/LiPb/PCA)

The geometrical model for this blanket is shown in Fig. D.2.4-1. Note in particular that $^6Li$ is 90% enriched and as expected, most of the contribution (99.8%) to the total tritium breeding ratio (TBR) comes from the $^6Li(N,\alpha)t$ reactions. The TBR in this blanket exhibits the highest value among the five blankets considered. The shield is cooled with water and the Fe1422 alloy is used since it has low activation level. The atomic densities for the constituents in the various zones of the blanket which were used in the calculation are shown in Table D.2.4-1.

The tritium breeding profiles throughout the blanket are shown in fig. D.2.4-2. Since neutrons are moderated in energy mostly through the Pb(n,inelastic) reactions, the spectrum is soft in this blanket and hence most of the breeding occurs through the $^6Li(n,\alpha)t$ reactions. The cross-section for this reaction is appreciably large at low neutron energies. Note also from Fig. D.2.4-2 the increase in the $T_6$ profiles near the reflector due to the enhanced increase in the number of slow neutrons reflected back to the breeding zone in that location.

The profiles for the total heat deposition rate and the contribution to this profile from both neutrons and gamm-rays heating are shown on Fig. D.2.4-3 for 5 $MW/m^2$ wall loading. In contrast to the $Li_2O$ blankets, the contribution to the total heating from gamma-rays interactons is appreciable ($\sim$ 43%). This emphasizes the high level of the gamma-ray flux in this blanket type produced through the inelastic processes and particularly from the Pb(n,inelastic) reactions. As shown in Fig. D.2.4-3, the gamma-ray heating level in the first wall in larger than the corresponding value for neutrons. The maximum value for the homogenized heating rate in the first wall is $\sim$ 90 $MW/m^3$ for 5 $MW/m^2$ wall loading. The corresponding value in the breeding zone is $\sim$ 70 $MW/m^3$. Notice also the peak in the profiles near the reflector boundaries and that the profile for the total heating is dominated by the contribution from gamma-rays heating in the reflector and the shield.

The displacement per atom per year of operation is shown in Fig. D.2.4-4 for the main constituents of the PCA structure and for 5 $MW/M^2$ wall loading. The maximum value in the first wall is $\sim$ 78 dpa/yr for a WL = 5 $MW/m^2$. On Fig. D.2.4-5 and Fig. D.2.4-6, the profiles for the hydrogen and the helium production rates are shown, respectively. The average value for the hydrogen

production rate from Fe, Ni, and Cr are displayed, respectively. In the first wall, the hydrogen production rate is ~ 4.8 x $10^3$ appm/yr. The corresponding value for the helium production rate is ~ 1.6 x $10^3$ appm/yr. These values are for a wall loading of 5 MW/$m^2$.

Table D.2.4-1. Constituents Atomic Density by Zone (atm/b•cm) in the $Li_{17}Pb_{83}$ Self-Cooled Blanket with PCA Structure (LiPb/LiPb/PCA)

| Constituent | First Wall | Breeding Zone | Reflector | Shield |
|---|---|---|---|---|
| Mo | 4.934-4 | 7.401-5 | 8.881-4 | --- |
| Fe | 2.749-2 | 4.124-3 | 4.949-2 | 6.258-2 |
| Pb | 1.378-2 | 2.549-2 | 2.756-3 | --- |
| $^7$Li | 2.823-4 | 5.222-4 | 5.645-5 | --- |
| $^6$Li | 2.540-3 | 4.699-3 | 5.081-4 | --- |
| Cr | 6.370-3 | 9.555-4 | 1.147-2 | 1.663-3 |
| Ni | 6.450-3 | 9.675-4 | 1.161-2 | 1.422-3 |
| Si | 4.214-4 | 6.320-5 | 7.584-4 | 3.524-4 |
| C | 9.855-5 | 1.478-5 | 1.774-4 | 2.078-3 |
| Ti | 1.483-4 | 2.274-5 | 2.669-4 | --- |
| H | --- | --- | --- | 6.700-3 |
| O | --- | --- | --- | 3.350-3 |
| Mn | --- | --- | --- | 1.097-2 |

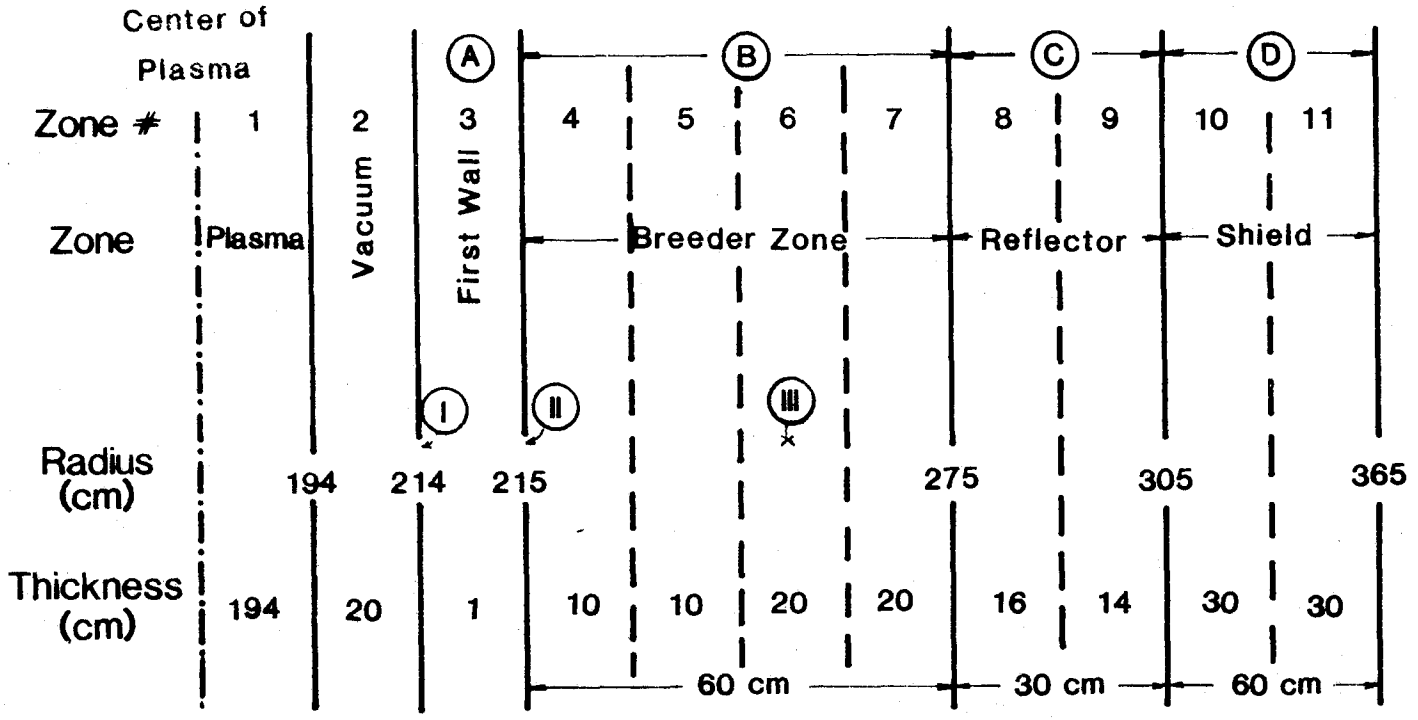


(A) 50% PCA, 50% $Li_{17}Pb_{83}$ (90% $^{6}Li$)
(B) 7.5% PCA, 92.5% $Li_{17}Pb_{83}$ (90% $^{6}Li$)
(C) 90% Fe 1422, 10% $H_2O$

Figure D.2.4-1 One-dimensional model for $Li_{17}Pb_{83}$ self-cooled blanket.

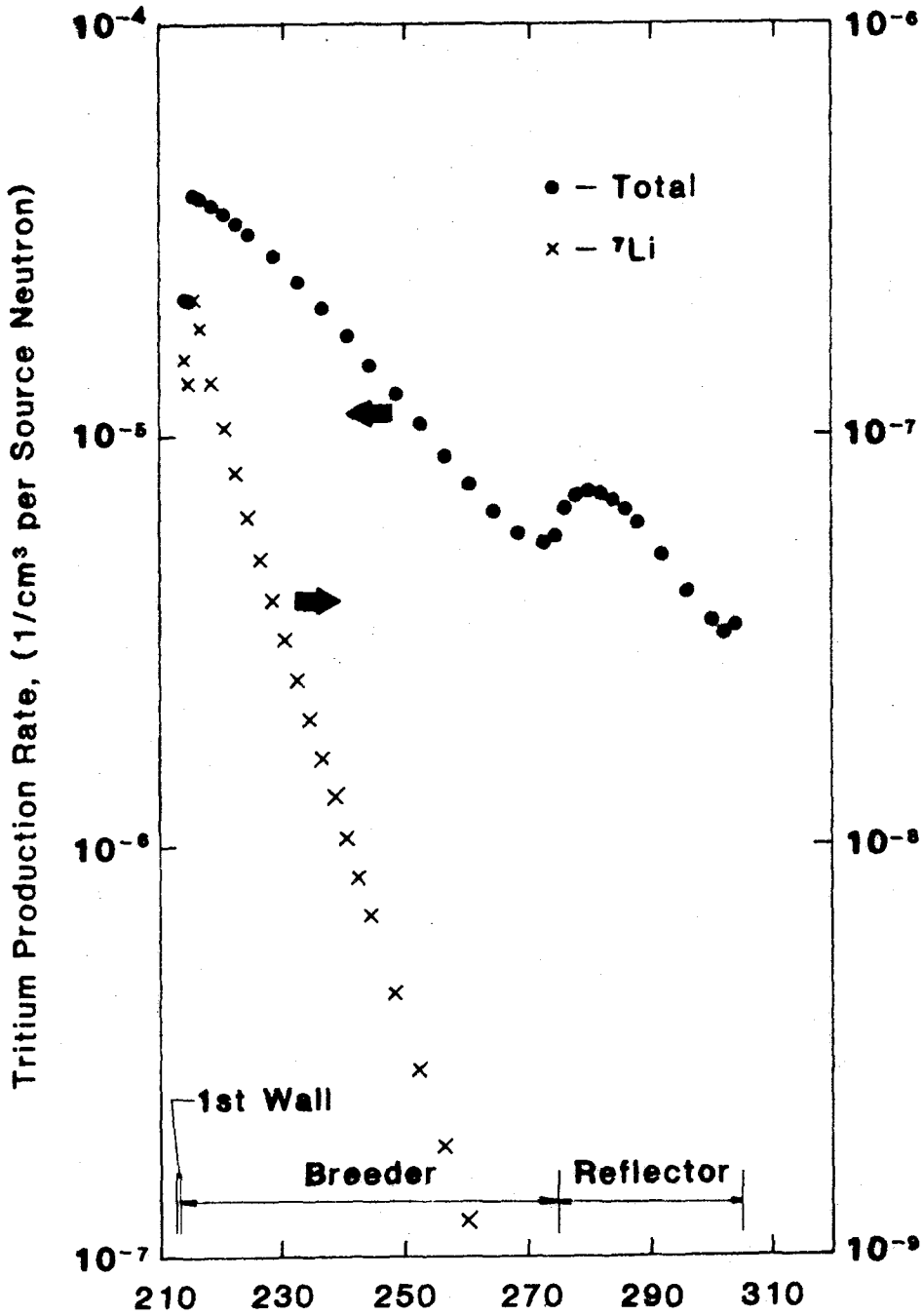


Figure D.2.4-2 Tritium Production Rate in the $L_{17}Pb_{83}$ self-cooled blanket.

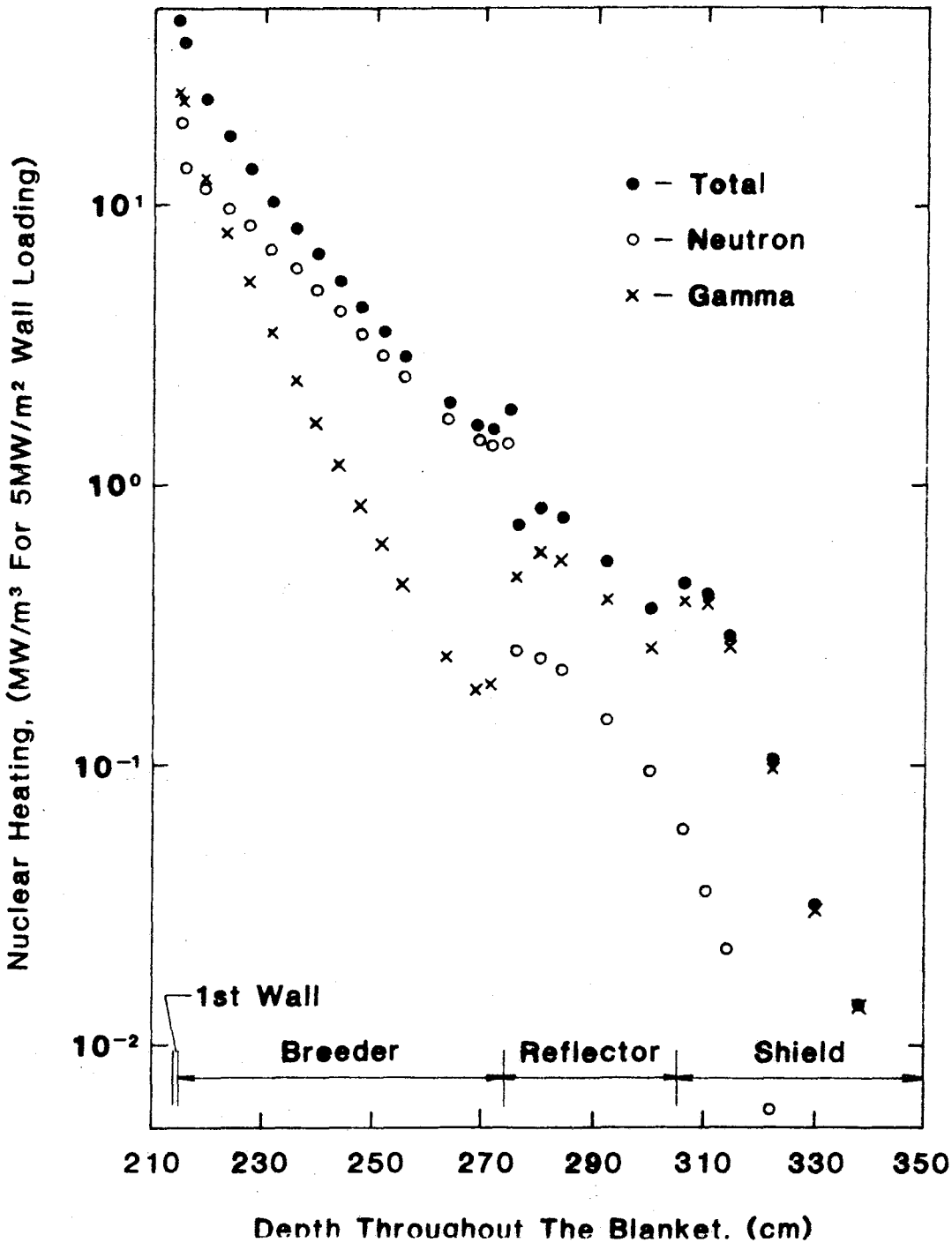


Figure D.2.4-3 Heat deposition rate in the $Li_{17}Pb_{83}$ self-cooled blanket.

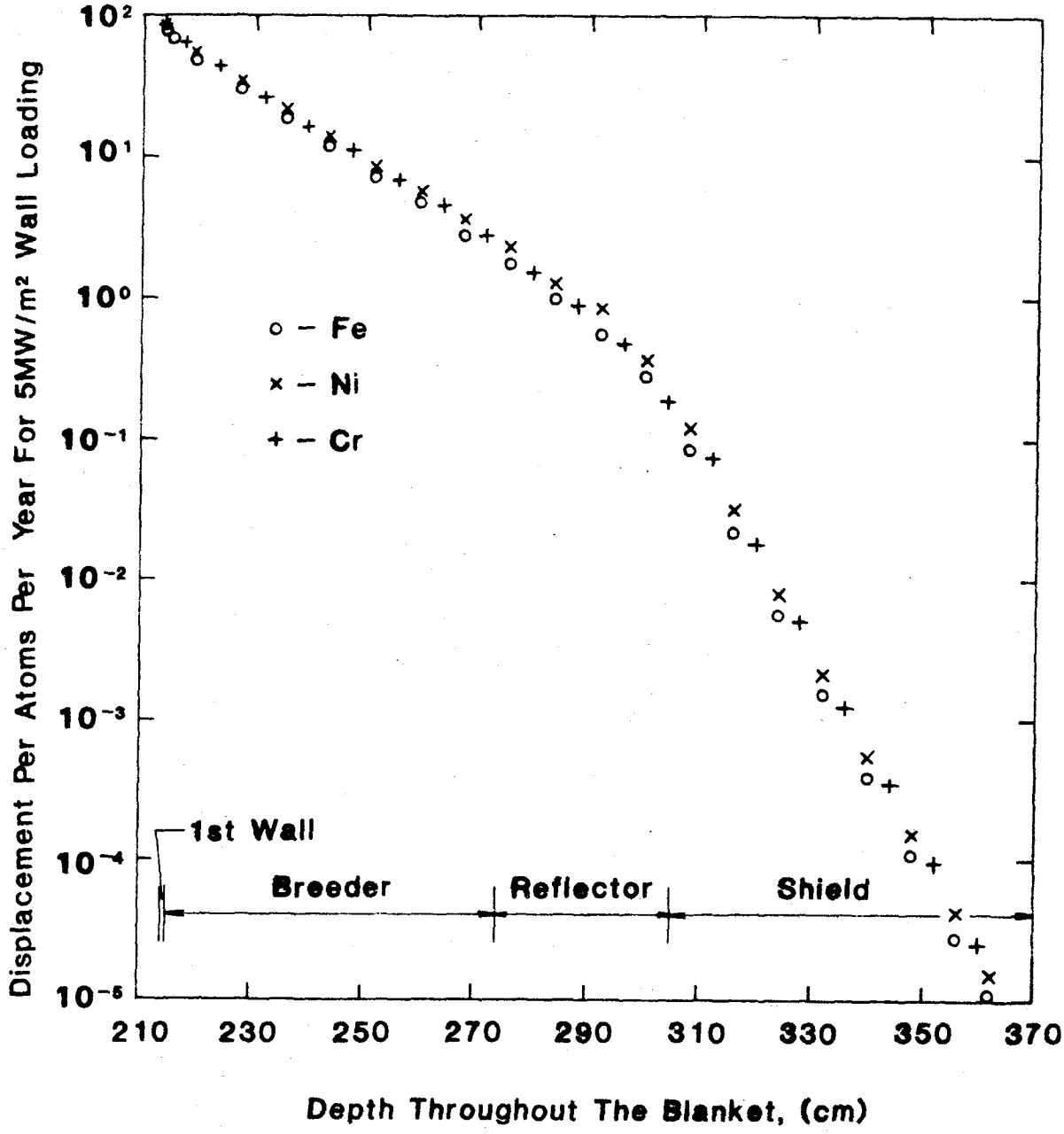


Figure D.2.4-4 Displacement per atom rate in the $L_{17}Pb_{83}$ self-cooled blanket.

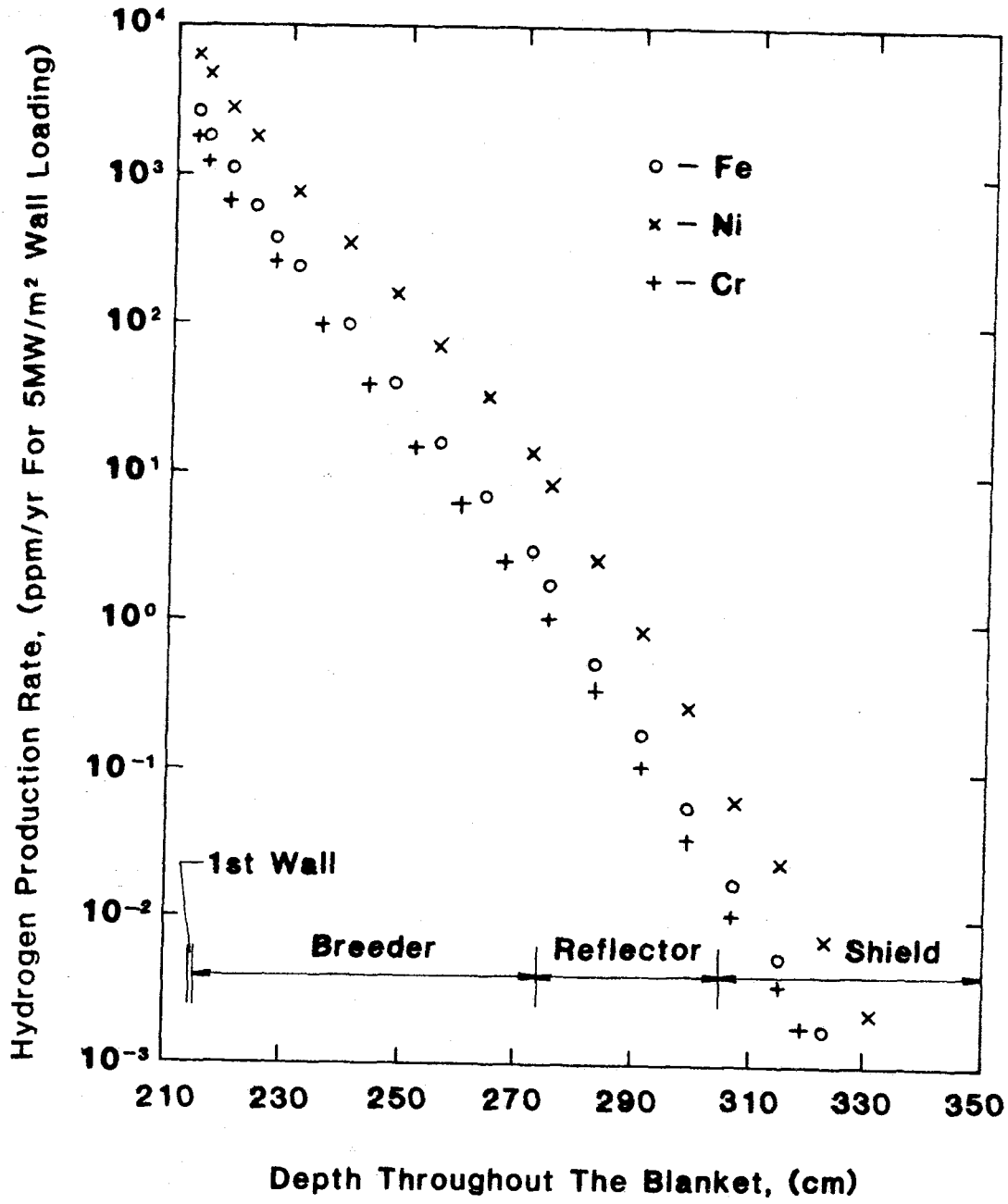


Figure D.2.4-5 Proton Production Rate in the $Li_{17}Pb_{83}$ self-cooled blanket.

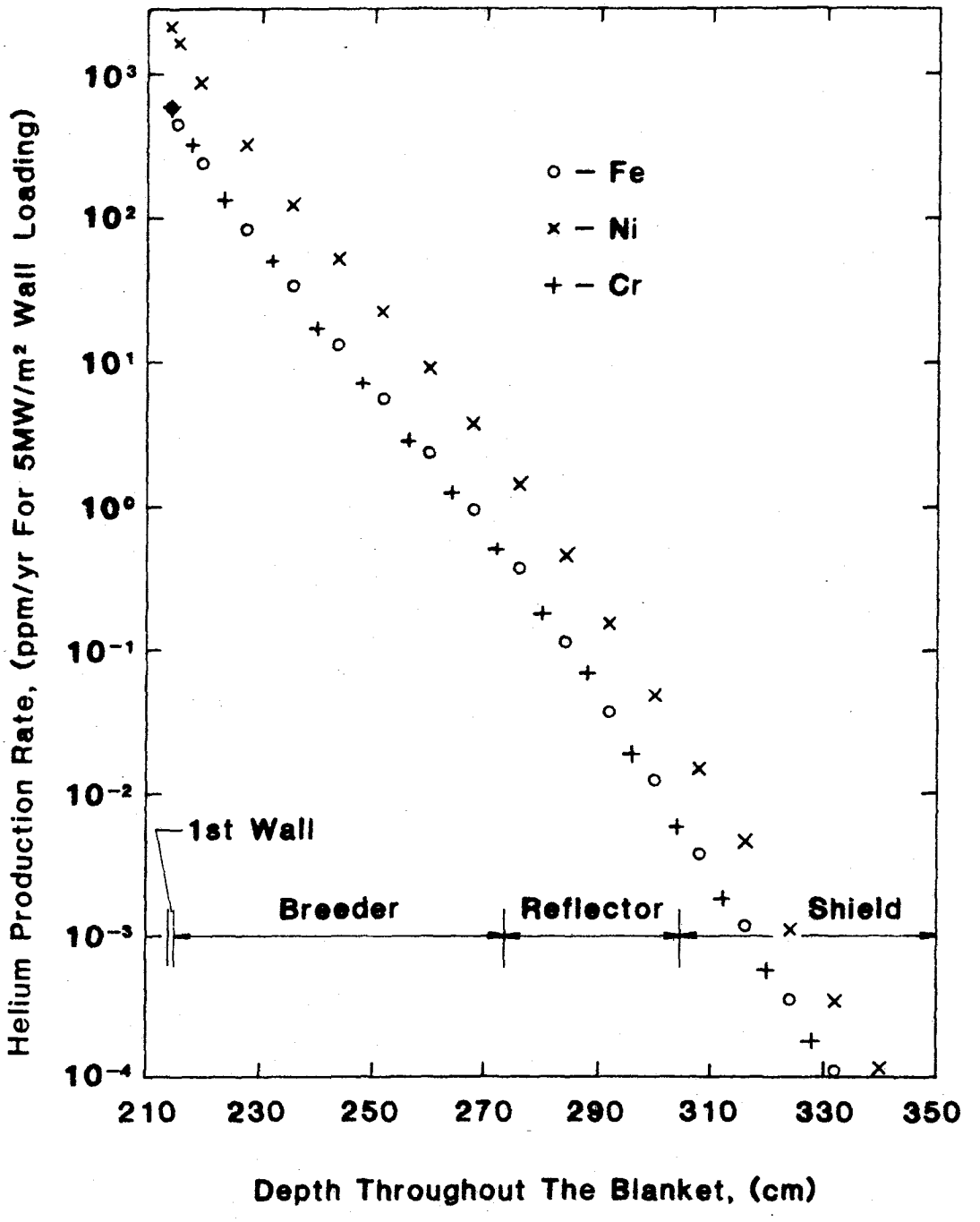


Figure D.2.4-6 He Production Rate in the $Li_{17}Pb_{83}$ self-cooled blanket.

## D.2.5 The Liquid Lithium Self-Cooled Blanket with V15Cr5Ti Structure (Li/Li/V)

The one-dimensional geometrical model and material arrangement for this blanket is shown in Fig. D.2.5-1. Detailed discussion on this blanket can be found in Chapter 6. Natural lithium is used as the breeding material and the Fe1422 steel as the reflector and shield. Elsewhere, the vanadium alloy V15Cr5Ti is used as the structure. The atomic densities for the constituents in various zones of the blanket are given in Table D.2.5-1.

The profiles for tritium production and heat generation rates are shown in Fig. D.2.5-2 for a wall load of 2 $MW/m^2$. Appreciable contribution (36%) to the total breeding ratio comes from $^7Li(n,\alpha n')t$ reactions. The tritium bred in the toroidal channel contributes about 15% to the total tritium breeding in the blanket. The maximum tritium production rate occurs at the front edge of the toroidal channel and reaches the value of $\sim 8.35 \times 10^{-3}$ T/yr. Li atom$\cdot cm^3$ for 5 $MW/m^2$ which corresponds to $\sim 3.68 \times 10^{-5}$ $T/cm^3$ per D-T source neutron. In the poloidal channel, the maximum tritium production rate for 5 $MW/m^2$ is $\sim 5.82 \times 10^{-3}$ T/yr. Li atom$\cdot cm^3$ or $2.84 \times 10^{-5}$ $T/cm^3$ per D-T neutron.

The heat production profiles from both neutrons and gamma-rays interactions are also shown in Fig. D.2.5-2. The blanket power multiplication is 1.25. Most of the heat produced in the entire blanket is due to neutrons interactions (72.3%). However, gamma-rays heating dominates in the first and second walls, the reflector, and the shield. The value shown in Fig. D.2.5-2 for the maximum heating rate in the first wall for 2 $MW/m^2$ wall load is $\sim 10$ $MW/m^3$. For 5 $MW/m^2$ wall load, the maximum heating rate is 25 $MW/m^3$. The maximum heating rate in the breeding zone occurs at the front edge of the toroidal channel and reaches the value of 21 $MW/m^3$ for a 5 $MW/m^2$ wall load.

The damage parameters (dpa, H and He production rates) in vanadium, chromium, and titanium are shown in Fig. D.2.5-3 through Fig. D.2.5-5, respectively, for a 2 $MW/m^2$ wall load (dpa cross-section data for titanium is not available). Considering a 5 $MW/m^2$ wall loading and averaging over the atomic densities of these elements, the maximum displacement per atom, hydrogen and helium production rates in the V15Cr5Ti structure are: 62 dpa/yr, $1.65 \times 10^3$ appm/yr, and $3.85 \times 10^2$ appm/yr, respectively.

Table D.2.5-1. Constituents Atomic Density by Zone (atom/b•cm) in the Lithium Self-Cooled Blanket with V15Cr5Ti Structure (Li/Li/V)

| Constituent | First Wall | Toroidal Channel | Second Wall | Poloidal Channel | Reflector | Shield |
|---|---|---|---|---|---|---|
| V | 5.754-2 | 6.157-3 | 5.754-2 | 5.754-4 | --- | --- |
| Cr | 1.060-2 | 1.134-3 | 1.060-2 | 1.060-4 | --- | --- |
| Ti | 2.835-3 | 3.033-4 | 2.835-3 | 2.835-5 | --- | --- |
| $^{6}Li$ | --- | 3.102-3 | --- | 3.435-3 | 3.472-4 | --- |
| $^{7}Li$ | --- | 3.824-2 | --- | 4.240-2 | 4.283-3 | --- |
| Fe | --- | --- | --- | --- | 6.258-2 | 6.953-2 |
| N | 1.311-4 | 1.403-5 | 1.311-4 | 1.311-6 | --- | --- |
| Cr | --- | --- | --- | --- | 1.663-3 | 1.848-3 |
| Ni | --- | --- | --- | --- | 1.422-3 | 1.580-3 |
| Mn | --- | --- | --- | --- | 1.097-2 | 1.219-2 |
| Si | --- | --- | --- | --- | 3.524-4 | 3.916-4 |
| C | --- | --- | --- | --- | 2.078-3 | 2.309-3 |
| $^{16}O$ | 1.148-4 | 1.228-5 | 1.228-5 | 1.148-6 | --- | --- |

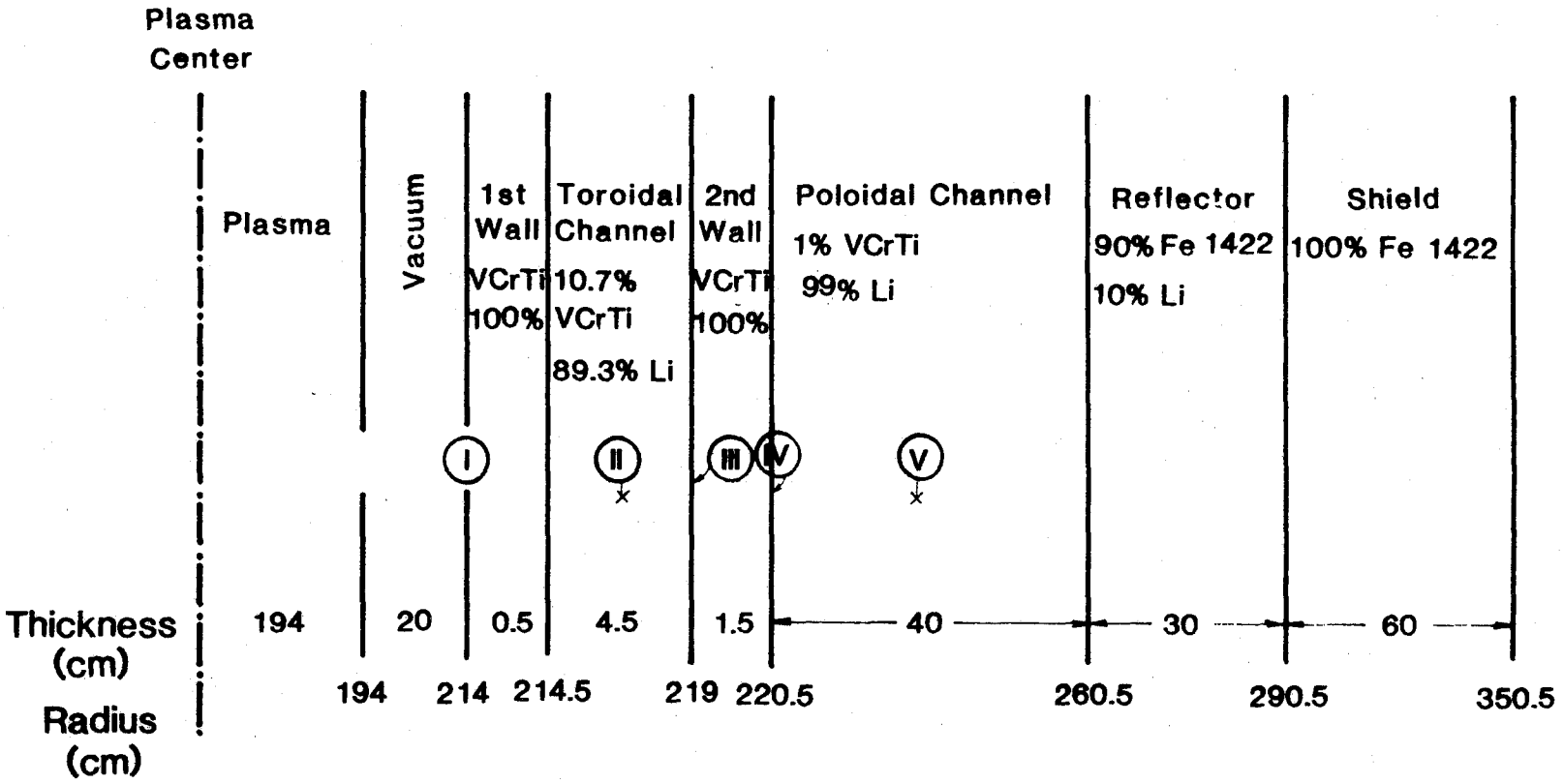


Figure D.2.5-1 One-dimensional model for the Lithium self-cooled blanket with V15Cr5Ti structure (Li/Li/V).

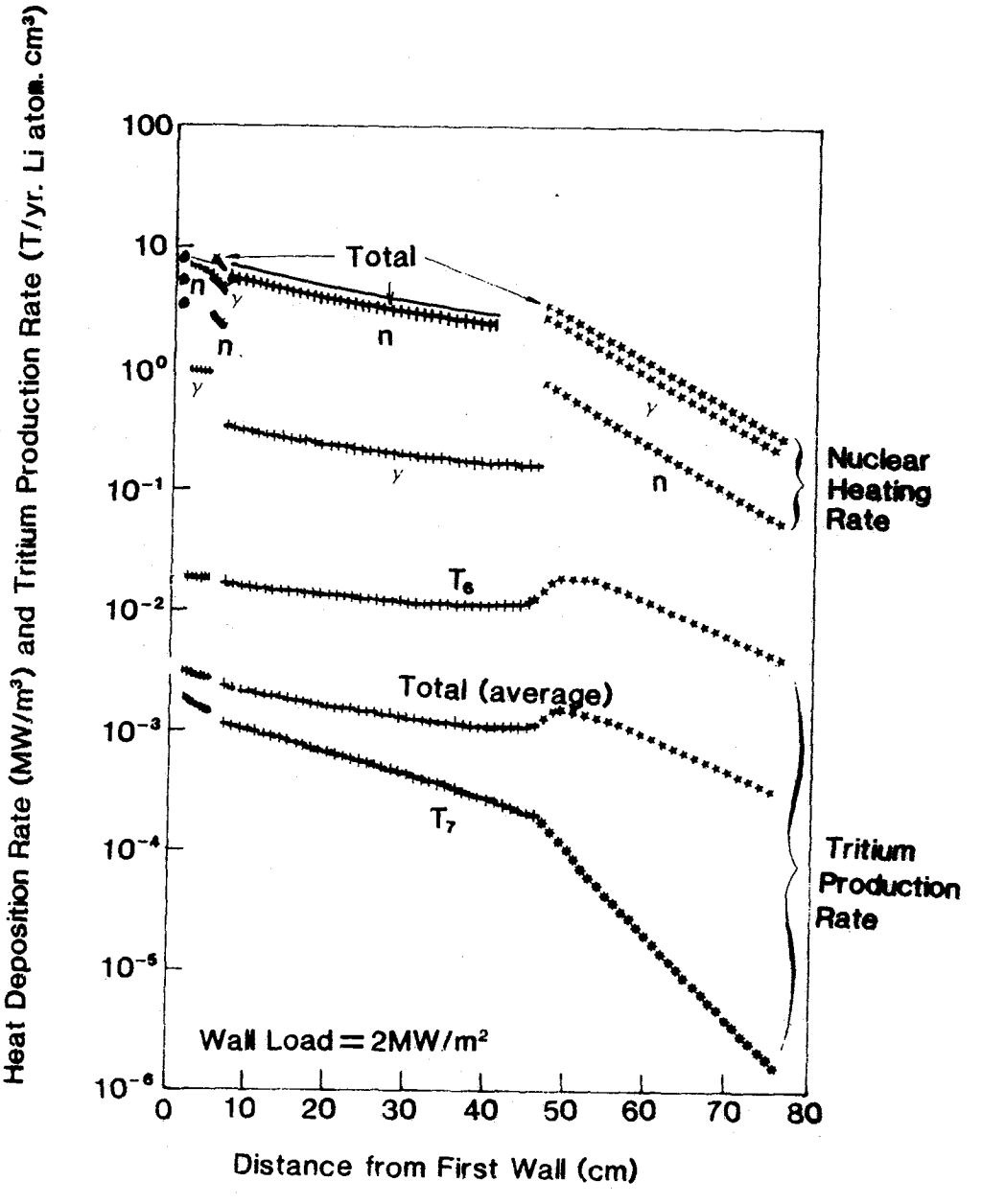


Figure D.2.5-2 Tritium production and heat deposition rates in the Lithium self-cooled blanket with Vanadium structure (Li/Li/V).

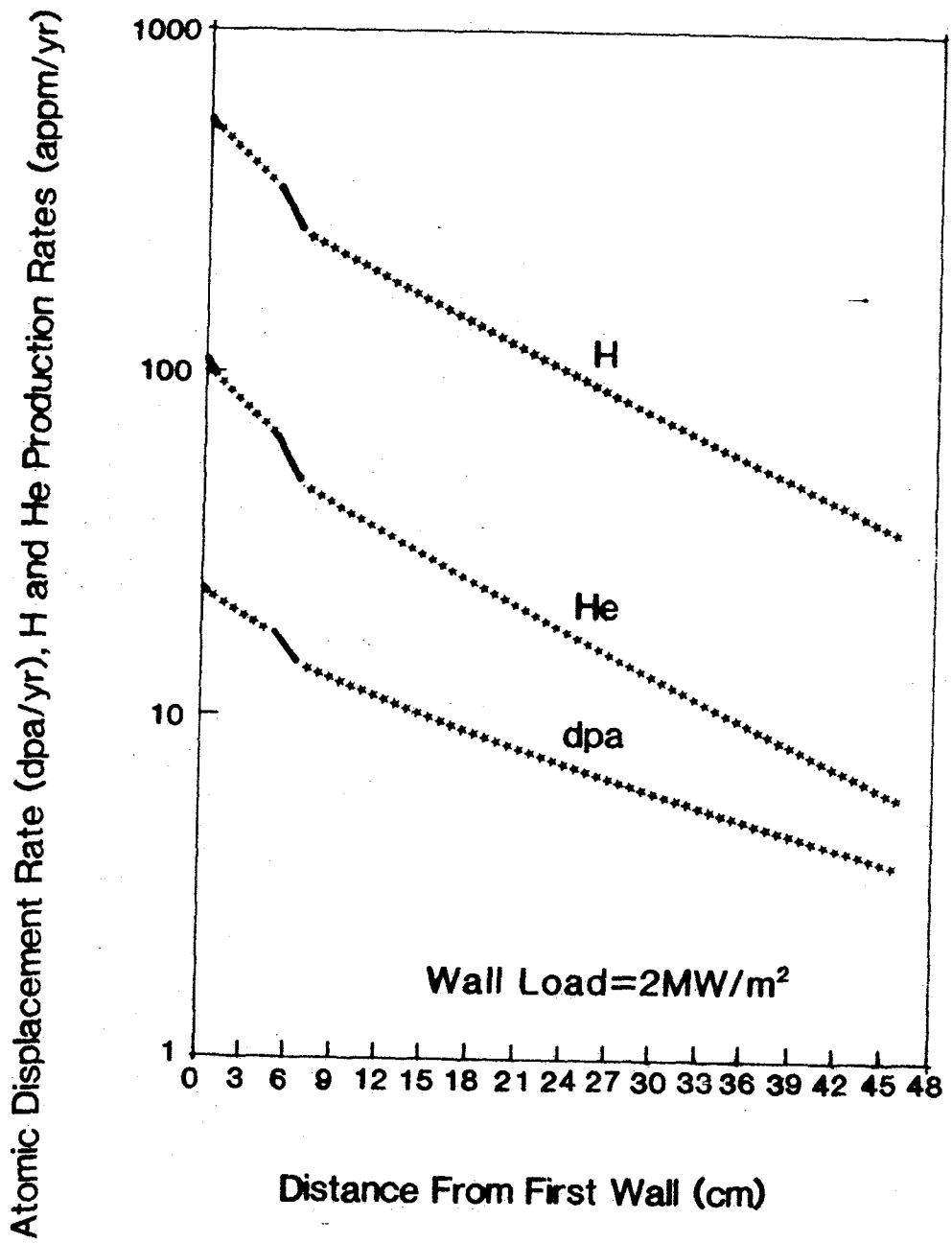


Figure D.2.5-3 Atomic displacement, hydrogen and helium production rates in Vanadium in the Li/Li/V blanket.

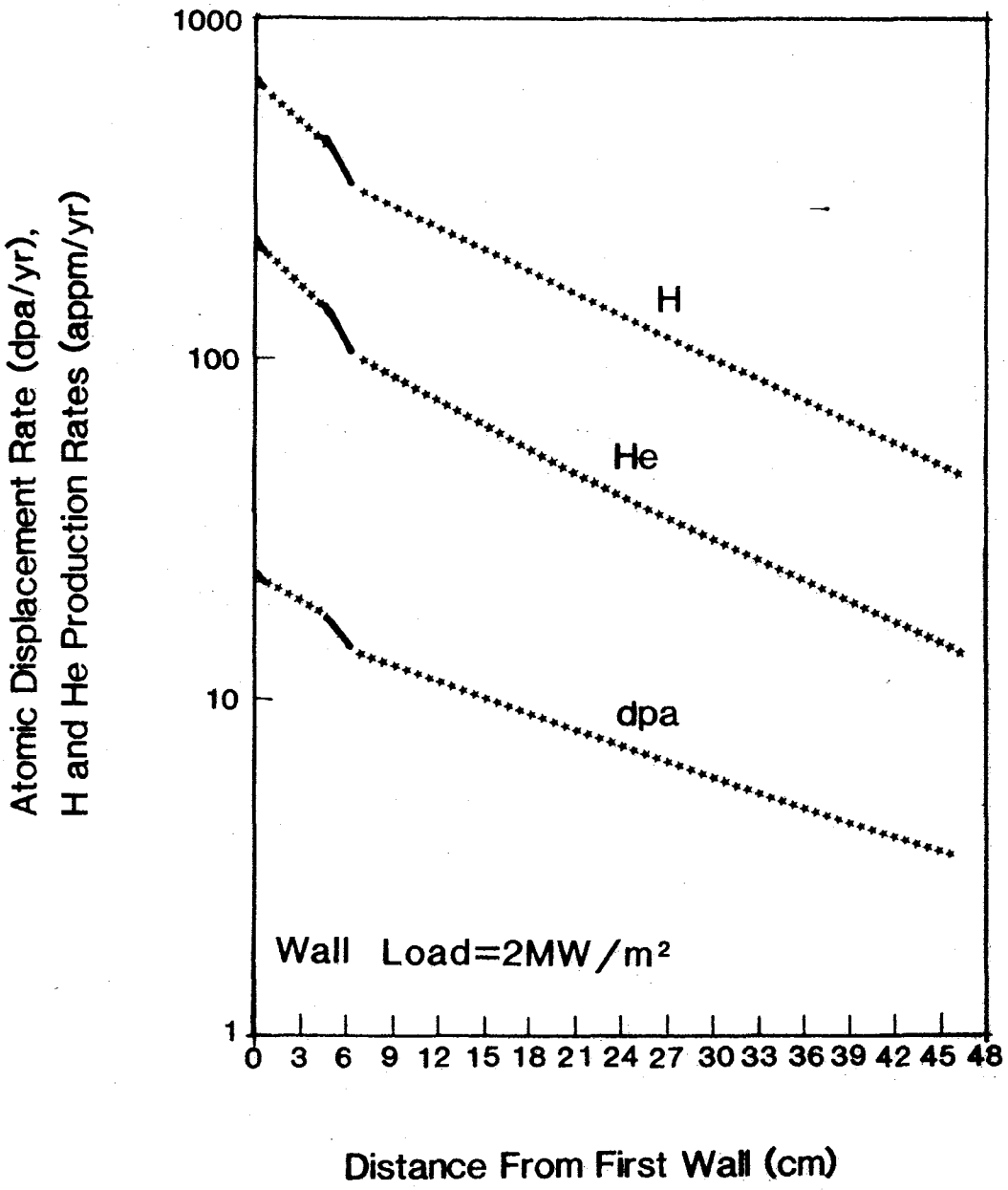


Figure D.2.5-4 Atomic displacement, hydrogen and helium production rates in chromium in the Li/Li/V blanket.

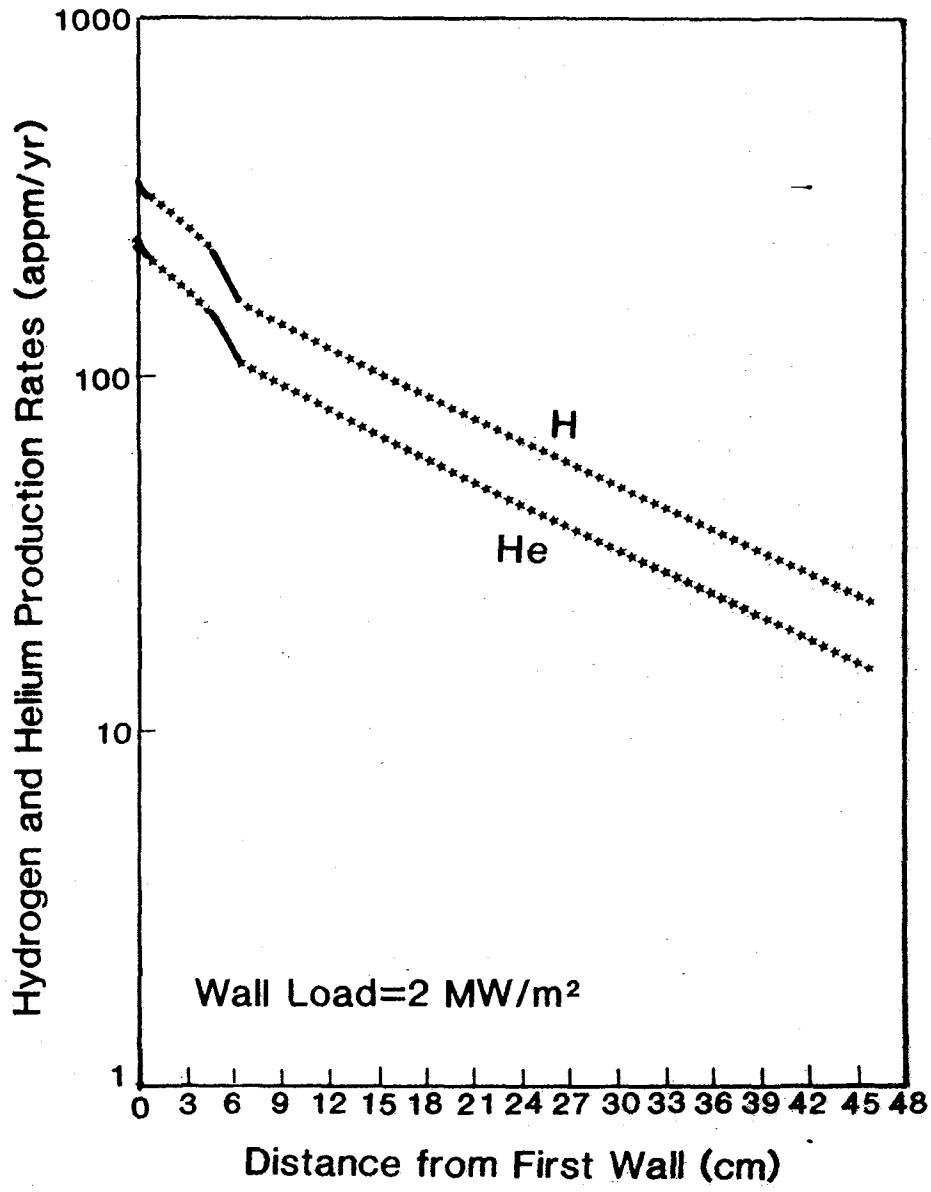


Figure D.2.5-5 Hydrogen and helium production rates in titanium in the Li/Li/V blanket.

### D.2.6 The $LiAlO_2$ Water-Cooled Blanket, with Ferritic Steel Structure ($LiAlO_2/H_2O/FS/Be$)

The geometrical model and material arrangement for this blanket type is shown in Fig. D.2.6-1. The breeding zone consists of three subzones, namely: blanket-1, blanket-2, and blanket-3 subzones. Each of these subzones has different volumetric ratio for its constituents. Beryllium, which is used as a neutron multiplier is located in blanket-1 with 87% theoretical density (TD). The $\gamma$-$LiAlO_2$ breeding material is also 87% TD and the $^6Li$ enrichment is 90%. The atomic densities for the blanket materials which were used in the calculation are given in Table D.2.6-1.

The tritium production rate profiles are shown in Fig. D.2.6-2 for $T_6$ and $T_7$. The unit used is triton atoms produced per year per Li atom ($^6Li$ or $^7Li$) per unit volume. The profile for the total tritium production is almost entirely dominated by the contribution from $T_6$ since $^6Li$ is enriched in this blanket (90% enrichment). The curve for the total breeding ratio is normalized to the total lithium atoms, $^6Li$ and $^7Li$, and their atomic densities are given in Table D.2.6-1. Note also from Fig. D.2.6-2 that the tritium production comes mostly from blanket-1 subzone where beryllium is located. The Be(n,2n') reactions enhance tritium production in that subzone since more neutrons are available for breeding. In addition, since the threshold for the Be(n,2n) reaction is only ~ 2.4 MeV, multiple (n,2n) reactions can occur leading to an increase in the neutron multiplication in that zone. The values shown in Fig. D.2.6-2 are for 1 $MW/m^2$ wall loading. The maximum tritium production rate is $1.25 \times 10^{-1}$ T/yr Li atom$\cdot cm^3$ for 1 $MW/m^2$ which translates to ~ $8.99 \times 10^{-5}$ $T/cm^3/s$ per one D-T source neutron.

The heat deposition rate profiles are shown in Fig. D.2.6-3. The contribution from gamma-rays heating in the first wall is larger than the contribution from neutrons. This is also true in the coolant manifold and the shield zones where heating from gamma-rays dominates. The values shown in the first wall are those obtained for the homogenized case where the maximum heating rate is ~ 4.4 $MW/m^3$ for 1 $MW/m^2$ wall load. If we consider the volume fraction as the ferritic steel in the first wall (32%), the maximum heat deposition rate in the structure would be 13.8 $MW/m^3$ for 1 $MW/m^2$ wall load (68.7 $MW/m^3$ for 5 $MW/m^2$ wall load).

The damage parameters (dpa, hydrogen, and helium production rate) are shown in Fig. D.2.6-4 through Fig. D.2.6-8 for the main constituents of the HT-9 structure (Fe,Cr,Mo) and for beryllium and aluminum. The results shown are for 1 $MW/m^2$ wall loading. The average values for the HT-9 structure (average over the atomic densities of Fe,Cr,and Mo) are shown in Fig. D.2.6-8 throughout the first wall and blanket-1. The average value for the maximum displacement per atom rate, hydrogen production rate, and helium production rate in the first wall are: 11 dpa/yr, 500 appm/yr, and 120 appm/yr, respectively for a 1 $MW/m^2$ wall load. A summary for the nuclear parameters in this blanket for a wall load of 5 $MW/m^2$ can be found in Table D.2.7-1.

Table D.2.6-1. Constituents Atomic Density by Zone (atom/b•cm) in the $LiAlO_2$ Water-Cooled Blanket ($LiAlO_2/H_2O$/FS/Be)

| Constituent | First Wall | BLNK-1 | BLNK-2 | BLNK-3 | Coolant Manifold | Shield |
|---|---|---|---|---|---|---|
| H | 4.690-3 | 1.441-2 | 7.705-3 | 2.680-3 | 4.489-2 | 1.340-2 |
| Mo | 1.547-4 | 9.424-5 | 6.041-5 | 3.383-5 | 1.595-4 | --- |
| Fe | 2.259-2 | 1.376-2 | 8.823-3 | 4.941-3 | 2.329-2 | 5.622-2 |
| O | 2.352-3 | 9.904-3 | 4.168-2 | 4.673-2 | 2.245-2 | 6.700-3 |
| Cr | 3.424-3 | 2.087-3 | 1.338-3 | 7.490-4 | 3.531-3 | 1.479-3 |
| Be | --- | 4.838-2 | --- | --- | --- | --- |
| $^7Li$ | --- | 1.351-4 | 1.892-3 | 2.269-3 | --- | --- |
| $^6Li$ | --- | 1.216-3 | 1.702-2 | 2.043-2 | --- | --- |
| Al | --- | 1.351-3 | 1.892-2 | 2.269-2 | --- | --- |
| Ni | --- | --- | --- | --- | --- | 1.265-3 |
| Mn | --- | --- | --- | --- | --- | 9.752-3 |

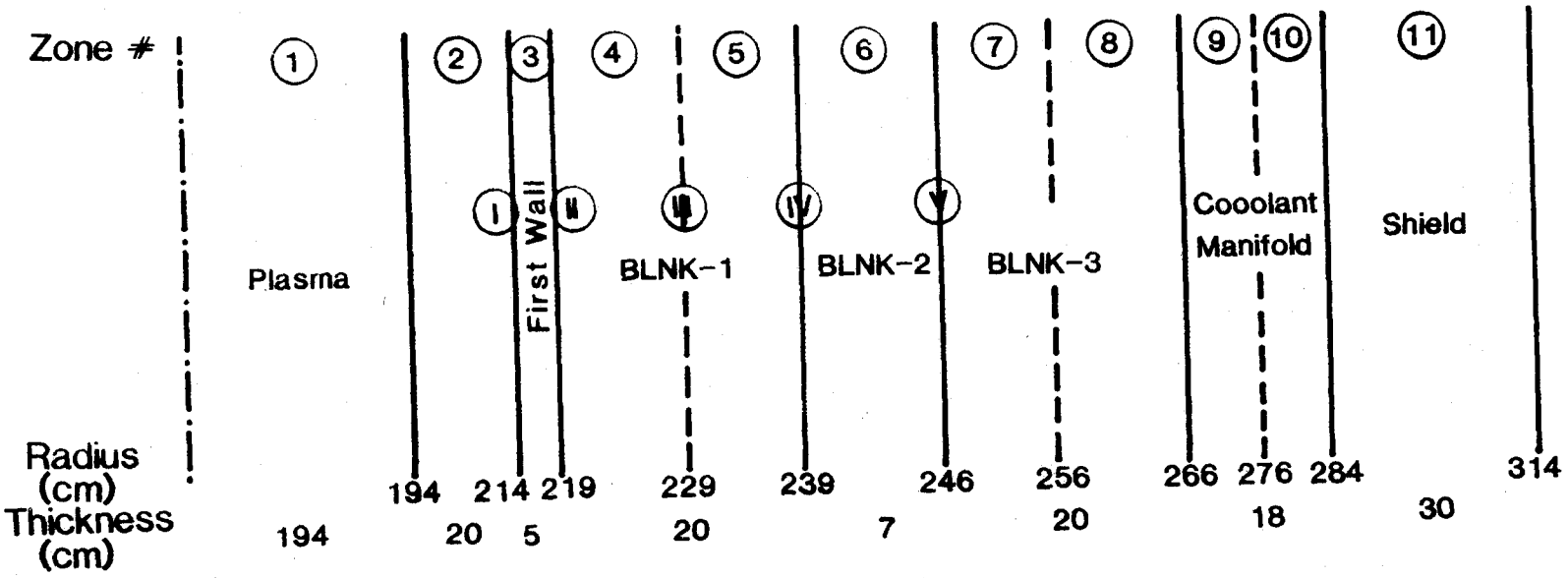


First Wall: 32% HT-9, 7% $H_2O$, 61% Void

BLNK-1: 19.5% HT-9, 21.5% $H_2O$, 5% $\gamma$-$LiAlO_2$*, 5% Be+, 9% Void

BLNK-2: 12.5% HT-9, 11.5% $H_2O$, 70% $\gamma$-$LiAlO_2$*, 6% Void

BLNK-3: 7% HT-9, 4% $H_2$), 84% $\gamma$-$LiAlO_2$*, 5% Void

Coolant Manifold: 33% HT-9, 17% $H_2O$, Shield: 80% Fe1422, 20% $H_2$)

*Breeder ($\gamma$-$LiAlO_2$), density = 87% TD, Li enrichment = 90%

+Be: 87% TD

Figure D.2.6-1 One-dimensional model for the $LiAlO_2/H_2O$/FS/Be blanket.

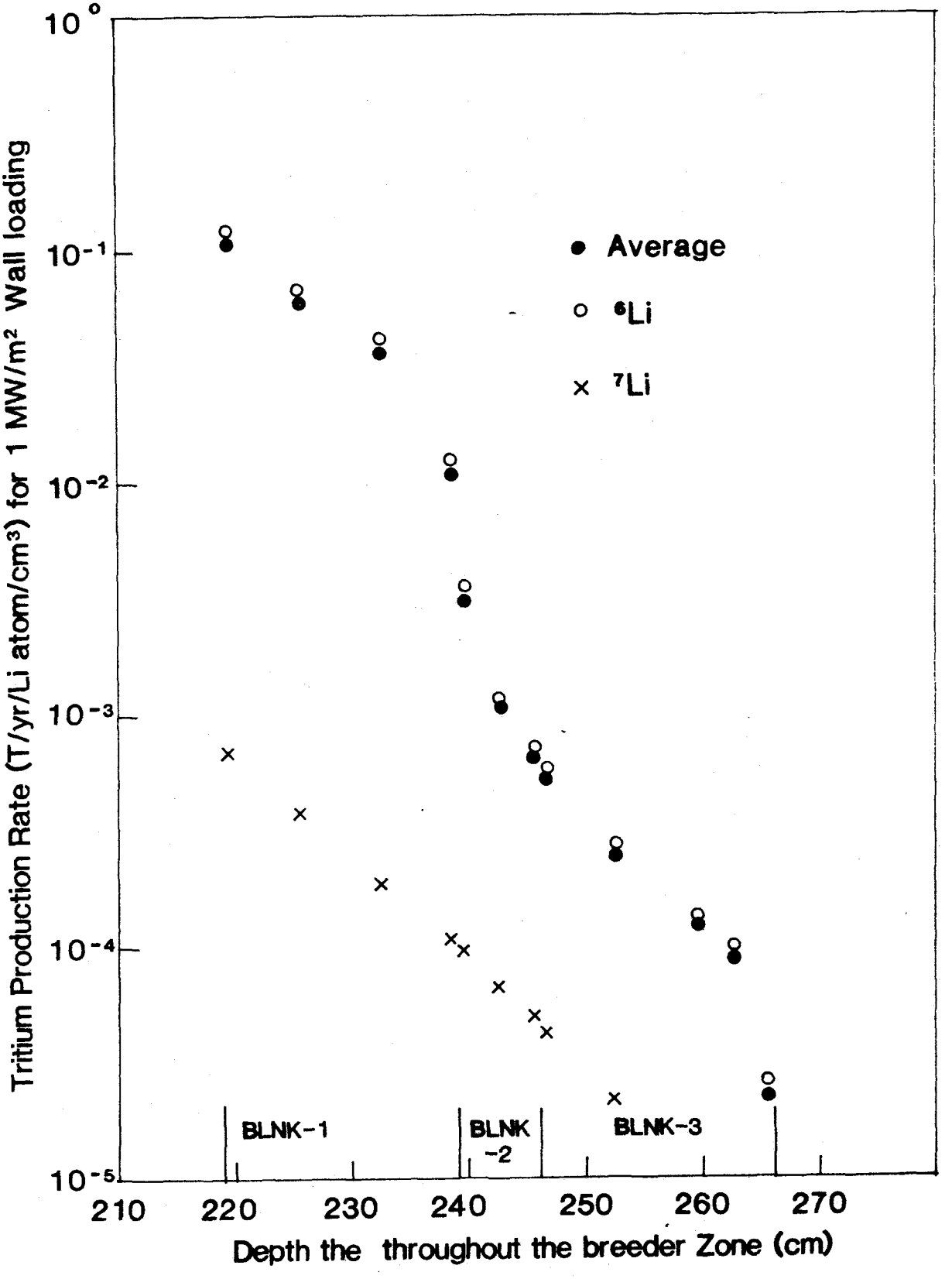


Figure D.2.6-2 Tritium production rate in the $LiAlO_2/H_2O$/FS/Be blanket.

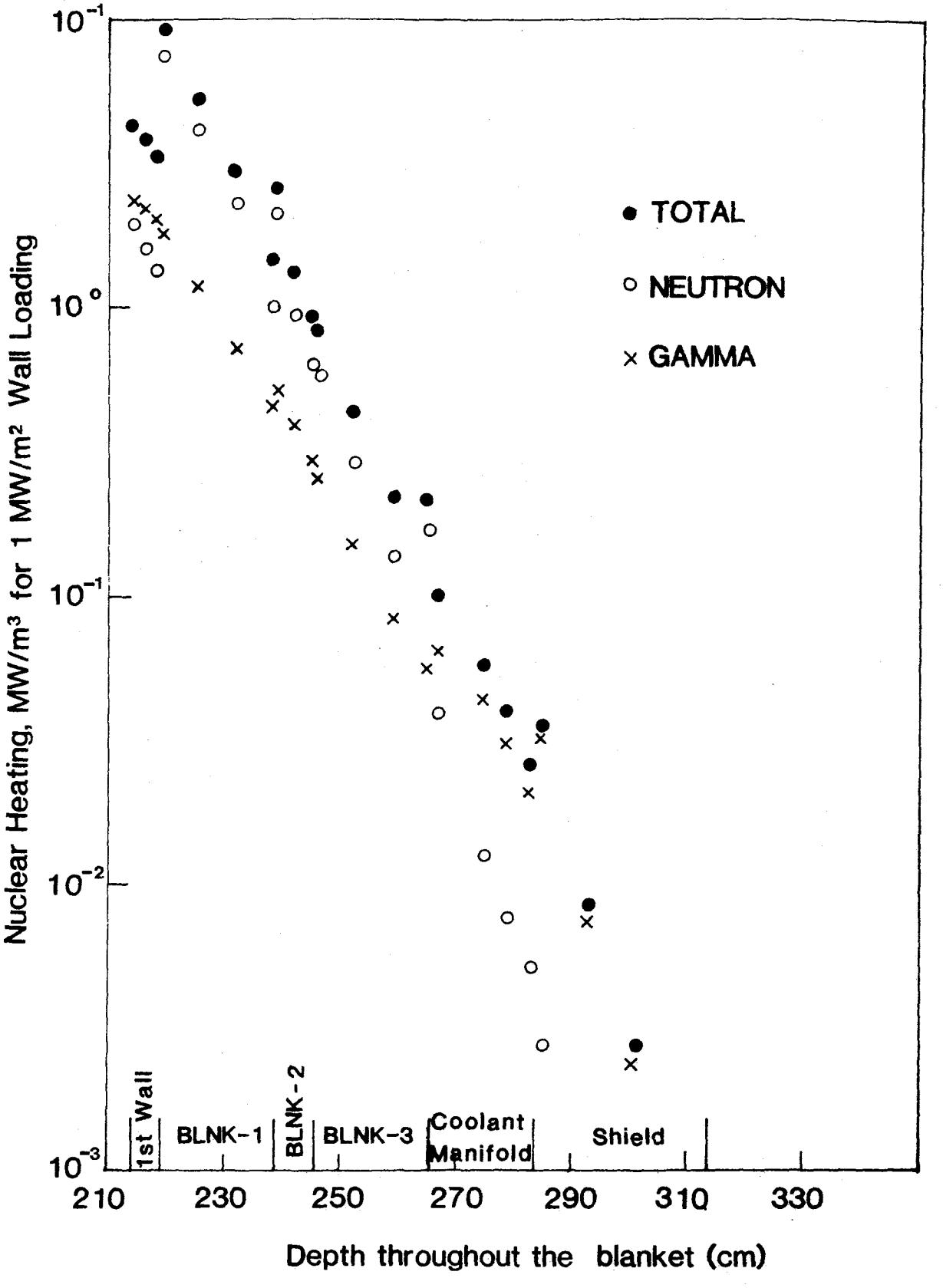


Figure D.2.6-3 Heat deposition rate in the $LiAlO_2/H_2O$/FS/BE blanket.

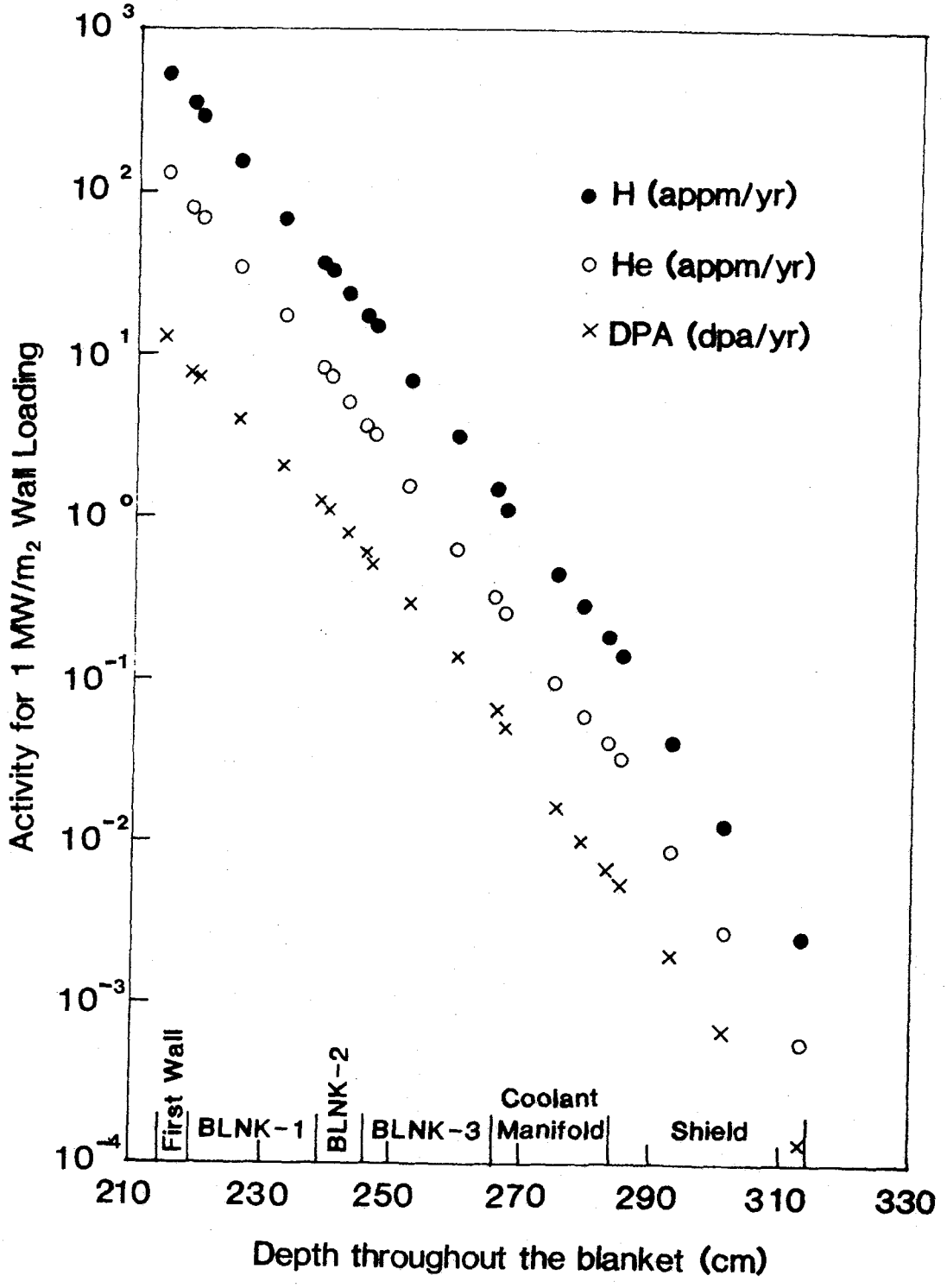


Figure D.2.6-4 The activities (dpa, hydrogen and helium production rate) for Iron in the $LiAlO_2/H_2O$/FS/Be blanket.

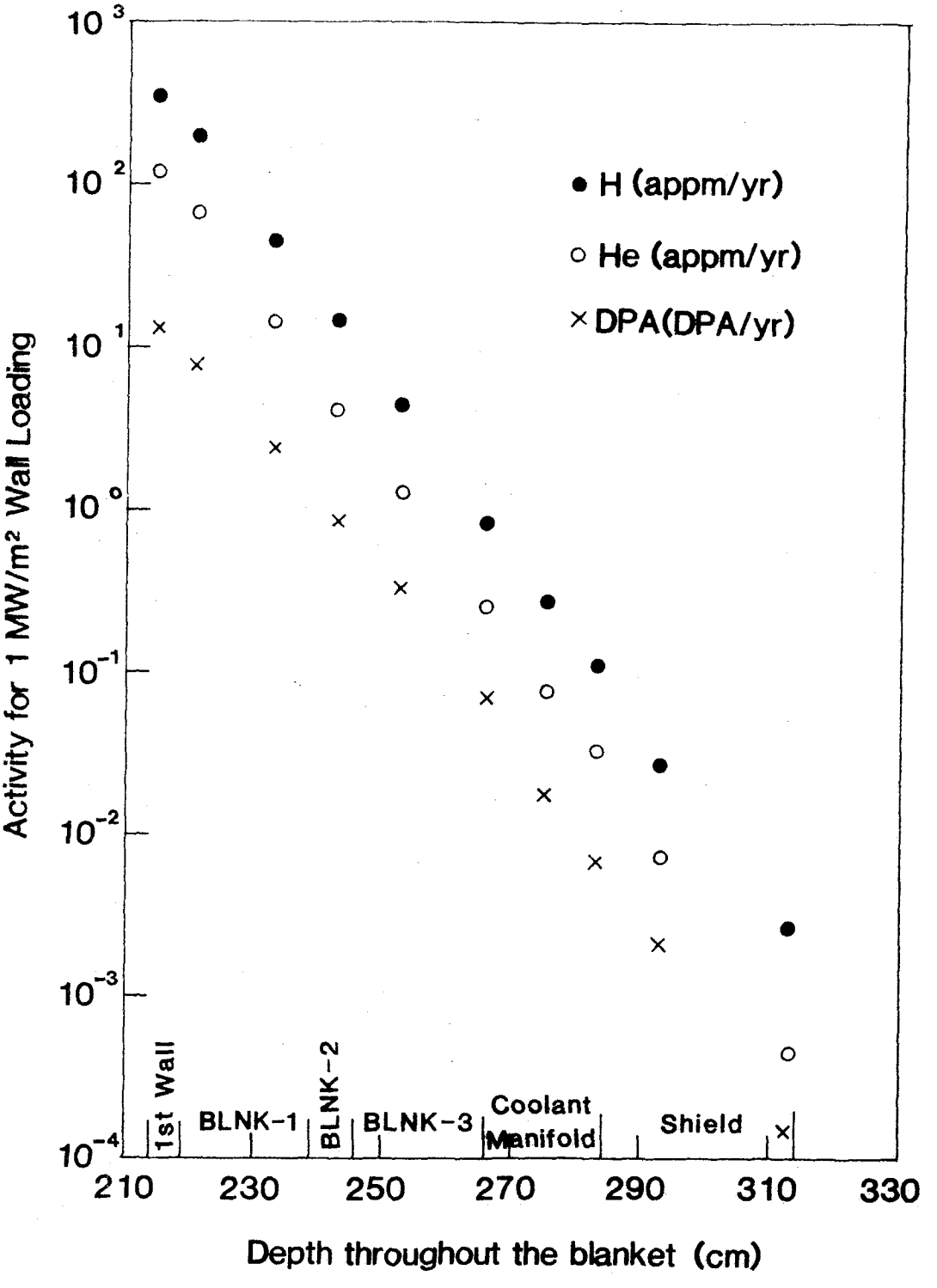


Figure D.2.6-5 The activities (dpa, hydrogen and helium production rate) for Chromium in the $LiAlO_2/H_2O$/FS/Be blanket.

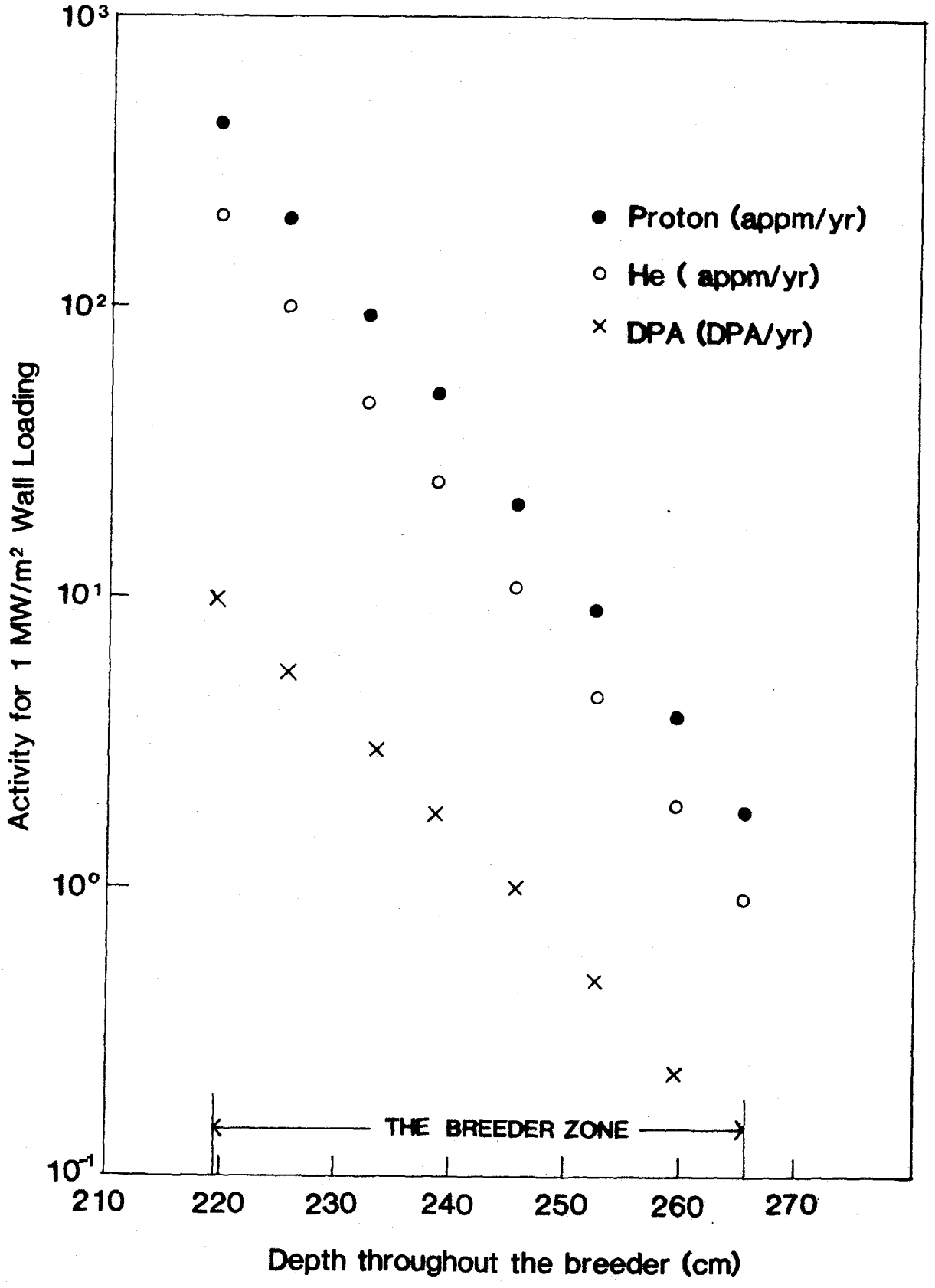


Figure D.2.6-6 The activities (dpa, hydrogen and helium production rate) for Aluminum in the $LiAlO_2/H_2O$/FS/Be blanket.

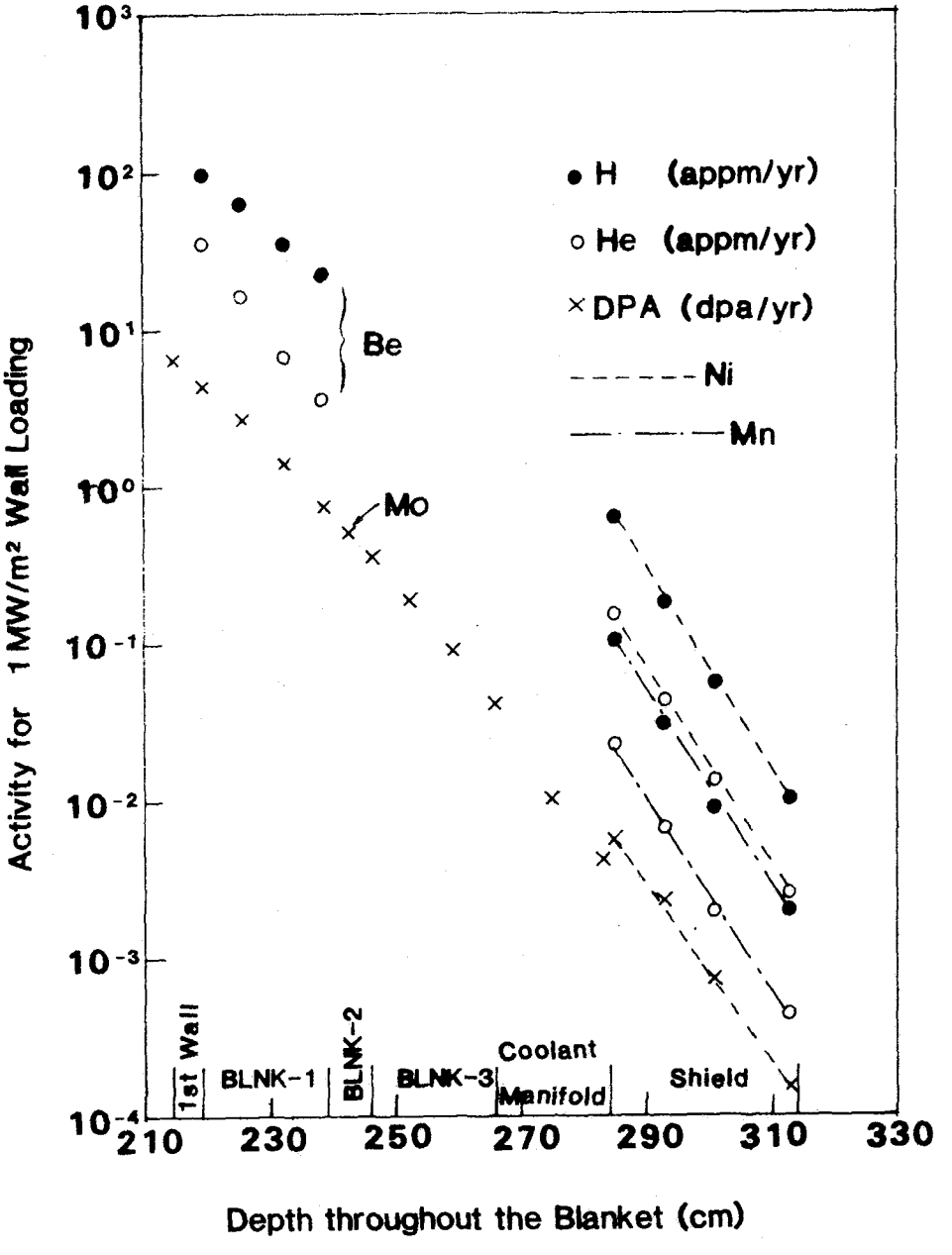


Figure D.2.6-7 The activities (dpa, Hydrogen and Helium production rate) for Beryllium, Molybdenum, Nickel and Manganese in the $LiAlO_2/H_2O$/FS/Be blanket.

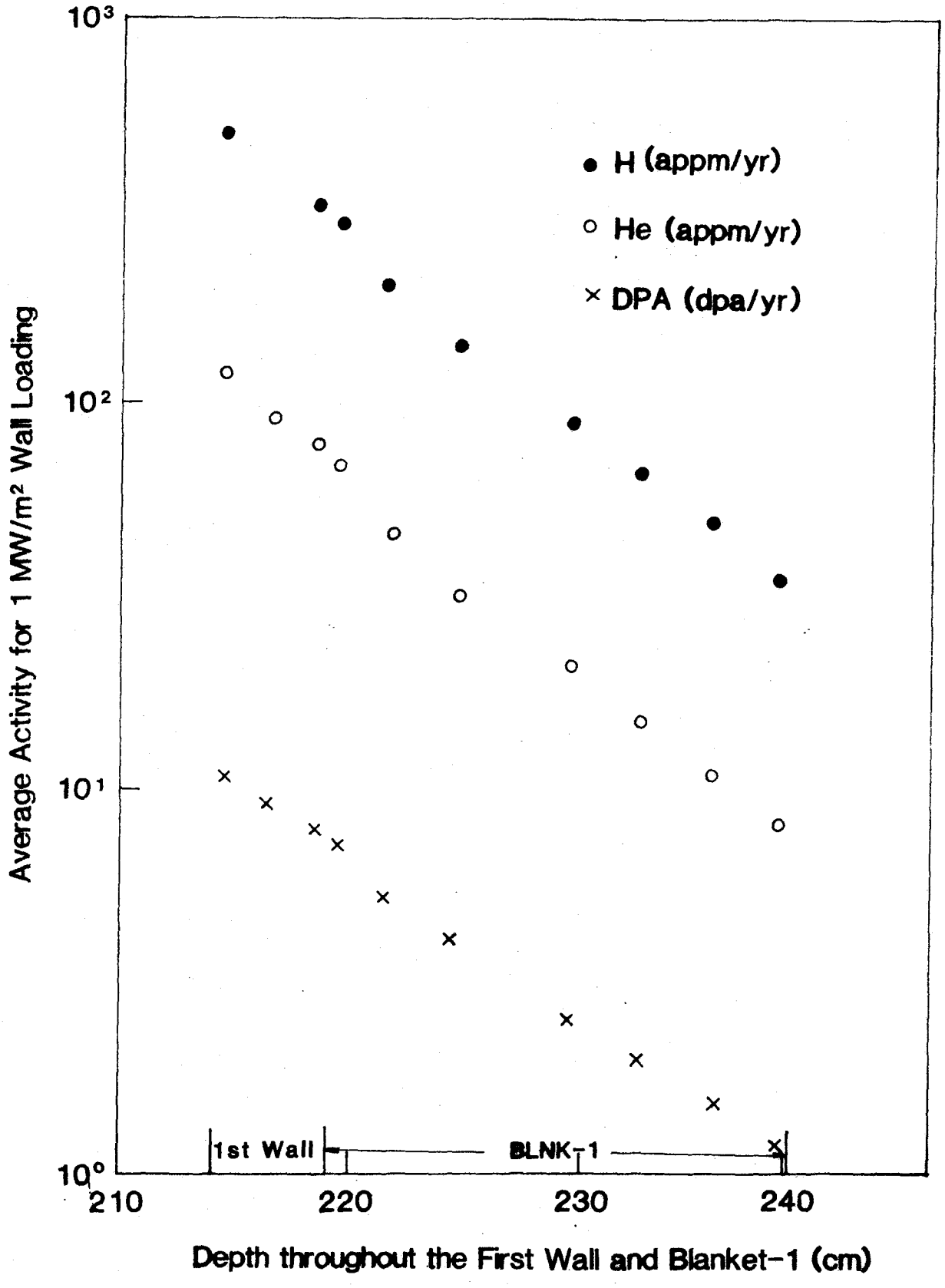


Figure D.2.6-8 The activities (dpa, hydrogen and helium production rate) for the ferritic steel (FS) average over the Fe, Cr and Mo constituents in the $LiAlO_2/H_2O$/FS blanket.

### D.2.7 Summary Table for the Nuclear Performance

A summary of the nuclear parameters in each blanket considered in the previous subsections are shown in Table D.2.7-1. Several observations can be made as follows.

#### D.2.7.1 Tritium Breeding

The LiPb/LiPb/PCA blanket has the largest tritium breeding ratio (TBR) followed by the Li/Li/V blanket. The TBR value in the $Li_2O$/He/Fs is the lowest. It appears that utilizing ferritic steel instead of PCA as the structural material reduces the total TBR. The lower TBR value in the $Li_2O$/He/Fs blanket as compared to the value found in the $Li_2O$/He/PCA blanket is due to the fact that Fs is 18% dense in the first wall of the first blanket as compared to the value of 6.6% in the later blanket. In addition, more structure in the breeding zone is used in the $Li_2O$/He/Fs blanket. Tritium breeding from $^7Li$ is almost negligible in the LiPb and the $LiAlO_2$ blankets since 90% enrichment for $^6Li$ is used. The maximum T-production rate in the $LiAlO_2$ blanket (see the unit used) is larger that the corresponding values in other blankets since the atomic densities for $^6Li$ and $^7Li$ are low in the $LiAlO_2$ material.

#### D.2.7.2 Heat Deposition and Power Multiplication

The blanket that exhibits the largest power multiplication is the $LiAlO_2$ one since beryllium is used as a multiplier. The margin among the power multiplication in the other blankets is small. The contribution to the total heat generation from gamma-rays interactions is the largest in the LiPb blanket. In addition, the first wall in this blanket is subject to the largest power density as compared to the other blankets. This is also true in the breeding zone. The lowest power density in both the structure of the first wall and the breeding zone is found in the Li/Li/V blanket.

#### D.2.7.3 Damage Parameters

Large displacement per atom in the first wall is obtained in the $Li_2O$ blanket with PCA structure while the lowest dpa value is in the $LiAl_2/H_2O$/FS/Be blanket. The LiPb blanket, however, exhibits the largest hydrogen and helium production rates in the first wall.

Table D.2.7-1. Summary of the Nuclear Parameters in the Five Blankets Considered in the Radiation Field Analysis (Wall Load = 5 $MW/m^2$)

| | $Li_2O$/He/PCA | $Li_2O$/He/FS | LiPb/LiPb/PCA | Li/Li/V | $LiAlO_2$/$H_2O$/FS/Be |
|---|---|---|---|---|---|
| Tritium Breeding Ratio (TBR): | | | | | |
| $T_6$ | 8.03-1 | 9.11-1 | 1.579 | 8.61-1 | 1.330 |
| $T_7$ | 4.25-1 | 2.83-1 | 2.64-3 | 4.92-1 | 1.17-2 |
| Total TBR | 1.228 | 1.194 | 1.582 | 1.353 | 1.342 |
| Maximum T-Production Rate[a] (T/yr. Li atom.$cm^3$)[f] | 8.64-3 | 7.5-3 | 7.12-2 | 8.35-3 | 6.25-1 |
| Heat Deposition per D-T neutron (MeV) | | | | | |
| Neutrons | 13.90 | 11.96 | 9.90 | 12.78 | 13.53 |
| Gamma-ray | 3.97 | 6.15 | 7.58 | 4.89 | 5.67 |
| Total | 17.87 | 18.11 | 17.48 | 17.67 | 19.20 |
| Power Multiplication | 1.27 | 1.28 | 1.24 | 1.25 | 1.36 |
| Maximum Heat Deposition[a] ($MW/m^3$) | | | | | |
| First Wall Structure | 53.03[b] | 45.6[b] | 90[e] | 25 | 68.7[b] |
| Breeding Zone[c] | 41 | 50 | 70 | 21 | 46 |
| Damage Parameters[a,d] | | | | | |
| • DPA (dpa/yr) in First Wall | 96 | 58 | 78 | 62 | 55 |
| • H Production (appm/yr) in First Wall | 3.35+3 | 2.00+3 | 4.84+3 | 1.65+3 | 2.5+3 |
| • He Production (appm/yr) in First Wall | 1.00+3 | 6.20+2 | 1.55+3 | 3.85+2 | 6.00+2 |

[a]Values given are for a wall load = 5 $MW/m^2$
[b]Values given are the value obtained from the homogenized results divided by the volume fraction of the structure.
[c]The homogenized result.
[d]Averaged over the structure constituents
[e]The homogenized value.
[f]For Li atomic densities, $^6Li$ and $^7Li$, see the constituents atomic density table for each blanket.

D.2.8 Reference Fluxes at Key Locations

In this subsection we give the neutron fluxes at the key locations in each blanket, individually. The fluxes are given in a tabulated form. The key locations are:

Location I: The first interval (centimeter) of the first wall. In the Li/Li/V blanket, location-I is in the first wall region (0.5 cm-thick).

Location II: The first interval (centimeter) at the front edge of the breeding zone. In the Li/Li/V blanket, location-II is in the middle of the toroidal channel. In the $LiAlO_2$ blanket, this location is in the first interval (centimeter) of Blanket-I zone).

Location III: The middle point of the breeding zone. In the Li/Li/V blanket, location III is in the first interval (centimeter) of the second wall. In the $LiAlO_2$ blanket, this location is at the mid-point of Blanket-I.

Location IV and V: In the Li/Li/V blanket these locations are at the first interval (centimeter) and the mid-point of the poloidal channel, respectively. In the $LiAlO_2$ blanket, they are at first interval (centimeter) of Blanket II and Blanket III, respectively.

These locations are marked in the figures that display the geometrical model of each blanket. The fluxes given are for those corresponding to a one source neutron from the (d-t) reaction. To convert these fluxes to those obtained for a given wall load, WL, the following formula is used.

$$(F)_{WL} = \frac{2\ \Pi\ R_{FW} \cdot (WL) \cdot (F)_{DT}}{10^4 \times 14.1 \times 1.602 \times 10^{-19}}$$

i.e.,

$$(F)_{WL} = 2.78 \times 10^{14} \quad (R_{FW}) \cdot (WL) \cdot (F)_{DT} \qquad \text{(D.2.8-1)}$$

where

$(F)_{DT} \equiv$ The tabulated neutron flux at a given location, neutrons/$cm^2 \cdot s$, which corresponds to one D-T neutron source.

$(F)_{WL} \equiv$ The neutron flux for a given wall load, WL, (neutrons/$cm^2 \cdot s$),

$R_{FW}$ = First wall radius, cm

WL = Wall load, $MW/m^2$,

and cylindrical geometry is assumed.

In the following table, the neutron fluxes are given for each neutron group at the specified location in each blanket. The neutron group structure used (25 group) is given in Table D.2.1-1.

Table D.2.8-1. Neutron Fluxes per D-T Source Neutron at the First Wall, Front Edge and Middle of the Breeding Zone in the $Li_2O$/He/PCA Blanket

| Neutron Group | Location I | Location II | Location III |
|---|---|---|---|
| 1 | 1.1048-3 | 8.4661-4 | 4.7379-5 |
| 2 | 7.4080-5 | 9.2723-5 | 4.1043-5 |
| 3 | 3.6358-5 | 3.8935-5 | 1.1683-5 |
| 4 | 3.6896-5 | 3.8219-5 | 1.0384-5 |
| 5 | 3.9303-5 | 3.9792-5 | 9.7214-6 |
| 6 | 3.7256-5 | 3.7104-5 | 9.1208-6 |
| 7 | 3.2346-5 | 3.3044-5 | 9.2820-6 |
| 8 | 2.8812-5 | 2.9921-5 | 9.3745-6 |
| 9 | 2.9999-5 | 3.0896-5 | 9.6763-6 |
| 10 | 2.8566-5 | 2.8950-5 | 8.8054-6 |
| 11 | 5.2038-5 | 5.2246-5 | 1.5822-5 |
| 12 | 5.3184-5 | 5.2812-5 | 1.5489-5 |
| 13 | 6.7858-5 | 6.7006-5 | 1.9911-5 |
| 14 | 9.0871-5 | 8.9919-5 | 2.8677-5 |
| 15 | 3.2093-4 | 3.1167-4 | 1.0268-4 |
| 16 | 4.7898-4 | 4.6417-4 | 1.6764-4 |
| 17 | 2.7512-4 | 2.6657-4 | 1.0096-4 |
| 18 | 3.7206-4 | 3.6291-4 | 1.4733-4 |
| 19 | 7.3798-4 | 7.4222-4 | 4.3433-4 |
| 20 | 5.4066-4 | 5.3892-4 | 3.6015-4 |
| 21 | 1.8954-4 | 1.9014-4 | 1.3697-4 |
| 22 | 4.3381-5 | 4.0326-5 | 2.5801-5 |
| 23 | 3.3742-6 | 2.9665-6 | 1.6816-6 |
| 24 | 1.2499-7 | 8.5437-8 | 3.7238-8 |
| 25 | 2.2445-9 | 4.9580-10 | 1.5791-10 |

Table D.2.8-2. Neutron Fluxes per D-T Source Neutron at the First Wall, Front Edge and Middle of the Breeding Zone in the $Li_2O$/He/FS Blanket

| Group | Location I | Location II | Location III |
|---|---|---|---|
| 1 | 1.0604-3 | 5.2451-4 | 2.6889-5 |
| 2 | 4.7345-5 | 5.5821-5 | 2.2353-5 |
| 3 | 2.0841-5 | 2.3439-5 | 6.1959-6 |
| 4 | 3.8949-5 | 3.4868-5 | 6.0753-6 |
| 5 | 4.9143-5 | 4.0003-5 | 6.2154-6 |
| 6 | 4.4811-5 | 3.6379-5 | 5.9413-6 |
| 7 | 3.3277-5 | 2.9658-5 | 5.9703-6 |
| 8 | 3.1510-5 | 2.7574-5 | 5.9354-6 |
| 9 | 2.7081-5 | 2.5101-5 | 6.0014-6 |
| 10 | 2.2249-5 | 2.1811-5 | 5.3684-6 |
| 11 | 4.3496-5 | 4.0688-5 | 9.6034-6 |
| 12 | 5.0753-5 | 4.4483-5 | 9.5702-6 |
| 13 | 6.4926-5 | 5.7015-5 | 1.2374-5 |
| 14 | 8.5757-5 | 7.6564-5 | 1.7947-5 |
| 15 | 3.7303-4 | 3.1428-4 | 6.9845-5 |
| 16 | 7.1413-4 | 6.1181-4 | 1.3337-4 |
| 17 | 4.0715-4 | 3.5725-4 | 8.4009-5 |
| 18 | 6.0697-4 | 5.3965-4 | 1.3070-4 |
| 19 | 1.0030-3 | 1.0003-3 | 4.3541-4 |
| 20 | 6.2289-4 | 6.3305-4 | 3.5168-4 |
| 21 | 3.3153-4 | 3.0057-4 | 1.5629-4 |
| 22 | 8.4006-5 | 6.8002-5 | 2.9478-5 |
| 23 | 1.0877-5 | 6.8224-6 | 2.0038-6 |
| 24 | 8.5105-7 | 3.2348-7 | 4.6248-8 |
| 25 | 2.9969-8 | 2.7939-9 | 2.0451-10 |

Table D.2.8-3. Neutron Fluxes per D-T Source Neutron at the First Wall, Front Edge and Middle of the Breeding Zone in the $Li_{17}Pb_{83}$ Self-Cooled Blanket (LiPb/LiPb/PCA)

| Group | Location I | Location II | Location III |
|---|---|---|---|
| 1 | 1.3907-3 | 1.0273-3 | 2.3496-5 |
| 2 | 3.2625-5 | 3.0877-5 | 2.6948-6 |
| 3 | 1.3438-5 | 1.3442-5 | 1.1805-6 |
| 4 | 1.5549-5 | 1.4846-5 | 1.1516-6 |
| 5 | 2.0893-5 | 1.9566-5 | 1.3638-6 |
| 6 | 2.0396-5 | 1.8676-5 | 1.1704-6 |
| 7 | 1.7874-5 | 1.6668-5 | 1.0929-6 |
| 8 | 1.7459-5 | 1.6208-5 | 1.0566-6 |
| 9 | 1.6208-5 | 1.5066-5 | 1.0026-6 |
| 10 | 1.6005-5 | 1.4993-5 | 1.0013-6 |
| 11 | 3.7895-5 | 3.5611-5 | 2.2845-6 |
| 12 | 5.7855-5 | 5.5288-5 | 3.8479-6 |
| 13 | 9.4585-5 | 9.2033-5 | 7.5977-6 |
| 14 | 1.5729-4 | 1.5514-4 | 1.6533-5 |
| 15 | 1.0396-3 | 1.0322-3 | 1.8669-4 |
| 16 | 2.2634-3 | 2.2412-3 | 6.8078-4 |
| 17 | 2.0329-3 | 2.0256-3 | 7.5911-4 |
| 18 | 1.6444-3 | 1.6009-3 | 5.1479-4 |
| 19 | 2.2744-3 | 2.2723-3 | 1.0163-3 |
| 20 | 8.6423-4 | 8.3591-4 | 3.6539-4 |
| 21 | 1.2301-4 | 1.1557-4 | 4.5549-5 |
| 22 | 7.7797-6 | 6.4536-6 | 1.7808-6 |
| 23 | 2.4097-7 | 1.5525-7 | 2.3441-8 |
| 24 | 3.7983-9 | 1.6222-9 | 1.0584-10 |
| 25 | 2.2039-11 | 6.4032-12 | 2.0942-13 |

Table D.2.8-4. Neutron Fluxes Per D-T Source Neutron at the First Wall and at Various Locations (see Fig. D.2.5-1) in the Li/Li/V Blanket

| Group | Location I | Location II | Location III | Location IV | Location V |
|---|---|---|---|---|---|
| 1 | 1.3859-3 | 9.2699-4 | 7.1111-4 | 5.0513-4 | 1.1610-4 |
| 2 | 8.5288-5 | 1.2368-4 | 1.3509-4 | 1.0355-4 | 8.4519-5 |
| 3 | 3.2699-5 | 3.6952-5 | 3.5593-5 | 3.1189-5 | 2.3599-5 |
| 4 | 3.9697-5 | 4.1098-5 | 3.7815-5 | 3.4904-5 | 2.2246-5 |
| 5 | 4.7219-5 | 4.6372-5 | 4.1425-5 | 3.8723-5 | 2.1551-5 |
| 6 | 4.4181-5 | 4.2532-5 | 3.7957-5 | 3.5973-5 | 2.0139-5 |
| 7 | 3.5013-5 | 3.4652-5 | 3.0938-5 | 2.9615-5 | 1.7640-5 |
| 8 | 2.6237-5 | 2.6607-5 | 2.4818-5 | 2.3512-5 | 1.5113-5 |
| 9 | 2.2850-5 | 2.3404-5 | 2.1824-5 | 2.0672-5 | 1.3631-5 |
| 10 | 2.1294-5 | 2.2004-5 | 2.0485-5 | 1.9597-5 | 1.3157-5 |
| 11 | 3.9005-5 | 3.9764-5 | 3.6985-5 | 3.5059-5 | 2.2754-5 |
| 12 | 4.2346-5 | 4.2166-5 | 3.9605-5 | 3.7059-5 | 2.3469-5 |
| 13 | 5.6608-5 | 5.4469-5 | 5.1660-5 | 4.7085-5 | 2.8317-5 |
| 14 | 8.1638-5 | 7.6199-5 | 7.2813-5 | 6.4107-5 | 3.5084-5 |
| 15 | 4.2525-4 | 3.9499-4 | 3.8127-4 | 3.2499-4 | 1.5377-4 |
| 16 | 6.7677-4 | 6.3969-4 | 6.1995-4 | 5.3212-4 | 2.5509-4 |
| 17 | 6.0317-4 | 5.8650-4 | 5.6717-4 | 5.0807-4 | 2.9743-4 |
| 18 | 5.8692-4 | 5.5660-4 | 5.4598-4 | 4.8809-4 | 2.6085-4 |
| 19 | 1.2479-3 | 1.2435-3 | 1.2202-3 | 1.1385-3 | 9.3252-4 |
| 20 | 4.5667-4 | 4.7570-4 | 4.6601-4 | 5.2049-4 | 5.1566-4 |
| 21 | 2.6709-5 | 2.5431-4 | 2.5506-4 | 2.1148-4 | 1.4827-4 |
| 22 | 3.0479-5 | 2.9109-5 | 2.8982-5 | 2.4973-5 | 1.7797-5 |
| 23 | 1.4277-6 | 1.2495-6 | 1.3411-6 | 1.1182-6 | 6.5259-7 |
| 24 | 2.8385-8 | 1.7814-8 | 2.8022-8 | 1.9658-8 | 7.4599-9 |
| 25 | 2.3727-10 | 4.2001-11 | 2.4314-10 | 6.5154-11 | 1.6133-11 |

Table D.2.8-5. Neutron Fluxes Per D-T Source Neutron at the First Wall and at Various Locations (see Fig. D.2.6-1) in the Breeding Zone of the $LiAlO_2/H_2O$/FS/Be Blanket

| Group | Location I | Location II | Location III | Location IV | Location V |
|---|---|---|---|---|---|
| 1 | 1.3404-3 | 7.2366-4 | 1.6237-4 | 4.5106-5 | 1.7159-5 |
| 2 | 6.1173-5 | 6.6233-5 | 5.2418-5 | 2.4210-5 | 1.1630-5 |
| 3 | 1.8397-5 | 2.2491-5 | 1.7495-5 | 8.2673-6 | 3.7563-6 |
| 4 | 2.7907-5 | 3.2944-5 | 2.2283-5 | 9.2889-6 | 3.8297-6 |
| 5 | 3.2472-5 | 3.3341-5 | 1.8537-5 | 7.4399-6 | 3.2499-6 |
| 6 | 3.1449-5 | 3.0664-5 | 1.6202-5 | 6.5266-6 | 2.9262-6 |
| 7 | 2.8698-5 | 2.8805-5 | 1.5675-5 | 6.4729-6 | 3.1634-6 |
| 8 | 2.7504-5 | 2.7260-5 | 1.6305-5 | 7.1315-6 | 3.6137-6 |
| 9 | 2.6862-5 | 2.6996-5 | 1.7202-5 | 8.0737-6 | 4.2499-6 |
| 10 | 2.6790-5 | 2.6889-5 | 1.6609-5 | 7.6986-6 | 3.9136-6 |
| 11 | 5.7537-5 | 5.6285-5 | 3.2379-5 | 1.4802-5 | 7.8334-6 |
| 12 | 6.5337-5 | 5.9884-5 | 3.1097-5 | 1.3686-5 | 7.0626-6 |
| 13 | 7.3035-5 | 6.1768-5 | 2.9512-5 | 1.4296-5 | 8.2119-6 |
| 14 | 8.8549-5 | 7.3739-5 | 3.4342-5 | 1.7922-5 | 1.1607-5 |
| 15 | 3.7423-4 | 3.2069-4 | 1.5521-4 | 7.1525-5 | 4.0845-5 |
| 16 | 5.1126-4 | 4.4046-4 | 2.0576-4 | 1.0479-4 | 6.7356-5 |
| 17 | 3.0917-4 | 2.6652-4 | 1.2124-4 | 4.7675-5 | 2.2172-5 |
| 18 | 3.7739-4 | 3.3749-4 | 1.6080-4 | 6.3783-5 | 2.8040-5 |
| 19 | 3.7082-4 | 3.6368-4 | 1.9425-4 | 7.8871-5 | 3.8141-5 |
| 20 | 3.9409-4 | 3.8167-4 | 2.1347-4 | 8.0348-5 | 3.7562-5 |
| 21 | 3.3611-4 | 3.3156-4 | 1.9546-4 | 5.5403-5 | 1.5431-5 |
| 22 | 3.0281-4 | 2.9048-4 | 1.7323-4 | 3.0767-5 | 3.0728-6 |
| 23 | 2.5135-4 | 2.2270-4 | 1.2637-4 | 1.1361-5 | 2.3756-7 |
| 24 | 1.6565-4 | 1.2189-4 | 5.9529-5 | 1.7158-6 | 8.2589-9 |
| 25 | 1.0407-4 | 3.6612-5 | 1.1264-5 | 6.1759-8 | 1.5352-10 |

## References for Appendix D.2


1. VITAMIN-C: 171 Neutrons, 36 Gamma Group Cross Section library in AMPX Interface Format for Fusion Neutronics Studies, Pkg DLC-41, Oak Ridge National Laboratory (1978).

2. W. W. Engle, Jr., "A User's Manual for ANISN", RISC-CCC-82, Oak Ridge National Laboratory (July 1973).

## D.3 First Wall/Blanket

Four reference blanket designs were selected early in the FINESSE study to facilitate quantifying the test requirements and developing engineering scaling relationships:

- o Blanket 1 (Li/Li/V)
  - Self-cooled liquid lithium (breeder/coolant)
  - Vanadium alloy structure

- o Blanket 2 ($Li_2O$/He/FS)
  - $Li_2O$ solid breeder
  - Helium coolant
  - Ferritic steel structure

- o Blanket 3 ($LiAlO_2$/$H_2O$/PCA/Be)
  - $LiAlO_2$ solid breeder
  - Be neutron multiplier
  - Pressurized water coolant
  - Austenitic stainless steel structure

- o Blanket 4 (LiPb/LiPb/FS)
  - Self-cooled 17Li-83Pb liquid metal alloy
  - Ferritic steel structure

This selection does not imply any endorsement of any of the concepts. The intent in making these particular choices was that most of the issues and problems generic to development and testing of fusion power reactor blankets would be represented inclusively by these four concepts.

The first two blankets are taken from the tokamak versions of the respective concepts reported in Ref. 1, the BCSS Interim Report. The third blanket, also for a tokamak, was developed early in the second year of the study, and represents a preliminary version of the concept to be described in the BCSS Final Report, Ref. 2. The fourth blanket, designed for use in a tandem mirror reactor (TMR), was taken from a preliminary draft of the MARS Final Report, Ref. 3.

It must be emphasized that the blanket designs described in this Appendix are only for purposes of the FINESSE study. Definitive descriptions of BCSS or MARS blankets must not be taken from this report and should be taken only from References 2 and 3, since in all four cases there are differences between the FINESSE blanket and the final blanket version from those design studies.

The following four sections briefly describe the general features and operation of each blanket concept, and present more detailed information in figures and tables. Additional information for each of the four blankets has been generated as part of the FINESSE study, and can be found in Chapters 5 and 6 and elsewhere in the body of this report.

### D.3.1 Li/Li/V Concept (Tokamak)

The reference design for the Li/Li/V blanket is the poloidal/toroidal flow module shown in Figs. D.3-1 through -4. Design features and parameters are presented in Table. D.3-1 and -2. This design is composed of slightly slanted poloidal manifolds and relatively small toroidal channels. Each manifold supplies a number of toroidal channels. The coolant velocity in the toroidal channels is relatively high whereas that in the poloidal manifolds can be maintained at low values. Consequently, sufficient cooling of the first wall can be achieved without significantly increasing the total pressure drop through the blanket, since the single largest pressure drop is due to the poloidal flow through the manifold which is nearly perpendicular to the toroidal magnetic field. It should be noted, however, that there are large uncertainties in the calculations for MHD pressure drops of flowing liquid metals in high magnetic fields for regions with bends, orifices, and flow area changes.

### D.3.2 $Li_2O$/He/FS Concept (Tokamak)

This concept is shown in Figures D.3-5 and -6. Design features and parameters are listed in Tables D.3-3 and -4. To achieve the maximum volume of solid breeder in the $Li_2O$/He blanket, a flat plate fuel element geometry was adopted. Solid breeder pellets are clad in HT-9 sheets to form plates. The coolant flows through the 1-mm coolant gaps between breeder plates and maintains the solid breeder temperature distribution within its specified temperature limits. The breeder plates are purged with a separate helium

stream with 1% $H_2$ added for positive control of tritium extraction. The purge stream operates at 1 atm pressure. This allows the 50 atm coolant pressure to clamp the cladding onto the $Li_2O$ pellets, giving good thermal contact. It also reduces the purge mass flow rate and avoids concerns about cladding deformation in case of a coolant depressurization accident.

### D.3.3 $LiAlO_2/H_2O$/PCA/Be Concept (Tokamak)

This blanket, described in Figures D.3-7 through -9 and in Tables D.3-5 through -7, is similar to that described in Ref. 2. The major exception is that PCA (Prime Candidate Alloy) austenitic stainless steel, a Ti-modified Type 316 steel, was selected for the structural material instead of the HT-9 ferritic steel selected for the concept by the BCSS. This was a deliberate choice by FINESSE, and was intended to assure that any development and testing concerns peculiar to austenitic stainless steel would be visible in the study results. The choice has a negligible effect otherwise on the blanket design and performance for purposes of the FINESSE study.

The blanket configuration is modular in nature, with a lobe-shaped semi-cylindrical actively cooled first wall. Nominal dimensions are 30 cm width poloidally (15 cm radius for the first wall) and 70 cm depth measured radially away from the plasma. The first 20 cm of the breeding zone is a 90:10 volume mixture ratio of beryllium (Be) and the $LiAlO_2$ ternary ceramic (TC) breeder. Both materials are fabricated in sphere-pac form; the Be and TC individual spheres are ~100% dense. Packing density for the sphere-pac is 86%. The remaining 32 cm of the breeding zone is $LiAlO_2$, again in sphere-pac form. The last 18 cm of the nominal module depth is coolant inlet and outlet manifolds which extend around all the blanket modules to form the blanket sector, with the manifold acting as sector structure.

The individual blanket modules contact each other along their side walls from the juncture of adjacent lobes radially back to the manifold zone. The side walls bear against each other, providing mutual support to reduce structural requirements for reacting loads due to the 6-atm maximum internal pressure of the helium purge gas.

### D.3.4 LiPb/LiPb/V Concept (TMR)

This self-cooled liquid metal blanket uses 17Li-83Pb (LiPb) as the breeder-coolant. The design, described in Figures D.3-10 through -13 and Tables D.3-8 through -17, is taken from a preliminary draft of Ref. 3 and should not be referenced as representing the MARS blanket.

The basic design of the blanket is quite simple. The 17Li-83Pb alloy is fed at 350$^0$C to the HT-9 blanket module through a large electrically-insulated coolant header at the top (Fig. D.3-10). From there, it flows in parallel through the rectangular HT-9 beam structure and the 10 cm-diameter circular HT-9 tube section (Fig. D.3-11). The tubes in the front ensure uniform flow in the regions where the neutron heating is the highest, and the rectangular sections are better suited to attain a low void fraction to increase the blanket multiplication factor, M. The LiPb exits at 500$^0$C through a large-diameter coolant pipe to a double-walled heat exchanger. The large pipes are necessary to reduce the MHD pumping power losses and they also lower the liquid metal velocity which in turn lowers the corrosion rate.

The neutron-produced energy is deposited in a 38.2 cm-thick blanket module and a 43 cm-thick reflector. The reflector is made from water-cooled low-activation austenitic steel because of the lower temperature and because the neutron damage rate is lower than in the blanket.

The tritium breeding ratio is 1.15 from the LiPb which is enriched to 90% Li-6. An important feature of LiPb is its low tritium solubility; only 7 g of tritium are in the entire blanket and heat transport system. Only 1 g of tritium is in the blanket modules at any time, and the rest is in the heat transport system.

TABLE D.3-1.
MAJOR PARAMETERS AND FEATURES OF
Li/Li/V CONCEPT (TOKAMAK)

| | |
|---|---|
| General Description | |
| Materials | |
| Coolant | Liquid Li (natural) |
| Breeder | Liquid Li (natural) |
| Neutron Multiplier | None |
| Structure | V-15Cr-5Ti |
| Purge gas | None |
| Major Design Parameters | |
| Average neutron wall load, $MW/m^2$ | 5.0 |
| Average first wall surface heat flux, $MW/m^2$ | 1.0 |
| Coolant | |
| Inlet/outlet temperature, $^0C/^0C$ | 300/550 |
| Maximum pressure, MPa | 3.1 |
| Breeder | |
| Minimum/maximum temperature, $^0C/^0C$ | 300/550 |
| Maximum pressure, MPa | 3.1 |
| Structure | |
| First wall/blanket maximum temperature, $^0C/^0C$ | 690 |
| Minimum/maximum temperature at: | |
| Coolant interface, $^0C/^0C$ | 350/615 |
| Breeder interface, $^0C/^0C$ | 350/615 |
| Neutronics | |
| Tritium breeding ratio | |
| 1-D, 100% coverage | -- |
| Net (3-D with all geometrical details and penetration)[a] | |
| Maximum nuclear heating rates | |
| Breeder, W/cc | 22.4 |
| Coolant, W/cc | 22.4 |
| Neutron multiplier, W/cc | -- |
| Structure, W/cc | 24.8 |
| Energy (1-D calculation) | |
| Multiplication factor | 1.26 |
| Deposited in heat recovery zone, MeV | 17.7 |
| Deposited in heat loss zone, MeV | 0.67 |
| First Wall/Blanket Design Description | |
| Inboard first wall/blanket | |
| Thickness (including manifolds), m | 0.64 |
| Manifold thickness, m | 0.575[c] |
| Percent structure/percent coolant in manifold region, %/% | 17/83 |
| Coolant $\Delta P$ (total), MPa | 3.0 |
| Outboard first wall/blanket | |
| Thickness (including manifolds), m | 0.84 |
| Manifold thickness, m | 0.775[c] |
| Percent structure/percent coolant in manifold region, %/% | 54/46 |
| Coolant $\Delta P$ (total), MPa | 3.0 |

TABLE D.3-1 (Continued)

| | |
|---|---|
| Primary coolant loop pumping power, % of blanket thermal power | 0.8 |
| First Wall | |
| Description | Toroidal flow channels 45 x 25 mm<br>- Inboard 250 channels<br>- Outboard 350 channels |
| Minimum/maximum coolant temperature, $^0C/^0C$ | 300/615 |
| Maximum structure temperature, $^0C$ | 690 |
| Blanket | |
| Description | Poloidal flow channels which serve as manifolding; 12 manifolds/ sector. |
| $^6Li$ enrichment, % | 7.4 (natural) |
| Minimum/maximum coolant temperature, $^0C/^0C$ | 300/585 |
| Maximum structure temperature, $^0C$ | 650 |
| Tritium removal from breeder | |
| Method | Molten salt |
| Power loss (thermal), % total | 0.01 |
| Steady-state breeder tritium inventory, g | 490 (in Li) |
| Purge gas | None |
| Material | |
| Temperature, $^0C$ | |
| Pressure, MPa | |
| Tritium barriers | None |
| Power Conversion System | |
| IHX description | |
| Type of system | Li-to-Na IHX (ferritic steel) |
| Intermediate coolant | Na |
| Material | Na |
| Inlet/Outlet temperature, $^0C/^0C$ | 275/525 |
| Maximum pressure, MPa | 0.4 |
| Tritium barriers | Natural oxide |
| Tritium recovery method | Cold trap |
| Coolant pumping power, MWe | 9 |
| Coolant flow rate, kg/h | $6.5 \times 10^7$ |
| Thermal storage provision (tokamak) | |
| Technique | IHX |
| Storage medium | Na |
| Steam generator | |
| Type | Na to $H_2O$ |
| Single or double wall tubes | Single |
| Steam | |
| Inlet/outlet temperature, $^0C/^0C$ | 245/510 |
| Maximum pressure, MPa | 16.6 |
| Tritium barriers | Natural oxide |

TABLE D.3-1 (Cont.)

| | |
|---|---|
| Thermal efficiency | |
| $\eta = \frac{(MW_e)_{out} - (MW_e)_{pump}}{MW_{th\ TOTAL}}$, % | 41.7 |
| Gross $(MW_e/MW_{th})$, % | 42.3 |
| Steady-State Tritium Losses, Ci/d | <10 |

[a]As calculated by Tritium Breeding Task Group, BCSS.

[b]Neutron energy multiplication only.

[c]Manifold/blanket thickness = (total thickness) - (FW thickness)

TABLE D.3-2. FWBS COMPOSITION AND DIMENSIONAL STACKUP

| | TOK INBOARD; TM UNDER COILS | | | | | TOK OUTBOARD; TM BETWEEN COILS | | | | |
|---|---|---|---|---|---|---|---|---|---|---|
| | Mat'l | Inner Radius (cm) | Outer Radius (cm) | Volume Fraction | Theor. Density | Mat'l | Inner Radius (cm) | Outer Radius (cm) | Volume Fraction | Theor. Density |
| FW Coating | None | -- | -- | -- | -- | None | -- | -- | -- | -- |
| FW Structure | V-15Cr-5Ti | 475 | 480 | 20% | 100% | V-15Cr-5Ti | 920 | 925 | 20% | 100% |
| FW Coolant | Li | 475 | 480 | 80% | 100% | Li | 920 | 925 | 80% | 100% |
| Bkt 1* Structure | V-15Cr-5Ti | 440 | 475 | 7.5% | 100% | V-15Cr-5Ti | 925 | 960 | 7.5% | 100% |
| Bkt 1 Refl (Bulk Mat'l) | -- | -- | -- | -- | -- | -- | -- | -- | -- | -- |
| Bkt 1 Coolant | Li | 440 | 475 | 92.5% | 100% | Li | 925 | 960 | 92.5% | 100% |
| Bkt 1 Breeder | Li | 440 | 475 | -- | 100% | Li | 925 | 960 | | 100% |
| Bkt 1 Multiplier | None | -- | -- | -- | -- | None | -- | -- | -- | -- |
| Bkt 2* Structure | V-15Cr-5Ti | 416 | 440 | 10% | 100% | V-15Cr-5Ti | 960 | 995 | 10% | 100% |
| Bkt 2 Refl (Bulk Mat'l) | | 416 | 440 | 40% | 100% | | 960 | 995 | 80% | 100% |
| Bkt 2 Coolant | Li | 416 | 440 | 50% | 100% | Li | 960 | 995 | 10% | 100% |
| Bkt 2 Breeder | Li | 416 | 440 | -- | -- | Li | 960 | 995 | -- | -- |
| Bkt 2 Multiplier | None | -- | -- | -- | -- | None | -- | -- | -- | -- |
| Plenum/Manifold Structure<br>Plenum/Manifold Coolant<br>Bkt/Shield Gap** | N/A | | | N/A | N/A | N/A | | | N/A | N/A |
| Shield Structure<br>Shield Moderator/Reflector<br>Shield Absorber<br>Shield Coolant<br>Shield/Vacuum Tank Gap** | N/A | | | N/A | N/A | N/A | | | N/A | N/A |

*Bkt 1 and Bkt 2 illustrate composition of unique blanket layers.

**Bkt/Shield Gap = 2 cm for Tok, Inboard
= 50 cm for Tok, Outboard
= 2 cm for TM

Shield/Vac Tank Gap = 2 cm for Tok, Inboard
= 50 cm for Tok, Outboard
= 10 cm for TM

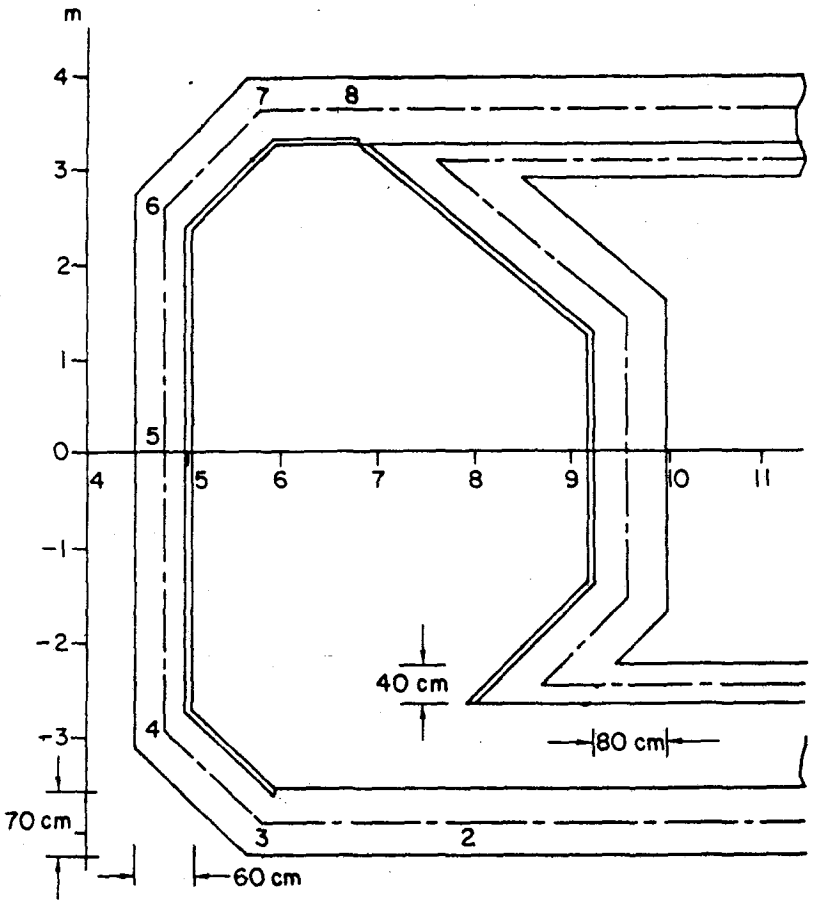


Fig. D.3-1. Poloidal View of Blanket.

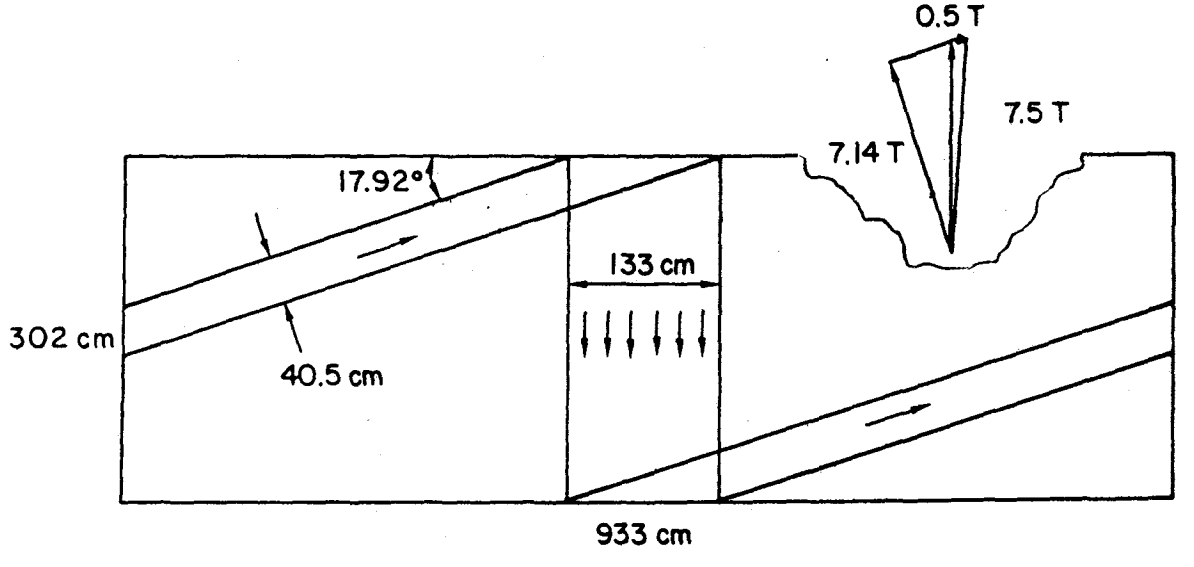


Fig. D.3-2. Diagram showing path of reference blanket concept.

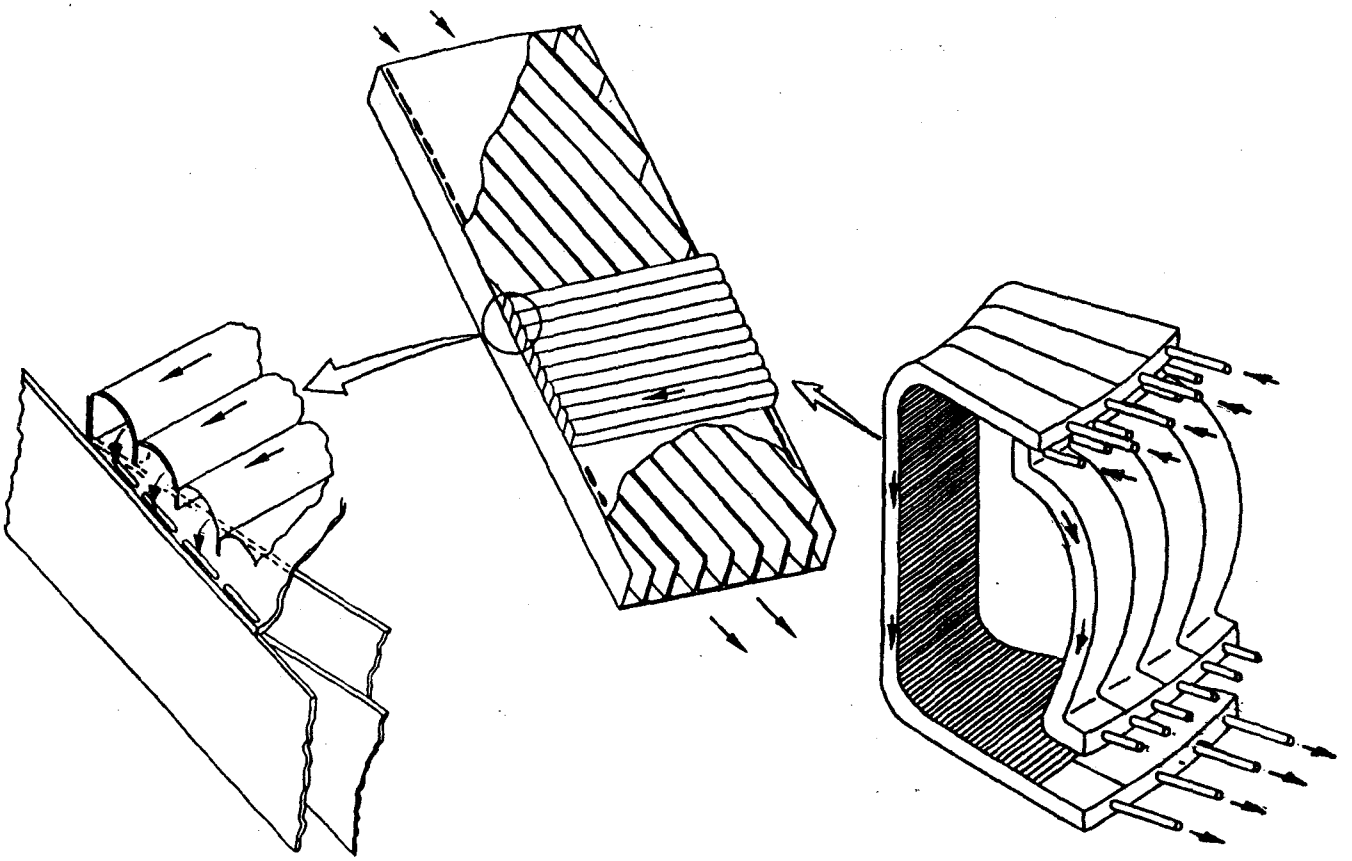

Fig. D.3-3. Liquid metal flow concept (poloidal/toroidal flow).

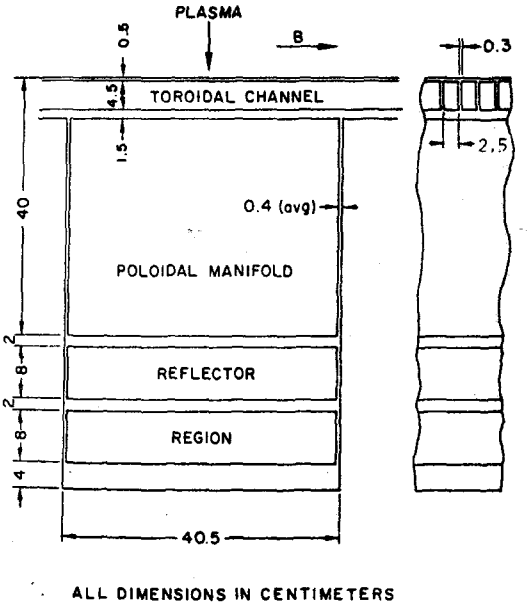


Fig. D.3-4. Cross-sectional view and dimensions of the toroidal/poloidal blanket (outboard).

TABLE D.3-3.
MAJOR PARAMETERS AND FEATURES OF
$Li_2O$/He/FS CONCEPT (TOKAMAK)

| | |
|---|---|
| General Description | |
| Materials | |
| Coolant | Gaseous He |
| Breeder | $Li_2O$ (natural Li) |
| Neutron multiplier | -- |
| Structure | HT-9 ferritic steel |
| Purge gas | Gaseous He |
| Major Design Parameters | |
| Average neutron wall load, $MW/m^2$ | 5.0 |
| Average first wall surface heat flux, $MW/m^2$ | 1.0 |
| Coolant | |
| Inlet/outlet temperature, $^0C/^0C$ | 275/510 |
| Maximum pressure, MPa | 5.2 |
| Breeder | |
| Minimum/maximum temperature, $^0C/^0C$ | 510/795 (EOL), 746 (BOL) |
| Maximum pressure, MPa | 0.1 |
| Structure | |
| First wall/blanket maximum temperature, $^0C/^0C$ | 547/515 |
| Minimum/maximum temperature at: | |
| Coolant interface, $^0C/^0C$ | 275/515 |
| Breeder interface, $^0C/^0C$ | 442/515 |
| Neutronics | |
| Tritium breeding ratio | |
| 1-D, 100% coverage | -- |
| Net (3-D with all geometrical details and penetration)[a] | -- |
| Maximum nuclear heating rates | |
| Breeder, W/cc | 47 |
| Neutron multiplier, W/cc | -- |
| Structure, W/cc | 50 |
| Energy (1-D calculation) | |
| Multiplication factor | 1.18 |
| Deposited in heat recovery zone, MeV | 16.65 |
| Deposited in heat loss zone, MeV | 0.44 |
| First Wall/Blanket Design Description | |
| Inboard first wall/blanket | |
| Thickness (including manifolds), m | 0.41 |
| Manifold thickness, m | 0.11 |
| Percent structure/percent coolant in manifold region, %/% | 20/80 |
| Coolant $\Delta P$ (total), MPa | 0.095 |
| Outboard first wall/blanket | |
| Thickness (including manifolds), m | 0.85 |
| Manifold thickness, m | 0.22 |
| Percent structure/percent coolant in manifold region, %/% | 20/80 |
| Coolant $\Delta P$ (total), MPa | 0.122 |

TABLE D.3-3 (Continued)

| | |
|---|---|
| Primary coolant loop pumping power, % of blanket thermal power | 4.9 |
| First Wall | |
| Description | Internal fins; semi-cylindrical wall forming module front. |
| Minimum/maximum coolant temperature, $^0C/^0C$ | 275/334 |
| Maximum structure temperature, $^0C$ | 547 (EOL) |
| Blanket | |
| Description | Pressurized module; $Li_2O$ in cladded 1.1-cm thick plates. |
| $^6Li$ enrichment, % | 7.4% (natural) |
| Minimum/maximum coolant temperature, $^0C/^0C$ | 334/507 |
| Maximum structure temperature, $^0C$ | 515 |
| Tritium removal from breeder | |
| Method | He purge gas flow |
| Power loss (thermal), % total | ~0 |
| Steady-state breeder tritium inventory, g | 1080 |
| Purge gas | |
| Material | He |
| Temperature, $^0C$ | 300-500 |
| Pressure, MPa | 0.1 |
| Tritium barriers | Natural oxides |
| Power Conversion System | |
| Thermal storage provision (tokamak) | |
| Technique | Packed bed thermal storage |
| Storage medium | Steel balls |
| Steam generator | |
| Type | Helical wound tube and shell |
| Single or double wall tubes | Single |
| Steam | |
| Inlet/outlet temperature, $^0C/^0C$ | 204/460 |
| Maximum pressure, MPa | 8.3 |
| Tritium barriers | Natural oxide on both sides |
| Thermal efficiency | |
| $\eta = \frac{(MW_e)_{out} - (MW_e)_{pump}}{MW_{th\ TOTAL}}$, % | 36.4 |
| Gross $(MW_e/MW_{th})$, % | 39.2 |
| Steady-State Tritium Losses, Ci/d | 103[c] |

[a]As calculated by Tritium Breeding Task Group, BCSS.

[b]Neutron energy multiplication only.

[c]Assumes 100% of tritium released as $T_2$.

TABLE D.3-4. FWBS COMPOSITION AND DIMENSIONAL STACKUP

| | TOK INBOARD; TM UNDER COILS | | | | | TOK OUTBOARD; TM BETWEEN COILS | | | | |
|---|---|---|---|---|---|---|---|---|---|---|
| | Mat'l | Inner Radius (cm) | Outer Radius (cm) | Volume Fraction | Theor. Density | Mat'l | Inner Radius (cm) | Outer Radius (cm) | Volume Fraction | Theor. Density |
| FW Coating | None | -- | -- | -- | -- | None | -- | -- | -- | -- |
| FW Structure | HT-9 | 214 | 220 | 0.12 | 1.0 | HT-9 | 214 | 220 | 0.12 | 1.0 |
| FW Coolant | He | 214 | 220 | 0.88 | 1.0 | He | 214 | 220 | 0.88 | 1.0 |
| Bkt 1* Structure | HT-9 | 220 | 232 | 7.9% | 1.0 | HT-9 | 220 | 265 | 7.9% | 1.0 |
| Bkt 1 Refl (Bulk Mat'l) | -- | -- | -- | -- | -- | -- | -- | -- | -- | -- |
| Bkt 1 Coolant | He | 220 | 232 | 11.5% | 1.0 | He | 220 | 265 | 11.5% | 1.0 |
| Bkt 1 Breeder | $Li_2O$ | 220 | 232 | 80.6% | 0.8 | $Li_2O$ | 220 | 265 | 80.6% | 0.8 |
| Bkt 1 Multiplier | -- | -- | -- | -- | -- | -- | -- | -- | -- | -- |
| Bkt 2* Structure | HT-9 | 232 | 244 | 28.6% | 1.0 | HT-9 | 265 | 277 | 28.6% | 1.0 |
| Bkt 2 Refl (Bulk Mat'l) | -- | -- | -- | -- | -- | -- | -- | -- | -- | -- |
| Bkt 2 Coolant | He | 232 | 244 | 8.9% | 1.0 | He | 265 | 277 | 8.9% | 1.0 |
| Bkt 2 Breeder | $Li_2O$ | 232 | 244 | 62.5% | 0.8 | $Li_2O$ | 265 | 277 | 62.5% | 0.8 |
| Bkt 2 Multiplier | -- | -- | -- | -- | -- | -- | -- | -- | -- | -- |
| Plenum/Manifold Structure | HT-9 | 244 | 255 | 0.20 | 1.0 | HT-9 | 277 | 299 | 0.2 | 1.0 |
| Plenum/Manifold Coolant | He | 244 | 255 | 0.80 | 1.0 | He | 277 | 299 | 0.8 | 1.0 |
| Bkt/Shield Gap** | N/A | 255 | 257 | N/A | N/A | N/A | 299 | 349 | N/A | N/A |
| Shield Structure | | 257 | | | | | 349 | | | |
| Shield Moderator/Reflector | | 257 | | | | | 349 | | | |
| Shield Absorber | | 257 | | | | | 349 | | | |
| Shield Coolant | $H_2O$ | 257 | | | | $H_2O$ | 349 | | | |
| Shield/Vacuum Tank Gap** | N/A | | | N/A | N/A | N/A | | | N/A | N/A |

*Bkt 1 and Bkt 2 illustrate composition of unique blanket layers.

**Bkt/Shield Gap = 2 cm for Tok, Inboard
= 50 cm for Tok, Outboard
= 2 cm for TM

Shield/Vac Tank Gap = 2 cm for Tok, Inboard
= 50 cm for Tok, Outboard
= 10 cm for TM

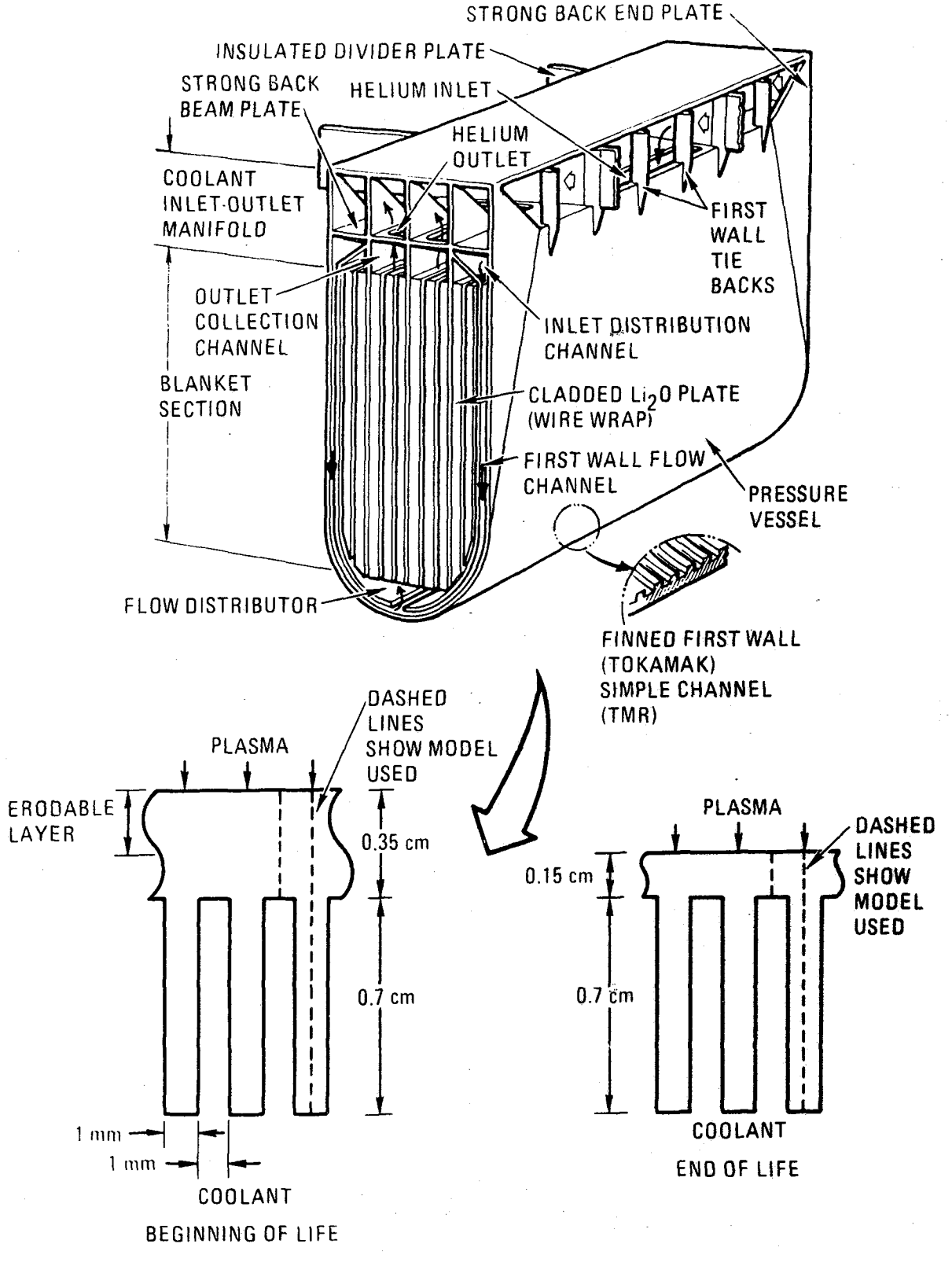


Fig. D.3-5. $Li_2O$/He/FS blanket configuration.

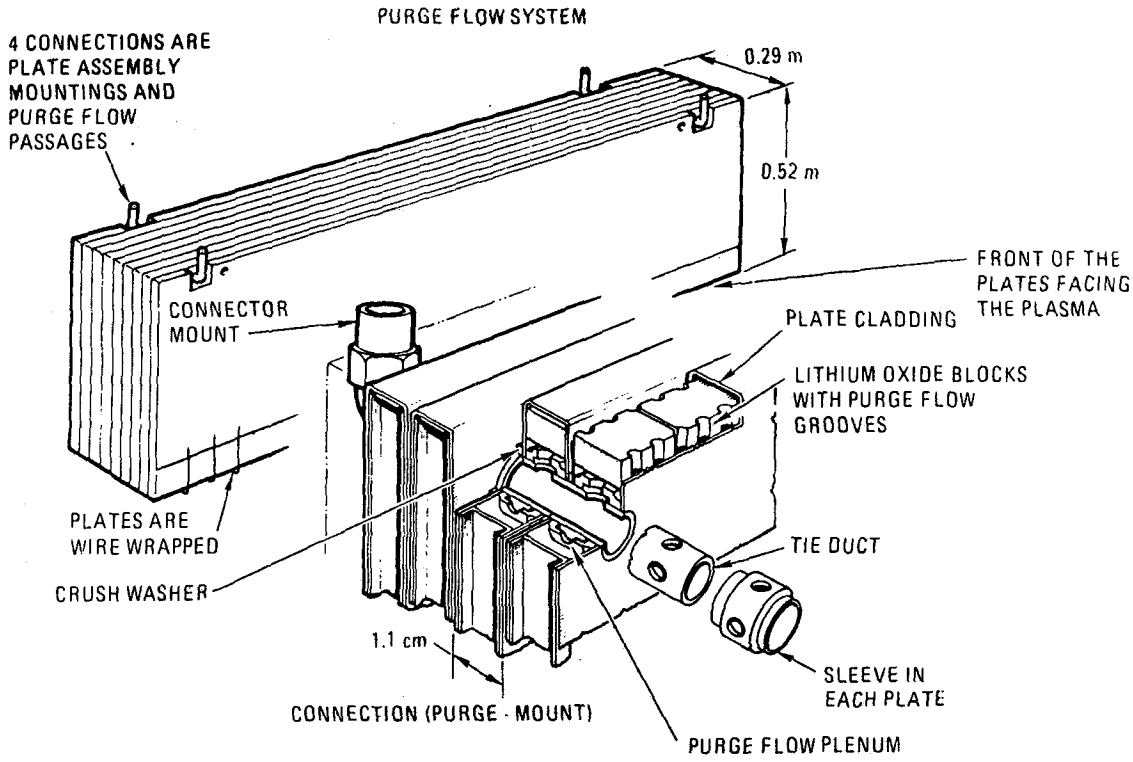


(a) Purge system connections inside blanket module.

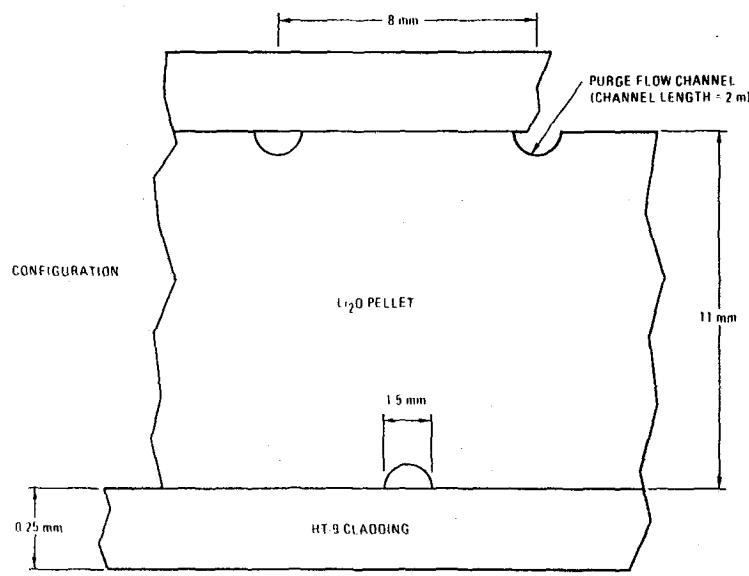


(b) Detail of cladded $Li_2O$ plate.

Fig. D.3-6. Gas purge system for $Li_2O$/He/FS blanket.

TABLE D.3-5.
MAJOR PARAMETERS AND FEATURES OF
$LiAlO_2/H_2O$/PCA/Be CONCEPT (TOKAMAK)

| | |
|---|---|
| **General Description** | |
| **Materials** | |
| Coolant | Pressurized $H_2O$ |
| Breeder | $\gamma$-$LiAlO_2$ @ 87% TD; 90% $^6Li$ |
| Neutron multiplier | Be @ 87% TD |
| Structure | PCA Aust. St. Stl. |
| Purge gas | He |
| **Major Design Parameters** | |
| Average neutron wall load, $MW/m^2$ | 5.0 |
| Average first wall surface heat flux, $MW/m^2$ | 1.0 |
| Coolant | |
| Inlet/outlet temperature, $^0C/^0C$ | 280/320 |
| Maximum pressure, MPa | 15.2 |
| Breeder | |
| Minimum/maximum temperature, $^0C/^0C$ | 350/1000 |
| Maximum pressure, MPa | ~0.1-0.6 |
| Structure | |
| First wall/blanket maximum temperature, $^0C/^0C$ | 465/~360 |
| Minimum/maximum temperature at: | |
| Coolant interface, $^0C/^0C$ | ~290/330 |
| Breeder interface, $^0C/^0C$ | ~350/350 |
| **Neutronics** | |
| Tritium breeding ratio | |
| 1-D, 100% coverage | -- |
| Net (3-D with all geometrical details and penetration)[a] | -- |
| Maximum nuclear heating rates | |
| Breeder, W/cc | -- |
| Neutron multiplier, W/cc | -- |
| Structure, W/cc | -- |
| Energy (1-D calculation) | |
| Multiplication factor | 1.372 |
| Deposited in heat recovery zone, MeV | 19.29 |
| Deposited in heat loss zone, MeV | 0.38 |
| **First Wall/Blanket Design Description** | |
| Inboard first wall/blanket | |
| Thickness (including manifolds), m | 0.35 |
| Manifold thickness, m | 0.07 |
| Percent structure/percent coolant in manifold region, %/% | 33/67 |
| Coolant $\Delta P$ (total), MPa | ~0.2 |
| Outboard first wall/blanket | |
| Thickness (including manifolds), m | 0.70 |
| Manifold thickness, m | 0.18 |
| Percent structure/percent coolant in manifold region, %/% | 20/80 |
| Coolant $\Delta P$ (total), MPa | ~0.2 |
| Primary coolant loop pumping power, % of blanket thermal power | 0.8 |

TABLE D.3-5 (Continued)

| | |
|---|---|
| First Wall | |
| Description | Lobe-shaped; flow in poloidal direction through 3.8 x 3.8 mm rectangular channels. |
| Minimum/maximum coolant temperature, $^0C/^0C$ | 280/320 |
| Maximum structure temperature, $^0C$ | ~465 |
| Blanket | |
| Description | Lobe-shaped module. Double-wall coolant tubes surrounded by sphere-pac breeder, or Be/breeder in 90:10 volume ratio. |
| $^6Li$ enrichment, % | 90 |
| Minimum/maximum coolant temperature, $^0C/^0C$ | 280/320 |
| Maximum structure temperature, $^0C$ | ~360 |
| Tritium removal from breeder | |
| Method | He purge gas flow |
| Power loss (thermal), % total | ~0 |
| Steady-state breeder tritium inventory, g | 2300 |
| Purge gas | |
| Material | He |
| Temperature, $^0C$ | ~350-400 |
| Pressure, MPa | ~0.1-0.6 |
| Tritium barriers | Natural oxides, tube ass'y annulus and inner tube inside surface. |
| Power Conversion System | |
| Thermal storage provision (tokamak) | |
| Technique | Circulating liquid |
| Storage medium | Pressurized water |
| Steam generator | |
| Type | Once-through horizontal |
| Single or double wall tubes | Single |
| Steam | |
| Inlet/outlet temperature, $^0C/^0C$ | 240/299 |
| Maximum pressure, MPa | -- |
| Tritium barriers | Natural oxides, both surfaces |
| Thermal efficiency | |
| $\eta = \frac{(MW_e)_{out} - (MW_e)_{pump}}{MW_{th\ TOTAL}}$, % | 34.9 |
| Gross $(MW_e/MW_{th})$, % | 35.7 |
| Steady-State Tritium Losses, Ci/d | 100[c] |

[a]As calculated by Tritium Breeding Task Group, BCSS.

[b]Neutron energy multiplication only.

[c]Assumes 1 Ci/ℓ concentration in primary coolant; losses to steam generator secondary side of 100 ℓ/day.

TABLE D.3-6. FWBS COMPOSITION AND DIMENSIONAL STACKUP

| | TOK INBOARD; TM UNDER COILS | | | | | TOK OUTBOARD; TM BETWEEN COILS | | | | |
|---|---|---|---|---|---|---|---|---|---|---|
| | Mat'l | Inner Radius (cm) | Outer Radius (cm) | Volume Fraction | Theor. Density (%) | Mat'l | Inner Radius (cm) | Outer Radius (cm) | Volume Fraction | Theor. Density (%) |
| FW Coating | -- | -- | -- | -- | -- | -- | -- | -- | -- | -- |
| FW Structure | PCA | 481 | 486 | .32 | 100 | PCA | 914 | 919 | .32 | 100 |
| FW Coolant | $H_2O$ | 481 | 486 | .07 | 100 | $H_2O$ | 914 | 919 | .07 | 100 |
| Bkt 1* Structure | PCA | 461 | 481 | .195 | 100 | PCA | 919 | 939 | .195 | 100 |
| Bkt 1 Refl (Bulk Mat'l) | -- | 461 | 481 | -- | -- | -- | -- | -- | -- | -- |
| Bkt 1 Coolant | $H_2O$ | 461 | 481 | .215 | 100 | $H_2O$ | 919 | 939 | .215 | 100 |
| Bkt 1 Breeder | $LiAlO_2$ | 461 | 481 | .050 | 87 | $LiAlO_2$ | 919 | 939 | .05 | 87 |
| Bkt 1 Multiplier | Be | 461 | 481 | .450 | 87 | Be | 919 | 939 | .45 | 87 |
| Bkt 2* Structure | PCA | 458 | 461 | .125 | 100 | PCA | 939 | 966 | .084 | 100 |
| Bkt 2 Refl (Bulk Mat'l) | -- | 458 | 461 | -- | -- | -- | -- | -- | -- | -- |
| Bkt 2 Coolant | $H_2O$ | 458 | 461 | .115 | 100 | $H_2O$ | 939 | 966 | .059 | 100 |
| Bkt 2 Breeder | $LiAlO_2$ | 458 | 461 | .70 | 87 | $LiAlO_2$ | 939 | 966 | .804 | 87 |
| Bkt 2 Multiplier | -- | 458 | 461 | -- | -- | -- | -- | -- | -- | -- |
| Plenum/Manifold Structure | PCA | 451 | 458 | .33 | 100 | PCA | 966 | 984 | .33 | 100 |
| Plenum/Manifold Coolant | $H_2O$ | 451 | 458 | .67 | 100 | $H_2O$ | 966 | 984 | .67 | 100 |
| Bkt/Shield Gap** | N/A | | | N/A | N/A | N/A | | | N/A | N/A |
| Shield Structure | Fe1422 | 419 | 449 | .80 | 100 | Fe1422 | 1034 | 1064 | .80 | 100 |
| Shield Moderator/Reflector | -- | -- | -- | -- | -- | -- | -- | -- | -- | -- |
| Shield Absorber | -- | -- | -- | -- | -- | -- | -- | -- | -- | -- |
| Shield Coolant | $H_2O$ | 419 | 449 | .20 | 100 | $H_2O$ | 1034 | 1064 | .20 | 100 |
| Shield/Vacuum Tank Gap** | N/A | | | N/A | N/A | N/A | | | N/A | N/A |

*Bkt 1 and Bkt 2 illustrate composition of unique blanket layers.

**Bkt/Shield Gap
= 2 cm for Tok, Inboard
= 50 cm for Tok, Outboard
= 2 cm for TM

Shield/Vac Tank Gap
= 2 cm for Tok, Inboard
= 50 cm for Tok, Outboard
= 10 cm for TM

TABLE D.3-7. BLANKET COOLANT TUBE SPACING DEFINITION

| Bank | $x_i$ | $x_j$ | Lateral and Vertical Spacing, d | n/meter[1] | Zone |
|---|---|---|---|---|---|
| 1 | 0 cm | 1.65 cm | 1.65 cm | 60.6 | |
| 2 | 1.65 cm | 3.4 cm | 1.75 cm | 57.1 | |
| 3 | 3.4 cm | 5.2 cm | 1.8 cm | 55.5 | |
| 4 | 5.2 cm | 7.05 cm | 1.85 cm | 54.0 | 90% Be : 10% $LiAlO_2$ |
| 5 | 7.05 cm | 9.0 cm | 1.95 cm | 51.3 | Spherepac @ 87% TD |
| 6 | 9.0 cm | 11.0 cm | 2.00 cm | 50 | |
| 7 | 11.0 cm | 13.05 cm | 2.05 cm | 48.8 | |
| 8 | 13.05 cm | 15.2 cm | 2.15 cm | 46.5 | |
| 9 | 15.2 cm | 17.55 cm | 2.35 cm | 42.5 | |
| 10 | 17.55 cm | 20 cm | 2.45 cm | 40.8 | |
| 11 | 20 cm | 22.4 cm | 2.4 cm | 41.7 | |
| 12 | 22.4 cm | 25.2 cm | 2.8 cm | 35.8 | |
| 13 | 25.2 cm | 28.35 cm | 3.15 cm | 31.7 | 100% $LiAlO_2$ |
| 14 | 28.35 cm | 31.85 cm | 3.50 cm | 28.6 | Spherepac 87% TD |
| 15 | 31.85 cm | 35.80 cm | 3.95 cm | 25.3 | |
| 16 | 35.80.cm | 40.30 cm | 4.50 cm | 22.2 | |
| 17 | 40.30 cm | 45.55 cm | 5.25 cm | 19.0 | |
| 18 | 45.55 cm | 47 cm | ---[2] | | |
| | | | | = 711 | |

(1) Tubes per meter poloidally, per sector (4 m avg. length).

(2) Cooled by conduction to rear wall.

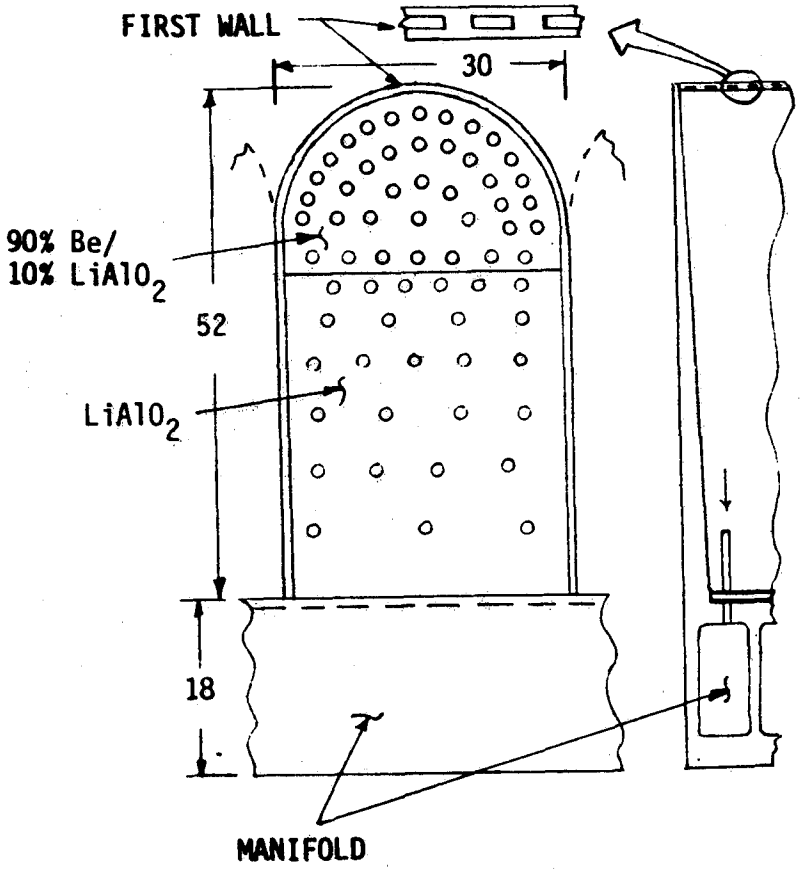


Fig. D.3-7. Design configuration for $LiAlO_2/H_2O$/PCA/Be concept.

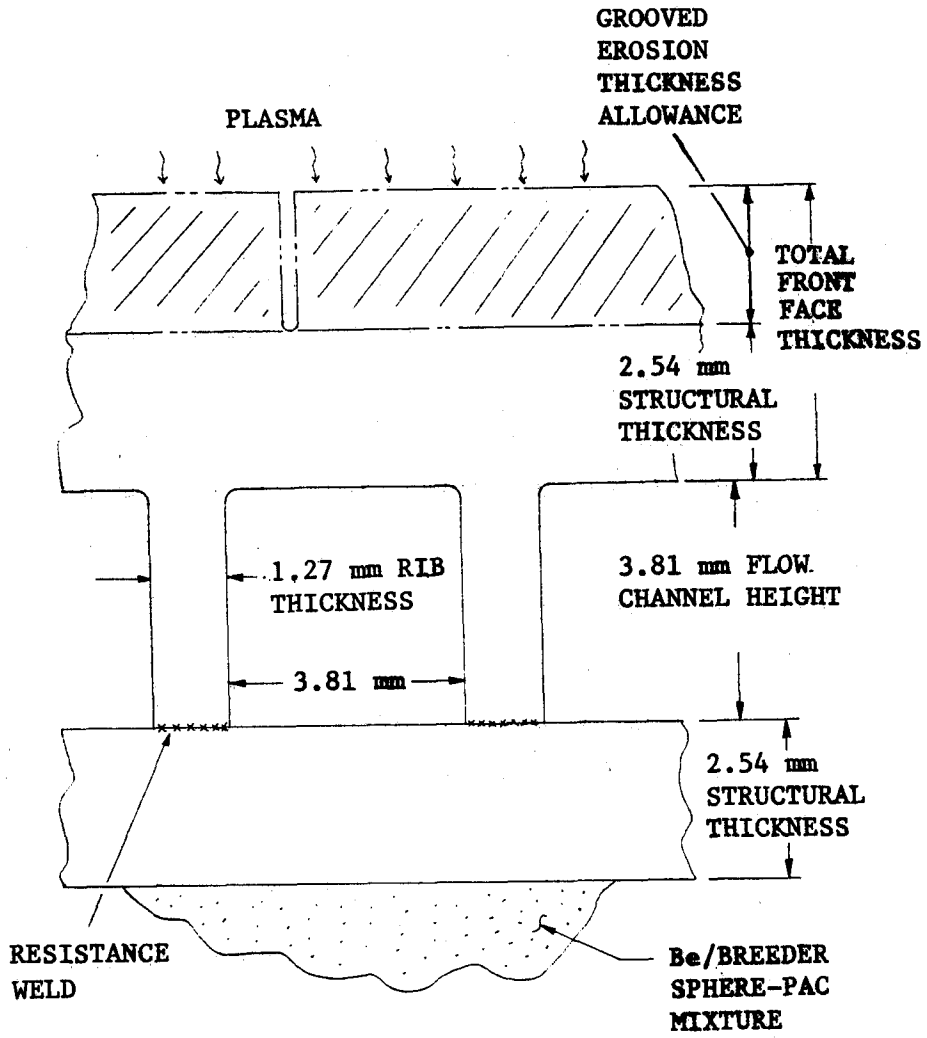


Fig. D.3-8. First wall configuration for $LiAlO_2/H_2O$/PCA/Be concept.

- DESIGN FOR PURGE FLOW CHANNEL
  - WIRE CLOTH SLEEVE SURROUNDING THIN-WALL, SMALL DIAMETER PERFORATED TUBE
  - WIRE CLOTH SPECIFICATIONS[a]:
    - SS MATERIAL
    - T ≃ 0.25 MM (.010 IN.)
    - 58% TD
    - 80 x 700 MESH, TWILLED DUTCH WEAVE
    - OPENINGS ARE TRIANGULAR, ~20-25 μM WIDTH (< 30 μM SPHERE-PAC MINIMUM PELLET SIZE)
  - TUBE SPECIFICATIONS:
    - 6 MM I.D. (~0.19 IN.)
    - 0.25 MM DIA. PERFORATIONS, ~10% OF SURFACE AREA
    - $t_w$ = .25 MM (.010 IN.)
  - CLOTH/TUBE ASSEMBLY WRAPPED AROUND EACH DWT IN GENTLE SPIRAL, TO KEEP IT IN PLACE

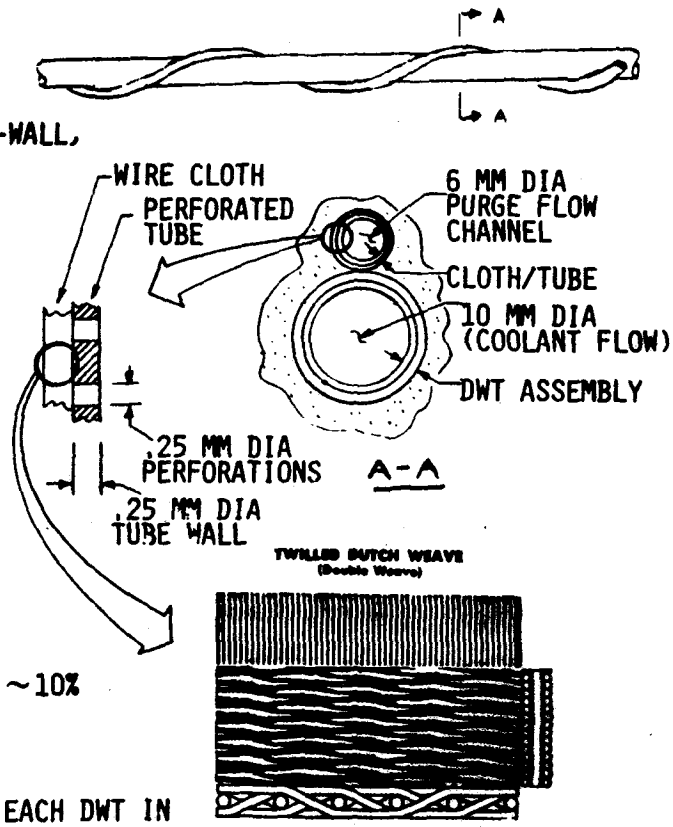


[a] TETKO CO., NEW YORK

Fig. D.3-9. Purge flow channel details for $LiAlO_2/H_2O$/PCA/Be blanket.

TABLE D.3-8.
MAJOR PARAMETERS AND FEATURES OF
LiPb/LiPb/HT-9 CONCEPT (TMR)[a]

| | |
|---|---|
| General Description | |
| Materials | |
| Coolant | 17Li83Pb (90% $^6$Li) |
| Breeder | 17Li83Pb (90% $^6$Li) |
| Neutron multiplier | (No separate multiplier) |
| Structure | HT-9 ferritic steel |
| Purge gas | None |
| Other | o Insulator at outlet header<br>o $H_2O$ (reflector coolant)<br>o Fe1422 (reflector structure) |
| Major Design Parameters | |
| Average neutron wall load, MW/m$^2$ | 4.3 |
| Average first wall surface heat flux, MW/m$^2$ | ~0 |
| Coolant | |
| Inlet/outlet temperature, $^0$C/$^0$C | 350/500 |
| Maximum pressure, MPa | 1.57 |
| Breeder | |
| Minimum/maximum temperature, $^0$C/$^0$C | 350/500 |
| Maximum pressure, MPa | 1.57 |
| Structure | |
| First wall/blanket maximum temperature, $^0$C/$^0$C | 550/550 |
| Minimum/maximum temperature at: | |
| Coolant interface, $^0$C/$^0$C | ~350/500 |
| Breeder interface, $^0$C/$^0$C | ~350/500 |
| Neutronics | |
| Tritium breeding ratio | |
| 1-D, 100% coverage | -- |
| Net (3-D with all geometrical details and penetration) | ~1.15 |
| Maximum nuclear heating rates | |
| Tube zone, MeV/Fusion | 9.145 |
| Beam zone, MeV/Fusion | 5.016 |
| Reflector, MeV/Fusion | 5.442 |
| Energy (1-D calculation) | |
| Multiplication factor | ~1.5 |
| Deposited in heat recovery zone, MeV/Fusion | 19.18 |
| Deposited in heat loss zone, MeV/Fusion | 0.151 |
| First Wall/Blanket Design Description | |
| First wall/blanket (LiPb) | |
| Thickness (including manifolds), m | 0.19 |
| Manifold thickness, m | NA |
| Percent structure/percent coolant | 7/74 |
| Coolant $\Delta$P (total), MPa | 1.57 |

TABLE D.3-8 (Continued)

| | | |
|---|---|---|
| Reflector ($H_2O$) | | |
| Thickness (including manifolds), m | | 0.19 |
| Manifold thickness, m | | NA |
| Percent structure/percent coolant | | 14/85 |
| Coolant $\Delta P$ (total), MPa | | -- |
| Primary coolant loop pumping power, % of blanket thermal power | | ~1.0 |
| First Wall | | |
| Description | | Two rows of staggered 10-cm dia. tubes, continuous between inlet and outlet headers. |
| Minimum/maximum coolant temperature, $^0C/^0C$ | | 350/500 |
| Maximum structure temperature, $^0C$ | | 550 |
| Blanket | | |
| Description | | Continuous row of coolant channels of rectangular cross section. |
| $^6Li$ enrichment, % | | 90 |
| | Blanket | Reflector |
| Minimum/maximum coolant temperature, $^0C/^0C$ | 350/500 | 280/320 |
| Maximum structure temperature, $^0C$ | ~520 | ~340 |
| Tritium removal from breeder | | |
| Method | | Vacuum pumping |
| Power loss (thermal), % total | | -- |
| Steady-state breeder tritium inventory, g | | ~1 |
| Purge gas | | NA |
| Tritium barriers | | Natural oxides |
| Power Conversion System | | |
| Steam generator | | |
| Type | | -- |
| Single or double wall tubes | | Double |
| Steam | | |
| Inlet/outlet temperature, $^0C/^0C$ | | -- |
| Maximum pressure, MPa | | -- |
| Tritium barriers | | Natural oxides |
| Thermal efficiency | | |
| $\eta = \frac{(MW_e)_{out} - (MW_e)_{pump}}{MW_{th\ TOTAL}}$, % | | -- |
| Gross ($MW_e/MW_{th}$), % | | -- |
| Steady-State Tritium Losses, Ci/d | | -- |

[a]Information extracted from draft of MARS Final Report and is not to be referenced.

[b]Neutron energy multiplication only.

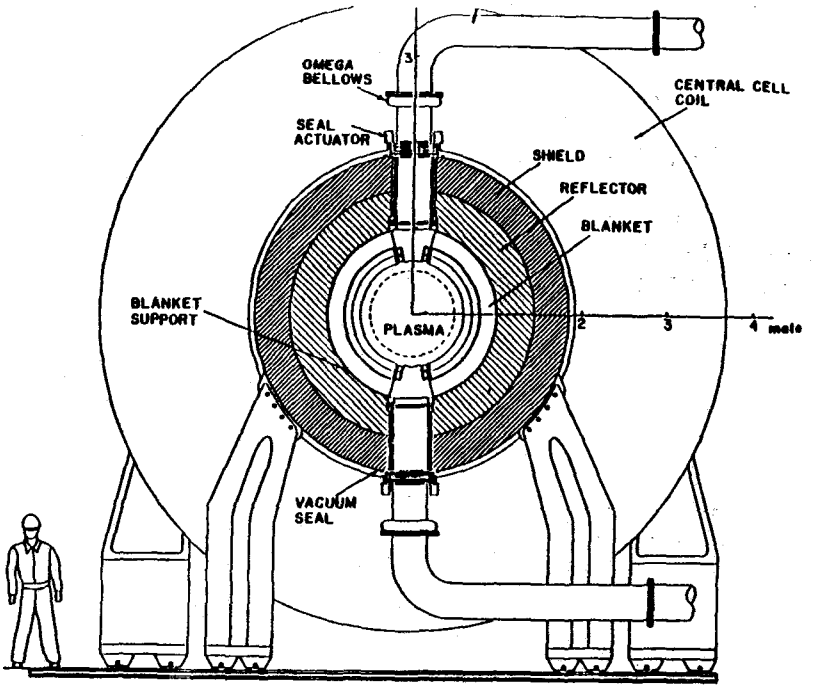


Fig. D.3-10. Vertical cross section of the central cell for the LiPb/LiPb/V **blanket concept.**

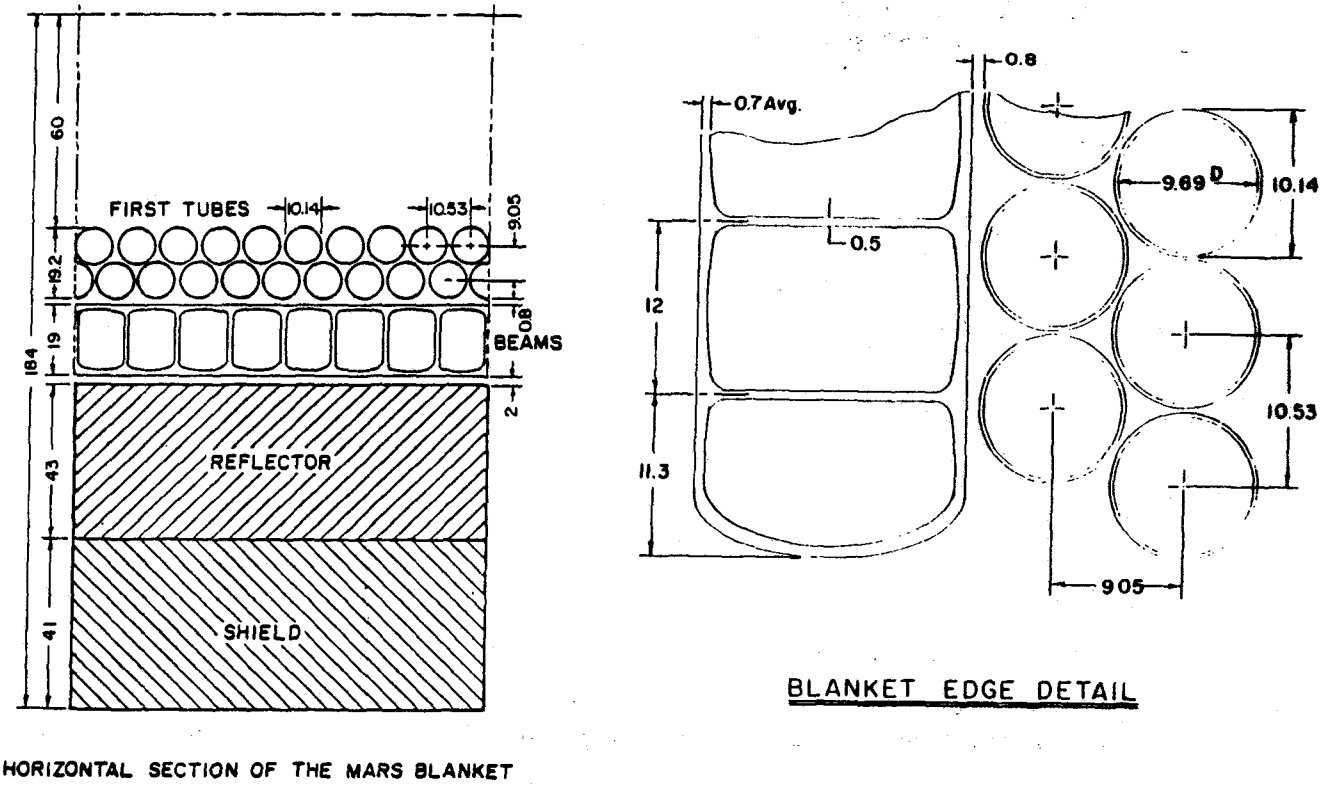


Fig. D.3-11. Horizontal cross section and edge detail of the LiPb/LiPb/V blanket.

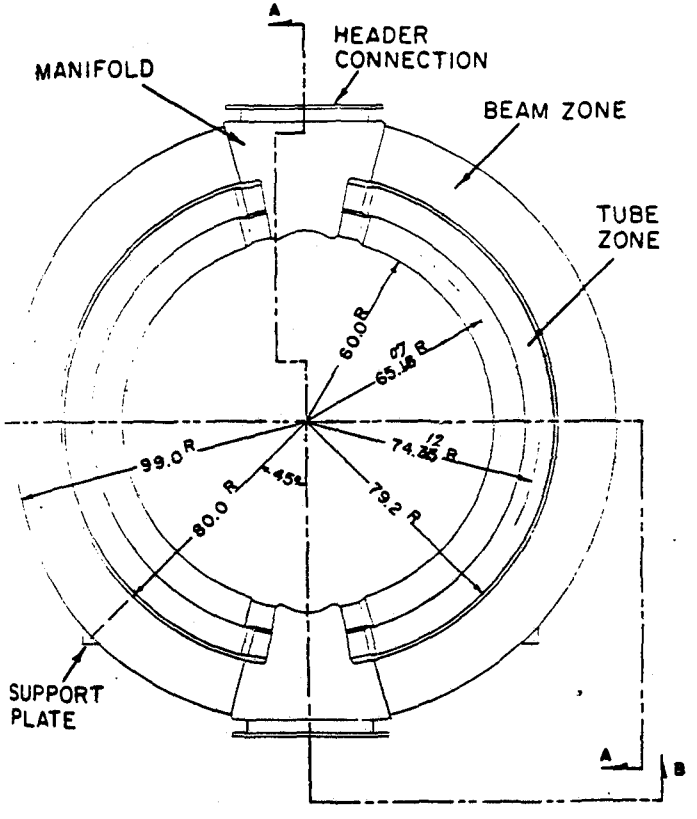


Fig. D.3-12. Axial view of LiPb/LiPb/V blanket.

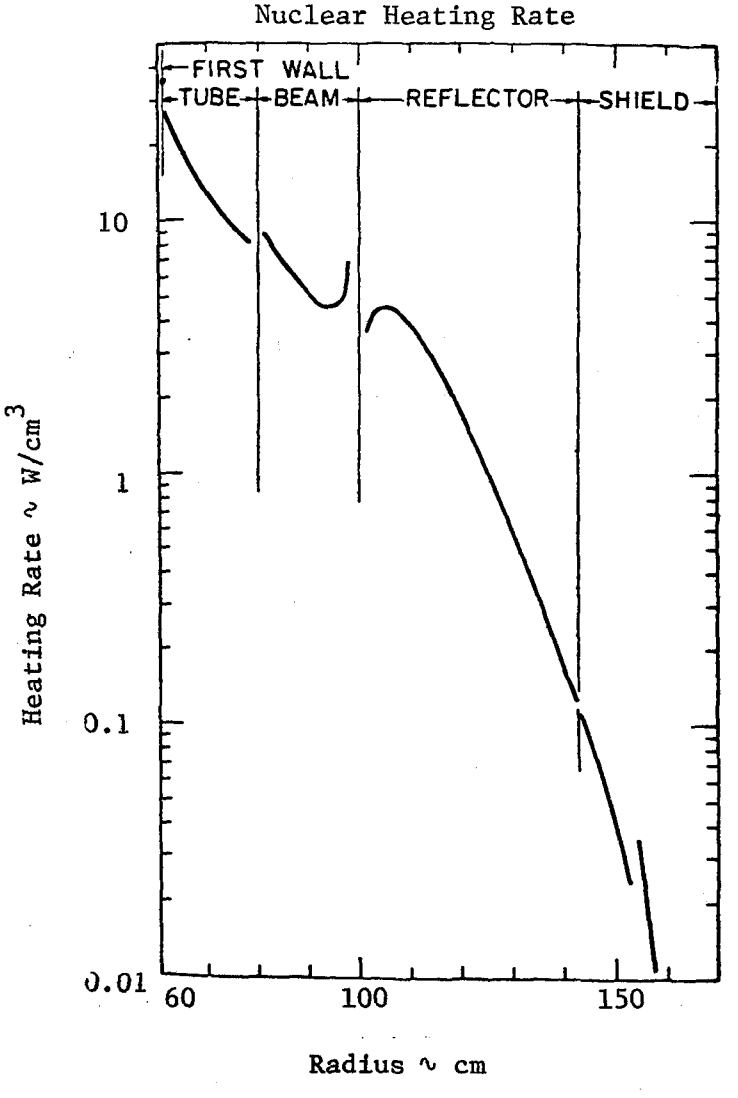


Fig. D.3-13. Nuclear heating rates for LiPb/LiPb/V blanket

TABLE D.3-9. BLANKET MODULE STRUCTURAL PARAMETERS

| | |
|---|---|
| Number of modules | 72 |
| Outer diameter (cm) | 198 |
| Axial length - cold (cm) | 179.2 |
| Axial length - hot (cm) | 180.25 |
| Number of tubes in first row | 34 |
| Number of tubes in second row | 32 |
| Tube outer diameter (cm) | 10.14 |
| Tube wall thickness (cm) | 0.23 |
| Tube axial spacing (cm) | 10.53 |
| Tube radial spacing (cm) | 9.05 |
| Web thickness in beam zone (cm) | 0.5 |
| Avg. flange thickness in beam zone (cm) | 0.7 |
| Number of rectangular passages | 30 |
| Dimension of rectangular passage (cm x cm) | 17.6 x 11.5 |
| Thickness of manifold material (cm) | 0.7 |
| Mass of empty blanket module (kg) | 2734 |
| Mass of module filled with $Li_{17}Pb_{83}$ (tonnes) | 29.47 |
| Compressive stress at support (MPa) | 2.7 |

TABLE D.3-10. STRUCTURAL PARAMETERS OF REFLECTOR

| | |
|---|---|
| Material of construction | Fe 1422 (Nonmagne -30) |
| Inner radius (cm) | 101 |
| Outer radius (cm) | 144 |
| Length of modules | |
| 19 modules (m) | 6.32 |
| 2 modules (m) | 5.08 |
| Maximum structure temp. C | 340 |
| Design coolant pressure (MPa) | 13.8 |
| Yield strength of Fe 1422 @ 340 C (MPa) | 245 |
| Max. design stress intensity (MPa) | 147 |
| Mass of reflector module | |
| 6.32 m long (tonnes) | 149 |
| 5.08 m long (tonnes) | 119.8 |
| Total mass of reflector (tonnes) | 3070.6 |

TABLE D.3-11. MECHANICAL PARAMETERS FOR THE BLANKET MODULE

| | |
|---|---|
| Structural material | HT-9 |
| Axial length, room temperature (cm) | 179.2 |
| Axial length, operating temperature (cm) | 180.25 |
| Inner radius (cm) | 60 |
| Outer radius (cm) | 99 |
| Tube zone thickness (cm) | 19.2 |
| Beam zone thickness (cm) | 19 |
| Tube outer diameter (cm) | 10.14 |
| Tube wall thickness (cm) | 0.23 |
| Axial tube spacing (cm) | 10.53 |
| Radial tube spacing (cm) | 9.05 |
| $Li_{17}Pb_{83}$ weight contained in a module (ton) | 29.5 |
| Structural material weight of a module, drained (ton) | 2.7 |

TABLE D.3-12. MATERIAL FRACTIONS IN THE BLANKET ZONES

| | |
|---|---|
| Tubular zone | |
| Inner radius, (cm) | 60 |
| Outer radius (cm) | 79.2 |
| Material fractions in v/o | |
| $Li_{17}Pb_{83}$ | 73.7 |
| HT-9 | 7.1 |
| VOID | 19.2 |
| Beam structural zone | |
| Inner radius (cm) | 80 |
| Outer radius (cm) | 99 |
| Material fractions in v/o | |
| $Li_{17}Pb_{83}$ | 85 |
| HT-9 | 14.4 |
| VOID | 0.6 |

TABLE D.3-13. 3-D RESULTS FOR TRITIUM PRODUCTION AND NUCLEAR HEATING

| | Tritium production (tritons/fusion) | Nuclear heating (MeV/fusion) |
|---|---|---|
| Front tubes | 0.248 | 4.71 |
| Back tubes | 0.230 | 2.88 |
| Beam zone | 0.461 | 4.02 |
| Manifolds | 0.213 | 2.53 |
| Reflector | -- | 5.27 |
| Total | 1.152 | 19.41 |

TABLE D.3-14. SPATIAL VARIATION OF dpa RATE (dpa/FPY) IN HT-9 BLANKET STRUCTURE

| | |
|---|---|
| Front tube | |
| Front | 60.0 |
| Side | 43.2 |
| Back | 30.9 |
| Back tube | |
| Front | 31.9 |
| Side | 24.2 |
| Back | 18.8 |
| Front of beam | |
| Behind front tube | 18.5 |
| Center | 17.7 |
| Behind back tube | 17.9 |

TABLE D.3-15. THERMAL HYDRAULIC PARAMETERS FOR EACH REFLECTOR MODULE

| | I | | II | III | IV | Reflector |
|---|---|---|---|---|---|---|
| | Zone 1 | Zone 2 | Zone 3 | Zone 4 | Zone 5 | Module |
| Inner/outer radius (cm) | 101/116 | | 116/120 | 120/130 | 130/144 | 101/144 |
| Nucl. heating (MW) | 22.03 | | 4.03 | 4.03 | 2.1 | 32.2 |
| % of nucl. htg. | 68.5 | | 12.5 | 12.5 | 6.5 | 100 |
| Water temp. in/out (°C) | 280/307.4 | | 307.4/320 | 307.4/320 | 307.4/320 | 280/320 |
| Coolant passage (mm) | 2 | | 2.5 | 2.5 | 1.35 | - |
| Mass flow (kg/s) | 179 | | 71 | 71 | 37 | 179 |
| Velocity (m/s) | .94 | | 1.03 | 1.03 | .64 | - |
| Pressure drop (k/Pa) | 1.94 | | 1.37 | 1.37 | 1.40 | 3.31 |

TABLE D.3-16. MARS BLANKET THERMAL-HYDRAULIC PARAMETERS

| | |
|---|---|
| Fusion power, MW | 2580 |
| Blanket power, MW | 2081 |
| Reflector power, MW | 730 |
| Blanket coolant | $Li_{17}Pb_{83}$ |
| Coolant temperature, °C | 350/500 |
| Structural temperature, °C | 350/550 |
| Maximum coolant velocity in blanket, m/sec | .17 |
| Coolant velocity in feed/discharge pipe, m/sec | 1.34 |
| Coolant flow rate, kg/hr | $3.2 \times 10^8$ |
| Reflector coolant | $H_2O$ |
| Coolant temperature, °C | 280/320 |
| Structural temperature, °C | 280/340 |
| Maximum coolant velocity, m/sec | 1.03 |
| Coolant pressure, MPa | 13.8 |
| Coolant flow rate, kg/hr | $1.15 \times 10^7$ |

TABLE D.3-17. SUMMARY OF MARS BLANKET MHD CALCULATIONS

| | V(m/s) | a(m) | $t_w$(mm) | L(m) | B(T) | k | $\Delta P_E$ (MPa) | $\Delta P_M$ (MPa) | $\Sigma\Delta P$ (MPa) |
|---|---|---|---|---|---|---|---|---|---|
| Feed pipe | 1.34 | .18 | 1 | 3 | 4.7 | .05 | .16 | .16 | .32 |
| Feed pipe turn to supply header | 1.34 | .18 | 1 | - | 4.7 | .10 | .32 | - | .32 |
| Supply header turn to blanket tube | .17 | .05 | 2 | - | 4.7 | .10 | .01 | - | .01 |
| Blanket tube | .17 | .05 | 2 | 1.88 | 4.7 | - | - | .27 | .27 |
| Blanket tube turn to return header | .17 | .05 | 2 | - | 4.7 | .10 | .01 | - | .01 |
| Return header turn to discharge pipe | 1.34 | .18 | 1 | - | 4.7 | .10 | .32 | - | .32 |
| Discharge pipe | 1.34 | .18 | 1 | 8 | 4.7 | .05 | .16 | .16 | .32 |
| Total | | | | | | | | | 1.57 |

TABLE D.3-18. MHD PARAMETERS

| | |
|---|---|
| Blanket power, MW | 2071 |
| Blanket coolant flow rate, $m^3/hr$ | $3.4 \times 10^4$ |
| Blanket velocity, m/sec | .17 |
| Magnetic field, Tesla | 4.7 |
| MHD pressure drop, MPa | 1.57 |
| Maximum blanket pressure, MPa | 0.73 |
| LiPb pumping power (80% efficiency), MW | 20 |

## References for Appendix D.3


1. M. A. Abdou et al., "Blanket Comparison and Selection Study," report ANL/FPP-83-1 (Vols. I and II), Argonne National Laboratory (October 1983).

2. D. L. Smith et al., "Blanket Comparison and Selection Study Final Report," report ANL/FPP-84-1 (Vols. I and II), Argonne National Laboratory (to be published).

3. "Mirror Advanced Reactor Study Interim Design Report," report UCRL-53480, Lawrence Livermore National Laboratory (September 1984).

## D.4 Plasma-Interactive Components

### D.4.1 Introduction

The design of components to be used in high heat and particle flux regions of fusion devices depends critically upon the operating conditions those components will experience. The most important conditions are the heat and particle fluxes, which govern the material selection, as for instance, with respect to heat conduction and the choice of high- versus low-Z materials. But other conditions including neutron irradiation, cycling, and the operating temperature further narrow the design options. Finally, the chemical and magnetic environmental conditions have to be considered.

There are three groups of components for which operating conditions must be defined. The first group are those components which are in direct contact with the plasma and experience a high heat flux, such as limiters or divertor plates in tokamaks, and halo scrapers, or direct convertors in mirror machines. The second group are those components associated with auxiliary heating, such as beam dumps, wall armor and RF windows. These components are exposed to a high heat flux but do not directly interact with the plasma. Finally, there are first wall components, which interact with the plasma over a large surface, but with a moderate heat load.

Those high heat flux components in direct contact with the plasma have the greatest uncertainty in operating conditions, particularly the limiter and divertor, due to the uncertainties in the plasma edge parameters. The auxiliary heating components have the best defined or predictable operating conditions, even for future devices. The operating conditions of the first wall are theoretically well defined, but there is no direct experimental support for the calculations because reactor relevant conditions have not yet been achieved. Thus the uncertainty is high, particularly with respect to disruption wall loadings and plasma related hot spots.

After a brief discussion in Section D-4.2 of the present data base for the determination of the operating environment, the operating parameters for plasma interactive components (PIC) and/or high heat flux components (HHFC) will be characterized in Section D.4.3. These are: (1) heat flux; (2) particle flux; (3) neutron flux and fluence; (4) burn time and number of cycles; (5) materials and temperature; and (6) magnetic environment.

D.4.2 Plasma Edge Conditions as the Base for Operating Parameters

The establishment of the plasma edge and scrape-off parameters represents the starting point in determining the operating environment for PIC/HHFC. For tokamaks, the critical parameters in the scrape-off layer are plasma density $n_e$, electron and iontemperature $T_e$ and $T_i$, and characteristic decay lengths $\lambda_\Gamma$ and $\lambda_q$ for particle and power fluxes, respectively. For reactor relevant plasma operation, the plasma density in the scrape-off layer can vary between $10^{18}$ - $10^{20}$ $m^{-3}$, with electron and ion temperatures on the order of 100 eV, and ion fluxes parallel to the magnetic field of $\Gamma_i = 3 \times 10^{23} m^{-2}$ $s^{-1}$ at the plasma boundary. Along with the corresponding electron flow, this can result in heat fluxes of $\gtrsim 10$ $MW/m^2$ perpendicular to the magnetic field. Particle and heat fluxes of this order are measured in present devices.

The transport of particles and energy in the edge, characterized by the decay lengths $\lambda_\Gamma$ and $\lambda_q$, involves a complex interaction between several important effects, such as electron and ion temperature profiles, magnetic field, neutral density profile, recycling coefficients, plasma thermal conductivity, particle diffusivity, impurity species and density, impurity generation rates, atomic and molecular cross sections. In the regions near the limiter or divertor, the parameters become highly two- or three-dimensional, depending on the configuration of these components. There are a number of one- and two-dimensional computer codes that have been used to describe the plasma transport into divertors and limiters.(1) Even three-dimensional codes are being developed. However, this does not mean that the phenomena are well enough understood to predict operating conditions in future devices with confidence. In particular, the heat and particle fluxes presented here should be considered as best estimates.

In mirror devices, there is a weaker coupling between the main plasma, the edge (halo), and the interacting structure (collector plates, direct convertor) than in tokamaks, which makes the particles and heat fluxes more predictable. There is significant uncertainty, though, in the determination of the radial parameter profiles, which depend on the achievement of control of the radial electric potential. However, due to the dispersion of the plasma in the end cells, the maximum heat and particle flux at the collector plates can be controlled by the choice of their axial position.

### D.4.3 Operating Parameters

In this section, the operating parameters will be characterized for typical components representing the three groups of PIC/HHFC distinguished in Section D.4.1. That is, the limiter/divertor group that sees plasma and high heat flux, a beam dump representing the HHFC of the auxiliary heating system with low plasma interaction, and the first wall where the concerns of plasma interaction dominate those of heat flux.

For the limiter/divertor the operating parameters have been reviewed in a recent study[1] for present machines, near-term devices, experimental test reactors, and long-term demonstration-type reactors. Table D.4-1 is essentially a reproduction from Ref. 1 with a few parameters added. This table might serve as a summary for the parameter discussion in the following subsections.

#### D.4.3.1 Heat Flux

The peak heat flux at limiters and divertor plates in existing devices ranges as high as 50-100 $MW/m^2$. However, these heat fluxes are only applied for several tenths of a second. In future devices, where steady-state or quasi-steady-state heat removal has to be achieved, the maximum heat fluxes are predicted to be 5-10 $MW/m^2$. It should be mentioned that in design studies such as INTOR[2] or DEMO[3], the heat flux has been limited to these values by shaping the limiter or angling the divertor plates relative to the magnetic field lines. Therefore, the 5-10 $MW/m^2$ values are determined more by the perception that this is an acceptable steady-state heat flux, rather than by device specific parameters.

The same rational applies to beam dumps where due to their external location, the design is more flexible. Up to 30 $MW/m^2$ have been achieved in steady-state laboratory tests[1] with a flat plate design. However, in future devices the maximum design heat flux will be driven by cost and reliability and is expected to be between 10 and 20 $MW/m^2$.

Typical first wall heat fluxes are predicted to be 0.5 - 1 $MW/m^2$ at the plasma surface in tokamaks. In tandem mirror reactors the first wall heat flux is very low, except in regions near neutral beam injection, where charge exchange processes might cause local peaks of up to several $MW/m^2$.

D.4.3.2 Particle Flux and Species

The peak particle flux at limiters and divertor plates depends on the plasma edge conditions. For example, with low electron temperature at the plasma edge ( $\lesssim$ 100 eV), the particle fluxes are high, and vice versa for the same extracted power. For ETR or INTOR[2]-type and DEMO-type[3] reactors, maximum particle fluxes of 3 x $10^{22}$ - 2 x $10^{23}$ $m^{-2}s^{-1}$ have been calculated at limiter leading edges and divertor plates. The impinging particle species are essentially duterium and tritium, with typically 5-7% helium and 0.01-0.1% other impurities. The helium and the impurity ions can significantly contribute to the sputtering behavior, despite their small fractions.

In tandem mirror reactors, peak particle fluxes at end collectors range between $10^{20}$-$10^{21}$ $m^{-2}s^{-1}$, however, at much higher particle energies (typically 20 - 100 keV). The same range applies also to beam dumps.

Typical first wall particle fluxes, mainly from charge exchange, are predicted to be 1 - 5 x $10^{20}$ $m^{-2}s^{-1}$,[2,3] again depending on the edge conditions.

D.4.3.3 Neutron Flux and Fluence

The target neutron flux for future fusion reaction will be a matter of cost optimization. It is presently believed be around 5 $MW/m^2$ at the first wall of commercial reactors.[4] In near-term devices and experimental test reactors, the achievable neutron flux will be in the order of 1-2 $MW/m^2$. In terms of material damage in typical structural materials during an operational period of one full power year (FPY), these fluxes correspond to a displacement rate of about 60 dpa/FPY for the commercial reactor and 12-24 dpa/FPY for the near-term device, respectively. For limiters/divertors, first wall components and other PICs, a minimum target life time of one FPY seems to be reasonable, resulting in component life time fluences of 60 dpa and 12-24 dpa, respectively. The same neutron flux and fluence levels apply to first wall components in tandem mirror devices. HHFC related to auxiliary heating are normally located in regions where the neutron flux is only a fraction of the first wall values, thus neutron damage is not a major concern.

D.4.3.4 Burn Time and Number of Cycles

Once thermal equilibrium is reached in any PIC/HHFC, (after a few seconds of full power operation), the burn time is of minor concern. Rather, it is the number of temperature cycles that is relevant with respect to structural failure. In near-term and ETR-type pulsed tokamaks, typical burn times of 200 - 300 s and $10^5$ - $10^6$ pulses during their lifetime are envisaged. Therefore, fatigue is a major concern, even at moderate neutron damage levels. In long-term devices with anticipated steady-state operation, the design has to focus on thermal ratcheting effects, including irradiation-induced swelling and creep, and low cycle fatigue at high neutron damage levels. The number of cycles during a component life time may be in the order of 10 - 1000.

D.4.3.5 Materials and Operating Temperature

Materials for PIC/HHFC are primarily chosen with respect to impurity introduction into the plasma, surface erosion, thermophysical properties, mechanical properties, resistance to neutron damage, fabricability, and compatibility with the coolant. In most cases, no single material can be identified that satisfies all of the requirements and therefore most conceptual component designs for future devices consist of composite material structures, i.e., a protective surface material bonded to the structural heat sink material. Candidate materials have been reviewed in reference 1 and are summarized in Table D.4-1. Facing the plasma either low-Z (beryllium or graphite) ceramics, or high-Z refractory metals (tungsten, tantalum, vanadium) are promising for limiter/divertor applications. The heat sink material can possibly be a copper alloy or, rather more speculative, a refractory metal. For RF antennas, there are additional electromagnetic requirements placed on the materials. Copper alloys will be used for both their high thermal and electrical conductivity, while ceramics will be used primarily for their electrical insulating properties.

Beam dumps for present systems are all composed of water-cooled, copper alloy heat sinks. Future beam dumps are likely to be of similar designs. Sputter resistant surface coating such as molybdenum to reduce sputtering erosion have been considered.

For first walls, candidate materials are stainless steel (PCA), ferritic steel (HT-9), and vanadium-base alloys.[4] Protection against excessive

Table D.4-1: Operating Parameters for Limiters/Divertors in Tokamaks

| Parameter | Present Machines (0 - 3 y) | Near Term (3 - 8 y) | ETR (1990s) | Long Term (After 2000) |
|---|---|---|---|---|
| Heat Flux | 4 $MW/m^2$, 1.5 s (TFTR)<br>70 $MW/m^2$, 0.25 s (TFTR) | $\lesssim$ 5 $MW/m^2$ | $\lesssim$ 5 $MW/m^2$ | $\lesssim$ 10 $MW/m^2$ |
| Ion Flux | --- | --- | 3 - 20 x $10^{22}$ $/m^2$-s (INTOR) | 3 x $10^{22}$ $/m^2$-s (DEMO) |
| Edge Temperature | 10 - 100 eV | ~ 100 eV (TFCX) | ~ 20 - 100 eV (INTOR) | 20 - 100 eV |
| Neutron Flux | 0 | 1 - 2 $MW/m^2$ | 1 - 2 $MW/m^2$ | 2 - 5 $MW/m^2$ |
| Neutron Fluence | 0 | < 1 dpa | ~ 25 dpa | ~ 60 dpa |
| Burn Time | 0.2 - 5 s | 20 - 300 s (TFCX) | 200 s (INTOR) | Continuous |
| Number of Cycles | $10^5$ | ~ $10^5$ (TFCX) | ~ $10^6$ (INTOR) | < $10^3$ |
| Structural Materials | Nickel Base Alloys<br>Stainless Steel | Copper Alloys | Copper Alloys<br>Refractory Metals | Copper Alloys<br>Refractory Metals |
| Surface Materials | Graphite<br>TiC, SiC Coated Graphite<br>Be | Be<br>SiC<br>BeO<br>C | Be<br>W<br>Ta | Be<br>W<br>Ta<br>V |
| Coolant | None | Water | Water | Water<br>Liquid Metals |
| Operating Temperature:<br>Surface<br>Heat Sink | <br>800°C - 1800°C<br>< 200°C | <br>$\lesssim$ 1000°C<br>$\lesssim$ 400°C | <br>$\lesssim$ 1000°C<br>$\lesssim$ 400°C | <br>$\lesssim$ 1000°C<br>$\lesssim$ 750°C |
| Magnetic Field at Limiter/Divertor | | | 5.5 T (INTOR) | ~ 4 T (DEMO) |
| Configuration | Tiles mechanically attached to heat sink | Coating/cladding bonded to heat sink | Coating/cladding bonded to heat sink | Coating/cladding bonded to heat sink |

sputtering erosion can be necessary in crucial first wall regions.

Once the material is chosen for a PIC/HHFC the operating temperature window is determined essentially by the mechanical material properties and the coolant. For a copper alloy HHFC structure, the maximum temperature is on the order of 400°C. There is at least a temperature drop of 150 - 200 °C from the maximum heat sink temperature to the bulk coolant temperature. Advanced refractory material alloys might allow maximum temperatures up to 750°C, which would be advantageous with respect to heat recovery. The surface temperature of the plasma side material could then approach 1000°C for limiter/divertor designs.

In beam dumps, thinner protection layers on the order of 1 mm are required and the surface temperature is only slightly higher than the maximum heat sink temperature, i.e., about 400°C.

Maximum allowable temperatures for the candidate first wall materials are 550°C for PCA and HT-9, and 750°C for the vanadium-base alloy V-15Cr-5Ti.

D.4.3.6 Magnetic Field

The magnetic field at PIC/HHFC locations is of interest with respect to the electromagnetic forces acting on the component structure during a plasma disruption, and in MHD pressure drop considerations in the case of liquid metal cooled components. For future tokamak reactors a maximum magnetic field of 12 T is considered feasible. This refers approximately to the inboard of the plasma chamber and reduces to about 4-7 T at the potential locations of limitors/divertors at the outboard and bottom of the plasma chamber, respectively.

In mirror devices, the maximum magnetic field is almost twice as strong as in tokamaks. However, at the beam dumps the field is on the order of 5 T near the axis, or less than 1 T outside the magnetic coils. RF antennas may be located in high field regions with up to 10 T. HHFC in the end cells such as halo scrapers, collector plates and direct convertors usually see $<<$ 1 T.

First wall components are, depending on their locations, exposed up to the maximum magnetic field mentioned above, i.e., approximately 12 T in tokamaks and 24 T in mirrors.

## References for Appendix D.4


1. M. A. Abdou et al., "Technical Assessment of the Critical Issues and Problem Areas in High Heat Flux Materials and Component Development", University of California at Los Angeles, UCLA-ENG-84-25, PPG-815 (1984).

2. "International Tokamak Reactor, Phase Two A", Part 1, IAEA, Vienna (1983).

3. M. A. Abdou et al., "A Demonstration Tokamak Power Plant Study (DEMO)", Argonne National Laboratory, ANL/FPP-82-1, (1982).

4. M. A. Abdou et al., "Blanket Comparison and Selection Study, Interim Report", Argonne National Laboratory, ANL/FPP-83-1 (September 1983).

## D.5 Tritium and Vacuum Systems

In this section, the basic characteristics of a commercial reactor tritium processing system are summarized. This system provides complete closed-loop tritium handling and processing, including: injection into plasma, vacuum exhaust from the plasma, extraction from the breeder, tritium cleanup from the plasma exhaust and breeder extractor, isotope separation, storage, secondary containment, waste treatment, air cleanup, and monitoring. The MARS[4] system, with flow rates, is shown in Figure D.5-1.

### D.5.1 Fuel Cycle

The largest flow of tritium is associated with the fuel cycle. Since not all the tritium injected into the plasma reacts before it is swept out by various transport processes, the reactor exhaust must be processed to remove the unburnt DT. Estimates for fractional burnups in tokamak and mirror reactors range from 0.1 - 10% (40% STARFIRE[1], 40% DEMO[2], 5% INTOR[3], 13% MARS[4], 0.04% TDF[5], 0.8% TASKA-M[6], 0.2% FRMR[7], others[14]) implying 5 - 500 kg/day of tritium throughout. The exact burnup fraction is clearly important in assessing inventory and sizing the tritium system.

Since this exhaust stream will contain helium ash and impurities (from plasma erosion, outgassing and leaks), it must be removed from the reactor chamber, filtered for debris, and chemically processed. For the base pressures, $10^{-5}$-$10^{-6}$ Pa,[1,4] and throughputs, 20-50 Pa-$m^3$/s,[1,4] expected, the favored vacuum pumps are cryopumps. These provide reliable, contaminant-free, high speed removal of hydrogen and impurities. However, due to the high vapor pressure of helium even at 4K, helium is normally pumped by additional cryosorption on molecular sieves, charcoal, or argon frost.[1] Such compound cryopumps capable of pumping hydrogen and helium in separate stages are under development.

Since cryopumps eventually saturate, they must be periodically regenerated by heating to restore their pumping ability and limit the proton tritium inventory. This will require isolating the pump from the chamber with valves so that the re-evaporated gases will be confined to a higher pressure and may be removed by transfer pumps such as turbomolecular pumps. Limits on valve lifetime suggest regeneration times of ~ 2 hrs.[1]

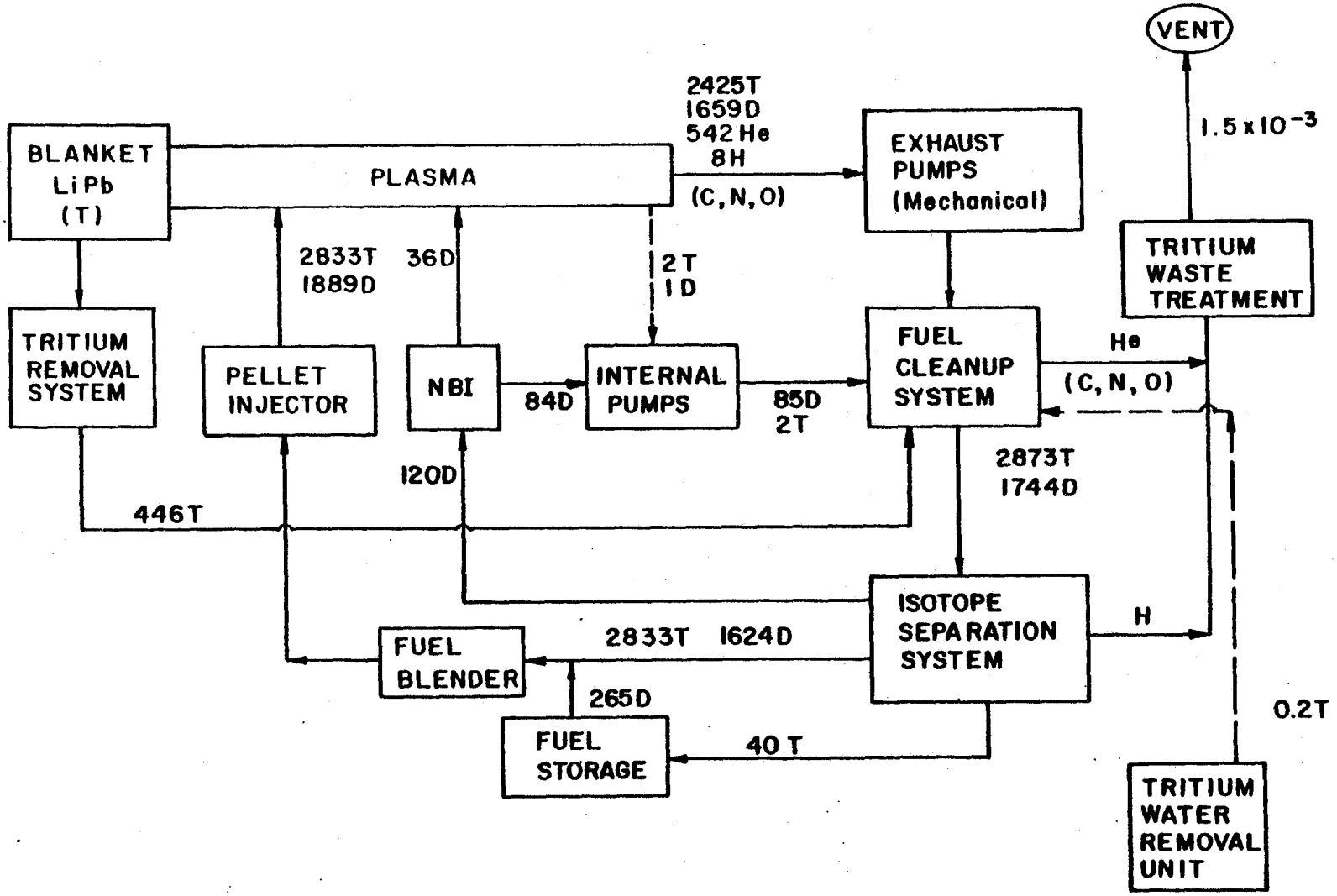


Figure D.5-1 MARS tritium processing system with gas flow rates, (g/d). (4)

Alternatives to cryopumps include turbomolecular pumps (up to ~ 1 Pa as with cryopumps) and Roots blowers (over ~ 0.1 Pa), depending on the operating gas pressure.[4] Both of these mechanical pumps remove helium and hydrogen readily and require no regeneration. However, they require tritium-proof seals, need development to large throughputs, and are more costly and complex than cryopumps.

Finally, a range of mechanical pumps are used to bring the gas pressure up to around 0.1 MPa (1 atm) where it can readily be transported to and through the rest of the tritium processing system. These include Roots blowers, Normatex scroll pumps and metal bellow pumps that can operate with minimal or no seals.[1,8] Tritiated gas transfer lines at these pressures are quite small (about 1 cm diameter). The largest concern is reducing tritium permeation, which can be accomplished through exacting attention to welds and joints, and the use of double walled piping with a sweep gas in the annulus.

From the vacuum pumps, the plasma exhaust is taken to the fuel cleanup unit and passed through some combination of activated metal getters, electrolysis, molecular sieves, cryogenic strippers, palladium diffusers[10] or catalytic oxidation in order to separate the hydrogen.

One proposed cleanup process[9] involves impurity absorption on molecular sieve (~ 75 K), catalytic oxidation of these impurities to form water and hydrogen-free compounds, condensation of the water, and electrolysis to recover the hydrogen. This cryogenic/electrolysis approach produces no waste problem and low operating costs, but reliable electrolysis cells with low DTO inventory are not available. An alternative process based on hot (~ 1000 K) uranium getters is presently available and minimizes handling the more hazardous tritium oxide, but has materials and permeation problems due to the high temperatures and requires periodic replacement and disposal of the uranium getter. A combined system, as shown in Figure D.5-2 is being tested at TSTA, for an ultimate capacity of 1 kg/d. Some impurities (e.g., iodine and nitrogen) may be more troublesome to remove, but feasible methods exist.

Afterwards, the cleaned hydrogen gas is passed to an isotope separation system where it is processed by an array of distillation columns. The purity requirements for this system (< 1 ppm impurities) are more stringent than those for the plasma.[9] Cryogenic distillation technology is relatively

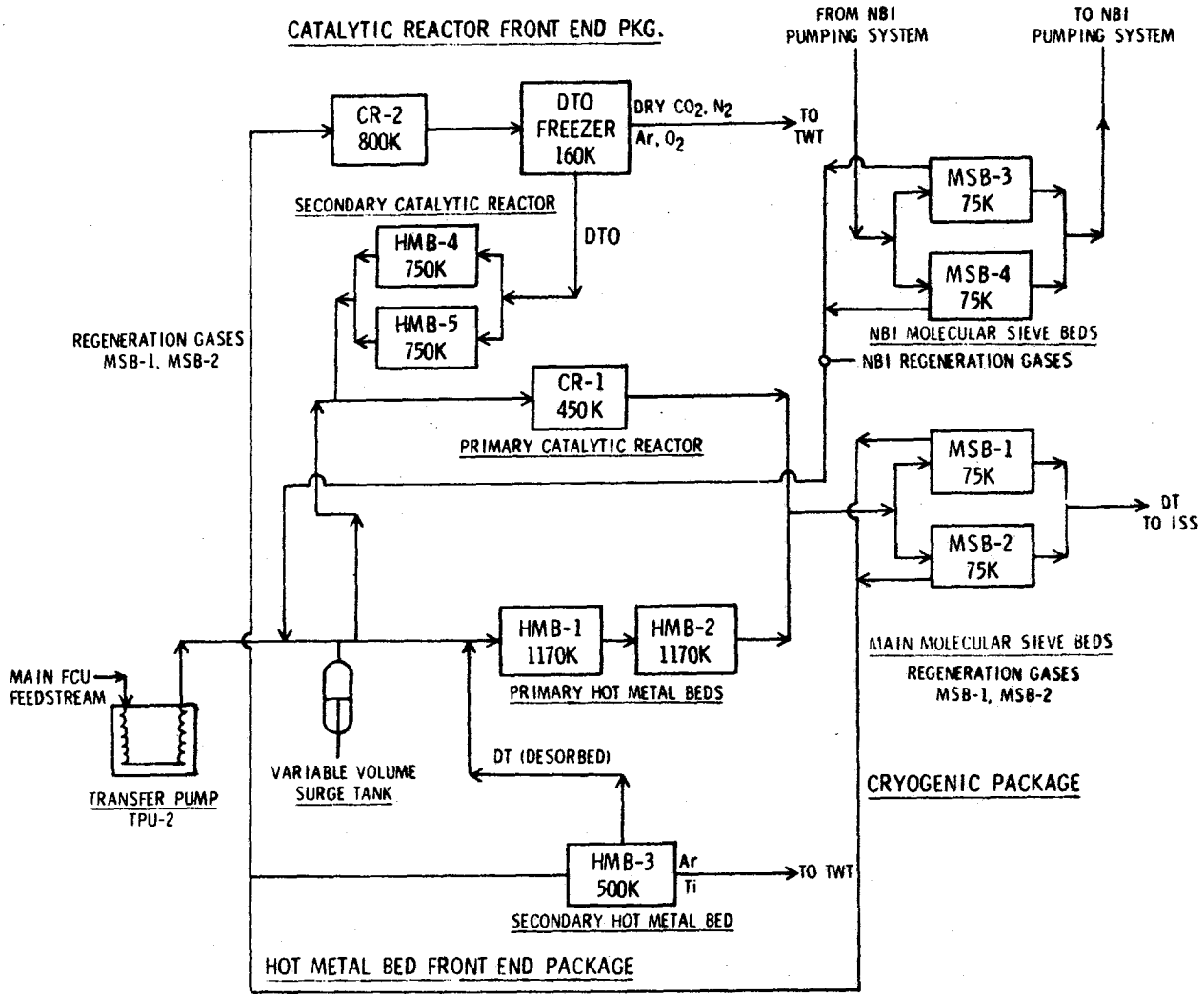


Figure D.5-2 Fuel cleanup system at TSTA.[9]

well-established, with large stills operating at Savannah River, U.S. and Grenoble, France. Reactor throughputs can be handled with systems of 4-5 columns, each on the order of 0.1 m diameter by 4 m high. Since some of the separated hydrogen gas is HT, additional separation through catalytic equilibrators are needed. These equilibrators split HT molecules by forcing the equilibrium reaction $HT + D_2 \rightleftarrows HD + DT$ to the right in the presence of large amounts of $D_2$. The product streams typically consist of high purity (> 99%) $T_2$, $D_2$ and/or DT and a waste stream (~ 50% $H_2$, 50% $D_2$, 0.1ppm $T_2$).

These $D_2$ and $T_2$ streams would generally be directed back to the plasma chamber, and blended and injected through gas puffers, pellet injectors or neutral beams, depending on the machine design, plasma conditions, and operating mode.

Some tritium storage is provided for startup purposes and to store excess tritium generated or tritium cleaned during maintenance processes. Typical tritium storage systems are based on uranium getter beds. This is a well-established technology that has a high storage capacity, holds tritium at room tempeature, and can be made to desorb the tritium above 400°C.[19]

### D.5.2 Breeder Cycle

Depending on the particular blanket design, this tritium produced in the blanket may be brought out of the reactor in a helium carrier gas (as in most solid breeder blankets) or directly with the breeding medium (as in most liquid metal blankets).

In the latter case, an additional extraction step is necessary. The basic choice for liquid metal tritium recovery techniques is largely governed by the tritium concentration in the liquid metal relative to its vapor partial pressure. For lithium, with a relatively high tritium solubility, direct contact methods such as molten salt extraction or yttrium gettering appear possible.[11] Both have been demonstrated in the laboratory. Concerns remain, besides scaling up to larger throughputs, on blanket corrosion due to trace halides from the salt and on shielding yttrium from oxygen and nitrogen impurities in the lithium.[11] For 17Li-83Pb, the solubility is very low and both direct and indirect methods are possible. The extraction system must produce very low tritium levels in order to control tritium permeation from the coolant loop. Molten salt extraction and yttrium getters have not been

experimentally established or are sensitive to lead. Vacuum extraction is probably not fast enough to control tritium levels, although mixing with a helium carrier might work. Permeation is possible if surface oxide barriers can be prevented.

The net result is a stream of tritium gas, usually in a helium carrier gas, with some impurities and water vapor. This is directed to the fuel cleanup unit and isotope separators as used for the fuel cycle. However, due to the differences in the inlet streams (~ 90% DT, 10% He from plasma versus ~ 10% $T_2$ and HT, 90% He from the breeder) and their impurities (solid breeder stream may have substantial H or O added to enhance tritium recovery and limit permeation), additional or separate fuel cleanup processes may be used.

From this point, the breeder tritium is treated in a similar manner as tritium from the fuel cycle - isotope separation with the product streams cycled back into the plasma or storage.

### D.5.3 Secondary Systems

Additional tritium processing is needed to account for tritium permeation, tritium leaks, or the tritium content in process waste streams in order to minimize losses and safety risks. A diagram of tritium flow in MARS secondary systems[12] is shown in Fig. D.5-3.

Tritium can potentially migrate into the primary coolant from the plasma or from the breeder. From here, it may escape through normal leakage or further permeation - especially through the steam generators and eventually the condensers where it can be released to containment or atmosphere. It is desirable to keep this coolant tritium level small since it is "vulnerable" or fairly readily releasable.

A particular concern is water since this is likely to be present in some components - blanket, shield, high heat flux components, general purpose coolant, or on the secondary steam side. Presently developed methods require some scaling in capacity. An existing commercial system at Grenoble, France processes about 20 kg/hr heavy water, extracting 16 g $T_2$/yr and maintaining 1.5 Ci/kg $D_2O$. A facility under construction at Darlington, Canada will process 400 kg/hr, extract about 2 kg/yr tritium from CANDU reactor heavy water and maintain 0.3 Ci/kg $D_2O$[13], although initially larger quantities

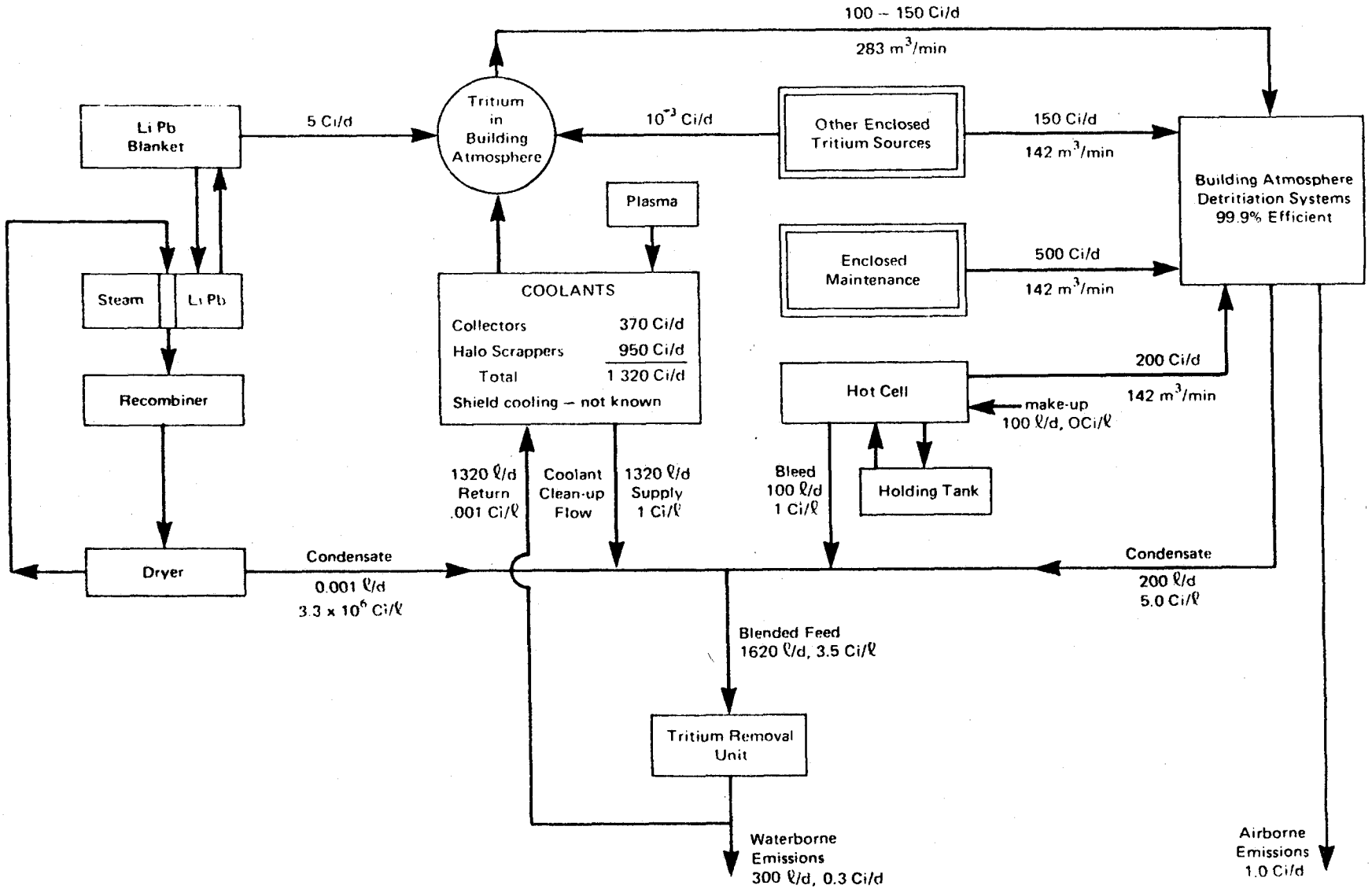


Figure D.5-3 Secondary system tritium flows in MARS.[15]

will be removed due to high inventories. While the cost is somewhat uncertain, a MARS-type tritiated coolant water extraction facility would be about 10 M$ based on the Darlington CANDU Tritium Removal Facility.[12]

In addition, it is expected that tritium will leak through piping, welds, valves, seals, pumps and any other components containing tritium. Careful design, including double-walled piping with sweep gas is necessary to control such tritium losses.

For a typical containment volume of ~ $10^6$ $m^3$, atmospheric processing of ~ 5 turnovers/d, and a tritium release rate of under 10 Ci/d, the normal atmospheric tritium level is < 1 $\mu Ci/m^3$.[1,9,12] In the event of an accidental release of, say, 10 g DT from a pump failure, the average tritium level becomes ~ 0.1 $Ci/m^3$. Thus, atmospheric tritium recovery systems are needed to control normal and accident tritium levels in the containment. These typically operate by converting any gaseous hydrogen (or tritium) into water, which is then trapped by condensation or molecular sieve adsorption. However, this converts tritiated gas into its much more hazardous (x25000) oxide form, and other methods are under consideration.[16] The collected water may be returned to the water cleanup system for tritium extraction. There is a trade-off between the atmospheric system throughput and the time to clean up a given accidental release. Reactor designs typically choose turnover rates of 2-3 times/day, allowing 1-10 days (or more) for cleanup of a $10^5$ Ci tritium leak, depending on the behavior of the released tritium (surface adsorption, HT/HTO conversion).[12] It is generally preferred to put tritium containing systems into nested compartments to minimize processing volume and leakage to atmosphere.[17]

Finally, a certain amount of tritium is lost through the process waste streams. For example, TSTA has about a 1% process loss in the primary fuel cleanup loop, with the secondary waste treatment system reducing the final process loss to about 100 Ci/yr.

Solutions include additional stages in the impurity removal step, improved waste treatment (e.g., recovery of tritiated water), baking of highly

tritiated components before disposal, and modifications to the fuel cycle (e.g., cleaning only 10% of plasma exhaust on each pass if the burnup is very low, or partially bypassing the isotope separator stage).

### D.5.4 Instrumentation and Control

An important aspect of the tritium system, in addition to all the process hardware, is monitoring and control over the tritium inventory. Present DOE criteria may call for 100 Ci (0.01 g) accuracy in tritium processing systems.[18] However, in a fusion reactor with 1 kg/d circulating tritium and several more kilograms in storage, this implies 0.0001% accuracy. Furthermore, tritium is subject to decay, burnup, creation and permeation over a large surface area of piping, and will occur in a variety of phases and chemical compounds. Present approaches to tritium management in fusion experiments are illustrated at TFTR[15], where tritium inventories are limited to 50,000 Ci on-site and tritium releases are controlled to remain within DOE dose limits.

The requirements for tritium control in reactors with 100 MCi will always be stringent, and reliable real-time tritium monitors with good resolution under reactor conditions are needed. Commercial ionization chambers with 10% accuracy are available for tritium flows with up to 100% $T_2$. PVT measurements of tritium level may be made to an accuracy of 0.2% under carefully controlled conditions. Mass spectrometry is useful (2%), but operates in a batch mode. Calorimeters may provide real-time measurements in concentrated tritium systems such as storage units. Accurate real-time tritium measurements in high pressure helium (5 MPa), or at very low effluent levels (1 $\mu Ci/m^3$) with HT/HTO and background radiation discrimination are needed.[18] Tritium inventory must also consider tritium trapped in components. For example, tritium implanted in limiters or divertors could be as much as 1 kg. At present, periodic shutdown might be necessary to check specific inventories.

Table D.5-1 summarizes the inventory distribution in MARS and STARFIRE. It should be noted that MARS uses a liquid lithium-lead coolant, while STARFIRE is based on solid $LiAlO_2$. As may be seen, tritium inventories on the order of 1-10 kg are likely, with the bulk of the tritium associated with the breeder, the storage vault, and the isotope separation system.

Table D.5-1: Typical Reactor Tritium Inventories

| Tritium Inventory (g) | MARS[4] | STARFIRE[1] |
|---|---|---|
| Total Site | 3264 | ~ 11225 |
| Blanket | 1.0 | ~ 10000 |
| Primary loop | 7.5 | NA |
| Blanket tritium extraction | <0.1 | 0.2 |
| Fuel cleanup | 0.6 | 30 |
| Isotope separator | 210.0 | 100 |
| Other fuel cycle components | - | 24 |
| Fueling system | 22.5 | 54 |
| Plasma | <0.1 | 0.1 |
| Reactor exhaust pumps | <0.1 | 63 |
| NBI cryopanels | 1.0 | 0 |
| Structure | 0.8 | NA |
| Water coolant | 21.6 | NA |
| Storage vault | 3000 | 1071 |
| Containment atmosphere | <0.1 | <0.1 |

## References for Appendix D.5


1. C. C. Baker et al., "STARFIRE - A Commercial Tokamak Fusion Power Plant Study", Argonne National Laboratory, ANL/FPP-80-1 (September 1980).

2. M. A. Abdou et al., "A Demonstration Tokamak Power Plant Study (DEMO)", Argonne National Laboratory, ANL/FPP-82-1 (September 1982).

3. "US FED-INTOR, Critical Issues", USA FED-INTOR/82-1 (October 1982).

4. "Mirror Advanced Reactor Study (Mars)", Final Design Workshop, LLNL, Livermore, August 29-31, 1983.

5. "A Tandem Mirror Technology Demonstration Facility", Lawrence Livermore National Laboratory, UCID-19328 (October 1983).

6. "TASKA-M: A Low Cost, Near Term Tandem Mirror Device for Fusion Technology Testing", FPA-83-7, KfK-3680, UWFDM-600 (December 1983).

7. G. Carlson et al., "Field-Reversed-Mirror Pilot Reactor", Electric Power Research Institute, EPRI AP-1544 (September 1980).

8. T. M. Dowell, "Survey of Pumps for Tritium Gas", Canadian Fusion Fuels Technology Project, CFFTP# F83021 (May 1983).

9. P. A. Finn, R. G. Clemmer and B. Misra, "Tritium Management Requirements for D-T Fusion Reactors (ETF, INTOR, FED)", Argonne National Laboratory, ANL-81-32 (October 1981).

10. H. Yoshida, S. Konishi and Y. Naruse, "Preliminary Design of a Fusion Reactor Fuel Cleanup System by the Palladium Alloy Membrane Method", Nucl. Tech./Fusion, 3, 471 (May 1983).

11. "Fuel Cycle Programs Quarterly Progress Report, April-June 1983", Argonne National Laboratory, ANL-83-78.

12. S. Sood and O. Kveton, "A Design Assessment of Tritium Removal Systems for the Mirror Advanced Reactor Study", Canadian Fusion Fuels Technology Project, CFFTP# F83018 (October 1983).

13. T. Drolet, K. Wong and P. Dinner, "Canadian Experience with Tritium - The Basis of a New Fusion Project", Nucl. Tech./Fusion, 5, 17 (1984).

14. M. Ortman, E. Larsen and S. Abdel-Khalik, "Characteristics of Unburned Tritium Exhaust, Recovery and Reprocessing Systems in Magnetic and Inertial Confinement Reactors", Proc. Top. Mtg. on Trit. Tech. in Fission, Fusion and Isotopic Appl., Dayton, Ohio, April 29-May 1, 1980.

15. H. Howe and K. Lind, "Environmental Control of Tritium Use at the Tokamak Fusion Test Reactor (TFTF)", Princeton Plasma Physics Laboratory, PPPL-1494 (January 1979).

16. C. Fokers and R. Cena, "Tritium Containment Systems. A Trade-off Study", Lawrence Livermore National Laboratory, UCRL-52627 (December 1978).

17. H. Weichselgartner and W. Swansiger, "Tritium in the Compact Ignition Experiment (ZEPHYR)", Proc. Top. Mtg. on Trit. Tech. in Fission, Fusion, and Isotopic Appl., Dayton, Ohio, April 29 - May 1, 1980.

18. L. J. Wittenberg et al, "Evaluation Study of the Tritium-handling Requirements of a Tokamak Experimental Power Reactor", Mound Laboratory, MLM-2259 (November 1975).

19. J. Gill, B. Anderson and R. Watkins, "Tritium Storage/Delivery and Associated Cleanup Systems for TFTR", J. Vac. Sci. Tech. A, 1(2), 856 (April-June 1983).

# APPENDIX E

## MODELING OF MFTF-$\alpha$+T HIGH GAMMA MODE PERFORMANCE

TABLE OF CONTENTS

PAGE

E.1 Introduction.....E-1
E.2 MFTF-α+T High Gamma Mode Operation.....E-1
E.2.1 Device Description.....E-1
E.2.2 Physics Description.....E-2
E.3 Description of the Physics Model.....E-5
E.4 Baseline Parameters.....E-11
E.4.1 Strong Effect.....E-11
E.4.2 Moderate Effect.....E-12
E.4.3 Mild Effect.....E-13
REFERENCES.....E-21

# E. MODELING OF MFTF-α+T HIGH GAMMA MODE PERFORMANCE

## E.1 Introduction

This appendix will describe recent work concerning physics modeling of the MFTF-α+T device in the high wall loading (High-Γ) mode of operation. The parameters for this mode, as originally proposed, can be found in Ref. 1. For the present studies, new models of the particle and energy balance in tandem mirrors with MARS-type end cell configurations and high-field beam-driven inserts in the central cell have been incorporated in the TMRBAR tandem mirror physics code[2]. These models, which reflect better understanding of MFTF-α+T plasma physics since the original proposal, have been used to obtain a new set of baseline parameters for the High Γ operating mode. In addition, some trade studies have been done and a partially optimized set of operating parameters has been obtained. Finally, plasma physics issues characteristic of high-field test cell operation of a tandem mirror device have been raised and the need for future work in several areas identified.

The remainder of this appendix is organized as follows. Section E.2 describes the physics of the High-Γ mode of MFTF-α+T operation. This section includes a review of some of the concepts from Ref. 1. In the following section a brief description of the physics models which have been incorporated in the TMRBAR code is presented. The details of the models will be presented in a separate report. Section E.4 will present a comparison of the reference parameters from with those obtained from the updated model which serves to benchmark the new model.

## E.2 MFTF-α+T High Γ Mode Operation

### E.2.1 Device Description

The α+T upgrade of MFTF-B requires a number of changes in the MFTF-B configuration.

1. The axicell and transition coils in the MFTF-B end cell are replaced by a second yin-yang coil pair, a high field choke coil and a

transition coil. The field magnitudes are modified so that the field profile resembles a MARS-type end cell.

2. Ions in the new "anchor" yin yang magnetic well are heated by ICRH to increase the pressure in this good curvature region. This pressure provides MHD stability for the central cell plasma.

3. The sloshing ion neutral beam energy is increased to 200 keV so that the sloshing ions remain mirror confined in the new plug magnetic field.

4. The new choke coil field is set to 18 T (larger than the MFTF-B axicell peak field) primarily to increase the confinement in the central cell ions.

5. A high field axisymmetric test-cell section is inserted at the midplane of the central cell. The test-cell assembly includes two 12 T coil assemblies featuring a superconducting coil and a normal copper coil insert for each, and a blanket test module on which integrated nuclear testing is to be performed.

Detailed descriptions and design drawings of these changes are given in Ref. 1.

### E.2.2 Physics Description

Before proceeding to a description of the phyics for the High-$\Gamma$ operating mode, a brief review of the High-Q mode will be given. In this mode, the MARS-like end cell magnets and the high field test cell section are in place and MFTF-$\alpha$+T is operated with high electrostatic confinement and small neutral beam current input to the test cell. This results in a device with high overall Q in which the test cell wall loading is not greatly different from the wall loading in the rest of the central cell. Further details for this mode of operation are given in Ref. 1. The contrasts between the High Q and High $\Gamma$ modes will be highlighted below.

The goal of the High-Γ operating mode is to achieve on high neutron wall loading on the blanket test module in the test cell. To accomplish this the density in the test cell is increased by more than a factor of two over the density of the central cell Maxwellian plasma by injecting large currents of neutral beam particles into the test cell. In steady state, the trapped particle current from these beams must eventually scatter out of the test-cell mirror confinement and provide a particle source for the central cell particle population. Finally, this current must escape the device either through neoclassical transport (usually small), radial losses induced by the drift pumping system, or axial (Pastukhov) end losses. To keep the required pumping currents for the drift pump coils as low as possible, the axial confinement is significantly decreased in High-Γ mode by reducing the electrostatic potential in the plug region. Thus, the particle current is removed axially rather than radially.

Finally, the finite plasma pressure in the bad curvature regions of the test cell during High-Γ operation requires that the central cell be operated at lower beta to satisfy the MHD stability criteria. At fixed anchor beta these stability criteria set an upper limit on the total pressure weighted normal curvature in the central cell region. When a finite beta test cell is introduced, MHD requires that some pressures in the central cell be given up whenever the pressure in the test cell is increased. The stability boundary for the baseline configuration, giving beta in the central cell as function of beta in the test cell for fixed anchor beta, is shown in Fig. E.2-1[3].

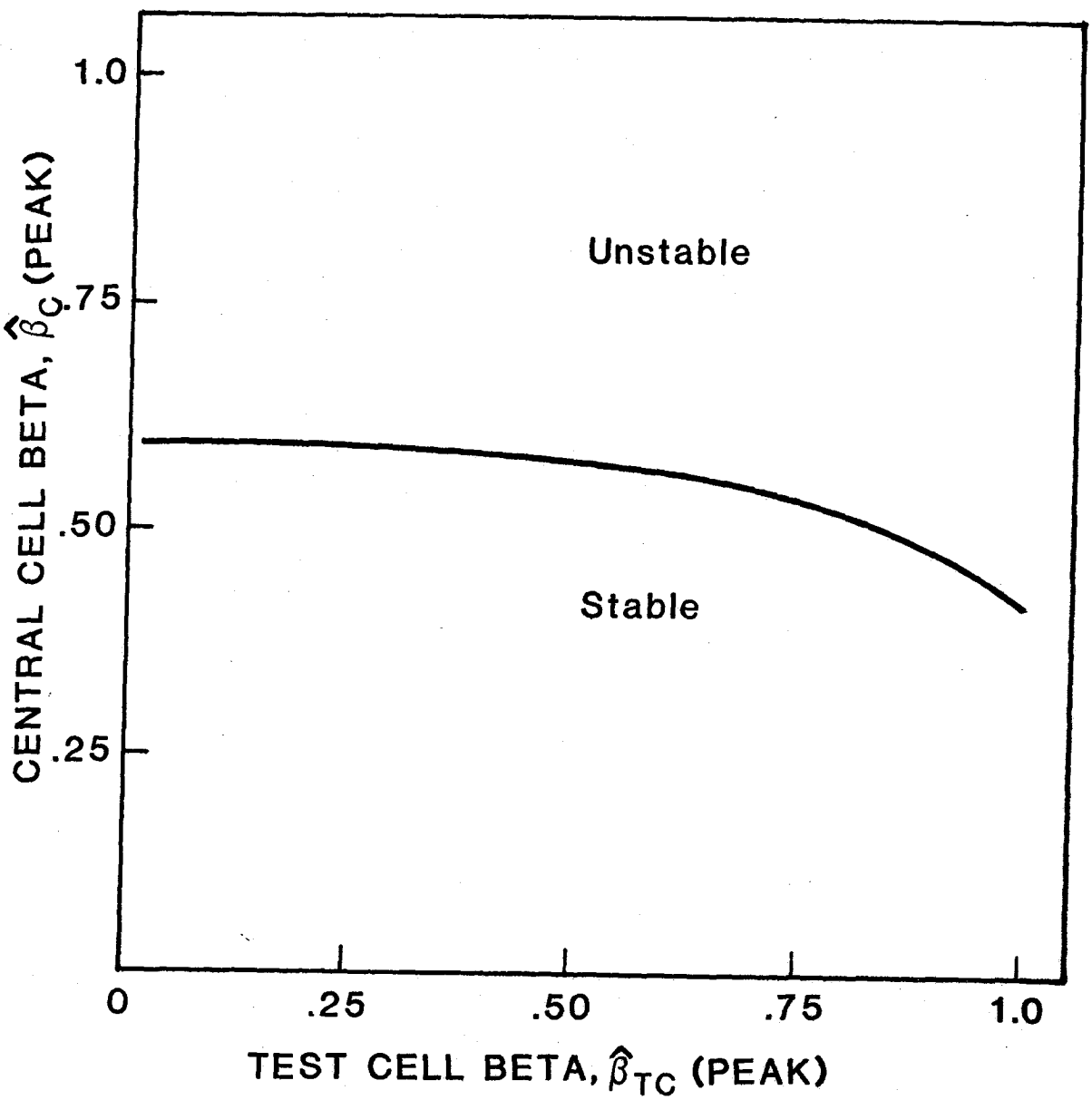


Figure E.2-1. Stability boundary for central cell peak beta vs. test cell peak beta from MHD calculations; $\hat{\beta}_{anchor} = 0.6$, $L_{eff,tc} = 2.8m$, $L_{tc} = 3.5m$.

## E.3. Description of the Physics Model

The physics models describing test-cell operation which have been developed for this study, focus on the energy and particle balances for the hot mirror trapped particles in the test cell and the sources provided by this class of particles in the energy and particle balances of the central cell population. These models have been incorporated in the TMRBAR tandem mirror physics code[2]. Diagrams of the magnetic field and potential profiles used in the code models, and the nomenclature used, are shown in Figs. E.3-1 and E.3-2. The test cell insert is treated in the model as a separate subsystem, similar to the treatment of the separate regions of the MARS type double yin yang end cells. Particle and energy balances are satisfied at a cardinal point on axis at the midplane of the test cell. The self-consistent plasma potential referenced to the potential in the rest of the central cell is calculated for the test cell cardinal point from a local quasi-neutrality condition. The axial magnetic field, plasma potential and density profiles corresponding to MFTF-$\alpha$+T in High-$\Gamma$ mode are shown in Fig. E.3-3.

The ion velocity space boundaries at the test cell cardinal point for this configuration are shown in Fig. E.3-4. Three classes of ions can be identified. HOT ions are those which are mirror trapped between the test cell peak mirror fields. HOT* ions are those with pitch angle and energy such that they are not mirror trapped in the test cell but remain trapped by the central cell choke coil fields. COLD ions form a Maxwellian distribution, part of which passes the choke coil point into the end cell regions and is electrostatically confined by the potential peak in the plug. To further distinguish the HOT* population from that part of the COLD Maxwellian which remains in the central cell (large pitch angle), the specification is made that a HOT* ion carries sufficient energy that if it pitch angle scatters, at fixed energy, into the loss cone for the central cell mirror, it is not confined by the electrostatic potential and is lost axially from the machine.

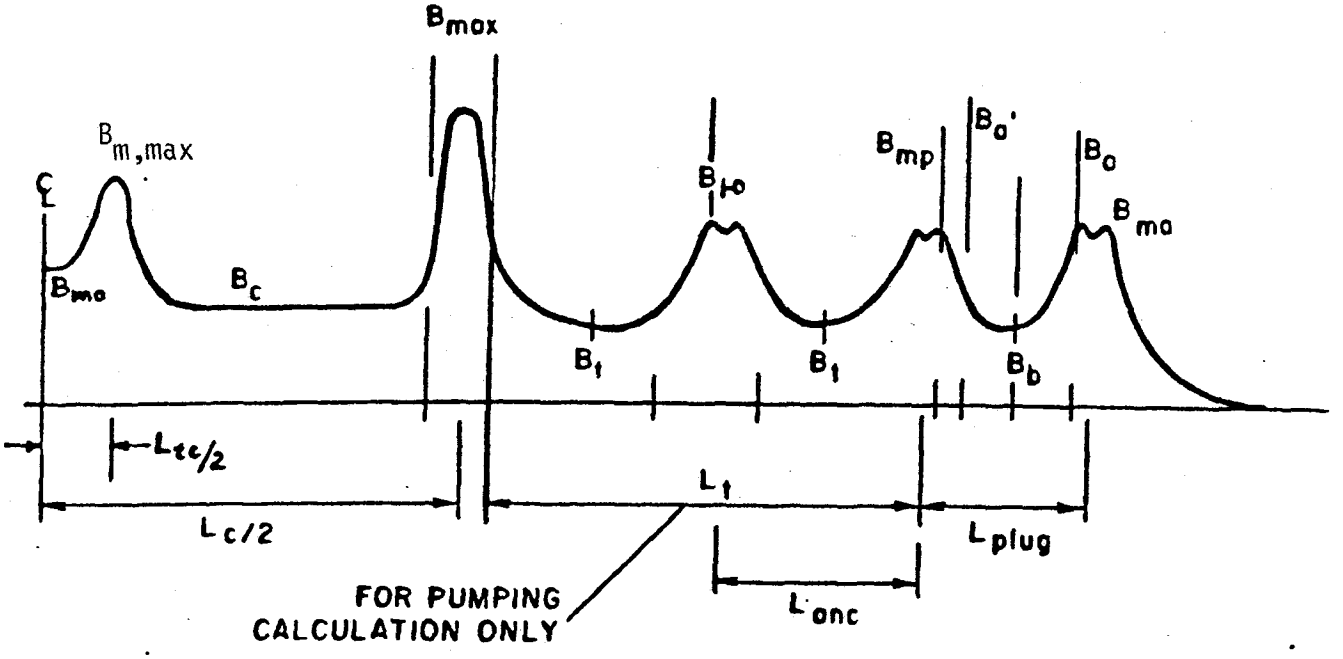


Figure. E.3-1. Axial magnetic field and length definitions (not to scale).

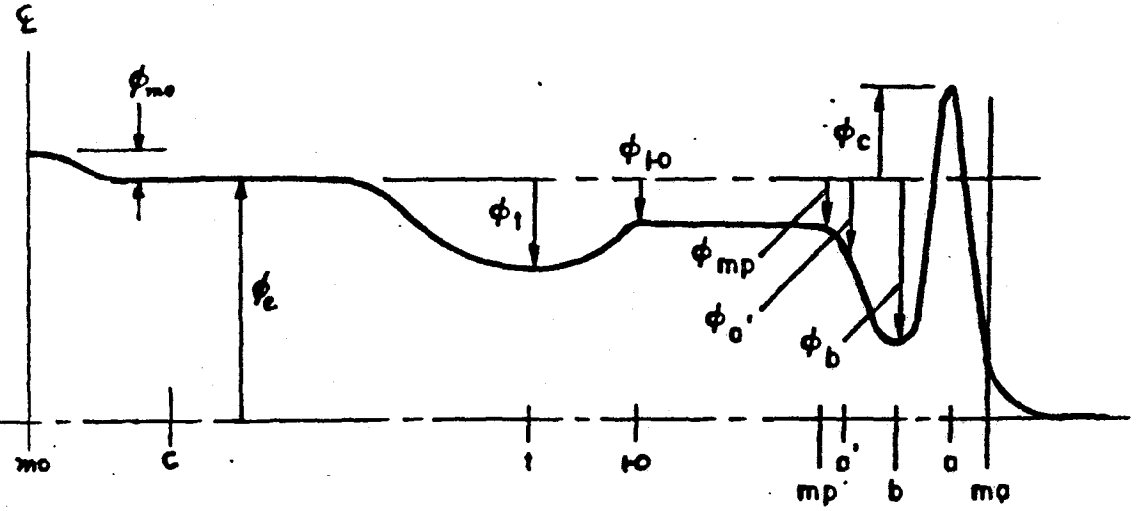


Figure. E.3-2. Axial potential and cardinal point definitions (not to scale).

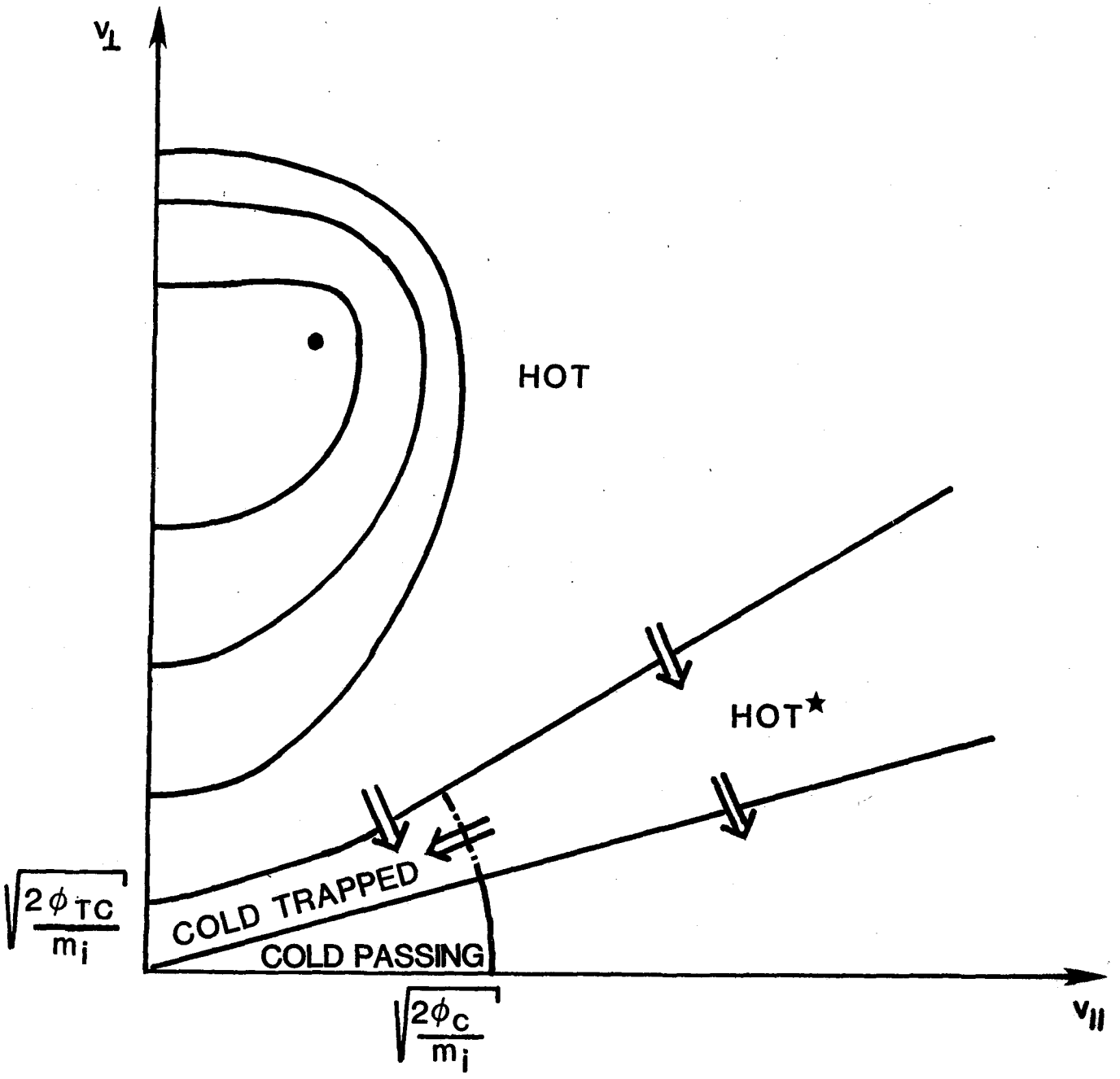


Figure. E.3-3. Velocity space for ions at the midplane of the test cell.

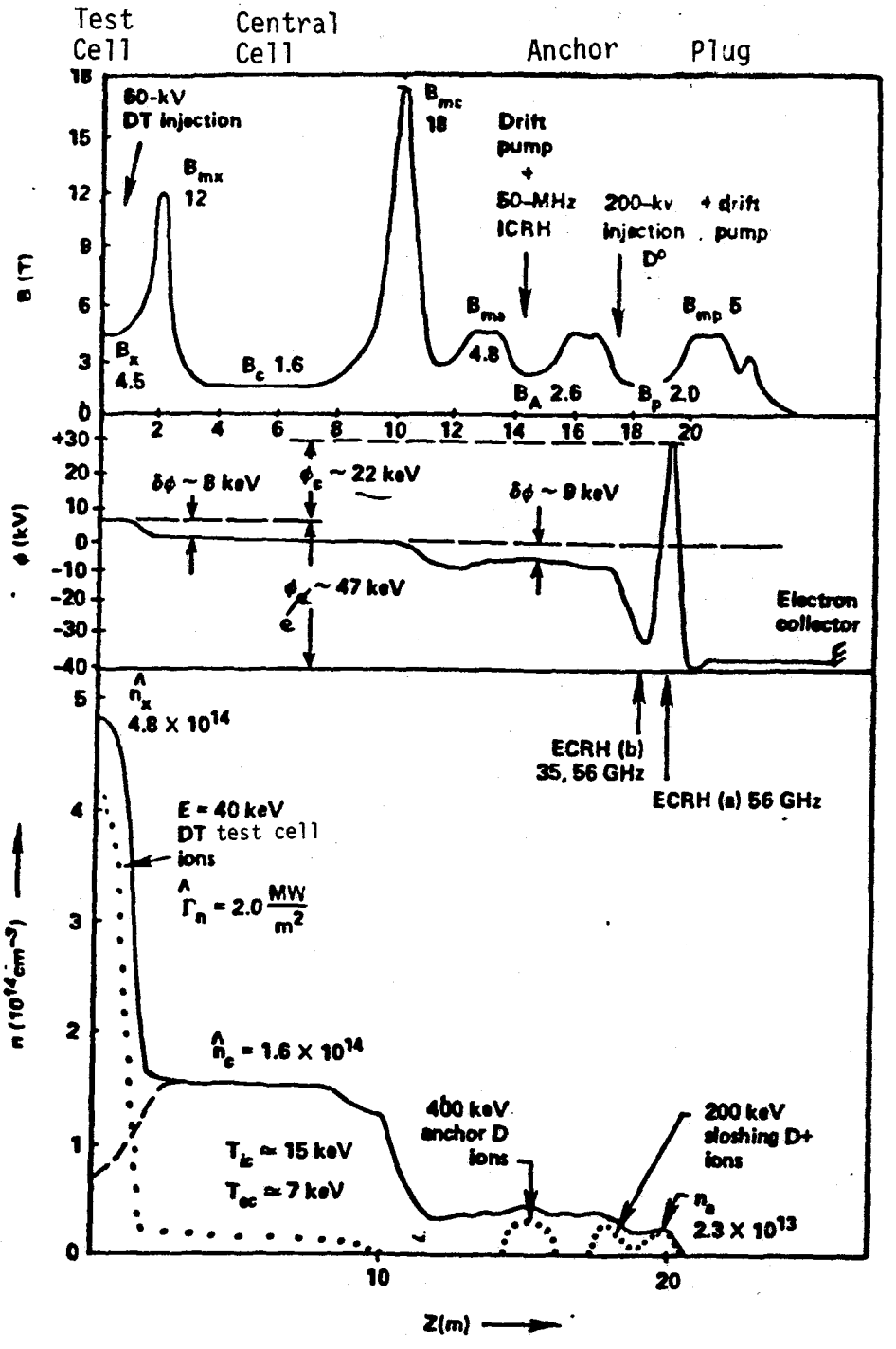


Figure E.3-4. Profiles of field, potential, and density in the high-Γ mode of MFTF-α+T (from Ref. 1)

The trapped ions from the neutral beams in the test cell provide the source for the HOT ion population. The sink for this class of particles is pitch angle scattering out of the test cell into the HOT* population. These HOT* particles are lost either by pitch angle scattering into the loss cone or energy slowing down into the COLD Maxwellian distribution. Finally, particles in the COLD population are lost from the device either by neo-classical transport (usually small), radial drift pumping or axial (Pastukhov) losses.

Separate particle and energy balances for the HOT and HOT* populations are included in the model. For the HOT particles the energy balance is determined by a Logan-Rensink plug model[4,5] in which neutral beam particles are injected at a specified average energy and injection angle into a mirror magnetic field. The effect of the positive potential which forms in the test cell region is taken into account in terms of an effective mirror ratio for the test cell region. This model yields the HOT average energy. The HOT density is then calculated from the equation for test-cell beta. The test-cell beta value must be input to the calculation.

The energy balance for the HOT* ions is also calculated using a Logan-Rensink model but with several modifications. First, the HOT* particles spend the majority of their time in the central cell region where the relative potential is zero. Second, the injection angle to be used is determined by assuming that a particle reaching the test cell peak field point with infinitesimal parallel velocity is represented as a particle injected into the HOT* distribution at the central cell minimum field. The effective mirror ratio for the HOT* particles in the Logan-Rensink model is simply the ratio of the choke coil field to the test cell peak field. The injection energy for the HOT* ions is taken to be a functional of the average loss energy of the HOT population (from the Logan-Rensink model for the HOT particles), the COLD temperature and the electrostatic potential, consistent with the models of convective energy flow described below. Particle balance of the HOT* population, yielding the HOT* density, is achieved by balancing the source currents and loss currents for the HOT* population using the confinement parameters ($n\tau$) obtained from the two Logan-Rensink model calculations.

The Logan-Rensink models used above do not take into account the fact that the velocity space loss cone for the particles of interest may be partially filled with other particles. In particular, the loss cone for the HOT* particles is partially filled with COLD passing particles. Multi-region Fokker-Planck models[6] have been used to calibrate the Logan-Rensink models for a single parameter point (electron temperature, passing and trapped density, and trapped ion energy). Work continues to further calibrate the models over a wide range of these parameters.

Energy transfer between the ion populations due to convection of particles from one population to another is also modeled. Detailed knowledge of the energy spectrum of particles crossing a particlular boundary in Fig. E.3-3 requires extensive Fokker-Planck calculations which are not available at this time. To take into account the changes in the net number of particles flowing from one population to another when the electrostatic potential $Q_c$ changes, the distribution of particles on the boundaries is calculated and the flow rate across any point on the boundary is taken proportional to the number of particles at that point. As an example, this model results in an energy source to the cold population due to HOT particles flowing across the HOT - COLD TRAPPED boundary in Fig. E.3-3 at an energy higher than the COLD particle energy.

Other aspects of test cell operation which are modeled include the energy transfer due to drag of the HOT and HOT* particles on the COLD ions and electrons in the ion and electron power balances of the COLD particles. The HOT and HOT* particles are also included in the global charge balance for the device which yields the central cell potential $\phi_e$. In addition, hot alpha effects from alphas born in HOT-HOT and HOT*-HOT* fusion reactions are included. Some fraction of these alphas, after slowing down, also contribute to the equilibrium concentration of thermal alpha ash in the device. The rate at which these alphas are produced and thermalized also affects the alpha pumping requirements for the transition and plug drift pumping systems.

## E.4 Baseline Parameters

The plasma physics models used in this study incorporate several improvements in the understanding of MFTF-$\alpha$+T High-$\Gamma$ mode physics (primarily in the end cell physics) compared with the models employed in Ref. 1. As a result, the physics parameters for a baseline device with approximately the same dimensions and other physical characteristics as in the reference case may be different from the reference values. Comparison of the reference physics values and the current results, for the reference design, serves to benchmark the new models.

The complete list of physics parameters for MFTF-$\alpha$+T is quite lengthy and will not be presented here. Instead, the critical parameters for test cell, central cell and end cell performance and those fundamental parameters which are significantly different between the previous work and present results will be compared. An effort will be made to explain the differences below in terms of the improvements in the physics understanding that have occurred between the two studies. Before proceeding to a parameter-by-parameter comparison of the two studies, some frequently used terminology will be presented. To a great extent, each of the following terms concerns an aspect of the MFTF-$\alpha$+T physics which has changed between the original study and the present work. The following list is organized with the terms which most strongly affect the test cell performance given first.

### E.4.1 Strong Effect

#### E.4.1.1 g and H Factors

Improved calibration of the Futch-Lodestro trapping formulas in the transition regions against Fokker-Planck code results indicates that g (ratio of [passing + trapped] density to passing density) must be greater than or equal to two for transition region resistance to two-stream instabilities. In addition, these results indicate that H (correction factor for non-square well magnetic field shape) is related to g by a scaling law.

#### E.4.1.2 Cutoff

Improved mapping formulas to calculate the passing density at cardinal points in the end cell regions include a cutoff in particle energy, which

depends on the electrostatic confining potential $\phi_c$, above which particles cannot exist in the end cells. For low potentials relative to the central cell temperature, as in MFTF-$\alpha$+T, these formulae produce lower passing densities in the end cell regions.

E.4.1.3 Calibrated ($n\tau$)

Recent calibration of the confinement parameters ($n\tau$) for the hot mirror trapped particles in the test cell from multi-region Fokker-Planck code results indicate that the Logan-Rensink plug model may underestimate the confinement by 50%. A correction coefficient has been used in the present study.

E.4.1.4 COLD Ion Drag

The energy balances for the HOT and HOT* particles have been modified to include drag of these ions on the COLD Maxwellian ions in the central cell and test cell regions. For the low background ion temperatures in MFTF-$\alpha$+T, this term may be comparable to drag on electrons.

E.4.1.5 Convection Terms

As previously described, the energy transfer from one population to another due to particles flowing across the boundaries in velocity space has been modeled, albeit crudely, in the present study.

E.4.2 Moderate Effect

1.4.2.1 Trapping Coefficients

The recent calibrations of the trapping formulas against Fokker-Planck results also indicate that several of the coefficients in the Futch-Lodestro formulas should be modified.

E.4.2.2 Plug Hot Electron Power

Recent calculations of the scattering and drag times for the hot electrons in the plug on the background electron population indicate that only

the drag power is coupled into the background energy balance. Previous models has also included the scattering power.

### E.4.3 Mild Effect

#### E.4.3.1 Alpha Effective Temperature

An effective temperature that is higher than the COLD particle temperature is used for alpha contributions to the central cell beta based on a model of alpha particles slowing down on both the COLD particles and the two hot populations. The temperature of alphas reaching the trapping region in the transition is taken to be the temperature of the COLD Maxwellian population.

#### E.4.3.2 Alpha Scrapeoff in the Halo

The fractions of alpha energy and alpha particles deposited in the halo plasma are calculated consistent with the plasma radius and alpha Larmor radius.

#### E.4.3.3 Charge Exchange

The fractions of test cell neutral beam particles which charge exchange or completely penetrate the test cell plasma are calculated based on a pencil beam model which includes re-ionization of some of the charge exchange neutrals[7].

#### E.4.3.4 First Wall Radius

The first wall in both the test cell and central cell regions is taken to be two alpha Larmor radii away from the edge of the plasma to ensure that alphas born at the plasma edge do not directly bombard the first wall.

Finally, it should be noted that the present model includes a loss channel for the HOT* particles due to pitch angle scattering out of the central cell mirror trap at energies above the electrostatic confining potential. When this occurs, the HOT* particle is lost rapidly from the device (one axial transit time). In the previous model it was assumed that all of the test cell beam particles which were trapped eventually fueled the

COLD Maxwellian population in the central cell. Since some of the HOT* particles leak out in the new model, the need for supplemental fueling of the COLD population, by a pellet injection system or low energy neutral beam line, may be indicated by the present model when it was not shown in Ref. 1. The amount of fueling current required depends on the electrostatic potential so that in cases like the Fusion Power Demonstration (FPD) device the potential may be high enough so that the test cell beam trapped current may be sufficient to completely fuel the COLD population[8].

The baseline parameters for MFTF-$\alpha$+T in High-$\Gamma$ mode from Ref. 1 are given in Table E.4-1. The corresponding parameters using the present models are given in Table E.4-2. In both cases the following physical dimensions and machine parameters are held constant in the test cell, central cell, and end cell regions: 1) mirror-to-mirror and plasma effective lengths; 2) peak and midplane on axis magnetic field values; 3) peak and volume averaged plasma beta values, and 4) the plasma radius at the various cardinal points used in the models. In addition, to benchmark the new physics models most efficiently, the central cell Maxwellian ion temperature, test cell trapped current from the neutral beam injectors, and end cell axial (Pastukhov) confinement parameter ($n\tau$) for the central cell ions have been fixed to the reference values.

Comparison of the parameters in Tables E.4-1. and E.4-2 shows that the current model benchmarks quite well against the reference results provided that the injection energy in the test cell is increased from 60 keV (average) to 83.2 keV. This result is consistent with the inclusion of cold ion drag terms in the energy balances for the hot ion populations in the present calculations. At balance this added power to the test cell ($P_{nb,trap}$ = 15.8 MW compared with 11.4 MW in Ref. 1) results in a higher density and average energy of the HOT mirror trapped population and, therefore, a higher test cell fusion power and wall loading. At fixed test cell and central cell beta the increased HOT ion pressure in the test cell produces a lower electron and HOT* pressure there (and in the central cell) primarily through lower electron temperature. The present results also indicate that particle balance of the cold central cell ion population requires 32.8 amps of supplemental fueling current from a pellet injector or low energy neutral beam system in the central cell. This is consistent with 71.3 amps of Pastukhov end loss of

HOT* ions from the central cell (not considered in the reference model) combined with the reduction of transition region trapping current from 97 amps to 55 amps.

Note that both the increase in test cell injection energy and the central cell supplemental fueling, current requirement are sensitive to the central cell ion temperature and test cell trapped beam current, both of which have been set at the reference values to provide a good benchmark of the present results. Preliminary results using an injection energy of 60 keV with COLD temperature $T_c \simeq 15$ keV indicate that for particle balance in the central cell without supplemental fueling the beam current delivered to the test cell may need to be as high as 300 amps. In addition, this balance has been obtained by lowering the beta values in both the central cell and test cell by 20% from the reference values and requires a g value of 1.3 in the transition region. Finally, some cases have been obtained at higher beta and g values (still lower than the reference values) by lowering the central cell ion temperature. In these cases, the beam current requirement is much larger because the electron temperature has decreased with the ion temperature and confinement (proportional to $T_e^{3/2}$).

Other parameters of the device which are somewhat different in the present study are the end cell passing densities and some of the end cell species energies. The passing densities for ions are lower in all of the end cell regions in the present study due to the cutoff which has been taken into account in the passing density formulas. As a result, for constant beta, the average energies of either the hot ions or hot electrons will increase so that the pressure is the same as in the reference study. In the anchor the hot ion average energy is up to 1.18 MeV (from 0.4 MeV) and in the barrier region the hot electron energy is up to 1.46 MeV (from 0.475 MeV). The required ECRH power in the plug and the required ICRH power in the anchor are all lower in the present study because the major contributions to these powers vary as $n^2E^{-3/2}$ where n is the appropriate particle density and E is the average energy. The required ECRH power in the barrier is higher in the present study because for high hot electron energies the dominant term in this power is due to synchrotron radiation which increases as $\eta E^2$.

Table E.4-1. Baseline Parameters for MFTF-α+T
High-Γ Mode From Reference 1

| | | | | |
|---|---|---|---|---|
| **DT TEST CELL** | | | | |
| $n_{HOT}$ | $4.75 \times 10^{14} cm^{-3}$ | | $P_{FUS,TC}$ | 11.0 MW |
| $E_{HOT}$ | 40 keV | $r_p$ | 15.0 cm | |
| $T_{ec}$ | 7 keV | $r_{WALL}$ | 25.0 cm | |
| $\phi_e$ | 47 kV | $\Gamma_{TC}$ | $2.0\ MW/m^2$ | |
| $\phi_c$ | 22 kV | $I_{TRAP,TC}/I_{TC}$ | 190 A/240 A | |
| $(n\tau)_{LOCAL}$ | $2.0 \times 10^{13} cm^{-3} s$ | | $P_{NB,TRAP}/P_{NB}$ | 11.4 MW/14.4 MW |
| $\langle\sigma v\rangle_{DT}$ | $6.6 \times 10^{-16} cm^3/s$ | | $E_{INJ}$ | 60 keV |
| $\Delta\phi_{TC}$ | 8.0 kV | $\theta_{INJ}$ | $75^o$ | |
| $\hat{\beta}_{TC}$ (PEAK) | 0.46 | | | |
| **CENTRAL CELL** | | | | |
| $n_c$ | $1.3 \times 10^{14} cm^{-3}$ | | $r_c$ | 25.0 cm |
| $n_{ec}$ | $1.6 \times 10^{14} cm^{-3}$ | | $r_{WALL}$ | 45.0 cm |
| $n_{HOT*}$ | $3.0 \times 10^{13} cm^{-3}$ | | $P_{FUS}$ | 5.9 MW |
| $T_c$ | 15.0 keV | $\Gamma$ | $0.14\ MW/m^2$ | |
| $T_{ec}$ | 7.0 keV | $C_\alpha$ | NEGLIGIBLE | |
| $E_H^*$ | 20.0 keV | $I_{c,PAST}$ | 90.0 A | |
| $\phi_{ic}$ | 30.0 kV | $I_{HOT*,PAST}$ | 0.0 A | |
| $\phi_{ec}$ | 39.0 kV | $I_{FUEL,COLD}$ | 0.0 A | |
| $\beta_c$ (PEAK) | 0.60 | | | |

Table E.4-1. Baseline Parameters for MFTF-α+T
High-Γ Mode From Reference 1 (Cont'd)

| | | | | |
|---|---|---|---|---|
| **ANCHOR** | | | | |
| $n_{PASS,ANC}$ | $7.75 \times 10^{12} cm^{-3}$ | | $E_{HOT,ANC}$ | 400 keV |
| $n_{HOT,ANC}$ | $2.4 \times 10^{13} cm^{-3}$ | | $P_{ICRH}$ | 1.14 MW (TOTAL) |
| **TRANSITION** | | | | |
| $I_{TRAP}$ | 97 A | $n_{PASS,t}$ | $1.2 \times 10^{13} cm^{-3}$ | |
| $I_{Neo}$ | 3 A | $g_{DT}$ | 1.7 | |
| $\delta\phi_t$ | 10 kV | $H_{DT}$ | 0.333 | |
| **PLUG/BARRIER** | | | | |
| $n_{PASS}(b)$ | $3.0 \times 10^{12} cm^{-3}$ | | $P_{ECRH,b}$ | 1.08 MW (TOTAL) |
| n(b) | $1.2 \times 10^{13} cm^{-3}$ | | $P_{ECRH,a}$ | 0.12 MW (TOTAL) |
| g | 1.7 | $T_{ew}$ | 60 keV | |
| G | 4.0 | $\delta\phi_{a' \to a}$ | 37 kV | |
| n(a) | $2.3 \times 10^{13} cm^{-3}$ | | $\delta\phi_a$ | 60 kV |
| $E_{eH}$ | 475 keV | $n_{SLOSH}/n(b)$ | 3.3 | |

Table E.4-2. Baseline Parameters for MFTF-α+T High-Γ Mode From Present Models

| | | | | |
|---|---|---|---|---|
| **DT TEST CELL** | | | | |
| $n_{HOT}$ | $5.08 \times 10^{14} cm^{-3}$ | | $P_{FUS,TC}$ | 14.6 MW |
| $E_{HOT}$ | 41.8 keV | $r_p$ | 15.0 cm | |
| $T_{ec}$ | 6.36 keV | $r_{WALL}$ | 27.0 cm | |
| $\phi_e$ | 46.8 kV | $\Gamma_{TC}$ | $2.46 MW/m^2$ | |
| $\Gamma_c$ | 23.4 kV | $I_{TRAP,TC}/I_{TC}$ | | 190 A/217 A |
| $(n\tau)_{LOCAL}$ | $2.76 \times 10^{13} cm^{-3}s$ | | $P_{NB,TC}/P_{NB}$ | 15.8 MW/18.1 MW |
| $\langle\sigma v\rangle_{DT}$ | $7.49 \times 10^{-16} cm^3/s$ | | $E_{INJ}$ | 83.2 keV |
| $\delta\phi_{TC}$ | 8.3 kV | $\theta_{INJ}$ | 75° | |
| $\hat{\beta}_{TC(PEAK)}$ | 0.46 | | | |
| **CENTRAL CELL** | | | | |
| $n_c$ | $1.49 \times 10^{14} cm^{-3}$ | | $r_c$ | 26.1 cm |
| $n_{ec}$ | $1.67 \times 10^{14} cm^{-3}$ | | $r_{WALL}$ | 59.8 cm |
| $n^*_{HOT}$ | $1.73 \times 10^{13} CM^{-3}$ | | $P_{FUS}$ | 6.11 MW |
| $T_C$ | 15.0 keV | $\Gamma$ | $0.14 MW/m^2$ | |
| $T_{ec}$ | 6.36 keV | $C_\alpha$ | $1.7 \times 10^{-3}$ | |
| $E^*_H$ | 36.2 keV | $I_{c,PAST}$ | 93.7 A | |
| $\phi_{ic}$ | 31.7 kV | $I_{HOT*,PAST}$ | 71.3 A | |
| $\Gamma_{ec}$ | 38.5 kV | $I_{FUEL,\ COLD}$ | 32.8 A | |
| $\hat{\beta}_{c(PEAK)}$ | 0.60 | | | |

Table E.4-2. Baseline Parameters for MFTF-α+T
High-Γ Mode From Present Modes (Cont'd)

| | | | | |
|---|---|---|---|---|
| ANCHOR | | | | |
| $n_{PASS,ANC}$ | | $E_{HOT,ANC}$ | 1181 keV | |
| $n_{HOT,ANC}$ | $1.07 \times 10^{13} cm^{-3}$ | $P_{ICRH}$ | | 0.583 MW (TOTAL) |
| TRANSITION | | | | |
| $I_{TRAP}$ | 55 A | $n_{PASS,t}$ | $3.58 \times 10^{12} cm^{-3}$ | |
| $I_{Neo}$ | 0.83 A | $g_{DT}$ | 1.62 | |
| $\delta\phi_t$ | 21.3 kV | $H_{DT}$ | 1.31 | |
| PLUG/BARRIER | | | | |
| $n_{PASS}(b)$ | $1.39 \times 10^{12} cm^{-3}$ | $P_{ECRH,b}$ | | 1.56 MW (TOTAL) |
| n(b) | $5.02 \times 10^{12} cm^{-3}$ | $P_{ECRH,a}$ | | 0.06 MW (TOTAL) |
| g | 1.62 | $T_{ew}$ | 25.2 keV | |
| G | 3.62 | $\delta\phi_{a' \to a}$ | 47.2 kV | |
| n(a) | $7.44 \times 10^{12} cm^{-3}$ | $\delta\phi_a$ | | 68.1 kV |
| $E_{eH}$ | 1463 keV | $n_{SLOSH}/n(b)$ | 2.68 | |

Another area showing some differences is in the transition region where the trapping current (that current which the drift pump coils must pump out of the device) is down to 55 A (from 97 A). The present study uses an H-factor which is 4 times greater than the reference calculation, which would tend to increase the trapping current. However, since this current is proportional to the square of the passing density in the transition region, the effect of the cutoff is to produce lower trapping current.

Finally, the first wall radius in the present study is taken to be two alphas Larmor radii away from the edge of the plasma in both the test cell and central cell to avoid direct bombardment of the surface by hot alpha particles. This may be overly conservative in the central cell where the alpha production rate and equilibrium concentration are low. If the central cell first wall were brought in to 45 cm, as in the reference study, the increased fusion power in the central cell, $P_{FUS}$ = 6.11 MW compared with 5.9 MW, would also result in higher wall loading there.

## References for Appendix E


1. Thomassen, K. I., and Doggett, J. N. eds., "Options to Upgrade the Mirror Fusion Test Facility," Lawrence Livermore National Laboratory, UCID-19743, April 1983.

2. Campbell, R. B., "TMRBAR - A Code to Calculate Plasma Parameters for Tandem Mirror Reactors Operating in the MARS Mode," Lawrence Livermore National Laboratory, UCID-19875 Aug. 1983.

3. Bulmer, R. H., Private communication.

4. Carlson G. A., et al., "Tandem Mirror Reactor with Thermal Barriers," Lawrence Livermore National Laboratory, UCRL-52836, Sept. 1979, pp. 48-50.

5. Logan, B. G., Mirin, A. A., and Rensink, M. E., "An Analytic Model for Classical Confinement in Tandem Mirror Plugs," Nuc. Fus. 20, 1613 (1980).

6. Matsuda, Y. and Stewart, J. J., in Proceedings of the Tenth Conference on Numberical Solutions of Plasmas, San Diego Jan. 4-6, 1983 (GA Technologies, Inc., San Diego 1983) paper 2B8.

7. Carlson, G. A. and Hamilton, G. W., "Wall Bombardment Due to Charge Exchange of Injected Neutrals into a Fusion Plasma," Lawrence Livermore National Laboratory, UCRL-75306, April 1974.

8. Haney, S. W. and Fenstermacher, M. E., "Test Cell Modeling and Optimization for FPD-II," (UCID to be published).

# APPENDIX F

## SMALL SCALE, MULTIPLE EFFECTS TESTING AT US/DOE BREEDER REACTOR IN-PILE FACILITIES

TABLE OF CONTENTS


| | | Page |
|---|---|---|
| F.1 | Introduction | F-1 |
| F.2 | Aims and Expectations | F-1 |
| F.3 | Cost in Money and Time | F-3 |
| F.4 | Strategy for Facility Use | F-4 |
| F.5 | Breeder Reactor In-Pile Test Facilities | F-5 |
| | F.5.1 EBR-II Instrumented Subassemblies | F-5 |
| | F.5.2 FFTF Test Subssemblies | F-7 |
| | F.5.3 TREAT | F-8 |
| | F.5.4 FNEL and FFTF Remote Handling Capability | F-11 |
| F.6. | Fusion Experiments in Breeder Reactor Facilities | F-13 |
| | F.6.1 General Features | F-13 |
| | F.6.2 EBR-II | F-14 |
| | F.6.3 FFTF | F-15 |
| | F.6.4 TREAT | F-16 |
| F.7 | Conclusions | F-17 |
| F.8 | References | F-18 |

# APPENDIX F. SMALL SCALE, MULTIPLE EFFECTS TESTING AT US/DOE BREEDER REACTOR IN-PILE FACILITIES

## F.1 Introduction

It is anticipated that many U.S. in-pile testing facilities currently with main missions in support of the fission breeder reactor program could well play a significant role in fusion technology development. In fact, fusion materials irradiation is already taking place at these facilities in parallel with other activities. However, it is the aim of this present discussion to propose in a general way a wider, future role for these facilities in fusion research that could help bridge the gap between simple materials testing and testing full scale (or true act-alike) components. Full use could then be made of the existing capabilities for integral test design, instrumentation and analysis as well as considerable experience in technology development accrued from the fission reactor program.

In-pile multiple effects testing at the Experimental Breeder Reactor-II (EBR-II), the Fast Flux Test Facility (FFTF), and the Transient Reactor Test Facility (TREAT) will be discussed. EBR-II and FFTF are both sodium cooled fast breeder reactors with individual subassemblies available for instrumented and controlled experiments. TREAT is an air cooled pulse reactor with a single, large test hole at its center for instrumented and controlled transient experiments. Features of these facilities relevant to test vehicle and experiment design will be described under the conservative assumption of no major facility alterations. Illustrative fusion test concepts will be given from a facility perspective which dovetail with those from other perspectives given elsewhere in the interim report, e.g., Chapter 12.

## F.2 Aims and Expectations

The breeder reactor facilities described here have the capapabilities of providing intense neutron and/or ionizing radiation fields in test volumes within a fission reactor core. The testing arrangements of interest are those that are primarily intended for fairly sophisticated, integral, multiple effects tests. Special arrangements exist so that experiments (which are isolated from the experimenter) can be well instrumented with away-from-

reactor capabilities for both real time data recording and experiment control. Maximum test dimensions are large by the standards of materials testing but small with respect to full scale components in fusion.

Based on fission program experience and anticipated fusion program needs, a reasonable aim in using these facilities would be to perform experiment simulations that lie within a scope of testing that overlaps the notions of "element" and "module" testing in a nuclear environment. Part of a full component could be simulated, and information on interactions of subcomponents (both qualitative and quantitative) could be generated. Experiments could be designed to test multiple effects or issues (including their interactions). Emphasis is most reasonably placed on enhancing the level of understanding, model development, and predictive ability relative to those issues and phenomena most critical to the engineering of the fusion machine.

It is not likely that testing full scale or true act-alike component behavior will be possible in these facilities. Priorities will have to be set to decide which conditions are the most useful out of those conditions which are achievable to best simulate the features of the fusion environment that are most important to test. To set these priorities fusion component modeling and experiment design and analysis will develop interactively. On one hand extrapolation of test results to the fusion environment will place considerable reliance on analysis. On the other hand development of the analytical tools themselves, will make strong use of "families" of experiments which will include not only in-pile series of tests that span useful ranges of key test conditions, but also related tests performed in other environments.

Thus, the envisioned test program that makes full use of breeder reactor facilities requires also a full-scale analytical program as well as integration within the fusion testing program as a whole. While these requirements might, at first thought, seem like an additional burden, in fact they will, if met, probably prove to be one of the program's strongest assets. In the fission program achieving defensible "act-alike" behavior in experiment modules has proven to be extremely elusive, despite the fact that a "unit cell" in a fission reactor is for many purposes as small as a single fuel pin. The essential difficulty with a purely "act-alike" philosophy is in not knowing a priori the sensitivity of the studied behavior to even the smallest changes in reference design, materials or conditions. By contrast, analytical models,

developed and supported through experiments, as suggested here for the fusion program, will prove very versatile and provide very powerful means of addressing technological issues.

## F.3 Cost in Money and Time

In the absence of any major facility modifications (an assumption) the cost of doing small scale, multiple effects experiments in the studied facilities can be roughly estimated to be the same as fission program experiments of similar sophistication. Costs for manpower and hardware are comparable to each other. Manpower costs include a facility safety analysis as well as experiment planning and analysis. Significant labor is involved in transporting and manipulating irradiated experimental devices (both pre- and post-test). Some, but probably not all irradiated hardware may be reusable. Calibration tests to determine the neutronic coupling of test materials to the reactor will probably be necessary for each series of tests involving similar configurations. If many experiments of the same type are run, experience at EBR-II and TREAT indicates a cost of about $1 M per experiment. One-of-a-kind or first-of-a-series tests are more expensive. The cost of testing at FFTF can be considered comparable to EBR-II and TREAT. In addition, for experiments containing only non-fissile materials, the initial preparation of a closed loop and experiment in FFTF could be accomplished for approximately $5 M. These cost estimates are not given so much for budgeting purposes as they are for contrast between simple in-pile materials test costs ($.01 M-$.1 M) and full-scale components test costs at a projected fusion test facility (many $ M).

If again guided by experience with fission program tests of similar sophistication, a lead time of one or more years is anticipated for planning, hardware construction, and test set-up. Test planning, the facility safety analysis, and the transporting/manipulation of irradiated experiment devices (both pre- and post-test) account for significant amounts of lead time. Again, this figure falls in between the lead times for testing simple materials and that projected for full scale components.

The individual testing facilities will be described in more detail later on, but it is worth noting here that a single experiment should not fully occupy a facility. In EBR-II and FFTF an experiment occupies only a single

subassembly of the reactor core so additional activities and experiments can procede in parallel. At TREAT there is only one test hole. But being a transient testing facility, different experiments can be rapidly swapped in and out.

## F.4 Strategy for Facility Use

Given constraints of money and time a strategy for optimal facility use will be needed. Also the "lifespan" and urgency of issues need to be considered in making experiments with long lead times sufficiently flexible as to be useful. The following "strategy" as learned from the fission program addresses these questions and was assumed implicitly in the preceeding cost estimates.

The test vehicle is the "empty" structure that contains the experiment and interfaces with both the reactor and away-from-reactor data collection and experiment control systems. The design of the test vehicle should have an anticipated useful lifespan of many experiments (decades) and should be flexible enough to contain many different experiments. (Note that the desired long lifespan refers to the design not to the individual piece of hardware.) Since the bulk of the facility safety analysis will be concerned with test vehicle performance and integrity, the time spent per experiment on this activity will be minimized. Additionally, time spent in analyzing or calibrating an experiment placed in a familiar, well-characterized test vehicle will also be minimal.

The design of the individual experiment to fit within the generic test vehicle described above may then procede with the minimum of lead time to address the most pressing technological issues. Families or series of tests with closely related appearance and objectives are desirable both from the point of view of model development and economics. The economies that arise from employing similar configurations of materials in many tests will still be very significant even if individual test objectives turn out to be very different.

Finally, if the issues to be tested are sufficiently short-lived or volatile, experiments may be designed to defer final decisions about test conditions until very late in test planning. While this situation is not yet anticipated in fusion, many safety issues in fission technology required this sort of flexibility in testing.

## F.5 Breeder Reactor In-Pile Test Facilities

### F.5.1 EBR-II Instrumented Subassemblies

EBR-II is a small, experimental liquid sodium cooled fast breeder reactor located at the Idaho National Engineering Laboratory (INEL). Almost from its first generation of power in the mid 1960's EBR-II has served as an in-pile irradiation facility in parallel with its other missions in the breeder reactor program. Developments in the course of its lifetime and the breeder reactor program as a whole have been in the direction of experiment irradiations becoming both more sophisticated and a greater part of the facility's mission.

EBR-II employs the pool concept of reactor design whereby the reactor core, reflector, blanket, primary sodium pumps, pipes, heat exchangers, and fuel handling equipment are completely submersed in the molten sodium of the reactor core. The pool design would make any major modification of the facility for other use very difficult, and indeed imposes significant constraints on concepts of experimental test vehicles to be placed in-pile. Test vehicles requiring instrumentation or control are accomodated in EBR-II as a substitute for a control rod and some associated hardware. This method allows tests leads to pass out upward through control rod penetrations in the reactor vessel cover, and allows for the mechanical means of manipulating the test vehicle. Outer dimensions in the horizontal plane of any test vehicle are thus constrained to be slightly smaller than the standard EBR-II subassembly (hexagonal- 5.8 cm flat-to-flat). Vertical dimensions are much less constrained, there being 6 m within the 370 deg-C sodium pool and nearly 3 m more available to the top of the control rod lifting platform. However, high neutron flux is available only for the 34 cm reactor core height. Cooling of test samples is possible principally through direct contact with or heat exchange with sodium from the core.

Since about 1970 a variety of such test vehicles have been in use at EBR-II, differing principally in types of instrumentation, characteristics of the experiment layout, and the means by which test articles are inserted or removed. Fig. F-1 shows a schematic of one such vehicle, the BFTF (breached fuel test facility), including a representative experiment. In the example

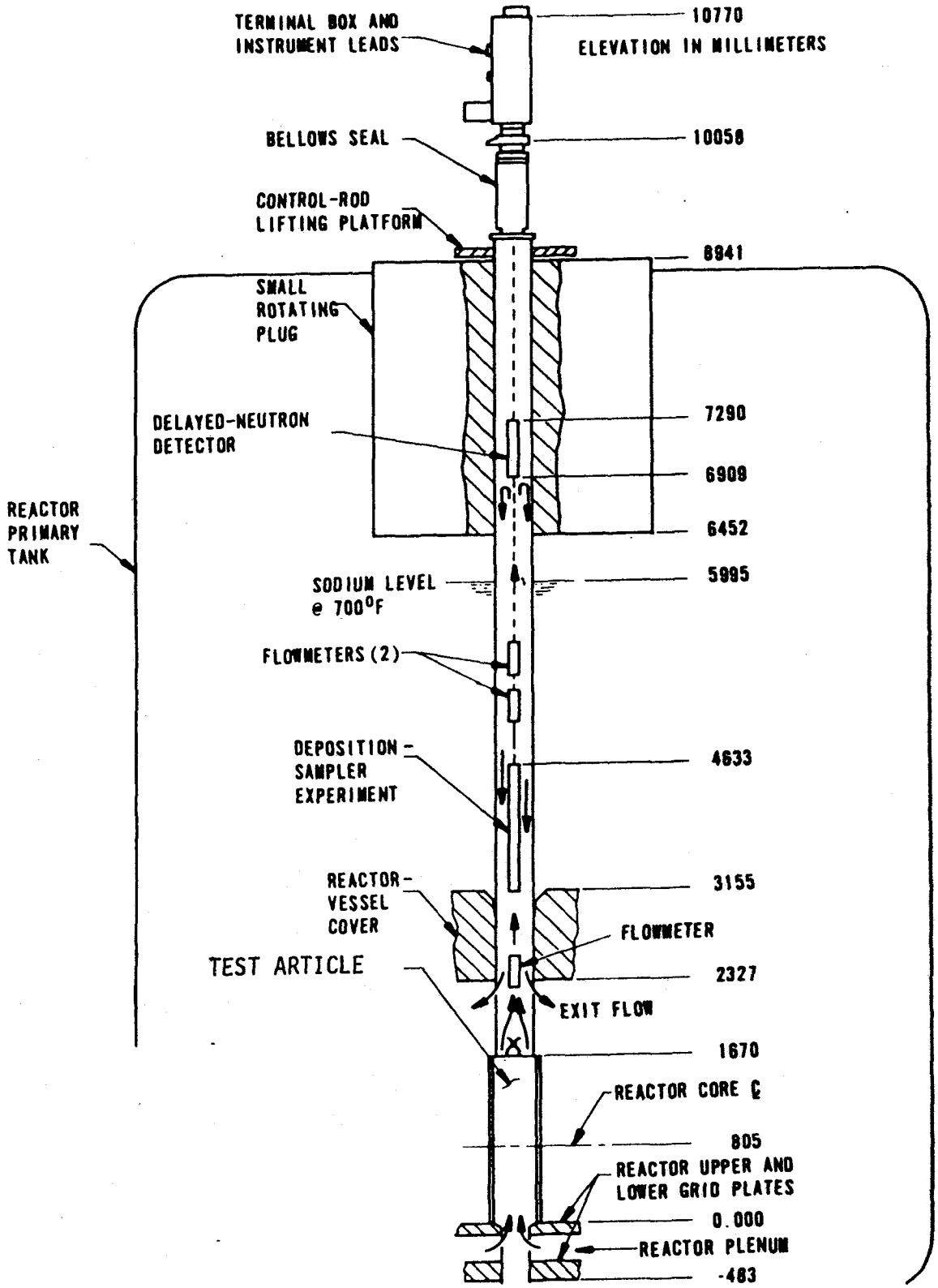


Figure F-1 EBR-II BFTF typical experiment configuration.

shown liquid sodium flows past fissioning, failed reactor fuel, followed downstream by instrumentation to study deposition and mobility of failed fuel debris. In order to study deposition during a long irradiation period this test vehicle features a remove-from-above instrument "stalk" containing the debris samplers.

Additional data concerning the EBR-II neutron and thermal environment at test vehicle locations as well as general features and constraints governing test vehicles are given and compared to that of the other breeder reactor facilities in Table 1.

F.5.2 FFTF Test Subassemblies

FFTF, like EBR-II, is a liquid sodium cooled fast breeder reactor but with a much larger core and power output; the core is 91 cm high. Coming into service in 1980 at the Hanford Engineering Development Laboratory (HEDL), its primary mission is that of a fast neutron flux irradiation test bed for full-scale fast reactor fuels, materials and components testing. The FFTF was designed as a testing facility and hence has considerable capability for a broad spectrum of testing. Unlike EBR-II, the FFTF reactor incorporates a loop design in which sodium coolant "loops" sequentially from the core to a pump to a heat exchanger and back again. For present purposes this loop system has advantages over the pool type design used in EBR-II in allowing components to be isolated from one another, leading to easier sub-system instrumentation and modifications.

Like EBR-II, the FFTF core is made up of hexagonal subassemblies, though much larger (11.1 cm flat-to-flat). An instrument tree positions thermocouples over most positions to measure outlet flow and temperature. Within core physics constraints, these positions are available for irradiation testing. The large subassembly cross section provides sufficient volume to perform relatively complex interactive effects tests. In addition to these "non-instrumented" positions, the current core configuration provides for eight fully instrumented assemblies. These assemblies occupy positions between those containing instrument trees and provide a method to bring test instrument and control lines out of the core.

One example of present testing capability is the Material Open Test Assembly (MOTA). This assembly currently carries the entire national breeder

duct and cladding materials irradiation program, as well as fusion and space reactor materials. It contains 48 specimen-carrying capsules, each instrumented with a thermocouple. Additionally, 30 of the capsules are tied to a temperature control system. Conceptual designs have been generated for solid breeder testing, including thermocouple, purge gas, and tritium monitoring devices within the vehicle.

Even greater test capability can be realized in FFTF through the use of the Closed Loop Irradiation Assemblies (CLIRA's). CLIRA's are primarily targeted here as potential test vehicles for very sophisticated integral, multiple effects tests. The CLIRA's are not yet opperational at FFTF, but a schematic is shown in Fig. F-2. Each CLIRA will have a complete cooling system, including primary loops, secondary loops, and heat exchangers that are completely independent of the FFTF main heat transport system. The in-reactor portion of the CLIRA can accommodate instrumented test articles of outer diameter up to 7 cm and 3.6 m high. High neutron flux is available for the 91 cm of in-core height. Current designs envision the possibility of changing instrumentation during interim test examinations. The unique feature of the CLIRA concept is the fact that the closed loop system transports coolant from in-pile to away-from-reactor locations where elaborate measurement and/or processing is feasible, including for example: sampling, analysis, purification, and heat exchange. The steady-state heat removal capability of a CLIRA is designed to be as high as 2 MW.

Additional data concerning the FFTF neutron and thermal environment at test vehicle locations along with other features and constraints are given and compared to that of the other breeder reactor facilities in Table F-1.

### F.5.3 TREAT

TREAT is a graphite moderated "pulse" reactor located at the INEL site near EBR-II. While air-cooling provides a limited steady-state capability, TREAT is best known for its operations in a transient mode. TREAT has been in service since 1959 with in-pile transient testing of breeder reactor fuel as its primary mission. Improvements made in the 1970's make computer controlled, shaped power transients possible. A further upgrade of TREAT's core and capabilities is currently underway which, when completed, will provide a larger test hole, facilities for larger test vehicles, and a "harder" (epithermal) incident neutron spectrum.

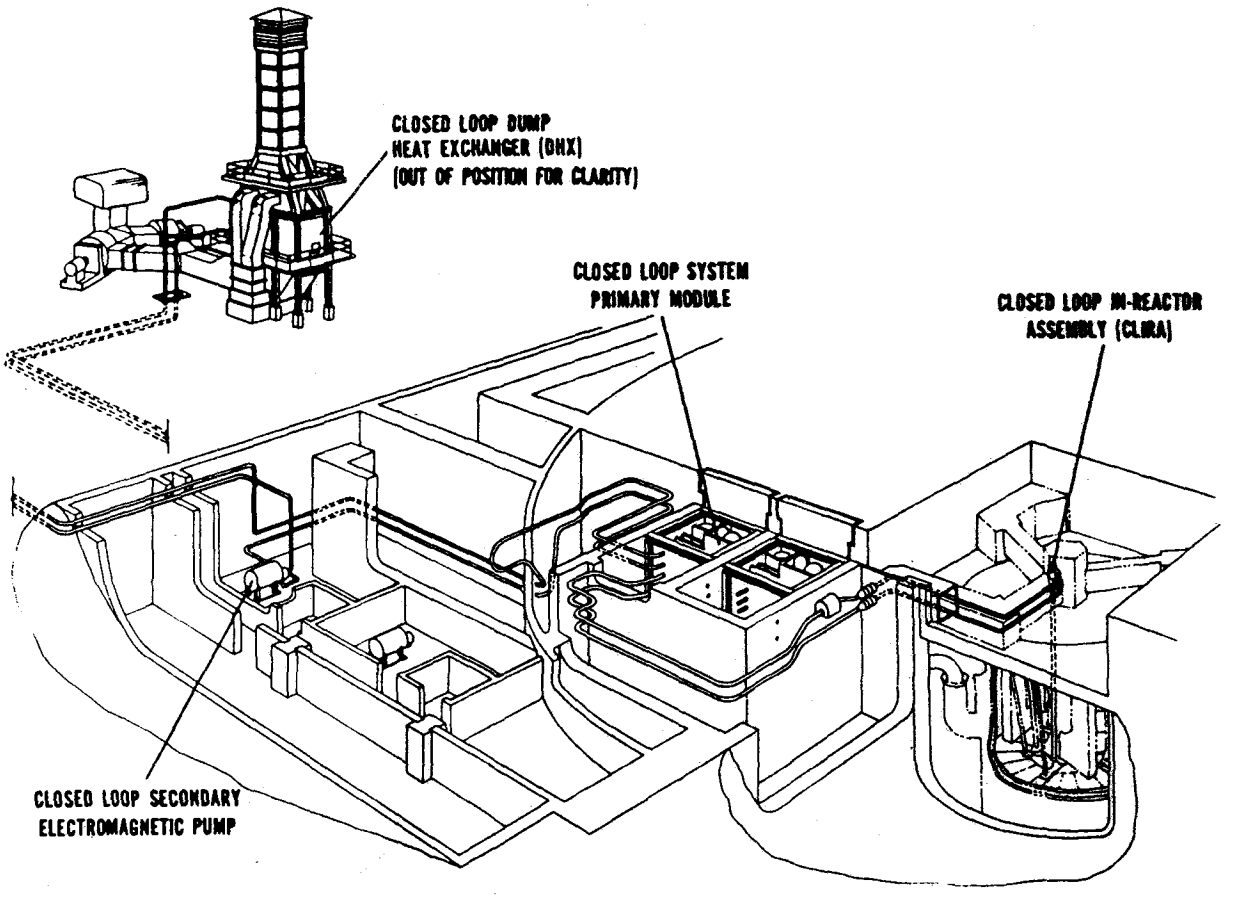


Figure F-2 FFTF CLIRA closed loop system.

Table F-1 Testing Environment in US/DOE Breeder Reactor Facilities

| | | EBR-II | FFTF | TREAT |
|---|---|---|---|---|
| nuclear: | peak flux ($n/cm^2$-s) | $2x10^{15}$ (fast) | $7x10^{15}$ (fast) | ~$8x10^{16}$ (thermal) |
| | max. fluence ($n/cm^2$) | unlimited | unlimited | ~$1x10^{16}$ (thermal) |
| | core height (cm) | 34 | 91 | 122 (present)<br>152 (after upgrade) |
| geometry: | test vehicle | (variety) | (variety), especially CLIRA | (variety) |
| | cross section | hex, 5.8 cm flat-to-flat (outer dimension of test vehicle) | hex, 11.1 cm flat-to-flat (outer dimension of test vehicle) | 10 cm x 20 cm (present)<br>20 cm diameter (upgrade) (outer dimension of test vehicle) |
| | height of experiment (cm) | 900 | 366 (in reactor portion only) | 800 |
| thermal: | ambient temperature (°C) | 370-473 (pool temperature inlet to outlet) | 360-527 (core temperature inlet to outlet) | 20-600 reactor cooling air from beginning to end of transient |
| | test vehicle cooling | heat exchange with pool sodium or independent | heat exchanger with bulk coolant or 2 MW independent loop | independent, self contained system |

transient

The reactor core is a stack of solid rectangular blocks containing a mixture of uranium and graphite as fuel and moderator. Removal of some of these blocks allows for a fairly large in-pile test hole at the center of the reactor to accomodate test vehicles. The maximum size of the test-hole cross section is limited primarily by neutronic considerations. Current test hole dimensions in the horizontal plane are 10 cm x 20 cm, at present, to be enlarged to ~20 cm circular inner diameter in the upgrade. The active core height is 122 cm, at present, to be enlarged to 152 cm in the upgrade. The core may also be "slotted" to view in real time events taking place within the test vehicle by either photographic or nuclear imaging techniques. (At present a fast neutron hodoscope is used to track the motion of fissioning test fuel.)

A wide variety of test vehicles have been used for tests in the TREAT reactor. All are totally separated from reactor components and are easily loaded into and removed from the reactor. Figure F-3 shows, for example, the advanced TREAT loop, slated for use in the upgraded core. This highly instrumented test vehicle includes a self-contained cooling system that circulates liquid sodium through a test pin bundle. Note that Fig. 3 indicates modification of the reactor's thermal neutron spectrum through neutron filters, a device that would probably be useful in fusion work.

Additional data concerning the TREAT neutron and thermal environment at the test hole location along with other test vehicle features and constraints are given and compared to that of the other breeder reactor facilities in Table F-1.

### F.5.4 INEL and FFTF Remote Handling Capability

Support for experiments to be performed at any of the above breeder reactor facilities exists at a multitude of US/DOE laboratories. However, special mention should be made of facilities at INEL and FFTF with capability of remote handling, assembling, and dismantling large irradiated test vehicles and experiments in-cell. HFEF (Hot Fuel Examination Facility) is located at the INEL site and has been used routinely for in-pile experiments performed at both EBR-II and TREAT. Noteworthy features include both air-filled and argon-filled cells. Capabilities exist for precision physical measurements in-cell, as well as neutron radiography, and gamma scanning. Facilities for remote

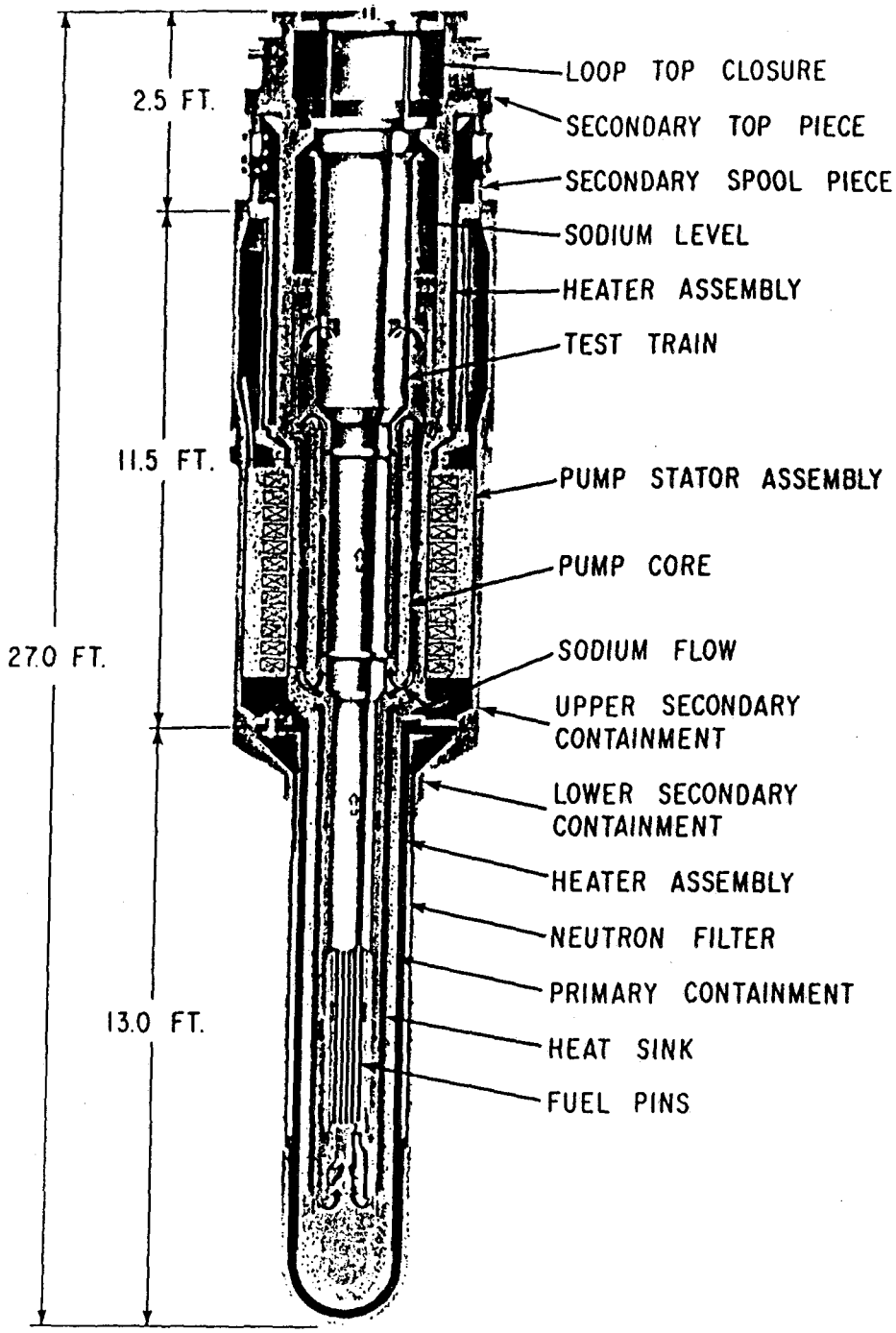


Figure F-3 Advanced Treat Loop (ATL) set-up for testing fuel pins in the upgraded TREAT reactor.

handling also exist at the FFTF complex. The Interim Examination and Maintenance (IEM) argon cell is equipped with a variety of remote handling devices and manipulators and is currently used for test assemblies removed from the reactor. Another FFTF facility, the Shielded Materials Facility (SMF), provides additional capability. Within this large hot cell complex, capability exists for precision specimen measurements, as well as large assembly and disassembly operations.

## F.6 Fusion Experiments in Breeder Reactor Facilities

### F.6.1 General Features

Present investigations, described elsewhere in the FINESSE interim report, point toward fission facilities being potentially very useful in testing certain issues and effects. Fusion materials testing is already underway in fission facilities, but attention in the future will be directed toward multiple effects testing. For solid breeder and blankets interactive material effects, thermal hydraulics and corrosion, and tritium permeation/-containment have been identified as relevent issues. For liquid metal breeders irradiation induced corrosion and embrittlement are effects identified as important to test in a neutron field. The response of instruments and control systems as well as the response of structure and failure modes to intense neutron fields are also deemed important. This rough summary of fusion issues appropriate for testing in fission reactors will, of course, change in time.

In seriously evaluating the strengths and weaknesses of breeder reactor in-pile testing facilities in the service of fusion program it will become evident that many individual limitations or non-prototypic features can be overcome. However, when this is done, some price is often paid in degrading some other aspect of the test. For example; fixing an incident fission neutron spectrum to produce heat distribution more prototypic of that produced in a fusion machine might be possible only by selective absorption of part of the neutron spectrum and at the expense of reducing the total heating rate. Thus, while some decisions concerning experiments and facilities may be fairly straightforward, it is anticipated that many, if not most, will reduce to an evaluation of "trade-offs" as to what features of a given experiment can be

modeled without the experiment, what features are most important to produce in the experiment, and what fusion issues are currently the most crucial. Hence, all such evaluations that are made here will be subject to change as fusion technology advances.

With these qualifications and considerations in mind, all three of the described facilities exhibit certain generic advantages. The expertise and equipment to perform sophisticated, well-instrumented, integral tests exists; so cost and lead time relative to a new facility would be minimal. Sophisticated support facilities capable of dealing with irradiated equipment and material are readily available. If dealing with liquid metal issues, liquid metal technology abounds.

Generic disadvantages are also identifiable. If the neutron spectrum is important, experiments at all three facilities must suffer the fission spectrum. Steps taken to modify the spectrum may improve some particular features, but never accurately produce a true fusion spectrum. With the possible exception of TREAT the test holes in all three facilities tend to be small with respect to typical test article dimensions as identified in other FINESSE analyses. Although present FINESSE analsyes have not indicated strong need for experiments involving both neutron and magnetic fields, if desired in the future, small test holes will make production of high magnetic fields in-pile rather difficult. In fact, any magnetic field desired in an EBR-II or FFTF experiment would probably be generated by a small permanent magnet. Because of a strong preoccupation with safety at fission facilities, a stringent facility safety analysis will be required of all experiments.

### F.6.2 EBR-II

Particular advantages to be had in performing experiments in EBR-II include a relatively hard fission neutron spectrum and virtually unlimited fluence. If a liquid metal breeder test is envisioned, the EBR-II liquid sodium coolant is a candidate substitute or, at least, a compatable material. On the other hand, multiple effects experiments in EBR-II are handicapped by the short core height and fairly small subassembly dimensions. Tests on water-cooled modules would have to overcome a significant incompatability problem with the reactor's sodium coolant. Because the test vehicle and article are in at least good thermal contact with the sodium from the whole reactor pool, precise temperature control of experiments may be difficult.

The sample EBR-II test vehicle and experiment shown in Fig. 1 has many features that could be representative of a typical wall, breeder, or blanket integral experiment in the fusion program. In particular, it depicts coolant flowing past a module being irradiated in the neutron field, where the coolant is subject to both continuous and periodic (through removable deposition samplers) analysis. Other arrangements of test modules and instrumentation are available with alternative test vehicles. Although Fig. 1 shows the module's coolant as sodium from the EBR-II pool, there is no such restriction in principle. An independently circulating system could be devised including, if desired, heat exchange with the sodium pool. Opportunities also exist for controlled variation of applied neutron flux with time to simulate, for example, possible periodicity in fusion reactor "burns". One way this is possible is through a limited power transient capability of the reactor. However, without altering the reactor power the test flux may also be changed with time by moving the test vehicle to another subassembly location in the core, or possibly by using the test vehicle removal/insertion mechanism to move the experiment in and out of core as it would a control rod. (In the latter case the experiment would have to be designed so that such movement would not neutronically disturb reactor operations.)

### F.6.3 FFTF

The neutron flux in FFTF is approximately three times that in EBR-II and the spectrum is just slightly softer. Possible test vehicle cross sections are considerably larger (four times the area), and the active core height is much larger (approximately three times). These features make FFTF a likely choice for some of the larger multiple effects experiments. The cross section is too small, however, for the larger submodule tests. In open test assembly postions reactor coolant flows past the experiment. As with EBR-II, precise temperature control of experiments may pose a problem. However, the CLIRA loops, when operational, have a unique advantage of separate cooling loops with away-from-reactor coolant monitoring and sampling. Test modules that are water cooled will need to take account of incompatability with the reactor's sodium coolant. The fact that a CLIRA is not yet operational is a disadvantage in the present that will become less significant in the longer term.

One obvious use of a CLIRA in the fusion program would be some sort of corrosion, or debris producing test on wall, breeder, or blanket modules. The away-from-reactor coolant analysis feature would permit a far more elaborate real-time, close monitoring of a coolant stream than could be possible in any of the other described facilities. In fact, if desired, away-from-reactor coolant processing concepts could be tested sumultaneously with the generation of corrosion products or debris in the neutron field. The fact that the CLIRA assembly is insulated from the bulk reactor coolant may also provide the opportunity to test materials and components at lower temperatures than available in the open positions.

F.6.4 TREAT

An obvious use of TREAT capabilities is in experiments where both transient behavior and a neutron field are desirable. Not only can transient behavior be driven by controlled power pulses but also the possibility exists for observing transient behavior in real time through both instrumentation as well as various imaging techniques. Alternatively, TREAT will also be useful in situations where dependence upon neutron flux rather than fluence is of prime interest. The TREAT test hole, especially after the upgrade is complete, can be large enough to contain reasonably sized modules, including, if the need existed, fully controllable magnetic fields. While the TREAT reactor produces a softer (thermal, epithermal after upgrade) neutron flux than does EBR-II or FFTF, its principal limitation, as described in Table 1, is in total irradiation fluence. This restriction limits transients to the equivalent fluence of only a few tens of seconds at full fission reactor power.

As identifiable in the present study, safety experiments designed to follow the generation and pathways of tritium release in a transient mode could make good use of simultaneous tritium production and heat generation taking place in a neutron field. Test vehicles such as shown in Fig. 3 or, alternatively, vehicles in which coolant passes through the test module only once could be used to study tritium release in real time. If desirable, materials which are not particularly radioactive could be "seeded" with tracers so their locations could also be monitored in real time. Components of test modules could be pre-damaged at any fluence level desired by pre-irradiation in a steady state high-fluence facility.

A second group of tests that would make good use of TREAT capabilities involves the electromagnetic response of fusion reactor instrumentation, control systems, and key plasma powering systems (such as RF windows) to intense neutron and ionizing radiation fields. This could be done by measuring the dependence of key electromagnetic parameters as a function of flux during a TREAT transient irradiation.

## F.7 Conclusions

The US/DOE breeder reactor facilities described above can play a role in performing small scale, but fairly sophisticated, multiple effects tests in a fusion reactor technology developement program. Experiments in these facilities could help bridge an information gap between simple materials testing and testing full scale (or true act alike) components. Indeed, costs and lead times are also likely to fall between these two extremes. While many test conditions of interest to the FINESSE project can be produced in these facilities, tests performed in these facilities will necessarily be on a small scale and suffer other features not prototypic of a true fusion environment. However, many strategies and techniques in experiment design can be borrowed from the breeder reactor developement program to circumvent prototypicality problems. Chief among these is the notion that a strong analytical program must advance interactively with experiment analysis and design.

## References for Appendix F

Sources of information for this report include the Guide for Irradiation Experiments in EBR-II, Guide for Irradiation Experiments in TREAT, and the Summary Description of the Fast Flux Test Facility available from ANL and WHC. A good deal of information on the subject can be found in the openly available Proceedings of the Conference on Fast Thermal and Fusion Reactor Experiments, (Salt Lake City, 1982) available from the American Nuclear Society.